Exploring Interstitial Mediators in Burn Injury

A Thesis Submitted in Accordance with the Requirements of the Degree of Doctor of Philosophy of Imperial College London

by

Dominic Friston

The Nociception Group

Department of Surgery and Cancer

APMIC
Imperial College,
Chelsea and Westminster Hospital Campus,
London, SW10 9NH

Supervised by:
Dr. Istvan Nagy, Dr. Elizabeth Want and Dr. Lakjaya Buluwela

Abstract

Burn injury remains a major clinical challenge to both survival and to quality of life. Its progressive, aberrant inflammation underlies the lethal dysfunction of various organs and the pain it induces is excruciating and notoriously difficult to manage. While it is known that burn injury's complex local and disseminating pathology is orchestrated from the burned tissue, few studies have sought to characterise the local signalling environment. An enhanced understanding of the local and acutely temporally-dynamic processes defining burn injury and its progression is required for the development of novel therapeutic interventions.

First, the viability of microdialysis as an interstitial sampling technique was established in a histologically-validated deep partial-thickness rat burn model before analysing the microdialysate's dynamic composition over three hours post-burn via metabolomics and a multiplex cytokine immunoassay. Next-Generation sequencing libraries of the burn and control microdialysis sites were prepared to measure transcriptional changes potentially underlying the interstitial profile characterising burn injury. The cytokines leptin and fractalkine, three lysophosphatidylcholine species (LPC(18:0), LPC(16:0) and LPC(14:0)), niacinamide and uric acid were all identified as molecules upregulated locally in the burn injury interstitium for the first time, which was further supported by the differential expression of their associated genes. *In vitro* study of LPC(18:0)'s possible contribution to inflammation and/or pain in burn injury elucidated its potentiation of TRPV1-mediated nociceptor responses, highlighting this interaction as a potential mechanism of lysophosphatidylcholine's established inflammatory and algogenic effects and implicating them in burn injury.

This project is the first exploratory analysis of the burn site interstitium, demonstrating the feasibility of combining local and continuous sampling with untargeted and multiplex molecular profiling for comprehensive study of any pathological state. Elucidating the functional relevance of the many elevated mediators and the nociceptor sensitisation reported presently in burn injury is an exciting prospect.

Contents

Abstract 2
Contents 4
Figure List 9
Table List 11
Declaration of Originality 12
Copyright Declaration 13
Acknowledgements 14
Abbreviations 15
1 CHAPTER 1 – GENERAL INTRODUCTION 17
1.1 Burn Injury 17
1.1.1 Definition 17
1.1.2 Epidemiology 18
1.1.2.1 Burn Injury: A World-Wide Clinical Challenge 18
1.1.2.2 Physical Rehabilitation 20
1.1.2.3 Psychological Aspects of Recovery 21
1.1.3 Burn Pathophysiology 22
1.1.3.1 Skin Anatomy and Clinical Burn Depth Classification 22
1.1.3.2 Mechanistic Bases of Burn Site Trauma 26
1.1.3.2.1 Denaturation 27
1.1.3.2.2 Free Radicals 28
1.1.3.2.3 Hypoperfusion 30
1.1.3.2.4 Burn Wound Progression - The Jackson Model 33
1.1.4 Clinical Priorities in Burn Treatment 35
1.1.4.1 Inflammation in Burn Injury 42
1.1.4.1.1 Inflammatory Mediators in Burn Injury 44
1.1.4.2 Burn Injury Pain 50

1.1.4.2.1 The Function of Pain 51
1.1.4.2.2 The Anatomy of Nociception 52
1.1.4.2.3 Nociceptive Signal Transduction 55
1.1.4.2.4 Nociception in Burn Injury 61
1.1.4.2.5 TRPV1: An Interface for Pain and Inflammation 67
1.1.4.2.6 Clinical Management of Burn Pain 73
1.1.4.3 Modelling burn injury in animals 77
1.2 Microdialysis 85
1.2.1 Experimental Considerations for Microdialysis 86
1.2.2 Microdialysis in Burns Research 92
1.3 Metabolomics 95
1.3.1 The Theory and Practise of Liquid Chromatography-Mass Spectrometry 98
1.3.1.1 Chromatography 99
1.3.1.2 Ionisation 101
1.3.1.3 Mass Analysers 102
1.3.1.4 Data Analysis 104
1.3.2 Metabolomics in Burns Research 106
1.4 Aims and Objectives 108
2 CHAPTER 2 – EXPERIMENTAL TECHNIQUES AND PROTOCOLS 109
2.1 Animals 109
2.2 Anaesthesia 109
2.3 Burn Model 110
2.4 Microdialysis 111
2.5 Metabolomics 113
2.5.1 Materials 113
2.5.2 Sample Preparation 113
2.5.3 UPLC-MS Analysis 114
2.5.4 Data Processing 115

2.5.5 Statistical Analysis of Metabolomics Data 116
2.5.5.1 PCA and PLS-DA 116
2.5.5.2 CVA 117
2.5.5.2.1 Executing CVA; Constructing the Batch Script 118
2.5.6 Structural Elucidation 126
2.5.6.1 Tandem Mass Spectrometry (MS/MS) 127
2.6 Lipidomics 129
2.7 Cytokine Panels 130
2.7.1 Statistical Analysis 132
2.8 Gene Sequencing 133
2.8.1 RNA Isolation 133
2.8.2 Next-Generation Sequencing Library Preparation 135
2.9 Tissue Sectioning and Histology 138
2.10 Cell Culture 139
2.10.1 DRG Primary Culture 139
2.10.2 HEK293T Cell Culture 140
2.10.3 Thawing, Passaging and Storage 140
2.10.4 Plasmid Amplification 141
2.10.5 Transfection 144
2.11 Calcium Imaging 145
2.11.1 LPC Preparation 146
2.11.2 Statistical Analysis 146
2.12 Whole-cell Voltage Clamp Electrophysiology 147
3 CHAPTER 3 – SAMPLING FROM SCALD-TYPE INJURY FOR MULTIPLE ANALYTICAL PLATFORMS 149
3.1 Introduction 149

3.2 Results and Discussion 153
3.2.1 Sample Collection 153
3.2.2 Sample Analysis 156
4 CHAPTER 4 – DEFINING THE BURN TRANSCRIPTOME 165
4.1 Introduction 165
4.2 Results and Discussion 168
5 CHAPTER 5 – THE INTERSTITIAL CYTOKINE PROFILE OF BURNED SKIN 183
5.1 Introduction 183
5.2 Results 185
5.3 Discussion 192
5.3.1 Leptin as an Inflammatory Mediator 192
5.3.2 Leptin in Burn Injury 194
5.3.3 Fractalkine as an Inflammatory Mediator 197
5.3.4 Further Considerations 201
6 CHAPTER 6 – TEMPORAL METABOLOMIC PROFILING OF THE BURN INJURY INTERSTITIUM 206
6.1 Introduction 206
6.2 Results 209
6.3 Discussion 223
6.3.1 Uric Acid in Disease States 224
6.3.2 The Protective Potential of Niacinamide in Burn Injury 226
7 CHAPTER 7 – LYSOPHOSPHATIDYLCHOLINE'S SENSITISATION OF TRPV1 AS A POTENTIAL NOVEL PRO-NOCICEPTIVE MECHANISM 229
7.1 Introduction 229
7.2 Results 233

7.3 Discussion 241
7.3.1 LPC and Immune Cells following Burn Injury 242
7.3.2 LPC and Cytokines 245
7.3.3 LPC and Burn Pathology 247
7.3.4 LPC and TRPV1 253
7.3.5 The Source of LPC 265
7.3.6 Further Targets for LPC 267
8 CHAPTER 8 – GENERAL DISCUSSION 273
8.1 Main Findings 273
8.2 Reflective Commentary: The Interpretation of Burn Injury Data 275
8.3 Project Shortcomings and Future Directions 279
8.4 Closing Remarks 287
9 References 289
10 Appendix 337

Figure List

Figure 1 The anatomy of the skin 23
Figure 2 Schematic of pathological factors underlying burn wound progression 34
Figure 3 Jackson's model of burn wound progression 36
Figure 4 The Wallace rule of nines 37
Figure 5 Key residues for TRPV1 function 69
Figure 6 The principles of microdialysis and probe style variants 92
Figure 7 Design matrix X 120
Figure 8 Matrix X0 120
Figure 9 Contrast matrix c 122
Figure 10 Skin histopathology following induction of a deep-partial thickness burn model 154
Figure 11 Metabolites are detectable via microdialysate UPLC-MS with both ESI+ and ESI- 157
Figure 12 PCA and PLS-DA scores plots indicate metabolite differences between burn and control microdialysate 159
Figure 13 High-VIP metabolites exhibit a clear burn effect 163
Figure 14 Expression distribution boxplots across all samples 173
Figure 15 Correlation matrix: pairwise comparison of normalised gene expression data 174
Figure 16 Principal component analysis of gene expression profiles of skin and DRG tissue 176
Figure 17 Heat map and HCA of genes differentially expressed between burn and control skin samples 177
Figure 18 Seven cytokines exhibited interesting temporal profiles 188
Figure 19 KEGG map of cytokine-cytokine receptor interaction pathway 191
Figure 20 KEGG map of the Jak-STAT signalling pathway 191
Figure 21 Canonical variates analysis of ESI+ UPLC-MS data 211
Figure 22 Canonical variates analysis of ESI- UPLC-MS data 212
Figure 23 Temporal concentration profiles of high canonical weight metabolite features. 216
Figure 24 Comparative fragmentation spectra of burn microdialysate metabolite features and previously-defined profiles available in metabolomics databases and publications 219

Figure 25 Comparative chromatograms and fragmentation spectra of target metabolite features and standard solutions of their expected structure 221
Figure 26 LPC(18:0), LPC(16:0) and LPC(14:0) are elevated in burn injury, as detectable by both metabolomics and lipidomics. 234
Figure 27 Various LPC-related genes are significantly differentially expressed in burned skin tissue 234
Figure 28 LPC(18:0) induces nonspecific membrane effects in untransfected HEK293T cells . 237
Figure 29 LPC(18:0) sensitises TRPV1 in HEK293T cells and DRG neurons 239
Figure 30 LPC(18:0) may further sensitise TRPV1 by enhancing its TrkA-mediated promotion of membrane insertion 256
Figure 31 Membrane perturbation by LPC 264

Table List

Table 1 RNA Yields measured in-house 155

Table 2 Quality Evaluations of total RNA 170

Table 3 Summary of RNA-Seq mapping statistics 172

Table 4 Group-wise correlation of expression data 173

Table 5 2-Way ANOVA statistics for 11 cytokines..... 187

Table 6 RNA comparisons of all cytokines and related genes discussed in this chapter 189

Declaration of Originality

I declare that the contents of this thesis are entirely my own work unless otherwise stated and that all additional sources of material are duly cited. As indicated in the text, significant contributions presented in this report were made by other individuals, notably including:

- Generating and constructing the figure presenting the histological validation of our burn model's depth (Fig. 10; Jose Valente Torres Perez)
- Preparation of Next-Generation gene sequencing libraries from RNA I isolated and provided (Chapter 4; Vienna Biocenter Core Facilities)
- Lipidomics analysis of microdialysate (which features only briefly in this report in contributing half of the data in Fig. 26; Dr. Tim Marczylo)

Copyright Declaration

The copyright of this thesis rests with the author and is made available under a Creative Commons Attribution Non-Commercial No Derivatives license. Researchers are free to copy, distribute or transmit the thesis on the condition that they attribute it, that they do not use it for commercial purposes and that they do not alter, transform or build upon it. For any reuse or redistribution, researchers must make clear to others the licence terms of this work.

Acknowledgements

First and foremost, I wish to thank Dr. Istvan Nagy. Under your supervision, I never felt anything less than completely supported in an often unpredictable environment. You never steered me wrong, and I could not have hoped to enjoy the company of a supervisor more. For the same reasons, I must thank Dr. Elizabeth Want, who guided me through difficult terrain with infallible (if rarely-shared) optimism to great reward. Thanks to both of your efforts, I can already look back over the past four years with extreme fondness.

Thank you to my research family; particularly Jose Torres, whose companionship was a rare and important constant over my PhD. Thank you to Dr. Helen Laycock, for your ongoing support and often uniquely valuable insight into my research. Thank you to Dr. João Valente and Dr. Anna Andreou for all the fun we had, and for being the first to teach me what it is to develop into a scientist. Thank you to everyone else who brightened the lab, including the Kim Lackenby, Sarah Gentry, Jacky Chen, Sara Ellen, Flavia Rosianu, Alina Miedzik, Ela Rapacz and particularly Faruq Noormohamed.

Finally, thank you to my family, particularly my inspirational father, for your unwavering love and ongoing support of my education.

Abbreviations

5-HT	Serotonin
AA	Arachidonic acid
ANOVA	Analysis of variance
APCI	Atmospheric pressure chemical ionisation
ASIC	Acid-sensing ion channel
ATP	Adenosine triphosphate
ATX	Autotaxin
AUC	Area under curve
BBA	British Burn Association
BK	Bradykinin
Ca_v	Voltage-gated calcium channel
CaM	Calmodulin
CaMKII	Ca^{2+}/Calmodulin-dependent protein kinase II
CGRP	Calcitonin gene-related peptide
CNS	Central nervous system
COX-2	Cyclooxygenase-2
CVA	Canonical variate analysis
DAG	Diacylglyceride
DC	Dendritic cell
ddH_2O	Double-distilled water
DRG	Dorsal root ganglia
ELISA	Enzyme-linked immunosorbent assay
EPSC	Excitatory post-synaptic currents
ERK	Extracellular signal-regulated kinase
ESI	Electrospray ionisation
FDR	False discovery rate
GC	Gas chromatography
G-CSF	Granulocyte colony-stimulating factor
GM-CSF	Granulocyte macrophage colony-stimulating factor
GO	Gene ontology
HEK293T	Human embryonic kidney cells 293 with T antigen of SV40
HIC	High income country
HILIC	hydrophobic interaction liquid chromatography
-HODE	-Hydroxyoctadecadienoic acid
-HPETE	-Hydroperoxyeicosatetraenoic acid
HPLC	High-performance liquid chromatography
HRQoL	Health-related quality of life
IFNγ	Interferon-γ
IASP	International Association for the Study of Pain
IL-	Interleukin-
IPA	Isopropyl alcohol
iNOS	Inducible nitric oxide synthase
JAK2	Janus kinase 2d-Signal Transducer
JNK	c-Jun N-terminal kinase
KEGG	Kyoto Encyclopaedia of Genes and Genomes
K_v	Voltage-gated potassium channel
LC	Liquid chromatography
LCAT	Lecithin-cholesterol acyltransferase
LMIC	Low-to-middle income country
LPA	Lysophosphatidic acid
LPC(14:0)	Lysophosphatidylcholine(14:0)
LPC(16:0)	Lysophosphatidylcholine(16:0)

LPC(18:0)	Lysophosphatidylcholine(18:0)
MAPK	Mitogen-activated protein kinase
MCP-1	Monocyte chemoattractant protein-1
MeOH	Methanol
MIP-1β	Macrophage inflammatory protein 1β
MODS	Multiple organ dysfunction syndrome
MS	Mass spectrometry
MS/MS	Tandem mass spectrometry
MW	Molecular weight
m/z	Mass-to-charge ratio
Na_v	Voltage-gated sodium channel
NF-κB	Nuclear factor kappa-light-chain-enhancer of activated B cells
NGF	Nerve growth factor
NIH	National Institutes of Health
NK cell	Natural killer cell
NMDAR	N-methyl-D-aspartate receptor
NMR	Nuclear magnetic resonance spectroscopy
NSAID	Non-steroidal anti-inflammatory
NO	Nitric oxide
PAR	Protease-activated receptor
PARP	Poly ADP ribose polymerase
PC	Phosphatidylcholine
PCA	Principal component analysis
PFA	Paraformaldehyde
PGE2	Prostaglandin E2
PI3K	Phosphatidylinositol-4,5-bisphosphate 3-kinase
PKA	Protein kinase A
PKC	Protein kinase C
PLA_2	Phospholipase A_2
PLS-DA	Partial least squares-discriminant analysis
PMN	Polymorphonuclear neutrophils
PSN	Primary sensory neuron
PUFA	Polyunsaturated fatty acid
QC	Quality control
Q-TOF	Quadrupole-Time of flight (mass analyser)
RA	Rheumatoid arthritis
RM	Repeated measures
ROS	Reactive oxygen species
RP	Reversed-phase (chromatography)
RT	Retention time
SIRS	Systemic Inflammatory Response Syndrome
STAT3	Activator of transcription 3
TBSA	Total body surface area
TNF-α	Tumour necrosis factor-α
TrkA	Tropomyosin receptor kinase A
TLR2	Toll-like receptor 2
TRPC5	Short transient receptor potential channel 5
TRPM8	Transient receptor potential M member 8
TRPV1	Transient receptor potential vanilloid type 1
TTX	Tetrodotoxin
UPLC	Ultra-performance liquid chromatography
VEGF	Vascular endothelial cell growth factor
VIP	Variable influence on projection
WHO	World Health Organisation

1 CHAPTER 1 – GENERAL INTRODUCTION

1.1 Burn Injury

1.1.1 Definition

“Burn” is a broad term that can refer to one of many types of injury. According to the International Society of Burn Injuries and the World Health Organisation (WHO), a burn can result from exposure to heat, cold, radiation, chemicals, electricity or friction (WHO, 2014). Despite their shared name and some mechanistic overlap, the pathogenesis and progression associated with each trauma is dependent on which of these sources induced them. This project is exclusively an investigation of heat-induced burn injury, in which energy is transferred from an external heat source to the body resulting in trauma of the skin and, in some cases, the underlying tissues. Such injuries, henceforth referred to simply as ‘burns’, include scalds, resulting from contact with hot liquids, contact burns, resulting from contact with hot solids, and flame burns, resulting from contact with flames; no other type of burn is discussed in this thesis beyond this point. This introductory chapter is an overview of burn injury, with particular focus on the inflammatory and nociceptive components of its pathophysiology, and of microdialysis and metabolomics, particularly as potential means of investigating these high clinical priority aspects of burn injury.

1.1.2 Epidemiology

1.1.2.1 Burn Injury: A World-Wide Clinical Challenge

The World Health Organisation (WHO) most recently estimated that 265,000 deaths are caused by fire-related injuries annually world-wide (WHO, 2014). Of these, 90-95% are estimated to occur in low and middle income countries (LMICs), with half occurring in Southeast Asia (Ahuja et al., 2009; Peck et al., 2013; WHO, 2014). However, the vast majority of burns are non-fatal. 2004 saw 11,000,000 burns requiring medical attention world-wide, ranking fourth among all injuries, and burns under 20% total body surface area (TBSA) occurred in 153 per 100,000 children aged 0-15 years and were hence the fifth most common non-fatal injury for this age group (WHO, 2008). Such wide-scale, grand summations are challenging; global evaluations of severity-, morbidity-, mortality-, source- (contact, liquid, flame), outcome- or risk factor-specific effects are complicated by inter-regional inconsistencies in data recording and availability and, indeed, the region-dependent interrelated nature of these multivariate factors themselves. Nonetheless, regional studies have offered great insight into the worldwide incidence, treatment and impact of burn injury.

Regarding LMICs, 1,000,000 people are moderately to severely burned in India each year (WHO, 2014). A meta-analysis of empirical studies within India, Pakistan, Bangladesh and Sri Lanka indicated that 80% of burns were flame- or scald-induced; they were more common among males aged 0-12 and among females over 14 with most burns occurring in the home. Low socioeconomic status, youth and flammable clothing were among the identified risk factors (Golshan et al., 2013). Of the 732

burn admissions in a South-eastern Iranian hospital over 2 years, 95.1% of the injuries were heat-induced (33.1% were scalds), 14.3% were intentional, age and sex correlated with the cause of the burn and a TBSA over 50% closely correlated with mortality (Ansari-Moghaddam et al., 2013). In Lebanon, a higher middle income country, during the 20 years leading up to March 2012, 1,524 patients were admitted to a burn unit in Geitawi; 47% were from rural areas, 36% had a 20-40% TBSA burn and TBSA correlated with mortality (Ghanime et al., 2013). In Istanbul, Turkey (of the same economic status as Lebanon), 1,590 burn patients presented to the burn clinic between January 2005 and January 2009. 975 of their number were children, 375 of which were hospitalised; scalding accounted for 85.6% of their injuries and 91.2% resided in urban areas. Their mean TBSA was 14.1%, with a range of 1-86% (Arslan et al., 2013).

Among the higher income countries (HICs), 220 per 100,000 of the US population required medical attention for their burns annually with 5% requiring hospitalisation or transfer between 1993 and 2004 (Fagenholz et al., 2007). In the UK, burn patients represent 1% of all presentations in accident and emergency departments at 175,000 cases per year and 10% of these require inpatient burn unit care. Further, 250,000 cases are managed outside hospitals by general practitioners or other healthcare professionals (Enoch et al., 2009). On average, 300 succumb to their injury each year (BBA, 2001). The improvement and stability of burn mortality rates among HICs, recorded between 4 and 7% (Bloemsma et al., 2008; Enoch et al., 2009), has prompted some shift in focus regarding outcome for empirical study from survival to quality of life (Pereira et al., 2004). Such analyses have assessed the

physical rehabilitative outcomes, the psychological consequences of the injury and the changes to quality of life these underlie.

1.1.2.2 Physical Rehabilitation

At the point of physical rehabilitation, contractures (a hardening of affected tissue) are among the most common causes of impaired mobility following burn injury (Leblebici et al., 2006). Between 1993 and 2002, 38.7% of 985 regional burn unit admissions developed at least one contracture at discharge where, among those with contractures, the mean amount was 3 (Schneider et al., 2006). Contracted tissue not only directly restricts movement but can lead to prolonged hyperextension (bending a joint beyond its normal range) and thereby dislocation, as has been observed with 19% of surgically treated post-burn metacarpophalangeal joint extension contractures (Graham et al., 1990; Stoddard et al., 2014). Functional range of the underlying joints is susceptible to further orthopaedic complications (Stoddard et al., 2014), such as the formation of osteophytes (Evans et al., 1959) or heterotopic ossification, observed in 1-2% of burn patients (Elledge et al., 1988; Hunt et al., 2006; Peterson et al., 1989) Functional compromise can also result from muscle weakness caused by various neuropathies, whether peripherally localised or generalised, as observed with 15-37% (Helm et al., 1977; Henderson et al., 1971) and 15-29% (Helm et al., 1977; Lee et al., 2009) of acute burn patients respectively. Further, a hypermetabolic response with concomitant muscle catabolism always occurs with a burn >40% TBSA and persists for a year after the injury (Hart et al., 2000a; Hart, et al., 2000b).

1.1.2.3 Psychological Aspects of Recovery

Two principally concerning psychological burn symptoms are depression and post-traumatic stress disorder, reported to prevail in 7-46% and 9-45% of burn survivors respectively (Difede et al., 1999; Dyster-Aas et al., 2008; Falder et al., 2009; Lawrence et al., 2006; Madianos et al., 2001; Perry et al., 1992; Thombs et al., 2007; Williams et al., 1991). It is widely accepted that, despite discrepancies in prevalence rates likely owing to measurement inconsistencies (Falder et al., 2009), facilitation of psychological recovery is key to rehabilitation (Blakeney et al., 2008; Yu et al., 1999). The practical and emotional implications of these culminating physical and psychological detriments are perhaps best indicated by broader health-related quality of life (HRQoL) measures, which focus on the daily impact of the injury and, crucially, reflect the patient's capability to compensate for physical or psychological setbacks (Palmieri et al., 2014). Regardless of the instruments used, prominent among which are the EQ-5D, the Short Form 36 Health Survey, the Burns-Specific Health Scale and their shorter variants, their measurements converge on the fact that burns cause an often unrecoverable and substantial loss in quality of life attributed to both physical and psychological detriments (Miller et al., 2013; Oster et al., 2011; Pavoni et al., 2010; Tirumala N et al., 2013; Wasiak et al., 2014; Xie et al., 2012).

Over the last century, enhancements in burn prevention strategies (Hunt, 2000), our understanding of burn pathophysiology (Marshall et al., 1983) and general critical care (Goretsky et al., 1995; Hickling et al., 1994; Pereira et al., 2004) have led to vastly improved survival rates (Esselman et al., 2006; Hoskin, 2000; Ilechukwu,

2002; Pereira et al., 2004). Mortality has declined from 54-100% at the beginning of the 20th century, plateauing over the last 30 years, to 5-6% (Hoskin, 2000; Jaskille et al., 2009; Sneve, 1905). Indeed, mortality is expected to further improve with enhanced management of the effects of systemic inflammation. However, it is evident that burn injury remains a global problem and, with improving mortality, attention must also address morbidity. The challenges faced in this endeavour are as complex, multifaceted and interrelated as the outcomes requiring improvement among burn survivors.

1.1.3 Burn Pathophysiology

Here, the characteristics and components of the trauma within the burn site along with their progressions and any further-reaching effects they have are overviewed. As is convention for experimental burn studies, the findings of the current work will be discussed in terms of the injury's clinical classifications, which are here used as a starting point to describe burn pathophysiology in the immediately affected anatomy: the skin.

1.1.3.1 Skin Anatomy and Clinical Burn Depth Classification

Regardless of the various pathological components inducing tissue damage, and the complexity of their temporal profiles following the initial trauma, burn wounds are principally and most simply categorised by their depth of the damage. Clinically-relevant burn depths are mapped to the layers of the skin (Fig. 1); superficial (first degree) burns do not extend past the epidermis, partial-thickness (second degree)

burns extend within the dermis and full-thickness (third degree) burns extend to full dermal trauma, reaching the subcutaneous tissue (Heimbach et al., 1992). Three further degrees of burn injury exist; fourth degree burns extend below the skin into muscle tissue, fifth degree burns extend beyond muscle and superficially affect bone and sixth degree burns char bone. These burn depths are typically induced by the same sources as third degree burns with greater durations of exposure, though they are less clinically relevant with mortality rates of nearly 100%.

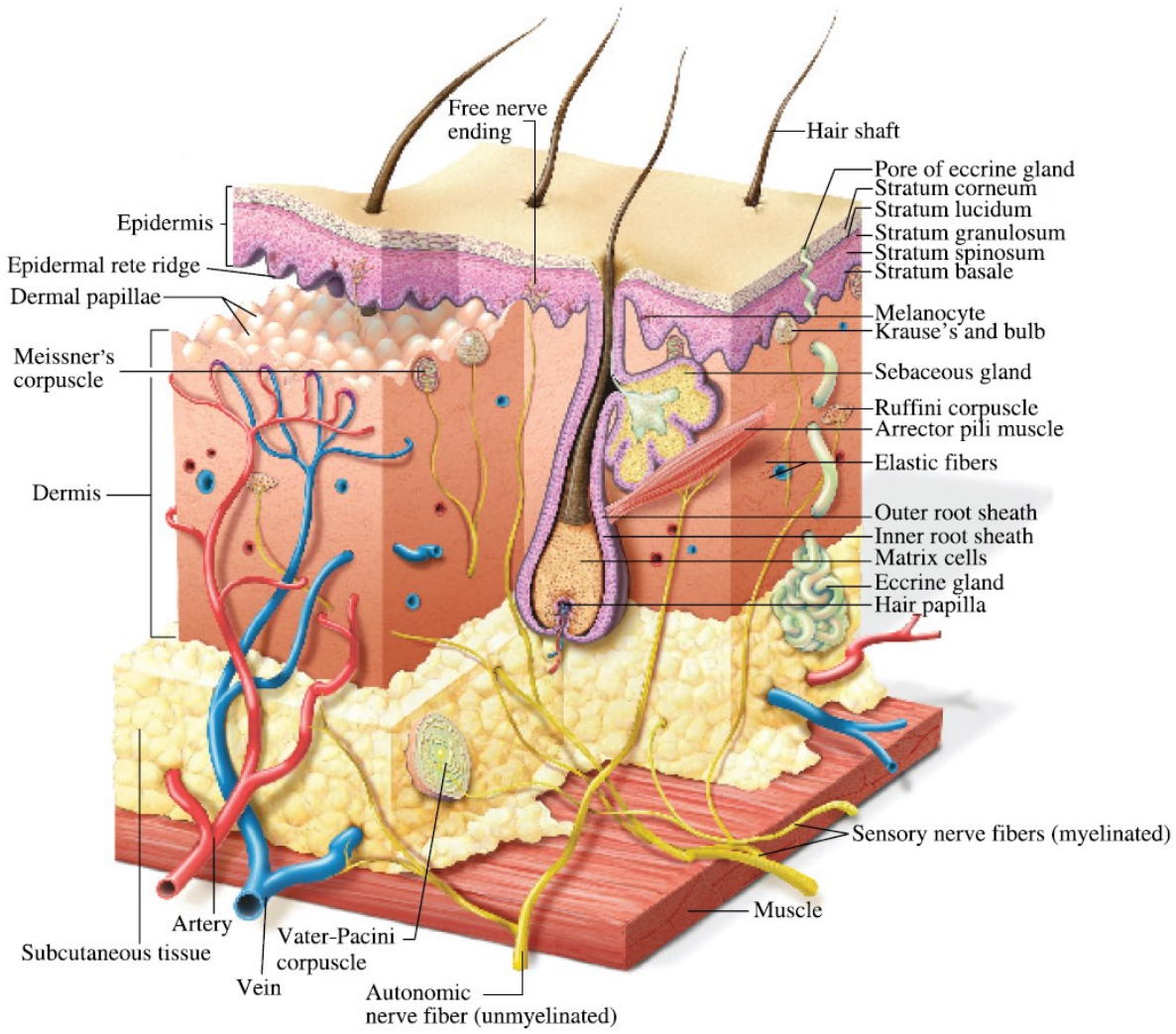


Figure 1 The anatomy of the skin. This schematic representation of the skin presents the layout of the epidermis, dermis and subcutaneous tissue and their constituent structures. It is by its descent through these layers that burn depth is classified and the pathological consequences progress. Image published by DeSanti (2005) and reproduced with permission of the rights holder, Wolters Kluwer Health, Inc.

Superficial burns are induced by minor exposure, whether restricted by duration or extremity of the temperature, and only damage the epidermis. The epidermis contains no blood vessels and is nourished both by diffusion of oxygen from the surrounding air and by the delivery of nutrients from the underlying dermis, which further serves as a channel for waste disposal. It is composed primarily of keratinocytes which progressively differentiate superficially with increasing keratinisation, ultimately reaching the outermost epidermis with no nuclei and eventually being shed as they are replaced. This progression defines 5 epidermal layers; from the deepest to the most superficial, they are the stratum basale, stratum spinosum, stratum granulosum, stratum lucidum and stratum corneum. The stratum corneum hence provides the outermost layer of the body's defense against trauma and infection, while the stratum basale, composed of a single layer of keratinocytes, is attached to the basement membrane. Retention of the stratum basale and basement membrane enables differentiation to replace every layer up to the stratum corneum, and hence complete regeneration of the tissue with no permanent changes. Prior to recovery, the affected epidermal layers may peel off and symptoms will include pain and minor inflammation, enabled in part by the presence of naked nerve endings terminating in the basal epidermal layers and the presence of Langerhans cells among the 5% of epidermal cells that are not keratinocytes (where the others are melanocytes and Merkel cells).

Second degree burns extend deeper, into the dermal skin layers. The dermis exists to maintain the epidermis and is structurally more complex, consisting of both the papillary dermis and the reticular dermis, where burns extending into either are respectively referred to as superficial-partial and deep-partial thickness burns. Both

layers are composed of the skin's outermost blood vessels, elastic fibres and Type I and III (reticular) collagen fibres, where these fibres constitute 70% of the dermis' protein content. The papillary dermis is thinner with its fibres arranged loosely, while the reticular dermis is denser with fibres organised parallel to the epidermis. These fibres are produced by fibroblasts, the principal cell type of the dermis, while macrophages and adipocytes constitute two further dermal major cell classes. The collagen fibres confer skin's tensile strength and resistance to mechanical forces and the elastin fibres (1% of the dermal protein content) resist deformation and maintain the skin's original shape (Debelle et al., 1999). The dermis also contains nerve endings, epidermal appendages, macrophages and mast cells, while the remainder is extracellular matrix composed of mucopolysaccharides, chondroitin sulfates, and glycoproteins. Burns extending this far induce a greater inflammation with capillary dilation and enhanced permeability; this fluid shift manifests as blister formation in superficial partial-thickness burns, in which only a thin layer of dermal cells is lifted from those underlying by the collection of fluid with inflammation. In such cases, deeper extensions of the epidermal rete ridge containing basal keratinocytes survive, and keratinocytes can proliferate to confluency before regenerating the epidermis, albeit in a thinner, weaker form. Superficial partial thickness burns (without infection) typically heal spontaneously within three weeks for a cosmetically satisfactory result. However, if the damage extends to the reticular dermis, the damaged skin layer is too thick for blister formation; it is either removed during the trauma, in which case the exposed reticular dermis weeps, or remains as a blanched, waxy layer. At this depth, rete ridge extensions are no longer viable and the only remaining basal keratinocytes will be sparsely located alongside epidermal appendages such as hair follicles and sweat glands (see Fig. 1). They remain viable for proliferation and

eventual convergence of their separate colonies, though spontaneous healing can take many weeks under these circumstances and the results are aesthetically inferior to those achieved with surgical wound closure.

In third degree or “full thickness” burns, the dermis and epidermis are lost in their entirety, leaving the subcutaneous tissue exposed. Subcutaneous tissue, the innermost layer of the integumentary system, is primarily composed of adipocytes and collagen and elastin fibres, and contains larger blood vessels and nerve endings than the dermis as well as the roots of some epidermal appendages such as hair follicles (Fig. 1). It functions as a source of energy and means of temperature regulation, as well as protecting the body from mechanical stress. When a burn extends to the subcutaneous tissue, a deep granulating wound (consisting of new connective tissue and microscopic blood vessels) remains, around which the epithelium will slowly proliferate inwards. Such spontaneous healing can only accomplish closure in small third degree burns though, without surgical intervention, scarring and contracture following a third-degree burn is of a debilitating severity in any case. As described below, burn depth classification, in combination with determining the burn total body surface area (TBSA), is crucial for directing the clinical response.

1.1.3.2 Mechanistic Bases of Burn Site Trauma

The above description of a primary aspect of burn classification outlines the affected structures with progressing damage depth, which directly affects patient outcome and required clinical intervention. The cause of this damage is multi-faceted and

progressive, and requires careful consideration in any attempt to delineate the mechanisms underlying burn pathology. Below, the fundamental traumatic processes underlying tissue damage within burn injury are described.

1.1.3.2.1 Denaturation

Every pathological effect induced by a burn ultimately stems from the simple transfer of energy to the skin. This is detrimental because proteins rely on their native formations, held at 37°C, to function. Conformational changes occur even within physiological temperatures, although they can be irreversible when induced with sufficient supraphysiological temperature leading to denaturation (Despa et al., 2005). This process is mediated by the disruption of secondary and tertiary protein structures; while the energy transferred is not sufficient to break peptide bonds, and the amino acid organisation remains unaffected, alpha-helix and beta sheet proteins are disrupted such that the protein uncoils into a random shape. Heat in particular denatures proteins by the elevation of kinetic energy causing molecules to vibrate with a frequency and strength sufficient to overpower hydrogen bonds and non-polar hydrophobic interactions, disrupting protein structure. Once the secondary and tertiary structure is compromised, denatured proteins precipitate or coagulate and are rendered irreversibly damaged (Despa et al., 2005). The temperature at which this occurs depends on the molecule or structure; for example, computational modelling indicates that, with 20 seconds of exposure, lipid bilayers are completely denatured at 48°C, while 60°C denatures 2% of collagen and 1% of RNA. Denaturation is the fundamental pathological mechanism in burn injury, disrupting proteins and cell membranes to induce coagulation necrosis such that they cease to

function and initiate a cascade of further pathological processes in the surrounding tissue, as described below.

1.1.3.2.2 Free Radicals

Following the initial transfer of energy, the formation and actions of free radicals represent a traumatic component of injury engaging various other aspects of the pathology. Free radicals are molecules with unpaired electrons, which confer to the compound a strong oxidising and/or reducing potential. The most influential products of free radicals are the reactive oxygen species (ROS) superoxide, hydroxyl radicals and hydrogen peroxide. Free radicals are generated and function physiologically in cells, for example in catalysing the action of certain enzymes (Reichard et al., 1983; Stubbe, 1990) and via their role in bactericidal phagocytosis (Rosen et al., 1995). However, free radicals can be toxic to host tissue. All major biomolecular classes are susceptible to damage by free radicals, though cell membranes in particular are at risk for their high polyunsaturated fatty acid (PUFA) content (Latha et al., 2001). Further, this oxidative membrane destruction, known as lipid peroxidation, is a self-sustaining, on-going process (Ayala et al., 2014). Collagen, protein enzyme systems (Weiss, 1986), organelle membranes (e.g. for lysosomes and mitochondria; Del Maestro et al., 1980) are also at risk. Free radicals, left unchecked, can thereby serve as a fundamental inducer of cell death (Malorni et al., 1993). In addition to general lipid peroxidation, ROS may induce apoptosis through poly ADP ribose polymerase (PARP) cleavage, elevation of mitochondrial permeability with cytochrome C release and caspase activation (Shupp et al., 2010). Free radicals mediate cell death in burn injury as a result of two principal factors. Firstly, immune

cells such as neutrophils and mast cells recruited post-burn induce the release of superoxide radicals (Babior, 1978) alongside various further oxidants (Weiss, 1986) in their bactericidal capacity via NAPDH and xanthine oxidase-dependent pathways (Horton, 2003); although it is an immune response, the molecules cannot discriminate between bacteria and host tissue when inducing damage. Secondly, while oxidative species are comfortably regulated by antioxidant enzyme systems, vitamins and specialised molecules under physiological conditions (Guemouri et al., 1991), this regulation is compromised in burn injury and free radicals are left unchecked (Aust et al., 1986; Tredget et al., 1992). Free radical scavenging enzyme systems such as superoxide dismutase (which catalyses superoxide → hydrogen peroxide), catalase and glutathione peroxidase (which catalyses hydrogen peroxide → water and oxygen) themselves operate by oxidation and reduction and are thereby powered by electron supply. In burn injury, tissue hypoperfusion induces hypoxia and therefore ATP depletion (which itself induces cell death via calcium overload; Tsujimoto, 1997), leading to insufficient energy supply for regeneration of free radical scavengers (Kaufman et al., 1989). Further, following sufficient duration of oxygen deprivation, resupply of oxygen with reperfusion paradoxically contributes to further free radical production, leading to another cycle of neutrophil infiltration and free radical release (Kalogeris et al., 2012). Free radical-mediated damage is therefore a fundamental mediator of tissue damage in burn injury (Horton, 2003; Latha et al., 2001), and can underlie the pathological contributions of compromised tissue perfusion and inflammation as described below.

1.1.3.2.3 Hypoperfusion

As exemplified by the influence of oxidative stress, impaired blood flow is a defining feature of burn injury. It is extensively multifaceted and informs the vast majority of local pathological components underlying burn wound progression following the initial denaturing trauma; indeed, the above-discussed direct denaturation of vasculature and the effect of free radicals (specifically on post-capillary venules following neutrophil aggregation; Cetinkale et al., 1997) both contribute to altered perfusion in burn tissue. However, many further factors compromise burn wound circulation and can induce further-reaching systemic effects of clinical significance, as discussed below.

The principal cause of hypoperfusion post-burn is oedema, which occurs both locally and systemically as a consequence of various underlying processes (Infanger et al., 2004). The net effect of these processes is the shift of fluid from the vascular to the interstitial space, which raises tissue pressure to the point of preventing blood flow (Baskaran et al., 2000). The formation of oedema results from three underlying factors; the first, increased capillary permeability, is mediated by a variety of mechanisms. Venule endothelial cell contraction, which increases the interendothelial cell space, is mediated by various inflammatory mediators such as histamine, bradykinin, leukotrienes, nitric oxide and substance P (Cotran, 1965; Kumar et al., 2005). Further, endothelial cells are susceptible to denaturation or oxidative stress in burn injury (Baskaran et al., 2001; Bucky et al., 1994; Kumar et al., 2005). It has also been suggested that elevated capillary permeability in burn injury is mediated by increased endothelial cell transcytosis (movement of protein

through endothelial cell pores) via the action of vascular endothelial cell growth factor (VEGF; Infanger et al., 2004; Kumar et al., 2005). Elevated vascular permeability alone is insufficient to generate the oedema observed post-burn; another factor it depends on is a decrease in interstitial hydrostatic pressure (Shupp et al., 2010). This is attributed primarily to two underlying processes; firstly, the denaturation of collagen as a result of thermal trauma inducing its transformation into a water-soluble gelatin (Lund et al., 1992) and, secondly, reduced fibroblast adhesion to collagen networks leading to compromised constraint of hyaluronan gel. Hyaluronan gel characteristically swells with the availability of fluid and the space to do so and, without the limitations imposed by collagen, draws from fluid in the vascular supply until the negative interstitial hydrostatic pressure is balanced (Rodt et al., 1994). Oedema is also partially attributed to a third factor, vasodilation, which is observed concomitantly with an increase in capillary hydrostatic pressure (Demling, 2005) and the availability of various inflammatory mediators capable of its mediation (Rawlingson, 2003; Taheri et al., 1994). However, the possibility that vasodilation's contribution to the fluid shift underlying oedema is negligible in comparison to that of capillary permeability and interstitial hydrostatic pressure is noted (Shupp et al., 2010).

Oedema is not the only cause of hypoperfusion. While its characteristic vasodilation may contribute to hypoperfusion by increasing interstitial pressure, vasoconstriction is also reported to contribute to burn wound progression (Demling, 2005; Shupp et al., 2010) though the relative contributions of vasodilation and vasoconstriction over time and spatially post-burn are not clear. Vasoconstriction is suggested to contribute to hypoperfusion simply through reducing fluid availability, and is

implicated in burn injury specifically by the vasoconstricting action of thromboxane A2 (which further elevates vascular permeability, platelet aggregation and neutrophil activation) which is elevated following thermal trauma (Barrow, Ramirez, et al., 2000). The assertion is supported by demonstrations that systemic vasoconstrictor administration enhances burn wound depth (Knabl et al., 1999) and indications that ibuprofen pre-treatment improves burn wound outcome via arachidonic acid cascade inhibition at the cyclooxygenase (COX) level reducing vasoconstriction (Barrow, Ramirez, et al., 2000), though contrasting results for this line of support have been published (Tan et al., 2002).

Beyond oedema and vasoconstriction, hypercoagulability is the final principal contributor to circulatory deficiency in burn injury. Platelet aggregation is increased following thermal trauma, leading to the promotion of thrombus formation and thereby the occlusion of blood vessels, as can be observed by histological examination (Bucky et al., 1994; Cotran, 1965). Further, thrombus formation in burn injury is potentiated by a concomitant reduction of fibrinolysis (Isik et al., 1998; Rockwell et al., 1990). These processes are attributed to decreased thrombomodulin activity, where thrombomodulin is a glycoprotein located on the endothelium and exerts inhibition of thrombosis and enhancement of fibrinolysis through the respective inhibition of thrombin and activation of protein S (Uygur et al., 2009). It has further roles in physiological states, including reducing the release of endothelial cell proinflammatory cytokines and leukocyte adhesion (Shupp et al., 2010). However, in pathological states such as burn injury (Uygur et al., 2009) and those involving shear stress or hypoxia (Shupp et al., 2010), thrombomodulin is down-regulated at a transcriptional level, contributing to hypercoagulability. This has

motivated several experimental approaches to addressing local circulatory deficiency. The capability of the lipid-lowering medication Simvastatin to restore blood flow in burn injury has been attributed to its maintenance of thrombomodulin expression (Uygur et al., 2009), demonstrating restoration of the body's endogenous regulation of coagulation. Alternative approaches have included the application of exogenous fibrinolytic agents (Isik et al., 1998), fibrin synthesis inhibitors (Mahajan et al., 2006) and platelet aggregation inhibitors (Battal et al., 1997). The success of all these approaches in reducing necrosis in experimental contexts suggests that hypercoagulability is a principal contributor to hypoperfusion-mediated tissue damage in burn injury, though aggressively targeting coagulation in patients undergoing frequent surgeries (see below) poses the risk of their bleeding out and there is little evidence supporting an improvement in patient outcome with the use of the more common clinical anticoagulant heparin (Oremus et al., 2007).

1.1.3.2.4 Burn Wound Progression - The Jackson Model

While the fundamental pathological processes contributing to the burn wound are described separately above, many of them are heavily interrelated as expressed schematically by Singh et al (Fig. 2; Singh et al., 2007). The onset and interaction of these processes define how the wound develops following the initial traumatic transfer of energy; while directly denatured tissue cannot be recovered, subsequent wound progression is open for therapeutic intervention. Understanding the contribution of the above-described processes over time is therefore crucial for informing the clinical approach to burn injury. The pathological progression as

mediated by these underlying processes are described by the Jackson Model of Burn Wound Progression, discussed below.

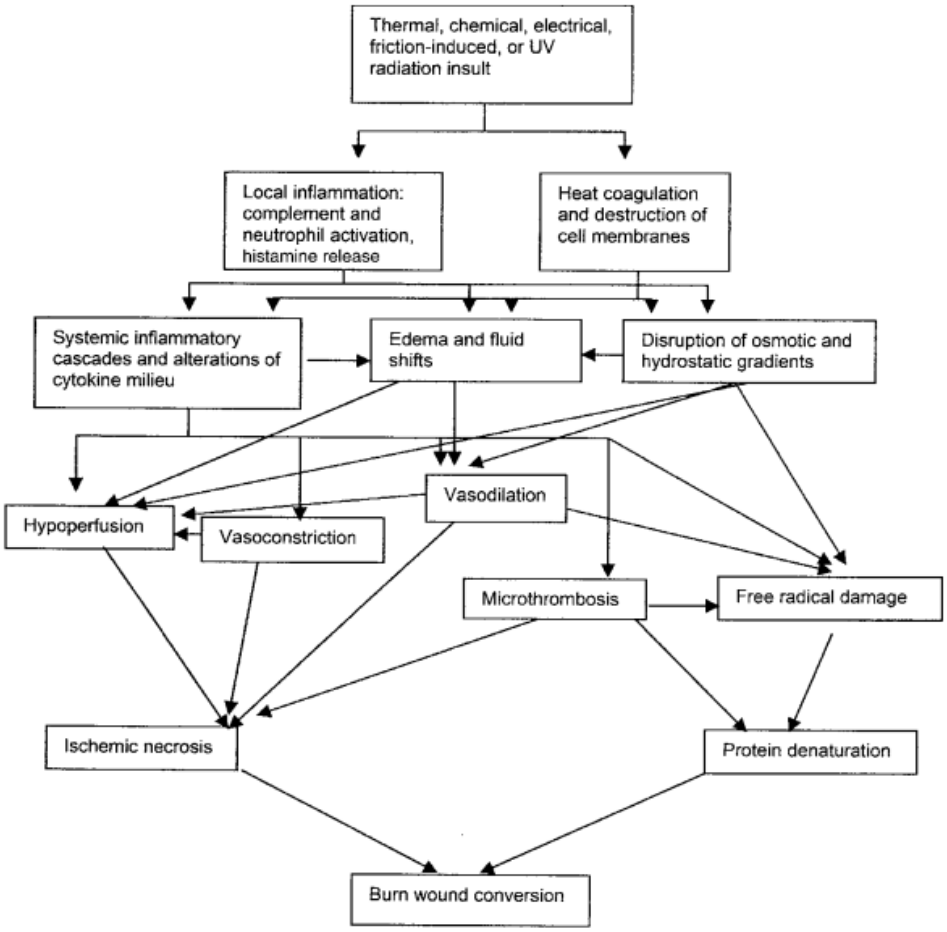


Figure 2 Schematic of pathological factors underlying burn wound progression. This schematic outlines the temporally-complex interplay of individual pathological factors underlying the development of the burn wound. Image published by Singh et al. (2007) and reproduced with permission of the rights holder, Wolters Kluwer Health, Inc.

The Jackson model divides areas of the local burn site by the viability of their tissue, and demonstrates that burn depth, despite constituting the primary axis of characterisation in clinical assessment, is dynamic during the acute phase of recovery. At its core, the zone of coagulation is characterised by denatured tissue for

which recovery is impossible as the coagulated proteins cannot be restructured at a secondary and tertiary level (Hettiaratchy et al., 2004). The immediately surrounding tissue is the zone of stasis, named for its characteristic circulatory deficiency and reflecting the pathological significance of hypoperfusion. Crucially, this tissue can be salvaged with adequate patient care; recovery of the zone of stasis depends on restoration of blood supply, as has been compromised by various factors inducing hypoperfusion as described above. Unsuccessful restoration of perfusion to the zone of stasis will eventually render it unsalvageable, converting it to an addition to zone of coagulation (Fig. 3). Finally, the outermost region defined by the model is the zone of hyperaemia. This tissue is generally expected to recover, but remains susceptible for conversion to zone of stasis and subsequently to zone of coagulation if circulatory deficiency or severe sepsis remains unresolved for an extended period of time (Hettiaratchy et al., 2004). Preventing wound progression, its underlying pathological components and the systemic effects being progressively orchestrated from the burn site are the defining objectives of therapeutic intervention, which is discussed below.

1.1.4 **Clinical Priorities in Burn Treatment**

It is the above-described fundamentally tissue-damaging processes, characterising both the initial trauma and the wound's progression, that dictates the need for the particularly complex and multi-disciplinary clinical response required for burn injury. Clinical intervention targets both local and systemic burn effects to address the greatest threats to survival and quality of life during and after recovery, and currently represents some areas with great demand for further research. As such, the clinical

management of and challenges in responding to burn injury are briefly outlined below.

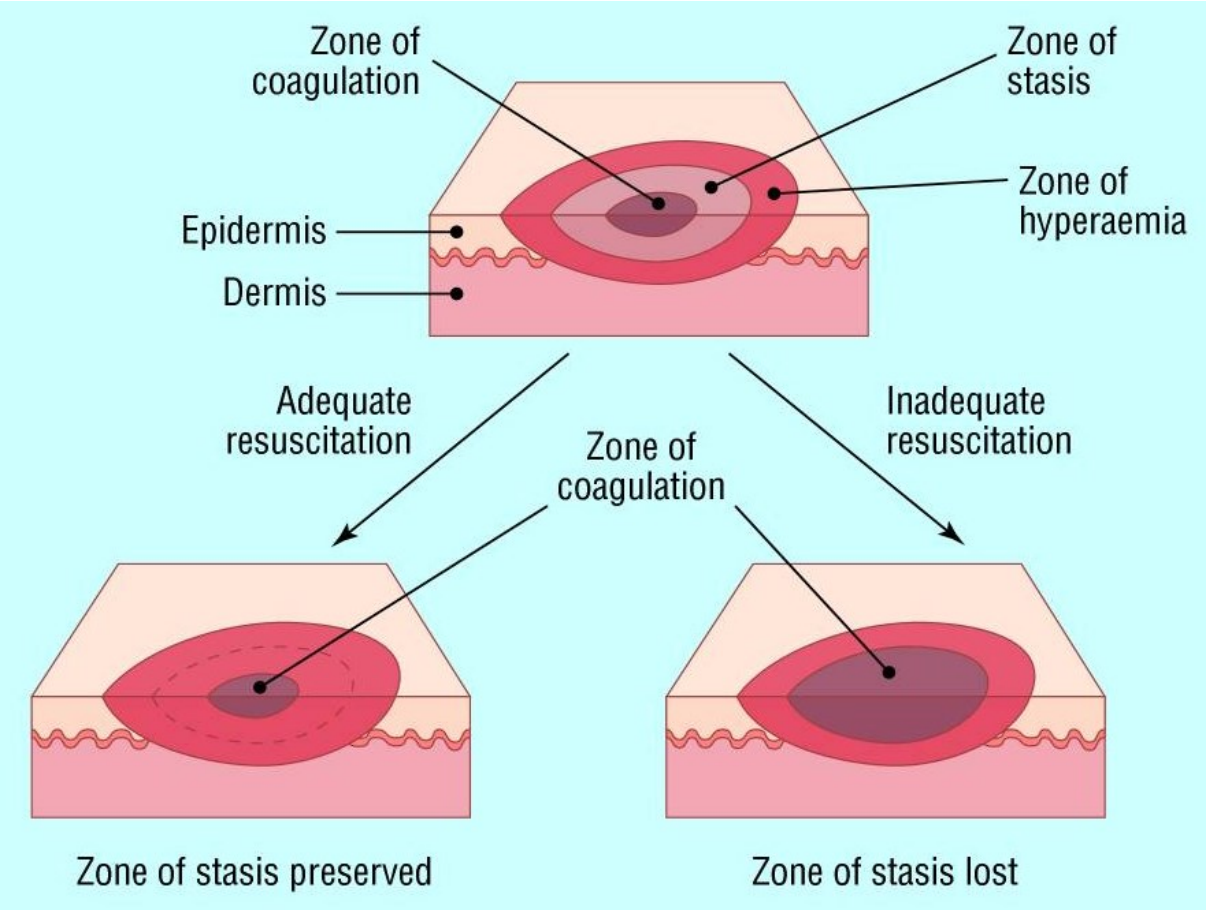


Figure 3 Jackson's model of burn wound progression. The model categorises areas in the burn site by their potential viability, from the irreparable zone of coagulation, to the potentially salvageable zone of stasis, to the outer zone of hyperaemia. This diagram presents the alternative wound progressions with either sufficient or insufficient wound resuscitation. Image published by Hettiaratchy and Dziewulski (2004) and reproduced with permission of the rights holder, BMJ Publishing Group Ltd.

Initial clinical evaluation of a burn categorises both the burn depth (as described above) and total body surface area (TBSA) as referral criteria, where management of severe burns (typically deep partial- or full-thickness, as is the subject of this project) is conducted in specialised burn units. TBSA is often judged by the Wallace rule of

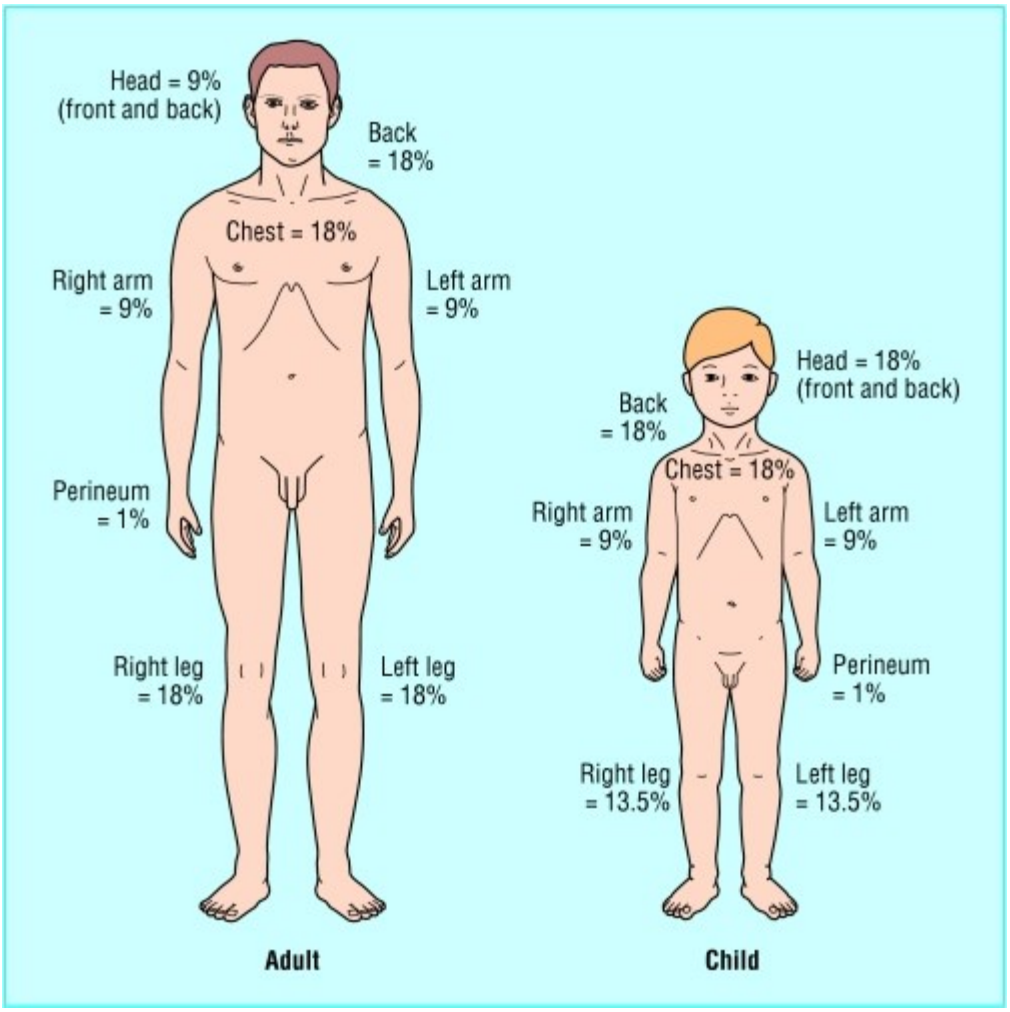


Figure 4 The Wallace rule of nines. A method for visually assessing burn TBSA when evaluating trauma severity and the need for referral. Image published by Hettiaratch et al. (2004) and reproduced with permission of the rights holder, BMJ Publishing Group Ltd.

nines (Fig. 4; Hettiaratchy et al., 2004), which defines major body components with TBSAs of 9% or 18%. Referral criteria vary by country though, as an example, the American Burn Association advises referral for partial-thickness burns of greater than 20% TBSA (or affecting the face, hands, feet, genitalia, perineum and/or major joints) or for full-thickness burns of 5% TBSA (American Burn Association, 2016).

One of the top clinical priorities in treating a major burn is fluid resuscitation; efforts to prevent burn shock, the systemic oxygen deprivation resulting from post-burn fluid

shifts, are thought to largely underlie the modern improvement in major burn mortality (Latenser, 2009). Locally-occurring processes contributing to post-burn hypovolaemia are outlined above; these changes in vascular permeability and aberrant hydrostatic pressures induce hypoperfusion locally by applying pressure on vasculature. However, systemically, the increase in interstitial volume with oedema induces intravascular volume depletion and haemoconcentration which mediates distributive hypovolaemia (Barton et al., 1997), ultimately preventing oxygenation throughout the body (Barton et al., 1997; Berger et al., 2001; Demling, 2005; Ipaktchi et al., 2006). This shock is compounded by reduced cardiac output following burn injury, resulting from decreased plasma volume and decreased cardiac contractility thought to be induced by circulating mediators such as TNFα and impaired cardiac Ca^{2+} signalling (Barton et al., 1997; Csontos et al., 2007; Maass et al., 2002; Willis et al., 2005). Fluid resuscitation is required for burns exceeding 15% TBSA (Mitra et al., 2006), and failure to initiate it within 2 hours post-burn when indicated significantly increases the chance of mortality (Barrow, Jeschke, et al., 2000; Schiller et al., 1996).

Alongside fluid resuscitation, the improvement in burn mortality observed over the last few decades is attributed to timely surgical intervention (Rashid et al., 2001). An immediate surgical requirement following admission is to prevent the combination of a circumferential deep partial- or full-thickness burn, wherein the skin is inelastic, and underlying oedema further compromising tissue perfusion or restricting respiration (Hettiaratchy et al., 2004). This is accomplished via an escharotomy, in which an incision is made to relieve the tissue's circumferential restriction. However, following this initial intervention, the majority of surgery will consist of debridement (excision of

the burn site), to prevent unviable tissue triggering systemic inflammatory response syndrome (SIRS) or sepsis (see below), and skin grafting of synthetic substitutes or from donor sites to accomplish wound closure (Hettiaratchy et al., 2004).

A key aspect of intensive care management following a severe burn is limiting the burn's systemic effects, where multiple organ dysfunction syndrome (MODS) remains a major threat to post-burn mortality (Marshall, Jr. et al., 1983). Despite their distance from the burn site, various organs are susceptible to damage by the systemic inflammatory hypermetabolic state that burn trauma induces (Aikawa et al., 1987; Cotran, 1965; Nuytinck et al., 1988), referred to as SIRS. As alluded to above in the description of burn shock, cardiovascular complications are not limited to hypovolaemia but include the compromise of cardiac function (Schultz et al., 1997). This is thought to result from the inflammation-induced hypermetabolic state elevating circulating catecholamines, which in turn can trigger myocardial infarction and cardiac arrhythmias by increasing adrenergic stimulation of the heart. The observed cardiac instability following burn injury is further attributed to the above-described post-burn hypercoagulability (Coumel, 1996; Falk et al., 1995; Goff et al., 1990) and myocardial oedema (Ansermino et al., 2004). Like the heart, the lungs are susceptible to damage in SIRS and their subsequent failure is characteristic of post-burn MODS, even in the absence of smoke inhalation (Till et al., 1983; Tranbaugh et al., 1980). The damage is attributed to inflammation and its associated oxidative stress (Demling et al., 1989; Oldham et al., 1988; Sener et al., 2002), which lasts for days post-burn but can be attenuated with early burn wound excision, highlighting the progression from local inflammation to SIRS to MODS (Demling et al., 1990; Demling et al., 1989). It should be noted that, while these inflammatory contributors

to pulmonary complications have been confirmed specifically in lieu of inhalation injury, many more have been identified concomitantly with lung damage and may apply in either case (Cakir, 2004). While early kidney failure normally results from the combination of hypoperfusion, haemolysis and muscle breakdown (Ansermino et al., 2004), delayed renal failure is likely a consequence of systemic inflammation and accompanied by the failure of other organs in MODS. It is attributed to a hypoperfusion-induced decrease in glomerular filtration rate and/or tubular dysfunction, and is particularly associated with high mortality rates when occurring as a result of SIRS or sepsis (Davies et al., 1994; Planas et al., 1982; Schiavon et al., 1988) and the release of oxygen radicals secondary to inflammation (Sener et al., 2002).

The heart, lungs and kidneys are but three examples of organs susceptible to acute failure in post-burn MODS; by the nature of its inflammatory pathogenesis, any organ prone to damage by hypoperfusion or oxidative stress could be affected, as has been observed in the brain (Ansermino et al., 2004) and intestines (Cakir, 2004). Each of the susceptible organs here exemplify the progression from local inflammation to SIRS to MODS and thereby, given its associated mortality rates, the need for improved therapeutic intervention. Crucially, any characteristic of SIRS described here is applicable to sepsis which is differentiated from SIRS only by the presence of infection and remains a significant factor in mortality (Fitzwater et al., 2003). While infection is common in and enhances the post-burn immune response, though the extent to which it increases conversion to MODS is not clear (Greenhalgh et al., 2007), SIRS rather than sepsis was deliberately discussed here as

inflammation is ultimately the underlying problem; infection is not required for a fatal progression to MODS.

Following haemodynamic stabilisation, overcoming the initial threats posed by systemic inflammation progressing to MODS and successful wound closure, which can take many months consisting of repeated wound debridement and redressing, the patient enters the rehabilitative phase of recovery where the clinical goal is to restore their former lifestyle to the greatest extent possible. It consists firstly of reconstructive surgery, in which the aim is to optimise function, comfort and wound appearance rather than preserve life, as is the case in the acute phase of recovery. Scarring, contractures, adjusting for amputations and skin decolouration are the features addressed here, though urgent (if nonlethal) issues such as contracted eyelids exposing the cornea take priority (Barret, 2004). Beyond surgically addressing the physical constraints enforced by wound contracture and scarring, regaining motility and function of the affected site relies extensively on physical rehabilitation. This challenge is compounded by the need to immobilise burned tissue to allow healing, as it is inelastic and routinely requires skin graft adherence (which, depending on the graft, can take between one and fourteen days to attach; Edgar et al., 2004). It is further compounded by pain, which remains a cornerstone of burn therapy throughout treatment and is discussed separately below. The rehabilitative phase also incorporates consideration of the complex psychosocial consequences of burn injury, from anxiety and depression associated with coming to terms with the implications of their injury, early surgical interventions and the intensive care environment (which correlates with resting pain and social support; Wiechman et al., 2004) to their reintegration into society which is challenged by the

physical limitations imposed by their wound, the change in their appearance, the psychological trauma of their injury, sexual dysfunction and the implications of these for social interaction with family, friends and restarting work (Palmieri et al., 2014; Stoddard, Jr. et al., 2014; Wiechman et al., 2004). Rehabilitation can understandably take years, requiring continued surgical and pharmacological intervention with ongoing psychotherapy (Stoddard, Jr. et al., 2014).

Over the last few decades, improved policy in acute burn care, particularly regarding wound excision and fluid resuscitation, has seen a significant increase in survival rates. This highlights the threat that pathological mediators disseminating from the burn site poses, alongside the continued challenges to mortality imposed by the progression of SIRS or sepsis to MODS. With therapeutic intervention principally directed toward symptom management, delineating the mechanisms underlying the effects of systemic inflammation is certainly an attractive avenue for work prioritising the improvement of wound progression and post-burn survival rates.

1.1.4.1 Inflammation in Burn Injury

Neither the extensive interest in inflammation as a therapeutic avenue in burn injury, nor its extensive implication in the immune system-mediated processes underlying the current principal threats to survival, is surprising. Aside from the immediate protein denaturation induced by the trauma, inflammation is implicated in every above-discussed pathological component of burn injury. Free radicals are generated by neutrophils and mast cells recruited in the immune response. Hypoperfusion is a consequence of increased capillary permeability and endothelial cell damage,

respectively mediated by inflammatory mediators and the free radicals produced in the immune response, alongside inflammatory vasoconstriction and hypercoagulability. These processes underlie burn wound progression and the development of fatal systemic consequences characterised by aberrant inflammation inducing distributive hypovolaemia and compromised organ function. The need to intervene with the body's response to burn injury is evident, but must be balanced with the need for its pathophysiological function. For example, inflammation is vital for successful wound healing; various inflammatory mediators recruit leukocytes and macrophages to initiate the proliferative phase wherein keratinocytes and fibroblasts differentiate to accomplish wound closure (Claudinot et al., 2005; Ito et al., 2005; Singer et al., 1999). This process mirrors the issue with regulating inflammation as, while its occurring in excess underlies hypertrophic scaring, interfering with it could limit the rate of tissue recovery (Curran et al., 2013; Shih et al., 2010; Tabas et al., 2013). Therapeutic intervention targeting the immune response to burn injury would have to be finely tuned to retain its necessary function and, given the particular pathological progression with inflammation's systemic dissemination, specifically preventing the development of systemic effects is an attractive prospect. As inflammation operates through circulatory and interstitial communication executed via the passage of inflammatory mediators, it is possible that these could effectively be targeted to regulate the response in a space-delimited manner. This is reflected in the extensive work defining the spatial and temporal profiles of the molecules mediating the immune response to burn injury and their functions, which is briefly outlined below.

1.1.4.1.1 Inflammatory Mediators in Burn Injury

Burn injury's characterisation as an inflammatory pathology has motivated comprehensive study of the molecules engaging the immune system post-burn. The combination of the relative accessibility of systemic samples (e.g. plasma) compared with local sampling techniques and the particular relevance of systemic inflammatory mediators to the highest priority clinical features of burn injury (e.g. distributive hypovolaemia, SIRS, MODS) has precipitated that the vast majority of studies evaluate molecules potentially underlying the pathology in circulation. Epidermal damage (Moran et al., 1987) and immune function dysregulation, as exhibited in macrophage hyperactivity and T-cell dysfunction observed post-burn and predicting systemic inflammatory effects (Dockrell; MacMicking et al., 1997), constitute a compromise in the first two lines of the body's immunological defense (Cakir, 2004). The resulting release of mediators, and the means by which they underlie the pathological consequences of immune dysregulation in burn injury, are continuously being elucidated, as outlined below.

Cytokines are a loosely-associated group of small (5-20 kDa) cell-signalling proteins (Kishimoto et al. , 1994). Although it is simply by these criteria and their mediation of autocrine, paracrine or endocrine signalling that they are categorised as a molecular class, in practise they are functionally defined by their varying roles as immunomodulatory agents (Kishimoto et al., 1994). As a result, they feature heavily in the profiling of molecules mediating the post-burn immune response. Three cytokines in particular have been consistently recorded as systemic regulators of the post-burn immune response: tumour necrosis factor-α (TNFα; Drost et al., 1993; Liu

et al., 1994), interleukin-1 (IL-1; Biffl et al., 1996; Drostet al., 1993; Kowal-Vern et al., 1994) and interleukin-6 (IL-6; Rodriguez et al., 1993; Struzyna et al., 1995; Yeh et al., 1999). These three cytokines are characteristic of the acute phase response, a complex systemic early-defense system activated in various pathological states including trauma, infection, stress and inflammation. TNFα, generated primarily by macrophages but also by lymphocytes, neutrophils, mast cells and neurons, is principally implicated in the systemic conversion of various inflammatory pathologies by inducing the upregulation of several other cytokines including IL-6 and IL-8 (Marano et al., 1988; Piguet et al., 1991). Acting via TNFR1 and TNFR2, where the latter is less ubiquitous but more localised to immune cells, it activates the nuclear factor kappa-light-chain-enhancer of activated B cells (NF-κB) protein complex and mitogen-activated protein kinase (MAPK) pathways (principally the c-Jun N-terminal kinase (JNK) and p38 cascades; extracellular signal–regulated kinase (ERK) is only minimally engaged), which respond to varying forms of cell stress to produce cytokines and regulate cell survival or apoptosis (Locksley et al., 2001). Consequences beyond cytokine release include endothelial cells assuming a procoagulant profile leading to increased immune cell adhesion and the suppression of lipolysis (Shehab El-Din, 1996). IL-1β contributes to the acute phase response by mediating the maturation and activation of T- and B-cells (Dinarello et al., 1986; Faunce et al., 1998; Fukushima et al., 1994). Like TNFα, it increases adhesion of neutrophils and lymphocytes to endothelial cells and can induce the production of secondary cytokines including IL-6 (Granowitz et al., 1992) and IL-2 (Von Hoegen et al., 1989). While TNFα concentration increases have been reported as both transient (Drost, et al., 1993) and prolonged (Yeh et al., 1999), post-burn serum elevations of IL-1β consistently remain at their highest over the first week and correlate with burn

severity (Drost et al., 1993). This temporal profile is shared by IL-6 which has both pro- and anti-inflammatory functions (Tilg et al., 1997). IL-6 has emerged as an indicator of mortality with plasma concentrations recorded as tenfold of those in surviving patients (Drost et al., 1993). It is produced in this context by various cells such as T- and B-cells, macrophages, fibroblasts and endothelial cells (Akira et al., 1993). Its association with mortality is thought to reflect its particular elevation in the presence of infection, though this feature of burn injury is often unclassified and this relationship remains unclear to date (Yeh et al., 1999).

While TNFα, IL-1β and IL-6 have remained the focus of burn cytokine research since their early recognition, further elevated circulating cytokines have been identified due largely to the development of multiplex platforms. Those identified include IL-8 (McMillen et al., 1996; Rodriguez et al., 1993), granulocyte colony-stimulating factor (G-CSF; Struzyna et al., 1995), IL-2 (Kowal-Vern et al., 1994), IL-10, GM-CSF, IL-15, monocyte chemoattractant protein-1 (MCP-1), macrophage inflammatory protein 1β (MIP-1β) and vascular endothelial growth factor (VEGF; Hur et al., 2015a). IL-8 induces chemotaxis specifically in neutrophils, with only weak effects on other immune cells in circulation, and thereby mediates inflammation and may contribute to oxidative stress in burn injury (Bickel, 1993). G-CSF, following its characterisation as one of the first cytokines to be identified, was quickly brought forwards for clinical usage for its ability to induce neutrophil production (Bendall et al., 2014); while it is still not clear if it induces this effect in physiological conditions, it is now known to exert this function as an emergency regulator under stress conditions (Basu et al., 2002) and may contribute to the immune response (and thereby oxidative stress) in burn injury. IL-2 regulates various lymphocytes during immune response,

maintaining regulatory T cells, inducing CD4+ T cell differentiation and optimising effector T cell generation and memory cell differentiation for CD8+ T cells (Boyman et al., 2012); IL-15 functions similarly, with additional functions such as natural killer (NK) cell activation (Budagian et al., 2006). IL-10 is principally associated specifically with promoting the endothelial immune response to viral and bacterial infection (Ouyang et al., 2011). As macrophages are crucial for wound healing through their clearance of tissue debris and promotion of repair (DiPietro et al., 1995; Kovacs, 1991), the elevations of GM-CSF, MCP-1 and MIP-1β, all of which attract monocytes that differentiate into macrophages among other immune cells (Menten et al., 2002; Shallo et al., 2003; Wicks et al., 2016), exemplify the necessity of the immune response and the consequences of its dysregulation. Evidently, while the implication of a subset of these cytokines is particularly specific to the presence of infection, cytokines are nonetheless crucial mediators of the immune response to burn injury without it. Note that this summary of cytokines implicated in burn injury is drawn from clinical studies, and excludes those identified only in rodent models; such cytokines will be discussed individually as their relevance emerges later in this thesis (Finnerty et al., 2009). While cytokines only represent one (albeit major) class of inflammatory signalling in burn injury, an exhaustive overview of all potentially-involved inflammatory mediators is beyond the scope of this report. However, two further notable topics include the implication of inducible nitric oxide synthase (iNOS) and eicosanoids (arachidonic acid metabolites) in post-burn inflammation. iNOS activity, an indicator of post-burn macrophage hyperactivity, is promoted by both various cytokine (IL-1β, TNFα) and non-cytokine (prostaglandin E2) inflammatory mediators post burn (Mauel et al., 1995; Milano et al., 1995; Renz et al., 1988; Salvemini et al., 1995); as iNOS induction has been found to underlie vascular hyperpermeability and

distal organ dysfunction post-burn (Chen et al., 1999; Inoue et al., 2001), and amelioration of these effects with iNOS inhibition (Güneysel, 2002), the targeting of inflammatory mediators potentiating nitric oxide (NO) synthesis is currently being pursued as a therapeutic avenue (Cakir, 2004). Eicosanoids such as prostaglandins, leukotrienes and thromboxanes are elevated post-burn and some have been suggested to exert aberrant immunosuppressive actions (Ricciotti et al., 2011; Stenson et al., 1980), consistent with the normalisation of immune function when reducing their synthesis via COX inhibition (Shoup et al., 1998; Strong et al., 2000). The elevated release of PGE_2 and NO from macrophages and its consequent T-cell suppression has been suggested as the defining factor mediating post-burn immune dysfunction (Allison, 1978; Bogdan, 2011; Metzger et al., 1980; Mills, 1991).

Given the importance of continuous sampling for evaluating the temporally-dynamic signalling environment in burn injury, the vast majority of studies measure inflammatory mediators in circulation as demonstrated above. However, a minority have prioritised profiling cytokines specifically in the burn site. One approach, employing an enzyme-linked immunosorbent assay (ELISA) of homogenised skin tissue, identified that elevations of the principal three cytokines associated with burn injury, TNFα, IL-1β and IL-6, also occur locally (Ipaktchi et al., 2006). Further, blocking these three cytokines with antibodies can reduce post-burn microvascular damage via the reduction of neutrophil-mediated oxidative stress (Ravage et al., 1998). These findings support the local generation and release of these cytokines, as is suggested for TNFα, IL-6 and, additionally, IL-8 in a similarly-designed study specifically examining the correlation of local and systemic cytokine levels (Rodriguez et al., 1993). A limited number of studies have utilised microdialysis for

characterisation of the signalling environment both locally and continuously. One determined the significant dermal elevation of IL-1β, IL-6, IL-8, IL-10, G-CSF, and MIP-1β following the minimal exposure to UV sufficient for complete erythema 24 hours post-burn and the significant elevation of IL-7 and IL-13 following the application of heat sufficient for nociception (Angst et al., 2008). IL-6, IL-8, IL-13, IL-1α, IL-1β, MCP-1, and TNF-α were found to be elevated in lysates of subcutaneous white adipose tissue damaged in full thickness burns, as measured with a bead-based multiplex immunoassay (Saraf et al., 2016). Another microdialysis study specifically measuring histamine, an inflammatory mediator rapidly released from mast cells following thermal trauma that increases capillary permeability and oxidative stress (Xie et al., 2005), identified its dermal elevation post-burn via a radiometric enzyme assay (Papp et al., 2005). An alternative approach has been evaluating the cytokine expression of keratinocytes harvested from a burn site in culture; this identified the release of IL-1α, IL-2, IL-4, IL-10, interferon-γ (IFNγ, a cytokine that primarily activates macrophages in response to viral or microbial pathogens; Schroder et al., 2004) and TNFα (Gauglitz et al., 2012).

Despite the clinical consequences of the overwhelming inflammation occurring after a major burn, the inflammation itself cannot currently be effectively therapeutically targeted and, as outlined above, clinical intervention focuses rather on treating the consequences via resuscitation and rapid wound excision. The major challenge is balancing the necessity of inflammation for wound healing with the systemic consequences (Rowan et al., 2015). For example, traditional anti-inflammatory therapies such as non-steroidal anti-inflammatories (NSAIDs) operate by inhibiting prostaglandin synthesis; as indicated above, this can correct immune dysregulation

post-burn to attenuate pro-inflammatory cytokines (Strong et al., 2000) and restore leukocyte counts in the presence of infection (Shoup et al., 1998). However, in practise, it impairs wound healing (Franz et al., 2007a). An exciting therapeutic prospect is the possibility of targeting specific components of the inflammatory response in order to selectively regulate mechanisms underlying pathological consequences, as is reflected in the many studies summarised above. However, to date none of these have translated to clinical practise, nor have non-traditional anti-inflammatories such as steroids (Rowan et al., 2015). With extensive systemic sampling not yielding an answer, attention could be drawn to our under-developed understanding of the acute local inflammation from which the systemic consequences develop. For example, while they have not been pursued in clinical trials, application of a topical p38-MAPK inhibitor has been shown to attenuate local inflammation and the systemic response (Ipaktchi, et al., 2006). While interest is evidently developing in this area, there has been no continuous local sampling of a severe burn to date; this approach may highlight key mediators operating during the acute phase of the injury that are susceptible to therapeutic intervention.

1.1.4.2 Burn Injury Pain

Just as inflammation emerges as a common theme underlying the threats to mortality following a severe burn, pain emerges as a common theme underlying the threats to quality of life. Despite burn injury's prevalence and the long-standing recognition of its pain as a major clinical issue (Perry et al., 1981; Perry, 1984), burn pain remains undertreated (Carrougher et al., 2006; Carrougher et al., 2003;

Choiniere et al., 1989). Beyond the immediate suffering its excruciating severity can cause (Summer et al., 2007), this is problematic for the long-term sensory dysfunction (Choiniere et al., 1991; Malenfant et al., 1998; Malenfant et al., 1996), chronic pain (Brenner et al., 2004; Dworkin, 2002; Ikeda et al., 2006; Kawasaki et al., 2004; Woolf et al., 1999) and stress-related psychological disorders it can induce (Caffo et al., 2003; Gilboa et al., 1994; Saxe et al., 2001). As current therapies are evidently inadequate, novel approaches influenced by a developed understanding of the algogenic signalling environment in burned tissue may offer burn patients a better quality of life. Here, the function of pain, the reasons for its challenging nature in burn injury and the current therapeutic approaches are overviewed.

1.1.4.2.1 The Function of Pain

According to the International Association for the Study of Pain (IASP), pain is defined as “an unpleasant sensory and emotional experience associated with actual or potential tissue damage, or described in terms of such damage” (IASP, 2016). Its unpleasantness is precisely its point; its function is to serve as a deterrent from exposure to potential sources of tissue damage. Nociception, the signal transduction that translates into the perception of pain, is set apart from other forms of sensation by its selective response to potentially damaging stimuli, such as noxious mechanical, chemical or heat stimuli; they contrast with the sensitivity of visual, auditory, olfactory, somatosensory and taste systems (Dubin, 2010). It is complex and highly subjective, with a variety of modalities, temporal profiles and severities depending on the stimulus, the responsive anatomy and modulation and various levels (Eccleston, 2001; Foulkes et al., 2008; Lacroix-Fralish et al., 2009; Price et al.,

1977). This brief overview will focus on the aspects of nociception and pain perception that pertain to burn injury. This pathology exemplifies the importance of understanding nociception, and the therapeutic potential of manipulating it; the evolutionary significance of pain as a biological warning system for dangerous environmental encounters and subsequently for limiting movement to enable tissue repair is self-evident, but it is not always representative of these functions. Pain can be experienced spontaneously without any harmful stimuli, in response to harmless stimuli (allodynia) or abnormally heightened in response to noxious stimuli (hyperalgesia). These states of pain perception develop by diverse, interrelated and/or progressive means, as exemplified by the varying contributions of tissue damage, inflammation, neuropathy and central sensitisation in burn injury discussed below.

1.1.4.2.2 The Anatomy of Nociception

Nociception begins with the detection of noxious stimuli by nociceptors (Kandel et al., 2000), specialised primary sensory neurons (PSNs). Their cell bodies are housed the dorsal root ganglia (DRG), or the trigeminal ganglia for the trigeminal nerve innervating the face, and project both peripherally in bundles forming dermatome-specific nerves and centrally to the spinal cord; both axons emanate from a single bifurcating projection, in a manner thought to maintain axonal continuity and reduce conduction failure (Amir et al., 2003). The two principal categories of nociceptors include Aδ and C fibres; the former are thinly myelinated and mediate fast, well-localised pain while the latter are slower and less spatially specific (Basbaum et al.,

2009). Both fibre types can be polymodal, responding to both heat and mechanical stimulation. Aδ fibres are therefore categorised as either Type I, responding to both modalities but with a relatively high heat activation threshold (though this is reduced with sustained exposure), or Type II, responding with lower heat thresholds and much higher mechanical threshold. Many C fibres exhibit sensitivity to both heat and mechanical stimuli (CMH fibres), though they are more heterogeneous than Aδ fibres; one particularly interesting subclass is that which becomes sensitive to mechanical or heat stimulation only in pathological states (Meyer et al., 1991), and is particularly sensitive to inflammatory chemical stimuli such as histamine (Schmidt et al., 1995). A third afferent type, Aβ fibres, are not nociceptors but are nonetheless capable of engaging nociceptive systems in pathological states; like Aδ fibres, they are myelinated and conduct signals quickly, though they respond to light touch rather than noxious stimuli physiologically. Aside from their response characteristics, nociceptors can be characterised by their molecular expression profile; C fibres can be divided into peptidergic and non-peptidergic populations (Snider et al., 1998). The former synthesises and releases neuropeptides such as substance P and calcitonin gene related peptide (CGRP) and expresses the tropomyosin receptor kinase A (TrkA) receptor for nerve growth factor (NGF), while the latter expresses the c-RET neurotrophin receptor for glial-derived neurotrophic factor (GDNF) and can be labelled with glycoprotein isolectin B4. Further, nociceptors exhibit differential ion channel expression dictating their sensitivity to various noxious stimuli such as heat (transient receptor potential cation channel subfamily V member 1; TRPV1), cold (TRPM8) and pH (acid-sensing ion channels; ASICs). Nociceptors can be categorised by their soma diameter, state of myelination, target tissue, trophic

dependency or molecular expression profile; these characterisations collectively determine the modality, localisation and function of distinct nociceptor populations.

The interface between a noxious environmental stimuli and the nervous system is the free nerve endings terminating peripheral projections from the DRG in the epidermis, dermis, connective tissue and arteriole walls (Dubin, 2010; Zylka et al., 2005). The fibres branch out upon termination (with A fibres becoming unmyelinated), A fibres doing so in tight clusters and C fibres doing so with a broader distribution; this confers their respective pain localisations and outlines their receptive fields (Dubin, 2010). While Aβ fibres innervate various non-neuronal structures conferring sensation for innocuous mechanical stimulation (Smith et al., 2009), nociceptive fibres terminate around keratinocytes, mast cells and Langerhans cells (Lumpkin et al., 2007), consistent with their functional dependence on the tissue's state. The centrally-projecting axon enters the spinal cord and likewise branches to innervate different rostrally- and caudally- directed spinal segments. They terminate primarily on relay neurons, which in turn project to the medulla, mesencephalon and thalamus which themselves project to the somatosensory and anterior cingulate cortices where sensory-discriminative and affective-cognitive aspects of pain are processed (Wall, 1992). Some central DRG projections terminate rather on interneurons in the dorsal horn which, together with descending pathways from the brain, can modulate nociceptive signals in excitatory or inhibitory manners (Basbaum et al., 2009; Wall, 1992).

1.1.4.2.3 Nociceptive Signal Transduction

Nociceptors are unified despite their modalities by the initiation of signal transduction at their free nerve endings; these terminals respond to their respective stimulus by receptor-mediated depolarisation, encoding the presence and intensity of a stimulus by the resulting train of action potentials. While the molecules producing the initial receptor potentials underlying nociception have received extensive attention, the identification of unknown receptors and characterisation of those already identified, particularly where polymodality is concerned (Dubin, 2010), remains an important pursuit. Our understanding of nociceptor activation by heat exemplifies the progress that has been made. The nociceptive threshold for heat is >42°C, as reflects the response profile of C and Type II Aδ fibres and can be reproduced in DRG neuron cultures with a subset of noxious heat responsive cells activated at >52°C (Cesare et al., 1996; Kirschstein et al., 1997; Leffler et al., 2007; Nagy et al., 1999). These response profiles would be first elucidated at a molecular level with the identification of TRPV1 as a nociceptive heat transducer (Caterina et al., 1997). TRPV1 is activated by temperatures exceeding 42°C, mediates a capsaicin (the active component in chilli peppers)-induced burning sensation via depolarisation of specific heat-activated nociceptor subsets, is expressed in most heat nociceptors and its knockout significantly impairs sensation of noxious heat (Caterina et al., 2000; Caterina et al., 1997; Davis et al., 2000). The remaining TRPV1-independent component of acute heat nociception could potentially be attributed to TRPV2; just as TRPV1 activation is thought to underlie the perception of pain with >42°C stimulation, TRPV2 is thought to underlie that with more extreme temperatures of >52°C. This is consistent with its activation threshold (Leffler et al., 2007; Nagy et al.,

1999), its expression in the subpopulation of Aδ neurons responding in this temperature range and the similarity between its biophysical properties and those of endogenous responses (Leffler et al., 2007; Rau et al., 2007).

While burn injury includes heat transfer, which itself initiates nociceptive signal transduction, post-burn pain is also a result of peripheral sensitisation (see below) implicating signal transduction by innocuous and noxious mechanical stimulation, potentially alongside conformational tissue changes. Mechanosensitive fibre termination can indicate its function and range of sensitivity; while high threshold mechanoreceptors (e.g. C fibres, slowly adapting Aδ mechanoreceptor fibres) terminate in the skin as free nerve endings, Aδ D-hair fibres (a subcategory of type II fibre) are considered the most sensitive Aδ mechanoreceptor and have large receptive fields and Aβ innervate Merkel cells, Pacinian corpuscles and hair follicles to function as stretch receptors in the detection of texture, light pressure and vibration (innocuous stimuli). While distinct temperature ranges have been identified for heat sensors, elucidating functional distinctions between mechanoreceptors has proven challenging; designing behavioural assays discriminating between the sensation of texture and vibration and between that of noxious and innocuous mechanical stimulation is difficult (Wetzel et al., 2007), and it is not clear which of the many means of physically applying pressure to a cell best replicates physiological conditions (Bhattacharya et al., 2008; Hawon Cho et al., 2006; Cho et al., 2002). However, the consensus is that mechanosensitive cation channel gating is induced by conformational changes to the cell, even if the above limitations have prevented elucidation of the precise mechanotransduction machinery and stimulation-specific mechanoreceptor characterisation (Basbaum et al., 2009).

Despite the current lack of clarity in the molecular characterisation of mechanosensation, there is evidence for various candidate ion channels potentially mediating the depolarisation of mechanoreceptors which are currently being pursued. These may induce the generation of action potentials in response to the innocuous and noxious stimuli underlying pain in burn injury and, interestingly, exhibit significant functional overlap with channels otherwise implicated in burn pathology. One such is example is the implication of ASIC 1, 2 and 3, the mammalian orthologues to the established *C. elegans* mechanotransducers mec-4 and mec-10 (Chalfie, 2009), which mediate pain in burn injury following the onset of ischaemia and consequent acidosis (see below). Deficiency of any of these channels has typically not translated to any significant change to mechanosensation (Price et al., 2000; Price et al., 2001; Roza et al., 2004), though mec-4 and mec-10 are proposed to form a complex with MEC-2; the deficiency of this protein's mammalian orthologue, SLP3, does compromise sensation of innocuous (but not noxious) mechanical stimuli via A fibres and therefore could feature in post-burn mechanical allodynia (see below; Wetzel et al., 2007). Another example is TRPV2 which, in addition to its activation by temperatures >52°C, responds to osmotic stretch upon heterologous expression and endogenously in cardiac myocytes (Muraki et al., 2003) and is predominantly expressed in medium- (Aδ) to large-diameter (Aβ) A fibres exhibiting sensitivity to heat and mechanical stimuli (Caterina et al., 1999; Muraki et al., 2003). TRPV4 is also gated by shear stress in a manner thought to mediate vascular regulation by its endothelial expression (Yin et al., 2010), while the mechanosensitivity of Piezo proteins is also being progressively elucidated (Zhao et al., 2016). Additionally, two potassium two pore domain channel subfamily K family

members, TREK-1 and TRAAK, are found in a subpopulation of nociceptive C fibres and are modulated by pressure and temperature, as is demonstrated by animals deficient in these channels (Noel et al., 2009), though little else has been reported on their significance *in vivo*. While mechanical hyperalgesia and allodynia contributes significantly to pathological pain states including that of burn injury, the intricacies of stimulus-specific mechanotransduction is little understood at a molecular level.

It is the gating of stimulation-specific ion channels, the expression of which is dictated by the class of neuron, that initiates nociceptive signal transduction. The current generated by this minor receptor potential in the periphery relies on signal conduction for transduction into an action potential and its communication towards the central nervous system (CNS), which is mediated by voltage-gated channels. Currently, mammals are known to have genes for nine Na_vs (voltage-gated sodium channels), ten Ca_vs (voltage-gated calcium channels) and forty K_vs (voltage-gated potassium channels) not including splice variants (Schulz et al., 2008); they each have their own functional characteristics which constitutively (along with other voltage-gated channels) determine a cell's excitability and firing profile, including its action potential generation threshold, action potential amplitude, hyperpolarisation and maximal firing frequency (Dubin, 2010), alongside channels controlling modulation of firing frequency such as the hyperpolarization-activated cyclic nucleotide-gated cation channel (Miller, 2001). This is significant because responses to particular stimuli will consequently recruit a particular subset of voltage-gated channels. For example, transduction of the receptor potential following noxious cold stimulation is dependent on $Na_v1.8$ which, uniquely among Na_vs, is not inactivated by the temperature (Zimmermann et al., 2007) and humans lacking $Na_v1.7$ are

congenitally incapable of feeling pain (Cox et al., 2006). Further, enhancement of PSN excitability is a fundamental pronociceptive mechanism in pathological pain states characterised by sensitisation such as burn injury, as discussed below. Both via the pharmacological inhibitory specificity they could enable, potentially rivalling that of the initially nociceptively-gated channel, and by their established involvement in nociceptive signal transduction and peripheral sensitisation, voltage gated channels are an attractive therapeutic target and are in any case a functionally-important consideration in any pain study (Dubin, 2010).

Peripheral sensitisation encapsulates various processes underlying alterations in the response profiles of nociceptors to promote pain signalling, broadly described to result from local inflammation and/or damage (Dubin, 2010); it is a crucial modulator of peripheral nociception. Peripheral sensitisation is ultimately a consequence of a pathophysiological shift in interstitial fluid composition; neurons, resident cells (keratinocytes, endothelial cells, fibroblasts (Dubin, 2010; McMahon et al., 2005) and immune cells (mast cells, basophils, macrophages, neutrophils; Basbaum et al., 2009) release a variety of signalling molecules such as neurotransmitters, peptides (e.g. CGRP, substance P, bradykinin), eicosinoids and lipids (e.g. prostaglandins, thromboxanes) and cytokines. Interaction of these inflammatory/ algogenic molecules with their respective nociceptor receptors alters the neuron's response profile to mediate peripheral sensitisation in pathological states such as burn injury, underlying the development of hyperalgesia and allodynia. Any individual molecule implicated induces nociception via direct activation of receptors, via sensitisation or both, often by various pathways and interrelated means; their particular involvement

in burn injury pain (and inflammation) are hence discussed on a case-by-case basis below.

Just as hyperexcitability underlying enhanced pain processing can develop peripherally, it can occur in the CNS in processes referred to collectively as central sensitisation. Three prominent mechanisms for this include sensitisation mediated via N-methyl-D-aspartate receptors (NMDARs), inhibitory interneuron disinhibition and glial cells. NMDAR-mediated central sensitisation occurs as an addition to physiological nociception, in which PSNs generate excitatory post-synaptic currents (EPSCs) in the relay neurons of the dorsal horn primarily via release of glutamate, which activates postsynaptic AMPA and kainate receptors to generate an action potential upon sufficient EPSC summation. Postsynaptic NMDARs do not feature in this process physiologically but, with sufficient relay neuron depolarisation, can become responsive to the released glutamate. The resulting elevation in calcium influx strengthens synaptic connections between PSNs and dorsal horn relay neurons, enhancing nociceptive transmission (Latremoliere et al., 2009). The inhibitory interneuron disinhibition mechanism of central sensitisation describes the impaired function of inhibitory interneurons, which tonically inhibit the relay neurons of the dorsal horn to regulate their depolarisation and excitation. It is supported by the observations that inhibition of such GABAergic and glycinergic interneurons replicates the sensitisation observed following peripheral nerve injury, and that such injuries decrease inhibitory post-synaptic currents (Basbaum et al., 2009; Malan et al., 2002; Sivilotti et al., 1994; Yaksh, 1989). Inhibitory interneuron disinhibition enhances nociceptive transmission to both innocuous and noxious stimuli, and hence contributes to both allodynia and hyperalgesia (Keller et al., 2007; Torsney et

al., 2006). Glial-cell mediated central sensitisation describes the pro-nociceptive central actions of microglia (the resident macrophages of the CNS) and astrocytes following peripheral nerve injury; interestingly, this form of central sensitisation is specific to PNS damage and is not observed with inflammation alone (Basbaum et al., 2009; Chessell et al., 2005; Tsuda et al., 2003). The activated microglia surround the central terminal of the damaged PSN within the dorsal horn and release a variety of inflammatory mediators such as BDNF, thought to act on relay neuron TrkB to reverse the Cl^- gradient and therefore switch GABA's action to depolarising. Their recruitment has been attributed to activation by ATP, released specifically following peripheral nerve injury (Basbaum et al., 2009; Chessell et al., 2005; Tsuda et al., 2003), and fractalkine, which is released centrally from activated PSNs (Milligan et al., 2004).

The train of action potentials mediating pain, generated peripherally by that initial ion channel gating with voltage-gated channel recruitment for transduction, is therefore subject to regulation by varying processes of peripheral and central sensitisation. Along with the various descending pathways of pain regulation, which are beyond the scope of this thesis, these processes define the sequential components of pain signalling potentially accessible for as of yet much-needed therapeutic intervention.

1.1.4.2.4 Nociception in Burn Injury

Algogenic processes in burn injury often contribute to pain via multiple mechanisms and at different levels of the nociceptive signalling process described above. Burn

injury pain is a combination of various components including exposure to heat, non-neuronal and neuronal cell damage, inflammation and ischemia. The implications of algogenic mediators and processes in the acute and inflammatory components of burn injury pain are therefore best discussed on a molecule-by-molecule basis, rather than in the context of nociceptive anatomy as overviewed above.

The channel TRPV1 is implicated in burn pain on multiple fronts. As discussed above, it is gated by noxious temperatures (>42°C) to which any tissue undergoing thermal trauma would be exposed (Caterina et al., 2000; Caterina et al., 1997). TRPV2 would similarly generate a receptor potential as it is gated in the presence of temperatures exceeding 52°C (Leffler et al., 2007; Nagy et al., 1999); both channels therefore mediate a simple acute nociceptive pain component to burn injury, wherein noxious temperatures themselves induce action potentials. However, TRPV1's involvement in burn pain extends far beyond this. Its activation results in the release of the neuropeptides CGRP and substance P from the neuron's peripheral terminal (Helme et al., 1986; Kessler et al., 1999; Zimmermann et al., 2005), and both are found elevated in burn injury (Onuoha et al., 2001). These are inflammatory mediators, respectively capable of mediating vasodilation and plasma extravasation with the activation of various immune cells (Scholzen et al., 1998). Aside from any sensitising effects of their inflammatory actions, CGRP and substance P can directly activate nociceptors (Natura et al., 2005; Segond von Banchet et al., 2002; Szucs et al., 1999). Aside from the heat itself, TRPV1 can be activated by lipids formed endogenously during exposure to noxious heat: the oxidised linoleic acid metabolites 9- and 13-hydroxyoctadecadienoic acid (9- and 13-HODE; Patwardhan et al., 2010). Additionally, following activation of the coagulation cascade by thermally-induced

vascular damage (Lippi et al., 2010), thrombin is released and may sensitise TRPV1 via activation of protease-activated receptors (PARs) 1 and 4 (Russell et al., 2010; Vellani et al., 2010).

Aside from directly gating ion channels, generating lipids and the release of any inflammatory mediators these may induce, heat exposure can contribute to pain via membrane denaturation and the consequent release of algogenic cell contents. These include adenosine triphosphate (ATP), which is present in the cytoplasm at a concentration of 1 mM, making it sufficiently abundant for activation of $P2X_3$ and $P2X_{2/3}$ channels on nociceptors (North, 2004). Evidence supporting the contribution of this mechanism to burn pain includes the channels' use-induced upregulation following burn injury (Gao et al., 2010; Xu et al., 2009) and compromised sensitivity to mechanical and thermal stimulation and inflammatory pain in mice lacking these channels (Cockayne et al., 2005; Cockayne et al., 2000; Souslova et al., 2000). P2X channels are further thought to contribute to burn pain via a separate mechanism resulting from ischaemia, another fundamental form of tissue damage in burn injury. In hypoxic conditions, ATP generation relies solely on anaerobic glycolysis; this precipitates an accumulation of protons characterising the onset of lactic acidosis (Kraut et al., 2014). P2X channels containing $P2X_2$ subunits are sensitised to ATP-mediated activation by low pH, with a five-fold increase in affinity at pH 6.5 (King et al., 1997). Several further channels are directly activated by sufficiently low pH, such as TRPV4 (Suzuki et al., 2003), ASICs (White et al., 2010) and TRPV1, which is sensitised between pHs of 6-7 and activated by pHs below 6 (Jordt et al., 2000). These interactions can mediate hyperalgesia to thermal stimuli and allodynia to both mechanical and thermal stimuli (Caterina et al., 2000; Cockayne et al., 2005;

Cockayne et al., 2000; Davis et al., 2000; Grant et al., 2007; Sluka et al., 2003; Souslova et al., 2000; Todaka et al., 2004).

Just like molecules released as a result of exposure to noxious heat, molecules released with the onset of inflammation can contribute to pain in burn injury in a variety of ways; the three cytokines with the longest-standing association to burn injury, IL-1β, IL-6 and TNFα are no exceptions. IL-1β, sourced from neutrophils, macrophages and neurons, is detectible in burn blister fluid (Copray et al., 2001; Ono et al., 1995) in addition to its above-described systemic upregulation and can mediate thermal hyperalgesia and mechanical allodynia (Fukuoka et al., 1994; Sachs et al., 2002; Safieh-Garabedian et al., 1995). Its nociceptive modulation is mediated in a p38-MAPK dependent manner to enhance Tetrodotoxin (TTX)-resistant Na_vs (where TTX-sensitivity is used to discriminate between Na_v subgroups; Binshtok et al., 2008), inhibit K_vs (Takeda et al., 2008), sensitise TRPV1 (Obreja et al., 2002) and bradykinin 2 receptors (BK2; von Banchet et al., 2011) and upregulate NGF (Safieh-Garabedian et al., 1995). IL-6, elevated locally in a manner correlating with mechanical hyperalgesia in burn injury (Ono et al., 1995; Summer et al., 2008), is known to sensitise TRPV1 (Obreja et al., 2005) and to be upregulated by PGE2 (St-Jacques et al., 2011). While no further mechanisms have been elucidated, burn injury mechanical hyperalgesia is attenuated by IL-6 antibodies (Summer et al., 2008). TNFα is also increased locally (Rhodes et al., 1999) as well as systemically, as is attributed to its inflammation-specific release from keratinocytes (Corsini et al., 1998), fibroblasts (Fujisawa et al., 1997), macrophages and neutrophils (Khanolkar-Young et al., 1995) on top of its physiological synthesis by mast cells (Ackermann et al., 1998). In addition to upregulating IL-1β, IL-6, IL-8

and prostaglandins (Cunha et al., 1992), it may directly activate nociceptors via TNF receptor 1 (TNFR1; Hasegawa et al., 2010). This would be consistent with exogenous TNFα inducing thermal hyperalgesia and mechanical allodynia and hyperalgesia (Fernandes et al., 2011), though it also sensitises TRPV1 in a COX-dependent manner (Nicol et al., 1997). Bradykinin, implicated in burn injury by its antagonist's reduction of tissue oedema following thermal trauma (Nwariaku et al., 1996), directly activates nociceptors via BK1 and BK2 receptors (Moreau et al., 2005; Oh et al., 2004), where the former is only expressed in pathological states (Fox et al., 2003; Marceau et al., 1998). It further acts via $Na_{v1.9}$, TRPA1 and TRPV1, where the latter is either sensitised to body temperature (Cesare et al., 1996; Sugiura et al., 2002) or activated indirectly via the production of the lipid 12-hydroperoxyeicosatetraenoic acid (12-HPETE; Shin et al., 2002). Serotonin (5-HT), identified as elevated in one of the few microdialysis studies of burn injury (Samuelsson et al., 2008), is released from mast cells (Kushnir-Sukhov et al., 2007) and platelets (Humphrey et al., 1955) and mediates hyperalgesia (Loyd et al., 2011; Tambeli et al., 2006) potentially directly through nociceptive 5-HT_3 receptors (Hicks et al., 2002), via an indirect prostaglandin-, norepinephrine- and 5-HT_2 dependent pathway (Oliveira et al., 2007) or via ASIC sensitisation (Qiu et al., 2012). Histamine's production in burn injury (Horakova et al., 1974) is comparable to 5-HT in its release from mast cells and platelets (Mannaioni et al., 1997; Riley et al., 1953); it activates nociceptors via the H1 receptor (Nicolson et al., 2002; Ting et al., 2007) in an at least partially TRPV1-dependent manner (Kajihara et al., 2010), while H4 receptors are involved in the development of inflammatory thermal hyperalgesia (Coruzzi et al., 2007). Further, various eicosanoids are implicated in burn injury, including prostanoids, thromboxanes and leukotrienes; among them, PGE_2 stands

out as a significant algogen. Its mediation of hyperalgesia (Kuhn et al., 1973) is exerted by potentiating the effects of bradykinin (Kumazawa et al., 1996) and histamine (Nicolson et al., 2007), sensitising Na_vs (England et al., 1996) and TRPV1 (Moriyama et al., 2005), inhibiting K_vs (England et al., 1996) and up-regulating IL-6, CGRP, substance P and substance P's neurokinin-1 receptor (Ma, 2010; Segond von Banchet et al., 2003; St-Jacques et al., 2011).

The nociceptive influence of inflammatory mediators is evidently extensive and discussing each of them in full detail is beyond the scope of this introduction. However, one particular inflammatory mediator, NGF, requires further consideration for its multifaceted interaction with TRPV1, which is considered a pivotal component of the molecular interface between pain and inflammation. NGF induces hyperalgesia and allodynia upon injection (Lewin et al., 1993; Thompson et al., 1995), and is known to be upregulated by various burn-elevated inflammatory mediators including IL-1β and TNFα (Abe et al., 2007; Hattori et al., 1993; Woolf et al., 1997), histamine (Lipnik-Stangelj, 2006) and prostaglandins (Toyomoto et al., 2004). The vast majority of nociceptors expressing CGRP and substance P (and thereby those mediating TRPV1 activation's principal contribution to neurogenic inflammation) express TrkA, the receptor through which NGF's effects on TRPV1 are exerted (McMahon et al., 1994). Its pronociceptive effect is exerted largely (though not exclusively; D'Arco et al., 2007; Mamet et al., 2003; Obata et al., 2005; Ramer et al., 2001) through at least three distinct mechanisms sensitising TRPV1. The first is a phosphatidylinositol-4,5-bisphosphate 3-kinase (PI3K)- and protein kinase C (PKC)- dependent phosphorylation of TRPV1 (Bonnington et al., 2003) which lowers the channel's thermal activation threshold and enhances its sensitivity to various

activators (Vellani et al., 2001). The second is a PKC-dependent phosphorylation that promotes the receptor's trafficking from the cytoplasm and insertion into the membrane, increasing its availability (Morenilla-Palao et al., 2004; Zhang et al., 2005). The third is NGF's promotion of TRPV1 transcription, facilitating an increase in the protein's expression (Xue et al., 2007).

1.1.4.2.5 TRPV1: An Interface for Pain and Inflammation

TRPV1's activation and modulation by such a vast range of endogenous mediators implicated in burn injury and other pathological states has highlighted it as a key effector molecule in both pain and inflammation, as is predicted by its role as a molecular integrator of thermal and molecular interstitial stimuli (Caterina et al., 2000; Davis et al., 2000); indeed, it is increasingly being evaluated for its inflammatory effects in pathological states alone (Alawi et al., 2010; Devesa et al., 2011). To summarise the underlying interactions discussed above, TRPV1 is activated by heat, releases the inflammatory mediators CGRP and substance P upon activation, is activated by lipids, is sensitised by thrombin, is activated or sensitised by protons depending on the pH, mediates nociceptive H1 receptor activation and is sensitised by IL-1β, IL-6, TNFα, bradykinin, PGE_2 and NGF. It has therefore generated extensive interest as a potential therapeutic target, with particular areas of focus including its structure, the relationship this has with its function and its stimulation-mediated desensitisation. These are briefly overviewed below, exploring the receptor's polymodality and the molecular aspects of its operation.

Regardless of its activation or modulation by alogogens released in pathological states, an interesting characteristic of TRPV1 is its reduction in response size upon repeated stimulation (Caterina et al., 1997; Liu et al., 1996), which is thought to at least share mechanisms with, if not occur as a result of, the channel's desensitisation (Nagy et al., 2014). TRPV1 desensitisation is Ca^{2+} dependent, occurring with the influx of Ca^{2+} following the channel's activation (Cholewinski et al., 1993; Koplas et al., 1997; Mohapatra et al., 2005; Piper et al., 1999), wherein the Ca^{2+} binds to calmodulin (CaM) and activates calcineurin and Ca^{2+}/calmodulin-dependent protein kinase II (CaMKII; Lishko et al., 2007; Numazaki et al., 2003; Rosenbaum et al., 2004). PKA, however, can reverse desensitisation as reflected in sensitisation to various stimuli including capsaicin and pH (Bhave et al., 2003; Di Marzo et al., 2002; Mohapatra et al., 2005); TRPV1's Ca^{2+}-dependent desensitisation is thought to be regulated by a balance of calcineurin-mediated dephosphorylation and the actions of various kinases such as PKA (Bhave et al., 2003; Cortright et al., 2004; Docherty et al., 1996; Jung et al., 2004; Mandadi et al., 2004; Mohapatra et al., 2005). However, PKA-dependent phosphorylation also mediates TRPV1 desensitisation via the channel's internalisation and lysosomal degradation (Sanz-Salvador et al., 2012).

While TRPV1's desensitisation has been utilised therapeutically for centuries (Nagy et al., 2014), topical capsaicin is available for the treatment of peripheral neuropathic and HIV-associated pain (Noto et al., 2009) and analogues are currently in various clinical trials (Jara-Oseguera et al., 2008; Mandadi et al., 2008), pharmacological intervention targeting TRPV1 may benefit from a fuller understanding of the molecular machinery with which the channel operates. Consequently, much progress

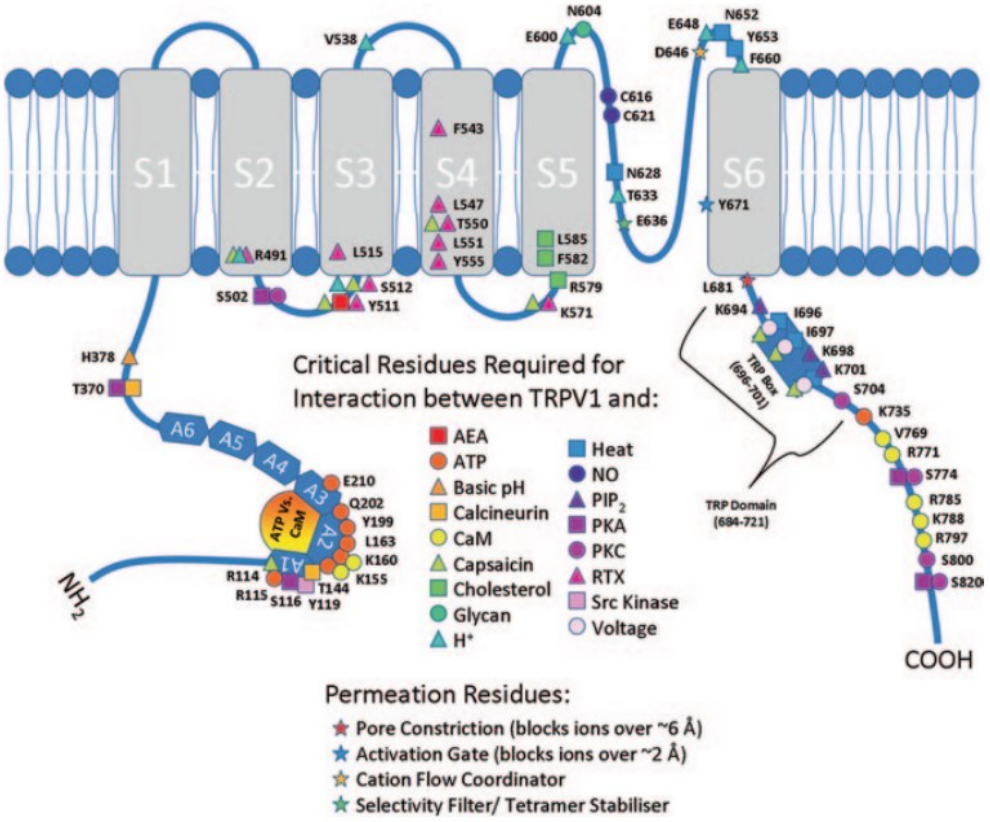


Figure 5 Key residues for TRPV1 function. TRPV1's topology representing crucial residues involved in the activation, sensitisation, desensitisation and gating of TRPV1; this figure was constructed by the author of this thesis for publication by Nagy et al. (2014) and reproduced with permission of the rights holder, Springer.

has been made in elucidating TRPV1's structure-function relationship (Fig. 5). The protein is composed of 839 amino acids in humans, forming an N-terminus, a C-terminus, six transmembrane-helices (S1-6) and a pore-forming loop between S5 and S6. TRPV1 complexes with other TRPV subunits to form a tetrameric ion channel; typically, this is by self-association with other TRPV1 molecules, but can include TRPV1 splice variants, TRPV2 (Rutter et al., 2005) or TRPV3 (Smith et al., 2002). The tetramer is then integrated into a transducisome, in which it is associated with elements of the channel's signalling pathways (such as PKC; Vennekens et al., 2002, CaM; Docherty et al., 1996, and PI3K; Stein et al., 2006) for efficient

transduction. In many cases, many of the above-described processes modulating TRPV1 function have been localised to particular residues or portions distributed throughout the molecule. The N-terminus contains the ankyrin repeat domain (consisting of six repeats of a 33-amino acid ankyrin sequence) which, in TRPV1, houses the binding site for CaM which regulates Ca^{2+}-dependent desensitisation (Fig. 5; Koplas et al., 1997). ATP is also thought to bind and potentiate TRPV1 currents here, as is abolished by D178 mutation (Kwak et al., 2000; Lishko et al., 2007; Mohapatra et al., 2005). The N-terminus also contains sites for post-transcriptional modification regulating sensitisation; these include Y200, which is ultimately phosphorylated by Src kinase to induce membrane insertion following NGF's activation of TrkA (Zhang et al., 2005), and both S116 and T370, PKA phosphorylation sites which attenuate stimulation-induced desensitisation (Bhave et al., 2003; Mohapatra et al., 2005). The C-terminus contains the TRP domain (E684-R721), which enables subunit tetramerisation and crucially couples stimulus reception with channel gating (Garcia-Sanz et al., 2007). Further, it determines the channel's required activation energy, particularly within the TRP box (a six-residue sequence conserved among TRP channels) it contains; alanine substitution of its constituent residues (I696, W697 and R701) compromises the channel's response to voltage, heat and capsaicin (Valente et al., 2008). The C-terminus' role in gating control is further supported by these effects also being observed progressively with truncation of the distal 31 or 72 amino acids (Vlachova et al., 2003). It also confers the channel's thermosensitvity, as indicated by reversal of temperature response profiles when swapping C-termini in TRPM8 chimaeras (Brauchi et al., 2006). Following earlier reports that PIP2 attenuates TRPV1 activation, and that its removal disinhibits the channel (Prescott et al., 2003), sufficient evidence has since been

collated to support PIP2 having a pronociceptive interaction with TRPV1 (Liu et al., 1998; Stein et al., 2006); this also occurs on the C-terminus (Brauchi et al., 2007). Just as the N-terminus is the major binding site for PKA, the C-terminus is the primary binding site for PKC; it contains both the major (S800; Numazaki et al., 2002) and minor (S774 and S820; Bhave et al., 2003) phosphorylation sites underlying PKC's sensitisation of the channel.

In addition to containing the constrictions that either block the ion conductance pathway or allow the passage of large (L681) and small (Y671) ions, constituting TRPV1's activation gate (Salazar et al., 2009), the pore domain contains E600 and E648. Upon protonation by decreases in extracellular pH, these residues respectively confer the channels sensitisation and activation by acidity such as that resulting from ischaemia in burn injury (Jordt et al., 2000). Further, S5 can bind lipids; it contains a cholesterol recognition amino acid consensus sequence, by which cholesterol binding decreases TRPV1 currents; the substitutions R579D and F582Q reduce this, while L585I prevents it (Picazo-Juarez et al., 2011). The pore region can also be a site of post-transcriptional modification, as demonstrated by the N604T mutant; this residue confers TRPV1's alteration of current amplitude and desensitisation by glycosylation state in wild type TRPV1, while responses are uniform in the N604T mutant (Veldhuis et al., 2012). In addition to containing the "vanilloid pocket" between the first intracellular loop and S4, the binding site for lipophilic compounds that cross the cell membrane including capsaicin (Jordt et al., 2002), the S1-S4 module contains several residues conferring TRPV1's pH sensitivity (Jordt et al., 2002) including those required for the hydrophobic reactions coupling proton binding to gating (Ryu et al., 2007). Further, while the molecular

determinants of TRPV1's gating by voltage are as of yet unconfirmed, it is known to rely at least on a series of positively charged amino acids within S4 (Papazian et al., 1991; Stuhmer et al., 1989). Finally, the S1-S4 module also enables post-transcriptional modification via its consensus PKC and PKA binding site found on the first intracellular loop, by which phosphorylation respectively potentiates heat- (Rathee et al., 2002) and capsaicin- (Numazaki et al., 2002) induced currents.

TRPV1's polymodality and our developing insight into its molecular operation raise interesting questions regarding the integration and/or independence of the means by which its activators and modulators exert their effects. Two principal lines of thought have emerged. The first is that the end point of any modulation or activation is a shift in the channel's voltage dependence from physiologically irrelevant to relevant ranges; that the channel is ultimately voltage-gated regardless of stimuli (Nilius et al., 2005). Here, mediators demonstrably operating by modification to temperature sensitivity are thought to be an indirect means of shifting voltage dependence (Gunthorpe et al., 2000; Vlachova et al., 2003). The second is an allosteric model, in which sensors for each of TRPV1's modalities are directly and individually linked to the channel's gating apparatus such that they can operate independently of one another (Latorre et al., 2007), as is supported by the fact that the C-terminus confers thermosensation without altering voltage-dependence (Brauchi et al., 2006). In any case, it is clear that the activation and regulation of TRPV1 is extremely complex and multifaceted, susceptible to modulation by a large range of mediators acting independently across the molecule; it is a characteristic that any study of TRPV1's operation must contend with, but likely that which confers its broad functional significance in pain and inflammation.

1.1.4.2.6 Clinical Management of Burn Pain

The complexity of burn pain is reflected in the difficulty of its management, which evolves throughout recovery and adapts to the dynamic contributions of distinct clinically-defined pain components (Summer et al., 2007). In brief, recovery from burn injury is divided into three phases; the acute phase, the healing phase and the rehabilitation phase, all of which are outlined by the above-described clinical priorities in burn injury. The acute phase consists of wound debridement and stabilisation by fluid resuscitation, and is bypassed with minor thermal trauma (Summer et al., 2007). The healing phase consists of accomplishing wound closure through maintenance of a clean wound bed, requiring frequent dressing changes and often surgical intervention. The rehabilitation phase consists of the resolution of the local inflammatory response and tissue remodelling, followed by completion of a treatment plan accomplishing optimal functional recovery and reintegration into society (Carrougher, 1998; Summer et al., 2007). Pain remains burn patients' most common complaint (Carrougher, 1998), and is clinically characterised by its presentation as one of three types; here, these characterisations and their prevalences over the course of recovery will be described.

The most intense burn pain component is procedural pain (Ashburn, 1995; Byers et al., 2001; Choiniere et al., 1989), defined as that resulting from therapeutic intervention which includes wound debridement, dressing changes and occupational therapy and is principally a result of mechanical hyperalgesia (Summer et al., 2007). Note that, while procedural pain certainly includes that from donor skin sites required

for grafting, and it is excruciating and susceptible to potentiation by systemic effects resulting from the burn, it is a separate pathology to burn injury and is not discussed in this thesis. During the acute phase of recovery, procedural pain is aggressively treated by pre-treatment with opioids, the effects of which coincide with the period of maximal stimulation of the burn site. Anxiolytics are typically used as an adjunct, as the emotional impact of extremely unpleasant first dressing changes has been found to underlie long-term psychological distress (Meyer Iii et al., 2012). The aggressive use of opioids continues into the healing phase of recovery, at which point procedural pain can vary unpredictably (Choiniere et al., 1989) and, in extreme cases, be further treated with local nerve blocks or general anaesthesia (Summer et al., 2007); local anaesthesia is avoided as its administration may create a channel for infection. While the advantages of topical analgesia are therefore clear, lidocaine has proven ineffective; its analgesia in burn injury is known to be dose- and nociceptor-dependent, with C fibres needing a much larger dose than Aδ fibres (Fink et al., 1983), but it is insufficient for procedural mechanical hyperalgesia (Summer et al., 2007). The limited success it has seen has applied to burns deep enough to require the generation of sensitive vascular granulation tissue, but the risk of cardiac arrhythmia following systemic dissemination is noted (Coleman, 2004; McLure et al., 2005; Weinberg et al., 2004). It has been suggested that, consistent with the observation that more inflamed tissue is less responsive to topical analgesia (Jellish et al., 1999), inflammation may reduce C-fibres' sensitivity to local anaesthetics (Aley et al., 2000). Other failed attempts at topical therapeutic intervention include NMDAR antagonists (Pedersen et al., 1998) and NSAIDs (Moiniche et al., 1994) where even morphine's effect does not reach statistical significance experimentally (Long et al., 2001) despite its (clinically unfeasible) success when administered subcutaneously

(Moiniche et al., 1993). In the rehabilitation phase, following wound closure, pain is far less severe and the limited procedural component is induced largely by physical or occupational therapy in the pursuit of optimal functional outcome, though this could also be defined as breakthrough pain (see below). Opioids are only indicated at this stage with complex surgical interventions such as the use of subcutaneous skin expanders and, like donor site trauma, could be considered a separate pathology and are not discussed here (Summer et al., 2007). The use of opioids is otherwise phased out prior to or early in the rehabilitation phase.

Background pain, characterised by its consistency and mild to moderate intensity, is described as a burning or throbbing sensation and occurs despite the patient remaining still (Jonsson et al., 1998); it could be described as a manifestation of allodynia. The general clinical approach is to continuously maintain a sufficient serum level of analgesic by its regular scheduled application (Kealey, 1995). It is highly variable in the acute phase; it ranges from absent to severe depending on the patient though, when severe, the continuous nature of background pain indicates the use of long half-life opioids such as methadone which, in addition to opioid receptor activation, inhibits NMDARs (Williams et al., 1998). While background pain is typically less severe than procedural or breakthrough pain during the healing phase, it is particularly variable (Summer et al., 2007). One of its more predictable aspects is its association with the ongoing process of re-epithelialisation; background pain increases with the emergence of epithelial skin “buds”, the skin appendages from which epithelial cells proliferate to cover the wound. Once coverage is complete, the pain drastically decreases. The clinical response continues to consist of maintaining a therapeutic serum concentration into this phase of recovery, though this must be

elevated with the onset of re-epithelialisation and several doses must be administered prior to stabilisation of this analgesic level (Kealey, 1995). Background pain ceases with wound closure, and therefore resolves prior to or early in the rehabilitation phase (Summer et al., 2007).

The final burn pain component, breakthrough pain, is transient pain that is not associated with surgical intervention. It is often categorised as pain induced by movement such as that observed in any post-operative patient; this is where breakthrough pain was originally defined. However, it can also occur spontaneously. This is known to result either from ongoing changes in nociception characteristic of the burn wound, taking place both peripherally and centrally, or from end-of-dose medication failure, in which the serum concentration of the analgesic falls below the therapeutic threshold (Portenoy et al., 1990). As breakthrough pain is classically defined as resulting in part from a combination of mechanical hyperalgesia and movement, the distinction between procedural and breakthrough pain is marred in the rehabilitation phase, where pain results from the movement required for physical and occupational therapy (Summer et al., 2007); its clinical management is the same. During the acute and healing phases, breakthrough pain is typically treated by reducing the interval between analgesic doses maintaining its therapeutic serum concentration, as is preferable to increasing the dose and thereby elevating the analgesic's peak concentration; this achieves a more stable serum analgesic level and fewer or lesser adverse effects (Portenoy et al., 1990).

The clinical response to burn pain at severities associated with under-treatment is therefore currently heavily reliant on the use of opioids. The fact that burn pain

remains undertreated results in part from the restrictions the adverse effects associated with the use of opioids incur; their common side effects include sedation, dizziness, nausea, vomiting, constipation, addiction and tolerance, which enforce at least temporary discontinuation of their use (Benyamin et al., 2008). The efficacy of opioids can be attributed to its broad spectrum nature; it acts both centrally and peripherally, mediating analgesia by inhibiting Ca_Vs (and thereby Ca^{2+} entry) and opening K_Vs to enhance outward K^+ currents in nociceptors. These effects are mediated intracellularly following binding of the opioid to its associated G-protein coupled receptors (GPCRs) and ultimately reduce pronociceptive signal transduction by inhibiting neurotransmitter release (Al-Hasani et al., 2011). However, it is the simplicity of their operating mechanism that underlies their interaction with unintended organ systems and the consequent adverse effects (Benyamin et al., 2008). If their analgesic efficacy could be achieved by a therapeutic intervention exclusively targeting nociceptive processing, such adverse effects could be avoided. However, despite great progress being made over the last few decades, our current understanding of the burn wound's nociceptive signalling environment is insufficient for development of such an approach; it must be further elucidated.

1.1.4.3 Modelling burn injury in animals

The complex and multifaceted nature of burn injury dictates the need for *in vivo* experiments, which can be used to evaluate its signalling environment in a setting capturing as many aspects of the pathology as possible. The ideal source of microdialysate would be humans in a strictly controlled modelling environment, though the use of animals can be justified on several counts. Principally, the severity

of the insult required for studying life-threatening trauma, and the long-term effects that would require enduring, is extreme enough to categorise the procedure as non-recovery in animals and it would therefore be unethical to induce them in a human. Sampling from burn patients with a pre-existing injury offer important insights into the pathology, as is reflected in the range of known mediators discussed above. However, the study of the immediate acute phase of burn injury in particular can impose requirements that conflict with the care of severely burned patients, and support the use of animal models. It requires sampling during the immediate stages of nociceptive generation and maintenance post-trauma; any time spent admitting the patient and addressing their greater needs of survival and comfort has already prevented this. Prioritising patient care enforces the sacrifice of complete sample series even where the proposed time course allows for sampling from severe burn patients, due to inevitable scheduling conflicts (Gatson et al., 2014). Further, where specific local sampling via microdialysis is needed, positioning a subcutaneous probe in a fresh burn injury is unethical not only for the pain it would induce but also for the risk of creating a channel for infection in an already-compromised skin barrier, a common consideration for any clinical transdermal device (Wolf et al., 2013). Additionally, the probe insertion is itself an injury and must be completed before the burn, such that mediators detected can be attributed specifically to the burn and pre-burn interstitial profiles can be compared. Further, analgesia interfering with peripheral nociceptive processing would be the priority in severely burned patients, but would compromise any insight into nociceptive processing. Further still, while burns are heterogeneous in their source, depth and surface area, empirical study of their underlying mechanisms would be facilitated by strict control of these factors.

The use of animals in burn studies is therefore primarily motivated by the experimental control they offer though, as in any translational research, the differences between animals and humans must be considered. Animal models have sustained in research due to their many successful clinical translations; for example, within the pain field, the clinical analgesic use of spinal opiate administration (Bennett et al., 2000; Onofrio et al., 1981; Yaksh et al., 1976), cyclooxygenase-2 (COX-2) inhibitors (Rao et al., 2008), tapentadol (Prommer, 2010), anti-nerve growth factor (NGF; Cattaneo, 2010; Watson et al., 2008) and pregabalin (Horga de la Parte et al., 2006) stemmed from the use of rodent models (Berge, 2011). However, convincing preclinical animal data can fail to translate clinically, as seen with tachykinin receptor 1 antagonists (Hill, 2000), the sodium channel blocker 4030W92 (Wallace et al., 2004) and the combination of dextromethorphan with morphine (Galer et al., 2005). Therefore, despite the overwhelming contributions enabled by the use of animals in a wide variety of fields, it requires cautious consideration.

Rodent models are frequently successfully used in burn research as they are extensively consistent with human burn pathology as described above. In brief, successfully modelled components of burn injury include but are not limited to the development of the gradient between zones of coagulation, stasis and hyperaemia (Eski et al., 2012; Nisanci et al., 2010), necrosis by denaturation (Wu et al., 2015), nociception (Gao et al., 2010; Huang et al., 2014; Summer et al., 2008), inflammatory response (Babcock et al., 2012; Summer et al., 2008), ischaemia (Firat et al., 2013) and oxidative stress (Bertin-Maghit et al., 2000; Feng et al., 2013), apoptosis (Xiao et al., 2013), aspects of tissue recovery including coagulation (Oksuz et al., 2013) and re-epithelialisation (Payne et al., 2010), cardiovascular

effects (Sayeed, 2005), fluid balance (Bao et al., 2010) and hypermetabolic response (Williams et al., 2009). The similarity between human and rodent burn pathophysiology naturally extends to the composition of samples analysed in targeted tissue profiling studies, with work for the identification of either novel signalling processes or biomarkers for pathological analysis and outcome prediction exemplifying this point, as described extensively elsewhere in this thesis (Claassen et al., 2014; Kraft et al., 2014; Maass et al., 2002; Orman et al., 2011; Pileri et al., 2008; Xiao et al., 2013). It is important to note that, despite these similarities, particular components of rodent recovery processes differ significantly from humans (Abdullahi et al., 2014). For example, human wounds heal primarily via re-epithelialisation, while rats and mice do so by wound contraction (Dorsett-Martin, 2004). However, this should not detract from the fact that rodent models have proven representative of human burn pathology with circulating sampling methods as shown above, particularly regarding the immune response.

While animal models therefore have the potential to recreate the majority of important aspects of human burn injury, fulfilment of this depends on the experiment's execution. A large variety of approaches are used and, while there is no single standardised burn model in widespread use, particular technologies and parameter ranges offering the greatest control have emerged as convention. The first consideration is the mechanism of injury, which can consist of direct contact with heated metal (Dahiya, 2009), electricity (Zelt et al., 1988), exposure to a flame (Dai et al., 2011) or a heated liquid (Andrews et al., 2016) among other heat sources. Despite their clinical prevalence (Golshan et al., 2013), flames are rarely used as a means of experimental heat transfer due to their associated risks and limited control

of heat capacity (Gurfinkel et al., 2010). The principal challenge associated with most common models is achieving a homogenous burn depth across the experimental site. This is especially true of direct contact models, executed by application of a heated metal instrument to a shaved area (usually the back) until the predetermined TBSA is reached (Abdullahi et al., 2014), and electrical burns, which are further complex to perform and require larger animals (e.g. monkeys) for the induction of lesions comparable to a human's (Zelt et al., 1988). Heated blocks in particular are attractive for the control they offer in regulating heat capacity, but the homogeneity of the skin contact itself, and therefore pressure and heat transfer, is compromised by anatomical contours, variances in tissue consistency and the presence of miniscule amounts of body fluids which vaporise on instrument contact (Gurfinkel et al., 2010). Heated liquids remain among the most common means of burn induction (Abdullahi et al., 2014) for their ability to circumvent these issues by adhering within the smallest crevices of the subject's cutaneous topography (Gurfinkel et al., 2010). They thereby accomplish the most reliable heat transfer and most homogenous burn depth. Scald-type models are also selected as they represent the most common mechanism of burn injury presenting clinically among the old and young, and remain among the most common mechanisms for the global population regardless of age (Battle et al., 2016; Arslan et al., 2013; Ansari-Moghaddam et al., 2013; Golshan et al., 2013). Despite their popularity, the drawbacks of scald models, namely lesser control over the affected area and the duration of exposure, should be noted (Abdullahi et al., 2014, Gurfinkel et al., 2010).

The selection of the burn mechanism, and the operation of its unique heat transfer characteristics, determines much of the remainder of the model design. The most

important aspect of experimental control a burn model offers is consistency in a required depth and area of the affected tissue (Abdullahi et al., 2014). This is regulated by the amount of heat transferred and consequent extent of tissue denaturation, which is strictly controlled via both the temperature and the duration of exposure. With scald models, the liquid tends to be heated to between 60°C (Niederbichler et al., 2011; Hoesel et al., 2009) and 100°C (Abdullahi et al., 2014; Wu et al., 2010; Wu et al., 2012) and the affected area exposed for between 2 seconds (Oliveira et al., 2009; Al-Mousawi et al., 2010) and 10 minutes (Andrews et al., 2016), where lower temperatures with longer durations can accomplish the same burn depths and areas as higher temperatures with shorter durations. Deep-partial or full thickness burns are the most commonly employed, requiring a greater extent of heat transfer which is accomplished with the higher temperatures and/or longer exposures within these ranges. In lieu of a standardised model, the each study's configuration and protocol is internally histologically validated. These parameters depend on the subject's anatomy and thereby the selection of a suitable species. Rats are the most widely used animal in pathophysiological studies and, for their representation of most aspects of human burn injury (described above) and the practicalities of their husbandry, this is true specifically of burns research (Santos Heredero et al., 1996). Their size indicates a lesser heat exposure than that required for larger animals also used in burns research, such as pigs (Martini et al., 2001, Santos Heredero et al., 1996). The most frequently used rat strains are Sprague-Dawley and Wistar; while the former are quite susceptible to infection, the latter are very resistant (Santos Heredero et al., 1996). The selection of either strain is therefore an important consideration for experiments requiring longer survival durations, as post-burn development of sepsis and MODS are clinically-interesting

but not ubiquitous among burn injuries (Greenhalgh et al., 2007). The influence of infection may therefore be desirable, problematic or less relevant in the many instances where the severity of the pathology requires that the procedure is non-recovery.

Beyond the mechanism of injury, exposure parameters and species, the anaesthetic selection must also be specific to the study. Conventional means of general anaesthesia are employed in the vast majority of animal burn studies, namely inhalational isoflurane (Hoesel et al., 2010; Wu et al., 2010; Wu et al., 2011, Baer et al., 2015), intraperitoneal (i.p.) sodium pentobarbital (Al-Ghoul et al., 2010; Hemilla et al., 2011) or an i.p. combination of ketamine and xylazine (Yang et al., 2013; Niederbichler et al., 2012). Isoflurane is widely used for its rapid rate of induction and recovery (Al-Mousawi et al., 2013), but is limited where prolonged deep anaesthesia is required by its associated ventilatory insufficiency as sufficient doses decrease tidal volume and respiratory rate (Steffey et al., 1977; Steffey et al., 1980). Pentobarbital is a short-acting barbiturate that is similarly attractive for its induction rate, but causes non-selective suppression of the CNS and, at surgical anaesthetic doses, induces cardiac and respiratory depression (Roth, 1935; Foulks, 1956). While pentobarbital use has been declining recently, the reported use of isoflurane and the ketamine/xylazine combination are on the rise (Stokes et al., 2009). Ketamine is an NMDAR antagonist with opioid receptor activity and therefore both analgesic and anaesthetic properties while xylazine, an adrenoceptor agonist and sedative, functions as a muscle relaxant and analgesic to facilitate smooth emergence from ketamine-induced anaesthesia (Al-Mousawi et al., 2013). Despite the combination's efficacy, its analgesic properties can preclude its use in the research of nociceptive

signalling. Where the use of isoflurane, pentobarbital or ketamine and xylazine is compromised, other less common anaesthetics with alternative benefits and contraindications can be viable. For example, where a long duration and minimal CNS interference are required, urethane may be suitable. Its anaesthetic duration exceeds 24 hours at 1.5 g/kg in adult rats (Field et al., 1993) and it has minimal effects on respiratory frequency and haemodynamic stability (Maggi et al., 1986a, 1986b). However, as with any anaesthetic, it will eventually paralyze the diaphragm and intercostal muscles and breathing must nonetheless be monitored closely. It has no analgesic activity and is therefore suitable for the retention of nociceptive signalling. However, its use is generally limited to non-recovery experiments by its carcinogenic properties (Tannenbaum et al., 1958; Miller, 1991). As the immune system is extensively engaged in burn injury, the potential immunomodulatory effects of any given anaesthetic must be considered. While pentobarbital, ketamine, and chloral hydrate all enhance basal IL-1β and TNFα mRNA expression (Fish et al., 2008), urethane is partially immunosuppressive and has been shown to reduce splenic IL-1β mRNA expression and basal TNFα mRNA levels.

1.2 Microdialysis

While continuously measuring biomarkers or mediators in circulation is relatively easy due to the accessibility of blood, they are generally not representative of the interstitium (extracellular space) within specific organs; systemic availability of an analyte often does not reflect functionally significant local elevations, and can even express the opposite (Papp et al., 2005). Where the signalling environment of an organ such as the skin is to be evaluated, it is far more informative to sample directly from the interstitium; microdialysis, as first conceived in its present form by Ungerstedt et al. (1974), is an effective means of accomplishing this (Ungerstedt, 1991). It is conducted via positioning a capillary-like probe into the tissue; its semi-permeable membrane allows passive bidirectional diffusion between the interstitium surrounding it and a solution perfused through it. Its advantages over other approaches to local sampling are clear; this would typically require the collection of biopsies which, by their destructive nature, do not allow for continuous sampling. Microdialysis is generally the only feasible option for continuous local sampling within the same subject and the probes are well-tolerated, enabling sampling over many days. Further, while the need for interstitial or whole tissue sampling depends on the study, microdialysis is commonly selected for its retention of the tissue's structure and distinction between intra- and extracellular components, making it ideal for the study of the signalling environment. Recent technological advances in microdialysis probe design have made it possible to sample from nearly any organ with inflow and outflow mediated via a single entry point and, while it is typically used for the recovery of interstitial molecules, the design allows the administration and diffusion of substances into the tissue by its inclusion in the perfusate. While measurement (if

not collection) of targeted elements of the interstitial fluid is possible by the use of *in vivo* detection methods such as implantable biosensors, these platforms are limited by their onboard analytical technology while the collection of microdialysate enables the application of conventional analytical approaches. Such applications are facilitated by the nature of microdialysate, in which the analytes are effectively purified in suspension and are already suitable for direct analysis with most analytical platforms, requiring minimal sample preparation. Further, the size threshold for recovered molecules and the length and localisation of the active uptake region is at the discretion of the researcher. While microdialysis is simple to conduct, it has several pitfalls and its correct execution requires an understanding of several of the technique's underlying principles.

1.2.1 Experimental Considerations for Microdialysis

The fundamental principle microdialysis relies on is the equilibration of the fluid within the tube with that outside it; this equilibration occurs by bidirectional diffusion and is determined by various methodological parameters and, ultimately, the known laws of physical chemistry (Ungerstedt, 1991). These dictate the interaction occurring between the perfusate, the interstitium and the probe, which must be carefully controlled for stable and reproducible sample collection and can be particularly problematic in responsive biological systems. One of the first considerations for *in vivo* microdialysis should be the effect of the probe's insertion. While only minimally traumatic, the insertion of a microdialysis probe is nonetheless an injury and the body responds accordingly; various inflammatory mediators are released, glucose metabolism increases and blood flow and the release of

neurotransmitters is altered, though this can be minimised by smooth insertion of a small probe (Ungerstedt, 1991). Any work employing microdialysis in the study of pathological states must allow time for stabilisation of the tissue, such that molecules released as a result of probe insertion are not erroneously attributed to the experimental condition. This varies by tissue type; inflammatory mediators released in rat skin following probe insertion, for example, stabilise within 20 minutes (Groth et al., 1998), though control data determining the duration of the probe response should be collected in every study. Once the tissue's response to the probe insertion has resolved, an extended period of stable sampling can be expected but is not unlimited; the duration of 'baseline' level recording varies by organ, analyte, equipment and its implementation (Osborne et al., 1990; Westerink et al., 1988) though, for example, subcutaneous tissue remains stable for a week (Ungerstedt, 1991). However, stabilisation of the sampling configuration is not solely dependent on resolution of the tissue's response to the probe; regardless of the sampling environment, it also depends on the fundamental equilibration of fluid movement and analyte diffusion, such that samples collected over time can be meaningfully compared. This depends on allowing sufficient time for changes in fluidics to resolve as the perfusate is introduced into the tissue, and on the selection of suitable perfusate that accommodates minimal introduction of unintended or unsuitable concentration gradients. For example, a non-physiological pH would continuously perpetuate the movement of protons, and a perfusate lacking calcium would deplete the surrounding tissue of it and compromise synaptic transmission (Imperato et al., 1984; Westerink et al., 1988). However, any molecule included in the perfusate will diffuse down its concentration gradient and may do so into the tissue, potentially exerting an effect on the sampling environment. Consequently, equilibration of

recovery (analyte collection via the probe) is facilitated by selection of a perfusate that best represents the tissue's physiological interstitial composition while consisting of only the bare essentials (Moghaddam et al., 1989). The stabilisation of a microdialysis configuration following probe insertion is therefore bipartite; depending on both stabilisation of the fluidics and of the tissue state. The time during which the changes in the former resolve is referred to as "equilibration", while that of the latter is the "flush" period. Unlike equilibration microdialysate, which must be discarded, flush fractions should have stable relative recovery (defined below) and can be used for comparison of metabolic profiles. While also allowing for resolution of the tissue's response to the probe insertion, such comparisons can ensure slight variations in the probe insertions do not contribute to any subsequently recorded differences in the tissues' interstitial profiles. However, it should be considered that this microdialysate fraction still represents the tissue in an injured state.

The amount of any given analyte recovered from the tissue by microdialysis depends on several variables, including the length of the portion of the microdialysis probe actively sampling from the interstitium, the permeability of the membrane, the rate of perfusate flow and the rate of the analyte's movement through the tissue (Bungay et al., 1990). The active probe length is generally maximised to increase the interface between the perfusate and the interstitium to increase recovery, while the membrane's permeability is determined primarily by the size of its pores; this can be restricted to regulate the sampling of larger interstitial components with negligible impact on the uptake of the smaller target molecules. However, beyond imposing a size threshold, the membrane is far less influential as a determinant of molecule recovery than the composition of the interstitial fluid. For example, relative to its

movement in water, average analyte diffusion across brain parenchyma is reduced by 50% while having to traverse a microdialysis probe membrane only reduces it by 20% (Amberg et al., 1989). Flow rate is also an important determinant of recovery, as is outlined in the distinction between relative and absolute recovery. Relative recovery refers to an analyte's concentration upon collection from a microdialysis probe expressed as a percentage of its concentration in the sampled tissue, while absolute recovery refers to the total amount of the analyte collected in a given timeframe (Chefer et al., 2009). The selection of a higher perfusion rate prioritises absolute recovery over relative recovery by providing the tissue with a greater volume of perfusate for the analyte to perfuse into; as the perfusate in the active recovery region is more rapidly replaced with its faster flow, the concentration of any incoming analytes within the probe is reduced, encouraging inward diffusion and increasing the total amount of analyte collected. The selection of a lower perfusion rate prioritises relative recovery over absolute recovery by allowing an analyte more time to diffuse down its concentration gradient into a particular volume of the perfusate; consequently, the microdialysate's analyte concentration is closer to that of the interstitium but has a lower volume. There are advantages to either approach; prioritising absolute recovery maximises the total amount of interstitial molecules collected such that the increased yield may facilitate the use of less sensitive analytical platforms or more analyses. However, the lower concentration of sample collected may indicate the need for extraction, requiring further investment of time and effort and introducing a potential source of variance in the data. Conversely, prioritising relative recovery increases the likelihood that the sample can be analysed "neat", without additional steps in its preparation for analysis though, should the absolute amount of the molecule fall below that required for the sensitivity/number of

measurement analyses, there would be no recourse. There is also an important distinction between absolute and relative recovery in that changes in relative recovery represent inconsistency in tissue perfusion resulting from lack of stabilisation, while changes in absolute recovery with a stable relative recovery represents real changes in the physiological or pathophysiological availability of the analyte in the interstitium (Ungerstedt, 1991). However, it is important to note that a major challenge with the use of microdialysis is determining an analyte's true interstitial concentration from that recorded in the microdialysate. This cannot be overcome by evaluating the probe's recovery rate *in vitro* as the design would have to perfectly match the tissue's *in vivo* diffusion coefficient and, even were that possible, recovery varies on an analyte-by-analyte basis. The only accurate means of determining the extracellular concentration of an analyte is to perfuse it into the tissue at varying concentrations, and identify that which remains the same upon outflow and collection; this indicates that no diffusion occurred as there was no concentration gradient between the perfusate and interstitium and identifies the *in vivo* concentration, though it is a costly approach depending on absolute interstitial stability of the analyte (Lonnroth et al., 1987; Ungerstedt, 1991). As with many biological measurements, in lieu of precise measurements, relative changes between experimental and control tissue states are sufficient to indicate an experimental effect with microdialysates.

Aside from the analytical platform and any instruments required for specialised applications, such as a stereotaxic frame for cerebral sampling (Ungerstedt, 1991), considerations for equipping a microdialysis study principally concern the perfusion system and the selection of microdialysis probe. Perfusion rates typically range

between 0.5 and 5 µl/min; the perfusion system must be able to stably control the passage of small volumes of fluid. While several dedicated systems have been manufactured, clinical or similar syringe pumps typically accommodate these flow rates. The selection of the probe is dictated by the criteria described above, such as the membrane pore size, and by the requirements of its design, which are normally determined by the target tissue type. The two designs conventionally used currently are the catheter probe (Fig. 6a) and the concentric probe (Fig. 6b). Catheter style probes are relatively simple and inexpensive, consisting of a semi-permeable tube with non-permeable tubing on the one end, by which it can be attached to a syringe for perfusion, and a guide needle on the other, by which it can be inserted into the tissue. However, it must then exit the tissue, such that the guide needle can be removed and the exposed opening used as an outlet for sample collection. This requirement generally limits catheter probes to superficial tissue microdialysis, though the active uptake length of the probe is up to the discretion of the researcher. Concentric probes are more expensive and complicated, consisting of a dialysis membrane containing an inner cannula. They are positioned in the tissue similarly to an intravenous catheter; an introducer is inserted via a needle and the needle is then removed before insertion of the probe into the introducer, which is then sutured in place (Zapata et al., 2009). Perfusate enters the probe via the proximal end of the inner cannula and enters the distal end of the active probe length before changing direction and travelling to the outlet via the space between the inner cannula and semi-permeable membrane, into which interstitial molecules diffuse. This probe type enables deeper sampling and has the advantage of requiring only one wound (on entry). The final consideration is to reduce the potential for deadspace between the syringe pump, the probe and the collection vessel (which should be replaced at

predetermined intervals for continuous sampling), which is an often overlooked consequence of high connecting tube diameters and therefore unnecessarily high inner volumes (Ungerstedt, 1991).

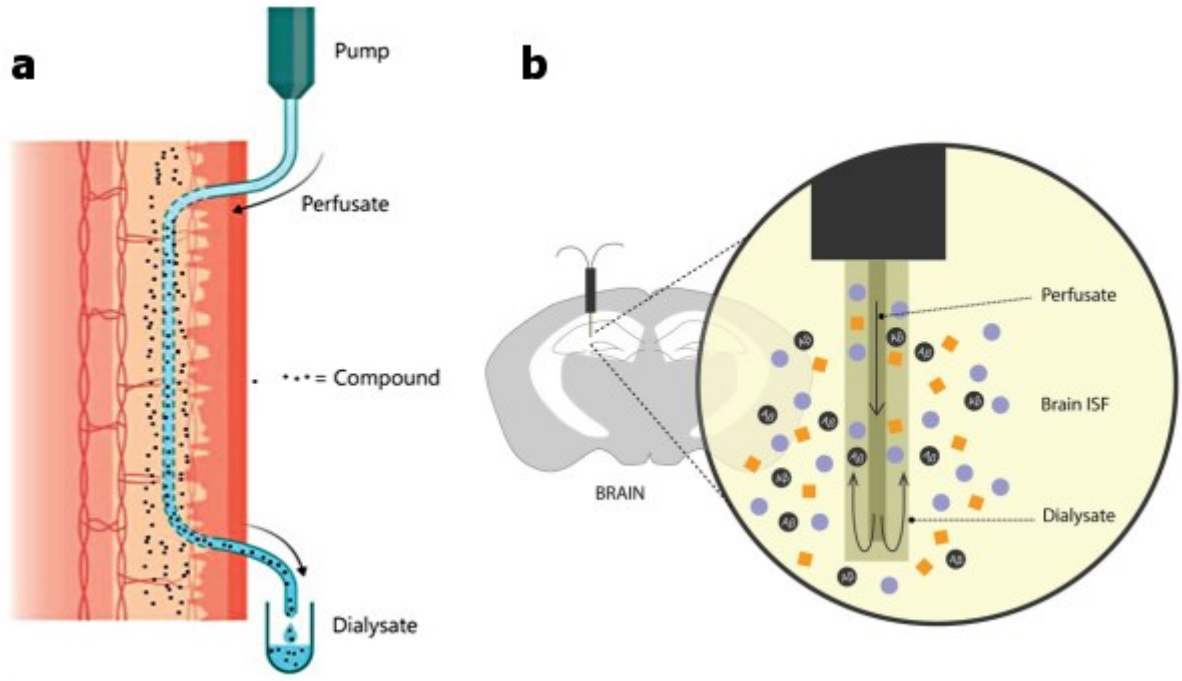


Figure 6 The principles of microdialysis and probe style variants. Fluid is perfused through a microdialysis probe; interstitial molecules passively diffuse into it and are carried externally for collection. Probes can resemble catheters (**a**) or concentric tubes (**b**), sampling by the same principles in either case. Images published by Melgaard et al. (2013) and Ramanathan et al. (2015) and reproduced with permissions of the rights holders, Karger Publishers and Frontiers.

1.2.2 Microdialysis in Burns Research

Addressing the above-described pitfalls and experimental design requirements has enabled successful experimental sampling by microdialysis throughout the body, particularly in the context of skin inflammation as is demonstrated by the elucidation of the dermal inflammatory response in allergy (Petersen et al., 1994; Petersen et

al., 1992), mediators of neurogenic inflammation (Schmelz et al., 2001), the vascular response to inflammation (Clough et al., 2002) and antioxidant status (Lee et al., 2005). Despite its clear viability for the study of inflammatory conditions and superficially-localising pathological states, microdialysis has only been used sparingly in burns research to date (Angst et al., 2008; Machens et al., 2006; Papp et al., 2005; Samuelsson et al., 2008). One of the above-discussed multiplex studies significantly contributing to our knowledge of the cytokine response to burn injury identified the elevation of IL-1β, IL-6, IL-8, IL-10, G-CSF, and MIP-1β following a UV burn and the elevation of IL-7 and IL-13 following the application of heat sufficient for nociception (Angst et al., 2008); the samples were dermal microdialysate. Similarly, a burn-induced rise in cutaneous 5-HT was identified following sampling with microdialysis, and further illustrated the need for local sampling by identifying no such effect systemically (Samuelsson et al., 2008). The post-burn elevation of the pro-inflammatory mediator complement 3a was also identified via subdermal microdialysis (Machens et al., 2006). The burn depth-dependent local elevation of histamine levels was also identified via microdialysis in pig models of superficial- to full-thickness burn injury (Papp et al., 2005), while an attempt to replicate the superficial burn component of this effect in a human microdialysis study did not find any histamine release (Petersen et al., 2009). While inflammation is a common theme in burn site microdialysis studies, they have also been used to evaluate metabolism (Samuelsson et al., 2006) and the distribution of antibiotics (Dalley et al., 2009). All these studies illustrate the potential of microdialysis for developing our understanding of the burn wound; it is clear that, even regarding the highest clinical priority components of the pathology such as inflammation, we have only scratched

the surface of what there is to be learned by continuously sampling from the burn site.

1.3 Metabolomics

Systems biology has enjoyed a boom in the development and application of various exploratory and targeted analytical technologies in recent decades, collectively forming the 'omics' fields of study. Omics approaches characterise and quantify the constituents within varying biological molecular pools, such that their potential function in different systems, physiological and/or pathological processes can be evaluated. They include genomics, transcriptomics, proteomics and, most recently, metabolomics. Where each omics class is defined by its target molecule class and the objects of their studies are their own respective 'omes', metabolomics can be defined as the multiparametric profiling of metabolites and the metabolome is the total metabolite complement of a biological system (Fiehn et al., 2002; Nicholson et al., 1999; Want et al., 2010b). Metabolites are distinguished from proteins in this context by their size (with the threshold generally considered to lie between 1200 and 2000 Da) and include lipids, small peptides, vitamins, nutrients, hormones, neurotransmitters and various substrates and products of ongoing metabolic processes (Goldsmith et al., 2010). The functional significance of these molecular classes is evident and reflected in metabolomics' modern wide-spread utilisation in studying toxicology, nutrition, the pharmaceutical industry, physiology, pathophysiology and clinically as a diagnostic tool (Robertson, 2005; Want et al., 2010b; Khoo et al., 2007; Goodacre et al., 2004).

Despite the established experimental and clinical influence of metabolomics, its relative youth and the enormity of its task is evident in the remaining unmet challenges to metabolome definition. The range of endogenous metabolite

concentrations comfortably surpasses nine orders of magnitude and includes an extensive variety of molecular classes, as alluded to above, and the difficulty in maximising metabolome coverage is compounded by challenges in subsequent data treatment and analysis (Nordström et al., 2006; Goodacre et al., 2004; Roessner et al., 2009; Want te al., 2010b). The progress made to date is largely a result of the development of the two principal metabolomics platforms: chromatography-coupled mass spectrometry (MS) and nuclear magnetic resonance (NMR) spectroscopy. MS and NMR spectroscopy have evolved concurrently with the development of the metabolomics field; following the initial developments of their current forms in 1918 (Griffiths, 2008) and the late 1940s (Becker, 1993) respectively, they developed rapidly and have been progressively applied within the modern conception of metabolomics since the 1960s and 70s (Dalgliesh et al., 1966; Hoult et al., 1974). Their status as the analytical mainstays is a result of their independent development and operation, which naturally confers different advantages and disadvantages and determines their suitability for different analyses. For example, a significant advantage of NMR is that it is non-destructive; it does not consume the sample, enabling its repeated use in further evaluations, and its analyses are further highly reproducible and inherently quantitative (Nicholson et al., 1999; Whitfield et al., 2004). However, MS, by comparison, is far more sensitive. While NMR typically only detects compounds exceeding 1-5 μM, MS can detect those within the femto- to attomolar range depending on the analyte and how well it ionises (Liu et al., 2011; Veenstra, 2012); indeed, single cell metabolomics is now possible with a suitable platform (Onjiko et al., 2015). Further, the varying chromatographic platforms coupled with MS typically require a sample volume of 10 – 50 μl, far lower than the 500 μl typically required for NMR. MS also offers greater selectivity as overlapping

resonances from different metabolites compromise NMR data interpretation (Keun et al., 2011; Veenstra, 2012); however, even among chromatographic techniques, liquid chromatography (LC)-MS is similarly compromised with overlapping elutions in untargeted studies. However, MS data is susceptible to an increased risk of sample loss and contamination imposed by the varying pre-treatments required for different chromatographic processing, which further requires greater investment of time (Dettmer et al., 2007). While there are further practical differences between NMR and MS, the major ones particularly apply to gas chromatography-MS (GC-MS) while NMR and LC-MS (Patti, 2011) are relatively more comparable; both are expensive, though NMR more so, both require minimal sample preparation, though LC-MS' is more complex, and both still face challenges in the identification of unknown target metabolites (Jansson et al., 2009; Bowen et al., 2010; Want et al., 2010b). Regardless, they are nonetheless effective in defining the metabolome via their easily-automatable, high-throughput and extremely multivariate metabolite measurement. Crucially, the selection of either platform - and its constituent technologies - characterises the analysed metabolite pool differentially, facilitating the detection and quantification of distinct areas within the metabolome and thereby enhancing its coverage. By their complementary nature, any platform could have been viable for use in this project, though MS' higher sensitivity would facilitate detection of lower-concentration analytes. LC-MS was ultimately utilised in the present work due to the advantages stated above; the relevant theory and practical considerations of its use is discussed below.

1.3.1 The Theory and Practise of Liquid Chromatography-Mass Spectrometry

The consecutive processes within a full LC-MS analysis include sample preparation, analyte separation, ionisation, mass analysis and detection and data analysis. The primary purpose of sample preparation is to separate metabolites from their containing experimental matrix. This avoids any potential interference this irrelevant component of the sample may have in the analysis, such as protein content suppressing the signal and blocking the column, though it also serves as an opportunity to concentrate low-abundance metabolites and raise their concentrations above the detection threshold in some circumstances (Dunn, 2011; Want et al., 2010b). The process must reflect the sample and the nature of its collection (Lu et al., 2008, Rabinowitz et al., 2007). For example, while simple fluids such as urine may only require dilution and centrifugation to remove particulates (Want et al., 2010a), samples collected or homogenised in a physiological buffer will require the removal of the salts contained and more complex samples such as those isolated from blood require thorough protein precipitation (Guo et al., 2015). LC-MS can be used to analyse solid tissue, though they require complete homogenisation prior to these same sample preparation steps (Want et al., 2010a). Protein precipitation is often executed by the addition of cold solvent (wherein lipids, another potentially undesirable molecular class, naturally form a layer on the sample surface and can be removed) and centrifuging with subsequent drying and resuspension in water. Unlike sample preparation for GC-MS, which requires chemical derivatisation upon metabolite extraction (Shackleton et al., 2006), the sample is ready for the next phase of analysis: Separation (Dettmer et al., 2007).

1.3.1.1 Chromatography

Separation prior to MS reduces sample complexity by minimising analyte co-elution and subsequent ion suppression, and can be accomplished by GC (Jellum et al., 1977), LC (Plumb et al., 2004; Swartz et al., 2005) or capillary electrophoresis (Ramautar et al., 2009). While the latter is not commonly employed for its lack of sensitivity, relatively underdeveloped structural elucidation resources and lack of reproducibility in larger scale studies (Want et al., 2010b), GC and LC remain popular and have distinct advantages. While GC is cheaper and has higher separation efficiency (Kopka, 2006; Krone et al., 2010), the development of ultra-performance LC (UPLC) seems to have motivated the current preferential use of LC-MS by its shortened run time in addition to its fewer target restrictions and simpler sample preparation (Swartz et al., 2005). Separation by LC-MS relies on the variation in chemical properties of individual metabolites within the sample; these properties determine that the molecules interact differentially with components of the chromatography apparatus, such that they require different amounts of time to pass through it (Dunn, 2011). The components in question are the mobile phase and the stationary phase. The mobile phase is effectively a dynamic solvent, into which the sample is entered, that then passes through the stationary phase and changes over time. The design of the progressive balance between the mobile phase's constituents, which typically progresses from a high concentration of one solvent to a high concentration of another, is referred to as a 'gradient'. The design typically depends on the stationary phase (the chromatography column itself), where selection of the gradient and column should reflect the chemical nature of the class of molecules. For example, the use of a reversed-phase (RP; Wilson et al., 2005;

Lenz et al., 2007) column prioritises the separation (i.e. the even spread of elution over time) of moderately polar to non-polar compounds and, for example, retains lipids better, while hydrophilic interaction LC (HILIC; Alpert, 1990; Hemstrom et al., 2006; Grumbach et al., 2004; Tolstikov et al., 2002; Spagou et al., 2010) columns are better suited for separation of very polar as well as non-polar molecules (Gika et al., 2008; Want et al., 2010b). Use of the former would typically indicate a gradient consisting of increasing organic (e.g. acetonitrile) and decreasing aqueous (water) content, while use of the latter would require the opposite. It is the varying adsorption of any given metabolite to the column in the dynamic chemical environment defined by the combination of the stationary and mobile phase that determines the time required for the molecule to pass through (the retention time) and thereby the separation of sample constituents. The growing popularity of LC-MS is largely a result of development in this stage of the analysis, wherein technological advances have progressively achieved smaller column particle sizes with more uniform packing and enabled the passage of samples through the column at higher pressures with greater efficiency, resolution and sensitivity. The methodological progression from LC-MS to high performance-LC (HPLC) to UPLC ultimately allows much faster chromatography with narrower chromatographic peaks which enhance peak concentrations and reduce ionisation suppression (see below) and signal-to-noise ratios (Wilson et al., 2005), all of which fundamentally translate to heightened sensitivity.

1.3.1.2 Ionisation

Following separation, the metabolites must be ionised for subsequent mass analysis. This is performed in a vacuum in GC-MS, wherein metabolites are either vaporised by thermal desorption and ionised by bombardment with electrons or ionised by chemical reaction in with reagent gas ions (Kopka, 2006; Want et al., 2010b). However, this is not possible with LC-MS as vaporisation of the liquid sample overwhelms the vacuum. While a vacuum is still required for the later stages of the analysis, metabolites are most commonly ionised at atmospheric pressure via the use of electrospray ionisation (ESI) before introduction into the vacuum within LC-MS (Dunn, 2011). The term electrospray refers to the process of dispersing a liquid as a fine aerosol; in ESI, it is applied as a means of ionisation and of delivering the analytes into the mass analyser (Yamashita et al., 1984). The atmospheric interface is held at a high temperature to evaporate the solvent within the aerosolised sample before the ions are delivered into the mass analyser (Metz et al., 2007). It is commonly referred to as a 'soft' ionisation technique for the characteristically low amount of fragmentation it induces. The ions formed either gain a hydrogen cation in positive mode ESI (ESI+) or lose a hydrogen nucleus in negative mode ESI (ESI-). It should therefore be noted that ESI only efficiently ionises molecules capable of this proton loss or gain, and is thereby dependent on their having acidic or basic functional groups (though no single ionisation method can optimally ionise every compound; Dunn, 2011). Just as samples can be chemically ionised in a vacuum within GC-MS, they can be chemically ionised at atmospheric pressure in LC-MS (Lee et al., 2003); while less common than ESI, atmospheric pressure chemical

ionisation (APCI) performs better in the analysis of non-polar and thermally stable neutral analytes such as lipids (Metz et al., 2007).

1.3.1.3 Mass Analysers

Following ionisation, molecules within the sample proceed to mass analysis. Mass analysers can be broadly categorised as low-mass resolution or high-mass resolution spectrometers. While either can be used for targeted metabolomics, wherein metabolites of pre-determined masses are detected, the former lacks the resolution to distinguish between co-eluting analytes of the same mass and are therefore unsuitable for global, exploratory metabolomics, wherein the analytes are scanned without bias (Dunn, 2011; Want et al., 2010b). The most common mass analyser, incorporated into low-mass and high-mass resolution systems alike, is the quadrupole. It is composed of four parallel metal rods; opposing rods are electrically coupled together and a radio frequency voltage is applied between one pair of rods and the other, such that only ionised metabolites of a particular mass-to-charge ratio (*m/z*) successfully pass through while others will veer off course and collide with the quadrupole (Hoffmann et al., 2003; Villas-Boas et al., 2007). Low-mass resolution systems can incorporate single quadrupoles, sets of three quadrupoles or quadrupole-ion trap combinations. Single quadrupole systems use the quadrupole simply as a mass filter prior to mass detection, while the three quadrupoles in a triple quadrupole system sequentially scan a pre-determined *m/z* ratio range, fragment the ion using a collision gas, then filter the collision products by their mass (Gross, 2004; Villas-Boas et al., 2007). They are particularly powerful in targeted analyses for their sensitivity and accuracy and are typically used for analyte quantification. Another low

mass-resolution approach to MS or MS/MS is the use of a quadrupole ion-trap mass analyser (March, 1997; Tolstikov et al., 2002). While the previously described application of quadrupoles operate on the continuous passage of ions, quadrupole ion traps apply their electrical fields to confine target ions within, such that they can be separated from others (which are ejected) and subsequently detected with or without collision fragmentation.

High-mass resolution instruments better suited for unbiased exploratory analyses include time of flight (TOF; Wang et al., 2003) or quadrupole-TOF (Q-TOF; Plumb et al., 2002; Lenz et al., 2004; Williams et al., 2005) systems which, while surpassed in resolution by Fourier transform ion cyclotron resonance (FTICR; Marshall et al., 1998) and Orbitrap (Hu et al., 2005) spectrometers, are the current mainstay of UPLC-MS. TOF MS determines an analyte's *m/z* ratio by the measure of time; the ion is accelerated by an electric field, travelling with a kinetic energy and velocity specific to its *m/z* ratio that is reflected in the time required for it to meet the mass detector (Dettmer et al., 2007). The function of the quadrupole in Q-TOF is to filter the target ion and to direct it into the collision cell, at which point the fragment *m/z* ratios are determined by the TOF component of the system (Gouveia et al., 2013). This enables simultaneous multivariate measurement across the entire mass range and demonstrates tandem mass spectrometry (MS/MS), wherein a molecule (the parent) is intentionally fragmented (into daughter ions) to quantify the analyte. The collision step, which is now typically performed with an octapole operating on the same principles as a quadrupole, generates a fragmentation profile containing specific *m/z* ratios and relative intensities which, in combination with the molecule's retention time, should be unique to a compound. These criteria can be compared

between a sample analyte and a separately analysed standard solution of its expected structural match to determine its identity. Mass analysis concludes with detection by a system such as an electron multiplier, at which point the *m/z* ratios and signal intensities are recorded and can be explored.

1.3.1.4 Data Analysis

MS generates highly multivariate, complex data which typically requires comparison between multiple individually analysed samples in biological contexts, for example, to identify changes in a tissue over time or in a pathological state. The first challenge to this is in processing the data, where comparing relative concentrations in different analyses relies on precise determination of its representation within each sample. This process, referred to as alignment, has to overcome the challenges presented by the presence of metabolite features sharing *m/z* ratios and the complexity of the data which, in addition to the parent and daughter ions, contains adducts, dimers and isotopes (Smith et al., 2006; Lange et al., 2008; Nielsen et al., 1998; Wang et al., 1987; Dunn, 2011). This, in addition to further processing functions such as filtration (e.g. excluding analytes only present in a certain percentage of samples or non-parent species; Jonsson et al., 2005) or normalisation (e.g. scaling gross measures of signal intensity to comparable ranges between samples for the removal of irrelevant variance; Sysi-Aho et al., 2007; Warrack et al., 2009; Lindon et al., 2001), can be controlled to varying degrees in different software packages made available either by manufacturers or as academic freeware such as XCMS (Smith et al., 2006) and MZmine 2 (Katajamaa et al., 2005; Pluskal et al., 2010). Following data treatment, the second analytical challenge is in the statistical identification of

metabolites discriminating between experimental groups. The multivariate nature of data generated via MS precludes the use of standard discrimination methods which calculate p-values under the assumption of low co-linearity (i.e. that the number of observations is greater than the number of variables). MS data analysis therefore requires multivariate analyses incorporating dimension reduction such as principal component analysis (PCA; Katajamaa et al., 2007; Jolliffe et al., 2016), which re-expresses the data as a set of linearly uncorrelated variables called principal components. This unsupervised approach indicates the presence of variance and structure within the data, meaning separation between variable groups exhibited in this unsupervised analysis can represent an experimental effect. PCA can then be followed by supervised PCA-related procedures such as partial least squares-discriminant analysis (PLS-DA; Jonsson et al., 2005; Worley et al., 2013), which quantify the contribution of individual metabolites to the separation and therefore the experimental effect. Such approaches are ideal for particular experimental designs, but do now allow for the incorporation of particular experimental factors such as linear temporal organisation of the data (Montana et al., 2011). Further, beyond preparing the data for statistical analysis of affected metabolites and executing it, structural elucidation is not complete until matching retention times and fragmentation profiles are confirmed by comparison between the analyte and a prepared standard solution of the compound. Structural elucidation therefore depends on the availability of information regarding that metabolite based on prior (experimental or theoretical) analyses for cross-reference. This is principally sourced from online databases such as HMDB (Wishart et al., 2013; Wishart et al., 2009) and Metlin (Smith et al., 2005) though, as a consequence of their relative youth, metabolomics databases are less comprehensive and well-annotated than those in

transcriptomics or proteomics (Want et al., 2010b). However, continuous use and investment in metabolomics drives the growth of these databases with every experiment and it is already an extremely powerful analytical tool. Indeed, the challenges metabolomics still face are collectively being progressively and continuously overcome with ongoing investment in the development of its technology and resources. As with the development of any revolutionary analytical platform, this is an exciting time; metabolomics has yet to be applied in many obvious yet novel biological contexts, such as in profiling the burn injury interstitium.

1.3.2 Metabolomics in Burns Research

Despite its general success as an analytical platform, metabolomics has been underutilised in burns research. To date, it has only been used in three studies and, as has been typical of other multivariate means of profiling complex molecular mixtures following burn injury, these have all evaluated systemic samples. Two analysed plasma; one identified the elevation of α-ketoisovaleric acid, 3-methylhistidine and β-hydroxybutyric acid via NMR in the early stages of severe human burn injury (Zhang et al., 2014), while another identified the post-burn elevation of trihydroxy cholanoic acid and uric acid in a 30% TBSA full thickness rodent model via UPLC-Q-TOF-MS (Liu et al., 2010). The third analysed human serum following a >15% TBSA burn (which is distinguished from plasma only by its containing clotting factors) and identified the burn-induced elevation of pyruvate, glycine, alanine, 3-hydroxybutyrate, glucose and lactate via NMR (Wearn, 2015). However, despite the viability of metabolomics for studying wounds (Forster et al., 2016), and despite the success of analysing both systemic (Finnerty et al., 2013;

Qian et al., 2010) and local (Pollins et al., 2007; Tan et al., 2015) burn injury samples via proteomics, metabolomics have not been used in the specific study of the burn site. Microdialysis may be a means of enabling this as, for example, metabolomic analysis of microdialysates has been successfully utilised in the study of peripheral inflammatory pathologies (Medina-Torres et al., 2015), muscle-based myalgia (Hadrevi et al., 2013), ischaemia (Povlsen et al., 2013), the central nervous system (Kao et al., 2015) and cancer (Wibom et al., 2010) though, even in this context, exploratory metabolomics has been seldom used. The potential for combining microdialysis and exploratory metabolomics for the elucidation of the extremely complex and little-understood signalling environment in burned tissue is clear.

1.4 Aims and Objectives

The hypothesis of this project is that the burn site is a complex, acutely temporally dynamic signalling environment characterised by the differential regulation of various interstitial pathological mediators, and thereby one that is suitable for exploratory analysis of localised samples. On this basis, the task was to perform the first multi-platform exploratory analysis of the burn tissue interstitium. The specific aims were to:

1. Establish the viability of microdialysis as a sampling method in burn injury
2. Analyse microdialysate fractions collected sequentially over the immediate acute phase of burn injury (0-3 hours) via multiplex immunoassays and exploratory (untargeted) metabolomics and lipidomics for the identification of burn-affected interstitial mediators with distinct temporal profiles
3. Prepare Next-Generation sequencing libraries for the microdialysis sites and their innervating DRG
4. Characterise the pathological significance of any novel up-regulated molecules via Ca^{2+} imaging- and electrophysiology-based *in vitro* study

2 CHAPTER 2 – EXPERIMENTAL TECHNIQUES AND PROTOCOLS

2.1 Animals

All procedures were performed in accordance with the UK Animals (Scientific Procedures) Act 1986, the revised National Institutes of Health Guide for the Care and Use of Laboratory Animals, Directive 2010/63/EU of the European Parliament and of the Council on the Protection of Animals Used for Scientific Purposes and the guidelines of the Committee for Research and Ethical Issues of IASP published in Pain, 16 (1983) 109-110. Further, Good Laboratory Practice and ARRIVE guidelines were observed. All procedures on animals were approved by veterinary services (Central Biological Services) at Imperial College London, UK. Every effort was taken to minimize the number of animals used. Male Sprague-Dawley rats (125-200 g) were housed in climate-controlled rooms, on a 12 h light/dark cycle and with food and water *ad libitum*.

2.2 Anaesthesia

General anaesthesia was induced with 1.5 g/kg urethane by i.p. injection. Prior to the initial anaesthetic injection, rats were sedated with 5% inhaled isoflurane to ensure smooth anaesthetic induction. Injections were performed with 25G needles, introduced at angles of 30°, between a third and half way up between the hind legs and the base of the ribcage. Slight negative pressure was applied to ensure the needle had not entered an organ or blood vessel; had this occurred, blood, urine or other matter rather than intraperitoneal air would be seen and the anaesthetic

preparation would be replaced. The initial anaesthetic doses were injected bilaterally, 1 cm either side of the midline, in order to aid systemic absorption of the initial urethane dose from the peritoneal cavity.

The depth of anaesthesia required for a 2 minute 60°C hind paw scald is beyond that of a typical surgical procedure, which is characterised by muscle relaxation, unconsciousness, loss of palpebral reflex and tail pinch response, maintenance of corneal reflex and normal to slightly decreased breathing and heart rates (Fish et al., 2008). The urethane dose used was its reported upper limit (according Imperial College London Central Biomedical Services and the manufacturer's protocol; U2500, Sigma) of 1.5 g/kg, in order to induce deep anaesthesia as determined by additional the loss of corneal reflex. After the injection of urethane, animals were placed in a comfortable position in a covered cage and noise was kept to a minimum to ease the induction of anaesthesia, which would typically require 10-40 minutes for loss of corneal reflex. Body temperature was monitored and maintained at 37°C with a heat blanket, rectal thermometer and homeothermic control unit (50-7061-F; Harvard Apparatus). Animals were terminally anaesthetised by intraperitoneal sodium pentobarbital (40 mg) and decapitated upon completion of microdialysis.

2.3 Burn Model

As described in Section 1.1.4.3, each burn model must be designed and validated in-house. The model used presently has previously been utilised by our group; the burn depth and spinal nociceptive processing induced were validated in mice (White et al., 2011) and, more recently, in rats undergoing the same procedure (data currently in

preparation for publication). The deep partial-thickness burn model was induced by submerging one hind paw in 60°C saline to the ankle for 2 minutes (NB: the probes withstand far higher temperatures than the 60°C of our model during sterilisation). The contralateral paw was simultaneously submerged in room temperature saline. The use of saline was motivated by the need to ensure that the burn solution was isotonic to the skin, preventing burn injury soup dilution, cell damage and hypotonicity-induced nociception (Alessandri-Haber et al., 2003). Submerging the paws in their respective solution was aided by the animal's suspension on a platform allowing easy access to their hind limbs for both experimental treatments and subsequent microdialysis. Practically, the treatment consisted of positioning 200 ml beakers of saline at the required temperatures beneath the platform. Burn depth was confirmed histologically following excision of the microdialysed region to a depth including subcutaneous tissue, which was divided and further used to evaluate probe depth and isolate RNA as described in their respective method descriptions below. The tissue used for histological analysis was stored in 1 ml 4% paraformaldehyde (PFA) at 4°C for 24 hours, before being moved to 30% sucrose in PBS with 0.01% sodium azide.

2.4 Microdialysis

Microdialysis probes were inserted prior to the burn in order to allow for two things: Firstly, a 20 minute equilibration period (ensuring steady flow, stabilisation of dead space and ultimately equal sampling from the subcutaneous interstitium between both microdialysis sites) which is discarded and, secondly, for a 30 minute collection of pre-burn "flush" microdialysate which is used for comparison of the pre-burn

metabolic profile (see Section 1.2.1 for an overview of the differences between, purposes of and considerations of designing equilibration and flush periods). All microdialysis was conducted using 400 μm 3 MDa cut-off microdialysis catheters (Dermal Dialysis, Erlanger, Germany) and a Model '22' syringe pump (Harvard Apparatus) perfusing Ringer's solution (Baxter, Northampton, UK) at 2 μl/min. After the induction of anaesthesia, probes were briefly perfused for lubrication and were then inserted into the dermis of the dorsal aspects of both hind paws, leaving the skin through an exit puncture with an active uptake distance of 10 mm via their attached 25 G needles, which were subsequently removed to expose the outlet for sample collection. The probe's depth, at the dermal border of the subcutaneous tissue, was validated following excision of the microdialysis site after the experiment. After probe insertion, the animal was carefully positioned on the microdialysis platform and the inlets of both microdialysis probes were attached to syringes of Ringer's solution fitted with 25G needles in the syringe pump. The probe was positioned such that the portion proximal to the active uptake site was entirely enclosed by the polypropylene tubing attached as part of the standard manufacturing process, and the probe length distal to the active uptake region was shortened to 2 cm. The probe outlets were positioned in tubes for collection of microdialysate, conducted for 0.5 hrs pre-burn, for collection of the above-described flush fraction, and then continuously for 3 hours post-burn. Over this 3 hours, microdialysates were divided into half hour fractions for time series analysis; each fraction was immediately stored on ice following conclusion of its collection, and complete microdialysate sets were stored at -80°C upon conclusion of the experiment. Individual fractions were consistently 50 μl in volume, as determined by their weight. It was at this stage that microdialysis sites were excised to verify probe depth after

the sacrifice of the animal as described above. Complete microdialysate sets were collected from 12 animals and divided into three groups of 4 sample sets for separate analyses by metabolomics, lipidomics and a multiplex cytokine immunoassay.

2.5 Metabolomics

2.5.1 Materials

Solvents for metabolite extraction from the microdialysate (LC-MS grade water and methanol) were obtained from Sigma (Gillingham, UK). Prepared samples were placed in Total Recovery Vials (Waters) for MS injection. The chromatography solvents used were water (LC-MS Chromasolv grade; Sigma) and methanol (LC-MS Chromasolv grade; Sigma) with a HSS T3 column (1.8 µm, 100 x 2.1 mm; Waters). Formic acid, leucine enkephalin and sodium formate were obtained from Sigma.

2.5.2 Sample Preparation

Sample preparation began with 1:3 dilution using -20°C methanol (MeOH) and vortexing for 20 seconds. The resulting 240 µl samples were then stored at -20°C for 20 minutes before being centrifuged for 10 minutes at 12000 x g for the removal of insoluble precipitates and protein. The supernatants were then placed in fresh eppendorfs and dried in a vacuum concentrator (Eppendorf Concentrator Plus 'Speed Vac') in V-AQ mode at 45°C for 2 hours. Dried samples were then

resuspended and sonicated in LC-MS grade water (Sigma) before being placed in Total Recovery Vials (Waters). Quality controls (QCs) were prepared by combining 5 µl from each sample.

2.5.3 UPLC-MS Analysis

UPLC was performed using an Acquity UPLC system (Waters) with a HSS T3 column (1.8 µm, 100 x 2.1 mm; Waters) coupled to a Synapt G2-S Q-ToF (Waters) operating in both positive (ESI+) and negative (ESI-) electrospray ionisation modes for metabolic profiling of four microdialysate sets. Chromatography was performed with a 5 µl injection volume at 40°C and a flow rate of 400 µl/min with solvents A) 0.1% formic acid in water and B) 0.1% formic acid in MeOH. The 12 minute gradient, including 2 mins of re-equilibration at the end, was structured as follows (and illustrated in Fig. 11c): 0-1 min, 1% B (hold); 1-3 mins, 1-15% B (linear); 3-6 mins, 15-50% B (linear); 6-9 mins, 50-95% B (linear); 9-10 mins, 95% B (hold); 10-10.1 mins, 1% B (linear), 10.1-12 mins, 1% B (hold). ESI+ and ESI- were both performed with a 30 V cone voltage, 120°C source temperature, 450°C desolvation temperature, 900 L/h desolvation gas flow and 50 L/h cone gas flow but with capillary voltages of 1 kV and -1 kV respectively. The Synapt was operated in sensitivity mode with acquisition between *m/z* 100-1200, a scan time of 0.1 s, an inter-scan delay of 0.01s and centroid mode data collection. Leucine enkephalin (MW 555.62; 200 pg/µl in 50:50 acetonitrile/water) was the LockSpray lock mass with an analyte-to-reference scan ratio of 10:1; lockmass scans were collected every 30 s and averaged over 3 scans to perform mass correction. Prior to the analysis, the instrument was calibrated using 0.5 mM sodium formate. To confirm that there

were no contaminants in the solvents or in the instrument, 5 consecutive injections of the LC-MS grade water and then the MeOH used during sample preparation were analysed. The quality control (QC), composed of 5 µl taken from every sample, was first used to condition the column with 10 consecutive injections, and then subsequently injected between every 10 sample injections to monitor system stability and effects of run time. This was executed by visual inspection of the PCA; QC measurements were not used formally for any recalculation. The sample run order was randomised.

2.5.4 Data Processing

Data was viewed and then exported from the MassLynx v4.1 (Waters) software package as two data sets, one for ESI+ and one for ESI- mode, which both required conversion to netCDF format using DataBridge within MassLynx v4.1 for use with the freeware XCMS Bentobox (Smith et al., 2006). XCMS detected peaks within these raw data using the centWave algorithm (Tautenhahn et al., 2008) with a 3-15 second peak width window and a 30 ppm mass accuracy window. A 0.1 *m/z* width was used for grouping. Prior to retention time (RT) correction, this employed a 10 second bandwidth; following RT correction, the bandwidth was determined by that feature's RT deviation profile. XCMS Bentobox ultimately produces a table of time-aligned features (with parent ions, isotopes, adducts and fragments listed as separate metabolite features), reporting their *m/z* ratio, retention time and signal intensity (as peak area) within each study sample and quality control sample. These data were normalised via median fold normalisation to control for any variation in overall sample concentration and underwent a variance-stabilising transformation to convert

multiplicative noise into additive noise (Veselkov et al., 2011); this scales the data by gross measures of signal intensity to comparable ranges, controlling for non-biological variance and thereby allowing for meaningful statistical comparison.

2.5.5 Statistical Analysis of Metabolomics Data

2.5.5.1 PCA and PLS-DA

XCMS Bentobox output was analysed in Simca P+ V. 13.0.3 (Umetrics) using Principal Component Analysis (PCA). Data underwent Pareto scaling (which scales the data such that the square root of the standard deviation is one for all metabolites) and a logarithmic transformation (10 log(peak height + 20)), which respectively adjust for differences in fold differences between metabolites and convert multiplicative relations into additive relations (van den Berg et al., 2006). Scores plots were used to examine the interrelationship or lack thereof between data grouped into 4 classes: QCs, pre-burn flush microdialysates (from both burn and control sites), burn microdialysates and control microdialysates. Upon recognising separation between the burn and control data, partial least squares discriminant-analysis (PLS-DA) was applied to identify the variables (metabolite features) underlying the difference via ranking of their variable influence on projection (VIP) values. Although PCA and PLS-DA were only used to identify a burn effect to confirm the viability of the sampling method, and hence metabolite features identified this way were not pursued in further analyses, whether or not a viable metabolite pool exhibiting a burn effect was present was assessed. In doing so, a VIP cut-off of 2< was selected.

2.5.5.2 CVA

We tested for effects of the burn using canonical variates analysis (as implemented in the SPM academic freeware) to find orthogonal mixtures of dependent variables, the metabolite signal intensities, that correlated with orthogonal mixtures of independent variables, the microdialysis site (with two levels: burn and control) and time (with seven levels: one pre-burn and six post burn levels). The effects of interest correspond to an interaction between microdialysis site and time, representing a difference in temporal profiles of a metabolite's concentration between the two microdialysis sites. Effects of time within each site were hence encoded as experimental factors, along with confounds as a constant term for each time series, within the design matrix. Fixed effects analysis pooling was used over the four animals and the effects of interest specified in terms of contrasts (linear mixtures of model parameters that contrasted the differences between burn and control sites at each time point). The significance of these effects was assessed with transformations of Wilks's Lambda expressed as multiple log p-values, representing the potential multidimensional dependency of the metabolite signal intensities on the independent variables. Each significant dimension represents a difference in temporal concentration profiles between burn and control microdialysis sites (a canonical variate) as exhibited by a corresponding subset of metabolites. The corresponding canonical vector expresses the contribution of each metabolite to that canonical correlation, with a higher value (i.e. a higher canonical weight) representing a greater contribution. Metabolites with high weights within the canonical vector hence exhibit the temporal profile defined by the canonical

correlation, and thereby the greatest effect of the burn site. Only metabolites among the top 5% following ranking by canonical weight were considered for structural elucidation, as is convention (and comparable to the arbitrary selection of a VIP threshold in PLS-DA). To ensure efficient parameter estimates, the dimensionality of the multivariate dependent variables was reduced to a quarter of the number of observations using singular value decomposition (after removing the effects of confounds and uninteresting experimental effects defined by the null space of the contrast matrix; see Fig. 9).

2.5.5.2.1 Executing CVA; Constructing the Batch Script

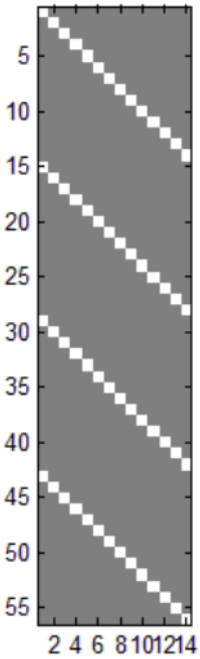
The analysis was conducted using MATLAB routines from the Statistical Parametric Mapping (SPM) 12b academic software (http://www.fil.ion.ucl.ac.uk/spm/). In practise, performing this analysis only requires knowledge of MATLAB syntax sufficient for constructing a batch script (written internally) that generates 4 matrices (required for **spm_CVA.m**), calls the required SPM routines and executes two other processes; random permutation of the data and the reporting and plotting of CVA output. Here, the execution of the batch script, presented below, is explained:

1. clear
2. X = kron(eye(2,2),eye(7,7)); % the effect of two sites measured seven times
3. X = kron(ones(4,1),X); % over four animals
4. X0 = kron(eye(8,8),ones(7,1)); % confounds are constants for each timeseries

Line 1 served to clear breakpoints from the current method; preventing any pauses placed in the script for the purposes of debugging from interfering in its execution. Executing the CVA routine required the input of 4 matrices; the first two were

generated between lines 2-4. These matrices, X and X0, contained the explanatory variables. Respectively, they encoded the experimental factors (i.e. effect of time for each site) and confounds (i.e. a constant term within each time series). The matrix X is called a design matrix. This specified the experimental design; here, the time point and experimental treatment (burn or control) over 56 rows, reflecting the organisation of data to be imported, as encoded by a 1 in the required column as opposed to a 0. As the experiment was conducted in 4 animals, each individual time point within each experimental condition (burn or control), of which there can be 14 as reflected by the number of columns, was repeated 4 times. Following the organisation of the data to be imported, 7 consecutively collected time point data from the burn site are followed by those of the control site within each diagonal of fourteen 1s with one diagonal per animal. Lines 2 and 3 generated this matrix, X, from two Kronecker Tensor products. The first, in line 2, incorporated two identity matrices, each representing one dependent variable (burn and control or time point; see Supplementary Material 4 for a demonstration of the use of Kronecker Tensor products and identity matrices). An identity matrix is a matrix with ones on the main diagonal and zeroes elsewhere; such a matrix with m rows and n columns is generated in Matlab via the syntax eye(m,n). Since the dependent variables had 2 and 7 levels presently, they were generated by eye(2,2) and eye(7,7) respectively. Hence, the output of line two is the Kronecker product of two identity matrices:

1	0	0	0	0	0	0	0	0	0	0	0	0	0
0	1	0	0	0	0	0	0	0	0	0	0	0	0
0	0	1	0	0	0	0	0	0	0	0	0	0	0
0	0	0	1	0	0	0	0	0	0	0	0	0	0
0	0	0	0	1	0	0	0	0	0	0	0	0	0
0	0	0	0	0	1	0	0	0	0	0	0	0	0
0	0	0	0	0	0	1	0	0	0	0	0	0	0
0	0	0	0	0	0	0	1	0	0	0	0	0	0
0	0	0	0	0	0	0	0	1	0	0	0	0	0
0	0	0	0	0	0	0	0	0	1	0	0	0	0
0	0	0	0	0	0	0	0	0	0	1	0	0	0
0	0	0	0	0	0	0	0	0	0	0	1	0	0
0	0	0	0	0	0	0	0	0	0	0	0	1	0
0	0	0	0	0	0	0	0	0	0	0	0	0	1



Line 3 generated another Kronecker Tensor product. Here, the *ones* function created a 4 x 1 array of ones, such that the Kronecker product is the above matrix repeated four times (for four animals). The result (where White = 1, Grey = 0 and Black = -1) is:

Figure 7 Design matrix X. This encodes the dependent variables (burn vs. control and microdialysate collection period) across 56 rows of data, as it is laid out in XCMS' output, as required by CVA as implemented in the SPM12 package. White = 1, Grey = 0.

The matrix X0 encoded experimental confounds as constant terms within each time series. It is therefore the Kronecker Tensor of an 8x8 identity matrix and a 7x1 vector of ones, and can be visualised as follows:

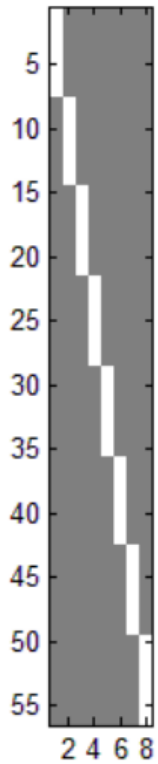


Figure 8 Matrix X0. This encodes experimental confounds as constant terms within each time series, as is required by CVA as implemented in the SPM12 package. Each column contains seven ones, reflecting the number of time points, and represents one time series among the eight analysed (two per animal x four animals). White = 1, Grey = 0.

This matrix X0 is used to project both the design matrix and data onto null space of confounding variables. In other words, confounding effects are removed from both the design matrix and data prior to canonical variates analysis.

```
5. data     = importdata('data.txt');
6. Y        = data.data;
7. MB       = data.textdata(1,:);
8. Y(1:2,:) = [];
```

The next matrix generated contained the data. These were arranged with single metabolites in columns with its measurements in every fraction over 56 rows (7 time points x 2 microdialysis sites x 4 animals = 56), as output from XCMS. Line 5 imported these data from a text file and line 6 defined its numerical values as variable matrix Y. Line 7 defined the first row of the text data within the imported file, the metabolite IDs, as a separate matrix MB. As the data were imported from raw XCMS output, the numerical component included two rows specifying each metabolite's median *m/z* ratio and median retention time. Line 8 removed these; they were not included in the CVA.

```
% for i = 1:size(Y,2)
%     for j = 1:(2*4)
%         k      = (1:7) + 7*(j - 1);
%         Y(k,i) = Y(k(randperm(7)),i);
%     end
% end
```

Lines 9-14 are an optional component of the script which serves to randomise the order of each metabolite's signal intensities within each time series. Performing CVA with random permutations of the data enable one to estimate the null distribution of any statistics (i.e. the distribution under the null hypothesis of no treatment effect). This can be useful to check that there have been no violations of distributional assumptions when using the analytic results for the p-values provided by CVA.

```
9.  Y   = log(Y);
```

Line 9 transformed the raw signal intensity values in matrix Y into their natural logs, as is typical for the conversion of multiplicative relations to additive relations when conditioning the influence of residuals within regression models.

```
10. c   = kron([1 -1],eye(7,7))';
```

In addition to the Y matrix (containing the data) and the X and X0 matrices of explanatory variables, the CVA script finally required a contrast matrix, c. This matrix specifies the effects to be tested for: in the present case, the interaction between microdialysis site and time. Here, burn and control data within these comparisons were respectively encoded by 1s and -1s. The contrast matrix *c* was constructed as a Kronecker Tensor product of an array simply containing a 1 and a -1 and a 7x7 identity matrix, and can be visualised as follows:

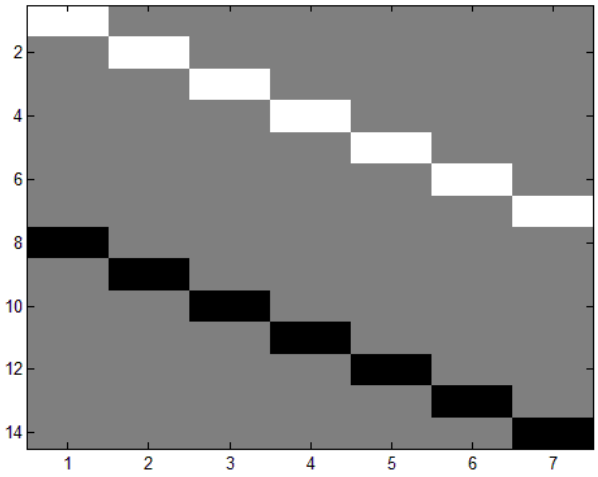


Figure 9 Contrast matrix c. This encodes the comparisons to be tested by CVA as those between time-matched burn (1s in the upper seven rows) and control data (-1s in the lower seven rows), as indicated within each column. White = 1, Grey = 0 and Black = -1.

The weights as specified in each column of the contrast matrix c were applied to the coefficients of the design matrix X. The control data in the eighth row, encoded as -1, were subtracted from the burn data in the first row, encoded as 1, as was the ninth from the second, and the tenth from the third etc. In doing so, the interesting subspace of the data was defined as any differences at any point in time between burn and control data, and anything else was determined to be uninteresting. This was the mixture of effects tested for using CVA.

```
11. CVA = spm_cva(Y,X,X0,c);
```

Having imported the data as matrix Y and having generated the design matrices X and X0 and the contrast matrix c, line 11 executed SPM12's CVA routine based on this input to perform the analysis.

```
12. spm_figure('GetWin','Figure 1'); clf

13. Xstr-1- = 'Dimensionality';
14. Xstr-2- = ['Chi-squared: ' sprintf('%6.1f ',  CVA.chi)];
15. Xstr-3- = ['           df: ' sprintf('%6.0f ',CVA.df) ];
16. subplot(2,2,1)
17. bar(log(CVA.p)); hold on
18. plot([0 (length(CVA.p) + 1)],log(0.05)*[1 1],'r:','LineWidth',4), hold off
19. xlabel(Xstr)
20. ylabel('log p-value')
21. axis square
22. title(-'Test of dimensionality';sprintf('minimum p = %.2e',min(CVA.p))-)
```

The remainder of the script plotted the results of the analysis, and in doing so highlighted the important elements of the output required for identifying interesting analytes within the metabolomics data. Line 12 generated an empty figure titled "Figure 1", while lines 13-15 set up strings (lists of characters in MATLAB) for values required for the subsequent plots. Namely, these were a chi squared distribution,

reflecting the amounts of variance explained, and the shape of the distribution as controlled by its degrees of freedom, which enabled computation of p-values. Lines 16-22 generated a plot of the log p-value for each dimensionality, where the response variables' dependency on the explanatory variables may be multi-dimensional. Each p-value was reported with its aforementioned chi squared statistic and degrees of freedom, where each p-value related to a different uncorrelated (orthogonal) mixture of differences in the data or, in other words, a different experimental effect, ranked in order of significance. In effect, the series of p-values tested for the dimensionality of the treatment effect by scoring the improbability of a canonical correlation between successive pairs of orthogonal mixtures. In other words, if two p-values are significant, the mapping between explanatory and response variables is (at least) two-dimensional. Practically, each p-value represented the significance of a different temporal profile that was conserved over the time courses of a subset of metabolites.

```
23. subplot(2,2,2)
24. plot(CVA.w,CVA.v,'.')
25. xlabel('prediction')
26. ylabel('response')
27. axis square
28. title('Canonical variates')
```

The second subplot, generated by lines 23-28, indicated the degree of correlation between the highest-correlating mixtures of explanatory (design) variables and response (data) variables. This allows one to visualise the correlation between mixtures of variables subtending the correlation whose significance is reported in the first subplot.

```
29. i   = 1;
30. str = 'first canonical contrast';
31. subplot(2,2,3)
32. est  = c'*CVA.C(:,i);
33. plot(est - est(1))
34. xlabel('Time')
35. ylabel('difference in trajectories')
36. axis square
37. axis([1,7,0,60])%i added this
38. title(str)
```

While a significant p-value and associated high canonical correlation in subplots 1 and 2 indicates a significant correlation between mixtures of explanatory and response variables, they do not tell us anything about the size, direction or relative contributions of individual metabolites within. The difference in burn and control data is represented rather by the canonical contrast (AKA canonical variate) which expresses the experimental effect that best explains the underlying significant canonical correlation, as reported by the CVA and plotted by lines 29-38. Line 29 defined the canonical contrast to be plotted as the first; in the event of multiple significant canonical correlations, i is increased accordingly for multiple contrast plots.

```
39. i       = find(CVA.p < 0.05);
40. t       = 1:7;
41. str     = 'Significant canonical vectors';
42. if isempty(i)
43.     i   = 1;
44.     str = 'first canonical contrast';
45. end
46. subplot(2,2,4)
47. hist(CVA.V(:,i),64)
48. xlabel('canonical weight')
49. ylabel('frequency')
50. axis square
51. title(str)
```

Having identified any significant canonical correlations (subplots 1 and 2) and their representative canonical contrasts (subplot 3); lines 39-51 plotted the distribution of metabolite contributions to the canonical correlation as a histogram. The metabolite contributions to a single canonical correlation and contrast, and thereby their similarity to the temporal profile, was quantified in a canonical vector composed of the canonical weights of individual metabolites; a higher weight reflects a greater contribution to the experimental effect. The skew of the canonical weights in the histogram suggests that a small number of metabolites contribute heavily to the treatment effect (site by time interaction), while a large number of metabolites contribute negligibly. This is important because it suggests the treatment effect is mediated in a relatively sparse fashion, engaging a relatively small number of metabolites. This provided a principled way to rank metabolites by their contribution to significant canonical correlations, i.e. the extent to which they exhibit an effect of the burn. To this end, their values could be compared with VIP values within PLS-DA.

2.5.6 Structural Elucidation

The *m/z* measurements of metabolite features exhibiting a burn-induced increase in concentration as determined by CVA were screened for parent ions by excluding isotopes, adducts and fragments among feature groups with a shared retention time (where such related features share a retention time reflecting the elution of their shared parent structure). Practically, executing this process manually involved ranking all metabolites contributing to this significant burn effect by retention time, grouping those with similar temporal profiles, and delineating the relationships

between the features within by the differences between their *m/z* ratios. From the suspected parents identified in this process, candidates for structural elucidation via tandem mass spectrometry (MS/MS) were then selected on the bases of signal and VIP strength and/or matching the molecular weights of interesting compounds potentially implicated in burn pathology. To determine features meeting the latter criteria, the HMDB (Wishart et al., 2013; Wishart et al., 2009) and Metlin (Smith et al., 2005) metabolomics databases were searched for the *m/z* measurements and returned ranked candidate structures.

2.5.6.1 Tandem Mass Spectrometry (MS/MS)

In order to gain more insight into the structure of the identified burn-elevated metabolite features, such that they may be compared with the profiles of known analytes, the microdialysates were re-analysed with intentional fragmentation of these metabolites features through the use of tandem mass spectrometry (MS/MS). MS/MS was performed using the same Acquity UPLC system (Waters) with a HSS T3 column (1.8 µm, 100 x 2.1 mm; Waters) coupled to a Synapt G2-S Q-ToF (Waters). Chromatographic and MS source parameters were the same as for the MS experiments in order to replicate the previously established RTs; however, a collision energy ramp of 10 - 40V was employed as standard. This was sufficient for fragmentation of all but one target metabolite, for which the collision energy ramp was subsequently extended from 10 - 50V, as described in the results. The fragmentation profiles obtained for each feature were compared with those available in the above metabolomics databases for entries with matching *m/z* measurements, or with profiles otherwise reported in publications.

Features with profiles matching the fragmentation of molecules in databases or previous publications underwent a final MS/MS analysis, with each sample analysis being immediately followed by injection of a prepared standard of the proposed compound under identical UPLC-MS/MS conditions. *m/z* measurement, chromatographic retention time and fragmentation profiles between the feature within the sample and its respective standard solution were then compared to confirm or rule out the feature's suspected molecular structure.

All standards for structural elucidation with MS/MS were purchased at the highest cost-effective purity possible. The standards for the seven metabolite features reaching this stage of the structural elucidation process were LPC(14:0), LPC(16:0), LPC(18:0) (85575P, 855675P and 855775P respectively; powder, >99% purity, Avanti Biolipids), niacinamide (72340, powder, >99.5% purity, Sigma) uric acid (U0881, powder, >99% purity, Sigma), arachidonic acid (10931, liquid, >95% purity, Sigma) and hypoxanthine (122010050, powder, >99.5% purity, ACROS Organics). For injection as a UPLC-MS/MS standard, each was prepared in a stock solution of 1 mg/ml before being diluted for the injection concentration of 10 µg/ml. The powdered standard preparations had different dissolution requirements (though all solvents used were MS-grade). The three LPC species and arachidonic acid required 50:50 water/MeOH, niacinamide only required water and uric acid and hypoxanthine required 1M NaOH. In order to minimise the NaOH concentration of the solvent, as NaOH is a strong base and pH changes might alter the analyte's RT, 150 mg of each was dissolved in as little NaOH as possible (6 ml for uric acid and 1.5 ml for hypoxanthine), before adding water to 15 ml for a 10 mg/ml preparation and

subsequent 10x dilution with water of an aliquot to the required 1 mg/ml stock solution. 5 µl aliquots of each standard stock solution were diluted in 495 µl of water for the 10 µg/ml injection standard solutions.

2.6 Lipidomics

The lipidomic analysis of microdialysate (which features only very briefly in this report; see Fig. 25) was conducted externally by Dr. Tim Marczylo of the Health Protection Research Unit within the National Institute for Health Research. Briefly, sample preparation began with protein precipitation, as it did with the metabolomics, though the methodology varied slightly to prioritise the recovery of lipids. 300 µl MeOH was added to each microdialysate fraction, followed by 1 ml methyl *tert*-butyl ether (MTBE; an organic solvent) and 312.5 µl water for phase separation. This mixture was incubated at room temperature for 10 minutes before centrifuging at 1000 x g for a further 10 minutes to remove protein. Unlike in the metabolomics sample preparation, only the upper (organic) layer of the supernatant was subsequently collected. In order to increase absolute recovery, the same extraction protocol was repeated on the remaining lower phase of the supernatant in 800 µl MTBE:MeOH:H_2O (10:3:2.5). Both extracts were combined before drying in a vacuum concentrator (Eppendorf Concentrator Plus 'Speed Vac') in V-AQ (for aqueous solution) mode at 45°C for 2.5 hours. Extracts were then resuspended in 20 µl 1:1 ACN:IPA (isopropyl alcohol).

For analysis, chromatography and mass spectrometry were conducted with an Ultimate 3000 Quaternary RSLC UHLPC system in line with a Q-Exactive Plus

Orbitrap Mass Spectrometer (Thermo). 5 µl of sample was injected onto an Accucore C_{18} 2.1 x 100 mm column with a solvent flow rate of 400 µl/min and a column temperature of 55°C. Solvent A consisted of 10mM $HCOONH_4$ in 50% ACN with 0.1% formic acid and solvent B consisted of 2mM HCOONH4 in ACN:IPA:H_2O (10:88:2) with 0.02% formic acid. The gradient was as follows: 0-6 min, 22-60% A (linear); 6-14 min, 60-85% A (linear); 14-23 min, 85-100% B (linear); 23-26 min, 100% A (hold); 26-26.1 min, 100-22% A (linear); 26.1-30 min, 22% A (hold). Data were aligned and assigned structural identities by LipidSearch (Thermo), the lipidomics platform for this UPLC-MS system, using both MS and MS/MS fragmentation data.

2.7 Cytokine Panels

The concentrations of 27 cytokines were measured in duplicate in each microdialysate fraction within four microdialysate sets using the FlexMAP 3D (Luminex) platform with xPONENT 4.2 plate reading Software (Luminex) and a Milliplex Rat Cytokine/Chemokine panel (RECYMAG65K27PMX; Merck Millipore) according to the manufacturer's protocol, briefly described here. This particular pre-prepared assay was selected for its competitive coverage among similar technologies (with 27 analytes) and what was, at the time, inclusion of every inflammatory antibody available for the FlexMAP 3D platform. The FlexMAP 3D system operates using colour-coded microspheres (beads) dyed with precise portions of both red and infrared fluorophores. This balance of dyes dictates the

bead's spectral signature, of which there can be up to 100 in a single assay. In the assay used presently, there were 27 spectral signatures corresponding with 27 chemokines/cytokines. Monoclonal antibodies against each cytokine were conjugated to beads with dyed that cytokine's respective spectral signature, allowing measurement of the concentrations of multiple analytes from a single mixed sample. This is accomplished via single file processing of the beads by flow cytometry; they simultaneously pass through a 635 nm solid state laser, which determines the bead's spectral signature (and further rules out bead aggregation) and hence the cytokine it measures, and a 532 nm laser which determines the signal strength corresponding with antibody binding and hence cytokine concentration.

Samples were prepared for this analysis by 2x dilution in Ringer's solution, both according to the manufacturer's protocol and further allowing elevation of the sample volume to an amount compatible with the assay. Along with the sample, background samples (consisting of Assay Buffer), two quality controls provided with the kit and seven serially-diluted standards were analysed; the first two confirm the reliability of the system and the standards allows for the generation of standard curves from which sample concentrations can be determined. All wells were analysed in duplicate, and a single dry well in each plate was used for probe height calibration. The plates were washed using 200 µl Assay Buffer with agitation before addition of 25 µl volumes of Assay Buffer (background), quality controls and standards to their respective wells. 25 µl of Ringer's solution was added to all background, quality control and standard wells in order to ensure that any effects of the Ringer's solution on the sample readings were induced equally across the analysis. To make up the volume in the sample wells, 25 µl of Assay Buffer was added. The beads, detection

antibodies, streptavidinphcoerythrin and sheath fluid were then added to all wells with required incubation and washing (by agitation) periods as described by the manufacturer's protocol before the plates were analysed.

2.7.1 Statistical Analysis

All data are expressed as means ± S.E.M. 16 cytokines, for which fewer than 20% of duplicate recordings over all animals were detectible, experimental conditions and time points were excluded from the analysis. For the remaining 11 cytokines, undetectable concentration means falling below the assay's minimum detectible concentration (i.e. the lowest expected concentration entered while generating the polynomial for the standard curve) were reassigned to the lower of either the lowest value recorded or the lower detection threshold, as reported by the plate reading xPONENT Software (Ver. 4.2 for FLEXMAP 3D Technology). In order to avoid introducing heteroscedasticity during this process, variance within each condition was calculated and applied to any reassigned data around the required mean. A single outlier was detected in the Eotaxin control pre-burn flush data by Grubb's test (maximum normed residual test) and was subsequently removed. Comparisons between burn and control cytokine concentrations were analysed by two-way analysis of variance (2-way ANOVA; Treatment [Burn or Control] x Time [Pre-burn or Post-burn]) on log transformed data. The Benjamini-Hochberg procedure (Benjamini et al., 1995) was used to adjust p-values for multiple testing correction. Significance was set at $P < 0.05$ following false discovery rate (FDR)-correction. Two-way ANOVAs and Grubb's tests were performed with Origin 9.1 and the Benjamini-Hochberg procedure was performed in Matlab R2014a.

2.8 Gene Sequencing

2.8.1 RNA Isolation

RNA was isolated from both the skin of the microdialysate site and the DRG at spinal levels L4 and L5 in order to genotype the local burn-affected signalling environment and its peripheral innervation. Each tissue type required a different isolation kit and protocol, due to the comparative structure and anticipated RNA yield of fibrous skin tissue and soft nervous tissue.

Skin from both burn and control microdialysate sites, including the depth of the subcutaneous tissue, was excised following the sacrifice of the animal and stored in RNAlater (Qiagen) at -80°C. The excised region was that spanning the metatarsals including subcutaneous tissue. The portion of excised tissue from which RNA was isolated (where the other half was used for validation of microdialysis probe and burn depth) typically weighed 130-150 mg. Oedema resulting from the burn increased the weight of tissue excised from the burn site, but this would not affect RNA quantification following normalisation to the expression of housekeeping genes such as glyceraldehyde 3-phosphate dehydrogenase (GAPDH). RNA was isolated from this tissue with both Midi (75742, Qiagen) and Mini (74704, Qiagen) RNeasy Fibrous Tissue Kits largely according to the manufacturers protocols (which differed only in scale), where discontinuation of the Midi-scale kit necessitated use of the Mini kit. Briefly, the maximum tissue mass possible, as required by skin's low RNA yield but restricted by the RNA binding capacity of the RNeasy spin column and the functional capacity of the lysis buffer, was processed. This equated to the entirety of the tissue

collected for RNA isolation with the Midi kit (which never exceeded 250 mg) and 30 mg for the Mini kit. The tissue was cut into 5-10 mg portions with micro-scissors before disruption and homogenisation with a rotor-stator homogeniser (Kinematica AG) in 2 ml/1ml (Midi/Mini) of lysis buffer. It was then diluted 3x in RNase-free water before adding 65µl/10µl of the protease Proteinase K (named for its breakdown of keratin, fibrous structural proteins), in the defining step of this kit's specialised application to fibrous tissue, and incubating at 55°C for 20/10 minutes. Remaining solid tissue and precipitates were then removed by centrifuging (2000/8400 x g, 5/3 min, RT) before lysates were diluted (1.5x) in EtOH and centrifuged three times (2000/8400 x g, 5/3 min, RT) through the RNeasy spin column for the binding of total RNA. Following DNase I digestion, washing (with buffers RW1 and RPE) and drying of the membrane, the RNA was eluted from the column twice in the same volume of RNase-free water to prioritise RNA concentration over volume.

DRG from both the burn and control sides of levels L4 and L5 (as identified by their position relative to the lowest rib), those innervating the hind paws, were excised and stored in RNAlater (Qiagen) at -80°C. Unlike the skin, this tissue could be used for gene sequencing in its entirety. However, due to the size of rat DRG and the need to sample exclusively from those innervating the microdialysis sites, each animal would yield only 10 mg of tissue from which RNA could be isolated. RNA was isolated from DRG with the RNeasy Plus Mini Kit (74134, Qiagen) according to the manufacturer's protocol. Briefly, all tissue was used as restrictions imposed by the DNA removal capacity of the gDNA spin column, the RNA binding capacity of the RNeasy spin column and the functional capacity of the lysis buffer do not apply to such low sample masses. Like the skin, DRG were disrupted and homogenised with a rotor-

stator homogeniser (Kinematica AG) and QIAshredder column (centrifuged at 8400 x g for 2 minutes) in 600 µl of lysis buffer. Solid tissue and precipitates were removed by centrifuging in a polypropylene tube (8400 x g, 3 minutes) and disposal of the pellet. The supernatant was spun through a gDNA elimination column (8400 x g, 30 seconds) before 2x dilution of the flow-through with 70% RNA-grade EtOH. The resulting RNA was centrifuged through the RNeasy spin column for the binding of total RNA in two aliquots. Following washing (with buffers RW1 and RPE) and drying of the membrane, the RNA was eluted from the column either twice in the same 30 µl volume of RNase-free water to prioritise RNA concentration over volume, or in two separate 30 µl volumes to be pooled for greater absolute recovery.

Total amounts of isolated RNA were quantified with a BioPhotometer (Eppendorf) at a 1:50 dilution; 2 µl of RNA suspension in 98 µl double distilled water (ddH_2O). Final elution volumes varied over the course of the project, as did RNA yields. These are reported in Chapter 3. While RNA purities reported in these analyses were noted, as indicated by A_{260}/A_{280} ratios, the quality of the RNA was ultimately determined and used for sample selection by Vienna Biocenter Core Facilities, who used the isolated RNA to perform the transcriptomic analyses in this project.

2.8.2 Next-Generation Sequencing Library Preparation

Following isolation of the RNA and their delivery to Vienna Biocenter Core Facilities, I played no further part in the gene sequencing and library preparation. In brief, Next-Generation sequencing libraries were prepared from the RNA samples I supplied by poly-A enrichment (New England Biolabs, USA), enriching mRNA and removing

ribosomal RNA (Zhao et al., 2014), using the manufacturer's instructions. The samples were sequenced with HiSeq2000 on two lanes using single-end sequencing with 50bp read length. A description of the workflow within this externally conducted process, to the level required for my interpreting the data, is described here.

Firstly, it is required that the transcriptome sequence reads are aligned with those of the reference genome. Reads were obtained with the HiSeq2500 using single-end sequencing with 50bp read length, with each sample sequenced in one run multiplexed on two lanes. These reads were base called using the HiSeq2500's coupled control software (Illumina), and reads aligning to ribosomal reads were filtered out. Remaining reads were aligned against the Rattus norvegicus genome (Ensembl Rnor 5.0 assembly) using TopHat v2.0.9 (Kim et al., 2013). The reads could then be associated with known genes based on annotations defined in the Ensembl rat genome, and number of reads for each gene could be counted with HTSeq tool version 0.5.4p3. These read counts were normalised in order to remove nonbiologically-derived variance in the data, allowing comparisons to be made between burn and control samples. This was executed using TMM normalisation as implemented in the edgeR R/Bioconductor package (R v3.0.1, Bioconductor v2.12), which defines sample-specific scaling factors from the variable number of total reads across samples.

The quality of this normalised data was evaluated by inspection of the expression distribution both between and within all samples, where expression over all samples should reflect the specificity of the tissue type and large variations in expression value distributions between samples may indicate issues with the RNA preparation

or analysis, where the earlier-applied normalisation should compensate for reasonable variance such that read counts of single genes can be compared on the same scale. Having established that overall expression distributions are sufficiently similar between samples, relationships within (and differences between) samples grouped by tissue type and experimental treatment are evaluated by means of Spearman's metrics and PCA. Data from within the same tissue and treatment groups should correlate well, while treatment effects may be indicated by separation between them.

Having evaluated the quality of the data, statistical comparisons were made to detect genes expressed differentially between burn and control samples in both the skin and DRG. These comparisons were performed with the R package Limma (Ritchie et al., 2015), which operates by generating gene-specific linear models (reportedly giving more reliable estimation of group average expression than simple arithmetic mean), using least-squares regression to identify the linear model with minimal sum of square errors. Modified t-test p-values are generated according to contrasts in these models between the tested sample groups, where the smallest p-values represent maximal difference between and minimal variance within sample groups. To address the multiple comparisons problem, as the library is so highly multivariate, p-values underwent FDR adjustment (as did those of the cytokine data) to control for the rate of false positive findings. The differentially expressed genes, as provided to us by Vienna Biocenter Core Facilities, were ranked by significance as determined by fold change in concentration and FDR-adjusted p-value. Overall differential expression of genes between burn and control samples could be evaluated by means of a heatmap visualising hierarchical clustering based on overall expression

measurement similarity, indicating overall differences between sample groups, and individual measurements of the underlying differentially expressed genes (one per row) over all samples (one per column). Having established that there is an effect induced by the treatment via these means, the significance-ranked differentially expressed genes can be explored and their functional implication in burn pathology considered. Finally, enrichment analyses were used to detect alterations in significant portions of functionally-associated gene networks. Here, these analyses were conducted against the most conventionally used Gene Ontology (GO) and Kyoto Encyclopaedia of Genes and Genomes (KEGG) databases, where the former organises genes by hierarchies based on their involvement in biological processes, molecular functions and cellular components and the latter defines pathways for biological interactions. Analyses testing for the representation of genes within a GO term or KEGG pathway were performed with the topGO and GOstats packages within R/Bioconductor. These were expressed visually with colour-coding of represented up- and down-regulated genes within the mapped pathways for KEGG matches.

2.9 Tissue Sectioning and Histology

Skin tissue specifically set aside for histological analysis was removed from storage in 30% sucrose, splayed out for sagittal sectioning and immersed in Optimal Cutting Temperature compound (OCT) before freezing. The cryostat was equilibrated from 30 to 14 μm upon emergence of the tissue within the OCT and was operated without an anti-roll bar as this damaged the skin tissue; sections were manually held flat to

the blade with a soft paint brush during cutting and subsequently positioned on polarised microscope slides.

For haematoxylin and eosin staining, sections were washed in distilled H_2O before 6 minutes of room temperature incubation in Harris Haematoxylin (HHS-32; Sigma). After another wash, they were counterstained in 1% Aqueous Eosin (Raymond A Lamb Ltd.) for 15 seconds before a final wash. The tissue was then sequentially dehydrated in 50%, 75%, 90% and 100% EtOH for 5 minutes each. Surplus dye was cleared with Histo-Clear II in two 5 minute washes before the slides were mounted in DPX Mountant (Sigma).

2.10 Cell Culture

2.10.1 DRG Primary Culture

DRG from the first cervical to the first sacral levels were collected from terminally anaesthetised male Sprague-Dawley rats (125-200 g) and stored in DMEM/F12 (Sigma) on ice. The tissue was then incubated at 37°C in 0.125% collagenase (Lorne Diagnostics) for 3 hours, and subsequently 0.05% trypsin-EDTA (Thermo) for 5 minutes, before being triturated and centrifuged at 200 x g atop a 1 ml cushion of bovine serum albumin (BSA; Sigma) for removal of debris. The pellet was resuspended and plated in DMEM (Sigma) supplemented with 50 IU/ml penicillin (Invitrogen), 50 µg/ml streptomycin, 2% Ultroser G (Pall France, St-Germain-en-Laye, Cedex France), 2 mM L-glutamine (Invitrogen) and 50 ng/ml nerve growth factor (Murine 2.5S; Promega) and on poly-DL-ornithine (Sigma)-coated glass

coverslips. Cells were cultured for 1 day at 37°C with 5% carbon dioxide prior to experiments.

2.10.2 HEK293T Cell Culture

HEK293T cells were grown at 37°C and 5% carbon dioxide on Nunclon surface 60 mm culture dishes in HEK293T growth medium (DMEM (Sigma) supplemented with 2% FBS (Sigma), 50 IU/ml penicillin (Invitrogen), 50 µg/ml streptomycin and 2 mM L-glutamine (Invitrogen)) and were passaged before reaching full confluency. Prior to experiments, HEK293T cells were seeded to poly-DL-ornithine (Sigma)-coated glass coverslips. Cells requiring transfection were allowed to attach for 8 hours before co-transfection using PLUS Reagent (Invitrogen) in conjunction with Lipofectamine 2000 (Invitrogen; see below for full transfection protocol). Cells were allowed to stabilise for at least 20 hours before use in experiments. The specifics of other techniques required for culture maintenance and experimental preparation are described below.

2.10.3 Thawing, Passaging and Storage

Following removal from cryostorage, cells were immediately warmed to 37°C and placed in a 15 ml Falcon tube, to which a further 4 ml of warmed HEK293T growth medium was slowly added. The suspension was centrifuged at 200 x g for 3 minutes and the pellet resuspended in 4 ml HEK293T growth medium before plating in its entirety on Nunclon Surface 60 mm culture dishes (Thermo) and incubation at 37°C, 5% CO_2. This preparation would require 24 hours to reach confluency.

HEK293T cells were seeded into fresh 60 mm culture dishes at 90% for general culture maintenance. The cells were washed in PBS twice to remove FBS before a 1 minute incubation in 2 ml 0.05% Trypsin-EDTA at 37°C. Cells were gently aspirated for easy removal and immediately added to 3 ml HEK293T growth medium (containing FBS). The cell suspension was centrifuged for 3 minutes at 200 x g and the pellet was resuspended in 4 ml fresh HEK293T growth medium. Cells were passaged into two new 60 mm culture dishes at ratios of 1:20 and 1:40, which would reach near-confluency after 3 and 4 days respectively. Cells were discarded upon reaching their 20th passage.

Surplus cells of low passage number obtained during seeding were stored in liquid nitrogen to retain the lab's stock of HEK293T cells. Cell counts within the suspensions from which cells are passaged as described above were determined with a haemocytometer, such that cryovials containing 1x10^{6} cells in 1.5 ml of freezing medium (70% HEK293T growth medium, 20% FBS, 10% DMSO (Sigma)) could be prepared. Cells to be frozen were sequentially stored at 4°C for 20 minutes, -20°C for 15 minutes and -80°C overnight before storage in the vapour phase of liquid nitrogen. Cells were stored no later than their 12th passage, given that the experimental use of cells within their first 2 passages following thawing was avoided and that cells were discarded on their 20th passage.

2.10.4 Plasmid Amplification

Amplifying the TRPV1 plasmid incorporating the high copy, ampicillin-resistant pcDNA3.1/V5-His-TOPO vector was a four day process. Lysogeny broth (LB) agar

plates were prepared on the first day. Miller's LB agar (Sigma) was suspended in distilled water at 40 g/l on a heated bar magnet stirrer before autoclaving both this and a 10 ml 30% glycerol preparation for 15 minute at 121°C. After autoclaving, the agar's temperature was maintained at 55°c to maintain its fluidity, such that 100 µg/ml ampicillin (Sigma) could be added and vortexed by hand. The preparation was then cooled to 50°C and distributed into 10 cm petri dishes at 20 ml/ dish. Plates were left to set overnight, having been inverted after 1 hour. Those not needed were sealed with parafilm and stored at 4°C for later use.

On day two, Subcloning-Efficiency DH5α Competent *E. coli* were thawed from -80°C on wet ice for 25 minutes before light mixing and division into two 50 µl aliquots. 5 µl of 2 ng/µl TRPV1 plasmid was added to the first, and 2.5 µl (250 pg) of pUC19 control (ampicillin-resistant) DNA to the second. Both were incubated on ice for 30 minutes before a 20 second heat shock at 42°C, after which they were immediately placed back on ice for 2 minutes. 950 µl pre-warmed Miller's LB medium was then added to each *E. coli* preparation before an hour of incubation at 37°C with 225 RPM agitation. Between 20 and 200 µl of both transformations were spread on the earlier-prepared selective plates before being covered loosely in foil and incubated upside-down overnight at 37°C.

On day three, colonies were selected on the quality of their formation as an indicator of successful *E. coli* transformation conferring ampicillin resistance, as colonies that are not well-rounded and smooth-edged may consist of untransformed *E. coli* growing in regions of depleted antibiotics. Such growth was noted from both the TRPV1 plasmid and the pUC19 control, indicating successful transformation. 2-3

well-formed colonies were selected from the TRPV1 plasmid plates with a sterile pipette tip and placed in 3 ml pre-warmed LB medium with 100 µg/ml ampicillin. This preparation was incubated at 37°C with 225 RPM agitation for 6 hours, such that it grew cloudy with the growth of *E. coli*. 500 µl of the suspension was mixed with 500 µl sterile 30% glycerol and frozen at -80°C to serve as a glycerol stock for later use. 200 µl of the remaining *E. coli* suspension was added to 150 ml pre-warmed LB-ampicillin in a 500 ml flask before being covered with foil and incubation at 37°C with 130 RPM agitation overnight.

Day four consisted of following the manufacturer's protocol for the HiSpeed Maxi Plasmid Purification Kit (Qiagen) for collection of the amplified plasmid. Briefly, the *E. coli* were harvested from their 150 ml suspension by centrifuging at 2500 x g for 30 mins at 4°C in four 50 ml falcon tubes. Using a centrifuge only capable of 2500 x g with 50 ml falcon tubes, while the protocol required 6000 x g, the duration was doubled. Pellets were then completely resuspended in 10 ml Buffer P1 with RNase A prior to addition of 10 ml Buffer P2 for lysis over 5 minutes at room temperature. 10 ml chilled Buffer P3 was then added to neutralise the solution in causing potassium dodecyl sulphate to precipitate, such that denatured proteins, chromosomal DNA and cellular debris become trapped in salt–detergent complexes while plasmid DNA remains in the solution. The lysate was then placed in a QIAfilter Cartridge for 10 minutes at room temperature with the outlet sealed, such that the precipitates would rise to the surface prior to filtration. After this period, the outlet was opened and a plunger used to filter the lysate through the cartridge directly into an equilibrated HiSpeed Maxi Tip, in which the lysate was allowed to passively filter into the resin by gravity flow. After washing with Buffer QC, DNA was eluted with 15 ml Buffer QF and

precipitated from this flow through using isopropanol. The eluate/isopropanol mixture was then filtered through a QIAprecipitator Maxi Module under constant pressure for the collection of DNA before washing with 70% EtOH and drying by the passage of air twice. The DNA was finally eluted in two passes of 1 ml Buffer TE before quantification by OD_{260}.

2.10.5 Transfection

Passaging, transfection and experiments were all conducted on a strict schedule, given the influence of cell density on the availability of LPC discussed in Chapter 7. Cells for experiments were passaged to poly-DL-ornithine-coated glass coverslips concomitantly while passaging for culture maintenance, as described above. The required amount of the 4 ml cell suspension (containing the cellular content of a 90% confluent 60 mm culture dish) was diluted 10x in HEK293T growth medium and divided plated at 500 µl/well. Following 9 hours of incubation at 37°C 5% CO_2, allowing for coverslip adhesion, these cells were transfected for experimentation the next day. This schedule generated cultures of sufficient cell count for high data yields with calcium imaging while maintaining cell separation ideal for avoiding the formation of networks and high transfection efficiency.

Transfection was conducted with the aid of the Thermo's Lipofectamine 2000/ Plus Reagent optimisation system according to the manufacturer's protocol. Briefly, for each well, 0.2 µg of TRPV1 and eGFP cDNA was incubated with 1 µl Plus Reagent in 25 µl DMEM for 15 minutes at RT. This preparation was then incubated with a further 25 µl DMEM containing 1 µl of Lipofectamine 2000 per well for another 15

minutes, during which the HEK293T growth medium in the wells of cells to be transfected was replaced with 200 µl DMEM per well. 50 µl of the transfection preparation was then added to each well and left overnight before use in experiments.

2.11 Calcium Imaging

Intracellular Ca^{2+} measurements were obtained with the ratiometric fluorescent dye Fura-2 AM. HEK293T and DRG cells were loaded with 100 nM Fura-2 AM (Sigma) for 20 minutes before being washed with extracellular buffer (in mM: NaCl 150, KCl 5, $MgCl_2$ 2, $CaCl_2$ 2, HEPES 10, glucose 10; pH corrected to 7.4 with NaOH). Images were recorded using an optiMOS Scientific CMOS Camera (QImaging) mounted to a Nikon Eclipse TE300 microscope and acquired with Winfluor (v3.7.3) ratiometric fluorescence imaging academic freeware (University of Strathclyde). Images were captured every 2 seconds throughout the experiment, with Fura-2 doubly excited at 355 nm and 380 nm and emissions recorded at 510 nm. Changes in intracellular Ca^{2+} concentrations are reported as the ratio of these intensities, F350/380, following background subtraction. All solutions were applied via a gravity flow perfusion system. Capsaicin was applied at varying concentrations in 10 second pulses at 4 minute intervals, a design found to produce distinct sequential responses. Capsaicin applications were made in the presence of either extracellular buffer or LPC, and experiments concluded with induction of a Ca^{2+} response by 500 nM ionomycin or 60 mM KCl for HEK293T and DRG cells respectively to confirm cell survival.

2.11.1 LPC Preparation

As a membrane lipid, LPC(18:0) is amphipathic and its use as an MS/MS standard required its dissolution in MeOH to 20 mM. At this concentration, LPC(18:0) would readily dissolve upon warming to RT. However, while MeOH is not known to interact with TRPV1, LPC(18:0) was reconstituted in extracellular buffer prior to each experiment to avoid any potential unreported or unintended effects of a solvent, such as the interaction between EtOH and TRPV1 (Trevisani et al., 2002). As lipids can be prone to oxidation (although It is unsaturated lipids that are principally susceptible to oxidation and LPC(18:0) is saturated), LPC was dried under N_2 before resuspension to 1 mM in extracellular buffer, where LPC(18:0) would readily dissolve in extracellular buffer at 4 mM at RT.

2.11.2 Statistical Analysis

All data are expressed as means ± S.E.M. Analyses evaluating the effects of LPC(18:0) on stimulation-induced desensitisation were performed on response sets from HEK293T cells (n = 48-78) and DRG neurons (n = 83-96). Cells had to distinctly respond to all 4 (for HEK293T cells) or 3 (for DRG neurons) capsaicin applications and the final depolarising stimulus (ionomycin or KCl) to be included in the analysis. Both peak amplitude and the Ca^{2+} transient AUC were analysed and, as this was an investigation of a potential sensitising effect of LPC, responses were normalised to the first capsaicin response in both cases. Baselines of fluorescence ratios measured in WinFluor (v3.7.3) were adjusted in Clampfit (v10.4), in which peak and AUC calculations were then performed following manual mapping of the response

start and end. Effects of LPC at varying concentrations, the number of capsaicin pulses and their interaction within the response peak amplitudes and AUCs of HEK293T cells and DRG were tested for by 2-way repeated measure (RM) ANOVA, wherein significance was set at $p < 0.05$. A significant effect of LPC concentration (including control data; 0 nM LPC) would indicate that the responses were altered by the amount of LPC present. A significant effect of the number of capsaicin pulses in this context would indicate stimulation-induced desensitisation of the response, while a significant LPC x capsaicin pulse count interaction here indicates a concentration-dependent effect of LPC on desensitisation. 2-way RM ANOVAs and post-hoc Bonferroni pairwise comparisons for exploring significant effects were performed in Origin (v9.1)

2.12 Whole-cell Voltage Clamp Electrophysiology

Whole-cell voltage clamp configuration HEK293T cell recordings were performed the day after transfection, with the same solutions and gravity flow perfusion system as in the calcium imaging experiments. Patch pipettes with a resistance of 2-4 MΩ were pulled from borosilicate glass capillaries (DMZ-Universal Puller, Harvard Apparatus Ltd). Recordings were obtained with an Axopatch 200B amplifier, Digidata 1200 digitizer (Molecular Devises, USA) and the Clampex within the pClamp 8.2 software package (Axon Instruments, USA). Whole-cell currents were recorded at 10 kHz with 2 kHz filtering and capacitance and series resistance were compensated by >60%. Cells were held at -60 mV with 10 second 30 nM capsaicin pulses applied at 4 minute intervals, as with the calcium imaging experiments. Current amplitudes were

measured following baseline subtraction in Clampfit (v10.4), though no formal statistical analyses were performed as discussed in Chapter 7.

3 CHAPTER 3 – SAMPLING FROM SCALD-TYPE INJURY FOR MULTIPLE ANALYTICAL PLATFORMS

3.1 Introduction

Microdialysis is a well-established sampling method enabling *in vivo* collection of solutes primarily from the extracellular interstitium. A porous probe is inserted into the skin and then perfused, enabling passive intake from the extracellular milieu as its constituents travel down their concentration gradient and across the probe's semipermeable membrane. It is ideal for the collection of continuous, longitudinal data from specific sites, and thereby for elucidating local, complex and temporally-dynamic pathophysiological processes. It has hence been used extensively for a variety of pathologies and tissues, including skin (Rackow et al., 1987), adipose tissue (Liffner et al., 2005) and heart (Farina et al., 2013).

The analysis of these samples has typically employed the use of platforms such as cytokine arrays or ELISAs in order to determine the concentrations of specific signalling components in select processes. Their targeted nature enforces a restricted analyte count which, while fit for purpose, limits the amount of information yielded from one sample. An assay equipped to measure preselected analytes will not identify further molecules present in the sample. "Omics" techniques applicable to the analysis of complex biological fluids, including metabolomics, can offer both an unprecedented data yield and exploration of all molecules present (i.e. global metabolomics) rather than fixation on predetermined targets (Johnson et al., 2016). These fields seek to characterise their respective "omes", the pools of molecules that

constitute the system or molecular class studied; the metabolome is an exhaustive list of small molecules, typically below 2000 Da, within a sample or system. Metabolomic approaches are therefore comprehensive, exploratory and viable tools for elucidating the skin's extracellular interstitium. Indeed, both proteomics (NIH, 2013; Rackow et al., 1987) and non-global (targeted) metabolomics with kit-prepared samples (Prout, 2014), have successfully been applied to dermal microdialysate, and global metabolomics have been applied to microdialysate sampled from other tissues (Constantian, 1978; Farina et al., 2013; Herndon et al., 1989; Liffner et al., 2005; Orman et al., 2011; Papp et al., 2003; Pileri et al., 2008; Rehberg et al., 2012). Global metabolomics remains a scarcely used tool in the analysis of skin microdialysate, yet is viable for the identification of metabolites discriminating between physiological and pathological conditions.

Global metabolomics typically employs one of two analytical platforms; mass spectrometry (MS) combined with a preceding separation method such as liquid or gas chromatography, or nuclear magnetic resonance (NMR) spectroscopy (Lanza et al., 2010; Nicholson et al., 1999; Want et al., 2010a). While NMR has generally proven more popular due in part to its non-destructive nature, the recent development of ultra-performance liquid chromatography (UPLC) as a separation technique has precipitated an increased focus on MS and its viability for new applications (Want et al., 2010a; Want et al., 2010b; Wilson et al., 2005). However, while a metabolome is a complete list of a system's small molecular constituents, no single technique within metabolomics can define one. An extensive range of parameters across all steps of the procedure must be optimised for each sample type and, to some extent, the metabolites' expected chemical characteristics.

The application of global metabolomics to a novel biofluid or tissue type therefore requires the evaluation of various methodological steps. Considerations for the microdialysis itself include probe selection, perfusate and perfusion rate, which will define the molecular recovery rate and sample volume; these selections should reflect the requirements for analysis by MS. Sample preparation has to be highly reproducible given the sensitivity of LC-MS, and must reflect the tissue constituent's expected characteristics, such as lipid-content and metabolite polarity, at each step. LC-MS analysis requires a fluid metabolite extract; microdialysate's liquid state precludes certain difficulties in the metabolite extraction process, though the sample type dictates the optimal aqueous metabolite extraction and resuspension protocol and nonetheless requires evaluation.

Following preparation, the separation techniques should ensure a maximal spread of elution over the duration of the analysis, allowing for better distinction between analytes. The techniques and equipment used should be tailored to the sample; for example, in selecting reversed-phase (RP; Wilson et al., 2005; Lenz et al., 2007) LC or hydrophobic interaction LC (HILIC; Alpert, 1990; Hemstrom et al., 2006; Grumbach et al., 2004; Tolstikov et al., 2002; Spagou et al., 2010), one prioritises the evenly spread elution of moderately polar to non-polar molecules or polar to non-polar molecules respectively (Want et al., 2010); the chromatography column should be selected on the basis of expected analyte polarity. Separation is accomplished by metabolites adsorbing to this column to different extents, depending on their chemical properties. This adsorption also depends on the solvent passing through the column, which typically increases in eluotropic strength over time. The time taken

to elute, the retention time (RT), of any single metabolite depends on its interaction with both the column and the solvent; the aim is to increase the spread of RTs, such that maximum detail for individual analytes can be recorded, as optimal separation reduces ion suppression and improves the quantitative ability of the method. The solvents, and their balance over time, need to be adjusted accordingly in order to maximise metabolome coverage. The overall duration of the separation is a compromise between throughput and detail, as shorter durations return less comprehensive metabolome coverage, though longer experiments are more susceptible to runtime effects (though the prevalence of this compromise is declining with technological advances; Gray et al., 2016). Additionally, parameters such as reconstitution solvent, sample injection volume, column flow rate and temperature still require evaluation for new sample types.

Following separation, the suitability of various aspects of the MS and data analysis for the sample must be confirmed but are largely predetermined by normal operating standards within metabolomics. MS parameters can be optimised for specific sample types using a quality control, a pooled sample representative of the entire sample set (Want et al., 2010a). Peak picking parameters during data analysis can also be optimised using this QC sample, in terms of signal:noise, chromatographic peak width, and mass accuracy. In addressing the questions raised to this point, the microdialysate's metabolites should now be detectable by MS and analysable as in any workflow for an established sample type, and the remaining considerations are universal to any metabolomics study. What follows here is a deconstruction of a workflow for the metabolomic analysis of skin microdialysate collected from rat subcutis. The suitability of UPLC-MS for microdialysate analysis is investigated in

what will be the first global metabolomics study of a local burn site sample. Approaches taken to all of the above-listed issues specific to a novel tissue analysis, and to those requiring consideration in any metabolomics study, are reported in a demonstration of their application to a study of the effects of burn injury on the extracellular interstitium's metabolic profile.

3.2 Results and Discussion

This study sought to determine the viability of combining microdialysis as a sampling method with metabolic profiling using UPLC-MS as a means of analysis. Pairing these techniques presented numerous challenges ranging across most steps of the intended workflow, resulting in various modifications from their standard applications. Here, an operational experimental setup for sampling, analysis and metabolite identification with these technologies is presented, and its viability demonstrated in the comparison of the extracellular interstitia in normal and burned tissue

3.2.1 Sample Collection

During manual insertion, the depth of the microdialysis probe could easily be judged by the resistance to the guide needle which was much lower in the subcutis than the dermis. Probes were positioned and shortened to minimise exposure of the semi-permeable membrane's surface area around the active uptake site; each half hour microdialysate fraction consistently lost 10 µl in volume, which is attributed to both solvent ultrafiltration into the tissue and evaporation, both of which must be accounted for in the selection of perfusion rate. Evaporation via the semipermeable

membrane is commonly prevented by enclosing the probe in tubing following its exit from the tissue, as was attempted in the preliminary stages of the present work. However, this was found to generate an unjustifiable amount of dead space and the consistent loss of 10 µl of microdialysate, due potentially in part to evaporation, was considered preferable. Excision of the microdialysis site after sacrifice of the animal allowed for histological confirmation of probe and burn depth. It also allowed for the isolation of RNA for subsequent tissue gene sequencing, which was further conducted in the DRG innervating the hind paws (L4+5). Histological analysis confirmed the positioning of the probe at the dermal border of the subcutaneous tissue (data not shown) and the deep partial-thickness of the burn, as indicated by the structure disruption, exfoliation, accumulation of eosinophilic material, karyopyknosis, karyorrhexis, oedema and vasodilation extending nearly into the

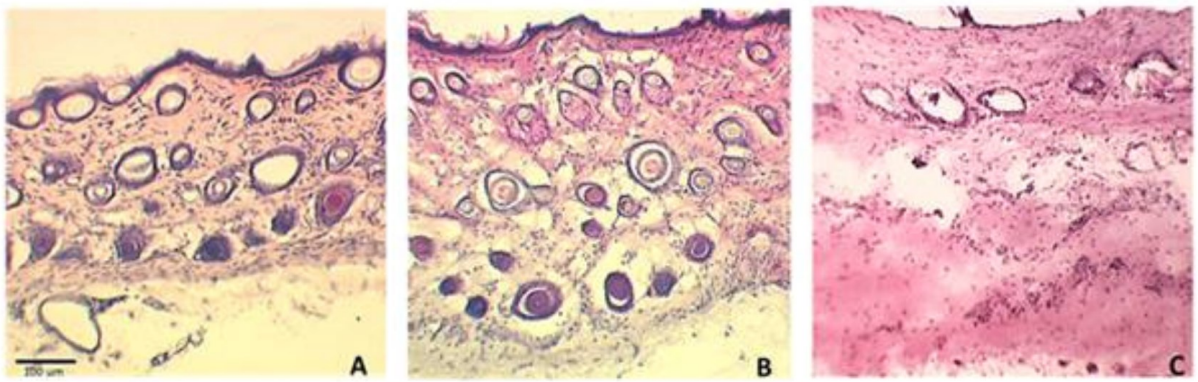


Figure 10 Skin histopathology following induction of a deep-partial thickness burn model. These microphotographs of H&E stained skin demonstrate the progression of the burn wound induced by 2 minute 60°C exposure after 5 minutes (**b**) and 3 hours (**c**) as compared with control tissue (**a**). The model induces structure disruption, exfoliation, accumulation of eosinophilic material, karyopyknosis, karyorrhexis, oedema and vasodilation extending into the reticular dermis, consistent with a deep partial-thickness model. Images provided by Jose Vicente Torres Perez.

Subject Number	Source Tissue	Treat-ment	Tissue Weight (mg)	Midi/ Mini Kit	Concentration (ng/µl)	Purity (A260/A280)
1	Skin	Burn	135	Midi	128.5	1.63
2	Skin	Burn	172	Midi	226	1.62
3	Skin	Burn	156	Midi	231.4	1.75
4	Skin	Burn	150	Midi	162.3	1.67
5	Skin	Burn	30	Mini	23.6	2.32
6	Skin	Burn	30	Mini	68.5	1.77
7	Skin	Burn	30	Mini	85.3	1.81
1	Skin	Control	164	Midi	607.4	1.68
2	Skin	Control	135	Midi	383.5	1.64
3	Skin	Control	153	Midi	302.6	1.71
4	Skin	Control	90	Midi	525.7	1.74
5	Skin	Control	30	Mini	330.3	1.78
6	Skin	Control	30	Mini	98.3	1.66
7	Skin	Control	30	Mini	169.2	1.65
2	DRG	Burn	-	-	21	1.04
3	DRG	Burn	-	-	118	1.71
5	DRG	Burn	-	-	0	-
6	DRG	Burn	-	-	16	3.88
7	DRG	Burn	-	-	0	-
8	DRG	Burn	-	-	16	3.88
9	DRG	Burn	-	-	22.2	1.83
10	DRG	Burn	-	-	8	1.97
11	DRG	Burn	-	-	0	-
2	DRG	Control	-	-	60.3	1.24
3	DRG	Control	-	-	197.2	1.81
5	DRG	Control	-	-	0	-
6	DRG	Control	-	-	0	-
7	DRG	Control	-	-	16	3.88
8	DRG	Control	-	-	16	3.88
9	DRG	Control	-	-	2	-
10	DRG	Control	-	-	6	-
11	DRG	Control	-	-	0	-

Table 1 RNA Yields measured in-house. While VBCF would evaluate the concentrations and quality of the RNA prior to library preparation, they were first evaluated internally to assess the isolation's execution and to indicate the number of samples required. These measurements can be directly compared with VBCF's evaluation in Table 2.

subcutaneous tissue (Figure 10a-c). These images, prepared by Jose Torres, indicate progressive wound development over the first 3 hours post-burn, which correlated with erythema (not shown) and oedema. The suitability of the skin and DRG collected for gene sequencing (to be conducted externally by Vienna Biocenter Core Facilities) could be evaluated internally at this stage by photometric quantification of RNA concentration following its isolation with Qiagen Mini and Midi RNeasy kits. As expected, the yields from skin samples were comfortably sufficient for gene sequencing despite the difficulty of isolating RNA from such fibrous tissue (see Table 1). Also as expected, RNA concentrations from single pairs of DRG were low. However, the higher readings were still theoretically sufficient for transcriptomics, which requires 1 µg of total RNA per sample, and all the samples were sent for evaluation of RNA concentration and quality in Vienna prior to their gene sequencing.

3.2.2 Sample Analysis

Assessing the metabolomic analysis began with evaluating chromatographic performance, as effective metabotype definition relies on successful analyte separation and detection. As indicated by the presence and intensity of the chromatogram peaks, and the spread of elution times, the approach proved suitable for the analysis of microdialysate with both positive and negative mode ionisation (Figs. 11a and b). It was apparent that ESI+ and ESI- generated independent metabolomic profiles, motivating the use of both modes. The quality of the chromatography (determined by visual chromatogram inspection confirming sharp, Gaussian peak shapes spreading over the gradient with no tailing and a high signal-

to-noise ratio) justified the prioritisation of retaining water-soluble rather than hydrophobic metabolites in selecting RP chromatography and the HSS T3 (C18) column, a decision motivated by the fluid state of the interstitium and therefore the likely solubility of recovered analytes. However, the rapid and overlapping early elutes justify the additional use of HILIC with microdialysate for maximising metabolome coverage. The peak separation further indicated the viability of the gradient, for which the solvents and their balance were adjusted to extend denser elution periods (Figs. 11a and b), along with various other parameters such as column flow rate and temperature.

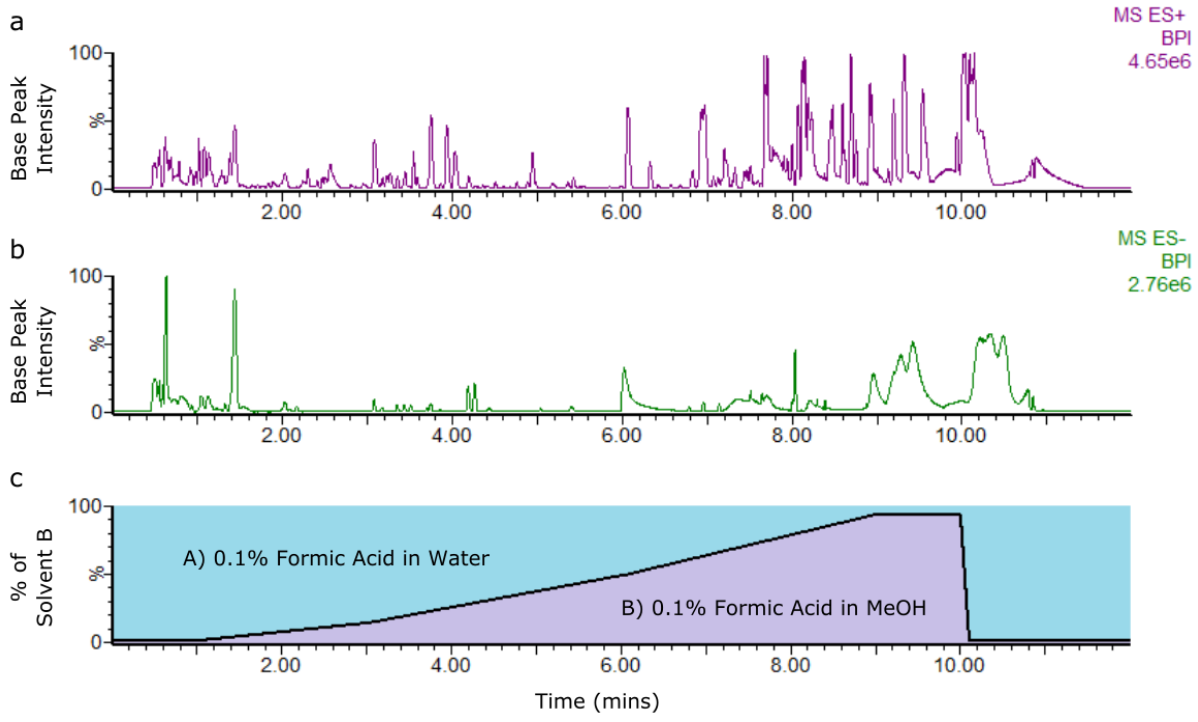


Figure 11 Metabolites are detectable via microdialysate UPLC-MS with both ESI+ and ESI-. The presence and intensity of peaks in the chromatogram of single burn site microdialysate fractions in ESI+ (**a**) and ESI- (**b**). As indicated by the presence and intensity of the peaks and the spread of elution times, both ionisation modes were worth pursuing for optimal metabolome coverage and the gradient (**c**) ensured sufficient elution spread in both modes.

Upon affirming the quality of the chromatography, PCA was applied to the burn and control sample UPLC-MS profiles (Figs. 12a and b). Whether utilising positive or negative mode ionisation, a clear separation can be observed between microdialysates collected from burned tissue and those collected either from the same site prior to the burn or from the control site. The clustering of the latter two sample types indicates that both microdialysis sites have a similar metabotype prior to the burn. However, in order to attribute variation in the data to an experimental effect, the stability of data acquisition must first be evaluated. Reliable metabolic profiling principally relies on the consistency of three analytical elements (Want et al., 2010a): 1. Retention time, ensuring accurate peak alignment during processing and chromatogram comparison between standards and samples; 2. Signal intensity, ensuring that the amplitude reflects relative analyte concentrations in the sample; 3. Mass accuracy, ensuring measurements are representative of the analyte's true *m/z* ratio. Of these, retention time and signal intensity prove inconsistent within the first few injections on a new column (Beal et al., 1994; Shults et al., 2015; Turnage et al., 2002); 10 consecutive QC injections were found to be sufficient in stabilising these parameters. The subsequent QC injections were interspersed between samples and included in the PCA; their clustering indicates the stability of acquisition over the course of the experiment (Figs. 12a and b).

Using microdialysis as a sampling method for UPLC-MS posed several questions regarding the collection of microdialysate, many of which can be addressed with these findings. The selection of a perfusion rate had to balance the inverse relationship between relative recovery (the solute concentration in the microdialysate

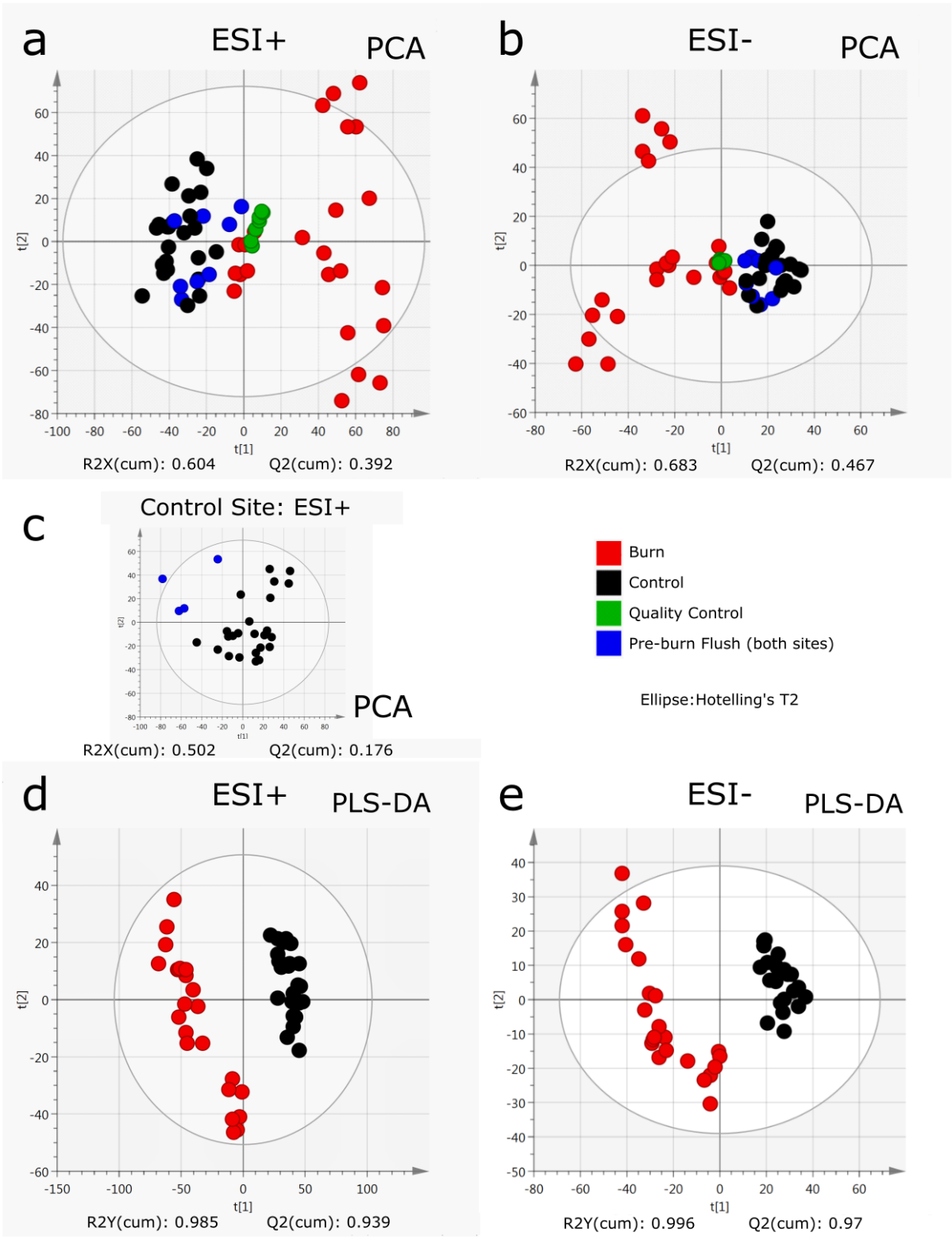


Figure 12 PCA and PLS-DA scores plots indicate metabolite differences between burn and control microdialysate. Upon unsupervised projection into two-dimensional spaces for visualisation of underlying structure and variance in the data, PCA of metabolite measurements collected with both ESI+ (**a**) and ESI- (**b**) demonstrate tight clustering of QCs, indicating stable sample analyses, and separation of burn samples from control and

pre-burn microdialysates (which group together), suggesting the presence of a burn effect. The separation of pre-burn microdialysates from subsequent fractions within the control data (**c**) indicates a difference in metabolite profiles likely resulting from the recovery of tissue from the probe insertion prior to induction of the burn. Following recognition of a burn effect via PCA, PLS-DA was utilised to identify discriminants accounting for the difference between burn and control metabolic profiles; the clear separation of post-burn burn and control site data was retained in the scores plots with both ESI+ (**d**) and ESI- (**e**). Red, Burn; Black, Control; Green, Quality Control; Blue, Pre-burn Flush.

relative to the tissue) and absolute recovery (the total amount of solute recovered), which is complicated by the increasing influence of solvent ultrafiltration and convection ('solvent drag') with higher perfusion speeds. Here, relative recovery was prioritised over absolute recovery, and hence sample concentration over volume, in utilising a low perfusion rate of 2 µl/min. The chromatograms demonstrate that the resulting metabolite concentrations were detectable, and the PCA demonstrates that they were sufficient for identification of an experimental effect following UPLC-MS analysis. Such sample volumes are enabled by the low requirements of UPLC-MS, for which more than enough material was collected with 50 µl per half hour fraction (with 10 µl lost to ultrafiltration or evaporation) despite repeated injections over several subsequent analytical steps in both ionisation modes. The quality of the chromatography and PCA also indicates that the probe's MW cut-off, which far exceeds the size of the intended analytes at 3 MDa, was suitable for the recovery of metabolites. It is further clear from these data that the perfusate selection (Ringer's solution), sample storage (at -80°C), active probe uptake length (of 10 mm) were suitable for UPLC-MS of microdialysate.

As demonstrated in Chapters 5 and 7 via the temporal profiles of select cytokines and metabolites, the probe insertion is itself a pathological event and therefore requires a half hour “flush” period for stabilisation of the extracellular interstitium. PCA of the control site microdialysate UPLC-MS profiles exhibits separation between the first microdialysate fraction and those following (Fig. 12c), indicating a shift in metabolic profile. While such a profile could suggest that the burn induces this separation via systemic effects, the PCA grouping of all pre-burn microdialysates with all control-site microdialysates in Figures 12a and b, and the spread observed with effects of the trauma in burn-site microdialysates, suggest that systemic effects are minimal. The separation in Figure 12c was therefore attributed to a transient increase in metabolites present only in the first fraction, indicating that the flush period is sufficient for stabilisation of the interstitium, consistent with previous measures of the inflammatory response to probe insertion (Groth et al., 1998; Stenken et al., 2010). A short stabilisation period relies on careful insertion of a sufficiently thin, lubricated probe.

The PCA scores plots (Figs. 12a and b) visualise variance and structure in the data prior to their classification in groups. The clarity of these unsupervised separations between burn and control samples indicates that the burn effect is an outstanding source of variance, far exceeding any influence of noise or run-time effects in both ESI+ (Fig. 12a) and ESI- modes (Fig. 12b). The spread within the burn and control groups is indicative of the inclusion of all time points, with the particular spread in the burn samples representing a diverging metabolic profile over time as the tissue’s response to the trauma develops. The separation of pre-burn microdialysates from subsequent fractions within the control data alone (Fig. 12c) indicates a difference in

metabolite profiles likely resulting from the recovery of tissue prior to induction of the burn; indicating that a 30 minute flush is sufficient. The burn vs control separation indicates that partial least squares-discriminant analysis (PLS-DA), a supervised approach to variable classification, can now be applied. Rather than simply projecting the maximum variance in the metabolomic profiles as PCA does, PLS-DA models covariance between these profiles and their categorisation as either burn or control samples (Want et al., 2011). Metabolic profile variables (i.e. features) can be ranked by their correlation with class separation, quantified as variable influence on projection (VIP) values, in order to identify those expressing the experimental effect. Features exceeding a predetermined threshold, set at 2 presently, are therefore typically prioritised for structural elucidation. Here, PLS-DA constructed well-fitting, highly predictive models for both ESI+ (Fig. 12d; R2Y(cum) 0.985, Q2(cum) 0.939) and ESI- (Fig. 12e; R2Y(cum) 0.996, Q2(cum) 0.97) data, which were consistent with PCA in the clear separation of burn and control samples, with a relative divergence of the former coinciding with the progression of the pathology.

The PCA and PLS-DA score plots indicate a clear effect of the burn in the metabolomics data. This statistical approach therefore fulfilled its purpose in supporting the combination of microdialysis and metabolomics in the exploration of superficial pathologies, as the separation between burn and control data presented depends upon contrasting metabolite concentrations within the samples that must have been detectible following use of the applied methodologies. Typically, this analysis would be followed by the identification of individual metabolite discriminants exhibiting burn-dependent differences in concentration within these PLS-DA models, as ranked by their VIP values. Indeed, the 2187 of 42364 and 757 of 13829

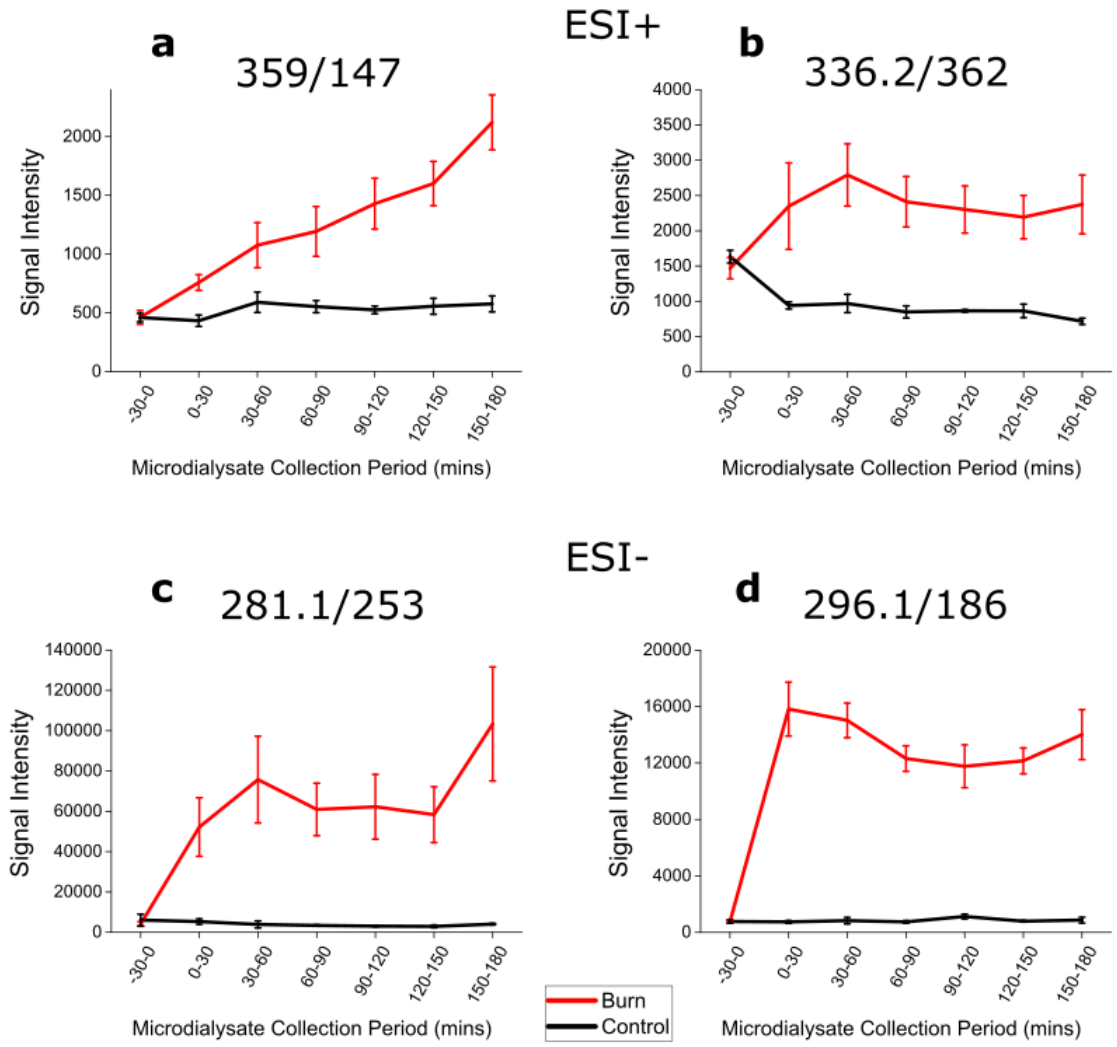


Figure 13 High-VIP metabolites exhibit a clear burn effect. These four metabolites, selected from those exceeding the VIP cut off within the PLS-DA of both ESI+ (**a** and **b**) and ESI- (**c** and **d**) data, demonstrate the successful execution of microdialysis and analysis by UPLC-MS. All four demonstrate varying concentration profiles characterised by a post-burn increase specific to the burn site while the control site remains stable (**a**, **c** and **d**) or fully recovers from the probe insertion prior to the burn (**b**). Metabolites such as these indicate that the applied methodology is feasible for the study of superficial pathologies, and that there are burn-elevated metabolites within the collected data set that can now be structurally elucidated.

metabolite features in ESI+ and ESI- mode respectively exceeding the VIP cut-off of 2 exhibit burn-dependent increases in concentration, as exemplified in Figure 13.

However, as discussed in the methods, this model does not account for the data's temporal arrangement, and hence may not detect metabolites with less consistent (e.g. transient) burn-induced elevations in concentration. To elucidate this potential multi-dimensionality of the burn effect, CVA was employed and further used for discriminant analysis as reported in Chapter 6.In summary, the data presented in this chapter support the application of various metabolomic experimental design elements to samples collected by microdialysis, including the use of RP chromatography and the HSS T3 column, the design of the solvent gradient, applying both ESI+ and ESI-, and various other parameters (e.g. column flow rate and temperature). Collectively, these constitute a novel metabolomic configuration for the analysis of interstitial fluid. In particular, its application to superficial pathologies is supported by demonstrating subcutaneous microdialysis' execution and the methodology's coverage of a deep partial-thickness burn tissue metabolome. Particularly in the context of this project, the data further validate the execution of the burn model. More importantly, they suggest that this novel combination of microdialysis with metabolomics has great potential for application both within burns research and further to other tissues and pathologies.

4 CHAPTER 4 – DEFINING THE BURN TRANSCRIPTOME

4.1 Introduction

It is via the transcription of RNA that the genetic instructions determining the growth, development, function and reproduction of any organism provide by DNA can be followed. There are as few as 19,000 genes in the human genome at current estimation, and this number will only decrease as sequencing and interpretation methodology improves (Ezkurdia et al., 2014). DNA can be transcribed into various classes of RNA, four of which code for protein synthesis (in most organisms) while many more can be broadly categorised as regulators of genes or cell structure (Bhattacharjee et al., 2013). Of those involved in the formation of protein, messenger RNA (mRNA) is the major class. In the 'translation' stage of protein synthesis, mRNA is delivered to ribosomes which construct proteins from amino acids using its genetic readout. The presence of transcripts for any particular genetic sequence reflects its active engagement in gene expression; while nearly every cell contains the same genetic information, it is differentially engaged depending on its environment. Characterising distinctive translation profiles within a specific cell type, organism, tissue type or state offers us insight into the operation of that system at one of its most fundamental levels. It is on this principle and in the pursuit of defining the functional element of the genome that the field of transcriptomics was formed (Wang et al., 2009).

Transcriptomics is the definition of a transcriptome: the sum total of mRNA transcribed in any given system (Wang et al., 2009). It depends on the quantification of individual gene transcripts as a measure of its expression, such that it can be compared between cell/tissue types or states and its contribution delineated. The two principle categories of technologies developed for defining and quantifying the transcriptome are microarray- or sequence-based approaches (Wang et al., 2009). Microarrays for gene expression studies utilise DNA spots, each containing picomoles of a specific DNA sequence (probes), attached to a solid surface. Transcription is typically measured by hybridisation of fluorescently-labelled cDNA to these microarrays, which can be customised to represent any level of detail up to the high-resolution interrogation of large genomes (Wang et al., 2016; Yamada et al., 2003). They yield large amounts of data and are relatively inexpensive (depending on the resolution and coverage), but are subject to several limitations. These include reliance on species- or transcript-specific probes, conferring a bias by which novel transcripts, gene fusions, single nucleotide variants and other previously unconsidered changes cannot be detected. Further, microarrays have a limited dynamic range resulting from the influence of background noise at the low end and signal saturation at the high end. Both limitations are overcome by the most recent implementation of the second principal approach to transcriptome definition, gene sequencing, also known as RNA-Seq Technology or Next-Generation Sequencing. Rather than measuring probe-cDNA hybridisation, gene sequencing operates by directly determining the cDNA's sequence. RNA-Seq supersedes its predecessors by measure of cost, its quantitative capacity and its specificity for shorter tags and isoforms (Wang et al., 2009). Briefly, it operates by conversion of RNA (total or polyadenylation (poly-A)-filtered, in which mRNA is selectively enriched) to a library

of cDNA fragments, with or without amplification. Adaptors are attached to one or both ends, enabling determination of that molecule's genetic code via single- or pair-end sequencing, at varying read lengths; all of these parameters depend on the technology employed, which can be any high-throughput sequencing technology (Wang et al., 2009). Reads are then aligned to the relevant genome or used to generate a novel assembly representing the transcriptional structure of the sample and the amount of gene expression for its constitutive transcripts. The advantages it confers already make it a financially viable alternative to microarrays and, with the cost of gene sequencing continuing to fall, it is expected to replace microarrays in contexts concerning transcriptome dynamics and structure.

While transcriptomics have been used to identify functionally significant contributors to various disease states detectible at a transcriptional level (Li et al., 2016; Twine et al., 2011), its utilisation in burn injury has been restricted to analysis of blood samples with either a focus on the transcriptional impact of concomitant infection (Kruczek et al., 2016; Yan et al., 2015) or the transcriptional response to inflammation as mediated by circulating leukocytes (Xiao et al., 2011). It is thereby comparable to the metabolomic analyses of burn injury to date; the use of high-throughput analytical omics technologies has so far only been applied to more accessible, systemic samples. In response, this project aimed to define the transcriptomes of the burn and control microdialysis sites such that differentially expressed genes may be explored to identify discriminants potentially underlying the burn's pathological progression. Further, the same RNA-Seq technology was applied to the DRG innervating these sites, such that any changes in expression induced by sensory transduction following the burn could be similarly identified.

After the isolation and delivery of RNA collected from these tissues, this analysis was conducted externally by Vienna Biocenter Core Facilities, where all sample and statistical analyses were executed; in return, databases of significantly differentially expressed genes and represented GO and KEGG pathways were returned. This chapter will serve to demonstrate the success or lack thereof in identifying an effect of the burn within the transcriptomes using RNA-Seq technology, and to deconstruct the implication of individual genes or networks of genes identified within. Genes or gene networks identified were interpreted in the context of otherwise-implicated functional processes as they emerged over the course of this project rather than independently. Indeed, a primary motivation behind this analysis was to identify transcriptional processes potentially influencing the burn interstitium, as evaluated in the metabolomics, cytokine profiling and lipidomics components of this project. Consequently, individual genes and most gene networks are not discussed in this chapter but are rather presented subsequently alongside protein-level data for cohesive discussion of their functional implications.

4.2 Results and Discussion

Consistent with the in-house analysis of the RNA content from microdialysis sites and their innervating DRG, VBCF deemed that RNA concentrations were sufficient for gene sequencing among all skin samples and enough DRG samples. While the internally measured RNA concentrations were not accurate predictions of VBCF's evaluations, they were accurate enough to affirm correct execution of the isolation from the skin samples. The limited dynamic range of the in-house photometer

dictated that RNA isolated from the limited amounts of DRG tissue could not be measured with this same accuracy; a greater number of DRG samples were sent to VBCF to increase the chances of having sufficient RNA. Further, while a sample is typically considered pure with a A_{260}/A_{280} of 2 as measured by a photometer and the in-house readings typically fell below this, VBCF's quality evaluation indicated that the purity was sufficient for the analysis across all skin samples and enough of the DRG samples. 4 burn and control samples were therefore selected for sequencing of the skin transcriptome by prioritising higher RNA concentrations. The problematically low RNA yields from DRG were identified during in-house analysis of the samples; despite the relative difficulty of isolating RNA from fibrous tissue over nervous tissue, the comparative amounts of starting material dictated that skin yields were far higher than those from the <10 mg masses of single DRG pairs. Consequently, the total RNA from 9 separate pairs of DRG with the highest concentrations were offered for VBCF's selection and only seven pairs of skin RNA were sent. Six of the eighteen DRG RNA samples failed VBCF's quality control evaluation and, while four burn and control samples were therefore still available for selection, one of the control samples was subsequently identified as problematic during the analysis and excluded. Libraries were therefore prepared from 4 samples within each condition and tissue type, except for that of the control DRG which was prepared from 3. Following sequencing of these 15 RNA samples, reads were base called and those identified as ribosomal were filtered out before alignment of the remaining reads to the rat genome. The mapping statistics are provided in Table 3, and were described as reasonably high over all samples by VBCF.

Subject Number	Source Tissue	Treatment	Tissue Weight (mg)	Midi/ Mini	RNA Quality Evaluation	Internally-measured Concentration (ng/µl)	Purity (A260/A280)	Concentration (ng/µl)	Volume (µl)	Total RNA Content (µg)
1	Skin	Burn	135	Midi	Ok	128.5	1.63	229	103	23.59
2	Skin	Burn	172	Midi	Ok	226	1.62	228	120	27.36
3	Skin	Burn	156	Midi	Ok	231.4	1.75	193	120	23.16
4	Skin	Burn	150	Midi	Ok	162.3	1.67	113	120	13.56
5	Skin	Burn	30	Mini	Ok	23.6	2.32	59	30	1.77
6	Skin	Burn	30	Mini	Ok	68.5	1.77	65	47	3.06
7	Skin	Burn	30	Mini	Ok	85.3	1.81	59	55	3.25
1	Skin	Control	164	Midi	Ok	607.4	1.68	295	120	35.4
2	Skin	Control	135	Midi	Ok	383.5	1.64	396	114	45.14
3	Skin	Control	153	Midi	Ok	302.6	1.71	171	112	19.15
4	Skin	Control	90	Midi	Ok	525.7	1.74	423	102	43.15
5	Skin	Control	30	Mini	Ok	330.3	1.78	263	27	7.1
6	Skin	Control	30	Mini	Ok	98.3	1.66	273	55	15.02
7	Skin	Control	30	Mini	Ok	169.2	1.65	203	55	11.17
2	DRG	Burn	-	-	Ok	21	1.04	7	25	0.18
3	DRG	Burn	-	-	Ok	118	1.71	45	25	1.13
5	DRG	Burn	-	-	Ok	0	-	3	55	0.17
6	DRG	Burn	-	-	Ok	16	3.88	28	55	1.54
7	DRG	Burn	-	-	Ok	0	-	7	50	0.35
8	DRG	Burn	-	-	Problematic	16	3.88	3	56	0.17
9	DRG	Burn	-	-	Ok	22.2	1.83	5	45	0.23
10	DRG	Burn	-	-	Problematic	8	1.97	4	52	0.21
11	DRG	Burn	-	-	Not Enough Material	0	-	n/a	48	n/a
2	DRG	Control	-	-	Not Enough Material	60.3	1.24	1	25	0.03
3	DRG	Control	-	-	Ok	197.2	1.81	85	25	2.13
5	DRG	Control	-	-	Ok	0	-	4	55	0.22
6	DRG	Control	-	-	Ok	0	-	6	56	0.34
7	DRG	Control	-	-	Ok	16	3.88	7	56	0.39
8	DRG	Control	-	-	Ok	16	3.88	4	56	0.22
9	DRG	Control	-	-	Problematic	2	-	2	56	0.11
10	DRG	Control	-	-	Not Enough Material	6	-	1	56	0.06
11	DRG	Control	-	-	Ok	0	-	8	48	0.38

Table 2 Quality Evaluations of total RNA. All RNA was quantified prior to and following delivery to VBCF; internal measurements were used as an indicator of the isolation's execution to inform the number of samples required, while VBCF's external analyses were used to select samples for gene sequencing library preparation.

Following read mapping, various aspects of the quality of the data and its treatment required evaluation. Firstly, to ascertain whether the normalisation successfully scales the data to comparable registers, enabling meaningful statistical analyses, expression distribution box plots of all samples were inspected. Their between-sample consistency indicates successful normalisation of the data, with no irreconcilable sources of variance that would suggest a problem in the RNA isolation, sequencing or data processing (Fig. 14). The data can therefore be explored for experimental effects, as drawn from relationships within and differences between samples grouped by tissue type and treatment. Here, this underlying structure within the data was evaluated by means of Spearman's metrics and PCA. Correlation values between all possible sample pairs vary between 0.78 and 0.97, as indicated in the pairwise correlation matrix (Fig. 15), indicating a relatively high correlation regardless of tissue type or experimental treatment. Within-group correlations, accounting for tissue type and experimental treatment, were very high as indicated in Table 4. This is expected, given the relative similarity of samples collected from the same tissue and undergoing the same treatment. The fact that the mean correlation within burned skin samples is relatively lower (with a mean of 0.934) than those of DRG or the control microdialysis site (0.954-0.967) may indicate a divergence in gene expression profiles resulting from the burn. However, these comparisons are primarily made to evaluate the quality of the data, which is affirmed by the high correlation of gene expression within sample type; with the exception of the burn skin (which may express a heterogeneous burn effect), the group-wise mean correlations all exceed 0.95, the correlation expected of biological replicates.

Subject	Sample Tissue	Treatment	Total Reads	Mapped Reads	Mapping Rate	Unique Reads	Non-unique Reads	Unmapped Reads
3	DRG	Burn	25,327,201	23,307,298	91.60%	20,940,047	2,267,251	2,119,903
6	DRG	Burn	26,706,113	24,009,181	89.90%	21,643,158	2,366,023	2,696,932
7	DRG	Burn	24,844,076	20,562,263	82.80%	18,124,094	2,438,169	4,281,813
9	DRG	Burn	27,604,916	19,971,747	72.30%	17,860,470	2,111,277	7,633,169
3	DRG	Control	28,720,428	27,253,436	94.90%	24,836,253	2,417,183	1,466,992
6	DRG	Control	24,454,552	22,115,666	90.40%	19,865,838	2,249,828	2,338,886
7	DRG	Control	32,035,298	25,616,875	80.00%	22,747,625	2,869,250	6,418,423
1	Skin	Burn	28,957,370	25,915,774	89.50%	21,130,347	4,785,427	3,041,596
2	Skin	Burn	35,631,699	32,075,730	90.00%	26,214,307	5,861,423	3,555,969
3	Skin	Burn	38,500,472	29,032,481	75.40%	23,662,262	5,370,219	9,467,991
4	Skin	Burn	32,279,594	29,549,360	91.50%	25,215,991	4,333,369	2,730,234
1	Skin	Control	36,382,639	34,764,004	95.60%	30,253,452	4,510,552	1,618,635
2	Skin	Control	42,142,089	40,298,749	95.60%	35,226,534	5,072,215	1,843,340
4	Skin	Control	28,534,897	26,978,286	94.50%	23,506,773	3,471,513	1,556,611
6	Skin	Control	37,858,572	36,097,287	95.30%	31,744,070	4,353,217	1,761,285

Table 3 Summary of RNA-Seq mapping statistics. Alignment of filtered reads to *Rattus norvegicus* reference genome (Ensembl Rnor 5.0 Assembly) using TopHat version 2.0.9. Total reads indicates the number of reads detected in the sample; Mapped reads indicates the number of reads mapped to the genome; Mapping rate is the percentage of mapped reads from the total number of reads; Unique reads is the number of uniquely aligned reads; Non-unique reads is the number of reads mapped to more than one location in the reference genome; Unmapped reads is the number of reads not mapped.

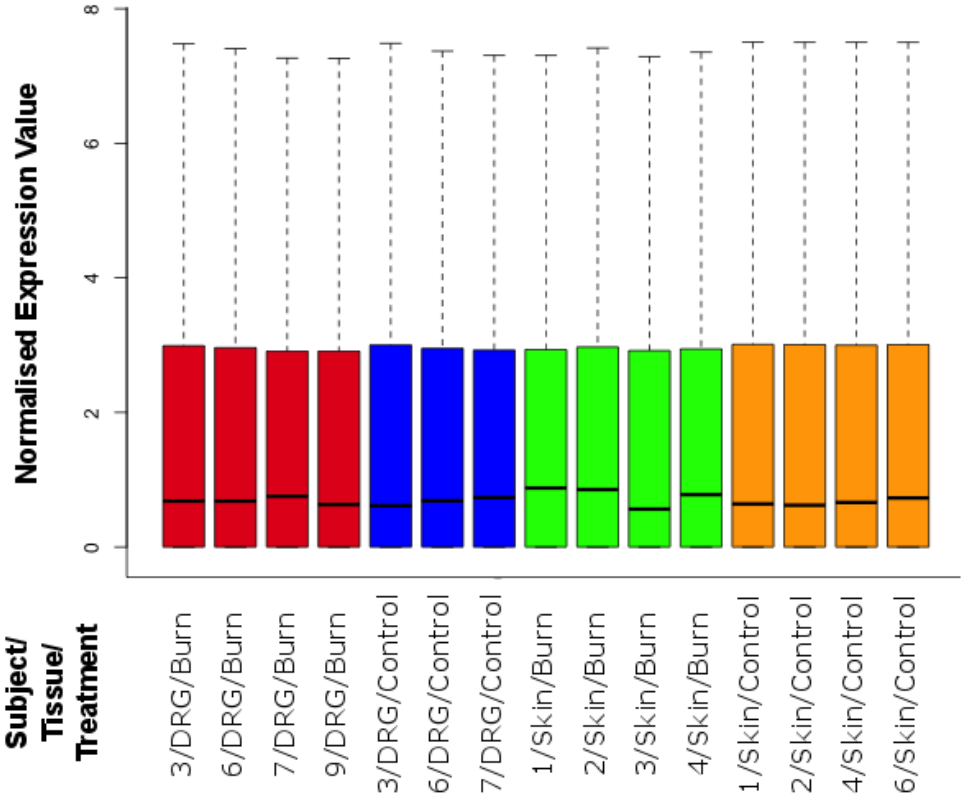


Figure 14 Expression distribution boxplots across all samples. The consistency of expression data between samples following normalisation indicates that there were no issues in the sampling or reading of the RNA, nor in the data's processing, and that the data have successfully been scaled to comparable registers, allowing for meaningful statistical analyses of experimental effects.

Group	Minimum Correlation	Mean Correlation
DRG (Burn)	0.943	0.954
DRG (Control)	0.952	0.958
Skin (Burn)	0.908	0.934
Skin (Control)	0.963	0.967

Table 4 Group-wise correlation of expression data. Spearman's metrics quantifying similarity between samples. These indicate a high correlation between gene expression data within tissue type and experimental treatment, reflecting a high quality of sample and library preparation. The highest correlations were within the DRG data and the control skin data; the relatively lower correlation of gene expression in the burned skin may reflect transcriptome divergence resulting from the burn.

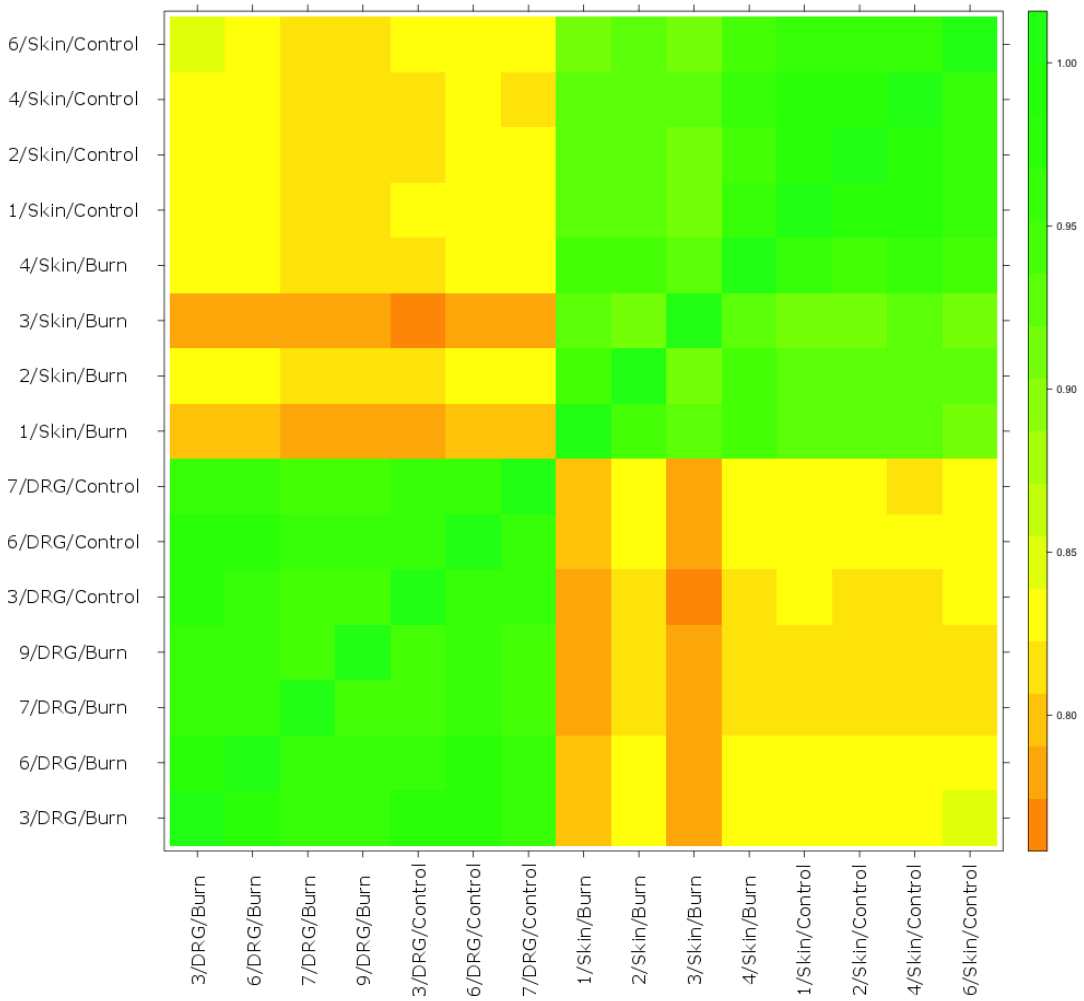


Figure 15 Correlation matrix: pairwise comparison of normalised gene expression data. A visualisation of all possible pairwise correlations over all samples. They range between 0.78 and 0.97; the lower correlations reflect between-tissue differences and are expected, while the higher correlations indicate the similarity between expression profiles within tissue type and suggest a high quality of sample and library preparation.

PCA, an ordination technique that re-expresses data to maximise its underlying structure and variance, allows for further inspection of the similarities and differences in the data indicated in the correlation analysis above and offers the first explicit representation of between-group relationships. The tight clustering of all DRG data (Fig. 16), regardless of whether they innervated burned or unburned skin, is the first indication that there may not be a burn effect detectible within DRG expression

profiles. The separation by tissue type is clear, with the skin data occupying a completely different subspace, indicating that whether the RNA was sourced from skin or DRG explains a substantial source of variance in the data. While the control skin data cluster within their group to an even greater extent than the DRG samples, the burn skin samples sit separately, suggesting the influence of a burn effect at skin-level, and spread within the group in a manner reflecting their relatively low within-group correlation (Table 4). At this stage, it is apparent that the quality of the RNA and library preparation was high, and that the differences in gene expression profiles between burn and unburned skin should be explored.

Having recognised the possibility of a burn effect, the contributions of single genes to the separation between burn and control expression profiles were quantified by means of modified t-test p-values generated via least-squares regression analyses within tissue type. Consistent with the degree of separation evident in the PCA (Fig. 16), 2610 genes were deemed differentially expressed in burn and control skin with a p-value cut-off of 0.01 following FDR-adjustment for multiple comparisons correction. A complete list of genes differentially expressed between burn and unburned skin samples with a p-value below 0.05 is presented in Supplementary Table 1 within the Appendix. With these criteria, only one gene was differentially expressed between DRG innervating the burn and unburned skin; while it is not uncommon to explore the data without multiple comparisons correction in these circumstances, it was decided that focus would be placed on the skin libraries; the DRG expression data would not be explored at this stage. Presenting the 2610 genes meeting these criteria in the comparison of skin samples as a heat map (Fig. 17) demonstrates the clarity of the differences in signal intensity between those contributing to overall

differences between samples as detectible by hierarchical clustering and reflected in the PCA; further, it indicates the mix of gene-specific upregulation and downregulation exhibited within the burned tissue.

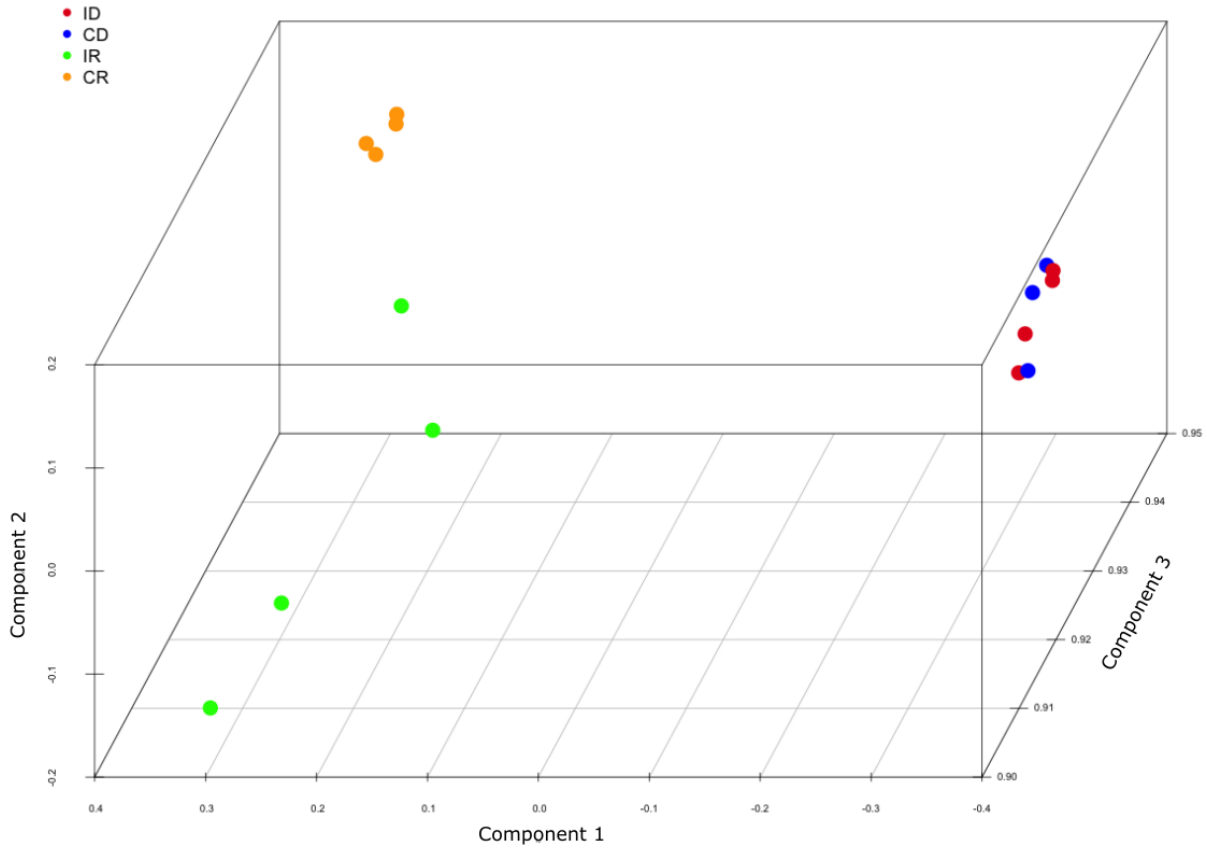


Figure 16 Principal component analysis of gene expression profiles of skin and DRG tissue. The tight clustering of data collected from the burn DRG (ID) and control DRG (CD) indicates a lack of detectible experimental effect between treatment groups. The separation between the burn skin (IR) and control skin (CR) data indicates an experimental effect, where the spread within the burn data may represent dynamic pathological transcriptional profiles while the tight clustering of the control data indicates a between-subject consistency in performing the experiment.

The clear separation between burn and control skin data justifies exploration of the genes underlying the differences in expression profiles, while the DRG libraries will not be pursued beyond this point. As described above, differentially expressed

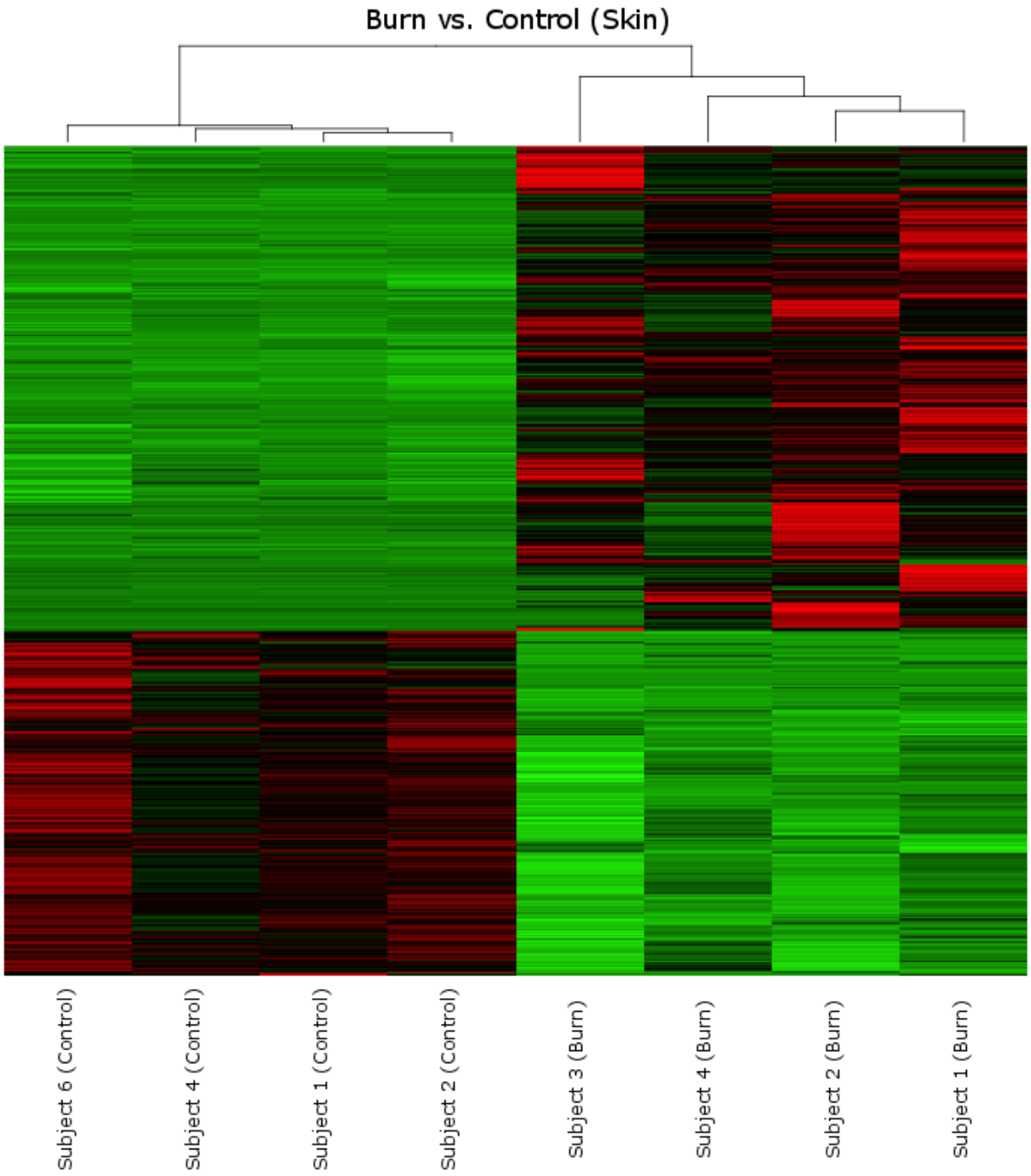


Figure 17 Heat map and HCA of genes differentially expressed between burn and control skin samples. A demonstration of the clarity of the difference in gene-by-gene (where each row is one gene) signal intensities between burn and control data; these contribute to an overall difference in expression profiles detectible by HCA, as indicated at the top of the figure. Further, this heatmap demonstrates the occurrence of both up- and down-regulation among different genes following the burn. Green = low intensity, Red = high intensity.

genes can be identified by the statistical significance of their contribution to the separation between burn and control expression profiles. However, these will not be discussed here; individual genes will be individually called upon over the coming chapters in the context of their functional implication alongside relevant protein-level data. Similarly, the significant results of enrichment analyses (used to detect alterations in significant portions of functionally-associated gene networks across entire libraries) will be discussed as they are implicated in burn pathology by data in the coming chapters. These analyses were conducted against the most conventionally used GO and KEGG databases, where the former categorises genes by biological processes, molecular functions and cellular components and the latter defines pathways for biological interactions. As is convention, these analyses mapped both up- and down-regulated genes collectively. This reflects the fact that mRNA and protein levels often do not correlate due to the conflicting influences of a wide repertoire of regulatory systems (e.g. smallRNA, regulatory R-proteins) and varying protein half-lives and stabilities (Maier et al., 2009); transcriptional changes in either direction can reflect translational changes in either direction. 178 GO terms and 34 KEGG pathways were significantly represented within the skin libraries generated in this study, and may hence play a role in burn injury; complete lists of these are presented in Supplementary Tables 2 and 3 within the Appendix respectively. The implication of these molecular interactions in any tissue state by gene sequencing is conventionally evaluated in the context of concomitant functional assays or protein-level studies, as is demonstrated in the present work (see Chapters 5 and 7). However, several pathways among those most significantly represented were not explicitly linked with any functional or molecular correlate reported in other chapters but nonetheless present avenues for further research of

burn injury. In particular, and consistent with the engagement of the immune system, these pertain to pathways representing the control of cell migration and adhesion, namely the Focal adhesion pathway ($p = 3.38E-6$), the Extracellular matrix (ECM)-receptor interaction pathway ($p = 6.23E-9$), the Cell adhesion molecules pathway ($p = 7.98E-6$) and the Cytokine-cytokine receptor interaction pathway ($p = 1.45E-6$). The Focal adhesion pathway represents the specialised structures that constitute the contact points between a cell and its surrounding ECM. These contact points, known as focal adhesions, are crucial for the regulation of various cellular processes such as motility, proliferation, differentiation, gene expression and survival (Wozniak et al., 2004). They contain both structural and signalling components which dynamically remodel depending on the tissue's state, initiating downstream events including PI3K (Reif et al., 2003) and MAPK (Carragher et al., 2004) signalling. Given the role of and signalling induced by focal adhesions, it is unsurprising that the Focal adhesion KEGG pathway extensively overlaps with both the ECM-receptor interaction and Cytokine-cytokine receptor interaction pathways (though the latter is discussed in the context of its implication by cytokine measurements collected presently; see Chapter 5). The ECM-receptor interaction pathway represents the molecules relating extracellular matrix macromolecular components, such as collagen, to transmembrane molecules, such as integrins (Geiger et al., 2001). In the same manner as the focal adhesion pathway, representation of the ECM-receptor interaction pathway reflects the regulation of genes associated with adhesion, migration, differentiation, proliferation and apoptosis (Kanehisa et al., 2017). The functional overlap of the Focal adhesion and ECM-receptor interaction pathways are explicitly represented by their shared genes, which largely consist of integrins. Integrins are heterodimers composed of α and β subunits, of which several variants

were differentially regulated in the present study; these included ITGA1 ($p = 0.005$), ITGA2 ($p = 0.001$), ITGA3 ($p = 0.006$), ITGA6 ($p = 0.009$) and ITGA11 ($p = 0.018$) α subunits and the ITGB1 ($p = 0.004$) β subunit (see Supplementary Table 1). Without correlating functional or protein-level data, the differential expression of any single gene is not meaningful out of the context of a functional network identified via enrichment analysis. Such correlates for these particular networks were not pursued within this project due to time restraints though, were this work to be undertaken, the single gene data may inform the hypothesis. A particular matter of interest they could inform in a continuation of the present study is the relative contribution of various cell types to differential expression within these signalling pathways, as RNA was isolated from whole skin tissue. For example, the cells with the highest expression of the integrin subunits as reported by the Human Protein Atlas are as follows: fibroblasts express ITGA1 and ITGB1, melanocytes express ITGA2, ITGA11 and ITGB1 while keratinocytes and Langerhans cells express ITGA11 (Uhlén et al., 2015). The differential expression of a gene exclusive to a particular skin cell type may implicate the activity of that cell in burn injury, though it is only a rudimentary estimation which can at best inform further study. Therefore, while significantly-represented pathways cannot be reliably reverse-engineered to implicate particular cell types within a complex sample or apply them to broader pathological processes in isolation, each of them represents an exciting avenue for further research which can develop their interpretation with functional and/or protein level data as demonstrated in the coming chapters. Beyond the Focal adhesion and ECM-receptor interaction pathways, the theme of structural and functional interaction between the cell and its surroundings is further represented in four of the sixteen most significant GO terms implicated presently, namely Collagen binding ($p = 1E\text{-}11$), Integrin

binding (p = 1.8E-8), Extracellular matrix binding (p = 1.7E-6) and Cell adhesion molecule binding (p = 1.9E5). Indeed, the Cell adhesion molecules KEGG pathway, consisting of membrane glycoproteins and their functionally-coupled proteins mediating the control of haemostasis, the immune response and inflammation (Kanehisa et al., 2017), ranked 6th among the most represented KEGG signalling pathways (p = 7.98E-6). Despite their functional similarity, its genetic overlap with the Focal adhesion and ECM-receptor interaction pathways is restricted mostly to several shared integrin subunits (only two of which, ITGA6 and ITGB1, were differentially regulated presently). It is nonetheless a viable point for further investigation. So too are two further KEGG pathways which, while not following the theme of cell-ECM interaction, nonetheless represent processes that are clinically relevant in burn injury; namely, the Complement and coagulation cascades (p = 0.0004) and Vascular smooth muscle contraction (p = 0.0007). The blood coagulation component of the former pathway is represented by a series of proenzyme-serine protease conversions which lead to the formation of thrombin, the enzyme responsible for the conversion of soluble fibrinogen to the insoluble fibrin (Kanehisa et al., 2017). Vascular smooth muscle cell contraction is mediated by increases in cytosolic Ca^{2+} activating the CaM-Myosin light-chain kinase, phosphorylation of Myosin light chain 20, myosin-actin interaction and thereby contractile force that reduces the blood vessel's diameter, as is reflected in the KEGG pathway's genes (Kanehisa et al., 2017). Both hypercoagulability and vasoconstriction contribute to hypoperfusion and the consequent ischaemia by which burn wound trauma progresses (see Section 1.1.3.2.3); their present implication could be of significant clinical interest and warrants further study.

In conclusion, the data presented in this chapter indicate global differences in gene expression between burn and control skin but not between their innervating DRG. This work is the first reported application of gene sequencing to these tissues or, importantly, to any local (rather than systemic) sample type in burns research. The data indicate a novel significant burn effect specifically at skin-level, while any possible changes in transcription induced by afferent signal transduction following the burn appear to be too minor for detection by global expression profile comparison. Several evaluation methods were employed to ensure the quality of the RNA and library preparation, which was found to be high as indicated by the high correlation between biological replicates and between samples from the same tissue where no experimental effect was apparent. Statistical analysis successfully identified discriminant genes underlying the separation between burn and control skin expression profiles. These, along with their functional networks as identified by enrichment analyses, can now be called upon in the following chapters as their potential roles in burn injury emerge in the context of related protein-level data.

5 CHAPTER 5 – THE INTERSTITIAL CYTOKINE PROFILE OF BURNED SKIN

5.1 Introduction

Burn injury induces a severe and immediate inflammatory response that can persist for weeks (Finnerty et al., 2009; Jeschke et al., 2007). Both locally and via the induction of systemic inflammatory response syndrome (SIRS), inflammation is thought to contribute to several aspects of the injury requiring high-priority clinical consideration. For example, systemic effects include hypermetabolism (Herndon et al., 1989; Orman et al., 2011), compromised organ function and structure (de Bandt et al., 1994; Finnerty et al., 2008; Wray et al., 2002), capillary permeability and peripheral/splanchnic vasoconstriction, leading to hypovolemia and thereby end organ hypoperfusion (Farina et al., 2013; Papp et al., 2003), bronchoconstriction, leading to respiratory problems (even in the absence of an inhalation injury; Liffner et al., 2005; Prout, 2014; Shults et al., 2015; Turnage et al., 2002), coagulopathy, leading to microvascular and subsequently organ pathogenesis (Farina et al., 2013; Rehberg et al., 2012) and immune system suppression (Constantian, 1978; Pileri et al., 2008). These pathologies underlie the development of SIRS (Constantian, 1978; Pileri et al., 2008; Schulte et al., 2013), shock (Farina et al., 2013; Papp et al., 2003; Rackow et al., 1987), and multiple organ dysfunction syndrome (MODS; Beal et al., 1994; Hatakeyama et al., 2014), conditions to which burn mortality is principally attributed (Goodarzi et al., 2014; NIH, 2013; Williams et al., 2009). These systemic effects develop from the local burn pathology, the necrotic progression of which is

advanced by inflammatory mediators via increased oxidative stress, cell death, hypoperfusion, vascular dysregulation, coagulation, neutrophil adherence and fibrin deposition (Coran, 2012; Dang et al., 2006; Latha et al., 2001; Shupp et al., 2010). Treating further and long-term consequences of the injury localised to the burn site, such as pain, compromised function and mobility, and their associated social and psychological problems, also remains a major clinical challenge (see Introduction).

Establishing the roles of cytokines as inflammatory mediators in burn pathology presents a clear novel therapeutic avenue. Progress has been made in elucidating the influence of a select few cytokines, most prominently TNF-α, IL-β and IL-6 (de Bandt et al., 1994; Drost et al., 1993), though our current understanding is insufficient for clinical influence and requires development on several fronts. Firstly, the synergistic nature of inflammatory mediators implicates cytokines beyond those previously established and supports exploration with multiplex platforms. Secondly, while systemic samples are attractive because of their accessibility and the advantages of continuous sampling, they do not necessarily reflect burn site inflammatory mediator levels (and can in fact be misleading; Papp et al., 2005); elucidating local pathology informs on both specific burn site effects and on systemic effects stemming from them. Thirdly, burn injury is a progressive, temporally complex pathology; the levels of inflammatory mediators should be assessed accordingly with as high a temporal resolution as possible, though most sampling methods enforce a compromise between temporal information and specificity to the burn site. Fourthly, regarding this temporal complexity, there is much to learn about the immediate post-burn inflammatory profile which cannot be defined in a clinical setting. This study aimed to address these issues by assessing the local time course concentration

profiles of 27 cytokines simultaneously in a deep partial-thickness rat model of scald-type burn injury, using subcutaneous microdialysis as a continuous sampling method for 0.5 hours pre- and 3 hours post-burn.

5.2 Results

Among the twenty-seven cytokines, eleven had a sufficient number of detectable readings for a meaningful comparison and were brought forward for analysis. A single outlier, within Eotaxin's control site pre-burn measurements, was detected by Grubb's testing (p = 0.00309) and removed from the analysis. Burn injury elevated the concentrations of two cytokines, leptin ($F(1,52) = 24.20935$, FDR-corrected p = 0.0002) and fractalkine ($F(1,52) = 7.04694$, FDR-corrected p = 0.0478), as indicated by the significance of the interaction between microdialysis site and time. Both had similar profiles, consisting of a rapid and sustained increase in concentration specific to the burn site that far exceeded any release due to probe insertion. The borderline statistically significant interactions for two further cytokines, GM-CSF and Eotaxin, did not survive the correction for multiple comparisons; this seems appropriate, with any stable burn-effects occurring over negligible concentration ranges.

One cytokine, EGF, had a significant site effect indicating a sustained difference in baseline between the burn and control microdialysate present before and after the burn. The higher average burn site concentrations are therefore not considered a burn effect. IL-18 and IL-1α had significant effects of time (p = 0.0002 and >0.0001 respectively), indicating that the probe insertion induced a similar release at both

Cytokine	Number of Recordings above Minimum Detection Threshold	2-Way RM ANOVA Term	Test Statistics	FDR-Adjusted P-Value
Leptin	38	Site	F(1,52) = 5.1819	0.0890
		Time	F(1,52) = 6.84894	0.0478
		Site*Time	F(1,52) = 24.20935	0.0002
Fractalkine	32	Site	F(1,52) = 13.86752	0.0040
		Time	F(1,52) = 0.44631	0.5976
		Site*Time	F(1,52) = 7.04694	0.0478
GM-CSF	18	Site	F(1,52) = 0.00776	0.9301
		Time	F(1,52) = 0.53569	0.5714
		Site*Time	F(1,52) = 4.53891	0.1136
Eotaxin	17	Site	F(1,51) = 0.10196	0.7992
		Time	F(1,51) = 0.58953	0.5663
		Site*Time	F(1,51) = 3.70434	0.1520
EGF	55	Site	F(1,52) = 9.29601	0.0238
		Time	F(1,52) = 6.40629	0.0529
		Site*Time	F(1,52) = 2.46763	0.2522
IL-18	48	Site	F(1,52) = 6.90986	0.0478
		Time	F(1,52) = 22.81937	0.0002
		Site*Time	F(1,52) = 1.56526	0.4068
IP-10	46	Site	F(1,52) = 0.77662	0.5045
		Time	F(1,52) = 4.35298	0.1151
		Site*Time	F(1,52) = 1.43926	0.4068
IL-2	11	Site	F(1,52) = 0.94578	0.4811
		Time	F(1,52) = 2.61669	0.2522
		Site*Time	F(1,52) = 0.1923	0.7291
IL-4	19	Site	F(1,52) = 1.51107	0.4068
		Time	F(1,52) = 0.84368	0.4986
		Site*Time	F(1,52) = 1.06596	0.4600
RANTES	43	Site	F(1,52) = 1.09071	0.4600
		Time	F(1,52) = 1.37353	0.4068
		Site*Time	F(1,52) = 2.48964	0.2522
Il-1α	13	Site	F(1,52) = 0.20792	0.7291
		Time	F(1,52) = 59.02708	<0.0001
		Site*Time	F(1,52) = 0.05398	0.8427
IL-12p70	8			
LIX	8			
IL-5	7			
IL-6	6			
TNFα	5			
IL-10	5			
GRO/KC/CINC-	2			
IL-1β	1			
IL-13	1			
MCP-1	1			
MIP-2	1			
IFNγ	0			
IL-17A	0			
G-CSF	0			
MIP-1a	0			
VEGF	0			

Table 5 2-Way ANOVA statistics for 11 cytokines. Cytokines for which concentrations were high enough to be unambiguous in at least 20% of microdialysate fractions were brought forward for statistical analysis. The terms were site (where a significant result indicates that there was a consistent difference between measurements reflecting a fundamentally different tissue state regardless of the burn), time (where a significant result indicates that both burn and control concentrations were altered similarly between the pre- and post- burn microdialysates) and their interaction (where a significant result indicates that the difference in one term depends on the difference in the other, in this case reflecting an effect of the burn).

sites that was unaffected by the burn. Their shared profile consists of a transient increase in concentration at both sites specific to the first and only pre-burn microdialysate fraction; it both supports the success of the half-hour flush period in minimising interference with burn effects and has interesting implications for the roles these cytokines may play following some types of trauma, even if not burn injury.

Next-Generation gene sequencing of RNA isolated from both burn and control microdialysis sites enabled detection of the expression of 26404 genes, 2610 genes of which were identified as differentially expressed as detailed in Chapter 4. These included 1186 up-regulated and 1424 down-regulated genes in burned skin compared to control skin (Fig. 17 and Appendix; Supplementary Table 1). Genes for all 11 cytokines included in the time course analyses were detected in the RNA sequencing, though only leptin and RANTES, had statistically significant differences between the burn and control measurements (Table 2). Leptin expression was lower in the burn microdialysis site than it was contralaterally, whereas RANTES RNA was recorded higher in the burned skin (Table 2). Leptin was therefore the only cytokine

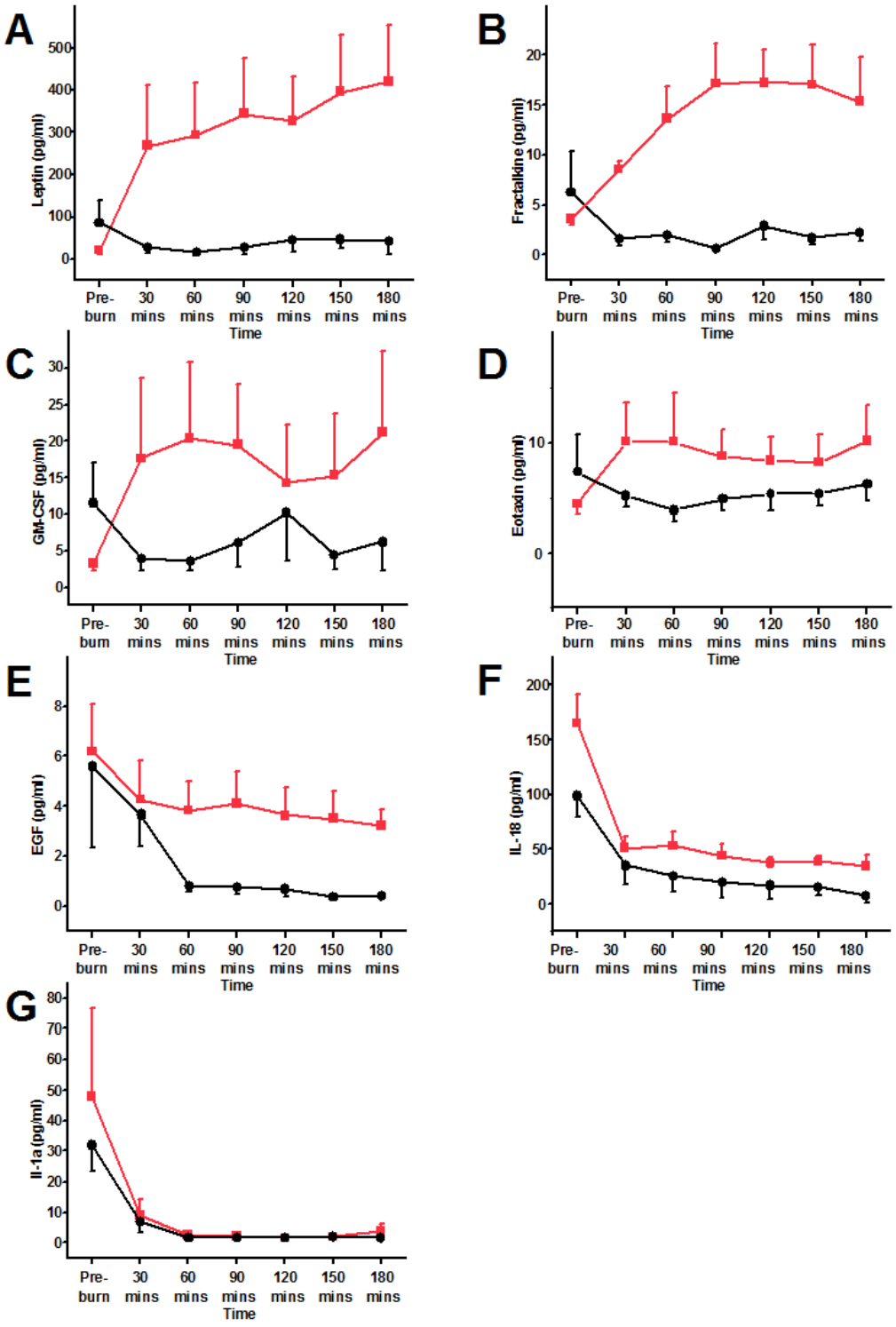


Figure 18 Seven cytokines exhibited interesting temporal profiles. Leptin (**a**) and fractalkine (**b**) were both significantly elevated by the burn, as indicated by their significant site x time interactions. GM-CSF (**c**) and eotaxin (**d**) both bordered significant interactions prior to FDR-adjustment; further study powered by more subjects may be worth pursuing. EGF (**e**) indicated the success of the analysis in its identification of microdialysis site as the

principal source of the evident difference in concentration profiles, despite what first appears to be a burn-specific elevation. Il-18 (**f**) and IL-1α (**g**) were both elevated by the probe insertion and recovered, but were seemingly not altered by the burn as is reflected in their extremely significant time effect p-values.

to be altered by the burn at both protein and RNA levels, as fractalkine transcription was apparently not altered and nor was protein expression of RANTES.

Enrichment analysis of pathways as described in the KEGG and Gene Ontology (GO) databases was also performed on the list of differentially expressed genes. A pathway is enriched where a significant proportion of the genes annotated to it are differentially expressed, and in such cases it is therefore likely that an enriched pathway is affected by the treatment. While comparing RNA levels of one gene can offer insight into specifically into a single protein's transcription, enrichment analyses are the primary utilisation of sequencing libraries such as that prepared in this study. Here, the significantly burn-enriched KEGG pathways included Cytokine-cytokine receptor interactions (p = 1.45E-6; Fig. 19) and the Jak-STAT signalling pathway (p = 0.0107; Fig. 20). Several cytokine-related GO terms, such as cytokine activity, cytokine binding and response to cytokine, were also significantly enriched in the biological process and molecular function categories (Supplementary Table 2).

Table 6 RNA comparisons of all cytokines and related genes discussed in this chapter. Comparing expression between burn and control microdialysis sites using gene sequencing can indicate the regulation of a protein at a transcriptional level; this table summarises the findings for all cytokines and related proteins discussed in this chapter. P-values are FDR-adjusted, rank indicates their position in ascending order of significance within the whole dataset.

Gene Name	Burn Mean	Control Mean	Burn StDev	Control StDev	Adjusted p-value	Rank
Lep	0.21316262	3.03482539	0.29621418	1.17808289	0.00040954	24
Cx3cl1	6.41431846	7.66708843	1.5350251	1.26099887	0.4501441	12986
Csf2	0	0	0	0	0	0
Ccl11	1.955853	2.4513641	2.4636665	0.33335325	0.16898033	3850
Egf	0.01681421	0.01438554	0.01258931	0.01339773	0.68764393	11991
Il18	81.3226357	73.7738312	64.4043336	14.706829	0.62279472	12976
Cxcl10	3.29117243	3.65233692	3.07506088	3.85381783	0.37180416	6307
Il2	0	0	0	0	0	0
Il4	0	0	0	0	0	0
Ccl5	15.2873322	0.96538362	6.61751593	0.699095	0.00147864	102
Il1a	2.57446798	3.86056081	1.82738903	0.48005844	0.056372	5097
Il12a	0.55799923	0.43280074	0.28074771	0.23820292	0.7212409	13503
Il12b	0	0	0	0	0	0
Lix1l	20.4316856	27.1330228	12.6462263	5.46614092	0.1963882	8528
Il5	0	0	0	0	0	0
Il6	26.7144794	3.53063278	48.9276017	4.23804029	0.54820902	7547
Tnf	0.57414863	0.30792822	0.67837223	0.1949945	0.90075334	15690
Il10	0.20908594	1.74913211	0.35431031	0.96929975	0.00515146	243
Cxcl1	167.704597	20.5209432	228.036002	8.66971026	0.80860304	13409
Il1b	90.8011644	10.9624338	81.22769	3.6518654	0.01319049	836
Il13	0	0	0	0	0	0
Ccl2	57.3292878	19.9154122	82.1573301	16.5970914	0.95413777	16972
Cxcl2	35.2049912	6.41167979	48.9490876	3.56556134	0.80458575	12709
Il17a	0	0	0	0	0	0
Csf3	21.3059759	3.41369707	39.1239251	3.71511236	0.76606861	12755
Vegfa	20.2163149	18.3399552	2.56926389	4.06171222	0.51476918	13956
Ccl3	4.78728485	0.48015166	4.90521559	0.09437962	0.04856042	1659
Il6r	19.720364	33.7753127	4.34447048	10.8077982	0.0137999	5773
Il12rb2	0.41532974	0.05090198	0.12408785	0.05353214	0.00054202	355
Il12rb1	0.53333898	0.1429444	0.12288385	0.05006038	0.00642466	1859
Jak2	13.3135521	23.3020375	4.02660966	3.20954097	0.00086344	3530
Stat3	51.8983791	83.2250292	7.89815494	14.1082477	0.00138206	4843
Nfkb1	23.2064228	32.3564083	7.08500454	6.85644115	0.0245734	8087
Bcl2l1	24.0003249	13.131359	10.1958061	2.76792338	0.00510545	4686
Tbx21	0.22782487	0.00388767	0.26735323	0.00777534	0.01323017	1610
Ifng	0	0	0	0	0	0
Jak3	7.73173404	1.79498681	1.74242464	0.29267644	2.02E-07	289
Jak1	35.4865851	62.2365747	7.56307903	7.14303784	0.00238127	4132

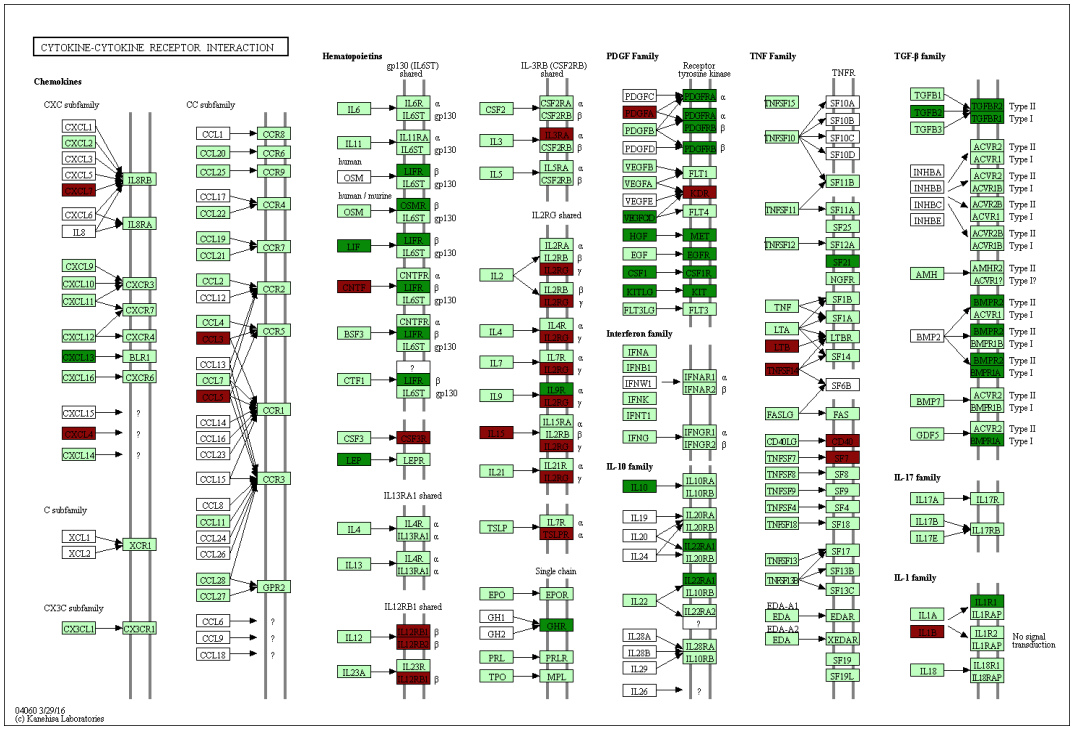


Figure 19 KEGG map of cytokine-cytokine receptor interaction pathway. 48 of the 156 genes annotated to this pathway as defined by the KEGG database were identified as differentially expressed between burn and control microdialysis site RNA. Differentially expressed genes are labelled green for down-regulation and red for up-regulation.

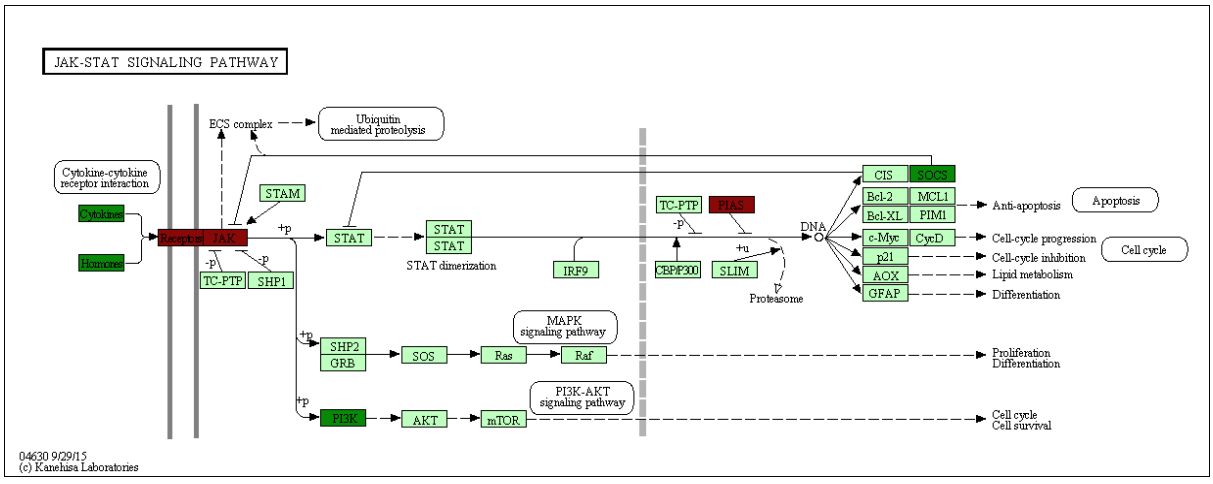


Figure 20 KEGG map of the Jak-STAT signalling pathway. 27 of the 110 genes annotated to this pathway as defined by the KEGG database were identified as differentially expressed between burn and control microdialysis site RNA. Differentially expressed genes are labelled green for down-regulation and red for up-regulation.

5.3 Discussion

5.3.1 Leptin as an Inflammatory Mediator

Continuous interstitial sampling is an important and underutilised approach to burn injury research. Here, it enabled the identification of two cytokines significantly increased following a deep-partial thickness burn injury, for which there is extensive support for several potential roles in the progression and resolution of the pathology. The first cytokine that the present study determined to be elevated locally in burn injury was leptin. To our knowledge, this is a novel finding. Leptin is a hormone principally known for its roles in regulating appetite and energy expenditure, though it draws attention in pathological states for its interaction with immune cells, as reviewed by Fernández-Riejos et al. (2010). In rodents, macrophage phagocytosis and proinflammatory cytokine expression is reduced with genetic abnormalities in leptin or leptin receptors but increased with the application of exogenous leptin (Loffreda et al., 1998). Further, leptin deficiency confers susceptibility to inflammatory stimuli and dysregulation of cytokine production, while circulating leptin levels increase with inflammation and infection (Faggioni et al., 2001; Sarraf et al., 1997). In cultured macrophages, leptin dose-dependently induces release of TNFα and IL-6 from monocytes alongside CC chemokine expression by activation of the Janus kinase 2d-Signal Transducer (JAK2)-Activator of Transcription 3 (STAT3) pathway. Leptin further activates circulating human monocytes (Santos-Alvarez et al., 1999) and it induces from them the secretion of interleukin 1 receptor antagonist and IP-10 upregulation (Gabay et al., 2001; Meier et al., 2003). Other supported actions on monocytes include preventing apoptosis (Najib et al., 2002), oxidative

burst stimulation (Sanchez-Pozo et al., 2003), regulation of oxidative stress (Maingrette et al., 2003) and chemotaxis (Gruen et al., 2007). Leptin acts on dendritic cells to increase IL-1β, IL-6, IL-12, TNFα, and MIP-1α production, promote cell survival, drive native T cell polarisation toward Th1 phenotype and protect from spontaneous and UV burn-induced apoptosis (with consistent NF-κB activation and up-regulation of bcl-x_L gene expression; Mattioli et al., 2005). Similarly, leptin promotes survival in human polymorphonuclear neutrophils (PMN; Bruno et al., 2005; Zarkesh-Esfahani et al., 2004) as well as regulating their chemotaxis (Caldefie-Chezet et al., 2003; Faggioni et al., 2001; Ottonello et al., 2004). It further increases eosinophil cell surface adhesion molecule expression and stimulates their release of IL-1β, IL-6, IL-8, growth-related oncogene-α and MCP-1 (Wong et al., 2007). Leptin's actions extend to natural killer cells, including development and differentiation, activation and cytotoxicity (Fernandez-Riejos et al., 2010; Matarese et al., 2005). Beyond these roles in the innate immune system, leptin has several functions in adaptive immunity such as its anti-apoptotic effect on T cells and consequent maintenance of lymphoid organs (Fantuzzi et al., 2000; Howard et al., 1999; Lord et al., 1998). It enhances lymphocyte and splenocyte proliferation in rodents (Demas, 2010), along with T cell levels and cytokine production in humans suffering endometriosis (Milewski et al., 2008). Beyond these proliferative effects, leptin enhances expression of early and late activation markers in human lymphocytes when co-stimulated with mitogens (Martin-Romero et al., 2001; Martin-Romero et al., 2000; Sanchez-Margalet et al., 2001; Sanchez-Margalet et al., 2002; Sarraf et al., 1997); T cells express the Ob receptor upon activation, possibly explaining the requirement of co-stimulation (Sanchez-Margalet et al., 2002), and leptin enhances T cell production of cytokines including IL-2 and IFNγ accordingly

(Martin-Romero et al., 2000). Leptin's polarisation of T cells toward a Th1 phenotype (described above) appears to be dependent on it effecting the up- and down-regulation of several cytokines (Martin-Romero et al., 2000; Napoleone et al., 2007; Santos-Alvarez et al., 1999), where reduced expression of key Th1 and Th2 transcription factors T-bet and GATA-3 confers protection from Th1 and Th2-dependent inflammation and leptin is a key regulator of CD4(+) T cell polarisation in this context (Batra et al., 2010; Liu et al., 2009). Consistent with the anti-apoptotic properties detailed above, leptin promotes T cell survival in stress-induced apoptosis, again via bcl-xL (Fernandez-Riejos et al., 2008; Fujita et al., 2002). Further, leptin can reduce regulatory T cell proliferation (Matarese et al., 2008). Between its roles in the innate and adaptive immune systems, leptin must be considered a proinflammatory mediator and potential therapeutic target within excessively-inflammatory conditions such as burn injury.

5.3.2 Leptin in Burn Injury

While this study is the first to identify leptin's local post-burn elevation, its systemic upregulation has been reported previously. Given the extensive mechanistic implication of leptin in immune regulation, it is unsurprising that circulating leptin has been found to increase with sepsis/ SIRS both in and out of a burn injury context (Abdel-Hafez et al., 2007; Arnalich et al., 1999; Greenhalgh, et al., 2007; Kino et al., 2003; Torpy et al., 1998); it has been suggested that leptin promotes survival in acute sepsis (Correia et al., 2001) and, if administered post-burn, attenuates inflammation and multiple organ failure (Cakir et al., 2005). Another post-burn function for leptin is suggested in metabolism, following the observation that it

increases with the ensuing of the anabolic state with the initiation of enteral feeding (Bar-Yosef et al., 2014). Its usual inverse association with body mass in plasma is reversed following burn injury; it is suggested that this is a result of secondary mediation by cytokines (Wade et al., 2013). Indeed, some conclude that, given the controversy surrounding leptin's association with IL-6 (which, notably, was not found to be elevated presently), and its apparent association with IGF-1, leptin levels may reflect metabolic state rather than that of inflammation (Bar-Yosef et al., 2014). Further, a role for leptin in angiogenesis following burn injury is well supported. Endothelial cells express the receptor Ob-R; its activation by leptin mediates endothelial cell proliferation, along with tyrosine phosphorylation of the receptor and STAT-3 and Erk1/2 activation (Bouloumie et al., 1998; Sierra-Honigmann et al., 1998). Leptin's angiogenic actions, including neovascularisation and capillary-like structure formation, have been observed both *in vivo* and *in vitro* (Bouloumie et al., 1998; Sierra-Honigmann et al., 1998), including with exogenous application following burn injury (Liapaki et al., 2008), and are not observed in ob/ob mice (Ring et al., 2000). Leptin has been implicated in further epithelial processes via its role as a potent mediator of keratinocyte proliferation. It acts directly on keratinocytes located at wound margins (Frank et al., 2000), putatively via the ObRb-receptor subtype that is specifically expressed in proliferating keratinocytes of non-wounded skin and hyperproliferative epithelia during repair; indeed, specific signalling deficiency for this subtype confers severe disorders in wound healing (Tsuboi et al., 1992). Beyond *in vivo* demonstration of leptin-ObRb signalling's importance in wound healing (Frank et al., 2000), leptin has shown mitogenic actions on human endothelial cells (Bouloumie et al., 1998), peripheral blood monocytes (Santos-Alvarez et al., 1999), tracheal epithelial cells (Tsuchiya et al., 1999), pancreatic beta cells (Islam et al.,

1997) and homopoietic cells (Gainsford et al., 1996) *in vitro*. It has been established that, at ObR, leptin activates Jak kinases to subsequently recruit and phosphorylate STAT proteins (Ghilardi et al., 1996; Vaisse et al., 1996). In-keeping with this, leptin has been shown to activate STAT3 in keratinocytes (Frank et al., 2000), while STAT3-deficient mice exhibit severely impaired wound healing (Sano et al., 1999). Leptin further increases corticotrophin-releasing factor expression alongside arterial pressure in rats (Correia et al., 2001; Mark et al., 1999). Following the observation of its increased plasma levels with post-burn hypovolaemia, it has been suggested that leptin's elevation may be a response to low blood pressure (Kino et al., 2003). Further, leptin levels are increased with surgical stress, for which it has been suggested as a candidate mediator (Ahima et al., 1996; Bornstein, 1997; Kino et al., 2003; Wallace et al., 2000). Finally, leptin's potential contribution to the generation of the neuropathic component of burn injury pain requires consideration. Leptin may act immediately on macrophages following its release from adipocytes in the periphery to facilitate the development of neuropathic pain. Indeed, it is by stimulation of the JAK-STAT pathway in macrophages, and the subsequent production of molecular substrates for neuropathic pain, that it has been shown to induce tactile allodynia (Maeda et al., 2009). However, leptin can also be transported to the central nervous system (Banks, 2004; Banks et al., 1996; Harvey, 2007; Myers, 2004), where it is also thought to contribute to neuropathic pain development by inducing the upregulation of spinal NMDARs following nerve injury, again in a manner dependent on JAK-STAT signalling (Lim et al., 2009; Tian et al., 2011). It is further worth noting that specific roles for leptin are being elucidated in the generation of chronic pain associated with particular pathologies; for example, via Ob-R and JAK2-STAT3 signalling and in an estrogen-dependent manner, it produces chronic pain in a rodent

model of endometriosis (Alvarez et al., 2014). Importantly, the involvement of several of leptin's above-mentioned potential post-burn activities is supported by the gene sequencing analysis. mRNA for JAK2 and STAT3 are significantly reduced while that of JAK3 is significantly increased (Table 6). Further, gene expression for NF-κB, bcl-xL and T-bet, which are responsible for leptin-induced T cell polarisation toward the Th1 phenotype (Batra et al., 2010; Liu et al., 2009; Mattioli et al., 2005), is elevated by the burn. Further still, mRNA expression of several leptin-regulated cytokines, including IL-1β and IFNγ, exhibit significant and nearly significant increases following burn injury in the skin.

5.3.3 Fractalkine as an Inflammatory Mediator

The second cytokine confirmed to be elevated locally in burn injury in the present study is fractalkine. A particularly interesting aspect of this cytokine within the context of this study is its implication in inflammatory processes, as reviewed by Jones et al. (2010). Fractalkine is synthesised as a transmembrane structure, consisting of an extracellular portion wherein a chemokine domain is attached, via a mucin-like stalk, to a transmembrane domain with a cytoplasmic tail (Umehara et al., 2004). The chemokine domain can be cleaved from the transmembrane portion at the mucin-like stalk by at least two enzymes, ADAM10 and ADAM17, which respectively function under normal and inflammatory conditions (Garton et al., 2001; Hundhausen et al., 2003; Hundhausen et al., 2007). As such, fractalkine can exist in a soluble or membrane-bound form (Garton et al., 2001; Hundhausen et al., 2003; Hundhausen et al., 2007). Its soluble form functions as a chemoattractant for monocytes, natural killer cells and T cells (Bazan et al., 1997; Imai et al., 1997; Lucas et al., 2003), while

its membrane-bound form, which can be induced on endothelial cells by proinflammatory cytokines including TNFα, IFNγ and IL-1 (Garcia et al., 2000) functions as a shear-resistant adhesion molecule for CX3CR1 leukocytes (Jones et al., 2010). CX3XR1 is hence a highly selective receptor and cytotoxic effector lymphocyte surface marker. This, alongside fractalkine's expression in inflammatory conditions, such as by monocytes, macrophages, fibroblasts, endothelial and dendritic cells in synovial tissue with rheumatoid arthritis (Ruth et al., 2001), has motivated interest in the fractalkine/CX3XR1 coupling's potential roles in immune control and inflammation. Putative roles for fractalkine have hence been identified in a variety of pathologies. Its chemoattractive action on and activation of NK cells at inflamed sites causes the lysis of local endothelial cells (Yoneda et al., 2000). The fractalkine consequently expressed on the inflamed epithelium is suggested to enable the capture of CX3XR1-expressing cytotoxic effector cells and their migration into tissue; this may be a fundamental vascular gateway mechanism for the immune system (Jones et al., 2010; Umehara et al., 2004). Atherosclerotic plaque formation depends in part on chemokines directing foam cell precursors to the vessel wall. Fractalkine, the infection-induced production of which is stimulated by IFNγ, TNFα and IL-1 in epithelial cells, is thought to contribute to the formation and rupture of atherosclerotic plaques (Glass et al., 2001; Hansson, 2001; Umehara et al., 2004) and is upregulated in atherosclerotic lesions of apolipoprotein E-deficient mice; the additional knockout of CX3CR1 reduces atherosclerotic lesion formation (Combadiere et al., 2003; Lesnik et al., 2002). Accordingly, increased fractalkine and CX3CR1 expression has been found in the monocytes, T lymphocytes and NK cells of ruptured coronary plaques in patients with unstable angina pectoris (Ikejima et al., 2010). Further, the absence of the M280 allele in CX3CR1, T280M being a CX3CR1

polymorphism that confers reduced cell adhesion, is associated with a fourfold increase in risk of carotid atherosclerosis (Kimouli et al., 2009). Rheumatoid arthritis (RA) is an inflammatory condition in which chemokines mediate the immune cell influx and subsequent cartilage degradation and pannus formation, along with the angiogenesis and cell proliferation, that underlies synovial hyperplasia within the pathology (Iwamoto et al., 2008). Fractalkine contributes to these processes, which ultimately destroy the joint, through both its roles in chemotaxis and adhesion. Supporting evidence includes the high percentage of synovial macrophages (Koch, 2005) and monocytes expressing CX3CR1 (Ruth et al., 2001), elevated soluble fractalkine in synovial fluid (Ruth et al., 2001), the expression of fractalkine by monocytes in synovial fluid and peripheral blood and by macrophages, fibroblasts, endothelial and dendritic cells in synovial tissue (Ruth et al., 2001) and the local increase of CX3CR1-expressing CD8+ T cells in RA (Nanki et al., 2002). Fractalkine's proangiogenic function has been demonstrated both *in vitro* and *in vivo*, and its immunodepletion results in both decreased human dermal microvascular endothelial cell chemotactic activity and decreased synovial fluid angiogenic activity (Volin et al., 2001). Fractalkine has further been implicated in HIV, which compromises the immune system and induces a gradual inhibition of adaptive immunity (Becker, 2007). Its expression is increased in the brain and lymph nodes of HIV patients (Foussat et al., 2001; Tong et al., 2000), and it has a neuroprotective effect when co-administered with the HIV-1 neurotoxin platelet activating factor or the regulatory HIV-1 product Tat *in vitro*; it is suggested that this effect could be exerted in the brain via the recruitment of peripheral macrophages, following focal inflammation induced by HIV (Tong et al., 2000). Further, where CX3CR1 functions as a co-receptor with CD4 for the viral envelope-target cell fusion step necessary for

HIV-1 infection, this fusion is potently and specifically inhibited by fractalkine (Combadiere et al., 1998). Further, CX3CR1 polymorphisms dictate the rate of HIV's progression into the development of AIDS (Faure et al., 2003; Moatti et al., 2001), and CX3CR1 inhibition has been proposed as one element of a novel treatment slowing the progression of HIV (Becker, 2007). Indeed, targeting fractalkine/CX3CR1 coupling offers a novel therapeutic avenue in many of the pathologies described above, as it may do within burn injury and many other associated pathologies not discussed here. There is currently no treatment specifically targeting fractalkine/CX3CR1, though synthetic analogues have successfully supressed fractalkine/CX3CR1-mediated chemotaxis *in vitro* (A. Inoue et al., 2005) and non-specific drugs now known to reduce fractalkine/CX3CR1 function include baclofen (Duthey et al., 2010), epigallocat-echin-3-O-gallate (Lee et al., 2009) and rosiglitazone (Wan et al., 2010). Importantly, it has previously been shown with a full-thickness murine contact burn model that compromised CX3CR1 function decreases recruitment of CX3CR1 positive cells in the burn site, myeloid cell recruitment, new blood vessel maintenance and burn wound healing (Clover et al., 2011). While the concentration of fractalkine is significantly increased in the interstitium, its mRNA is not significantly changed (Table 6). It is possible that a proportion of fractalkine found in the interstitium is cleaved from fractalkine-synthesising cells invading the injured skin, and that its interstitial availability is not regulated at a transcriptional level in burn injury. The present study is the first demonstration of fractalkine's increased availability in burn injury, bringing its many above-listed pathophysiological roles into context. Elucidation of this chemokine and its potential therapeutic manipulation is motivated by its implication in a growing list of pathologies, to which burn injury can now be added.

5.3.4 Further Considerations

Beyond the two significantly elevated cytokines, the findings may warrant further study of GM-CSF and eotaxin; they exhibited interesting concentration profiles, though the statistical significance of GM-CSF's burn x site interaction did not survive the multiple comparisons correction and eotaxin narrowly missed out on significance prior to FDR adjustment (p = 0.06). GM-CSF has drawn particular interest for its influence on microvessel hyperpermeability, an element of burn pathology that precipitates the interstitial oedema leading to dysfunction of multiple organs and hypovolaemic shock in the acute phase of recovery (Kremer et al., 2008). After it was determined that GM-CSF accelerates epithelisation, vascularisation and contraction of various injuries (Groves et al., 2000; Mery et al., 2004), GM-CSF treatment was shown to increase angiogenesis and reduce microvessel permeability in a deep partial-thickness burn model (Zhao et al., 2015; Zhao et al., 2014) and reduce healing time in human deep partial-thickness burns, prompting a call for clinical trials (Zhang et al., 2016). A functional parallel can hence be drawn between GM-CSF, leptin and fractalkine. Blood GM-CSF levels have been shown to increase in humans following a >20% TBSA burn (Hur et al., 2015b), though others report the comparison being compromised by concentrations falling below quantifiable levels (Shelhamer et al., 2015), as is arguably the case with the microdialysates in the present study. Eotaxin has also been shown to induce angiogenesis via endothelial cells *in vivo* and it has been suggested that this contributes to wound healing in pathologies characterised by eotaxin's upregulation (Salcedo et al., 2001), though previous multiplex assays have not found a significant burn vs control increase in

eotaxin in blood samples from humans (Hur et al., 2015b) or rodent full thickness models (Orman et al., 2011).

Two cytokines, IL-18 and IL-1α, exhibited extremely statistically significant concentration increases induced by the insertion of the microdialysis probe; interestingly, their concentrations and RNA expression were unaffected by the burn. Both cytokines are members of the same structural IL-1 family and have pro-inflammatory functions. IL-18 is notable for both its implication in the progression of an extensive range of inflammatory and immune pathologies and protective effects in some disease models (Dinarello et al., 2013). Consistent with the present findings, IL-18 has not been found elevated locally in burn tissue to date, though has received interest in the field of burn injury research for its ability to delay neutrophil apoptosis following alcohol intoxication and burn injury (Akhtar et al., 2011), for its therapeutic potential in combating bacterial infection in burn patients (Kinoshita et al., 2011; Kinoshita et al., 2004) and ameliorating burn-induced acute lung injury (Sekine et al., 2009) and as a urinary indicator of acute kidney injury in burn patients (Ren et al., 2015). Its elevated presence in some but not all inflammatory conditions is intriguing and warrants further investigation. IL-1α is synthesised physiologically in its precursor form within epithelial cells and is abundant in the epidermis. It is released from cells upon damage or necrosis and subsequently contributes to the induction of inflammation and is hence considered a damage-associated molecular pattern molecule (Jensen, 2010). It is therefore interesting and perhaps telling that a deep partial-thickness burn did not increase its local interstitial concentration while the damage to the skin caused by the microdialysis probe insertion did. IL-1α is dynamic within the nuclei of living cells and is extravasated in necrotic conditions. However,

during apoptosis, it concentrates in dense nuclear foci, is rendered less mobile, and is hence not released with the cell's other cytoplasmic contents (Cohen et al., 2010). Our understanding of the dynamic cell death mechanism balance in burn injury is limited, though it has previously been shown that the ischemic zone adjacent to a third degree burn becomes necrotic 24 hours post-burn, having shown no signs of necrosis after only 30 minutes (Singer et al., 2008). The relative contribution of apoptosis and necrosis in the early stages of burn injury is an important and little-understood consideration for progressing therapeutic approaches. The IL-1α concentration profile exhibited in the present study extends what we understand to the "apoptotic period" of the pathology, indicating that a deep partial-thickness burn remains apoptotic for at least 3 hours following the insult.

The cytokine panel used in the present study was selected for its extensive coverage of immunomodulatory signalling molecules. Of the 27 analytes, only 11 were recorded at detectible concentrations in at least 20% of the microdialysate fractions. It is notable that the present measurements of IL-1β, IL-6 and TNFα, while insufficient for statistical analysis, are not necessarily inconsistent with the extensive prior implication of these cytokines in burn injury. All three may have been consistently detected post-burn previously, though the majority of these reports detail systemic levels of the analyte in circulation (Drost et al., 1993; Liu et al., 1994; Biffl et al., 1996; Kowal-Vern et al., 1994; Rodriguez et al., 1993; Struzyna et al., 1995; Yeh et al., 1999) as opposed to local burn-site concentrations. Approaches to local burn site sampling reporting elevation of these cytokines have included homogenised skin (Ipaktchi et al., 2006), adipose tissue lysate (Saraf et al., 2016) and blister fluid (Rhodes et al., 1999; Ono et al., 1995), none of which maintain or represent the

interstitium as a signalling environment to as great an extent as microdialysis. Even if they did, the concentration elevations reported occur over days or more; the present work is unique in its characterisation of the immediate post-burn signalling environment, and may reflect that more time is required for the immune response to engage in upregulating these particular immunomodulatory agents. Indeed, the previous applications of microdialysis to burns research reporting elevations of IL-1β and IL-6 (Angst et al., 2008) among other inflammatory mediators (Samuelsson et al., 2008; Machens et al., 2006) recorded beyond the presently-reported time frame. Their findings are consistent with the time course of the acute phase response, to which IL-1β, IL-6 and TNFα contribute, which far exceeds the three hours modelled presently (Colley et al., 1983). The relatively short duration of the experiment may therefore explain the limited number of consistently detectible cytokines measured, though may further highlight potential roles of leptin and fractalkine among the earliest mediators of the inflammatory response in burn injury.

In conclusion, two novel local inflammatory mediators, leptin and fractalkine, have here been identified in burn injury. The upregulation of the former at a transcriptional level is supported by the accompanying gene sequencing data and the elevation of the latter has never before been recognised in any tissue following burn injury. These cytokines have various potential roles in burn pathology, principally relating to the immune system and inflammation, and the results of the RNA-seq functional enrichment analyses indicate that cytokine functions are affected by the burn injury. The fact that IL-18 and IL-1α are elevated by the probe insertion but not the burn is interesting; in the context of this study, it supports the proposed rapid recovery of the interstitium from the probe insertion (by which inducing the burn after ~45 minutes is

justified) but calls attention to the fact that some of the response variables may be influenced by the sampling method. In any case, given the destructive, inflammatory nature of burn injury, the potential of leptin and fractalkine as targets for therapeutic intervention must be considered, albeit with a healthy appreciation for the potentially nonspecific nature of leptin's release and its pleiotropy.

6 CHAPTER 6 – TEMPORAL METABOLOMIC PROFILING OF THE BURN INJURY INTERSTITIUM

6.1 Introduction

Chapter 3 described the successful analysis of microdialysate by metabolomics using conventional multivariate analyses for metabolomics data (PCA and PLS-DA) to identify a difference between the burn and control metabolite profiles. This model could have been used for the selection of individual metabolites exhibiting the burn effect, but it was not; the analysis ended after establishing that there was a global difference in metabolite profiles, having fulfilled its intended purpose of validating the sampling methodology. This model was not pursued further as the data contain valuable information regarding the temporal progression of metabolite concentrations over the three hours immediately following a burn injury; the organisation of data over time would be ignored with PCA and its related methods. Having identified a burn effect and the success of the sampling technique, an analysis which could retain the temporal organisation of the data was required.

Metabolomics experiments generate high volumes of data which, while rich in information, can present analytical challenges. Standard discrimination methods, which identify response variables exhibiting an experimental effect, require multivariate data with low co-linearity. In this setting, the p-value is calculated under the assumption that the number of observations (e.g., measurements of each metabolite) is greater than the number of variables observed (e.g., metabolites). This is rarely the case for omics data, and in this case there are 56 observations (7 time

points x 2 microdialysis sites x 4 animals) of 42364 and 13829 metabolites for positive and negative mode ionisation respectively.

This identification problem is typically addressed in the analysis of metabolomics data by dimension reduction procedures such as PCA or discriminant-PLS. This enables the contribution of explanatory variables to be identified on the bases of the response variable scores (Nørgaard et al., 2006). Indeed, this approach was employed for the early analyses evaluating the feasibility of combining microdialysis with metabolomics. However, a drawback of PCA and related procedures is that they can, in principle, overlook interesting subspaces of the data. For example, retaining the major principal components assumes that the treatment effect is the largest source of variance in the response variable. In other words, the first few principal components may not reflect variation in the data resulting from a burn effect. Further, while substantial progress has been made in developing algorithms for both low level data processing (e.g. peak detection and alignment, baseline correction) and higher level modelling including classification and regression (Montana et al., 2011), the same cannot be said for the integration of temporal profiling in regression models.

Temporal metabolome profiling can provide vital insights into the pathogenesis or progression of disease states and many studies produce time course data, typically in the form of a repeated measures design. Nonetheless, typical metabolomic analyses do not include the organisation of the data over time, largely because of the high collinearity of the data, missing data and/or assumptions that the same results would be obtained when ignoring time effects (Montana et al., 2011). However, with a suitable analysis, retaining time course information should allow for the recognition

of different temporal profiles and increase the tests power. To this end, canonical variates analysis was used to model the multivariate effects of treatment effects over time.

Canonical variates analysis (CVA; also known as canonical correlation analysis, multivariate analysis of variance) finds mixtures of dependent (response) variables that correlate with mixtures of independent (explanatory) variables. Here, it was used to test for an effect of the burn in the metabolomics data. CVA shares the beneficial characteristics of other multivariate analyses, such as avoiding the need for multiple comparisons correction and addressing the high collinearity of the data (albeit accomplishing this differently, via singular value decomposition). Crucially, CVA is predicated on an explicit statistical model of the mapping between explanatory and response variables that incorporates random effects or error. In other words, unlike partial least-squares and related techniques, it has an explicit model of observation error that enables an optimal (in the maximum likelihood sense) identification of how treatment effects are expressed. Furthermore, CVA can incorporate time effects, and enables the detection of multiple temporal profiles. The particular effects of interest corresponded to interaction between microdialysis site (with two levels; burn and control) and the time of observation (with seven levels: the 30 mins pre-burn, then six half hour fractions post-burn for 3 hours). Put simply, the interaction of interest corresponds to a difference in metabolite concentrations over time between the burned and unburned skin. MATLAB routines from the Statistical Parametric Mapping 12b academic software (http://www.fil.ion.ucl.ac.uk/spm/), called by (in-house) batch scripts, were used to conduct the analysis.

This chapter presents the results of analysing the data with CVA, and thereby the selection of discriminant metabolite features exhibiting the burn effect. However, determination of a molecule's up- or down-regulation by the burn is meaningless without confirmation of the molecule's structure. The highly multivariate data obtained via exploratory MS, generated as described in Chapter 3 and analysed here, allows only for rudimentary structural estimates based primarily on the metabolite feature's *m/z* ratio, and perhaps partially on the feature's retention time and accidental fragmentation, which presents a fundamental problem in that different molecules can share the same *m/z* ratio. After presenting the application of CVA for the selection of burn-affected metabolite features to be explored, this chapter describes the elucidation of the discriminant metabolite structures as conducted via comparison of their chromatographic properties and fragmentation profiles with those of prepared standards.

6.2 Results

CVA, used to test for effects corresponding with interaction between microdialysis site and time among the concentration trajectories of the metabolites, identified significant effects consisting of an increasing then maintained contrast between burn and control concentrations over time in both ESI+ (Figs. 21a-c) and ESI- data (Figs. 22a-c). The burn effect was multi-dimensional in the positive-mode data, where a second canonical contrast representing a transient difference between burn and control metabolite concentrations was detected (Fig. 21e). Just as the contribution of any single metabolite to a separation expressed in PLS-DA can be quantified by their VIP value, the contribution of any single metabolite to these burn effects as identified

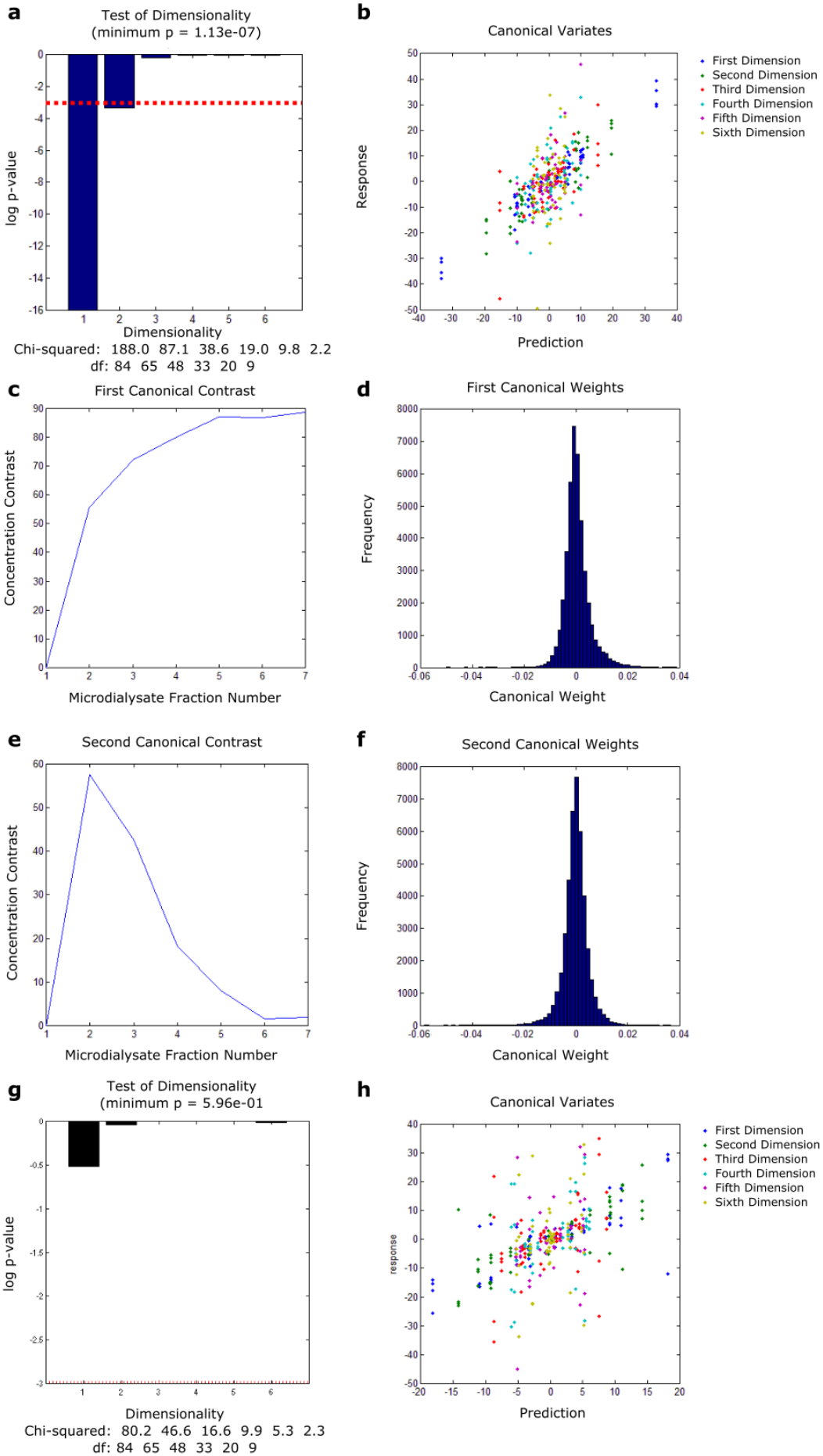

a
Test of Dimensionality
(minimum p = 1.13e-07)
log p-value
Dimensionality
Chi-squared: 188.0 87.1 38.6 19.0 9.8 2.2
df: 84 65 48 33 20 9
b
Canonical Variates
Response
Prediction
First Dimension
Second Dimension
Third Dimension
Fourth Dimension
Fifth Dimension
Sixth Dimension
c
First Canonical Contrast
Concentration Contrast
Microdialysate Fraction Number
d
First Canonical Weights
Frequency
Canonical Weight
e
Second Canonical Contrast
Concentration Contrast
Microdialysate Fraction Number
f
Second Canonical Weights
Frequency
Canonical Weight
g
Test of Dimensionality
(minimum p = 5.96e-01
log p-value
Dimensionality
Chi-squared: 80.2 46.6 16.6 9.9 5.3 2.3
df: 84 65 48 33 20 9
h
Canonical Variates
response
Prediction
First Dimension
Second Dimension
Third Dimension
Fourth Dimension
Fifth Dimension
Sixth Dimension

Figure 21 Canonical variates analysis of ESI+ UPLC-MS data. (**a**) expresses the log p-values, and the respective chi squared distributions and degrees of freedom on which they are based, where the red dash line indicates statistical significance. Each p-value represents a potential dimension of the metabolite concentrations' dependency on the explanatory variables; practically, each represents a different temporal profile that is conserved over the time courses of a subset of metabolites. (**b**) indicates the degree of correlation between mixtures of variables subtending the correlation whose significance is reported in the first subplot; a high correlation indicates a consistent temporal profile across explanatory variables. Where (**a**) indicates the significance of two temporal profiles, constituting a two-dimensional burn effect, (**c**) expresses the contrast in concentration trajectories in the first dimension; it consists of a sustained increase in difference between burn and control concentrations over time. (**d**) is a histogram of the metabolite contributions to the canonical correlation, and thereby their similarities to the temporal profile in (**c**); the skew suggests that a small number of metabolites contribute heavily to the treatment effect (site by time interaction), while most contribute negligibly. (**e**) and (**f**) respectively express the same as (**c**) and (**d**) for the second dimension of the burn effect; it is characterised by a transient increase in difference between burn and control concentrations. (**g**) and (**h**) respectively present p-values and variable mixture correlations for the same analysis of the data following randomisation of its order within individual metabolite time series; the lack of a significant result here, with treatment effects removed by randomisation, indicates that the significant results for the un-randomised data does not result from violations of distributional assumptions.

by CVA can be quantified by their canonical weight. The skews when plotting these weights within each effect dimension as histograms indicate that all three canonical contrasts were exhibited strongly in the concentration profiles of subsets of metabolites while most contributed to the canonical contrast negligibly (Figs. 21d and f, Fig. 22d). Metabolites were hence ranked by their canonical weights for each canonical contrast, and the top 5% in each were explored as discriminants altered by the burn.

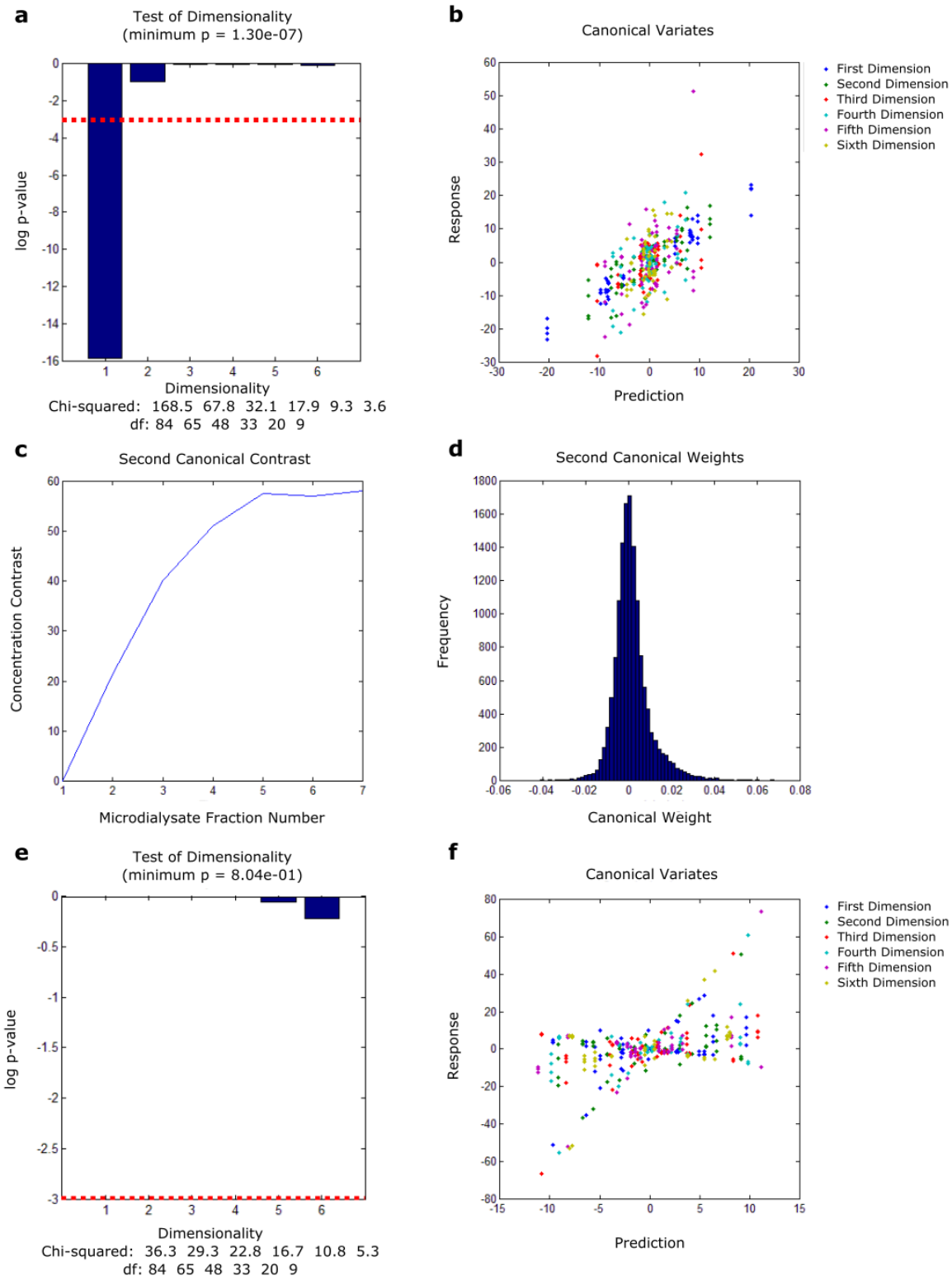


Figure 22 Canonical variates analysis of ESI- UPLC-MS data. (**a**) expresses the log p-values, and the respective chi squared distributions and degrees of freedom on which they are based, where the red dash line indicates statistical significance. Each p-value represents

a potential dimension of the metabolite concentrations' dependency on the explanatory variables; practically, each represents a different temporal profile that is conserved over the time courses of a subset of metabolites. (**b**) indicates the degree of correlation between mixtures of variables subtending the correlation whose significance is reported in the first subplot; a high correlation indicates a consistent temporal profile across explanatory variables. Where (**a**) indicates the significance of one temporal profile, constituting a one-dimensional burn effect, (**c**) expresses the contrast in concentration trajectories in this dimension; it consists of a sustained increase in difference between burn and control concentrations over time. (**d**) is a histogram of the metabolite contributions to the canonical correlation, and thereby their similarities to the temporal profile in (**c**); the skew suggests that a small number of metabolites contribute heavily to the treatment effect (site by time interaction), while most contribute negligibly. (**e**) and (**f**) respectively present p-values and variable mixture correlations for the same analysis of the data following randomisation of its order within individual metabolite time series; the lack of a significant result here, with treatment effects removed by randomisation, indicates that the significant results for the un-randomised data does not result from violations of distributional assumptions.

Structural Identification

Having determined which features exhibited an effect of the burn, targets for structural elucidation could be established. However, they had to meet several additional criteria to be viable for further analysis. Candidate structural IDs for any feature can be returned by searching metabolomics databases such as HMDB (Wishart et al., 2013; Wishart et al., 2009) and Metlin (Smith et al., 2005), as used in the present study, for its molecular weight. However, a metabolite will often yield the measurement of several features, owing to the potential formation of isotopes, adducts, fragments and multimers. The association of each feature to the parent compound was deduced from the raw spectra, such that the databases could be searched accordingly. This step precluded the selection of many features on the basis of signal intensity, as delineating their relationships required that each

important component of the profile recorded distinctly above background level. This highlights the importance of effective chromatography, as overlapping metabolite elution can compromise accuracy in measuring features of lower intensity due to ion suppression, precluding the recognition or pursuit of compounds relevant to the experiment.

With these criteria in mind, a subset of features was selected for structural elucidation using MS/MS. These were principally selected either for having functionally-relevant potential structures, as returned by the online metabolomics databases or in published literature, or for the combined clarity of the burn effect and fragmentation profile, where the latter quality offers the possibility of elucidating important, previously uncharacterised compounds. In the present study, these criteria dictated the selection of 84 target metabolites. Seven included features were ESI+ *m/z* 123.1/83, 137/189, 524.4/536, 468.3/504 and ESI- *m/z* 167/85. They were identified in spectra following determination of a burn effect by CVA, with respective canonical weights of 0.011, 0.0172, 0.017, 0.0148 and 0.0193, which is evident in their temporal profiles (Figs. 23a-g). 305.2/539 and 496.6/52 (Figs. 23c and e) also had high canonical weights of 0.0109 and 0.012 and could have been selected for identification at this stage, but were later selected on alternative criteria as discussed below.

In exploratory MS, the entire *m/z* ratio range (here, 50-1200 *m/z*) is rapidly scanned, such that each *m/z* ratio is analysed for only a fraction of the time. It is untargeted in nature and prioritises metabolome coverage over the detail of individual analytes, and is hence useful for initially identifying experimental effects and candidate targets

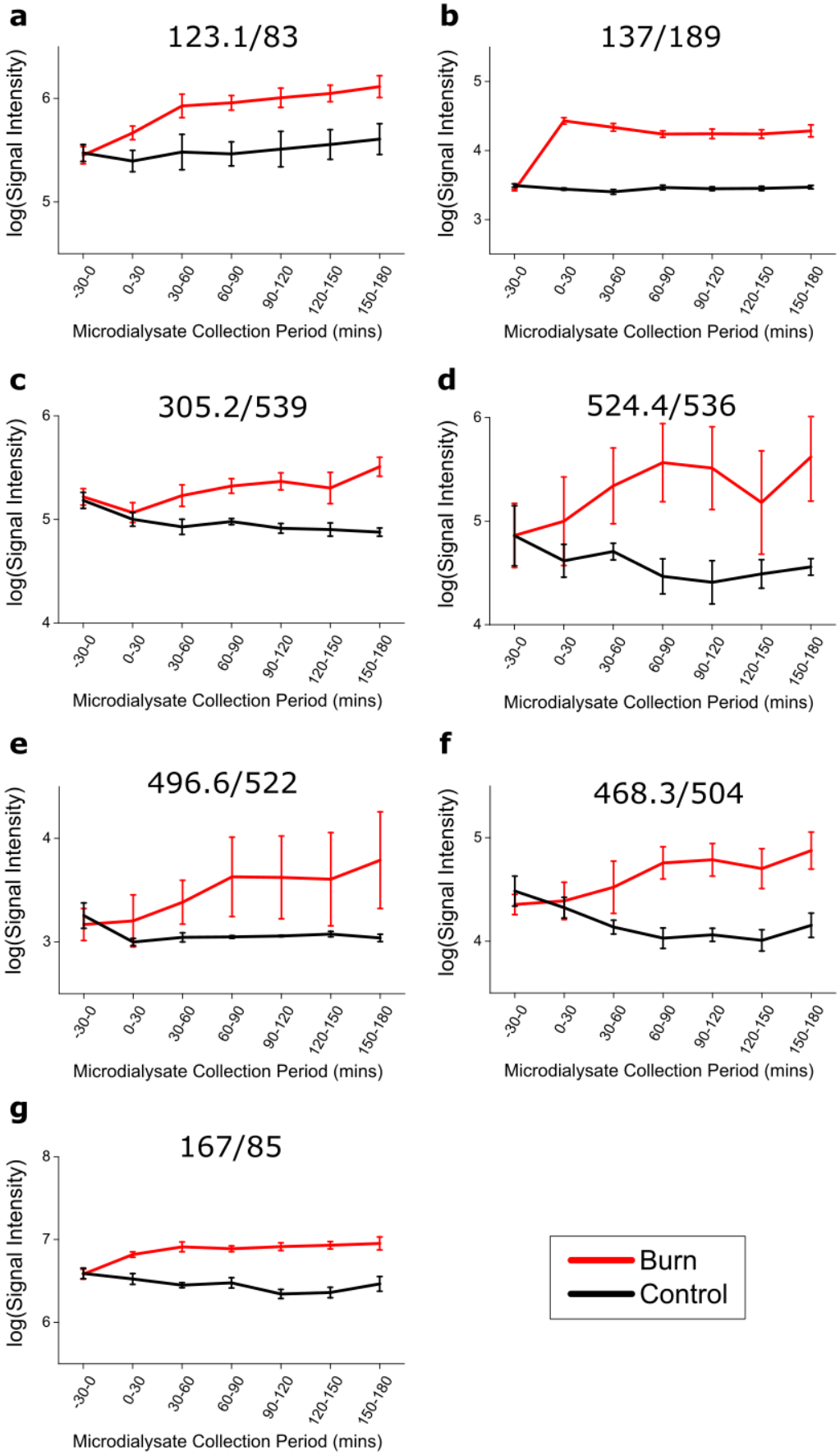

a
123.1/83
log(Signal Intensity)
Microdialysate Collection Period (mins)
b
137/189
log(Signal Intensity)
Microdialysate Collection Period (mins)
c
305.2/539
log(Signal Intensity)
Microdialysate Collection Period (mins)
d
524.4/536
log(Signal Intensity)
Microdialysate Collection Period (mins)
e
496.6/522
log(Signal Intensity)
Microdialysate Collection Period (mins)
f
468.3/504
log(Signal Intensity)
Microdialysate Collection Period (mins)
g
167/85
log(Signal Intensity)
Microdialysate Collection Period (mins)
-30-0
0-30
30-60
60-90
90-120
120-150
150-180
Burn
Control

Figure 23 Temporal concentration profiles of high canonical weight metabolite features. These metabolites recorded high canonical weights, indicating the extent to which they exhibit the temporal profile in the first dimension of the burn effect as defined by CVA, and were therefore selected for structural elucidation. These concentration profiles indicate the success of using CVA to identify burn-effected metabolites from highly multivariate data, as all expressed a burn-induced increase in concentration. Six were selected from ESI+ data, including 123.1/83, 137/189, 305.2/539, 524.4/536, 496.6/522 and 468.3/504, while 167/85 was selected from the ESI- data. Signal intensities are log transformed and expressed as mean ± SEM.

for MS/MS. However, assigning structures based on parent *m/z* ratio alone can yield a high number of viable candidate identities and is also susceptible to subtle mass inaccuracies characteristic of exploratory MS. The subsequent use of MS/MS represents a leap forward in reliability of metabolite identification. MS/MS accomplishes this via intentional deconstruction of a compound with a select *m/z* ratio to which data acquisition is dedicated, hence maximising scan time for and fragmentation of that analyte in order to attain detailed relative fragment intensity measurements. The detection range extends from 50 Da to 50 Da above the target *m/z* ratio, measuring all products of the metabolite's fragmentation (or lack thereof). While accuracy depends on scan time dedicated to that particular feature, experimental designs should accommodate efficient sample usage by maximising the number of features fragmented from one injection (e.g. 10-13 parent compounds per 5 µl in the present study). This often leads to some overlap between acquisition windows, which extend 1 minute either side of the feature's RT. The sequence of acquisition windows should be designed to minimise feature overlap by selecting targets with a spread of retention times, and should be executed with injection of a sample in which each feature was sufficiently abundant for a strong MS/MS signal.

Several fragmentation profile matches were recognised in the present study, including those for features 123.1/83, 137/189, 167/85, 524.4/536 and 468.3/504 (Fig. 24a-e). These exemplify an ideal progression towards identification, wherein the list of viable candidate structures is significantly reduced by the newer, more detailed feature profile and a provisional structure can often be assigned with near certainty. Nonetheless, even the concomitant use of the mass accuracy and fragmentation data offered by MS/MS as search criteria cannot provide an unequivocal match. This initial analysis serves rather to hone in on a single most likely identity, such that the sample can be injected again alongside a solution of a prepared standard of the provisional structure. Upon exhibiting a matching fragmentation profile and retention time, the structure is confirmed to be that of the authentic standard. The candidate structures with fragmentation profiles matching those of *m/z* 123.1/83, 137/189, 167/85, 524.4/536 and 468.3/504 (Fig. 24a-e) during the first stage of MS/MS were niacinamide, hypoxanthine, uric acid, lysophosphatidylcholine (LPC)(18:0) and LPC(14:0) respectively. All five would therefore be later reanalysed with prepared authentic standards for structural elucidation. Despite not initially being recognised for their high canonical weights (although they both had one), 496.6/522 and 305.2/539 would also be further pursued following selection from the initial exploratory MS data on alternative criteria. As metabolites thought to be LPC(18:0) and LPC(14:0), two LPC species varying only by the length of their carbon chain, were present, the initial exploratory MS data were searched for a metabolite feature potentially reflecting the presence of LPC(16:0); 496.6/522 was identified as a likely representative by its *m/z* ratio, its retention time (falling between those of LPC(18:0) and LPC(14:0)) and the presence

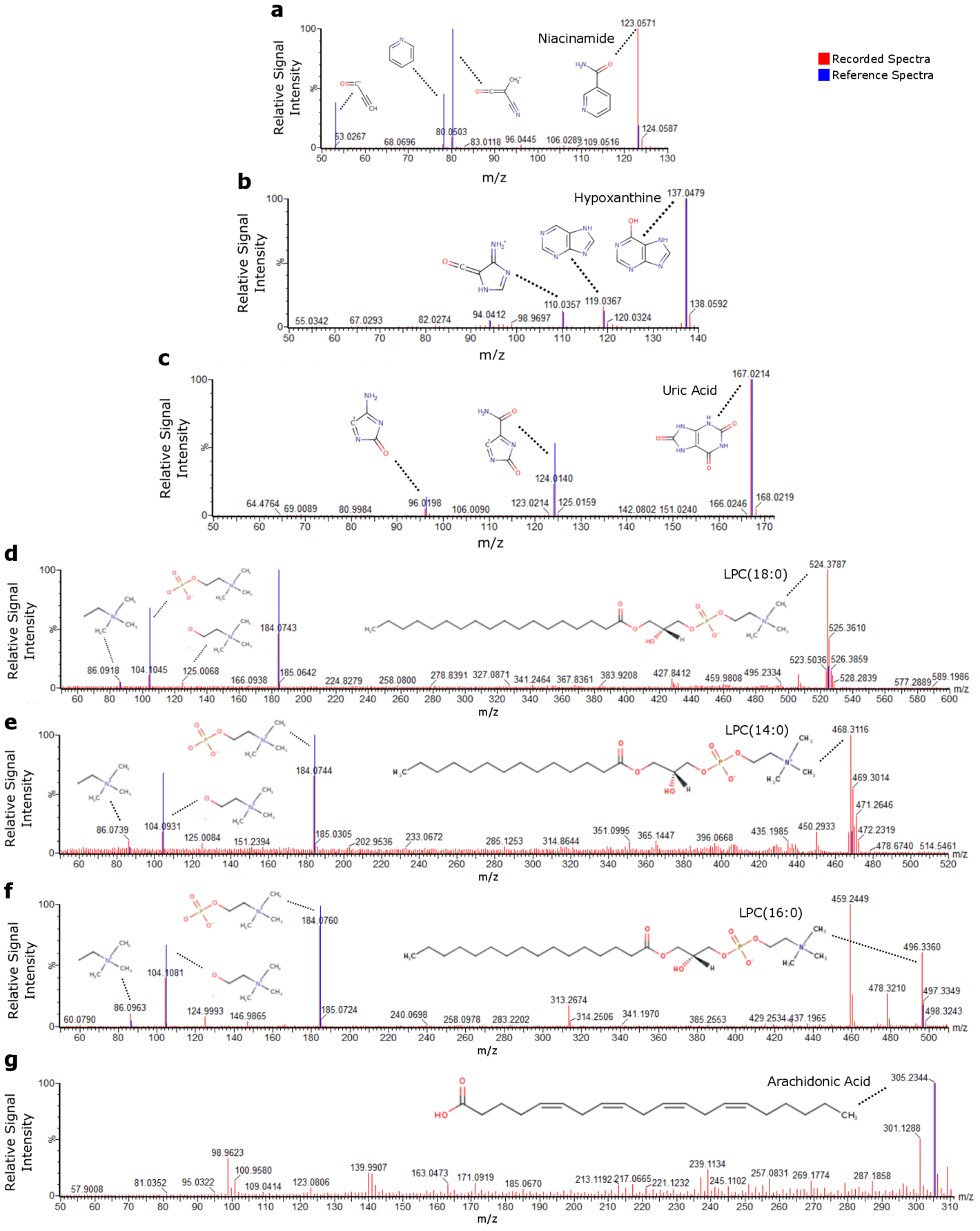

a
Niacinamide
123.0571
124.0587
80.0503
53.0267
68.0696
83.0118
96.0445
106.0289
109.0516
Recorded Spectra
Reference Spectra
b
Hypoxanthine
137.0479
138.0592
110.0357
119.0367
55.0342
67.0293
82.0274
94.0412
98.9697
120.0324
c
Uric Acid
167.0214
168.0219
124.0140
96.0198
64.4764
69.0089
80.9984
106.0090
123.0214
125.0159
142.0802
151.0240
166.0246
d
LPC(18:0)
524.3787
525.3610
184.0743
86.0918
104.1045
125.0068
166.0938
185.0642
e
LPC(14:0)
468.3116
469.3014
471.2646
472.2319
184.0744
86.0739
104.0931
125.0084
151.2394
185.0305
f
LPC(16:0)
459.2449
496.3360
497.3349
498.3243
184.0760
104.1081
86.0963
124.9993
146.9865
185.0724
g
Arachidonic Acid
305.2344
301.1288
98.9623
57.9008
81.0352
95.0322
100.9580
109.0414
123.0806
139.9907
163.0473
171.0919
185.0670
239.1134
Relative Signal Intensity
m/z

Figure 24 Comparative fragmentation spectra of burn microdialysate metabolite features and previously-defined profiles available in metabolomics databases and publications. These spectra overlays indicate the structural similarity between burn-elevated metabolite features within the sample and previously-characterised molecules, including niacinamide (**a**), hypoxanthine (**b**), uric acid (**c**), LPC(18:0) (**d**), LPC(14:0) (**e**), LPC(16;0) (**f**) and arachidonic acid (**g**). It is on the basis of their shared molecular constituents that the features were assigned these respective expected structures. The spectra are annotated with *m/z* ratios of major features and their expected molecular compositions. Red, recorded spectra; Blue, externally-sourced profile.

of fragments *m/z* 184, 104 and 86, which are shared with the other LPC species (Fig. 24f). 305.2/539 (Fig. 24g) was also selected for further structural elucidation as it shared a monoisotopic mass with arachidonic acid, though its fragmentation (or lack thereof) within the initial exploratory MS data was not matched with any prior analysis of the molecule. This was attributed to the fact that fragmentation profiles were scarce, as this metabolite is typically analysed with ESI- and it was presently identified with ESI+, and that the molecule may not have been optimally fragmented at the exploratory stage of the analysis. This metabolite feature was nonetheless attractive for its signal strength, the clarity of the burn effect exhibited, and the functional relevance of its potential structure, and was therefore selected for further analysis in the hopes that a higher collision energy or ESI- mode analysis could yet generate a discernible fragmentation profile.

Of the seven example features presented, ESI+ 123.1/83, ESI- 167/85, ESI+ 524.4/536, ESI+ 468.3/504 and 496.6/522 shared fragmentation profiles and retention times with their respective provisional structure standards (Fig. 25). Fragmentation of 123/83 generated daughter features at *m/z* 80.1, 78.1 and 53, coinciding with that for niacinamide as reported on HMDB (Wishart et al., 2009); Fig.

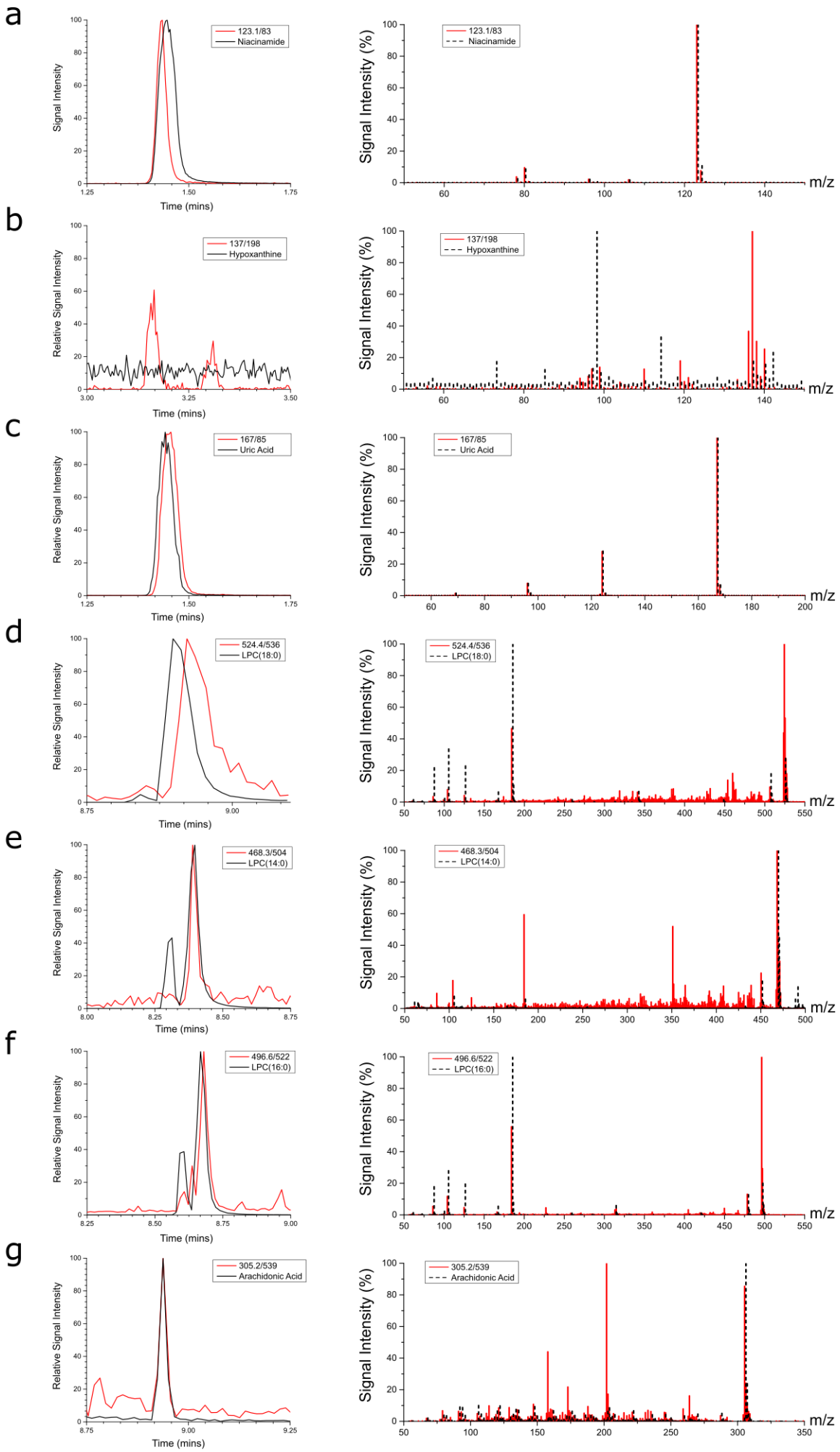

a
123.1/83
Niacinamide
Signal Intensity
Time (mins)
Signal Intensity (%)
m/z
b
137/198
Hypoxanthine
Relative Signal Intensity
c
167/85
Uric Acid
d
524.4/536
LPC(18:0)
e
468.3/504
LPC(14:0)
f
496.6/522
LPC(16:0)
g
305.2/539
Arachidonic Acid

Figure 25 Comparative chromatograms and fragmentation spectra of target metabolite features and standard solutions of their expected structure. Chromatographic overlap reflects a shared elution time, indicating that that there are no differentiating chemical properties leading to varied column binding between the two compounds. The fragmentation profile overlay indicates the structural similarity between the analysed metabolite feature within the sample and the prepared standard solution of its expected molecular structure. Of the 7 target metabolites, niacinamide (**a**), uric acid (**c**), LPC(18:0) (**d**), LPC(14:0) (**e**) and LPC(16:0) (**f**) shared both retention times and fragmentation spectra, confirming the features' structural identities as those of the standards. The hypoxanthine standard (**b**) did not share a retention time with the target metabolite feature, indicating that 137/198 is not hypoxanthine. Arachidonic acid (**g**) and 305.2/539 shared a retention time and appear to share a fragmentation profile though, despite increasing the collision energy, neither was effectively fragmented; the metabolite is likely to be arachidonic acid, though this cannot be confirmed to the same standard as the other 5 target features without a clear fragmentation profile comparison.

25a) and the prepared niacinamide standard. Fragmentation of metabolite feature 167/85 and uric acid generated the same daughter ions at *m/z* 124 and 96 with matching intensities, indicating their shared structure (Fig. 25c). Fragmentation of 524.4/536, 468.3/504 and 496.6/522 generated three daughter ions (*m/z* 184, 104 and 86; Fig. 25d-f) characteristically formed following dissociation from the phosphocholine headgroup following collision of LPC; this profile is not available in any major metabolomics database, but is widely reported (Liebisch et al., 2002). Alongside their shared retention time with their respective standard solutions, this confirmed the structures of metabolite features 524.4/536, 468.3/504 and 496.6/522 as LPC(18:0), LPC(14:0) and LPC(16:0). This structural identification of niacinamide, uric acid, LPC(18:0), LPC(16:0) and LPC(14:0) demonstrates the viability of both ESI+ and ESI- for microdialysate analysis and the value of maximising metabolome coverage via the concurrent use of different analytical techniques. However, the

other target MS/MS metabolite structures could not be confirmed. 137/189 and hypoxanthine eluted 68 seconds apart on the same gradient (Fig. 25b presents the lack of overlap), indicating differing interaction with the column and solvents, and hence precluding them from sharing a structure despite also recording matching parent and daughter ions (Fig. 25b). Features with lower *m/z* ratios tend to share more fragmentation profiles as a result of many smaller, simpler compounds being composed of different arrangements of the same structural elements which do not fragment differentially. Further steps to elucidate the true structure of this compound would consist of injecting the sample alongside standard solutions of these other compounds known to share the fragmentation profile or previously-uncharacterised theoretical matches. Finally, *m/z* 305.2/539 was further likened to arachidonic acid in one aspect by way of their shared retention time with ESI+ (Fig. 25g), though their shared structural identity could not be confirmed. Even with a collision energy of 50V, which enhances the fragmenting capacity of the analysis, the sample profile remained unchanged and therefore their fragmentation could not be compared (Fig. 25g). Further, the system could not detect the compound within the sample using ESI- (data not shown), the mode commonly used for MS/MS analysis of arachidonic acid. However, the fact that the prepared standard could not be fragmented in either ESI+ or ESI- suggests that, were feature 505.2/539 arachidonic acid, the analysis in its current form would have been incapable of proving it. Conventionally, further attempts to elucidate its structure would start with elevating the collision energy further then, if unsuccessful, analysing the sample with a different technique such as gas chromatography-MS (GC-MS) or NMR.

6.3 Discussion

Following on from the validation of the sampling method and confirmation of a burn effect in Chapter 3, the present data demonstrate the application of CVA, a novel analytical approach to metabolomics data, that retains the data's temporal organisation, allowing for the identification of multiple distinct changes in concentration over time and ultimately the successful structural elucidation of at least five metabolites exhibiting upregulation following burn injury. These were elucidated in pursuing of only a fraction of the metabolite features found to exhibit a burn effect, within just one complete pass through the described metabolomics workflow. Exploring the many more metabolites exhibiting a burn effect as identified by CVA, whether in the first dimension (a maintained increase in concentration) or the second (a rapid, transient increase in concentration which was not investigated during this project), has now resumed following conclusion of experiments within this PhD. Having presently confirmed the structure and burn-induced elevation of at least five molecules, the conclusion of the project would consist of delineating any of their potential implications in burn pathology through *in vitro* study. The molecules available for further study were LPC(14:0), LPC(16:0), LPC(18:0), uric acid, niacinamide and arachidonic acid (though, without successful fragmentation, the latter's structure was not confirmed to the same standard as the others), as hypoxanthine was ruled out as the seventh metabolite's identity. For their prior association with inflammatory conditions and the TRP channel family and thereby their potential implication in burn injury, as discussed extensively in Chapter 7, the three LPC species were selected for further study over the closing stages of this project. However, the burn-induced elevation of uric acid and niacinamide, the other

two compounds for which structural elucidation was completed, is nonetheless interesting.

6.3.1 Uric Acid in Disease States

Uric acid is a heterocyclic compound formed during the metabolism of purine nucleotides. Approximately two thirds of uric acid is excreted by the kidneys; an individual's circulating uric acid levels depend on their relative rate of purine metabolism and their renal clearance efficiency (Liu et al., 2010). Uric acid crystallises at high concentrations, as underlies its principal pathological implication in the pathogenesis of gout; high blood concentrations of uric acid leads to the formation of crystals and their deposition in joints, tendons and surrounding tissues, leading to inflammation (Martinon, 2010). Elevated circulating uric acid concentrations have further been associated with hypertension, metabolic syndrome, coronary artery disease, cerebrovascular disease, vascular dementia, preeclampsia and kidney disease (Feig et al., 2008). It is only by its association with compromised kidney function that uric acid has been associated with burn injury to date. The kidneys, like many organs susceptible in MODS, are prone to dysfunction following a severe burn. Acute kidney injury (AKI) is among the most common post-burn complications with both immediate and long-term consequences (Brusselaers, Monstrey, Colpaert, et al., 2010; Chertow et al., 2005; Emara et al., 2013). Several lines of evidence support roles for uric acid in AKI's pathogenesis, including its activation of the renin-angiotensin system, suppressing nitric oxide to cause systemic vasoconstriction and hypotension (Lapsia et al., 2012), its impairment of renal blood autoregulation and its induction of inflammation (Ejaz et al., 2007).

Hyperuricemic patients exhibited a 35-fold increase in risk of AKI following cardiovascular surgery (Lapsia et al., 2012) while reducing uric acid in an animal AKI model has been shown to reduce its associated inflammatory response (Sanchez-Lozada et al., 2005). Despite the mechanisms underlying uric acid's induction of AKI still requiring elucidation, a raised uric acid concentration is now commonly accepted as a risk factor for AKI (Ejaz et al., 2012). Following the initial recognition that uric acid is elevated in the plasma of severely burned patients (Zhi et al., 2014), its elevation was specifically explored in the context of post-burn AKI pathogenesis; it was found that circulating uric acid concentrations reflect the severity of the trauma and predict the onset of post-burn AKI in addition to the AKI's severity. It was concluded that, while hypovolaemia-induced compromise of end-organ perfusion is the primary risk factor in AKI pathogenesis, as is the case for many organs exhibiting post-burn dysfunction (Beal et al., 1994), a secondary risk factor is the inflammation resulting from global tissue hypoxia-induced elevation of xanthine oxidase activity, leading to increased uric acid concentration (Liang et al., 2015). Further, one of very few metabolomic studies of burn injury conducted prior to ours identified elevated uric acid in rat plasma (Liu et al., 2010). Interestingly, while the only failed structural elucidation of an elevated compound reported presently was that of the metabolite feature expected to be hypoxanthine, Liu et al. (2010) also identified elevated plasma hypoxanthine when combining the thermal injury with a model of sepsis. As uric acid's burn-induced elevation has only been identified systemically to date, this is the first report of its specifically local increase in burn injury. The proposed hypoxia-induced elevation of uric acid is supported by the present findings, as the damage observed in the deep partial-thickness burn model is consistent with local hypoperfusion; this association between hypoxia and uric acid in burn injury has only

been supported systemically to date. Similarly, unlike previous implications of uric acid in burn injury, the present data support its production specifically at the burn site. The lack of an elevation in control microdialysate suggests either that uric acid is not systemically distributed from the burn site within three hours, or that uric acid does not perfuse into the subcutis from circulation. In the latter case, it would be possible that uric acid disseminating from the burn site, rather than that produced with global hypoxia, accounts for its previously described systemic elevations and consequences. Establishing the impact of local hypoxia and locally sourced uric acid on its turnover, and the resultant influences on inflammation and kidney function, could present an exciting avenue for therapeutic intervention in burn injury.

6.3.2 The Protective Potential of Niacinamide in Burn Injury

Niacinamide (AKA nicotinamide) is the amide and *in vivo* product of nicotinic acid (AKA niacin, vitamin B3), and is a precursor in the synthesis of the coenzymes nicotinamide adenine dinucleotide and nicotinamide adenine dinucleotide phosphate. While it is generated endogenously, and it is known to be protective as its sufficient bioavailability confers antipruritic, antimicrobial and vasoactive properties (Wohlrab et al., 2014), these functions have primarily been elucidated through niacinamide's pharmaceutical application and the extent to which they occur endogenously is not clear (Wohlrab et al., 2014). However, protective niacinamide bioavailability is easily obtainable with pharmaceutical intervention, as is reflected in its therapeutic use in the treatment of various inflammatory cutaneous conditions such as bullous phemigold and dermatitis herpetiformis (Fivenson et al., 1994; Zemtsov et al., 1993), blister-inducing autoimmune diseases, and necrobiosis lipoidica (Handfield-Jones et

al., 1988), an inflammatory necrotising skin condition characterised by collagen degeneration, by epidermal application as a gel. While it has not been used clinically for burn injury, systemic administration has been shown to significantly enhance wound healing, as evaluated by granulation and capillary density at the burn site (Smith et al., 1989), and correct post-burn imbalances in the nicotinamide coenzyme system (Galimov Sh et al., 1991). While burn-induced effects on the products for which it is a precursor have been identified, and its systemic administration has been shown to be protective in burn injury, the present data appear to constitute the first demonstration of niacinamide's elevation in burn injury.

In its anti-inflammatory capacity (Lappas et al., 2011), it opposes the function of the other burn-elevated compounds identified in this chapter and may represent an endogenous regulatory mechanism for local inflammation. Its anti-inflammatory function is clear from its clinical use and its reduction of inflammation induced by potassium iodide in humans (Bernstein, 1980) and 12-O-tetradecanoyl-phorbol-13-acetate in mice (Ludwig et al., 1990), though the means by which this is executed are not clear (Shalita et al., 1995). Supported underlying mechanisms include inhibition of histamine release from mast cells (Bekier et al., 1974), reduction of inflammatory mediator synthesis and neutrophil chemotaxis (Bekier et al., 1974), histamine receptor inhibition (Berk et al., 1986) and lymphocyte transformation suppression (Burger et al., 1976). By any of these means, niacinamide may endogenously regulate local inflammation in burn injury and eventually contribute to its resolution. Its pharmacological benefits have also been attributed to its electron scavenging properties, by which it may reduce oxidative damage (Hamoud et al., 2013); again, this may be occurring endogenously in burn injury. Further, the fact

that niacinamide has been long-established as a safe clinical intervention for various inflammatory skin conditions via epidermal gel application is interesting; it is possible that the endogenous local elevation reported here may be bolstered with a topical application of the compound to therapeutic effect.

The application of CVA, informing the manual selection of metabolite features for MS/MS, and the unequivocal structural elucidation of LPC(14:0), LPC(16:0), LPC(18:0), uric acid and niacinamide was a pivotal stage of this project. It proved the viability of a novel statistical approach to metabolomics data, which here returned a database of burn-affected metabolites so vast that much within it remains to be evaluated. On the weight of these findings, this novel application of CVA to temporal profiling of metabolomics data shows great potential. The present identification of burn-elevated molecules, all of which are implicated in the pathological processes underlying burn injury, dictated the structure of the remainder of this project, in which the role of LPC in burn injury would be explored. Having briefly discussed uric acid's and niacinamide's identification and their potential associations with thermal trauma presently, Chapter 7 describes the pursuit of LPC as a pathological mediator in burn injury.

7 CHAPTER 7 – LYSOPHOSPHATIDYLCHOLINE'S SENSITISATION OF TRPV1 AS A POTENTIAL NOVEL PRO-NOCICEPTIVE MECHANISM

7.1 Introduction

Burn injury remaining a major and multidisciplinary clinical challenge (Brusselaers et al., 2010; Pavoni et al., 2010) results not only from the heterogeneity of the patient profile, which varies by age, mechanism of injury, depth, surface area, complications and co-morbidity (Brusselaers et al., 2010), but also from the temporal progression of the injury and the need for evolving clinical intervention (Bloemsma et al., 2008; Brown et al., 2003; Brusselaers et al., 2010; Falder et al., 2009). However, burns are unified by one factor; the destructive transfer of energy and consequent tissue denaturation, which initiates the local barrage of physiological and pathological effects that eventually lead to every manifestation of the burn. This acute phase of the injury is the subject of this project as its defining mechanisms present an avenue for novel therapeutic targets. In the previous chapter, the burn-dependent elevation of three species of LPC species was identified, and their potential implication in burn pathology will now be considered.

Characteristic of a burn's progression, single mechanisms implicated in the early local pathology can have multiple diverging or interrelated roles in the development of the injury. One such example is the activation of TRPV1. TRPV1 is a nonselective cationic channel allowing calcium influx upon activation that is expressed primarily in small- to medium-diameter neurons (Richardson et al., 2002). It is gated by

capsaicin, heat (42oC<), low pH, endogenous lipids and hypertonic challenges. In-keeping with the channel's initial characterisation as a pain transducer (Caterina et al., 1997), activation by any of these modalities evokes pain in humans and nocifensive behaviour in animals (Ciura et al., 2006; Garcia-Hirschfeld et al., 1995; Montell et al., 2002; Steen et al., 1992). Further, TRPV1 can be sensitised by heat, multiple phosphorylation processes and the inflammatory mediator nerve growth factor (Huang et al., 2006). It is by these activating and sensitising processes that TRPV1, upon exposure to heat, protons, endogenous lipids and inflammation, mediates acute thermal nociception alongside mechanical and thermal allodynia and hyperalgesia in inflammatory pain such as that of burn injury (Bolcskei et al., 2005; Caterina et al., 1997; Green et al., 2013; Planells-Cases et al., 2005; Woolf et al., 2007). Beyond its principal characterisation as a nociceptor, TRPV1 contributes to the initiation and maintenance of neurogenic inflammation via the release of neuropeptides such as substance P, calcitonin gene related peptide (CGRP), neurokinin A and somatostatin upon activation (Buck et al., 1986; Caterina et al., 2001; Holzer, 1988; Tsuji et al., 2012). Again, the implications for burn injury, the pathology of which is largely defined by extensive inflammation, are clear (Farina et al., 2013; van de Goot et al., 2009).

TRPV1 therefore has definitive roles in both inflammation and pain transduction within burn injury. Both aspects of the injury remain high priority clinical targets. Local inflammation can underlie the development of SIRS; indeed, this is the justification for early excision of burn tissue, which attenuates the circulation of inflammatory mediators (Farina et al., 2013; Ong et al., 2006). SIRS can lead to MODS, which is reportedly the most frequent cause of death following burn injury

(Bloemsma et al., 2008; Farina et al., 2013). Fortunately, recent advances in burn care have improved mortality rates (Brusselaers et al., 2005; Pavoni et al., 2010), yet pain following burn injury remains undertreated among the survivors (Summer et al., 2007; WHO, 2008). Elucidation of TRPV1's involvement in burn pain and inflammation, which is still little understood, may reveal processes underlying the injury's pathophysiology that are suitable for therapeutic intervention.

LPC is a proinflammatory mediator that constitutes the major bioactive phospholipid component of oxidised low-density lipoprotein (LDL) and is elevated in a variety of pathophysiological states (Matsumoto et al., 2007). It is primarily generated via two phosphatidylcholine (PC) hydrolysis pathways; either by lecithin-cholesterol acyltransferase (LCAT) transferring a fatty acid from a PC to cholesterol (Chen et al., 1997; Subbaiah et al., 1996), or by phospholipase A_2 (PLA_2) hydrolysis generating one molecule of LPC and one of a fatty acid (Kougias et al., 2006; McHowat et al., 1993). LPC is an amphipathic compound consisting of a hydrophobic fatty acid, a hydrophilic polar choline head group and a glycerol backbone arranged in a wedge-like conformation that exhibits detergent- and surfactant-like properties (Liu et al., 1991; Saunders, 1966). Physiologically, it exists either as single molecules or within micelles at sufficient concentrations (Saunders, 1966). It can insert itself into the membrane in either form, where single molecules are noted not to easily transfer to the inner lipid layer (Mohandas et al., 1982) and LPC's lysing and detergent effects are attributed mostly to micelles (Weltzien, 1979). Further, LPC can exert another nonspecific membrane effect in inducing the formation of transient calcium pores (Wilson-Ashworth et al., 2004). While LPC exists at high concentrations in different biological fluids physiologically, between 5-180 μM depending on the tissue (Croset

et al., 2000; Okajima et al., 1998), its bioavailability is regulated by reversible binding to albumin, erythrocytes and lipoproteins (Kohno et al., 2000; Kugiyama et al., 1993; Vuong et al., 2001). When studying LPC, the influences of its selective interactions, nonspecific membrane effects and dynamically controlled availability must therefore be considered.

LPC has previously been linked with the TRP channel family by its sensitisation and activation of the cold-sensing receptor TRP subfamily M member 8 (TRPM8; Abeele et al., 2006; Andersson et al., 2007). The change in membrane tension and curvature resulting from LPC's insertion (Patel et al., 2001) has been suggested as a potential mechanism for its effects on TRPM8, as it is for other channels (Abeele et al., 2006; Lundbaek et al., 1994; van den Brink-van der Laan et al., 2004) including the thermosensitive K^+ channel TREK-1 (François Maingret et al., 2000). Other effectors similarly partitioning the membrane, such as volatile anaesthetics, also modulate TRPM8 (Török et al., 2014; Vanden Abeele et al., 2013). However, LPC's relationship with TRPV1, a receptor with various endogenous lipid effectors (Nieto-Posadas et al., 2012), is unclear. Lysophosphatidic acid (LPA), an enzymatic product of LPC, is an established TRPV1 activator, acting on the C-terminus following efficient transbilayer movement (Nieto-Posadas et al., 2012; Tanaka et al., 2011). However, LPC itself is generally not reported to activate TRPV1 directly (Nieto-Posadas et al., 2012) and, where activation is reported, indirect effects are not excluded (Nieto-Posadas et al., 2012; Schilling et al., 2009b). LPC levels have been reduced in erythrocytes (Harris et al., 1981) and increased in burned muscle following burn injury (Turinsky et al., 1985), consistent with data supporting impaired

lipoprotein metabolism early post-burn (Pratt et al., 2001). While both TRPV1 and LPC are implicated in burn injury, their potential interaction remains little-understood.

The present study sought to elucidate whether or not LPC(18:0) may modulate TRPV1 in burn injury, following the demonstration that multiple LPCs are elevated in a validated deep partial-thickness scald-type burn model (see Chapter 6). In addition to demonstrating LPC's previously described non-specific membrane and calcium transient effects, its concentration-dependent sensitisation of TRPV1, as exhibited with calcium imaging and explored with electrophysiology, is identified. The data indicate that TRPV1 is modulated by LPC(18:0), and that their interaction may contribute to the pathophysiology of burn injury.

7.2 Results

Following confirmation of the identities of these three LPC species, and their elevation within burn injury, the metabolomic signal intensities were pooled with those of a lipidomic analysis designed to prioritise the detection of lipids. Their burn-specific increases in concentration over time, as reflected in their contributions to the extremely significant first dimension of the ESI+ burn effect identified by CVA (Fig. 21c, $p = 1.13E-7$), is evident for all three species (Fig. 26).

Gene sequencing using RNA isolated from the microdialysis sites revealed the differential expression of several genes involved in the production of LPC (Fig. 27). These included Lcat ($p = 0.001008$) and several PLA_2-related genes including those encoding its receptor Pla2r1 ($p = 0.002836$), its cytosolic form (Pla2g4d, p =

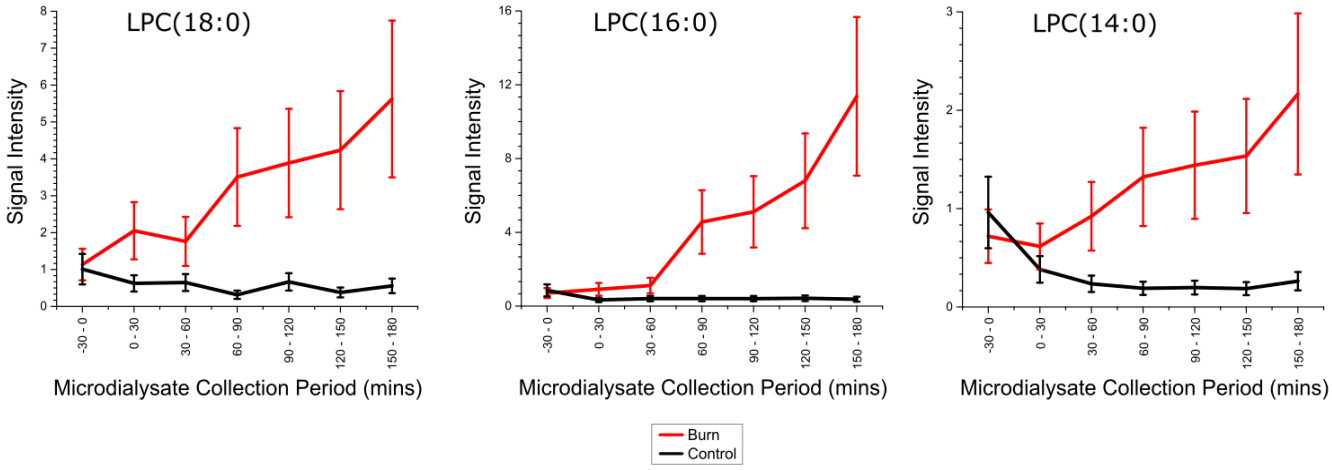


Figure 26 LPC(18:0), LPC(16:0) and LPC(14:0) are elevated in burn injury, as detectable by both metabolomics and lipidomics. After identifying these three LPC species in burn microdialysate using metabolomics (as described in Chapter 6), they were further found in the lipidomics data. Here, in order to present both data sets together, doubling the number of biological replicates (n = 8), the signal intensities were normalised to the average flush fraction within their respective methodology (metabolomics or lipidomics). Data expressed as mean ± SEM.

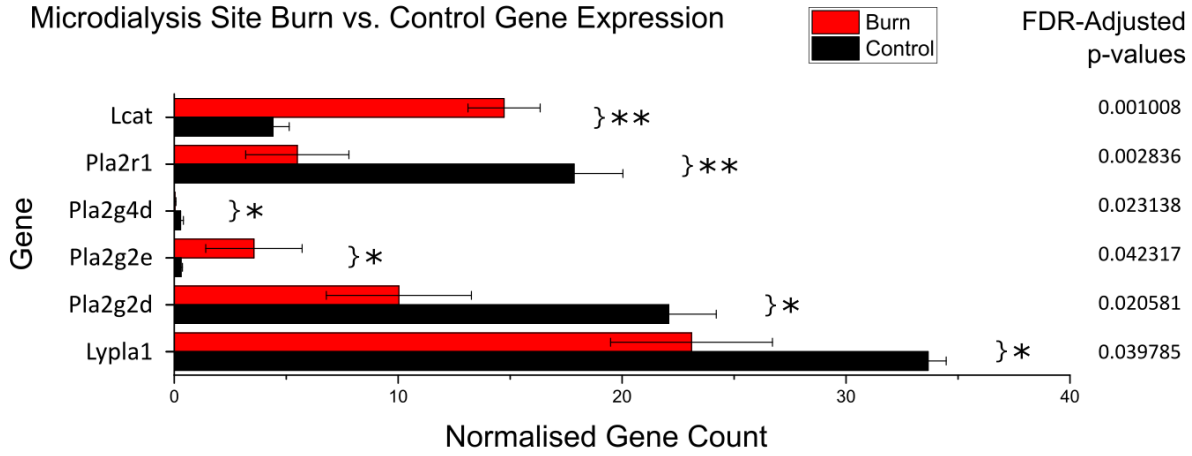
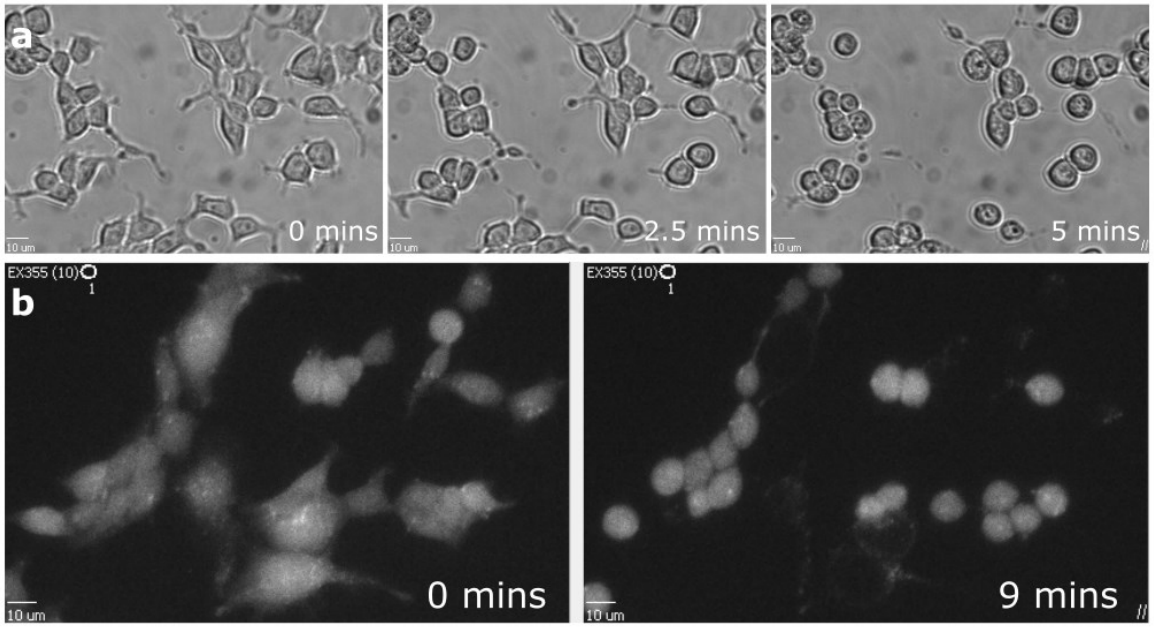
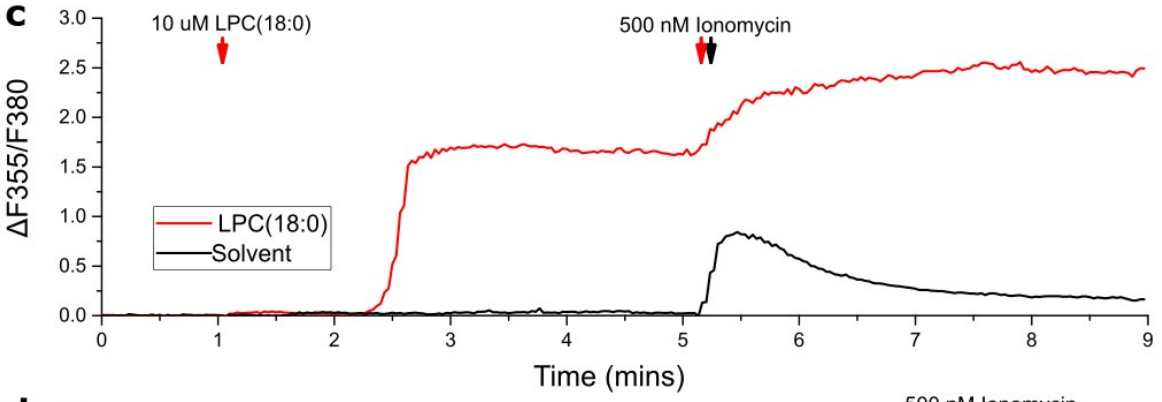


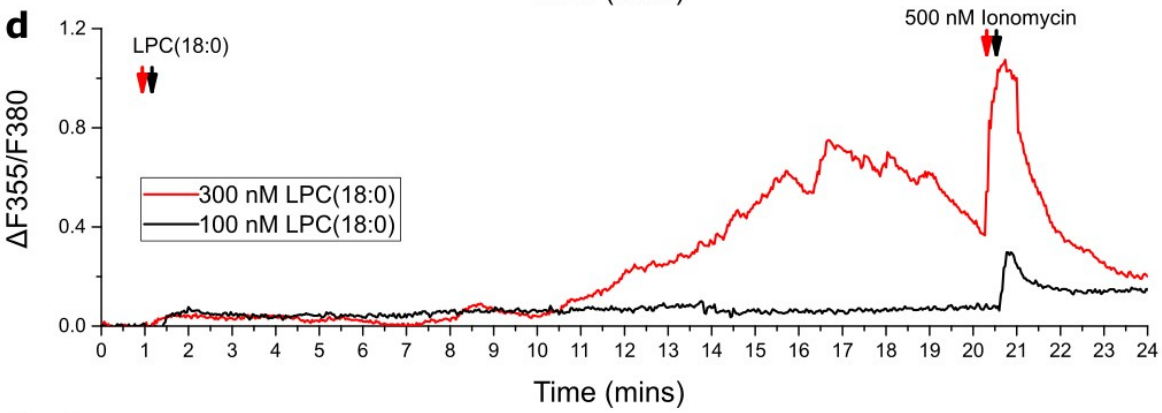
Figure 27 Various LPC-related genes are significantly differentially expressed in burned skin tissue. 6 genes regulating LPC availability were identified among those significantly altered, as reported by VBCF and presented with their FDR-adjusted p-values. Gene counts are expressed as RPKM values, which are normalised both between samples and between genes comparable by taking variable gene lengths into account. Data are expressed as mean ± SEM. *, $p < 0.05$; **, $p < 0.01$; ***, $p < 0.001$.

0.023138) and its secretory forms (Pla2g2e, p = 0.042317; Pla2g2d, p = 0.020581). Lypla1, which encodes acyl-protein thioesterase 1, a phospholipase that hydrolyses LPC in either its monomeric or micellar form to produce a glycerophosphocholine and a fatty acid, was also differentially expressed (p = 0.039785). Further, LPC's proinflammatory functions and regulation of cytokines may contribute to the significant representation of differential expression within the Jak-STAT signalling pathway and Cytokine-cytokine receptor interaction KEGG terms as described in Chapter 5 (Fig. 20) and discussed below.

Application of LPC(18:0) induced several concentration-dependent effects in untransfected HEK293T cells. After 5 minutes, 10 μM LPC(18:0) induced a marked change in the morphology of most cells, characterised by a rounded cell body and withdrawal or detachment of processes from the culture surface (Fig 28a). Similar LPC-induced cell rounding has been reported in fibroblasts (Colles et al., 2000) and macrophages (Kritharides et al., 1995; Sakai et al., 1996), and has been attributed to membrane destabilisation (Colles et al., 2000). Maximal cell rounding coincided with the onset LPC(18:0)-induced lysis, which occurred in a subset of cells exhibiting the morphological changes between 4 and 6 minutes of exposure to 10 μM LPC(18:0) (Fig. 28b). These effects were preceded by an increase in intracellular calcium. As with the morphological changes, such increases induced by LPC have been observed in a variety of cell types (Chaudhuri et al., 2003; Rolin et al., 2013; Tanaka et al., 2011; Wang et al., 2015; Yu et al., 1998) and can be attributed to spatial disruption of lipid packing with changes in membrane fluidity (Fink et al., 1984; Ghosh et al., 2002) or permeability (Colles et al., 2000; Katz et al., 1981) or ion


a
0 mins
2.5 mins
5 mins
b
EX355 (10)
0 mins
9 mins


c
10 uM LPC(18:0)
500 nM Ionomycin
LPC(18:0)
Solvent
ΔF355/F380
Time (mins)


d
LPC(18:0)
500 nM Ionomycin
300 nM LPC(18:0)
100 nM LPC(18:0)
ΔF355/F380
Time (mins)

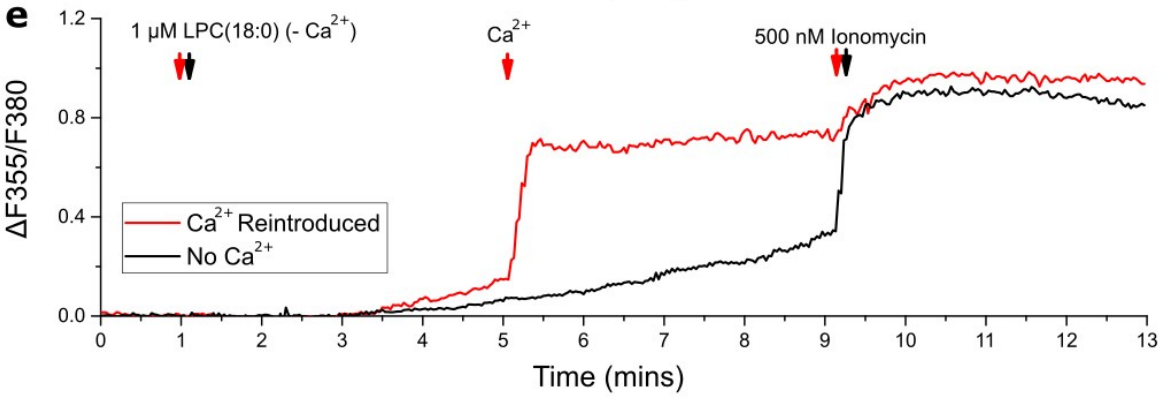

e
1 μM LPC(18:0) (- Ca2+)
Ca2+
500 nM Ionomycin
Ca2+ Reintroduced
No Ca2+
ΔF355/F380
Time (mins)

Figure 28 LPC(18:0) induces nonspecific membrane effects in untransfected HEK293T cells. Sufficient exposure to LPC(18:0) progressively induces cell rounding (**a**) and lysis (**b**) at a rate dependent on its concentration. Lysis is preceded by an intracellular Ca^{2+} overload, occurring less than 2 minutes following the onset of 10 μM LPC(18:0) (**c**), which can be delayed or prevented with sufficient reduction in LPC(18:0) concentration (**d**). This overload is dependent on an influx of extracellular calcium, as indicated following its reintroduction in Ca^{2+}-free conditions (**e**).

channel alteration (Inoue et al., 1992; Lundbaek et al., 1994). The increase in intracellular calcium was delayed following onset of application; higher concentrations would require less time to induce the response, would require less time to reach maximum intracellular calcium and would induce responses of greater amplitude (Figs. 28c and d). This profile is consistent with that of cells in which LPC has structurally compromised the membrane (Golfman et al., 1999). Importantly, this increase in intracellular calcium could be avoided with a sufficiently low LPC(18:0) concentration (Fig. 28d). Further, to test whether the effect was dependent on extracellular calcium or that of intracellular stores, the response was measured both in the complete absence of extracellular calcium and with the reintroduction of previously withheld extracellular calcium. The immediate $[Ca^{2+}]_i$ increase following the reintroduction of Ca^{2+}, and its prevention in the absence of $[Ca^{2+}]_e$, supports this response relying on an influx of extracellular calcium (Fig. 28e). This, along with the morphological changes, lysis, their relative timings, the delay observed in the response and the profile's similarity with that of previously reported structurally compromised cells (Golfman et al., 1999), is consistent with this particular effect of LPC(18:0) resulting from disruption of the membrane.

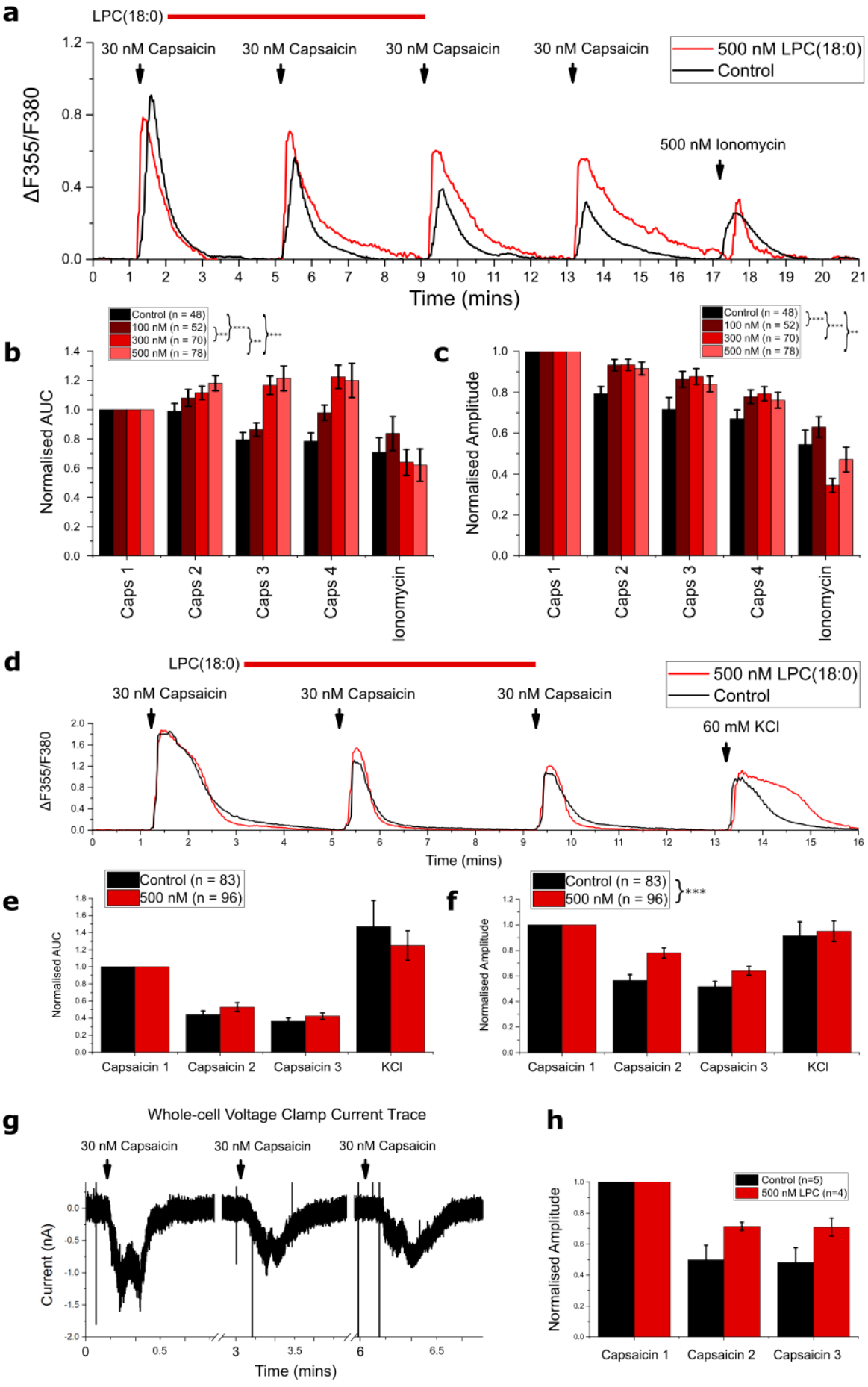

a
LPC(18:0)
30 nM Capsaicin
30 nM Capsaicin
30 nM Capsaicin
30 nM Capsaicin
500 nM LPC(18:0)
Control
500 nM Ionomycin
ΔF355/F380
Time (mins)
b
Control (n = 48)
100 nM (n = 52)
300 nM (n = 70)
500 nM (n = 78)
Normalised AUC
Caps 1
Caps 2
Caps 3
Caps 4
Ionomycin
c
Normalised Amplitude
d
LPC(18:0)
30 nM Capsaicin
30 nM Capsaicin
30 nM Capsaicin
500 nM LPC(18:0)
Control
60 mM KCl
ΔF355/F380
Time (mins)
e
Control (n = 83)
500 nM (n = 96)
Normalised AUC
Capsaicin 1
Capsaicin 2
Capsaicin 3
KCl
f
Normalised Amplitude
g
Whole-cell Voltage Clamp Current Trace
30 nM Capsaicin
30 nM Capsaicin
30 nM Capsaicin
Current (nA)
Time (mins)
h
Control (n=5)
500 nM LPC (n=4)
Normalised Amplitude
Capsaicin 1
Capsaicin 2
Capsaicin 3

Figure 29 LPC(18:0) sensitises TRPV1 in HEK293T cells and DRG neurons. In the presence of LPC(18:0), TRPV1-sensitisation manifested as a reduction in its stimulation-induced desensitisation to sequential capsaicin pulses in both HEK293T cells (**a**) and DRG neurons (**d**). Response Ca^{2+} transients were analysed by means of both their AUCs (**b**) and peak amplitudes (**c**) normalised to the first capsaicin response, both of which were significantly altered by LPC(18:0) in HEK293T cells while only peak amplitudes were significantly increased in DRG neurons (**e** and **f**). Few attempts to measure this effect via whole-cell voltage clamp electrophysiology were successful due to LPC(18:0)'s disruption of the gigaseal; a representative current trace exhibiting the desensitisation profile is shown (**g**) with the peak amplitudes indicating a similar sensitisation (**h**) but falling short of the required sample size for meaningful statistical analysis. Data are expressed as mean ± SEM. *, $p < 0.05$; **, $p < 0.01$; ***, $p < 0.001$.

Having identified these apparent membrane effects, and the extent of LPC(18:0) exposure required to induce them, LPC(18:0)'s potential effect on TRPV1-mediated responses was investigated. Changes in the amplitude and area under curve (AUC) of capsaicin-induced calcium transients were evaluated at varying LPC(18:0) concentrations in TRPV1-expressing HEK293T cells (n = 48-78) over repeated capsaicin pulses. In the absence of LPC(18:0), sequential 30 nM capsaicin pulses every 4 minutes exhibited a typical profile consistent with stimulation-induced TRPV1-desensitisation, characterised by the progressive decline of response amplitude and AUC (Fig. 29a; p = <0.001, effect of no. of capsaicin applications). However, in the presence of LPC(18:0), these declines in amplitude and AUC were reduced (p = 5.39223E-5; effect of concentration) and concentration-dependently reversed with successive capsaicin applications (p = 0.00446; 2-way ANOVA, concentration x no. of caps. applications) respectively (Fig 29a-c). Two minutes of LPC(18:0) exposure, initiated mid-way between the first two capsaicin pulses and not itself activating TRPV1, were sufficient for the onset of these effects. The respective reduction and reversal of peak and AUC decline escalated after 6 minutes

of LPC(18:0) exposure and did not recover with a 2 minute wash (Fig. 29a-c). Post-hoc analyses indicated significant effects of concentration on AUC in all pairwise comparisons, except for control and 100 nM LPC(18:0) ($p = 0.46765$), and 300 and 500 nM LPC(18:0) ($p = 1$). Unlike the increase in AUC, the reduction in desensitisation exhibited in the peak amplitudes was not concentration-dependent; there was no significant difference between response profiles in the presence of LPC(18:0), though all three LPC(18:0) concentrations elicited significantly elevated calcium transients when compared with control recordings (100 nM, $p = 7.74874E-4$; 300 nM, $p = 6.80231E-5$; 500 nM, $p = 0.00208$). Nor was the reduced desensitisation expressed by response amplitudes dependent on the duration of exposure, with the effect remaining stable after the onset of LPC(18:0) application ($p = 0.52107$, concentration x no. of applications interaction). Nonetheless, LPC(18:0) clearly elicits a reduction in TRPV1 desensitisation.

To investigate these effects in a model more representative of *in vivo* nociceptive processing, the same experimental design (excluding the fourth capsaicin pulse) was employed with small- to medium-diameter DRG neurons with 500 nM LPC(18:0) ($n = 83-96$). These neurons exhibited the expected desensitisation profile with repeated capsaicin application (peak $p > 0.0001$, AUC $p > 0.0001$; effect of number of capsaicin applications), as did the HEK293T cells, though AUC was not significantly affected by 500 nM LPC(18:0) ($p = 0.08449$; Fig. 29e and f). However, LPC(18:0)'s effect on peak response amplitudes remained significant in DRG ($p = 2.7E-5$, effect of LPC) and was further found to progress over time ($p = 0.00461$, LPC x number of capsaicin applications interaction). As in HEK293T cells, LPC(18:0) reduces stimulation-induced desensitisation in TRPV1-expressing DRG neurons.

LPC modulates various membrane proteins via altered bilayer tension (Abeele et al., 2006; Lundbaek et al., 1994; van den Brink-van der Laan et al., 2004), notably including voltage gated calcium channels (Ben-Zeev et al., 2010). As the reduction in desensitisation demonstrated above may depend rather on endogenously-expressed voltage-gated channels recruited following TRPV1's activation than TRPV1 itself, any potential voltage-dependent component of the response required controlling. To this end, whole-cell voltage-clamp recording was attempted with TRPV1-transfected HEK293T cells but proved unviable as a technique due to LPC(18:0)'s membrane effects typically compromising the seal within 4 minutes. Consequently, even while reducing the capsaicin pulse interval to 3 minutes and restricting LPC(18:0)'s concentration to 100 nM, only four complete response sets could be collected from cells in the presence of LPC(18:0) and the effects shown cannot be generalised to any wider cell population, nor would any statistical analysis be meaningful. Nonetheless, within the small cohort successfully recorded from here, the same reduced desensitisation as that observed by calcium imaging was recorded with consecutive capsaicin applications in the presence of LPC(18:0) via electrophysiology (Fig. 29g and h).

7.3 Discussion

Collectively, the present findings implicate a novel mechanism of nociception and neurogenic inflammation in burn injury. Three species of LPC, LPC(18:0), LPC(16:0) and LPC(14:0), were found to be elevated in the subcutaneous interstitium following induction of the deep partial thickness burn model. These increased metabolite

concentrations were accompanied by the differential expression of several genes associated with their generation. With sufficient exposure, LPC(18:0) induced deleterious membrane effects resulting in HEK293T cell rounding, calcium overload and lysis. With curtailed exposure, precluding effects compromising the model system, LPC(18:0) was found to concentration-dependently sensitise TRPV1, manifesting as a reduction of activation-induced desensitisation. This effect was observed in both HEK293T cells and primary small- to medium-diameter DRG neurons as indicated by peak response amplitude, the conventional measure of receptor activation (Charlton et al., 2010). AUCs, analysed as a secondary measure, can reflect receptor activation but can further depend on subsequent mechanisms of resting intracellular Ca^{2+} level restoration, namely extrusion and sequestration (Clapham, 2007). As LPC(18:0) also significantly altered the capsaicin response AUC in HEK293T cells, it may have further effects than that on TRPV1, though this cannot be ascertained from the present data. Regardless, LPC(18:0) did not significantly alter the capsaicin response AUC in DRG neurons. Attempts to exclude the potential contribution of voltage-gated response components via the use of voltage-clamp electrophysiology were hindered by LPC(18:0)'s membrane effects preventing attainment of whole-cell configuration. LPC(18:0) is nonetheless capable of sensitising TRPV1, and may thereby contribute to burn pathophysiology.

7.3.1 LPC and Immune Cells following Burn Injury

Our finding that subcutaneous LPC is increased following burn injury is consistent with its prominent characterisation as a proinflammatory lipid, driven by its implication in various inflammatory pathologies and mechanisms (Ha et al., 2012;

Matsumoto et al., 2007; Mehta et al., 1990; Sasagawa et al., 1999; Yoder et al., 2014). The relevance of these processes to burn injury must now be considered as, while burn-induced modulation of LPC levels has previously been reported systemically (Harris et al., 1981) and in muscle (Turinsky et al., 1985), LPC is here implicated in burn pathology at skin-level and specifically with increased interstitial availability for the first time. LPC's *in vitro* regulation of immune cell function is a key theme in its role as an inflammatory mediator. Amongst the cells affected are monocytes, which are recruited into the wound following burn injury (Shallo et al., 2003). LPC is capable of enacting this recruitment of circulating monocytes in a manner similar to monocyte chemoattractant protein-1 (MCP1; Schilling et al., 2009a); indeed, LPC's chemoattractant actions on monocytes are mediated in part indirectly via inducing MCP1 production (Takahara et al., 1996), which increases following burn injury (Daniel et al., 2007), as well as directly (Jing et al., 2000; Quinn et al., 1988; Tan et al., 2009). LPC has further been linked with monocytes differentiating into both macrophages and dendritic cells (Coutant et al., 2002). Macrophage activity, which is stimulated by LPCs (Gomez-Munoz et al., 1999; Yamamoto et al., 1987), is markedly enhanced following burn injury and is considered a key contributor to immune system dysfunction following the trauma (Fayazov et al., 2009; Schwacha, 2003), serving as the major source of inflammatory mediators during systemic inflammatory response syndrome (SIRS; Calum et al., 2009; Loose et al., 1984; Rodeberg et al., 1999; Winslow et al., 1996). This innate immune system phenotype, to which macrophages principally contribute, therefore contrasts with the post-burn adaptive immune system (Shen et al., 2012), which becomes immunosuppressive as indicated by the regulation of various T cells (Kelly et al., 1997; Kelly et al., 1999; Lederer et al., 1999). The interaction between immune

system components is thought to be mediated by dendritic cells (DCs), in part by T cell priming that relies on DC maturation (Shen et al., 2012). The fact that LPC can induce the generation of mature DCs from differentiating monocytes, increasing the T cell-stimulatory capacity of DCs (Coutant et al., 2002), appears to be insufficient to overcome the adaptive immune system acquiring an immunosuppressive phenotype post-burn (Kelly et al., 1997; Kelly et al., 1999; Lederer et al., 1999), which is specifically attributed to compromised Toll-like receptor-mediated activation of DCs (Shen et al., 2012) and augmented MafB expression in CD14+ monocytes with reduced maturation (Williams et al., 2012). LPC is further reported to directly induce chemotaxis (Radu et al., 2004) and activation of T lymphocytes as indicated by expression of an IL-2R receptor subunit (Asaoka et al., 1992) and IFNγ (Nishi et al., 1998). LPC also acts on neutrophils, increasing adhesion and CD11b and fMLP receptor expression, eliciting degranulation, regulating chemotaxis and, importantly, priming NAPDH oxidase activation which leads to ROS generation (Silliman et al., 2003). LPC enhancing ROS production via NADH/NADPH oxidase has further been demonstrated in endothelial cells (Takeshita et al., 2000), though it should be noted that LPC has also been reported to inhibit superoxide generation in neutrophils (Lin et al., 2005). Oxidative stress has been heavily implicated in burn pathophysiology, with ROSs known to be elevated in burn tissue by both xanthine oxidase and neutrophil activation and antioxidant strategies still considered to be a potential therapeutic avenue (Parihar et al., 2008); LPC's potential contribution to oxidative stress must be considered. Additionally, LPC's induction of adhesion molecule expression, including ICAMs, VCAMs and selectins, underlying monocyte adhesion to smooth muscle cells (Li et al., 2006) and endothelial cells (Zou et al., 2007) may represent a key component of its immune system interaction following burn injury.

7.3.2 LPC and Cytokines

In keeping with this influence on the immune system, LPC is known to increase the concentrations of various cytokines. Of particular interest are those primarily associated with elevation in burn injury; Il-1β (Drost et al., 1993; Finnerty et al., 2009), IL-6 (de Bandt et al., 1994; Drost et al., 1993; Finnerty et al., 2009; Shehab El-Din, 1996) and TNFα (de Bandt et al., 1994; Drost et al., 1993; Finnerty et al., 2009; Shehab El-Din, 1996). IL-1β, principally known as a leukocytic pyrogen, activates T-lymphocytes (Houssiau et al., 1989), enhances endothelial neutrophil and lymphocyte adherence, modulates the production of other cytokines such as IL-6 and has been implicated in various inflammatory pathologies (Drost et al., 1993; Libert et al., 1990; Shalaby et al., 1989). In addition to the above-listed effects of LPC on monocytes, LPC may contribute to burn injury progression via dose- and time-dependently inducing their production of IL-1β (Liu-Wu et al., 1998). IL-6 similarly plays various roles in the immune system, in addition to the acute phase response and haematopoiesis, including extensive modulation of immune cell chemotaxis and differentiation (Scheller et al., 2011). Elevated serum IL-6 has been reported extensively following burn injury, both with and without concomitant infection (de Bandt et al., 1994; Yeh et al., 1999), and could be contributed to by LPC's induction of IL-6 release from endothelial cells (Morita et al., 2015; Takabe et al., 2004) following thermal trauma. Studies identifying lysophospholipid-induced IL-6 production have also identified the release of IL-8 from both maturing DCs (Oz-Arslan et al., 2006; Rodriguez et al., 1993; Vindenes et al., 1995) and endothelial cells (Morita et al., 2015), where post-burn IL-8 levels have been found to mirror

those of IL-6 (Kraft et al., 2014; Takabe et al., 2004; Yeh et al., 1999) though the extent of elevation depends on the presence of concomitant infection (Yeh et al., 1997a, 1997b). It is thought to recruit neutrophils and induce angiogenesis, cell growth and tissue remodelling (Kraft et al., 2014). Inducing the release of IL-6 and IL-8 is among the many functions of TNFα, another inflammatory mediator known to be elevated in burn injury (Huang et al., 1999; Shehab El-Din, 1996; Yeh et al., 1999), alongside neutrophil chemotaxis (Lauterbach et al., 2008), inducing a procoagulant phenotype in endothelial cells (Nawroth et al., 1986) and enhancing immune cell adhesion (Xia et al., 1998). LPC has been reported to induce the release of TNFα from macrophages in a TLR2-dependent manner (Magalhaes et al., 2010), perhaps contributing to these processes in burn injury. While the roles of these cytokines in burn injury have received the most attention, further cytokines also linked with LPC have been implicated. The expression of IFNγ, a macrophage-activating cytokine critically involved in both innate and adaptive immunity, is suppressed following severe burn injury (Hultman et al., 1995; Toliver-Kinsky et al., 2002), potentially contributing to immunosuppression underlying burn pathophysiology (Toliver-Kinsky et al., 2002). However, LPC has been shown to enhance IFNγ secretion and gene expression from T lymphocytes (Huang et al., 1999; Nishi et al., 1998). These interactions can be dependent on IL-2 (Nishi et al., 1998), an IFNγ-inducing cytokine (Toliver-Kinsky et al., 2002) also released from T lymphocytes following LPC exposure (Coutant et al., 2002) and similarly implicated in severe burn injury by its reduction reportedly contributing to post-burn immunosuppression (Kowal-Vern et al., 1994). While LPC's effect on these cytokines may be at odds with reported release profiles in severe burns, both are elevated in relatively smaller burns (Hultman et al., 1995; Kowal-Vern et al., 1994). Further, LPC

exposure induces the production of MIP-2 (Olofsson et al., 2008), a neutrophil chemoattractant found to be elevated locally and systemically in burn injury (Carter et al., 2014). Given the variety of immune cells and inflammatory mediators it modulates, LPC's involvement in the complex immune component of burn injury must be considered. Its general characterisation as an inflammatory mediator, and indeed many of its relationships with specific immune cells and inflammatory processes, stem largely from its implication in pathologies comprising local and systemic inflammatory components such as atherosclerosis (Matsumoto et al., 2007), psoriasis (Ryborg et al., 1995) and rheumatoid arthritis (Fuchs et al., 2005). In summary, LPC's extensive characterisation as an inflammatory mediator, bolstered by findings that its injection in normal skin induces erythema, oedema, recruitment of T-lymphocytes, monocytes and macrophages and adhesion molecule expression (Ryborg et al., 2000), certainly supports its potential role as a mediator of burn pathophysiology.

7.3.3 LPC and Burn Pathology

Although contributing to inflammation is LPC's best characterised putative contribution to burn injury, LPC is implicated in components of various other pathological states that may apply to thermal trauma. For example, it has long been established that LPC accumulating with cardiac tissue ischaemia (Mock et al., 1990), such as that induced by pacing in the myocardium (Sedlis et al., 1993), exerts deleterious effects following membrane incorporation in the sarcolemma and consequently induces electrophysiological changes leading to arrhythmia (McHowat et al., 1993; Sedlis et al., 1997). Ischaemia-induced LPC accumulation is not

restricted to the heart, having also been observed in the brain (Inose et al., 2015) and kidneys (Matthys et al., 1984); it is considered a pathogenic factor in both cases. The subcutaneous LPC elevation following burn injury presently reported may be induced partly by local ischaemia, an important clinical consideration following thermal trauma (Noble et al., 1977; Singer et al., 2008). Indeed, although the data do not support locally-sourced systemic distribution of LPC within 3 hours post-burn, both myocardial function and the kidneys are compromised following burn injury, in-keeping with the implications of ischaemia. Whether by the resulting deleterious membrane effects (McHowat et al., 1993), consistent with present observations, or inflammatory mediator release (Inose et al., 2015), ischaemia-induced LPC-mediated processes observed in other tissues may contribute to burn injury progression.

While the present data cannot support a role for LPC in post-burn myocardial dysfunction, it may nonetheless be involved in the cardiovascular component of burn pathology. One of the primary clinical considerations in early post-burn management is fluid resuscitation to correct for hypovolaemia (Yowler et al., 2000) resulting in part from increased capillary permeability (Demling, 2005). Unlike LPA (Alexander et al., 1998), LPC increases endothelial cell permeability (Huang et al., 2005; Qiao et al., 2006); its local elevation may thereby contribute to the generation of interstitial oedema and ultimately to the intravascular fluid deficits observed post-burn. Other effects including the decreased cardiac contractility discussed above and peripheral vasoconstriction also contribute to post-burn hypotension (Hettiaratchy et al., 2004), and the ultimate depth of post-burn necrosis has been experimentally increased with the application of vasoconstrictors (Knabl et al., 1999). LPC can induce endothelium-

dependent vasoconstriction and inhibit endothelium-dependent relaxation (Ceylan et al., 2004; Murohara et al., 1994), and may thereby mediate various cardiovascular pathogenic effects in burn injury.

Neuropathy is another pathological component of burn injury (Tamam et al., 2013) in which LPC is implicated. While there is evidence for other central neurodegenerative effects mediated through inflammation (Sundaram et al., 2012), the vast majority highlight both peripheral (Nishimoto et al., 2015) and central (Vereyken et al., 2009) demyelination as LPC's neuropathic mechanism. This generally stems from its use as a well-established model of demyelination (Nishimoto et al., 2015; Vereyken et al., 2009), though the same effect as induced by endogenous LPC has been observed following peripheral nerve injury and is thought to contribute to the pathology (Nagai et al., 2010). LPC induces the breakdown of the myelin sheath via progressive vesiculation in a Ca^{2+}-influx dependent process (Allt et al., 1988; Hollis et al., 2015) that can be replicated by PLA_2 incubation (Smith et al., 1985). The importance of LPC's membrane effects here, whether on the membrane's curvature or simply its composition, is supported here by the finding that cholesterol, which induces an opposing negative membrane curvature (Chernomordik, 1996; McMahon et al., 2005), attenuates LPC's myelin toxicity. While it is accepted that LPC concomitantly recruits immune cells, leading to rapid monocyte influx and macrophage-mediated myelin debris phagocytosis (Ousman et al., 2000), antibody-mediated neutralisation of LPC-induced IL-2 upregulation reduces phagocytic macrophage count and demyelination, suggesting that the immune cells also contribute to demyelination (Ghasemlou et al., 2007). While the reduced nerve conduction velocity and abnormal compound muscle action potentials resulting from

demyelination (Tamam et al., 2013) as induced by LPC likely contribute to neuromuscular deficits, which are prevalent after thermal trauma (Tomera et al., 1988), this is not LPC's primary implication in post-burn neuropathy. This is rather its contribution to neuropathic pain, occurring after conversion to LPA (Inoue et al., 2008; Nagai et al., 2010; Wang et al., 2013). LPA, proposed by some to be the true mediator of demyelination (Nagai et al., 2010), is produced from LPC via the enzyme autotaxin (ATX) and acts on the lysophosphatidic acid (1) receptor (LPA1R) to induce mechanical allodynia and thermal hyperalgesia (Inoue et al., 2008; Nagai et al., 2010). Studies not excluding the contribution of autotaxin and LPA1R report LPC inducing the same neuropathic pain behaviours (Wallace et al., 2003; Wang et al., 2013) and further identify elevated neuronal nitric oxide synthase as a component of the mechanism (Wang et al., 2013). Although demyelination is not as prevalent as axonotmesis following thermal trauma, it is nonetheless an important neuropathic component given the potential functional implications of compromised nerve signalling (Lee et al., 2009; Tamam et al., 2013) and reportedly contributes to neuropathic pain itself (Gillespie et al., 2000; Nagai et al., 2010). Between LPC's demyelination and neuropathic pain induction, related or otherwise, and the significant neuropathic component of burn injury, it is clear that neuropathy should be further investigated as one of LPC's post-burn effects.

LPC's deleterious effects extend far beyond demyelination; with the precise mechanisms of action for many of the above-described processes still unknown, the possibility that they are initiated by a fundamentally injurious effect of LPC must be considered. In any case, LPC is known to be capable of inducing apoptosis in various cell types. For example, this is thought to underlie the development and

progression of atherosclerosis, with LPC-induced apoptosis observed in human endothelial cells, occurring through a p38-MAPK-dependent mechanism (Takahashi et al., 2002), and vascular smooth muscle cells (Hsieh et al., 2000). LPC induces lipoapoptosis in hepatocytes in both a PLA_2- and Gαi-dependent mechanism in a process thought to underlie non-alcoholic steatohepatitis (Han et al., 2008) and a JNK, glycogen synthase kinase-3 and CAAT/enhancer binding homologous protein-dependent manner (Kakisaka et al., 2012). Leading on from the PLA_2's implication in the pathogenesis of acute pancreatitis, LPC's induction of apoptosis in pancreatic acinar cells has been identified (Masamune et al., 2001). Further, LPC has received clinical interest for its anti-tumour function as it reportedly induces chronic myeloid leukemia K562 cell apoptosis via suppression of HDAC3/STAT3 activation and their interaction with bcl-xL (hoon Jung et al., 2012). LPC's cytotoxicity has also been observed in osteoblast-like MG-63 cells, and is here attributed largely to a TRPV2-activation dependent signalling cascade (Fallah et al., 2013). While LPC's induction of apoptosis in an extensive range of cells is established, there is currently little evidence to support a unifying underlying mechanism. However, the induction of a calcium influx has nonetheless emerged as a generally common them within LPC cytotoxicity in a variety of cell types (Chen et al., 1995; Qin et al., 2009; Song et al., 2010; Zhou et al., 2006), consistent with the general implication of calcium mobilisation in apoptosis (Orrenius et al., 2003). Yet, as with its induction of apoptosis itself, our understanding of LPC's mediation of this influx is exemplary of the difficulty in delineating the relative contribution of its different potential mechanisms of action. The influx has been attributed to membrane disruption in varying cell types (Chen et al., 1995; Li et al., 2007; Watanabe et al., 2003; Zhou et al., 2006), as is generally, but not always (Wang et al., 2016), the case with

endothelial cells and cardiac muscle as a putative component of atherosclerosis. However, LPC-induced influxes have also been attributed to other means such as membrane receptor-dependent signalling cascades (Fallah et al., 2013; Wang et al., 2016) and voltage-gated calcium channels, even within the same cell type (Li et al., 2007; Qin et al., 2009; Wang et al., 2016). While apoptosis is a significant contributor to cell death following burn injury (Duan et al., 2009; McNamara et al., 2010; Yasuhara et al., 2000), we can only speculate as to the contribution of LPC and the balance of mechanisms by which it is induced with the present findings. Nonetheless, there are multiple lines of inquiry worth pursuing even within the dermis; LPC induces apoptosis in fibroblasts by membrane disruption (Colles et al., 2000), as observed in many of the above-described studies, and it has been suggested that post-burn adipocyte apoptosis may contribute to altered lipid metabolism, including hyperlipidemia (Yasuhara et al., 2006) which is characterised by increased LPC levels (Chen et al., 1997).

LPC's complex implication in apoptosis is exemplary of the difficulty in delineating its operation in any given effect. LPC operates via a range of modes with varying specificity, from initiating selective protein interaction-dependent signalling cascades, to its indirect effects induced by its physiological membrane presence to its cytotoxic compromise of membrane structure. Any attempted definition of its effects must be approached with an awareness of the potential relative contributions of each of these three generic categories, and of the many possible mechanisms contained within. However, the mechanisms underlying the presently observed LPC-induced TRPV1 sensitisation could not be delineated within this project due to time constraints. Here,

the elements of our understanding of LPC function which may underlie the presented data, and which should direct further study, are discussed.

7.3.4 LPC and TRPV1

LPC has not been reported to activate TRPV1, though only few data affirming that it does not have been published (Nieto-Posadas et al., 2012; Tanaka et al., 2011; Torok et al., 2014). Studies reporting TRPV1 activation concomitant with LPC exposure (Schilling et al., 2009b, 2010) remain ambiguous about how this occurs, which is understandable given the above-described complexity of delineating LPC's function. Between the lack of data confirming activation, the plausibility of indirect mechanisms where activation is reported (Knowlden et al., 2014) and the fact that activations specifically by LPC have been explicitly demonstrated and well-established with other TRP channels (Andersson et al., 2007; Flemming et al., 2006), LPC itself is not thought to activate TRPV1, as is consistent with the present data. As LPC nonetheless exerts its effects on monocytes (Schilling et al., 2009b) and, specifically, macrophages (Schilling et al., 2010) through TRPV1 activation, the known relationship between these molecules should be explored. The best characterised link is via LPA, produced from LPC via autotaxin (Okudaira et al., 2010). LPA directly activates TRPV1 via C-terminus interaction and consequently induces nocifensive behaviours which are reduced with TRPV1 knockout; it is thought to contribute to the development of neuropathic pain (Nieto-Posadas et al., 2012). While building on LPA's pre-existing implication in neuropathic pain, which characterised its activation of LPA1R following conversion from LPC (Inoue et al., 2008), the authors also identified that LPA's binding site overlaps with that of PIP2

and that PIP2 allosterically modulates LPA's TRPV1 activation; it has since been suggested that TRPV1 and LPA1R respectively confer LPA's induction of acute inflammatory and neuropathic pain (Tigyi, 2011). In any case, TRPV1's activation could occur following LPC's conversion to LPA, and its generation of nociception thereby implicates LPC in burn injury pain both via TRPV1 and other mechanisms.

TRPV1 sensitisation can also underlie elevated nociceptive signal transduction (Malek et al., 2015) and serve as a functional equivalent of the channel's activation upon its threshold reaching physiological conditions (Crandall et al., 2002; Premkumar et al., 2000). While it is therefore as interesting as activation, TRPV1 sensitisation, whether mediated by membrane availability or by modulated gating, has not been previously identified as an effect of LPC. Nonetheless, there are avenues to pursue. For example, LPA sensitises TRPV1 in a PKCϵ-dependent process (Pan et al., 2010), as bradykinin does to potentiate gating (Bonnington et al., 2003; Cesare et al., 1999), and is thereby thought to mediate chronic bone cancer pain. The present finding that the LPA precursor LPC is elevated in burn injury may implicate this mechanism in its associated pain. Another avenue which actively pursued in this project was LPC's potential modulation of TRPV1 function via its action on TrkA receptors. Via TrkA, NGF sensitises TRPV1 primarily by inducing the receptor's translocation into the membrane and increasing its availability (Ji et al., 2002; Zhang et al., 2005). The means by which this is accomplished are unclear as none of the major biochemical pathways TrkA typically operates by, the PLCγ, ERK or PI3K pathways (Zhu et al., 2007), are unanimously supported. This is likely a result of the variety of expression systems, functional endpoints and intervention specificities employed between studies (Zhu et al., 2007). Nonetheless, the ERK

pathway has been implicated in NGF's TrkA-mediated TRPV1 sensitisation (Zhu et al., 2007; Zhuang et al., 2004), and LPC has been reported to enhance MAPK signals via extracellular action on TrkA as measured by phosphorylation of the ERK pathway components MEK1/2 (Wuhanqimuge et al., 2013). To determine whether or not LPC enhances NGF's TrkA-mediated TRPV1 sensitisation, experiments (not reported above) were conducted within the present project. They consisted of determining whether or not the increase in DRG neuron capsaicin responses observed after NGF-induced TRPV1 translocation to the membrane, which was reproducible presently (Fig. 30), would be enhanced by prior exposure to LPC. However, the execution of this endeavour was problematic and remains incomplete. The design of the experiment required that all capsaicin responses in the presence of LPC or LPC + NGF were normalised to a response prior to either exposure. Therefore, only cells expressing TRPV1 in the absence of NGF, which only constituted 44.74% of the (post-NGF exposure) capsaicin-responsive cell population, could be recorded from. Further, adding the requirement of TrkA expression, which was clearly indicated in the response profile, reduced the usable cell population to 30.92% of all capsaicin-responsive cells, where overall cell count had already been compromised by the NGF deprivation. Further, while the experience of constructing a new calcium imaging system was overall beneficial, it led to several teething problems, particularly regarding operation of the gravity-powered perfusion system. These issues manifested in the earlier-collected control data, prior to being overcome by minimising passive, unintentional perfusion of solutions and dead space. The earlier inconsistent capsaicin pulses prevented meaningful measurement and comparison of desensitisation and sensitisation profiles, and dictated the exclusion of responses from all but 8 cells in the control group. While LPC appeared

to potentiate NGF's effect, no comparison was made due to an unjustifiably small control sample size. This effect was not pursued further as the experiment also allowed for identification of an LPC effect prior to NGF exposure, which was evidently the relatively better-supported LPC response profile (Fig. 30). On the weight of these data, the possibility that LPC enhances NGF's sensitisation of TRPV1 via its extracellular TrkA action has important implications for burn injury pain

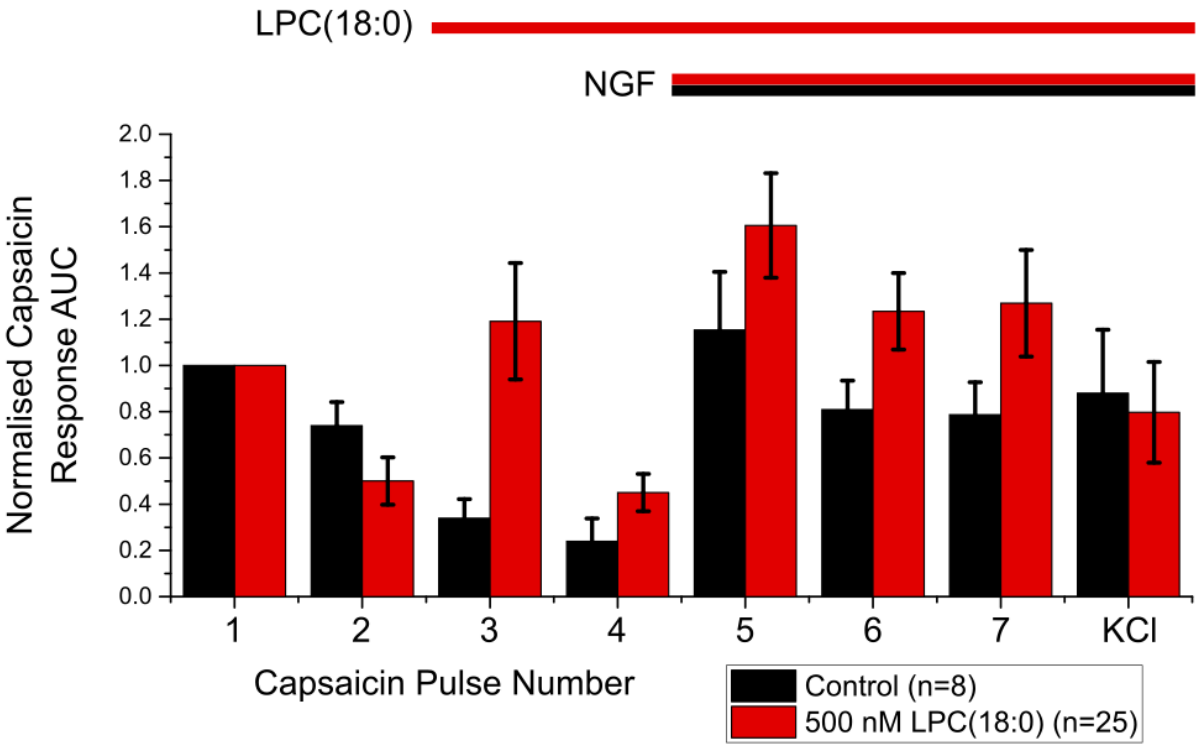


Figure 30 LPC(18:0) may further sensitise TRPV1 by enhancing its TrkA-mediated promotion of membrane insertion. The first calcium imaging experiments indicated that LPC(18:0) had a clear sensitising effect on TRPV1 regardless of TrkA function as seen in the third capsaicin response, motivating the above-described *in vitro* study. TrkA-mediated NGF-induced membrane insertion of TRPV1 was nonetheless reliably induced in the model system and perhaps enhanced by the presence of LPC(18:0), though whether the enhanced responses simply resulted from LPC's TrkA-independent sensitising effect alone is not clear. Various restrictions enforced by the study design made investigating this effect problematic; this comparison is based on a limited sample size and was dropped as a lower priority than LPC(18:0)'s TrkA-independent sensitising effect.

and inflammation, and must be pursued. However, rather than contend with the inefficiency of the TrkA-focused design, LPC's apparent potentiation of TRPV1-mediated responses was investigated instead presently.

LPA's activation and sensitisation of TRPV1 and the channel's role in LPC's effects on macrophages and monocytes constitute the entirety of the published relationship between LPC and TRPV1. Given the extensive concomitant prior use of LPC and TRPV1, and its established effects on other TRP channels, LPC was not expected to activate TRPV1; this study instead sought to determine whether it exerts any sensitising effect. Indeed, LPC did not activate TRPV1 between the concentrations used presently, though possible sensitising mechanisms both independent of and dependent on NGF's action on TrkA were identified. Evaluating the former effect in a dedicated experimental design demonstrated LPC-induced TRPV1 sensitisation occurring in both HEK293T cells and DRG neurons. However, the project's time constraints dictated that work identifying the underlying mechanism was limited to ill-fated attempts at whole-cell voltage clamp electrophysiology. The application of LPC would disrupt the gigaseal, presumably by altering membrane conformation at the points of pipette contact, preventing collection of sufficient recordings for a meaningful comparison. Nonetheless, the mechanism of LPC's TRPV1-sensitising effect must be elucidated and there are many possibilities to pursue. The known relationships between LPC and channels related to TRPV1 may offer valuable insight into this sensitisation and should influence the experimental design in the next stages of elucidating this mechanism.

One such group of related proteins are the other members of TRPV1's cation channel superfamily, the TRP channels. TRP channels are activated by a variety of changes in their local milieu to function as physiological sensors for vision, taste, olfaction, touch, hearing, osmosensation and, of particular interest here, thermosensation (Venkatachalam et al., 2007). Several channels are unified by this latter capability, exhibiting activation by varying temperature ranging from noxious heat to noxious cold (Jordt et al., 2003; Patapoutian et al., 2003). These include TRPV2 (<52°C; Nagy et al., 1999), TRPV1 (<42°C; Caterina et al., 1997), TRPV3 (34-38°C; Smith et al., 2002) and TRPV4 (27-35°C; Guler et al., 2002), TRPM4 and TRPM5 (15-35°C; Talavera et al., 2005), TRPM8 (25-28°C; Peier et al., 2002) and TRPA1 (<17°C; Story et al., 2003). Additionally, many TRP channels are further unified in being modulated by endogenous lipids. For example, PIP2 regulates the function of at least TRPV1 (Qin, 2007), TRPV5 (Rohacs et al., 2005), TRPM4 (Qin, 2007), TRPM5 (Liu et al., 2003), TRPM7 (Runnels et al., 2002) and TRPM8 (Liu et al., 2005) in addition to TRP/TRPL channels in *Drosophila* photoreceptors (Qin, 2007). Diacylglycerides (DAGs) and PUFAs, where the latter can be incorporated into or generated from the former, similarly modulate various TRP channels including TRPV1 (Motter et al., 2012; Woo et al., 2008). TRPV1 in particular is known to be activated or otherwise modulated by a variety of endogenous lipids including the arachidonic acid metabolites anandamide (Ross, 2003), hydroxyoctadecadienoic acids (Alsalem et al., 2013) and eicosatetraenoic acids (Kelly et al., 2015). Given the homology and functional overlap of TRP channels, the potential implications of LPC's known modulation of TRPM8 and TRPC5 for TRPV1 will be discussed.

TRPM8 is of particular interest not only in being thermosensitive, but also due to its pharmacological similarity to TRPV1; the same position is critical for their respective activations by AG-3-5 and capsaicin, indicating that they share a conserved ligand activation mechanism (McKemy, 2007). Andersson et al. (2007) found that the cold receptor's activation threshold was raised to physiological temperatures by 3 μM LPC. They interpreted the many tens of seconds required for this effect as representative of LPC's translocation across the membrane towards an intracellular site of action (Andersson et al., 2007), as opposed to a rapid extracellular interaction such as that between LPC and TREK-1 (François Maingret et al., 2000). Although the lack of effect in untransfected cells excluded this response reflecting the formation of transient non-protein calcium pores (Wilson-Ashworth et al., 2004), the means by which LPC modulates TRPM8 remain unclear. However, as the effect was maintained with inside-out configuration electrophysiology, it appears to be exerted in a membrane-delimited manner. This precludes the contribution of sensitising mechanisms such as rapid vesicular translocation and membrane insertion of the TRP channel (Bezzerides et al., 2004). The authors noted that LPC's effect could be mediated either by direct binding to TRPM8 or other channel-associated proteins, or otherwise indirectly via interaction with the phospholipid bilayer. Further, both LPC's carbon chain length and the biochemical properties of its head-group were independently affirmed. Their findings were consistent with another study reporting LPC generation as the basis of TRPM8 regulation by $iPLA_2$ and demonstrating LPC's activation of TRPM8 in HEK293 cells (Abeele et al., 2006). The report of LPC's ability to activate TRPC5 by Flemming et al. (2006) shared several similarities with Andersson et al.'s study. The time required for activation was consistent with translocation across the membrane, and activation was observed with both inside-

out and outside-out electrophysiology which further served to support LPC's effect being membrane-delimited. Through the use of a tetracycline-induced expression system, LPC's effect was shown to be dependent on TRPC5 rather than any unrelated membrane effect. The finding that the carbon chain length dictates TRPC5 activation was interpreted as an indicator of LPC's interaction either with the phospholipid bilayer or a lipid-interaction site associated with the channel. The activation was induced at concentrations towards the lower end of the 5-180 μM physiological concentration range reported for LPC (Ishii et al., 2004; Okita et al., 1997), with the influence of the dynamic equilibrium resulting from the balance of its free and protein-bound form noted. LPC's effect, as observed in HEK293T cells, was then found to have a similar time course in vascular smooth muscle cells endogenously expressing TRPC5. The electrophysiological response profile was consistent with TRPC5 responding both in homomeric and heteromeric assemblies with other TRP channels, as is representative of smooth muscle cells' expression profile (Beech et al., 2004). The authors note the possibility that LPC might represent a point of convergence between the many modes of TRPC5 activation including calcium store depletion (Zeng et al., 2004), an event that induces the activation of $iPLA_2$ and LPC generation to refill internal stores (Singaravelu et al., 2006). They conclude in discussing the difficulty in distinguishing between the effect's exertion either by a direct agonist interaction or by phospholipid bilayer LPC content, but suggest that the inefficacy of arachidonic acid and palmitoleic acids indicate the necessity of a bulky head-group for physical distortion the membrane.

Both reports inform interpretation of the present data and the direction for development of this study. TRPM8's activation occurring by sensitisation towards

physiological temperatures may reflect a similar effect in TRPV1; while LPC's cytotoxicity restricted its concentration in the present TRPV1 experiments to 1 μM (Fig. 28), observations indicate that larger cells more representative of *in vivo* thermosensation, such as those in the DRG cultures, were more resistant to LPC's detergent effect. At higher LPC concentrations, TRPV1's presently-reported sensitisation may reduce the thermal threshold to 37°C and thereby extend to gating by temperature; it is certainly encouraging that the present effect was induced at concentrations below LPC's reported physiological range. Both studies reported requiring durations in the many tens of seconds for LPC's effect; here, TRPV1's sensitisation is measured after 2 minutes of LPC exposure and subsequently at 4 minute intervals. While an immediate effect therefore cannot be excluded, its progressive development over sequential recordings and irreversibility with washing is consistent with LPC's ongoing integration into or translocation across the membrane. While TRPV1's sensitisation manifests here as a modulation of capsaicin responses, no insight can be gained into how directly LPC interacts with TRPV1 by comparison of response profiles with untransfected cells. However, the formation of calcium pores which such an analysis typically precludes would not exclusively contribute to ion flow during TRPV1 responses and nonspecific membrane effects were not observed at the lower concentrations of the TRPV1 experiments (Fig. 28). In only presently attempting whole-cell configuration electrophysiology, no insight into whether or not LPC's TRPV1 sensitisation is membrane-delimited can be drawn. Indeed, if disruption of the gigaseal was a consequence of cell positioning resulting from LPC-induced rounding rather than a detergent effect at the point of pipette contact, inside-out or outside-out electrophysiology would have yielded far more usable data. This presents an attractive option for the next experiment, as does

evaluating the influence of the bound-unbound LPC balance and its true interstitial availability in the model system. Further, as this sensitisation has presently been demonstrated in cells endogenously expressing TRPV1, the influence of the receptor's incorporation into either homomeric or heteromeric assemblies on this effect is an interesting concept. Additionally, as intracellularly-expressed TRPV1 mediates the release of calcium from a subset of internal stores upon activation (Turner et al., 2003; Wisnoskey et al., 2003), but does not induce store-operated Ca^{2+} entry as TRPC5 does (Zeng et al., 2004), the functional relationship between these channels and the implication of LPC's interaction with both should be explored.

The identification of LPC's effects on TRPM8 and TRPC5 exemplify the extent of elucidation required to demonstrate a TRP channel's activation by LPC. Due to the range of potential means by which it can modulate a channel, with varying levels of specificity, establishing whether or not the process is membrane delimited is an important step in narrowing down potential mechanisms. A common theme in the speculation as to how LPC's effect is exerted is by its physical perturbation of the membrane (illustrated in Fig. 31) and the resultant effects on the proteins it contains, as is broadly predicted by the membrane's lateral pressure profile. Ion channel gating by bilayer lateral profile changes are typically associated with dedicated mechanosensitive channels; for example, the best-described is the large conductance channel from *Escherichia coli* (MscL). Its ion flow is restricted physically at a five-fold symmetrical axis of constriction lined with hydrophobic residues, and is gated by increases in transbilayer pressure such as by that from a patch pipette's negative pressure (Berrier et al., 1989; Chang et al., 1998; Sukharev et al., 1994; Sukharev et al., 1993). Following the demonstration that channels can be gated by

tension transmitted exclusively via the lipid bilayer (Sukharev et al., 1994), efforts to delineate the contribution of the membrane's intrinsic curvature to this effect have experimentally utilised LPC for its conical structure and consequent modulation of the transbilayer lateral tension gradient (Perozo et al., 2002). MscL strongly favours its open state following external application of LPC. At 1.5 μM, it enhances its single MscL channel activity in the presence of minor transbilayer pressure. At 3 μM, MscL activity gradually increases over time without any applied pressure, consistent with the ongoing incorporation of LPC into the outer layer of the membrane. Similarly, amphipaths or lysophospholipids reduce the activation threshold of the mechanosensors MscS (Martinac et al., 1990), TREK-1 and TRAAK (François Maingret et al., 2000). Ultimately, it was described that mechanical transduction is initiated in MscL specifically by an asymmetry in lateral pressure profile between the outer and inner membrane leaflets, where symmetrical distributions of LPC failed to induce an open conformation. Further, LPC's effect could be reversed by the presence of phosphatidylethanolamine which, despite itself also being conical, forms hexagonal phases geometrically opposing LPC's impact on the membrane (Perozo et al., 2002).

Responding to mechanical stress in the membrane is a fundamental requirement of certain proteins, including mechanosensitive channels such as those described above. However, modulation by changes in membrane tension is not restricted to these molecules, having been observed in various voltage gated channels (Calabrese et al., 2002; Morris et al., 2007; Schmidt et al., 2008). Indeed, this is the mechanism by which LPC is thought to activate ryanodine receptor channels (Nakamura et al., 2007) and capsaicin modulates voltage-dependent sodium

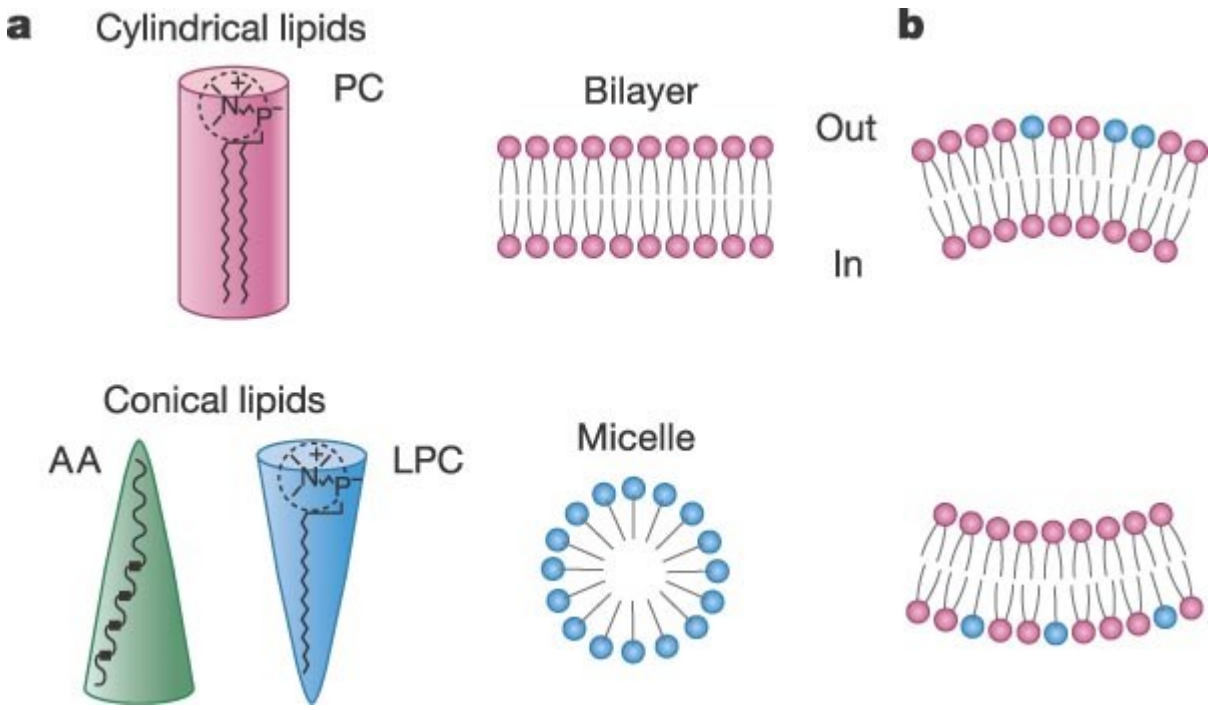


Figure 31 Membrane perturbation by LPC. With the loss of a fatty acid, an approximately cylindrical phosphatidylcholine is converted to an approximately conical lysophosphatidylcholine (**a**), comparable to the inverted conical structures of PUFAs such as arachidonic acid. This confers LPC's conformity within micelles and its ability to induce curvature in phospholipid bilayers by asymmetrical distribution between the outer and inner membrane leaflets (**b**). Image published by Kung, 2005 and reproduced with permission of the rights holder, Nature Publishing Group.

channels (Lundbaek et al., 2005). Despite sporadic implication in mechanosensing roles (Bielefeldt et al., 2008; Birder et al., 2001; Birder et al., 2002; Kiyatkin et al., 2013), TRPV1 is not currently thought to be gated by mechanical force in any classical sense (Christensen et al., 2007). However, as with any membrane protein (Phillips et al., 2009), TRPV1 could in principle be regulated by membrane bilayer tension. This concept was first investigated specifically within the TRP family in its implication in mechanosensitive TRP and TRPL channels (Hardie et al., 2012),

which prompted interest in its application to TRPV1's thermosensitivity. However, there has only been one study of TRPV1's modulation by membrane tension to date. The experiment evaluated TRPV1 thermosensitivity in liposomes with increased membrane fluidity or curvature, as accomplished by application of cholesterol and lysophosphatidylcholine respectively (Cao et al., 2013). The authors noted no change in TRPV1's temperature response profile. However, this particular component of the otherwise well-received study may have been better executed in avoiding the use of liposomes containing sphingomyelin, which sequesters cholesterol (Harder et al., 1997). Further, its use of a model system in which TRPV1 may orient itself bidirectionally, and in which PIP2 localises to either the inner or outer leaflet, may warrant further study. Currently, the question of whether or not TRPV1 may be regulated by membrane tension remains unanswered.

7.3.5 The Source of LPC

Much like its mode of action, LPC's generation is multifaceted. Though the relative contribution of each potential source is not typically addressed holistically in reports of LPC's function, individual pathways are known to contribute to particular components of other pathological states that could conceptually apply to burn injury. Where LCAT and PLA_2 constitute the best-characterised sources, circulating LPC is thought to be generated predominantly by LCAT, which generates LPC by transferring a fatty acid from PC to cholesterol (Subbaiah et al., 1996), following the recognition of increased LPC levels and LCAT activity in atherosclerotic patients (Matsumoto et al., 2007; Wells et al., 1986). Atherosclerosis is similar to burn injury in its combination of local and systemic inflammatory components; LCAT likely

contributes to elevated LPC concentrations at both levels in burn injury, as is consistent with the present finding that LCAT RNA is among that most upregulated in burned tissue (Fig. 27). While both secretory (Kougias et al., 2006) and lipoprotein-associated (also known as PAF-acetylhydrolase; Zalewski et al., 2005) forms of PLA_2, which operates by hydrolysing phosphatidylcholine to generate fatty acids and LPC, have also been implicated in inflammatory conditions, secretory PLA_2 ($sPLA_2$) in particular has previously been reported to contribute to inflammation (Yamada et al., 1998) and reflect disease severity (Nakae et al., 1995) in burn injury. Consistent with this, RNA for two secretory forms of PLA_2, Pla2g2e and Pla2g2d, were presently significantly altered in burned tissue, as was that of PLA_2's receptor, Pla2r1. Further, Pla2g4d was also altered; this is a cytosolic form of PLA_2, where cytosolic PLA_2 ($cPLA_2$) is thought to contribute to post-burn disruption of cardiac phospholipid bilayers (Zhang et al., 2007). The present data therefore support the contribution of LCAT, secretory and cytosolic PLA_2 to the observed elevation of LPC in burn injury, and implicate all three enzymes in its deleterious effects. While phospholipids are reported to undergo spontaneous deacylation in physiological conditions (Choi et al., 2011), no insight into the contribution of this source of LPC in burn injury can be drawn from the present data. Further, Ca^{2+}-independent PLA_2 ($iPLA_2$) in particular appears to be important for the above-described gating of TRPM8 by lysophospholipids (Abeele et al., 2006), a function of LPC from which we may draw parallels for TRPV1, yet no evidence of altered $iPLA_2$ expression was found presently.

7.3.6 Further Targets for LPC

LPC is extensively pleiotropic, as is likely a consequence of its fundamental and far-reaching actions regulating membrane-bound proteins, mobilising Ca^{2+} and lysing cells. It therefore has several further functions worth noting. For example, TRPV1 and TRPM8 are not the only thermosensitive channels affected by LPC. Another is the two-pore domain mechano-gated K^+ channel TREK-1 (Maingret et al., 2000), where LPC's putatively extracellular interaction with TREK-1 informed the interpretation of temporal response profiles as indicators of LPC's intracellular interaction with TRPM8 (Andersson et al., 2007). TREK-1 is highly expressed in DRG sensory fibres, particularly in small- to medium-diameter neurons, reflecting the expression profile of TRPV1 and other thermosensitive channels (Maingret et al., 2000). Given the potential implication of mechanically-mediated signal transduction in LPC's effect on TRPV1, the identification of mechanosensitive channels modulated by LPC is certainly interesting; however, unlike LPC's effects on TRPM8, its rapid activation of TREK-1 is lost with membrane excision, suggesting the requirement of a cytosolic factor (François Maingret et al., 2000). AA's similar activation of TREK-1, on the other hand, is maintained in excised membrane patches. The authors postulate that the cytosolic factor may nonetheless exert its effect as AA does; by altering membrane curvature (François Maingret et al., 2000). In any case, despite sharing similar expression profiles and both exhibiting thermosensitivity, TREK-1 would not functionally complement TRPV1. Its maximal dynamic range of heat sensitivity lies between 32-37^oC, with the strongest currents recorded at 37^oC. As an outward rectifying K^+ channel, higher physiological temperatures therefore optimise its polarising capacity and oppose the generation of

action potentials. Cooling, however, decreases its capacity to maintain depolarisation; the channel is therefore suggested to function as a negative feedback mechanism within heat-activated neurons, tonically limiting AP firing at physiological temperatures but enabling responses to colder temperatures (Maingret et al., 2000). On the basis of its hyperpolarisation reducing Ca^{2+} influx via VGCCs and NMDA receptor-associated Ca^{2+} channels, TREK-1 is therefore thought to have a neuroprotective role. As TREK-1 is activated by LPC, the present data implicate this mechanism in burn injury, as does TREK-1's activation by cell swelling and intracellular acidosis such as that in ischemic tissue (François Maingret et al., 2000). A further thermosensitive channel modulated by LPC is TRPV2. LPC has been shown to induce Ca^{2+} influx via TRPV2 in a manner dependent on the head-group properties and side-chain length, acting via G-proteins and PI3,4K to induce channel translocation to the membrane and thereby migration in a prostate cancer cell line (Monet et al., 2009). Further, LPC-induced cytotoxicity is reportedly dependent on TRPV2 in osteoblast-like MG-63 cells, where the preceding Ca^{2+} influx was abolished and cytotoxicity was reduced with TRPV2 inhibition (Fallah et al., 2013). While there is no evidence for modulation of TRPV2 by LPC specifically in a thermosensitive capacity, as there is for TRPV1 and TREK-1, an LPC-related functional comparison between TRPV2 and other TRP channels can be drawn from this cytotoxic role. While the present data indicate that LPC does not require TRP channels to induce cell death, consistent with its established detergent effect (Matsumoto et al., 2007), LPC may still contributing to cell death via Ca^{2+} influx-mediated apoptotic processes as is suggested for TRPV2 (Fallah et al., 2013) and further TRP channels. Silencing TRPC1 or TRPC3, which were concomitantly shown to interact, opposed the induction of Ca^{2+} influx and apoptosis alongside activation of

the pro-apoptotic proteins Bax and cleaved caspase-3 and the decrease of the anti-apoptotic protein bcl-2 and the survival kinase pAkt, as induced by LPC in smooth muscle cells (Wang et al., 2016). Hence, LPC may depend on different TRP channels for its Ca^{2+} influx-mediated pro-apoptotic action in a cell type-dependent manner. Beyond its dependence on TRPC1 and TRPC3 for these particular functions, and its above-described activation of TRPC5, LPC is further associated with the TRPC family by elevating intracellular Ca^{2+} ultimately via TRPC6 activation in corporal smooth muscle cells (So et al., 2005). Additionally, LPC-induced TRPC6-mediated Ca^{2+} influx in aortic endothelial cells induces the translocation of TRPC5 into the membrane (Chaudhuri et al., 2008). While LPC's modulation of the TRP channel family is extensive, the potential involvement of these processes in burn injury has not been investigated to date. LPC's eventual activation of TRPV2 may contribute to apoptosis within burned tissue, as it does in the MG-63 cell line (Fallah et al., 2013), and the possibility that it sensitises the channel to physiological temperatures is worth exploring. In atherosclerosis, downregulation of TRPC5 was shown to reduce LPC-induced Ca^{2+} influx and enhance endothelial cell migration (Chaudhuri et al., 2008); LPC-induced TRPC5 activation is therefore suggested to contribute to atherosclerosis by inhibiting endothelial cell migration (Earley et al., 2010), where the same process could contribute to burn pathology by compromising post-burn angiogenesis (Busuioc et al., 2011). Further, where mechanical hyperalgesia is a significant component of post-burn pain, treatment with TRPC6 antisense oligodeoxynucleotide reversed mechanical hyperalgesia as induced by a thermal injury where that for TRPC1 did not (Alessandri-Haber et al., 2009). The authors concluded that TRPC6 and TRPC1 cooperate with TRPV4 to mediate mechanical hyperalgesia and nociceptor sensitisation with diverse etiologies, where

TRPC6 and TRPV4 in particular mediate these processes in thermal injury (Alessandri-Haber et al., 2009).

LPC is therefore involved in inflammation, cardiovascular regulation and complications, ischaemia, oedema, demyelination, apoptosis and various signalling cascades within these and further processes such as pain transduction. All of these are important known pathological components of burn injury, and the present data support LPC as a potential underlying contributor to those occurring locally within or being mediated via the burn site. Should LPC serve as a common factor among various pathological burn injury components, or even contribute significantly to one, it could emerge as an exciting therapeutic target. Its implication in these processes in other pathologies has identified it as such, leading to various studies investigating the potential of controlling LPC availability as a means of clinical intervention. As one of the two principal enzymes generating LPC, PLA_2 has received some attention in this regard while, interestingly, LCAT has not. PLA_2 has specifically been identified as a potential therapeutic target for inflammatory skin diseases, though the complexity of delineating its pathology-specific isoenzymes and the potential ramifications of systemic inhibition have been recognised (Mruwat et al., 2013). Specifically targeting $sPLA_2$, a class of PLA_2 implicated in burn injury (Nakae et al., 1995) and found to be altered in the present gene sequencing data, via topical inhibitor application has been shown to reduce disease severity in those suffering allergic contact dermatitis (Ingber et al., 2007). Another topically-applied $sPLA_2$ inhibitor was also found to attenuate symptom severity in a murine dermatitis model (Otuki et al., 2011). The effect of an inhibitor targeting $sPLA_2$, or other PLA_2 forms implicated by the present data such as $cPLA_2$, applied to burn tissue would certainly

be worth evaluating. By their topical application avoiding systemic distribution, such PLA_2 inhibitors could constitute a feasible clinical response to LPC's post-burn elevation. Alternatively, targeting the effects of LPC rather than its generation has shown promise *in vitro*. LPC's pro-inflammatory effect, as measured by leukotriene B4 synthesis and chemotaxis in macrophages, is attenuated in the presence of the endogenous antithrombotic plasma protein annexin A5. While its mechanism of action in this particular context has not been confirmed, annexin A5 exerts its antithrombotic effect by crystallising over anionic membrane phospholipids, rendering them inaccessible for coagulation processes (Rand et al., 2003). When identifying annexin a5's inhibition of LPC, the authors noted that it was not accomplished via direct binding and postulated that it may result from annexin A5's formation of a protective shield and determination of membrane lipid composition (Cederholm et al., 2005; Domeij et al., 2013; Rand et al., 2003), consistent with LPC exerting pathological effects via membrane insertion. While LPC's implication in any particular signalling cascade has prompted calls for that process' therapeutic manipulation, such as G-protein inhibition (Han et al., 2008), targeting LPC's generation, or perhaps a unifying component of its many actions (e.g. membrane insertion), represents an efficient and potentially clinically viable approach. More specific approaches many nonetheless be necessary and TRPV1 would now be an interesting target for the treatment of burn injury, and could perhaps be investigated in the context of LPC's intracutaneous injection inducing both inflammation and a burning sensation (Ryborg et al., 2000).

In summary, this work is the first to describe the burn-induced subcutaneous elevation of multiple bioactive LPC species previously implicated in various

pathological processes applicable to burn injury. Through *in vitro* study specifically of LPC(18:0), its cyotoxicity was recognised and a novel effect was identified in its sensitisation of TRPV1 to ligand-mediated activation, particularly drawing attention to its roles in inflammation and pain transduction. Further, the preliminary data for LPC's potential enhancement of NGF-mediated TRPV1 sensitisation and for excluding the contribution of voltage-gated channels to LPC's TRPV1 sensitisation by voltage-clamp electrophysiology are encouraging. Future work should follow convention for delineating LPC's effects on TRP channels in determining whether or not they are membrane-delimited via excised patch electrophysiology. The range of LPC's pathological implications is huge, and exploring it is an exciting prospect.

8 CHAPTER 8 – GENERAL DISCUSSION

8.1 Main Findings

Burn injury is a major clinical challenge. It remains a threat to survival and to quality of life despite long-standing recognition of this fact. While it can only be overcome by improving the clinical response to burn injury, the development of novel therapeutic interventions depends on an enhanced understanding of burn pathology. Whether they are consequences of systemically disseminating effects or are localised exclusively to the burn site, the high clinical priority components of the injury which remain challenging to treat are all orchestrated from the locally-affected tissue. It is largely by recognition of the local pathology's influence that the clinical progression to date has been made, and it will be by further elucidation of the local burn site signalling environment that further progress will continue. In pursuit of this elucidation, this project applied multiple analytical platforms to the evaluation of the burn site with particular focus on its interstitial mediators. What follows is a summary of the principal findings over the full progression of the project, followed by a reflective commentary on their implication in the field of burn injury research and a discussion of the future work they might motivate.

Microdialysis has only been used sparingly in burn injury research, and never before has an "exploratory" analytical platform such as metabolomics, capable of unbiased, untargeted analyte detection, been applied to burn tissue microdialysate. Establishing the viability of their combination, which depended on the design of the sampling method (e.g. probe selection, perfusion rate, equilibration schedule), burn

model (e.g. temperature, means and duration of exposure, depth consistency) and analysis (e.g. chromatographic and detection parameters), was the initial success in this project that set everything else in motion. It ultimately indicated the presence of a detectible experimental effect, reflecting successful execution of the (now histologically-validated) burn model and microdialysis, which would then be further explored with lipidomics, multiplex cytokine panels and a novel approach to temporal metabolomics data analysis. The concomitant success in preparing a library of genes exhibiting burn-dependent differential expression from the microdialysis sites would continually offer insight into the production of subsequently-identified interstitial mediators at a transcriptional level as they emerged with additional microdialysate analyses. The first analysis to be completed employed a 27-plex cytokine panel, identifying the burn-induced elevation of leptin and fractalkine at the burn site; leptin had never been implicated locally in the burn wound before and fractalkine had never been implicated in burn injury regardless of localisation. While the lipidomics analysis is ongoing, analysing the metabolomics data with a novel approach incorporating canonical variates analysis, retaining the organisation of the multivariate data in timeseries, facilitated the generation of the greatest yield of confirmed burn-upregulated interstitial molecules in this project. Three lysophosphatidylcholine species (LPC(18:0), LPC(16:0) and LPC(14:0)), uric acid and niacinamide were unequivocally identified among the elevated metabolites. From these cytokines and metabolites, LPC(18:0) was selected as the focus of the concluding *in vitro* component of this project, which explored its potential interaction with TRPV1 as a possible mechanism underlying its known inflammatory and algogenic properties. It was found to enhance TRPV1-mediated Ca^{2+} responses both upon heterologous expression in HEK293T cells and in neurons within DRG primary

cultures, which could enhance pain signalling and neurogenic inflammation in burn injury.

8.2 Reflective Commentary: The Interpretation of Burn Injury Data

Having discussed the results of each major component of this thesis independently in their respective chapters, their interpretation in the wider contexts of the whole project and, more importantly, in the field of burn injury research will be very briefly overviewed here. Regarding the former, there are very few known molecular-level interactions between analytes identified by the different analytical platforms in this project (with the exception of those within the gene sequencing analysis, which were discussed as their relevances emerged within each chapter). The links between interstitial mediators identified by different platforms are rather thematic in general, drawing functional comparisons with no clear molecular relation. For example, bioactive LPC, fractalkine and leptin all have pro-inflammatory functions, and both LPC and fractalkine exhibit similar chemotactic properties for phagocytes upon their release from apoptotic cells (Ravichandran, 2010). Just as endothelial fractalkine release is proposed to mediate the capture of circulating cytotoxic effector cells (Jones et al., 2010; Umehara et al., 2004), LPC released from the endothelium following trauma may do the same; both may thereby serve as a fundamental vascular gateway mechanism for the immune system. It is evident that different mediators identified in this project may functionally cooperate in burn injury, though more direct, explicit mechanistic relationships integrating their implications in the pathology are few in number. They include the observation that exogenous LPC has been shown to dose-dependently mobilise leptin (Shimizu et al., 2005) and a

potential endogenous response to dyslipidemia. Dyslipidemia refers to abnormal circulating lipid balances that are common in burn injury; it is thought to result from the injury's characteristic hypermetabolism and inflammation. LPC is among the lipids enriched in blood during dyslipidemia as a result of the actions of proinflammatory phospholipases (Stahlman et al., 2013) and this occurring in burn injury is consistent with the present findings. However, niacinamide was also found to be upregulated; this is a product of the hypolipidemic action of nicotinic acid (vitamin B3; Jaconello, 1992), which is expressed endogenously but applied pharmacologically in the treatment of dyslipidemia (McKenney, 2003). The concomitant upregulation of LPC and niacinamide may therefore reflect the onset of dyslipidemia and the subsequent activation of an endogenous protective response to its induction by the burn. However, conversely, niacinamide is also a precursor of $NADP^+$, which constitutes the oxidase system by which LPC enhances superoxide production to enhance oxidative stress (Takeshita et al., 2000). Relationships that may have been expected to emerge between these chapters but did not are also interesting. For example, TNFα is reported to be elevated both systemically and locally post-burn and to induce lipolysis (the breakdown of lipids; Zhang et al., 2002), which itself is associated with the accumulation of LPC (Kleinman et al., 1988). Burn-induced local upregulation of TNFα would have therefore been thought to contribute to LPC's post-burn elevation had it been observed, but it was not.

While the relationships between analytes identified via different analytical platforms are limited, the analytes have an extensive range of functional implications to explore in their own rights, as is discussed in their respective chapters. This requires interpreting the present data in the wider context of our current understanding of

burn injury and the development of novel therapeutic interventions, which has several pitfalls. For example, burn injury and therapy is laden with contradictions; the principal pathological process in wound progression is hypoperfusion which results in part from the pressure induced by burn oedema, yet the most effective treatment is aggressive fluid resuscitation. Further, while administration of an inotrope promoting contraction would be better for a failing myocardium than aggressive fluid resuscitation, they can worsen hypoperfusion in the burn site and compromise tissue viability (Ansermino et al., 2004). The complexity of the local burn injury and the dissemination of its effects dictate that therapeutic intervention can have unintended effects both locally and distally, epitomising the importance of *in vivo* study as a means of elucidating the functional consequences of any intervention; this must be considered, particularly when targeting pleiotropic agents such as LPC and leptin. However, while addressing the complexity of such potentially multi-faceted involvements of single mediators in a pathology like burn injury requires an awareness of the potential for adverse effects, it also requires a realistic appreciation of the potential clinical relevance of modulating particularly specific mechanisms. NSAIDs, by the anti-inflammatory effect of their inhibition of COX-mediated prostaglandin and thromboxane synthesis, exemplify the potential impact such targeted approaches can have in far-reaching, complex tissue states (Harder et al., 2003). However, while LPC's extensive range of implications is encouraging, the prospect that it may only be effectively targeted therapeutically as a single component of a multi-faceted pharmacological intervention must be considered. The issue is particularly complicated with inflammatory mediators in burn injury, whereby disrupting endogenous processes can be harmful in excess such as in the NSAID-induced impairment of wound healing (Franz et al., 2007b). However, this presents

the possibility that targeting single mediators among many with over-lapping functions may hit a therapeutic “sweet-spot”, in which inflammation can be limited to its protective capacity. Again, the delicate balances determining therapeutic efficacy cannot be determined *in vitro*. A further particularly complicated aspect of interpreting data in the context of burn injury is that key characteristics of its systemic effects are determined by the presence of infection (and thereby the systemic inflammatory state’s classification as either sepsis or SIRS). Despite this, the presence of infection often goes unreported, as has previously complicated interpretation of the elevations of IL-6, IL-8 and TNFα in burn injury (Yeh et al., 1999), and will likely continue to complicate interpretation of the roles of any mediators related to the immune system. The present study only modelled the extreme acute period of burn injury (0-3 hours post-burn) and the scald was induced with saline, which will have sterilised the burn site; while infection would not affect the present data, the onset of sepsis is known to reduce systemic LPC levels outside the context of burn injury. Interestingly, this is consistent with LPC having a protective role in preventing sepsis, which has been suggested to occur by disinhibition of $sPLA_2$s resulting from reduced circulating LPC (Cunningham et al., 2008). Further, TRPV1 knockout has been found to accelerate sepsis (Fernandes et al., 2012). Both molecules are pro-inflammatory, but appear to have protective roles in pathological states defined by excessive inflammation. It is possible that the nature of the dysregulation leading to systemic inflammatory states is altered by the presence of infection and consequently differentially implicates TRPV1 and LPC, though this is far from clear. In any case, they exemplify the significance of infection as a confounding factor in burn injury research; this could equally apply to any mediator identified presently. Further, the present work adds significantly to our

particular knowledge of the local signalling environment in the burn site, which has fallen far behind the profiling of mediators found in circulation. It is interesting to consider the possibility that mediators known to be elevated in circulation post-burn such as leptin are sourced directly and immediately from the burn site, which highlights the importance of considering the nature of the sample whether it be interstitial (e.g. microdialysis), whole tissue (including intracellular components) or systemic (e.g. plasma).

8.3 Project Shortcomings and Future Directions

This project has raised many paths for research progression which should be pursued, ranging from fundamental requirements for additional data that would combine with that presented to generate complete, cohesive narratives suitable for publication, to addressing further questions organically resulting from the information this work has provided. Some further incomplete aspects of the project would require significant recourse, and were instead perhaps ill-conceived. Here, the shortcomings of the project are recognised and the exciting prospects for progression of this research are overviewed.

At the beginning of the study, the aim was to temporally profile the burn injury interstitium using a variety of platforms selected for their “exploratory” nature. 12 complete microdialysate sample sets were hence divided into three groups, with 4 sets going to each of metabolomics, multiplex cytokine and lipidomics analyses. Prioritising the use of as many multivariate analytical platforms as possible over sample size within each platform had its advantages and disadvantages. The

cytokine panels and metabolomics identified distinct upregulated mediators within the burn site; each of them is a novel finding with exciting research prospects. The statistical analyses were suitably controlled for the confirmation of burn effects with restricted sample sizes, such that it is evident that the reported analytes were consistently upregulated in burn injury with statistical significance within the recorded popoulation. However, with the exception of LPC, which could also be detected in the lipidomics and was therefore supported by profiling in double the number of animals, the analytes identified presently should be pursued with a larger sample size to confirm the burn effect's generalisation to the whole population. In hindsight, dedicating eight complete sample sets to the initial metabolomic analysis would have been more beneficial to the specific progression of this project than dividing them between metabolomics and lipidomics. While the lipidomics data show promise prior to any formal multivariate analysis, the metabolomics and multiplex cytokine profiling analyses were completed earlier in the project and dictated the remainder of the research activities in this project. Their complexity mirrored that of the metabolomics data (reflecting their similarity as an analytical platform), and simultaneously analysing them alongside dedicated *in vitro* study of already-identified analytes was not feasible. Consequently, despite the investment of a large number of important samples in this component of the project, the lipidomics results only feature briefly in this thesis to bolster the measurements of three LPC species, lipids identified in the metabolomics, as described in Chapter 7 (Fig. 25). However, full analysis of the lipidomics data will be conducted shortly and may yet justify the decision to divide samples between metabolomic and lipidomic analyses by significantly extending metabolome coverage.

Regardless of the division of sample sets between analytical platforms, the decision to restrict the number of animals used for the collection of microdialysate to 12 was a defining and successful feature of the project. As in any study, the size of the cohort heavily influences statistical efficiency and the ensuing confidence about effect size estimates. While greater sample sizes ensure that confidence intervals of effect size estimators are as small as possible, this is not the sole consideration of a study's design. Another is the ethical aspect of using larger sample sizes, particularly in studies inducing severe trauma and the potential for extreme suffering such as the present one. This project was funded by the National Centre for the Replacement, Refinement and Reduction of Animals in Research on the premise that a maximal amount of data would be generated from a minimal number of animals. Naturally, avoiding unnecessary loss of life and suffering was a high priority, as is reflected in the use of only four microdialysate sets per analytical platform. Another consideration is the pitfalls of excessively high sample sizes. Beyond the fact that over-powered studies are inefficient in their wasting of resources (Case et al., 2007), which equate to animal lives presently, they can be sensitised to the detection of trivially small effects of little scientific importance (Lenth, 2001). This is particularly relevant for analyses screening large numbers of potential aetiological factors. The approach taken presently in the search for interstitial mediators warranting further scrutiny was the prioritisation of those with larger effect sizes; namely, those that are statistically significant even in a relatively under-powered (but suitably controlled) design. The success of this focus on low-quantity, high-quality data is evident in the time courses of the mediators identified in the analyses.

Despite its many qualities, microdialysis presents a challenge in accurately determining the interstitial concentrations of molecules recovered. Sampling enabling meaningful comparison between different microdialysate fractions depends on a stable recovery rate which, as in this study, can be reflected in the consistency of concentrations of the majority of analytes not altered by experimental effects. However, due to the difficulty of replicating the *in vivo* recovery environment, the recovery rate is typically not known. Labour-intensive approaches to its determination can elucidate it (as discussed in Chapter 1) but, as in the present study, comparisons of mediator concentrations between experimental states often do not account for the reduced concentration resulting from that analyte's recovery rate, which need only be consistent between microdialysis sites and sequentially collected microdialysate fractions rather than defined. Therefore, the cytokine concentrations reported reflect a set percentage of the true interstitial concentration rather than the interstitial concentration itself. Further, determining actual concentrations from the metabolomics signal intensities (with arbitrary units) would have yielded values still subject to an unknown recovery rate; doing so was therefore not necessary or pursued.

In hindsight, two elements of this project could have been conducted differently and have emerged as missed opportunities which will be taken into account in further study. The first is that careful planning of microdialysate usage would have prevented discarding of potentially interesting sample components. Sample preparation for both the metabolomics and lipidomics study components included protein precipitation, whereby molecules too large for processing were removed. The proteins could have been analysed via proteomics or used to bolster sample sizes in

the cytokine profiling component of the project, but were instead discarded. Further, the DRG gene sequencing was compromised by the exclusion of a single sample which, after passing initial quality control checks, was determined to be problematic. The low RNA yields from such small amounts of tissue were a continuous problem. A better approach, rather than attempting to select the four highest quality individual DRG pair samples, may have been to pool three individual DRG pairs by condition prior to RNA isolation as has been successful elsewhere (Flegel et al., 2015). While the statistical analysis was perhaps unsuitable for evaluating transcriptional changes induced simply by nociceptive signalling in DRG, it will have been weakened by the exclusion of a quarter of the control data and may have benefited from a stronger signal. In any case, the conventional statistical design was applied to the DRG data to maintain consistency with the analysis of the skin RNA, which successfully identified many differentially expressed genes. Although this incorporates corrections for multiple comparisons which no differential expression within the DRG data could overcome, there are nonetheless interesting expression profiles which, in a targeted experimental and statistical design, may yield important insights into nociceptive signalling.

One of the most exciting open-ended aspects of this project, and that which is the highest priority for further research, is the investigation of LPC's potentiating effect on capsaicin responses. The experimental designs used in this pursuit can draw inspiration from previous work ascertaining LPC's interaction with other TRP channels, and will likely do so from the characterisation of its sensitisation of TRPM8 (Abeele et al., 2006; Andersson et al., 2007). Despite the present application of electrophysiology being unsuccessful, it is clear from these works that it is a viable

tool for exploring LPC's effects. The particular challenges in this project were likely a result of the decision to conduct the experiments in HEK293T cells and the means of transfection. It is not clear how exactly LPC compromised the seal in the present electrophysiological experiments, though the DRG cultures were apparently more resilient to LPC's membrane effects and may have withstood their application sufficiently for electrophysiological recording. Indeed, LPC's sensitisation of TRPM8 was successfully characterised in DRG cultures via electrophysiology in whole-cell, cell-attached and inside-out configurations (Andersson et al., 2007). However, despite the difficulties encountered presently, HEK cells have also been successfully used in electrophysiological study of LPC's TRPM8 sensitisation previously (Abeele et al., 2006). The fact that these authors generated a HEK293 cell line stably expressing TRPM8 may have played a part in their success. While a typically sufficient (Senatore et al., 2011) post-transfection membrane stabilisation period was allowed for with overnight recovery in the present study, the possibility that the combination of lipofection with subsequent application of LPC, both of which are incorporated into the membrane, particularly destabilises the membrane cannot be ruled out. However, LPC's membrane effects appeared to be consistent between transfected and untransfected HEK293T cells at higher concentrations.

Once a reliable model system is established, whether it be cultured DRG neurons or a stably TRPV1-expressing cell line, electrophysiology will be useful in elucidating the capsaicin response potentiation. At this stage, it is not clear whether LPC is exerting this effect via actions on TRPV1 or voltage-gated channels recruited following the initial TRPV1-mediated Ca^{2+} influx, where the latter would be precluded with successful voltage-clamp recording as was attempted presently. It will also be

important to determine that this effect is observed in TRPV1-mediated responses to heat rather than capsaicin, though it is encouraging that TRPM8 (which is sensitised to physiological temperatures by LPC) and TRPV1 have a conserved ligand activation site (McKemy, 2007) and that TRPV1's activation by both capsaicin and heat appears to depend on a shift in voltage-dependence (Gunthorpe et al., 2000; Nilius et al., 2005; Vlachova et al., 2003). Particular approaches employed the TRPM8 studies should include determination of concentration-dependent sensitisation to physiological temperatures (where 3 μM LPC, the concentration required for activation of TRPM8 in DRG, was not applied presently) and determination of whether or not this occurs via LPC's translocation across the membrane (Andersson et al., 2007). The particular use of excised patch configuration recording, or cell-attached recording with the LPC applied via the pipette solution, would also prevent any seal disruption resulting from gross morphological changes to the cell in addition to, crucially, precluding the contribution of sensitising mechanisms such as rapid vesicular translocation and membrane insertion of the TRP channel (Bezzerides et al., 2004); ultimately, this approach would determine if the process was membrane-delimited. Further, neither the mechanism of LPC's generation in burn injury nor that of its sensitisation of TRPV1 are elucidated at a molecular level presently; the PLA_2-dependence of its TRPM8 sensitisation has been supported by the use of PLA_2 inhibitors (Andersson et al., 2007) and PLA_2 activity assays (Abeele et al., 2006), highlighting an attractive starting point for investigating its possible effect on TRPV1. Further, regardless of involvement in potentiating capsaicin responses, the relative contributions of PLA_2 and LCAT (where the latter was among the most burn-affected genes in the

sequencing library generated presently) to elevated interstitial burn site LPC concentrations will be exciting to elucidate.

Alongside elucidating the mechanism of LPC's action, the initiation of behavioural studies is a high priority in the continuation of this work. This is due in part to the unknown extent to which any given model system represents the *in vivo* signalling environment (Dubin, 2010). For example, the study of cell bodies, such as in the use of DRG primary cultures, has been invaluable in the elucidation of nociceptive signal transduction and transmission to the CNS and neurotransmitter and neuropeptide release at central and peripheral terminals (Malin et al., 2007). However, whether by differential distribution of transduction molecules or by the lack of non-neuronal signalling components only present *in vivo*, *in vitro* and *in vivo* data have on occasion opposed each other in responses to heat (Caterina et al., 2000; Davis et al., 2000; Zimmermann et al., 2005) and acidity (St Pierre et al., 2009). Further, *in vitro* data can identify opposing effects of a single mediator by different mechanisms, such as LPC's presently reported potentiation of nociceptor responses to capsaicin and its previously-reported activation of TREK-1 (François Maingret et al., 2000) which, as an outward rectifying K^+ channel, would oppose the generation of action potentials. The net effect of LPC's elevation must therefore be determined *in vivo*. Mechanisms elucidated should then be pursued in human studies given potential species-dependent differences in mechanisms, as exhibited by the phenotypes of $Na_V1.7$ deficiency wherein mice retain mechanosensory and formalin-induced nocifensive behaviour (Nassar et al., 2005) while humans are completely insensitive to pain (Cox et al., 2006). Given LPC's extensive characterisation as a demyelinating agent upon focal application to the nervous system (Allt et al., 1988), its exogenous application

in humans must be carefully controlled. However, the prospect of exploring the therapeutic potential of disrupting LPC generation is exciting; several PLA_2 inhibitors are in on-going clinical trials for various conditions not including burn injury (Yarla, 2015), and targeting LCAT may offer another therapeutic avenue. Regarding the possibility that LPC does not mediate a functionally-significant component of inflammation or pain in burn injury despite its clear upregulation and nociceptor sensitisation in the present work, it is extremely encouraging that a rare study investigating its effect upon intracutaneous injection observed erythema, oedema and a transient burning sensation (Ryborg et al., 2000).

8.4 Closing Remarks

There is a wealth of opportunity in pursuing the data generated in this project. Not the least among these are two large databases of metabolites and lipids, represented by the second dimension of the CVA-identified burn effect and the exploratory lipidomics analysis output respectively, which could not be explored within this project's time frame. They each have potential equalling the that of the data yielding the identification of the various metabolites discussed presently, which itself presented far more research potential than could be pursued in three years. Further, even within the statistically-analysed portion of the metabolome defined presently, there were too many potentially functionally-relevant metabolite features to be structurally elucidated in a single pass; many more may yet be identified with successive analyses. The range of possibilities for progressing this research is a positive reflection on the project's exploratory approach, and it is exciting to consider

the impact the work achieved and enabled presently will have in advancing our understanding of burn injury.

9 References

Abdel-Hafez, N. M., Saleh Hassan, Y., & El-Metwally, T. H. (2007). A study on biomarkers, cytokines, and growth factors in children with burn injuries. Ann Burns Fire Disasters, 20(2), 89-100.

Abdullahi, A., Amini-Nik, S., & Jeschke, M. G. (2014). Animal models in burn research. Cell Mol Life Sci, 71(17), 3241-3255. doi:10.1007/s00018-014-1612-5

Abe, Y., Akeda, K., An, H. S., Aoki, Y., Pichika, R., Muehleman, C., . . . Masuda, K. (2007). Proinflammatory cytokines stimulate the expression of nerve growth factor by human intervertebral disc cells. Spine (Phila Pa 1976), 32(6), 635-642. doi:10.1097/01.brs.0000257556.90850.53

Abeele, F. V., Zholos, A., Bidaux, G., Shuba, Y., Thebault, S., Beck, B., . . . Prevarskaya, N. (2006). Ca2+-independent Phospholipase A2-dependent Gating of TRPM8 by Lysophospholipids. Journal of Biological Chemistry, 281(52), 40174-40182.

Ackermann, L., & Harvima, I. T. (1998). Mast cells of psoriatic and atopic dermatitis skin are positive for TNF-alpha and their degranulation is associated with expression of ICAM-1 in the epidermis. Archives of Dermatological Research, 290(7), 353-359.

Ahima, R. S., Prabakaran, D., Mantzoros, C., Qu, D., Lowell, B., Maratos-Flier, E., & Flier, J. S. (1996). Role of leptin in the neuroendocrine response to fasting. Nature, 382(6588), 250-252. doi:10.1038/382250a0

Ahuja, R. B., Bhattacharya, S. K., & Rai, A. (2009). Changing trends of an endemic trauma. Burns, 35(5), 650-656. doi:DOI 10.1016/j.burns.2009.01.008

Aikawa, N., Shinozawa, Y., Ishibiki, K., Abe, O., Yamamoto, S., Motegi, M., . . . Sudoh, M. (1987). Clinical analysis of multiple organ failure in burned patients. Burns Incl Therm Inj, 13(2), 103-109.

Akhtar, S., Li, X., Kovacs, E. J., Gamelli, R. L., & Choudhry, M. A. (2011). Interleukin-18 delays neutrophil apoptosis following alcohol intoxication and burn injury. Mol Med, 17(1-2), 88-94. doi:10.2119/molmed.2010.00080

Akira, S., Taga, T., & Kishimoto, T. (1993). Interleukin-6 in biology and medicine. Adv Immunol, 54, 1-78.

Al-Ghoul, W. M., Abu-Shaqra, S., Park, B. G., Fazal, N. (2010). Melatonin plays a protective role in postburn rodent gut pathophysiology. Int J Biol Sci 6(3): 282-293.

Al-Hasani, R., & Bruchas, M. R. (2011). Molecular Mechanisms of Opioid Receptor-Dependent Signaling and Behavior. Anesthesiology, 115(6), 1363-1381. doi:10.1097/ALN.0b013e318238bba6

Al-Mousawi, A. M., Kulp, G. A., Branski, L. K., Kraft, R., Mecott, G. A., Williams, F. N., Herndon, D. N., Jeschke, M. G. (2010). Impact of anesthesia, analgesia, and euthanasia technique on the inflammatory cytokine profile in a rodent model of severe burn injury. Shock 34(3): 261-268.

Alawi, K., & Keeble, J. (2010). The paradoxical role of the transient receptor potential vanilloid 1 receptor in inflammation. Pharmacol Ther, 125(2), 181-195. doi:10.1016/j.pharmthera.2009.10.005

Alessandri-Haber, N., Dina, O. A., Chen, X., & Levine, J. D. (2009). TRPC1 and TRPC6 channels cooperate with TRPV4 to mediate mechanical hyperalgesia and nociceptor sensitization. J Neurosci, 29(19), 6217-6228. doi:10.1523/jneurosci.0893-09.2009

Alessandri-Haber, N., Yeh, J. J., Boyd, A. E., Parada, C. A., Chen, X., Reichling, D. B., & Levine, J. D. (2003). Hypotonicity induces TRPV4-mediated nociception in rat. Neuron, 39(3), 497-511.

Alexander, J. S., Patton, W. F., Christman, B. W., Cuiper, L. L., & Haselton, F. R. (1998). Platelet-derived lysophosphatidic acid decreases endothelial permeability in vitro. Am J Physiol, 274(1 Pt 2), H115-122.

Aley, K. O., Messing, R. O., Mochly-Rosen, D., & Levine, J. D. (2000). Chronic hypersensitivity for inflammatory nociceptor sensitization mediated by the epsilon isozyme of protein kinase C. J Neurosci, 20(12), 4680-4685.

Allison, A. C. (1978). Mechanisms by which activated macrophages inhibit lymphocyte responses. Immunol Rev, 40, 3-27.

Allt, G., Ghabriel, M. N., & Sikri, K. (1988). Lysophosphatidyl choline-induced demyelination. A freeze-fracture study. Acta Neuropathol, 75(5), 456-464.

Alpert, A. J. (1990). Hydrophilic-interaction chromatography for the separation of peptides, nucleic acids and other polar compounds. J Chromatogr 499: 177-196.

Alsalem, M., Wong, A., Millns, P., Arya, P. H., Chan, M. S., Bennett, A., . . . Kendall, D. A. (2013). The contribution of the endogenous TRPV1 ligands 9-HODE and 13-HODE to nociceptive processing and their role in peripheral inflammatory pain mechanisms. Br J Pharmacol, 168(8), 1961-1974. doi:10.1111/bph.12092

Alvarez, P., Bogen, O., Chen, X., Giudice, L. C., & Levine, J. D. (2014). Ectopic Endometrium-Derived Leptin Produces Estrogen-Dependent Chronic Pain in a Rat Model of Endometriosis. Neuroscience, 258, 111-120. doi:10.1016/j.neuroscience.2013.11.008

Amberg, G., & Lindefors, N. (1989). Intracerebral microdialysis: II. Mathematical studies of diffusion kinetics. J Pharmacol Methods, 22(3), 157-183.

Amir, R., & Devor, M. (2003). Electrical excitability of the soma of sensory neurons is required for spike invasion of the soma, but not for through-conduction. Biophys J, 84(4), 2181-2191. doi:10.1016/s0006-3495(03)75024-3

Andersson, D. A., Nash, M., & Bevan, S. (2007). Modulation of the Cold-Activated Channel TRPM8 by Lysophospholipids and Polyunsaturated Fatty Acids. J Neurosci, 27(12), 3347-3355. doi:10.1523/jneurosci.4846-06.2007

Andrews, C. J., Kempf, M., Kimble, R., Cuttle, L. (2016). Development of a Consistent and Reproducible Porcine Scald Burn Model. PLoS One 11(9): e0162888.

Angst, M. S., Clark, J. D., Carvalho, B., Tingle, M., Schmelz, M., & Yeomans, D. C. (2008). Cytokine profile in human skin in response to experimental inflammation, noxious stimulation, and administration of a COX-inhibitor: A microdialysis study. Pain, 139(1), 15-27. doi:DOI 10.1016/j.pain.2008.02.028

Ansari-Moghaddam, A., Baghbanian, A., Dogoonchi, M., Chooban, B., Mostaghim-Roudi, M., & Torkfar, G. (2013). Epidemiology of burn injuries in south-eastern Iran: a retrospective study. J Pak Med Assoc, 63(12), 1476-1481.

Ansermino, M., & Hemsley, C. (2004). Intensive care management and control of infection. BMJ, 329(7459), 220-223.

Arnalich, F., Lopez, J., Codoceo, R., Jimenez, M., Madero, R., & Montiel, C. (1999). Relationship of plasma leptin to plasma cytokines and human survival in sepsis and septic shock. Journal of Infectious Diseases, 180(3), 908-911. doi:Doi 10.1086/314963

Arslan, H., Kul, B., Derebasinlioglu, H., & Cetinkale, O. (2013). Epidemiology of pediatric burn injuries in Istanbul, Turkey. Ulus Travma Acil Cerrahi Derg, 19(2), 123-126. doi:10.5505/tjtes.2013.44442

Asaoka, Y., Oka, M., Yoshida, K., Sasaki, Y., & Nishizuka, Y. (1992). Role of lysophosphatidylcholine in T-lymphocyte activation: involvement of phospholipase A2 in signal transduction through protein kinase C. Proc Natl Acad Sci U S A, 89(14), 6447-6451.

Ashburn, M. A. (1995). Burn pain: the management of procedure-related pain. J Burn Care Rehabil, 16(3 Pt 2), 365-371.

Association, A. B. (2016). Burn Unit Referral Criteria. Retrieved from http://www.ameriburn.org/BurnUnitReferral.pdf

Aust, S. D., Thomas, C. E., Morehouse, L. A., Saito, M., & Bucher, J. R. (1986). Active Oxygen and Toxicity. In J. J. Kocsis, D. J. Jollow, C. M. Witmer, J. O. Nelson, & R. Snyder (Eds.), Biological Reactive Intermediates III: Mechanisms of Action in Animal Models and Human Disease (pp. 513-526). Boston, MA: Springer US.

Ayala, A., Mu, #xf1, oz, M. F., Arg, #xfc, & elles, S. (2014). Lipid Peroxidation: Production, Metabolism, and Signaling Mechanisms of Malondialdehyde and 4-Hydroxy-2-Nonenal. Oxidative Medicine and Cellular Longevity, 2014, 31. doi:10.1155/2014/360438

Babcock, G. F., Hernandez, L., Yadav, E., Schwemberger, S., & Dugan, A. (2012). The Burn Wound Inflammatory Response Is Influenced by Midazolam. Inflammation, 35(1), 259-270. doi:DOI 10.1007/s10753-011-9313-9

Babior, B. M. (1978). Oxygen-dependent microbial killing by phagocytes (first of two parts). N Engl J Med, 298(12), 659-668. doi:10.1056/nejm197803232981205

Baer, L. A., Wu, X., Tou, J. C., Johnson, E., Wolf, S. E., Wade, CE. (2013). Contributions of severe burn and disuse to bone structure and strength in rats. Bone 52(2): 644-650.

Banks, W. A. (2004). The many lives of leptin. Peptides, 25(3), 331-338. doi:10.1016/j.peptides.2004.02.014

Banks, W. A., Kastin, A. J., Huang, W. T., Jaspan, J. B., & Maness, L. M. (1996). Leptin enters the brain by a saturable system independent of insulin. Peptides, 17(2), 305-311. doi:Doi 10.1016/0196-9781(96)00025-3

Bao, C., Hu, S., Zhou, G., Tian, Y., Wu, Y., & Sheng, Z. (2010). Effect of carbachol on intestinal mucosal blood flow, activity of Na+-K+-ATPase, expression of aquaporin-1, and intestinal absorption rate during enteral resuscitation of burn shock in rats. J Burn Care Res, 31(1), 200-206. doi:10.1097/BCR.0b013e3181c89eba

Bar-Yosef, O., Haik, J., Hilly, O., Levy, R., Efrati, O., Bujanover, Y., . . . Modan-Moses, D. (2014). Leptin, ghrelin, and adiponectin in the metabolic adjustment to burn injury in children. Wounds-a Compendium of Clinical Research and Practice, 26(6), 178-185.

Barret, J. P. (2004). Burns reconstruction. BMJ, 329(7460), 274.
Barrow, R. E., Jeschke, M. G., & Herndon, D. N. (2000). Early fluid resuscitation improves outcomes in severely burned children. Resuscitation, 45(2), 91-96.
Barrow, R. E., Ramirez, R. J., & Zhang, X. J. (2000). Ibuprofen modulates tissue perfusion in partial-thickness burns. Burns, 26(4), 341-346.
Barton, R. G., Saffle, J. R., Morris, S. E., Mone, M., Davis, B., & Shelby, J. (1997). Resuscitation of thermally injured patients with oxygen transport criteria as goals of therapy. J Burn Care Rehabil, 18(1 Pt 1), 1-9.
Basbaum, A. I., Bautista, D. M., Scherrer, G., & Julius, D. (2009). Cellular and Molecular Mechanisms of Pain. Cell, 139(2), 267-284. doi:10.1016/j.cell.2009.09.028
Baskaran, H., Toner, M., Yarmush, M. L., & Berthiaume, F. (2001). Poloxamer-188 improves capillary blood flow and tissue viability in a cutaneous burn wound. J Surg Res, 101(1), 56-61. doi:10.1006/jsre.2001.6262
Baskaran, H., Yarmush, M. L., & Berthiaume, F. (2000). Dynamics of tissue neutrophil sequestration after cutaneous burns in rats. J Surg Res, 93(1), 88-96. doi:10.1006/jsre.2000.5955
Basu, S., Dunn, A., & Ward, A. (2002). G-CSF: function and modes of action (Review). International Journal of Molecular Medicine, 10(1), 3-10.
Batra, A., Okur, B., Glauben, R., Erben, U., Ihbe, J., Stroh, T., . . . Siegmund, B. (2010). Leptin: A Critical Regulator of CD4(+) T-cell Polarization in Vitro and in Vivo. Endocrinology, 151(1), 56-62. doi:10.1210/en.2009-0565
Battal, M. N., Hata, Y., Matsuka, K., Ito, O., Matsuda, H., Yoshida, Y., & Kawazoe, T. (1997). Reduction of progressive burn injury by using a new nonselective endothelin-A and endothelin-B receptor antagonist, TAK-044: an experimental study in rats. Plast Reconstr Surg, 99(6), 1610-1619.
Battle, C. E., Evans, V., James, K., Guy, K., Whitley, J., Evans, P. A. (2016). Epidemiology of burns and scalds in children presenting to the emergency department of a regional burns unit: a 7-year retrospective study. Burns Trauma 4: 19.
Bazan, J. F., Bacon, K. B., Hardiman, G., Wang, W., Soo, K., Rossi, D., . . . Schall, T. J. (1997). A new class of membrane-bound chemokine with a CX3C motif. Nature, 385(6617), 640-644. doi:10.1038/385640a0
BBA. (2001). National Burn Care Review. National burn injury referral guidelines. (Vol. Standards and strategy for burn care.). London: 68-9.: British Burn Association.
Beal, A. L., & Cerra, F. B. (1994). Multiple organ failure syndrome in the 1990s. Systemic inflammatory response and organ dysfunction. JAMA, 271(3), 226-233.
Becker, E. D. (1993). A BRIEF HISTORY OF NUCLEAR MAGNETIC RESONANCE. Analytical Chemistry, 65(6), 295A-302A. doi:10.1021/ac00054a716
Becker, Y. (2007). The spreading of HIV-1 infection in the human organism is caused by fractalkine trafficking of the infected lymphocytes - a review, hypothesis and implications for treatment. Virus Genes, 34(2), 93-109. doi:10.1007/s11262-006-0056-x
Beech, D. J., Muraki, K., & Flemming, R. (2004). Non-selective cationic channels of smooth muscle and the mammalian homologues of Drosophila TRP. J Physiol, 559(Pt 3), 685-706. doi:10.1113/jphysiol.2004.068734
Bekier, E., & Maslinski, C. (1974). Antihistaminic action of nicotinamide. Agents and Actions, 4(3), 196.
Bekier, E., Wyczolkowska, J., Szyc, H., & Maslinski, C. (1974). The inhibitory effect of nicotinamide on asthma-like symptoms and eosinophilia in guinea pigs, anaphylactic mast cell degranulation in mice, and histamine release from rat isolated peritoneal mast cells by compound 48-80. Int Arch Allergy Appl Immunol, 47(5), 737-748.
Ben-Zeev, G., Telias, M., & Nussinovitch, I. (2010). Lysophospholipids modulate voltage-gated calcium channel currents in pituitary cells; effects of lipid stress. Cell Calcium, 47(6), 514-524. doi:10.1016/j.ceca.2010.04.006
Bendall, L. J., & Bradstock, K. F. (2014). G-CSF: From granulopoietic stimulant to bone marrow stem cell mobilizing agent. Cytokine Growth Factor Rev, 25(4), 355-367. doi:10.1016/j.cytogfr.2014.07.011
Benjamini, Y., & Hochberg, Y. (1995). Controlling the False Discovery Rate: A Practical and Powerful Approach to Multiple Testing. Journal of the Royal Statistical Society. Series B (Methodological), 57(1), 289-300.
Bennett, G., Serafini, M., Burchiel, K., Buchser, E., Classen, A., Deer, T., . . . Yaksh, T. (2000). Evidence-based review of the literature on intrathecal delivery of pain medication. J Pain Symptom Manage, 20(2), S12-36.
Benyamin, R., Trescot, A. M., Datta, S., Buenaventura, R., Adlaka, R., Sehgal, N., . . . Vallejo, R. (2008). Opioid complications and side effects. Pain Physician, 11(2 Suppl), S105-120.
Berge, O. G. (2011). Predictive validity of behavioural animal models for chronic pain. Br J Pharmacol, 164(4), 1195-1206. doi:10.1111/j.1476-5381.2011.01300.x

Berger, M. M., Bernath, M.-A., & Chioléro, R. L. (2001). Resuscitation, anaesthesia and analgesia of the burned patient. Current Opinion in Anesthesiology, 14(4), 431-435.
Berk, M. A., & Lorincz, A. L. (1986). The treatment of bullous pemphigoid with tetracycline and niacinamide. A preliminary report. Arch Dermatol, 122(6), 670-674.
Bernstein, J. E. L., A.L. (1980). The effects of topical nicotinamide, tetracycline, and dapsone on potassium iodide-induced inflammation. Journal of Investigative Dermatology, 74, 257–258.
Berrier, C., Coulombe, A., Houssin, C., & Ghazi, A. (1989). A patch-clamp study of ion channels of inner and outer membranes and of contact zones of E. coli, fused into giant liposomes. Pressure-activated channels are localized in the inner membrane. FEBS Lett, 259(1), 27-32.
Bertin-Maghit, M., Goudable, J., Dalmas, E., Steghens, J. P., Bouchard, C., Gueugniaud, P. Y., . . . Delafosse, B. (2000). Time course of oxidative stress after major burns. Intensive Care Med, 26(6), 800-803.
Bezzerides, V. J., Ramsey, I. S., Kotecha, S., Greka, A., & Clapham, D. E. (2004). Rapid vesicular translocation and insertion of TRP channels. Nat Cell Biol, 6(8), 709-720. doi:10.1038/ncb1150
Bhattacharjee, S., Renganaath, K., Mehrotra, R., & Mehrotra, S. (2013). Combinatorial Control of Gene Expression. Biomed Res Int, 2013. doi:10.1155/2013/407263
Bhattacharya, M. R. C., Bautista, D. M., Wu, K., Haeberle, H., Lumpkin, E. A., & Julius, D. (2008). Radial stretch reveals distinct populations of mechanosensitive mammalian somatosensory neurons. Proc Natl Acad Sci U S A, 105(50), 20015-20020. doi:10.1073/pnas.0810801105
Bhave, G., Hu, H. J., Glauner, K. S., Zhu, W., Wang, H., Brasier, D. J., . . . Gereau, R. W. t. (2003). Protein kinase C phosphorylation sensitizes but does not activate the capsaicin receptor transient receptor potential vanilloid 1 (TRPV1). Proc Natl Acad Sci U S A, 100(21), 12480-12485. doi:10.1073/pnas.2032100100
Bickel, M. (1993). The role of interleukin-8 in inflammation and mechanisms of regulation. J Periodontol, 64(5 Suppl), 456-460.
Bielefeldt, K., & Davis, B. M. (2008). Differential effects of ASIC3 and TRPV1 deletion on gastroesophageal sensation in mice. Am J Physiol Gastrointest Liver Physiol, 294(1), G130-138. doi:10.1152/ajpgi.00388.2007
Biffl, W. L., Moore, E. E., Moore, F. A., & Peterson, V. M. (1996). Interleukin-6 in the injured patient. Marker of injury or mediator of inflammation? Ann Surg, 224(5), 647-664.
Binshtok, A. M., Wang, H., Zimmermann, K., Amaya, F., Vardeh, D., Shi, L., . . . Samad, T. A. (2008). Nociceptors are interleukin-1beta sensors. J Neurosci, 28(52), 14062-14073. doi:10.1523/jneurosci.3795-08.2008
Birder, L. A., Kanai, A. J., de Groat, W. C., Kiss, S., Nealen, M. L., Burke, N. E., . . . Caterina, M. J. (2001). Vanilloid receptor expression suggests a sensory role for urinary bladder epithelial cells. Proc Natl Acad Sci U S A, 98(23), 13396-13401. doi:10.1073/pnas.231243698
Birder, L. A., Nakamura, Y., Kiss, S., Nealen, M. L., Barrick, S., Kanai, A. J., . . . Caterina, M. J. (2002). Altered urinary bladder function in mice lacking the vanilloid receptor TRPV1. Nature Neuroscience, 5(9), 856-860. doi:10.1038/nn902
Blakeney, P. E., Rosenberg, L., Rosenberg, M., & Faber, A. W. (2008). Psychosocial care of persons with severe burns. Burns, 34(4), 433-440. doi:10.1016/j.burns.2007.08.008
Bloemsma, G. C., Dokter, J., Boxma, H., & Oen, I. M. (2008). Mortality and causes of death in a burn centre. Burns, 34(8), 1103-1107. doi:10.1016/j.burns.2008.02.010
Bogdan, C. (2011). Regulation of lymphocytes by nitric oxide. Methods Mol Biol, 677, 375-393. doi:10.1007/978-1-60761-869-0_24
Bolcskei, K., Helyes, Z., Szabo, A., Sandor, K., Elekes, K., Nemeth, J., . . . Szolcsanyi, J. (2005). Investigation of the role of TRPV1 receptors in acute and chronic nociceptive processes using gene-deficient mice. Pain, 117(3), 368-376. doi:10.1016/j.pain.2005.06.024
Bonnington, J. K., & McNaughton, P. A. (2003). Signalling pathways involved in the sensitisation of mouse nociceptive neurones by nerve growth factor. J Physiol, 551(Pt 2), 433-446. doi:10.1113/jphysiol.2003.039990
Bornstein, S. R. (1997). Is leptin a stress related peptide? Nat Med, 3(9), 937-937. doi:Doi 10.1038/Nm0997-937
Bouloumie, A., Drexler, H. C., Lafontan, M., & Busse, R. (1998). Leptin, the product of Ob gene, promotes angiogenesis. Circ Res, 83(10), 1059-1066.
Boyman, O., & Sprent, J. (2012). The role of interleukin-2 during homeostasis and activation of the immune system. Nat Rev Immunol, 12(3), 180-190. doi:10.1038/nri3156
Brauchi, S., Orta, G., Mascayano, C., Salazar, M., Raddatz, N., Urbina, H., . . . Latorre, R. (2007). Dissection of the components for PIP2 activation and thermosensation in TRP channels. Proc Natl Acad Sci U S A, 104(24), 10246-10251. doi:10.1073/pnas.0703420104

Brauchi, S., Orta, G., Salazar, M., Rosenmann, E., & Latorre, R. (2006). A hot-sensing cold receptor: C-terminal domain determines thermosensation in transient receptor potential channels. J Neurosci, 26(18), 4835-4840. doi:10.1523/jneurosci.5080-05.2006

Brenner, G. J., Ji, R. R., Shaffer, S., & Woolf, C. J. (2004). Peripheral noxious stimulation induces phosphorylation of the NMDA receptor NR1 subunit at the PKC-dependent site, serine-896, in spinal cord dorsal horn neurons. European Journal of Neuroscience, 20(2), 375-384. doi:10.1111/j.1460-9568.2004.03506.x

Brown, T., Mills, S., & Muller, M. (2003). If it can't be measured it can't be managed - The paucity of outcome measures in burn care. Burns, 29(8), 757-757. doi:DOI 10.1016/j.burns.2003.09.006

Bruno, A., Conus, S., Schmid, I., & Simon, H. U. (2005). Apoptotic pathways are inhibited by leptin receptor activation in neutrophils. J Immunol, 174(12), 8090-8096.

Brusselaers, N., Hoste, E. A., Monstrey, S., Colpaert, K. E., De Waele, J. J., Vandewoude, K. H., & Blot, S. I. (2005). Outcome and changes over time in survival following severe burns from 1985 to 2004. Intensive Care Med, 31(12), 1648-1653. doi:10.1007/s00134-005-2819-6

Brusselaers, N., Monstrey, S., Colpaert, K., Decruyenaere, J., Blot, S. I., & Hoste, E. A. (2010). Outcome of acute kidney injury in severe burns: a systematic review and meta-analysis. Intensive Care Med, 36(6), 915-925. doi:10.1007/s00134-010-1861-1

Brusselaers, N., Monstrey, S., Vogelaers, D., Hoste, E., & Blot, S. (2010). Severe burn injury in Europe: a systematic review of the incidence, etiology, morbidity, and mortality. Crit Care, 14(5), R188. doi:10.1186/cc9300

Buck, S. H., & Burks, T. F. (1986). The neuropharmacology of capsaicin: review of some recent observations. Pharmacol Rev, 38(3), 179-226.

Bucky, L. P., Vedder, N. B., Hong, H. Z., Ehrlich, H. P., Winn, R. K., Harlan, J. M., & May, J. W., Jr. (1994). Reduction of burn injury by inhibiting CD18-mediated leukocyte adherence in rabbits. Plast Reconstr Surg, 93(7), 1473-1480.

Budagian, V., Bulanova, E., Paus, R., & Bulfone-Paus, S. (2006). IL-15/IL-15 receptor biology: a guided tour through an expanding universe. Cytokine Growth Factor Rev, 17(4), 259-280. doi:10.1016/j.cytogfr.2006.05.001

Bungay, P. M., Morrison, P. F., & Dedrick, R. L. (1990). Steady-state theory for quantitative microdialysis of solutes and water in vivo and in vitro. Life Sci, 46(2), 105-119.

Burger, D. R., Vandenbark, A. A., Daves, D., Anderson, W. A., Jr., Vetto, R. M., & Finke, P. (1976). Nicotinamide: suppression of lymphocyte transformation with a component identified in human transfer factor. J Immunol, 117(3), 797-801.

Busuioc, C. J., Popescu, F. C., Mogosanu, G. D., Lascar, I., Pirici, I., Pop, O. T., & Mogoanta, L. (2011). Angiogenesis assessment in experimental third degree skin burns: a histological and immunohistochemical study. Rom J Morphol Embryol, 52(3), 887-895.

Byers, J. F., Bridges, S., Kijek, J., & LaBorde, P. (2001). Burn Patients' Pain and Anxiety Experiences. Journal of Burn Care & Research, 22(2), 144-149.

Caffo, E., & Belaise, C. (2003). Psychological aspects of traumatic injury in children and adolescents. Child Adolesc Psychiatr Clin N Am, 12(3), 493-535.

Cakir, B., Cevik, H., Contuk, G., Ercan, F., Eksioglu-Demiralp, E., & Yegen, B. C. (2005). Leptin ameliorates burn-induced multiple organ damage and modulates postburn immune response in rats. Regul Pept, 125(1-3), 135-144. doi:10.1016/j.regpep.2004.08.032

Cakir, Y. (2004). Systemic responses to burn injury. Turk J Med Sci, 34, 215－226.

Calabrese, B., Tabarean, I. V., Juranka, P., & Morris, C. E. (2002). Mechanosensitivity of N-type calcium channel currents. Biophys J, 83(5), 2560-2574. doi:10.1016/s0006-3495(02)75267-3

Caldefie-Chezet, F., Poulin, A., & Vasson, M. P. (2003). Leptin regulates functional capacities of polymorphonuclear neutrophils. Free Radic Res, 37(8), 809-814.

Calum, H., Moser, C., Jensen, P. O., Christophersen, L., Maling, D. S., van Gennip, M., . . . Hoiby, N. (2009). Thermal injury induces impaired function in polymorphonuclear neutrophil granulocytes and reduced control of burn wound infection. Clin Exp Immunol, 156(1), 102-110. doi:10.1111/j.1365-2249.2008.03861.x

Cao, E., Cordero-Morales, J. F., Liu, B., Qin, F., & Julius, D. (2013). TRPV1 channels are intrinsically heat sensitive and negatively regulated by phosphoinositide lipids. Neuron, 77(4), 667-679. doi:10.1016/j.neuron.2012.12.016

Carragher, N. O. and M. C. Frame (2004). Focal adhesion and actin dynamics: a place where kinases and proteases meet to promote invasion. Trends Cell Biol 14(5): 241-249.

Carrougher, G. J. (1998). Burn care and therapy. St. Louis, Mo. [u.a.]: Mosby.
Carrougher, G. J., Ptacek, J. T., Honari, S., Schmidt, A. E., Tininenko, J. R., Gibran, N. S., & Patterson, D. R. (2006). Self-reports of anxiety in burn-injured hospitalized adults during routine wound care. J Burn Care Res, 27(5), 676-681. doi:10.1097/01.bcr.0000238100.11905.ab
Carrougher, G. J., Ptacek, J. T., Sharar, S. R., Wiechman, S., Honari, S., Patterson, D. R., & Heimbach, D. M. (2003). Comparison of patient satisfaction and self-reports of pain in adult burn-injured patients. J Burn Care Rehabil, 24(1), 1-8. doi:10.1097/01.bcr.0000039743.42589.7f
Carter, D., Warsen, A., Mandell, K., Cuschieri, J., Maier, R. V., & Arbabi, S. (2014). Delayed topical p38 MAPK inhibition attenuates full-thickness burn wound inflammatory signaling. J Burn Care Res, 35(2), e83-92. doi:10.1097/BCR.0b013e31828a8d6e
Case, L. D. and W. T. Ambrosius (2007). Power and Sample Size. Topics in Biostatistics. W. T. Ambrosius. Totowa, NJ, Humana Press: 377-408.
Caterina, M. J., & Julius, D. (2001). The vanilloid receptor: a molecular gateway to the pain pathway. Annu Rev Neurosci, 24, 487-517. doi:10.1146/annurev.neuro.24.1.487
Caterina, M. J., Leffler, A., Malmberg, A. B., Martin, W. J., Trafton, J., Petersen-Zeitz, K. R., . . . Julius, D. (2000). Impaired nociception and pain sensation in mice lacking the capsaicin receptor. Science, 288(5464), 306-313.
Caterina, M. J., Rosen, T. A., Tominaga, M., Brake, A. J., & Julius, D. (1999). A capsaicin-receptor homologue with a high threshold for noxious heat. Nature, 398(6726), 436-441. doi:10.1038/18906
Caterina, M. J., Schumacher, M. A., Tominaga, M., Rosen, T. A., Levine, J. D., & Julius, D. (1997). The capsaicin receptor: a heat-activated ion channel in the pain pathway. Nature, 389(6653), 816-824.
Cattaneo, A. (2010). Tanezumab, a recombinant humanized mAb against nerve growth factor for the treatment of acute and chronic pain. Curr Opin Mol Ther, 12(1), 94-106.
Cederholm, A., Svenungsson, E., Jensen-Urstad, K., Trollmo, C., Ulfgren, A. K., Swedenborg, J., . . . Frostegard, J. (2005). Decreased binding of annexin v to endothelial cells: a potential mechanism in atherothrombosis of patients with systemic lupus erythematosus. Arterioscler Thromb Vasc Biol, 25(1), 198-203. doi:10.1161/01.atv.0000150415.18759.36
Cesare, P., Dekker, L. V., Sardini, A., Parker, P. J., & McNaughton, P. A. (1999). Specific involvement of PKC-epsilon in sensitization of the neuronal response to painful heat. Neuron, 23(3), 617-624.
Cesare, P., & McNaughton, P. (1996). A novel heat-activated current in nociceptive neurons and its sensitization by bradykinin. Proc Natl Acad Sci U S A, 93(26), 15435-15439.
Cetinkale, O., Demir, M., Sayman, H. B., Ayan, F., & Onsel, C. (1997). Effects of allopurinol, ibuprofen and cyclosporin A on local microcirculatory disturbance due to burn injuries. Burns, 23(1), 43-49.
Ceylan, A., Karasu, C., Aktan, F., & Ozansoy, G. (2004). Simvastatin treatment restores vasoconstriction and the inhibitory effect of LPC on endothelial relaxation via affecting oxidizing metabolism in diabetic rats. Diabetes Nutr Metab, 17(4), 203-210.
Chalfie, M. (2009). Neurosensory mechanotransduction. Nat Rev Mol Cell Biol, 10(1), 44-52. doi:10.1038/nrm2595
Chang, G., Spencer, R. H., Lee, A. T., Barclay, M. T., & Rees, D. C. (1998). Structure of the MscL homolog from Mycobacterium tuberculosis: a gated mechanosensitive ion channel. Science, 282(5397), 2220-2226.
Charlton, S. J. and G. Vauquelin (2010). Elusive equilibrium: the challenge of interpreting receptor pharmacology using calcium assays. Br J Pharmacol 161(6): 1250-1265.
Chaudhuri, P., Colles, S. M., Bhat, M., Van Wagoner, D. R., Birnbaumer, L., & Graham, L. M. (2008). Elucidation of a TRPC6-TRPC5 channel cascade that restricts endothelial cell movement. Mol Biol Cell, 19(8), 3203-3211. doi:10.1091/mbc.E07-08-0765
Chaudhuri, P., Colles, S. M., Damron, D. S., & Graham, L. M. (2003). Lysophosphatidylcholine inhibits endothelial cell migration by increasing intracellular calcium and activating calpain. Arterioscler Thromb Vasc Biol, 23(2), 218-223.
Chefer, V. I., Thompson, A. C., Zapata, A., & Shippenberg, T. S. (2009). Overview of Brain Microdialysis. Curr Protoc Neurosci, Chapter, Unit7.1. doi:10.1002/0471142301.ns0701s47
Chen, L., Liang, B., Froese, D. E., Liu, S., Wong, J. T., Tran, K., . . . Choy, P. C. (1997). Oxidative modification of low density lipoprotein in normal and hyperlipidemic patients: effect of lysophosphatidylcholine composition on vascular relaxation. J Lipid Res, 38(3), 546-553.
Chen, L. W., Hsu, C. M., Cha, M. C., Chen, J. S., & Chen, S. C. (1999). CHANGES IN GUT MUCOSAL NITRIC OXIDE SYNTHASE (NOS) ACTIVITY AFTER THERMAL INJURY AND ITS RELATION WITH BARRIER FAILURE. Shock, 11(2), 104-110.

Chen, Y., Morimoto, S., Kitano, S., Koh, E., Fukuo, K., Jiang, B., . . . Ogihara, T. (1995). Lysophosphatidylcholine causes Ca2+ influx, enhanced DNA synthesis and cytotoxicity in cultured vascular smooth muscle cells. Atherosclerosis, 112(1), 69-76.

Chernomordik, L. (1996). Non-bilayer lipids and biological fusion intermediates. Chem Phys Lipids, 81(2), 203-213.

Chertow, G. M., Burdick, E., Honour, M., Bonventre, J. V., & Bates, D. W. (2005). Acute kidney injury, mortality, length of stay, and costs in hospitalized patients. Journal of the American Society of Nephrology, 16(11), 3365-3370. doi:10.1681/asn.2004090740

Chessell, I. P., Hatcher, J. P., Bountra, C., Michel, A. D., Hughes, J. P., Green, P., . . . Buell, G. N. (2005). Disruption of the P2X7 purinoceptor gene abolishes chronic inflammatory and neuropathic pain. Pain, 114(3), 386-396. doi:10.1016/j.pain.2005.01.002

Cho, H., Koo, J. Y., Kim, S., Park, S. P., Yang, Y., & Oh, U. (2006). A novel mechanosensitive channel identified in sensory neurons. European Journal of Neuroscience, 23(10), 2543-2550. doi:10.1111/j.1460-9568.2006.04802.x

Cho, H., Shin, J., Shin, C. Y., Lee, S. Y., & Oh, U. (2002). Mechanosensitive ion channels in cultured sensory neurons of neonatal rats. J Neurosci, 22(4), 1238-1247.

Choi, J., Zhang, W., Gu, X., Chen, X., Hong, L., Laird, J. M., & Salomon, R. G. (2011). Lysophosphatidylcholine is generated by spontaneous deacylation of oxidized phospholipids. Chem Res Toxicol, 24(1), 111-118. doi:10.1021/tx100305b

Choiniere, M., Melzack, R., & Papillon, J. (1991). Pain and paresthesia in patients with healed burns: an exploratory study. J Pain Symptom Manage, 6(7), 437-444.

Choiniere, M., Melzack, R., Rondeau, J., Girard, N., & Paquin, M. J. (1989). The pain of burns: characteristics and correlates. J Trauma, 29(11), 1531-1539.

Cholewinski, A., Burgess, G. M., & Bevan, S. (1993). The role of calcium in capsaicin-induced desensitization in rat cultured dorsal root ganglion neurons. Neuroscience, 55(4), 1015-1023.

Christensen, A. P., & Corey, D. P. (2007). TRP channels in mechanosensation: direct or indirect activation? Nat Rev Neurosci, 8(7), 510-521. doi:10.1038/nrn2149

Ciura, S., & Bourque, C. W. (2006). Transient receptor potential vanilloid 1 is required for intrinsic osmoreception in organum vasculosum lamina terminalis neurons and for normal thirst responses to systemic hyperosmolality. J Neurosci, 26(35), 9069-9075. doi:10.1523/jneurosci.0877-06.2006

Claassen, L., Papst, S., Reimers, K., Stukenborg-Colsman, C., Steinstraesser, L., Vogt, P. M., Niederbichler, A. D. (2014). Inflammatory response to burn trauma: nicotine attenuates proinflammatory cytokine levels. Eplasty, 14, e46.

Clapham, D. E. (2007). Calcium signaling. Cell 131(6): 1047-1058.

Claudinot, S., Nicolas, M., Oshima, H., Rochat, A., & Barrandon, Y. (2005). Long-term renewal of hair follicles from clonogenic multipotent stem cells. Proc Natl Acad Sci U S A, 102(41), 14677-14682. doi:10.1073/pnas.0507250102

Clough, G. F., & Church, M. K. (2002). Vascular responses in the skin: an accessible model of inflammation. News Physiol Sci, 17, 170-174.

Clover, A. J. P., Kumar, A. H. S., & Caplice, N. M. (2011). Deficiency of CX3CR1 delays burn wound healing and is associated with reduced myeloid cell recruitment and decreased sub-dermal angiogenesis. Burns, 37(8), 1386-1393. doi:10.1016/j.burns.2011.08.001

Cockayne, D. A., Dunn, P. M., Zhong, Y., Rong, W., Hamilton, S. G., Knight, G. E., . . . Ford, A. P. (2005). P2X2 knockout mice and P2X2/P2X3 double knockout mice reveal a role for the P2X2 receptor subunit in mediating multiple sensory effects of ATP. J Physiol, 567(Pt 2), 621-639. doi:10.1113/jphysiol.2005.088435

Cockayne, D. A., Hamilton, S. G., Zhu, Q. M., Dunn, P. M., Zhong, Y., Novakovic, S., . . . Ford, A. P. (2000). Urinary bladder hyporeflexia and reduced pain-related behaviour in P2X3-deficient mice. Nature, 407(6807), 1011-1015. doi:10.1038/35039519

Cohen, I., Rider, P., Carmi, Y., Braiman, A., Dotan, S., White, M. R., . . . Apte, R. N. (2010). Differential release of chromatin-bound IL-1alpha discriminates between necrotic and apoptotic cell death by the ability to induce sterile inflammation. Proc Natl Acad Sci U S A, 107(6), 2574-2579. doi:10.1073/pnas.0915018107

Coleman, L. S. (2004). Bupivacaine and Ventricular Fibrillation. Anesthesia & Analgesia, 99(4), 1269. doi:10.1213/01.ane.0000133953.14237.13

Colles, S. M., & Chisolm, G. M. (2000). Lysophosphatidylcholine-induced cellular injury in cultured fibroblasts involves oxidative events. J Lipid Res, 41(8), 1188-1198.

Colley, C. M., Fleck, A., Goode, A. W., Muller, B. R. Myers, M. A. (1983). Early time course of the acute phase protein response in man. Journal of Clinical Pathology 36(2): 203-207.

Combadiere, C., Potteaux, S., Gao, J. L., Esposito, B., Casanova, S., Lee, E. J., . . . Mallat, Z. (2003). Decreased atherosclerotic lesion formation in CX3CR1/apolipoprotein E double knockout mice. Circulation, 107(7), 1009-1016. doi:10.1161/01.Cir.0000057548.68243.42

Combadiere, C., Salzwedel, K., Smith, E. D., Tiffany, H. L., Berger, E. A., & Murphy, P. M. (1998). Identification of CX3CR1. A chemotactic receptor for the human CX3C chemokine fractalkine and a fusion coreceptor for HIV-1. Journal of Biological Chemistry, 273(37), 23799-23804.

Constantian, M. B. (1978). Association of sepsis with an immunosuppressive polypeptide in the serum of burn patients. Ann Surg, 188(2), 209-215.

Copray, J. C., Mantingh, I., Brouwer, N., Biber, K., Kust, B. M., Liem, R. S., . . . Boddeke, H. W. (2001). Expression of interleukin-1 beta in rat dorsal root ganglia. J Neuroimmunol, 118(2), 203-211.

Coran, A. G., Caldamone, A.A., Adzick, S.N., Krummel, T.M. and Laberge, J.-M. (2012). Coran, A.G., Caldamone, A.A., Adzick, S.N., Krummel, T.M. and Laberge, J.-M. (2012) Pediatric surgery, 2-Volume set: Expert consult - online and print (7th ed.). United States: Elsevier Health Sciences.

Correia, M. L., Morgan, D. A., Mitchell, J. L., Sivitz, W. I., Mark, A. L., & Haynes, W. G. (2001). Role of corticotrophin-releasing factor in effects of leptin on sympathetic nerve activity and arterial pressure. Hypertension, 38(3), 384-388.

Corsini, E., & Galli, C. L. (1998). Cytokines and irritant contact dermatitis. Toxicology Letters, 102-103, 277-282.

Cortright, D. N., & Szallasi, A. (2004). Biochemical pharmacology of the vanilloid receptor TRPV1. An update. European Journal of Biochemistry, 271(10), 1814-1819. doi:10.1111/j.1432-1033.2004.04082.x

Coruzzi, G., Adami, M., Guaita, E., de Esch, I. J., & Leurs, R. (2007). Antiinflammatory and antinociceptive effects of the selective histamine H4-receptor antagonists JNJ7777120 and VUF6002 in a rat model of carrageenan-induced acute inflammation. European Journal of Pharmacology, 563(1-3), 240-244. doi:10.1016/j.ejphar.2007.02.026

Cotran, R. S. (1965). THE DELAYED AND PROLONGED VASCULAR LEAKAGE IN INFLAMMATION. II. AN ELECTRON MICROSCOPIC STUDY OF THE VASCULAR RESPONSE AFTER THERMAL INJURY. Am J Pathol, 46, 589-620.

Coumel, P. (1996). Autonomic influences in atrial tachyarrhythmias. J Cardiovasc Electrophysiol, 7(10), 999-1007.

Coutant, F., Perrin-Cocon, L., Agaugue, S., Delair, T., Andre, P., & Lotteau, V. (2002). Mature dendritic cell generation promoted by lysophosphatidylcholine. J Immunol, 169(4), 1688-1695.

Cox, J. J., Reimann, F., Nicholas, A. K., Thornton, G., Roberts, E., Springell, K., . . . Woods, C. G. (2006). An SCN9A channelopathy causes congenital inability to experience pain. Nature, 444(7121), 894-898. doi:http://www.nature.com/nature/journal/v444/n7121/suppinfo/nature05413_S1.html

Crandall, M., Kwash, J., Yu, W., & White, G. (2002). Activation of protein kinase C sensitizes human VR1 to capsaicin and to moderate decreases in pH at physiological temperatures in Xenopus oocytes. Pain, 98(1-2), 109-117.

Croset, M., Brossard, N., Polette, A., & Lagarde, M. (2000). Characterization of plasma unsaturated lysophosphatidylcholines in human and rat. Biochemical Journal, 345 Pt 1, 61-67.

Csontos, C., Foldi, V., Fischer, T., & Bogar, L. (2007). Factors affecting fluid requirement on the first day after severe burn trauma. ANZ J Surg, 77(9), 745-748. doi:10.1111/j.1445-2197.2007.04221.x

Cunha, F. Q., Poole, S., Lorenzetti, B. B., & Ferreira, S. H. (1992). The pivotal role of tumour necrosis factor alpha in the development of inflammatory hyperalgesia. Br J Pharmacol, 107(3), 660-664.

Cunningham, T. J., Yao, L., & Lucena, A. (2008). Product inhibition of secreted phospholipase A2 may explain lysophosphatidylcholines' unexpected therapeutic properties. J Inflamm (Lond), 5, 17. doi:10.1186/1476-9255-5-17

Curran, T. A., & Ghahary, A. (2013). Evidence of a role for fibrocyte and keratinocyte-like cells in the formation of hypertrophic scars. J Burn Care Res, 34(2), 227-231. doi:10.1097/BCR.0b013e318254d1f9

D'Arco, M., Giniatullin, R., Simonetti, M., Fabbro, A., Nair, A., Nistri, A., & Fabbretti, E. (2007). Neutralization of nerve growth factor induces plasticity of ATP-sensitive P2X3 receptors of nociceptive trigeminal ganglion neurons. J Neurosci, 27(31), 8190-8201. doi:10.1523/jneurosci.0713-07.2007

Dahiya, P. (2009). Burns as a model of SIRS. Front Biosci (Landmark Ed) 14: 4962-4967.

Dai, T., Kharkwal, G. B., Tanaka, M., Huang, Y. Y., Bil de Arce, V. J., Hamblin, M. R. (2011). Animal models of external traumatic wound infections. Virulence 2(4): 296-315.

Dalgliesh, C. E., Horning, E. C., Horning, M. G., Knox, K. L., & Yarger, K. (1966). A gas-liquid-chromatographic procedure for separating a wide range of metabolites occuring in urine or tissue extracts. Biochemical Journal, 101(3), 792-810.

Dalley, A. J., Lipman, J., Deans, R., Venkatesh, B., Rudd, M., Roberts, M. S., & Cross, S. E. (2009). Tissue accumulation of cephalothin in burns: a comparative study by microdialysis of subcutaneous interstitial fluid cephalothin concentrations in burn patients and healthy volunteers. Antimicrob Agents Chemother, 53(1), 210-215. doi:10.1128/aac.00718-08

Dang, P. M., Elbim, C., Marie, J. C., Chiandotto, M., Gougerot-Pocidalo, M. A., & El-Benna, J. (2006). Anti-inflammatory effect of interleukin-10 on human neutrophil respiratory burst involves inhibition of GM-CSF-induced p47PHOX phosphorylation through a decrease in ERK1/2 activity. Faseb Journal, 20(9), 1504-1506. doi:10.1096/fj.05-5395fje

Daniel, E.E., Fulton, J. B., Hiddleston, M., Martin, W., Foulks, J. G. (1957). An analysis of the mechanism of barbiturate-induced cardiovascular depression and its antagonism by sympathomimetic amines. Survey of Anesthesiology 1(4): 287-293.

Daniel, T., Thobe, B. M., Chaudry, I. H., Choudhry, M. A., Hubbard, W. J., & Schwacha, M. G. (2007). Regulation of the postburn wound inflammatory response by gammadelta T-cells. Shock, 28(3), 278-283. doi:10.1097/shk.0b013e318034264c

Davies, M. P., Evans, J., & McGonigle, R. J. S. (1994). The dialysis debate: acute renal failure in burns patients. Burns, 20(1), 71-73. doi:http://dx.doi.org/10.1016/0305-4179(94)90111-2

Davis, J. B., Gray, J., Gunthorpe, M. J., Hatcher, J. P., Davey, P. T., Overend, P., . . . Sheardown, S. A. (2000). Vanilloid receptor-1 is essential for inflammatory thermal hyperalgesia. Nature, 405(6783), 183-187. doi:10.1038/35012076

de Bandt, J. P., Chollet-Martin, S., Hernvann, A., Lioret, N., du Roure, L. D., Lim, S. K., Vaubourdolle, M., Guechot, J., Saizy, R., Giboudeau, J. (1994). Cytokine response to burn injury: relationship with protein metabolism. J Trauma, 36(5), 624-628.

Debelle, L., & Tamburro, A. M. (1999). Elastin: molecular description and function. Int J Biochem Cell Biol, 31(2), 261-272.

Del Maestro, R., Thaw, H. H., Bjork, J., Planker, M., & Arfors, K. E. (1980). Free radicals as mediators of tissue injury. Acta Physiol Scand Suppl, 492, 43-57.

Demas, G. E. (2010). In vivo but not in vitro leptin enhances lymphocyte proliferation in Siberian hamsters (Phodopus sungorus). Gen Comp Endocrinol, 166(2), 314-319. doi:10.1016/j.ygcen.2009.10.011

Demling, R. H. (2005). The burn edema process: current concepts. J Burn Care Rehabil, 26(3), 207-227.

Demling, R. H., & Lalonde, C. (1990). Systemic lipid peroxidation and inflammation induced by thermal injury persists into the post-resuscitation period. J Trauma, 30(1), 69-74.

Demling, R. H., LaLonde, C., Liu, Y. P., & Zhu, D. G. (1989). The lung inflammatory response to thermal injury: relationship between physiologic and histologic changes. Surgery, 106(1), 52-59.

DeSanti, L. (2005). Pathophysiology and current management of burn injury. Adv Skin Wound Care, 18(6), 323-332; quiz 332-324.

Despa, F., Orgill, D. P., Neuwalder, J., & Lee, R. C. (2005). The relative thermal stability of tissue macromolecules and cellular structure in burn injury. Burns, 31(5), 568-577. doi:10.1016/j.burns.2005.01.015

Dettmer, K., Aronov, P. A., & Hammock, B. D. (2007). Mass spectrometry-based metabolomics. Mass Spectrom Rev, 26(1), 51-78. doi:10.1002/mas.20108

Devesa, I., Planells-Cases, R., Fernandez-Ballester, G., Gonzalez-Ros, J. M., Ferrer-Montiel, A., & Fernandez-Carvajal, A. (2011). Role of the transient receptor potential vanilloid 1 in inflammation and sepsis. J Inflamm Res, 4, 67-81. doi:10.2147/jir.s12978

Di Marzo, V., Blumberg, P. M., & Szallasi, A. (2002). Endovanilloid signaling in pain. Curr Opin Neurobiol, 12(4), 372-379.

Difede, J., & Barocas, D. (1999). Acute intrusive and avoidant PTSD symptoms as predictors of chronic PTSD following burn injury. Journal of Traumatic Stress, 12(2), 363-369. doi:Doi 10.1023/A:1024788812393

Dinarello, C. A., Cannon, J. G., Wolff, S. M., Bernheim, H. A., Beutler, B., Cerami, A., . . . O'Connor, J. V. (1986). Tumor necrosis factor (cachectin) is an endogenous pyrogen and induces production of interleukin 1. Journal of Experimental Medicine, 163(6), 1433-1450.

Dinarello, C. A., Novick, D., Kim, S., & Kaplanski, G. (2013). Interleukin-18 and IL-18 binding protein. Front Immunol, 4, 289. doi:10.3389/fimmu.2013.00289

DiPietro, L. A., Polverini, P. J., Rahbe, S. M., & Kovacs, E. J. (1995). Modulation of JE/MCP-1 expression in dermal wound repair. Am J Pathol, 146(4), 868-875.

Docherty, R. J., Yeats, J. C., Bevan, S., & Boddeke, H. W. (1996). Inhibition of calcineurin inhibits the desensitization of capsaicin-evoked currents in cultured dorsal root ganglion neurones from adult rats. Pflugers Arch, 431(6), 828-837.

Dockrell, H. M. Cytokines in Health and Disease: Immunology. 1993 Aug;79(4):685.

Domeij, H., Hua, X., Su, J., Backlund, A., Yan, Z., Frostegard, A. G., . . . Frostegard, J. (2013). Annexin A5 inhibits atherogenic and pro-inflammatory effects of lysophosphatidylcholine. Prostaglandins Other Lipid Mediat, 106, 72-78. doi:10.1016/j.prostaglandins.2013.01.004

Dorsett-Martin, W. A. (2004). Rat models of skin wound healing: a review. Wound Repair Regen, 12(6), 591-599. doi:10.1111/j.1067-1927.2004.12601.x

Drost, A. C., Burleson, D. G., Cioffi, W. G., Jr., Jordan, B. S., Mason, A. D., Jr., & Pruitt, B. A., Jr. (1993). Plasma cytokines following thermal injury and their relationship with patient mortality, burn size, and time postburn. J Trauma, 35(3), 335-339.

Drost, A. C., Burleson, D. G., Cioffi, W. G., Jr., Mason, A. D., Jr., & Pruitt, B. A., Jr. (1993). Plasma cytokines after thermal injury and their relationship to infection. Ann Surg, 218(1), 74-78.

Duan, H., Chai, J., Sheng, Z., Yao, Y., Yin, H., Liang, L., . . . Lin, J. (2009). Effect of burn injury on apoptosis and expression of apoptosis-related genes/proteins in skeletal muscles of rats. Apoptosis, 14(1), 52-65. doi:10.1007/s10495-008-0277-7

Dubin, A. E. (2010). Nociceptors: the sensors of the pain pathway. 120(11), 3760-3772. doi:10.1172/jci42843

Dunn, W. B. (2011). Mass spectrometry in systems biology an introduction. Methods Enzymol, 500, 15-35. doi:10.1016/b978-0-12-385118-5.00002-5

Duthey, B., Hubner, A., Diehl, S., Boehncke, S., Pfeffer, J., & Boehncke, W. H. (2010). Anti-inflammatory effects of the GABA(B) receptor agonist baclofen in allergic contact dermatitis. Experimental Dermatology, 19(7), 661-666. doi:10.1111/j.1600-0625.2010.01076.x

Dworkin, R. H. (2002). An overview of neuropathic pain: syndromes, symptoms, signs, and several mechanisms. Clin J Pain, 18(6), 343-349.

Dyster-Aas, J., Willebrand, M., Wikehult, B., Gerdin, B., & Ekselius, L. (2008). Major depression and posttraumatic stress disorder symptoms following severe burn injury in relation to lifetime psychiatric morbidity. J Trauma, 64(5), 1349-1356. doi:10.1097/TA.0b013e318047e005

Earley, S., & Brayden, J. E. (2010). Transient receptor potential channels and vascular function. Clin Sci (Lond), 119(1), 19-36. doi:10.1042/cs20090641

Eccleston, C. (2001). Role of psychology in pain management. British Journal of Anaesthesia, 87(1), 144-152. doi:10.1093/bja/87.1.144

Edgar, D., & Brereton, M. (2004). Rehabilitation after burn injury. BMJ, 329(7461), 343-345.

Ejaz, A. A., Dass, B., Kambhampati, G., Ejaz, N. I., Maroz, N., Dhatt, G. S., . . . Johnson, R. J. (2012). Lowering serum uric acid to prevent acute kidney injury. Med Hypotheses, 78(6), 796-799. doi:10.1016/j.mehy.2012.03.011

Ejaz, A. A., Mu, W., Kang, D. H., Roncal, C., Sautin, Y. Y., Henderson, G., . . . Johnson, R. J. (2007). Could uric acid have a role in acute renal failure? Clin J Am Soc Nephrol, 2(1), 16-21. doi:10.2215/cjn.00350106

Elledge, E. S., Smith, A. A., McManus, W. F., & Pruitt, B. A., Jr. (1988). Heterotopic bone formation in burned patients. J Trauma, 28(5), 684-687.

Emara, S., & Alzaylai, A. (2013). Renal failure in burn patients: a review. Ann Burns Fire Disasters, 26(1), 12-15.

England, S., Bevan, S., & Docherty, R. J. (1996). PGE2 modulates the tetrodotoxin-resistant sodium current in neonatal rat dorsal root ganglion neurones via the cyclic AMP-protein kinase A cascade. J Physiol, 495 (Pt 2), 429-440.

Enoch, S., Roshan, A., & Shah, M. (2009). Emergency and early management of burns and scalds. BMJ, 338, b1037. doi:10.1136/bmj.b1037

Eski, M., Ozer, F., Firat, C., Alhan, D., Arslan, N., Senturk, T., & Isik, S. (2012). Cerium nitrate treatment prevents progressive tissue necrosis in the zone of stasis following burn. Burns, 38(2), 283-289. doi:DOI 10.1016/j.burns.2011.08.008

Esselman, P. C., Thombs, B. D., Magyar-Russell, G., & Fauerbach, J. A. (2006). Burn rehabilitation: state of the science. Am J Phys Med Rehabil, 85(4), 383-413. doi:10.1097/01.phm.0000202095.51037.a3

Evans, E. B., & Smith, J. R. (1959). Bone and joint changes following burns; a roentgenographic study; preliminary report. J Bone Joint Surg Am, 41-A(5), 785-799.

Ezkurdia, I., Juan, D., Rodriguez, J. M., Frankish, A., Diekhans, M., Harrow, J., . . . Tress, M. L. (2014). Multiple evidence strands suggest that there may be as few as 19,000 human protein-coding genes. Hum Mol Genet, 23(22), 5866-5878. doi:10.1093/hmg/ddu309

Fagenholz, P. J., Sheridan, R. L., Harris, N. S., Pelletier, A. J., & Camargo, C. A., Jr. (2007). National study of Emergency Department visits for burn injuries, 1993 to 2004. J Burn Care Res, 28(5), 681-690. doi:10.1097/BCR.0B013E318148C9AC

Faggioni, R., Feingold, K. R., & Grunfeld, C. (2001). Leptin regulation of the immune response and the immunodeficiency of malnutrition. Faseb Journal, 15(14), 2565-2571. doi:DOI 10.1096/fj.01-0431rev

Falder, S., Browne, A., Edgar, D., Staples, E., Fong, J., Rea, S., & Wood, F. (2009). Core outcomes for adult burn survivors: a clinical overview. Burns, 35(5), 618-641. doi:10.1016/j.burns.2008.09.002

Falk, E., Shah, P. K., & Fuster, V. (1995). Coronary plaque disruption. Circulation, 92(3), 657-671.

Fallah, A., Pierre, R., Abed, E., & Moreau, R. (2013). Lysophosphatidylcholine-induced cytotoxicity in osteoblast-like MG-63 cells: involvement of transient receptor potential vanilloid 2 (TRPV2) channels. Mol Membr Biol, 30(5-6), 315-326. doi:10.3109/09687688.2013.828855

Fantuzzi, G., & Faggioni, R. (2000). Leptin in the regulation of immunity, inflammation, and hematopoiesis. J Leukoc Biol, 68(4), 437-446.

Farina, J. A., Jr., Rosique, M. J., & Rosique, R. G. (2013). Curbing inflammation in burn patients. Int J Inflam, 2013, 715645. doi:10.1155/2013/715645

Faunce, D. E., Gregory, M. S., & Kovacs, E. J. (1998). Acute ethanol exposure prior to thermal injury results in decreased T-cell responses mediated in part by increased production of IL-6. Shock, 10(2), 135-140.

Faure, S., Meyer, L., Genin, E., Pellet, P., Debre, P., Theodorou, I., . . . Group, S. S. (2003). Deleterious genetic influence of CX3CR1 genotypes on HIV-1 disease progression. J Acquir Immune Defic Syndr, 32(3), 335-337.

Fayazov, A. D., Shukurov, S. I., Shukurov, B. I., Sultanov, B. C., Namazov, A. N., & Ruzimuratov, D. A. (2009). Disorders of the immune system in severely burned patients. Ann Burns Fire Disasters, 22(3), 121-130.

Feig, D. I., Kang, D. H., & Johnson, R. J. (2008). Uric Acid and Cardiovascular Risk. N Engl J Med, 359(17), 1811-1821. doi:10.1056/NEJMra0800885

Feng, Y., Liu, Y., Wang, L., Cai, X., Wang, D., Wu, K., . . . Lei, W. (2013). Sustained oxidative stress causes late acute renal failure via duplex regulation on p38 MAPK and Akt phosphorylation in severely burned rats. PLoS One, 8(1), e54593. doi:10.1371/journal.pone.0054593

Fernandes, E. S., Liang, L., Smillie, S. J., Kaiser, F., Purcell, R., Rivett, D. W., . . . Brain, S. D. (2012). TRPV1 deletion enhances local inflammation and accelerates the onset of systemic inflammatory response syndrome. J Immunol, 188(11), 5741-5751. doi:10.4049/jimmunol.1102147

Fernandes, E. S., Russell, F. A., Spina, D., McDougall, J. J., Graepel, R., Gentry, C., . . . Brain, S. D. (2011). A distinct role for transient receptor potential ankyrin 1, in addition to transient receptor potential vanilloid 1, in tumor necrosis factor alpha-induced inflammatory hyperalgesia and Freund's complete adjuvant-induced monarthritis. Arthritis Rheum, 63(3), 819-829. doi:10.1002/art.30150

Fernandez-Riejos, P., Goberna, R., & Sanchez-Margalet, V. (2008). Leptin promotes cell survival and activates Jurkat T lymphocytes by stimulation of mitogen-activated protein kinase. Clin Exp Immunol, 151(3), 505-518. doi:10.1111/j.1365-2249.2007.03563.x

Fernandez-Riejos, P., Najib, S., Santos-Alvarez, J., Martin-Romero, C., Perez-Perez, A., Gonzalez-Yanes, C., & Sanchez-Margalet, V. (2010). Role of leptin in the activation of immune cells. Mediators Inflamm, 2010, 568343. doi:10.1155/2010/568343

Fiehn, O. (2002). Metabolomics--the link between genotypes and phenotypes. Plant Mol Biol 48(1-2): 155-171.

Field, K. J., White, W. J., & Lang, C. M. (1993). Anaesthetic effects of chloral hydrate, pentobarbitone and urethane in adult male rats. Lab Anim, 27(3), 258-269.

Fink, B. R., & Cairns, A. M. (1983). Differential peripheral axon block with lidocaine: unit studies in the cervical vagus nerve. Anesthesiology, 59(3), 182-186.

Fink, K. L., & Gross, R. W. (1984). Modulation of canine myocardial sarcolemmal membrane fluidity by amphiphilic compounds. Circ Res, 55(5), 585-594.

Finnerty, C. C., Jeschke, M. G., Herndon, D. N., Gamelli, R., Gibran, N., Klein, M., . . . the Host Response Glue, G. (2008). Temporal cytokine profiles in severely burned patients: a comparison of adults and children. Mol Med, 14(9-10), 553-560. doi:10.2119/2007-00132.Finnerty

Finnerty, C. C., Jeschke, M. G., Qian, W. J., Kaushal, A., Xiao, W., Liu, T., . . . Herndon, D. N. (2013). Determination of burn patient outcome by large-scale quantitative discovery proteomics. Critical Care Medicine, 41(6), 1421-1434. doi:10.1097/CCM.0b013e31827c072e

Finnerty, C. C., Przkora, R., Herndon, D. N., & Jeschke, M. G. (2009). Cytokine expression profile over time in burned mice. Cytokine, 45(1), 20-25. doi:10.1016/j.cyto.2008.10.005

Firat, C., Samdanci, E., Erbatur, S., Aytekin, A. H., Ak, M., Turtay, M. G., & Coban, Y. K. (2013). beta-Glucan treatment prevents progressive burn ischaemia in the zone of stasis and improves burn healing: an experimental study in rats. Burns, 39(1), 105-112. doi:10.1016/j.burns.2012.02.031

Fish, R. E., & American College of Laboratory Animal, M. (2008). Anesthesia and analgesia in laboratory animals. Amsterdam; London: Academic.

Fitzwater, J., Purdue, G. F., Hunt, J. L., & O'Keefe, G. E. (2003). The risk factors and time course of sepsis and organ dysfunction after burn trauma. J Trauma, 54(5), 959-966. doi:10.1097/01.ta.0000029382.26295.ab

Fivenson, D. P., Breneman, D. L., Rosen, G. B., Hersh, C. S., Cardone, S., & Mutasim, D. (1994). Nicotinamide and tetracycline therapy of bullous pemphigoid. Arch Dermatol, 130(6), 753-758.

Flegel, C., Schobel, N., Altmuller, J., Becker, C., Tannapfel, A., Hatt, H., & Gisselmann, G. (2015). RNA-Seq Analysis of Human Trigeminal and Dorsal Root Ganglia with a Focus on Chemoreceptors. PLoS One, 10(6), e0128951. doi:10.1371/journal.pone.0128951

Flemming, P. K., Dedman, A. M., Xu, S. Z., Li, J., Zeng, F., Naylor, J., . . . Beech, D. J. (2006). Sensing of lysophospholipids by TRPC5 calcium channel. Journal of Biological Chemistry, 281(8), 4977-4982. doi:10.1074/jbc.M510301200

Forster, Y., Schmidt, J. R., Wissenbach, D. K., Pfeiffer, S. E., Baumann, S., Hofbauer, L. C., . . . Rammelt, S. (2016). Microdialysis Sampling from Wound Fluids Enables Quantitative Assessment of Cytokines, Proteins, and Metabolites Reveals Bone Defect-Specific Molecular Profiles. PLoS One, 11(7), e0159580. doi:10.1371/journal.pone.0159580

Foulkes, T., & Wood, J. N. (2008). Pain Genes. PLoS Genet, 4(7), e1000086. doi:10.1371/journal.pgen.1000086

Foussat, A., Bouchet-Delbos, L., Berrebi, D., Durand-Gasselin, I., Coulomb-L'Hermine, A., Krzysiek, R., . . . Emilie, D. (2001). Deregulation of the expression of the fractalkine/fractalkine receptor complex in HIV-1-infected patients. Blood, 98(6), 1678-1686. doi:DOI 10.1182/blood.V98.6.1678

Fox, A., Wotherspoon, G., McNair, K., Hudson, L., Patel, S., Gentry, C., & Winter, J. (2003). Regulation and function of spinal and peripheral neuronal B1 bradykinin receptors in inflammatory mechanical hyperalgesia. Pain, 104(3), 683-691.

Frank, S., Stallmeyer, B., Kampfer, H., Kolb, N., & Pfeilschifter, J. (2000). Leptin enhances wound re-epithelialization and constitutes a direct function of leptin in skin repair. Journal of Clinical Investigation, 106(4), 501-509. doi:Doi 10.1172/Jci9148

Franz, M. G., Steed, D. L., & Robson, M. C. (2007a). Optimizing healing of the acute wound by minimizing complications. Curr Probl Surg, 44(11), 691-763. doi:10.1067/j.cpsurg.2007.07.001

Franz, M. G., Steed, D. L., & Robson, M. C. (2007b). Optimizing healing of the acute wound by minimizing complications. Curr Probl Surg, 44. doi:10.1067/j.cpsurg.2007.07.001

Fuchs, B., Schiller, J., Wagner, U., Hantzschel, H., & Arnold, K. (2005). The phosphatidylcholine/lysophosphatidylcholine ratio in human plasma is an indicator of the severity of rheumatoid arthritis: investigations by 31P NMR and MALDI-TOF MS. Clinical Biochemistry, 38(10), 925-933. doi:10.1016/j.clinbiochem.2005.06.006

Fujisawa, H., Wang, B., Kondo, S., Shivji, G. M., & Sauder, D. N. (1997). Costimulation with ultraviolet B and interleukin-1 alpha dramatically increase tumor necrosis factor-alpha production in human dermal fibroblasts. J Interferon Cytokine Res, 17(5), 307-313. doi:10.1089/jir.1997.17.307

Fujita, Y., Murakami, M., Ogawa, Y., Masuzaki, H., Tanaka, M., Ozaki, S., . . . Mimori, T. (2002). Leptin inhibits stress-induced apoptosis of T lymphocytes. Clin Exp Immunol, 128(1), 21-26. doi:DOI 10.1046/j.1365-2249.2002.01797.x

Fukuoka, H., Kawatani, M., Hisamitsu, T., & Takeshige, C. (1994). Cutaneous hyperalgesia induced by peripheral injection of interleukin-1 beta in the rat. Brain Res, 657(1-2), 133-140.

Fukushima, R., Alexander, J. W., Wu, J. Z., Mao, J. X., Szczur, K., Stephens, A. M., . . . Ogle, C. K. (1994). Time course of production of cytokines and prostaglandin E2 by macrophages isolated after thermal injury and bacterial translocation. Circ Shock, 42(3), 154-162.

Gabay, C., Dreyer, M. G., Pellegrinelli, N., Chicheportiche, R., & Meier, C. A. (2001). Leptin directly induces the secretion of interleukin 1 receptor antagonist in human monocytes. Journal of Clinical Endocrinology & Metabolism, 86(2), 783-791. doi:Doi 10.1210/Jc.86.2.783

Gainsford, T., Willson, T. A., Metcalf, D., Handman, E., McFarlane, C., Ng, A., . . . Hilton, D. J. (1996). Leptin can induce proliferation, differentiation, and functional activation of hemopoietic cells. Proceedings of the National Academy of Sciences of the United States of America, 93(25), 14564-14568. doi:DOI 10.1073/pnas.93.25.14564

Galer, B. S., Lee, D., Ma, T., Nagle, B., & Schlagheck, T. G. (2005). MorphiDex (morphine sulfate/dextromethorphan hydrobromide combination) in the treatment of chronic pain: three multicenter, randomized, double-blind, controlled clinical trials fail to demonstrate enhanced opioid analgesia or reduction in tolerance. Pain, 115(3), 284-295. doi:10.1016/j.pain.2005.03.004

Galimov Sh, N., & Kamilov, F. (1991). [The nicotinamide coenzyme system in experimental burn disease during prepubescence]. Vopr Med Khim, 37(3), 62-64.

Gao, Y., Xu, C., Yu, K., Li, G., Wan, F., Liu, S., . . . Liang, S. (2010). Effect of tetramethylpyrazine on DRG neuron P2X3 receptor involved in transmitting pain after burn. Burns, 36(1), 127-134. doi:10.1016/j.burns.2009.04.032

Garcia-Hirschfeld, J., Lopez-Briones, L. G., Belmonte, C., & Valdeolmillos, M. (1995). Intracellular free calcium responses to protons and capsaicin in cultured trigeminal neurons. Neuroscience, 67(1), 235-243.

Garcia-Sanz, N., Valente, P., Gomis, A., Fernandez-Carvajal, A., Fernandez-Ballester, G., Viana, F., . . . Ferrer-Montiel, A. (2007). A role of the transient receptor potential domain of vanilloid receptor I in channel gating. J Neurosci, 27(43), 11641-11650. doi:10.1523/jneurosci.2457-07.2007

Garcia, G. E., Xia, Y., Chen, S., Wang, Y., Ye, R. D., Harrison, J. K., . . . Feng, L. (2000). NF-kappaB-dependent fractalkine induction in rat aortic endothelial cells stimulated by IL-1beta, TNF-alpha, and LPS. J Leukoc Biol, 67(4), 577-584.

Garton, K. J., Gough, P. J., Blobel, C. P., Murphy, G., Greaves, D. R., Dempsey, P. J., & Raines, E. W. (2001). Tumor necrosis factor-alpha-converting enzyme (ADAM17) mediates the cleavage and shedding of fractalkine (CX3CL1). Journal of Biological Chemistry, 276(41), 37993-38001.

Gatson, J. W., Liu, M. M., Rivera-Chavez, F. A., Minei, J. P., & Wolf, S. E. (2014). Serum Levels of Neurofilament-H are Elevated in Patients Suffering From Severe Burns. J Burn Care Res. doi:10.1097/BCR.0000000000000176

Gauglitz, G. G., Zedler, S., v. Spiegel, F., Fuhr, J., v. Donnersmarck, G. H., & Faist, E. (2012). Functional Characterization of Cultured Keratinocytes after Acute Cutaneous Burn Injury. PLoS One, 7(2). doi:10.1371/journal.pone.0029942

Geiger, B., Bershadsky, A., Pankov, R., Yamada, K. M. (2001). Transmembrane crosstalk between the extracellular matrix--cytoskeleton crosstalk. Nat Rev Mol Cell Biol 2(11): 793-805.

Ghanime, G., Rizkallah, N., & Said, J. M. (2013). Epidemiology of major burns at the Lebanese Burn Center in Geitawi, Lebanon. Ann Burns Fire Disasters, 26(2), 59-62.

Ghasemlou, N., Jeong, S. Y., Lacroix, S., & David, S. (2007). T cells contribute to lysophosphatidylcholine-induced macrophage activation and demyelination in the CNS. Glia, 55(3), 294-302. doi:10.1002/glia.20449

Ghilardi, N., Ziegler, S., Wiestner, A., Stoffel, R., Heim, M. H., & Skoda, R. C. (1996). Defective STAT signaling by the leptin receptor in diabetic mice. Proceedings of the National Academy of Sciences of the United States of America, 93(13), 6231-6235. doi:DOI 10.1073/pnas.93.13.6231

Ghosh, P. K., Vasanji, A., Murugesan, G., Eppell, S. J., Graham, L. M., & Fox, P. L. (2002). Membrane microviscosity regulates endothelial cell motility. Nat Cell Biol, 4(11), 894-900. doi:10.1038/ncb873

Gika, H. G., Theodoridis, G. A., Wilson, I. D. (2008). Hydrophilic interaction and reversed-phase ultra-performance liquid chromatography TOF-MS for metabonomic analysis of Zucker rat urine. J Sep Sci 31(9): 1598-1608.

Gilboa, D., Friedman, M., & Tsur, H. (1994). The burn as a continuous traumatic stress: implications for emotional treatment during hospitalization. J Burn Care Rehabil, 15(1), 86-91; discussion 91-84.

Gillespie, C. S., Sherman, D. L., Fleetwood-Walker, S. M., Cottrell, D. F., Tait, S., Garry, E. M., . . . Brophy, P. J. (2000). Peripheral demyelination and neuropathic pain behavior in periaxin-deficient mice. Neuron, 26(2), 523-531.

Glass, C. K., & Witztum, J. L. (2001). Atherosclerosis: The road ahead. Cell, 104(4), 503-516. doi:Doi 10.1016/S0092-8674(01)00238-0

Goff, D. R., Purdue, G. F., Hunt, J. L., & Cochran, R. P. (1990). Cardiac disease and the patient with burns. J Burn Care Rehabil, 11(4), 305-307.

Goldsmith, P., Fenton, H., Morris-Stiff, G., Ahmad, N., Fisher, J., & Prasad, K. R. (2010). Metabonomics: a useful tool for the future surgeon. J Surg Res, 160(1), 122-132. doi:10.1016/j.jss.2009.03.003

Golfman, L. S., Haughey, N. J., Wong, J. T., Jiang, J. Y., Lee, D., Geiger, J. D., & Choy, P. C. (1999). Lysophosphatidylcholine induces arachidonic acid release and calcium overload in cardiac myoblastic H9c2 cells. J Lipid Res, 40(10), 1818-1826.

Golshan, A., Patel, C., & Hyder, A. A. (2013). A systematic review of the epidemiology of unintentional burn injuries in South Asia. J Public Health (Oxf), 35(3), 384-396. doi:10.1093/pubmed/fds102

Gomez-Munoz, A., O'Brien, L., Hundal, R., & Steinbrecher, U. P. (1999). Lysophosphatidylcholine stimulates phospholipase D activity in mouse peritoneal macrophages. J Lipid Res, 40(6), 988-993.

Goodacre, R., Vaidyanathan, S., Dunn, W. B., Harrigan, G. G., Kell, D. B. (2004). Metabolomics by numbers: acquiring and understanding global metabolite data. Trends Biotechnol 22(5): 245-252.

Goodarzi, M., Reisi-Dehkordi, N., Daryabeigi, R., & Zargham-Boroujeni, A. (2014). An epidemiologic study of burns: Standards of care and patients' outcomes. Iran J Nurs Midwifery Res, 19(4), 385-389.

Goretsky, M. J., Greenhalgh, D. G., Warden, G. D., Ryckman, F. C., & Warner, B. W. (1995). The Use of Extracorporeal Life-Support in Pediatric Burn Patients with Respiratory-Failure. Journal of Pediatric Surgery, 30(4), 620-623. doi:Doi 10.1016/0022-3468(95)90145-0

Gouveia, M. J., Brindley, P. J., Santos, L. L., Correia da Costa, J. M., Gomes, P., & Vale, N. (2013). Mass spectrometry techniques in the survey of steroid metabolites as potential disease biomarkers: a review. Metabolism, 62(9), 1206-1217. doi:10.1016/j.metabol.2013.04.003

Graham, T. J., Stern, P. J., & True, M. S. (1990). Classification and treatment of postburn metacarpophalangeal joint extension contractures in children. J Hand Surg Am, 15(3), 450-456.

Granowitz, E. V., Clark, B. D., Vannier, E., Callahan, M. V., & Dinarello, C. A. (1992). Effect of interleukin-1 (IL-1) blockade on cytokine synthesis: I. IL-1 receptor antagonist inhibits IL-1-induced cytokine synthesis and blocks the binding of IL-1 to its type II receptor on human monocytes. Blood, 79(9), 2356-2363.

Grant, A. D., Cottrell, G. S., Amadesi, S., Trevisani, M., Nicoletti, P., Materazzi, S., . . . Bunnett, N. W. (2007). Protease-activated receptor 2 sensitizes the transient receptor potential vanilloid 4 ion channel to cause mechanical hyperalgesia in mice. J Physiol, 578(Pt 3), 715-733. doi:10.1113/jphysiol.2006.121111

Gray, N., Adesina-Georgiadis, K., Chekmeneva, E., Plumb, R. S., Wilson, I. D., & Nicholson, J. K. (2016). Development of a Rapid Microbore Metabolic Profiling Ultraperformance Liquid Chromatography-Mass Spectrometry Approach for High-Throughput Phenotyping Studies. Analytical Chemistry, 88(11), 5742-5751. doi:10.1021/acs.analchem.6b00038

Green, D. P., Ruparel, S., Roman, L., Henry, M. A., & Hargreaves, K. M. (2013). Role of endogenous TRPV1 agonists in a postburn pain model of partial-thickness injury. Pain, 154(11), 2512-2520. doi:10.1016/j.pain.2013.07.040

Greenhalgh, D. G., Saffle, J. R., Holmes, J. H., Gamelli, R. L., Palmieri, T. L., & Horton, J. W. (2007). American Burn Association consensus conference to define sepsis and infection in burns. J Burn Care Res, 28. doi:10.1097/BCR.0b013e3181599bc9

Greenhalgh, D. G., Saffle, J. R., Holmes, J. H. t., Gamelli, R. L., Palmieri, T. L., Horton, J. W., . . . Latenser, B. A. (2007). American Burn Association consensus conference to define sepsis and infection in burns. J Burn Care Res, 28(6), 776-790. doi:10.1097/BCR.0b013e3181599bc9

Griffiths, J. (2008). A Brief History of Mass Spectrometry. Analytical Chemistry, 80(15), 5678-5683. doi:10.1021/ac8013065

Gross, J. H. (2004). Fragmentation of Organic Ions and Interpretation of EI Mass Spectra. Mass Spectrometry: A Textbook. Berlin, Heidelberg, Springer Berlin Heidelberg: 223-330.

Groth, L., Jorgensen, A., & Serup, J. (1998). Cutaneous microdialysis in the rat: insertion trauma and effect of anaesthesia studied by laser Doppler perfusion imaging and histamine release. Skin Pharmacol Appl Skin Physiol, 11(3), 125-132.

Groves, R. W., & Schmidt-Lucke, J. A. (2000). Recombinant human GM-CSF in the treatment of poorly healing wounds. Adv Skin Wound Care, 13(3 Pt 1), 107-112.

Gruen, M. L., Hao, M., Piston, D. W., & Hasty, A. H. (2007). Leptin requires canonical migratory signaling pathways for induction of monocyte and macrophage chemotaxis. Am J Physiol Cell Physiol, 293(5), C1481-1488. doi:10.1152/ajpcell.00062.2007

Grumbach, E. S., Wagrowski-Diehl, D. M., Mazzeo, E. R., Alden, B., Iraneta, P. C. (2004). Hydrophilic interaction chromatography using silica columns for the retention of polar analytes and enhanced ESI-MS sensitivity. LC-GC North Am., 22(10), 1010–1023.

Guemouri, L., Artur, Y., Herbeth, B., Jeandel, C., Cuny, G., & Siest, G. (1991). Biological variability of superoxide dismutase, glutathione peroxidase, and catalase in blood. Clin Chem, 37(11), 1932-1937.

Guler, A. D., Lee, H., Iida, T., Shimizu, I., Tominaga, M., & Caterina, M. (2002). Heat-evoked activation of the ion channel, TRPV4. J Neurosci, 22(15), 6408-6414. doi:20026679

Güneysel, O., Yeğen. (2002). Inhibition of nitric oxide synthesis ameliorates burn-induced remote organ injury in rats: A light microscopic study. Marmara Medical Journal, 15, 155-160.

Gunthorpe, M. J., Harries, M. H., Prinjha, R. K., Davis, J. B., & Randall, A. (2000). Voltage- and time-dependent properties of the recombinant rat vanilloid receptor (rVR1). J Physiol, 525 Pt 3, 747-759.

Guo, L., Milburn, M. V., Ryals, J. A., Lonergan, S. C., Mitchell, M. W., Wulff, J. E., . . . Caskey, C. T. (2015). Plasma metabolomic profiles enhance precision medicine for volunteers of normal health. Proc Natl Acad Sci U S A, 112(35), E4901-4910. doi:10.1073/pnas.1508425112

Gurfinkel, R., Singer, A. J., Cagnano, E., Rosenberg, L. (2010). Development of a novel animal burn model using radiant heat in rats and swine. Acad Emerg Med 17(5): 514-520.

Ha, C. Y., Kim, J. Y., Paik, J. K., Kim, O. Y., Paik, Y. H., Lee, E. J., & Lee, J. H. (2012). The association of specific metabolites of lipid metabolism with markers of oxidative stress, inflammation and arterial stiffness in men with newly diagnosed type 2 diabetes. Clin Endocrinol (Oxf), 76(5), 674-682. doi:10.1111/j.1365-2265.2011.04244.x

Hadrevi, J., Ghafouri, B., Sjors, A., Antti, H., Larsson, B., Crenshaw, A. G., . . . Hellstrom, F. (2013). Comparative metabolomics of muscle interstitium fluid in human trapezius myalgia: an in vivo microdialysis study. Eur J Appl Physiol, 113(12), 2977-2989. doi:10.1007/s00421-013-2716-6

Hamoud, S., Kaplan, M., Meilin, E., Hassan, A., Torgovicky, R., Cohen, R., & Hayek, T. (2013). Niacin administration significantly reduces oxidative stress in patients with hypercholesterolemia and low levels of high-density lipoprotein cholesterol. Am J Med Sci, 345(3), 195-199. doi:10.1097/MAJ.0b013e3182548c28

Han, M. S., Park, S. Y., Shinzawa, K., Kim, S., Chung, K. W., Lee, J. H., . . . Lee, M. S. (2008). Lysophosphatidylcholine as a death effector in the lipoapoptosis of hepatocytes. J Lipid Res, 49(1), 84-97. doi:10.1194/jlr.M700184-JLR200

Handfield-Jones, S., Jones, S., & Peachey, R. (1988). High dose nicotinamide in the treatment of necrobiosis lipoidica. Br J Dermatol, 118(5), 693-696.

Hansson, G. K. (2001). Immune mechanisms in atherosclerosis. Arteriosclerosis Thrombosis and Vascular Biology, 21(12), 1876-1890. doi:DOI 10.1161/hq1201.100220

Harder, A. T., & An, Y. H. (2003). The mechanisms of the inhibitory effects of nonsteroidal anti-inflammatory drugs on bone healing: a concise review. J Clin Pharmacol, 43(8), 807-815.

Harder, T., & Simons, K. (1997). Caveolae, DIGs, and the dynamics of sphingolipid-cholesterol microdomains. Curr Opin Cell Biol, 9(4), 534-542.

Hardie, R. C., & Franze, K. (2012). Photomechanical responses in Drosophila photoreceptors. Science, 338(6104), 260-263. doi:10.1126/science.1222376

Harris, R. L., Cottam, G. L., Johnston, J. M., & Baxter, C. R. (1981). The pathogenesis of abnormal erythrocyte morphology in burns. J Trauma, 21(1), 13-21.

Hart, D. W., Wolf, S. E., Chinkes, D. L., Gore, D. C., Mlcak, R. P., Beauford, R. B., . . . Herndon, D. N. (2000a). Determinants of skeletal muscle catabolism after severe burn. Ann Surg, 232(4), 455-465.

Hart, D. W., Wolf, S. E., Mlcak, R., Chinkes, D. L., Ramzy, P. I., Obeng, M. K., . . . Herndon, D. N. (2000b). Persistence of muscle catabolism after severe burn. Surgery, 128(2), 312-319. doi:10.1067/msy.2000.108059

Harvey, J. (2007). Leptin: a diverse regulator of neuronal function. Journal of Neurochemistry, 100(2), 307-313. doi:10.1111/j.1471-4159.2006.04205.x

Hasegawa, S., Kohro, Y., Shiratori, M., Ishii, S., Shimizu, T., Tsuda, M., & Inoue, K. (2010). Role of PAF receptor in proinflammatory cytokine expression in the dorsal root ganglion and tactile allodynia in a rodent model of neuropathic pain. PLoS One, 5(5), e10467. doi:10.1371/journal.pone.0010467

Hatakeyama, N., & Matsuda, N. (2014). Mechanisms of Inflammatory Response and Organ Dysfunction: Organ-Protective Strategy by Anesthetics. Curr Pharm Des.

Hattori, A., Tanaka, E., Murase, K., Ishida, N., Chatani, Y., Tsujimoto, M., . . . Kohno, M. (1993). Tumor necrosis factor stimulates the synthesis and secretion of biologically active nerve growth factor in non-neuronal cells. Journal of Biological Chemistry, 268(4), 2577-2582.

Hemmila, M. R., Mattar, A., Taddonio, M. A., Arbabi, S., Hamouda, T., Ward, P. A., Wang, S. C., Baker, J.R. Jr. (2010). Topical nanoemulsion therapy reduces bacterial wound infection and inflammation after burn injury. Surgery 148(3): 499-509.

Heimbach, D., Engrav, L., Grube, B., & Marvin, J. (1992). Burn depth: a review. World J Surg, 16(1), 10-15.

Helm, P. A., Johnson, E. R., & Carlton, A. M. (1977). Peripheral neurological problems in the acute burn patient. Burns, 3(2), 123-125.

Helme, R. D., Koschorke, G. M., & Zimmermann, M. (1986). Immunoreactive Substance-P Release from Skin Nerves in the Rat by Noxious Thermal-Stimulation. Neuroscience Letters, 63(3), 295-299. doi:Doi 10.1016/0304-3940(86)90373-3

Hemstrom, P. and K. Irgum (2006). Hydrophilic interaction chromatography. J Sep Sci 29(12): 1784-1821.

Henderson, B., Koepke, G. H., & Feller, I. (1971). Peripheral polyneuropathy among patients with burns. Arch Phys Med Rehabil, 52(4), 149-151.
Herndon, D. N., Barrow, R. E., Rutan, R. L., Rutan, T. C., Desai, M. H., & Abston, S. (1989). A comparison of conservative versus early excision. Therapies in severely burned patients. Ann Surg, 209. doi:10.1097/00000658-198905000-00006
Hettiaratchy, S., & Dziewulski, P. (2004). ABC of burns: pathophysiology and types of burns. BMJ, 328(7453), 1427-1429. doi:10.1136/bmj.328.7453.1427
Hettiaratchy, S., & Papini, R. (2004). Initial management of a major burn: II--assessment and resuscitation. BMJ, 329(7457), 101-103. doi:10.1136/bmj.329.7457.101
Hickling, K. G., Walsh, J., Henderson, S., & Jackson, R. (1994). Low Mortality-Rate in Adult-Respiratory-Distress-Syndrome Using Low-Volume, Pressure-Limited Ventilation with Permissive Hypercapnia - a Prospective-Study. Critical Care Medicine, 22(10), 1568-1578.
Hicks, G. A., Coldwell, J. R., Schindler, M., Ward, P. A., Jenkins, D., Lynn, P. A., . . . Blackshaw, L. A. (2002). Excitation of rat colonic afferent fibres by 5-HT(3) receptors. J Physiol, 544(Pt 3), 861-869.
Hill, R. (2000). NK1 (substance P) receptor antagonists--why are they not analgesic in humans? Trends Pharmacol Sci, 21(7), 244-246.
Hoesel, L. M., Mattar, A. F., Arbabi, S., Niederbichler, A. D., Ipaktchi, K., Su, G. L., Westfall, M. V., Wang, S. C., Hemmila, M. R. (2009). Local wound p38 MAPK inhibition attenuates burn-induced cardiac dysfunction. Surgery 146(4): 775-785; discussion 785-776.
Hoffmann, E. d., & Stroobant, V. (2003). Mass spectrometry : principles and applications. Chichester: John Wiley & Sons.
Hollis, E. R., 2nd, Ishiko, N., Tolentino, K., Doherty, E., Rodriguez, M. J., Calcutt, N. A., & Zou, Y. (2015). A novel and robust conditioning lesion induced by ethidium bromide. Exp Neurol, 265, 30-39. doi:10.1016/j.expneurol.2014.12.004
Holzer, P. (1988). Local effector functions of capsaicin-sensitive sensory nerve endings: involvement of tachykinins, calcitonin gene-related peptide and other neuropeptides. Neuroscience, 24(3), 739-768.
hoon Jung, J., Jeong, S.-J., Kim, J.-H., Lee, H.-J., Lee, H.-J., Lee, E.-O., . . . Kim, S.-H. (2012). Abstract 2015: Lysophosphatidylcholine induces apoptosis via suppressing STAT3 and HDAC3 activities and binding to the Bcl-x_L promoter in K562 chronic myelogenous leukemia cells. Cancer Research, 72(8 Supplement), 2015-2015. doi:10.1158/1538-7445.am2012-2015
Horakova, Z., & Beaven, M. A. (1974). Time course of histamine release and edema formation in the rat paw after thermal injury. European Journal of Pharmacology, 27(3), 305-312.
Horga de la Parte, J. F., & Horga, A. (2006). [Pregabalin: new therapeutic contributions of calcium channel alpha2delta protein ligands on epilepsy and neuropathic pain]. Rev Neurol, 42(4), 223-237.
Horton, J. W. (2003). Free radicals and lipid peroxidation mediated injury in burn trauma: the role of antioxidant therapy. Toxicology, 189(1-2), 75-88.
Hoskin, A. F. (2000). Trends in unintentional-injury deaths during the 20th century. Stat Bull Metrop Insur Co, 81(2), 18-26.
Hoult, D. I., Busby, S. J., Gadian, D. G., Radda, G. K., Richards, R. E., & Seeley, P. J. (1974). Observation of tissue metabolites using 31P nuclear magnetic resonance. Nature, 252(5481), 285-287.
Houssiau, F. A., Coulie, P. G., & Van Snick, J. (1989). Distinct roles of IL-1 and IL-6 in human T cell activation. J Immunol, 143(8), 2520-2524.
Howard, J. K., Lord, G. M., Matarese, G., Vendetti, S., Ghatei, M. A., Ritter, M. A., . . . Bloom, S. R. (1999). Leptin protects mice from starvation-induced lymphoid atrophy and increases thymic cellularity in ob/ob mice. Journal of Clinical Investigation, 104(8), 1051-1059. doi:10.1172/JCI6762
Hsieh, C. C., Yen, M. H., Liu, H. W., & Lau, Y. T. (2000). Lysophosphatidylcholine induces apoptotic and non-apoptotic death in vascular smooth muscle cells: in comparison with oxidized LDL. Atherosclerosis, 151(2), 481-491.
Hu, Q., Noll, R. J., Li, H., Makarov, A., Hardman, M., Graham Cooks, R. (2005). The Orbitrap: a new mass spectrometer. J Mass Spectrom 40(4): 430-443.
Huang, F., Subbaiah, P. V., Holian, O., Zhang, J., Johnson, A., Gertzberg, N., & Lum, H. (2005). Lysophosphatidylcholine increases endothelial permeability: role of PKCalpha and RhoA cross talk. Am J Physiol Lung Cell Mol Physiol, 289(2), L176-185. doi:10.1152/ajplung.00003.2005
Huang, J., Zhang, X., & McNaughton, P. A. (2006). Inflammatory Pain: The Cellular Basis of Heat Hyperalgesia. Curr Neuropharmacol, 4(3), 197-206.

Huang, S. H., Wu, S. H., Chang, K. P., Cheng, K. I., Lee, S. S., Kwan, A. L., . . . Lai, C. S. (2014). Autologous fat grafting alleviates burn-induced neuropathic pain in rats. Plast Reconstr Surg, 133(6), 1396-1405. doi:10.1097/PRS.0000000000000169

Huang, Y. H., Schafer-Elinder, L., Wu, R., Claesson, H. E., & Frostegard, J. (1999). Lysophosphatidylcholine (LPC) induces proinflammatory cytokines by a platelet-activating factor (PAF) receptor-dependent mechanism. Clin Exp Immunol, 116(2), 326-331.

Hultman, C. S., Napolitano, L. M., Cairns, B. A., Brady, L. A., Campbell, C., deSerres, S., & Meyer, A. A. (1995). The relationship between interferon-gamma and keratinocyte alloantigen expression after burn injury. Ann Surg, 222(3), 384-389; discussion 392-383.

Humphrey, J. H., & Jaques, R. (1955). The release of histamine and 5-hydroxytryptamine (serotonin) from platelets by antigen-antibody reactions (in vitro). J Physiol, 128(1), 9-27.

Hundhausen, C., Misztela, D., Berkhout, T. A., Broadway, N., Saftig, P., Reiss, K., . . . Ludwig, A. (2003). The disintegrin-like metalloproteinase ADAM10 is involved in constitutive cleavage of CX3CL1 (fractalkine) and regulates CX3CL1-mediated cell-cell adhesion. Blood, 102(4), 1186-1195. doi:10.1182/blood-2002-12-3775

Hundhausen, C., Schulte, A., Schulz, B., Andrzejewski, M. G., Schwarz, N., von Hundelshausen, P., . . . Ludwig, A. (2007). Regulated shedding of transmembrane chemokines by the disintegrin and metalloproteinase 10 facilitates detachment of adherent leukocytes. J Immunol, 178(12), 8064-8072.

Hunt, J. L. (2000). The 2000 Presidential Address - Back to the Future: The ABA and Burn Prevention. Journal of Burn Care & Rehabilitation, 21(6), 474-483. doi:DOI 10.1067/mbc.2000.1009667

Hunt, J. L., Arnoldo, B. D., Kowalske, K., Helm, P., & Purdue, G. F. (2006). Heterotopic ossification revisited: a 21-year surgical experience. J Burn Care Res, 27(4), 535-540. doi:10.1097/01.BCR.0000226023.58438.14

Hur, J., Yang, H. T., Chun, W., Kim, J. H., Shin, S. H., Kang, H. J., & Kim, H. S. (2015a). Inflammatory Cytokines and Their Prognostic Ability in Cases of Major Burn Injury. Annals of Laboratory Medicine, 35(1), 105-110. doi:10.3343/alm.2015.35.1.105

Hur, J., Yang, H. T., Chun, W., Kim, J. H., Shin, S. H., Kang, H. J., & Kim, H. S. (2015b). Inflammatory cytokines and their prognostic ability in cases of major burn injury. Annals of Laboratory Medicine, 35(1), 105-110. doi:10.3343/alm.2015.35.1.105

IASP. (2016). IASP Taxonomy. Retrieved from http://www.iasp-pain.org/Education/Content.aspx?ItemNumber=1698&&navItemNumber=576#Pain

Ikeda, H., Stark, J., Fischer, H., Wagner, M., Drdla, R., Jager, T., & Sandkuhler, J. (2006). Synaptic amplifier of inflammatory pain in the spinal dorsal horn. Science, 312(5780), 1659-1662. doi:10.1126/science.1127233

Ikejima, H., Imanishi, T., Tsujioka, H., Kashiwagi, M., Kuroi, A., Tanimoto, T., . . . Akasaka, T. (2010). Upregulation of Fractalkine and Its Receptor, CX3CR1, is Associated With Coronary Plaque Rupture in Patients With Unstable Angina Pectoris. Circulation Journal, 74(2), 337-345. doi:10.1253/circj.CJ-09-0484

Ilechukwu, S. T. (2002). Psychiatry of the medically ill in the burn unit. Psychiatr Clin North Am, 25(1), 129-147.

Imai, T., Hieshima, K., Haskell, C., Baba, M., Nagira, M., Nishimura, M., . . . Yoshie, O. (1997). Identification and molecular characterization of fractalkine receptor CX(3)CR1, which mediates both leukocyte migration and adhesion. Cell, 91(4), 521-530. doi:Doi 10.1016/S0092-8674(00)80438-9

Imperato, A., & Di Chiara, G. (1984). Trans-striatal dialysis coupled to reverse phase high performance liquid chromatography with electrochemical detection: a new method for the study of the in vivo release of endogenous dopamine and metabolites. J Neurosci, 4(4), 966-977.

Infanger, M., Schmidt, O., Kossmehl, P., Grad, S., Ertel, W., & Grimm, D. (2004). Vascular endothelial growth factor serum level is strongly enhanced after burn injury and correlated with local and general tissue edema. Burns, 30(4), 305-311. doi:10.1016/j.burns.2003.12.006

Ingber, A., Cohen, Y., Krimsky, M., & Yedgar, S. (2007). A novel treatment of contact dermatitis by topical application of phospholipase A2 inhibitor: a double-blind placebo-controlled pilot study. Int J Immunopathol Pharmacol, 20(1), 191-195.

Inose, Y., Kato, Y., Kitagawa, K., Uchiyama, S., & Shibata, N. (2015). Activated microglia in ischemic stroke penumbra upregulate MCP-1 and CCR2 expression in response to lysophosphatidylcholine derived from adjacent neurons and astrocytes. Neuropathology, 35(3), 209-223. doi:10.1111/neup.12182

Inoue, A., Hasegawa, H., Kohno, M., Ito, M. R., Terada, M., Imai, T., . . . Fujita, S. (2005). Antagonist of fractalkine (CX3CL1) delays the initiation and ameliorates the progression of lupus nephritis in MRL/lpr mice. Arthritis Rheum, 52(5), 1522-1533. doi:10.1002/art.21007

Inoue, H., Ando, K., Wakisaka, N., Matsuzaki, K., Aihara, M., & Kumagai, N. (2001). Effects of nitric oxide synthase inhibitors on vascular hyperpermeability with thermal injury in mice. Nitric Oxide, 5(4), 334-342. doi:10.1006/niox.2001.0350

Inoue, M., Xie, W., Matsushita, Y., Chun, J., Aoki, J., & Ueda, H. (2008). Lysophosphatidylcholine induces neuropathic pain through an action of autotaxin to generate lysophosphatidic acid. Neuroscience, 152(2), 296-298. doi:10.1016/j.neuroscience.2007.12.041

Inoue, N., Hirata, K., Yamada, M., Hamamori, Y., Matsuda, Y., Akita, H., & Yokoyama, M. (1992). Lysophosphatidylcholine inhibits bradykinin-induced phosphoinositide hydrolysis and calcium transients in cultured bovine aortic endothelial cells. Circ Res, 71(6), 1410-1421.

Ipaktchi, K., & Arbabi, S. (2006). Advances in burn critical care. Critical Care Medicine, 34(9 Suppl), S239-244. doi:10.1097/01.ccm.0000232625.63460.d4

Ipaktchi, K., Mattar, A., Niederbichler, A. D., Hoesel, L. M., Hemmila, M. R., Su, G. L., . . . Arbabi, S. (2006). Topical p38MAPK inhibition reduces dermal inflammation and epithelial apoptosis in burn wounds. Shock, 26(2), 201-209. doi:10.1097/01.shk.0000225739.13796.f2

Ipaktchi, K., Mattar, A., Niederbichler, A. D., Hoesel, L. M., Vollmannshauser, S., Hemmila, M. R., . . . Arbabi, S. (2006). Attenuating burn wound inflammatory signaling reduces systemic inflammation and acute lung injury. J Immunol, 177(11), 8065-8071.

Ishii, I., Fukushima, N., Ye, X., & Chun, J. (2004). Lysophospholipid receptors: signaling and biology. Annu Rev Biochem, 73, 321-354. doi:10.1146/annurev.biochem.73.011303.073731

Isik, S., Sahin, U., Ilgan, S., Guler, M., Gunalp, B., & Selmanpakoglu, N. (1998). Saving the zone of stasis in burns with recombinant tissue-type plasminogen activator (r-tPA): an experimental study in rats. Burns, 24(3), 217-223.

Islam, M. S., Morton, N. M., Hansson, A., & Emilsson, V. (1997). Rat insulinoma-derived pancreatic beta-cells express a functional leptin receptor that mediates a proliferative response. Biochem Biophys Res Commun, 238(3), 851-855. doi:10.1006/bbrc.1997.7399

Ito, M., Liu, Y., Yang, Z., Nguyen, J., Liang, F., Morris, R. J., & Cotsarelis, G. (2005). Stem cells in the hair follicle bulge contribute to wound repair but not to homeostasis of the epidermis. Nat Med, 11(12), 1351-1354. doi:http://www.nature.com/nm/journal/v11/n12/suppinfo/nm1328_S1.html

Iwamoto, T., Okamoto, H., Toyama, Y., & Momohara, S. (2008). Molecular aspects of rheumatoid arthritis: chemokines in the joints of patients. Febs Journal, 275(18), 4448-4455. doi:10.1111/j.1742-4658.2008.06580.x

Jaconello, P. (1992). Niacin versus niacinamide. CMAJ, 147(7), 990.

Jansson, J., Willing, B., Lucio, M., Fekete, A., Dicksved, J., Halfvarson, J., Tysk, C., Schmitt-Kopplin, P. (2009). Metabolomics reveals metabolic biomarkers of Crohn's disease. PLoS One 4(7): e6386.

Jara-Oseguera, A., Simon, S. A., & Rosenbaum, T. (2008). TRPV1: on the road to pain relief. Curr Mol Pharmacol, 1(3), 255-269.

Jaskille, A. D., Shupp, J. W., Pavlovich, A. R., Fidler, P., Jordan, M. H., & Jeng, J. C. (2009). Outcomes from burn injury-should decreasing mortality continue to be our compass? Clin Plast Surg, 36(4), 701-708. doi:10.1016/j.cps.2009.05.003

Jellish, W. S., Gamelli, R. L., Furry, P. A., McGill, V. L., & Fluder, E. M. (1999). Effect of topical local anesthetic application to skin harvest sites for pain management in burn patients undergoing skin-grafting procedures. Ann Surg, 229(1), 115-120.

Jellum, E. (1977). Profiling of human body fluids in healthy and diseased states using gas chromatography and mass spectrometry, with special reference to organic acids. J Chromatogr 143(5): 427-462.

Jensen, L. E. (2010). Targeting the IL-1 family members in skin inflammation. Curr Opin Investig Drugs, 11(11), 1211-1220.

Jeschke, M. G., Mlcak, R. P., Finnerty, C. C., Norbury, W. B., Gauglitz, G. G., Kulp, G. A., & Herndon, D. N. (2007). Burn size determines the inflammatory and hypermetabolic response. Crit Care, 11(4), R90. doi:10.1186/cc6102

Ji, R. R., Samad, T. A., Jin, S. X., Schmoll, R., & Woolf, C. J. (2002). p38 MAPK activation by NGF in primary sensory neurons after inflammation increases TRPV1 levels and maintains heat hyperalgesia. Neuron, 36(1), 57-68.

Jing, Q., Xin, S. M., Zhang, W. B., Wang, P., Qin, Y. W., & Pei, G. (2000). Lysophosphatidylcholine activates p38 and p42/44 mitogen-activated protein kinases in monocytic THP-1 cells, but only p38 activation is involved in its stimulated chemotaxis. Circ Res, 87(1), 52-59.

Johnson, C. H., Ivanisevic, J., & Siuzdak, G. (2016). Metabolomics: beyond biomarkers and towards mechanisms. Nat Rev Mol Cell Biol, 17(7), 451-459. doi:10.1038/nrm.2016.25

Jolliffe, I. T., & Cadima, J. (2016). Principal component analysis: a review and recent developments. Philosophical Transactions of the Royal Society A: Mathematical, Physical and Engineering Sciences, 374(2065).

Jones, B. A., Beamer, M., & Ahmed, S. (2010). Fractalkine/CX3CL1: A Potential New Target for Inflammatory Diseases. Mol Interv, 10(5), 263-270. doi:10.1124/mi.10.5.3

Jonsson, C. E., Holmsten, A., Dahlstrom, L., & Jonsson, K. (1998). Background pain in burn patients: routine measurement and recording of pain intensity in a burn unit. Burns, 24(5), 448-454.

Jonsson, P., Bruce, S. J., Moritz, T., Trygg, J., Sjöström, M., Plumb, R., Granger, J., Maibaum, E., Nicholson, J. K., Holmes, E., Antti, H. (2005). Extraction, interpretation and validation of information for comparing samples in metabolic LC/MS data sets. Analyst 130(5): 701-707.

Jordt, S. E., & Julius, D. (2002). Molecular basis for species-specific sensitivity to "hot" chili peppers. Cell, 108(3), 421-430.

Jordt, S. E., McKemy, D. D., & Julius, D. (2003). Lessons from peppers and peppermint: the molecular logic of thermosensation. Curr Opin Neurobiol, 13(4), 487-492.

Jordt, S. E., Tominaga, M., & Julius, D. (2000). Acid potentiation of the capsaicin receptor determined by a key extracellular site. Proc Natl Acad Sci U S A, 97(14), 8134-8139. doi:10.1073/pnas.100129497

Jung, J., Shin, J. S., Lee, S. Y., Hwang, S. W., Koo, J., Cho, H., & Oh, U. (2004). Phosphorylation of vanilloid receptor 1 by Ca2+/calmodulin-dependent kinase II regulates its vanilloid binding. Journal of Biological Chemistry, 279(8), 7048-7054. doi:10.1074/jbc.M311448200

Kajihara, Y., Murakami, M., Imagawa, T., Otsuguro, K., Ito, S., & Ohta, T. (2010). Histamine potentiates acid-induced responses mediating transient receptor potential V1 in mouse primary sensory neurons. Neuroscience, 166(1), 292-304. doi:10.1016/j.neuroscience.2009.12.001

Kakisaka, K., Cazanave, S. C., Fingas, C. D., Guicciardi, M. E., Bronk, S. F., Werneburg, N. W., . . . Gores, G. J. (2012). Mechanisms of lysophosphatidylcholine-induced hepatocyte lipoapoptosis. Am J Physiol Gastrointest Liver Physiol, 302(1), G77-84. doi:10.1152/ajpgi.00301.2011

Kalogeris, T., Baines, C. P., Krenz, M., & Korthuis, R. J. (2012). Cell biology of ischemia/reperfusion injury. Int Rev Cell Mol Biol, 298, 229-317. doi:10.1016/b978-0-12-394309-5.00006-7

Kandel, E. R., Schwartz, J. H., & Jessell, T. M. (2000). Principles of neural science. New York: McGraw-Hill, Health Professions Division.

Kanehisa, M., Furumichi, M., Tanabe, M., Sato, Y., Morishima, K. (2017). KEGG: new perspectives on genomes, pathways, diseases and drugs. Nucleic Acids Res 45(D1): D353-d361.

Kao, C. Y., Anderzhanova, E., Asara, J. M., Wotjak, C. T., & Turck, C. W. (2015). NextGen Brain Microdialysis: Applying Modern Metabolomics Technology to the Analysis of Extracellular Fluid in the Central Nervous System. Mol Neuropsychiatry, 1(1), 60-67. doi:10.1159/000381855

Katajamaa, M. and M. Oresic (2005). Processing methods for differential analysis of LC/MS profile data. BMC Bioinformatics 6: 179.

Katz, A. M., & Messineo, F. C. (1981). Lipid-membrane interactions and the pathogenesis of ischemic damage in the myocardium. Circ Res, 48(1), 1-16.

Kaufman, T., Neuman, R. A., & Weinberg, A. (1989). Is postburn dermal ischaemia enhanced by oxygen free radicals? Burns, 15(5), 291-294.

Kawasaki, Y., Kohno, T., Zhuang, Z. Y., Brenner, G. J., Wang, H., Van Der Meer, C., . . . Ji, R. R. (2004). Ionotropic and metabotropic receptors, protein kinase A, protein kinase C, and Src contribute to C-fiber-induced ERK activation and cAMP response element-binding protein phosphorylation in dorsal horn neurons, leading to central sensitization. J Neurosci, 24(38), 8310-8321. doi:10.1523/jneurosci.2396-04.2004

Kealey, G. P. (1995). Pharmacologic management of background pain in burn victims. J Burn Care Rehabil, 16(3 Pt 2), 358-362.

Keene, O. N. (1995). The log transformation is special. Stat Med, 14(8), 811-819.

Keller, A. F., Beggs, S., Salter, M. W., & De Koninck, Y. (2007). Transformation of the output of spinal lamina I neurons after nerve injury and microglia stimulation underlying neuropathic pain. Mol Pain, 3, 27. doi:10.1186/1744-8069-3-27

Kelly, J. L., Lyons, A., Soberg, C. C., Mannick, J. A., & Lederer, J. A. (1997). Anti-interleukin-10 antibody restores burn-induced defects in T-cell function. Surgery, 122(2), 146-152.

Kelly, J. L., O'Suilleabhain, C. B., Soberg, C. C., Mannick, J. A., & Lederer, J. A. (1999). Severe injury triggers antigen-specific T-helper cell dysfunction. Shock, 12(1), 39-45.

Kelly, S., Chapman, R. J., Woodhams, S., Sagar, D. R., Turner, J., Burston, J. J., . . . Chapman, V. (2015). Increased function of pronociceptive TRPV1 at the level of the joint in a rat model of osteoarthritis pain. Ann Rheum Dis, 74(1), 252-259. doi:10.1136/annrheumdis-2013-203413

Kessler, F., Habelt, C., Averbeck, B., Reeh, P. W., & Kress, M. (1999). Heat-induced release of CGRP from isolated rat skin and effects of bradykinin and the protein kinase C activator PMA. Pain, 83(2), 289-295. doi:Doi 10.1016/S0304-3959(99)00108-6

Keun, H. C., & Athersuch, T. J. (2011). Nuclear magnetic resonance (NMR)-based metabolomics. Methods Mol Biol, 708, 321-334. doi:10.1007/978-1-61737-985-7_19

Khanolkar-Young, S., Rayment, N., Brickell, P. M., Katz, D. R., Vinayakumar, S., Colston, M. J., & Lockwood, D. N. (1995). Tumour necrosis factor-alpha (TNF-alpha) synthesis is associated with the skin and peripheral nerve pathology of leprosy reversal reactions. Clin Exp Immunol, 99(2), 196-202.

Khoo, S. H. and M. Al-Rubeai (2007). Metabolomics as a complementary tool in cell culture. Biotechnol Appl Biochem 47(Pt 2): 71-84.

Kim, D., Pertea, G., Trapnell, C., Pimentel, H., Kelley, R., & Salzberg, S. L. (2013). TopHat2: accurate alignment of transcriptomes in the presence of insertions, deletions and gene fusions. Genome Biol, 14(4), R36. doi:10.1186/gb-2013-14-4-r36

Kimouli, M., Miyakis, S., Georgakopoulos, P., Achimastos, A. D., Neofytou, E. N., & Spandidos, D. A. (2009). Polymorphisms of Fractalkine Receptor CX3CR1 gene in patients with symptomatic and asymptomatic carotid artery stenosis. International Journal of Molecular Medicine, 24, S70-S70.

King, B. F., Wildman, S. S., Ziganshina, L. E., Pintor, J., & Burnstock, G. (1997). Effects of extracellular pH on agonism and antagonism at a recombinant P2X2 receptor. Br J Pharmacol, 121(7), 1445-1453. doi:10.1038/sj.bjp.0701286

Kino, Y., Kato, M., Ikehara, Y., Asanuma, Y., Akashi, K., & Kawai, S. (2003). Plasma leptin levels in patients with burn injury: a preliminary report. Burns, 29(5), 449-453. doi:10.1016/S0305-4179(03)00062-7

Kinoshita, M., Miyazaki, H., Ono, S., Inatsu, A., Nakashima, H., Tsujimoto, H., . . . Seki, S. (2011). Enhancement of neutrophil function by interleukin-18 therapy protects burn-injured mice from methicillin-resistant Staphylococcus aureus. Infect Immun, 79(7), 2670-2680. doi:10.1128/IAI.01298-10

Kinoshita, M., Seki, S., Ono, S., Shinomiya, N., & Hiraide, H. (2004). Paradoxical effect of IL-18 therapy on the severe and mild Escherichia coli infections in burn-injured mice. Ann Surg, 240(2), 313-320.

Kirschstein, T., Busselberg, D., & Treede, R. D. (1997). Coexpression of heat-evoked and capsaicin-evoked inward currents in acutely dissociated rat dorsal root ganglion neurons. Neuroscience Letters, 231(1), 33-36.

Kishimoto, T., Taga, T., & Akira, S. (1994). Cytokine signal transduction. Cell, 76(2), 253-262. doi:10.1016/0092-8674(94)90333-6

Kiyatkin, M. E., Feng, B., Schwartz, E. S., & Gebhart, G. F. (2013). Combined genetic and pharmacological inhibition of TRPV1 and P2X3 attenuates colorectal hypersensitivity and afferent sensitization. Am J Physiol Gastrointest Liver Physiol, 305(9), G638-648. doi:10.1152/ajpgi.00180.2013

Kleinman, Y., Krul, E. S., Burnes, M., Aronson, W., Pfleger, B., & Schonfeld, G. (1988). Lipolysis of LDL with phospholipase A2 alters the expression of selected apoB-100 epitopes and the interaction of LDL with cells. J Lipid Res, 29(6), 729-743.

Knabl, J. S., Bauer, W., Andel, H., Schwendenwein, I., Dado, P. F., Mittlbock, M., . . . Frey, M. (1999). Progression of burn wound depth by systemical application of a vasoconstrictor: an experimental study with a new rabbit model. Burns, 25(8), 715-721.

Knowlden, S., & Georas, S. N. (2014). The autotaxin-LPA axis emerges as a novel regulator of lymphocyte homing and inflammation. J Immunol, 192(3), 851-857. doi:10.4049/jimmunol.1302831

Koch, A. E. (2005). Chemokines and Their Receptors in Rheumatoid Arthritis Future Targets? Arthritis and Rheumatism, 52(3), 710-721. doi:10.1002/art.20932

Kohno, M., Yasunari, K., Maeda, K., Kano, H., Minami, M., Hanehira, T., & Yoshikawa, J. (2000). Effects of cardiac natriuretic peptides on oxidized low-density lipoprotein- and lysophosphatidylcholine-induced human mesangial cell migration. Hypertension, 35(4), 971-977.

Kopka, J. (2006). Gas Chromatography Mass Spectrometry. Plant Metabolomics. K. Saito, R. A. Dixon and L. Willmitzer. Berlin, Heidelberg, Springer Berlin Heidelberg: 3-20.

Koplas, P. A., Rosenberg, R. L., & Oxford, G. S. (1997). The role of calcium in the desensitization of capsaicin responses in rat dorsal root ganglion neurons. J Neurosci, 17(10), 3525-3537.

Kougias, P., Chai, H., Lin, P. H., Lumsden, A. B., Yao, Q., & Chen, C. (2006). Lysophosphatidylcholine and secretory phospholipase A2 in vascular disease: mediators of endothelial dysfunction and atherosclerosis. Med Sci Monit, 12(1), Ra5-16.

Kovacs, E. J. (1991). Fibrogenic cytokines: the role of immune mediators in the development of scar tissue. Immunol Today, 12(1), 17-23. doi:10.1016/0167-5699(91)90107-5

Kowal-Vern, A., Walenga, J. M., Hoppensteadt, D., Sharp-Pucci, M., & Gamelli, R. L. (1994). Interleukin-2 and interleukin-6 in relation to burn wound size in the acute phase of thermal injury. J Am Coll Surg, 178(4), 357-362.

Kraft, R., Herndon, D. N., Finnerty, C. C., Cox, R. A., Song, J., & Jeschke, M. G. (2014). Predictive Value of IL-8 for Sepsis and Severe Infections After Burn Injury - A Clinical Study. Shock. doi:10.1097/SHK.0000000000000294

Kraut, J. A., & Madias, N. E. (2014). Lactic Acidosis. New England Journal of Medicine, 371(24), 2309-2319. doi:10.1056/NEJMra1309483

Kremer, T., Abe, D., Weihrauch, M., Peters, C., Gebhardt, M. M., Germann, G., . . . Walther, A. (2008). Burn plasma transfer induces burn edema in healthy rats. Shock, 30(4), 394-400. doi:10.1097/SHK.0b013e3181673908

Kritharides, L., Jessup, W., Mander, E. L., & Dean, R. T. (1995). Apolipoprotein A-I-mediated efflux of sterols from oxidized LDL-loaded macrophages. Arterioscler Thromb Vasc Biol, 15(2), 276-289.

Krone, N., Hughes, B. A., Lavery, G. G., Stewart, P. M., Arlt, W., & Shackleton, C. H. L. (2010). Gas chromatography/mass spectrometry (GC/MS) remains a pre-eminent discovery tool in clinical steroid investigations even in the era of fast liquid chromatography tandem mass spectrometry (LC/MS/MS)(). J Steroid Biochem Mol Biol, 121(3-5), 496-504. doi:10.1016/j.jsbmb.2010.04.010

Kruczek, C., Kottapalli, K. R., Dissanaike, S., Dzvova, N., Griswold, J. A., Colmer-Hamood, J. A., & Hamood, A. N. (2016). Major Transcriptome Changes Accompany the Growth of Pseudomonas aeruginosa in Blood from Patients with Severe Thermal Injuries. PLoS One, 11(3), e0149229. doi:10.1371/journal.pone.0149229

Kugiyama, K., Sakamoto, T., Misumi, I., Sugiyama, S., Ohgushi, M., Ogawa, H., . . . Yasue, H. (1993). Transferable lipids in oxidized low-density lipoprotein stimulate plasminogen activator inhibitor-1 and inhibit tissue-type plasminogen activator release from endothelial cells. Circ Res, 73(2), 335-343.

Kuhn, D. C., & Willis, A. L. (1973). Proceedings: Prostaglandin E2, inflammation and pain threshold in rat paws. Br J Pharmacol, 49(1), 183p-184p.

Kumar, V., Abbas, A. K., Fausto, N., Robbins, S. L., & Cotran, R. S. (2005). Robbins and Cotran pathologic basis of disease. Philadelphia: Elsevier Saunders.

Kumazawa, T., Mizumura, K., Koda, H., & Fukusako, H. (1996). EP receptor subtypes implicated in the PGE2-induced sensitization of polymodal receptors in response to bradykinin and heat. Journal of Neurophysiology, 75(6), 2361-2368.

Kung, C. (2005). A possible unifying principle for mechanosensation. Nature 436(7051): 647-654.

Kushnir-Sukhov, N. M., Brown, J. M., Wu, Y., Kirshenbaum, A., & Metcalfe, D. D. (2007). Human mast cells are capable of serotonin synthesis and release. J Allergy Clin Immunol, 119(2), 498-499. doi:10.1016/j.jaci.2006.09.003

Kwak, J., Wang, M. H., Hwang, S. W., Kim, T. Y., Lee, S. Y., & Oh, U. (2000). Intracellular ATP increases capsaicin-activated channel activity by interacting with nucleotide-binding domains. J Neurosci, 20(22), 8298-8304.

Lacroix-Fralish, M. L., & Mogil, J. S. (2009). Progress in genetic studies of pain and analgesia. Annu Rev Pharmacol Toxicol, 49, 97-121. doi:10.1146/annurev-pharmtox-061008-103222

Lange, E., Tautenhahn, R., Neumann, S., Gröpl, C. (2008). Critical assessment of alignment procedures for LC-MS proteomics and metabolomics measurements. BMC Bioinformatics 9: 375.

Lanza, I. R., Zhang, S., Ward, L. E., Karakelides, H., Raftery, D., & Nair, K. S. (2010). Quantitative Metabolomics by (1)H-NMR and LC-MS/MS Confirms Altered Metabolic Pathways in Diabetes. PLoS One, 5(5). doi:10.1371/journal.pone.0010538

Lappas, M., & Permezel, M. (2011). The anti-inflammatory and antioxidative effects of nicotinamide, a vitamin B(3) derivative, are elicited by FoxO3 in human gestational tissues: implications for preterm birth. J Nutr Biochem, 22(12), 1195-1201. doi:10.1016/j.jnutbio.2010.10.009

Lapsia, V., Johnson, R. J., Dass, B., Shimada, M., Kambhampati, G., Ejaz, N. I., . . . Ejaz, A. A. (2012). Elevated uric acid increases the risk for acute kidney injury. Am J Med, 125(3), 302.e309-317. doi:10.1016/j.amjmed.2011.06.021

Latenser, B. A. (2009). Critical care of the burn patient: the first 48 hours. Critical Care Medicine, 37(10), 2819-2826. doi:10.1097/CCM.0b013e3181b3a08f

Latha, B., & Babu, M. (2001). The involvement of free radicals in burn injury: a review. Burns, 27(4), 309-317.

Latorre, R., Brauchi, S., Orta, G., Zaelzer, C., & Vargas, G. (2007). ThermoTRP channels as modular proteins with allosteric gating. Cell Calcium, 42(4-5), 427-438. doi:10.1016/j.ceca.2007.04.004

Latremoliere, A., & Woolf, C. J. (2009). Central Sensitization: A Generator of Pain Hypersensitivity by Central Neural Plasticity. J Pain, 10(9), 895-926. doi:10.1016/j.jpain.2009.06.012

Lauterbach, M., O'Donnell, P., Asano, K., & Mayadas, T. N. (2008). Role of TNF priming and adhesion molecules in neutrophil recruitment to intravascular immune complexes. J Leukoc Biol, 83(6), 1423-1430. doi:10.1189/jlb.0607421

Lawrence, J. W., Fauerbach, J. A., & Thombs, B. D. (2006). A test of the moderating role of importance of appearance in the relationship between perceived scar severity and body-esteem among adult burn survivors. Body Image, 3(2), 101-111. doi:10.1016/j.bodyim.2006.01.003

Leblebici, B., Adam, M., Bagis, S., Tarim, A. M., Noyan, T., Akman, M. N., & Haberal, M. A. (2006). Quality of life after burn injury: the impact of joint contracture. J Burn Care Res, 27(6), 864-868. doi:10.1097/01.BCR.0000245652.26648.36

Lederer, J. A., Rodrick, M. L., & Mannick, J. A. (1999). The effects of injury on the adaptive immune response. Shock, 11(3), 153-159.

Lee, A. S., Jung, Y. J., Kim, D. H., Lee, T. H., Kang, K. P., Lee, S., . . . Kim, W. (2009). Epigallocatechin-3-O-gallate decreases tumor necrosis factor-alpha-induced fractalkine expression in endothelial cells by suppressing NF-kappaB. Cell Physiol Biochem, 24(5-6), 503-510. doi:10.1159/000257494

Lee, M. Y., Liu, G., Kowlowitz, V., Hwang, J. H., Lee, J. H., Choi, K. H., & Lee, E. S. (2009). Causative factors affecting peripheral neuropathy in burn patients. Burns, 35(3), 412-416. doi:DOI 10.1016/j.burns.2008.08.009

Lee, S. H., Williams, M. V., DuBois, R. N., Blair, I. A. (2003). Targeted lipidomics using electron capture atmospheric pressure chemical ionization mass spectrometry. Rapid Commun Mass Spectrom 17(19): 2168-2176.

Lee, Y. S., Yang, J. H., Choi, J. C., & Eun, H. C. (2005). Age-dependent change of uric acid level in the dermis using cutaneous microdialysis. Gerontology, 51(4), 231-233. doi:10.1159/000085119

Leffler, A., Linte, R. M., Nau, C., Reeh, P., & Babes, A. (2007). A high-threshold heat-activated channel in cultured rat dorsal root ganglion neurons resembles TRPV2 and is blocked by gadolinium. European Journal of Neuroscience, 26(1), 12-22. doi:10.1111/j.1460-9568.2007.05643.x

Lenth, R. V. (2001). Some Practical Guidelines for Effective Sample Size Determination. The American Statistician 55(3): 187-193.

Lenz, E. M., Bright, J., Knight, R., Wilson, I. D., Major, H. (2004). A metabonomic investigation of the biochemical effects of mercuric chloride in the rat using 1H NMR and HPLC-TOF/MS: time dependent changes in the urinary profile of endogenous metabolites as a result of nephrotoxicity. Analyst 129(6): 535-541.

Lenz, E. M., Wilson, I. D. (2007). Analytical strategies in metabonomics. J Proteome Res 6(2): 443-458.

Lesnik, P., Charo, I., & Haskell, C. A. (2002). Decreased atherosclerosis in CX3CR1(-/-) mice reveals a role for fractalkine in atherogenesis. Circulation, 106(19), 217-217.

Lewin, G. R., Ritter, A. M., & Mendell, L. M. (1993). Nerve growth factor-induced hyperalgesia in the neonatal and adult rat. J Neurosci, 13(5), 2136-2148.

Li, X. H., Long, D. X., Li, W., & Wu, Y. J. (2007). Different mechanisms of lysophosphatidylcholine-induced Ca(2+) mobilization in N2a mouse and SH-SY5Y human neuroblastoma cells. Neuroscience Letters, 424(1), 22-26. doi:10.1016/j.neulet.2007.07.020

Li, Y. F., Xin, F., & Altman, R. B. (2016). Separating the causes and consequences in disease transcriptome. Pac Symp Biocomput, 21, 381-392.

Li, Z., Song, T., Liu, G. Z., & Liu, L. Y. (2006). Inhibitory effects of cariporide on LPC-induced expression of ICAM-1 and adhesion of monocytes to smooth muscle cells in vitro. Acta Pharmacol Sin, 27(10), 1326-1332. doi:10.1111/j.1745-7254.2006.00412.x

Liang, J., Zhang, P., Hu, X., & Zhi, L. (2015). Elevated serum uric acid after injury correlates with the early acute kidney in severe burns. Burns, 41(8), 1724-1731. doi:10.1016/j.burns.2015.09.001

Liapaki, I., Anagnostoulis, S., Karayiannakis, A., Korkolis, D., Labropoulou, M., Matarasso, A., & Simopoulos, C. (2008). Burn wound angiogenesis is increased by exogenously administered recombinant leptin in rats. Acta Cirurgica Brasileira, 23(2), 118-124. doi:Doi 10.1590/S0102-86502008000200002

Libert, C., Brouckaert, P., Shaw, A., & Fiers, W. (1990). Induction of interleukin 6 by human and murine recombinant interleukin 1 in mice. Eur J Immunol, 20(3), 691-694. doi:10.1002/eji.1830200333

Liebisch, G., Drobnik, W., Lieser, B., & Schmitz, G. (2002). High-throughput quantification of lysophosphatidylcholine by electrospray ionization tandem mass spectrometry. Clin Chem, 48(12), 2217-2224.

Liffner, G., Bak, Z., Reske, A., & Sjoberg, F. (2005). Inhalation injury assessed by score does not contribute to the development of acute respiratory distress syndrome in burn victims. Burns, 31(3), 263-268. doi:10.1016/j.burns.2004.11.003

Lim, G., Wang, S. X., Zhang, Y., Tian, Y. H., & Mao, J. R. (2009). Spinal leptin contributes to the pathogenesis of neuropathic pain in rodents. Journal of Clinical Investigation, 119(2), 295-304. doi:10.1172/JCI36785

Lin, P., Welch, E. J., Gao, X. P., Malik, A. B., & Ye, R. D. (2005). Lysophosphatidylcholine modulates neutrophil oxidant production through elevation of cyclic AMP. J Immunol, 174(5), 2981-2989.

Lindon, J. C., Holmes, E., Nicholson, J. K. (2001). Pattern recognition methods and applications in biomedical magnetic resonance. Prog Nucl Magn Reson Spectrosc. 39(1), 1-40

Lipnik-Stangelj, M. (2006). Multiple role of histamine H1-receptor-PKC-MAPK signalling pathway in histamine-stimulated nerve growth factor synthesis and secretion. Biochem Pharmacol, 72(11), 1375-1381. doi:10.1016/j.bcp.2006.06.028

Lippi, G., Ippolito, L., & Cervellin, G. (2010). Disseminated intravascular coagulation in burn injury. Semin Thromb Hemost, 36(4), 429-436. doi:10.1055/s-0030-1254051

Lishko, P. V., Procko, E., Jin, X., Phelps, C. B., & Gaudet, R. (2007). The ankyrin repeats of TRPV1 bind multiple ligands and modulate channel sensitivity. Neuron, 54(6), 905-918. doi:10.1016/j.neuron.2007.05.027

Liu-Wu, Y., Hurt-Camejo, E., & Wiklund, O. (1998). Lysophosphatidylcholine induces the production of IL-1beta by human monocytes. Atherosclerosis, 137(2), 351-357.

Liu, B., & Qin, F. (2005). Functional control of cold- and menthol-sensitive TRPM8 ion channels by phosphatidylinositol 4,5-bisphosphate. J Neurosci, 25(7), 1674-1681. doi:10.1523/jneurosci.3632-04.2005

Liu, D., & Liman, E. R. (2003). Intracellular Ca2+ and the phospholipid PIP2 regulate the taste transduction ion channel TRPM5. Proc Natl Acad Sci U S A, 100(25), 15160-15165. doi:10.1073/pnas.2334159100

Liu, E., Goldhaber, J. I., & Weiss, J. N. (1991). Effects of lysophosphatidylcholine on electrophysiological properties and excitation-contraction coupling in isolated guinea pig ventricular myocytes. Journal of Clinical Investigation, 88(6), 1819-1832. doi:10.1172/jci115503

Liu, G., Wang, Y., Wang, Z., Cai, J., Lv, X., & Zhou, A. (2011). Nuclear magnetic resonance (NMR)-based metabolomic studies on urine and serum biochemical profiles after chronic cysteamine supplementation in rats. J Agric Food Chem, 59(10), 5572-5578. doi:10.1021/jf104129k

Liu, L., & Simon, S. A. (1996). Capsaicin-induced currents with distinct desensitization and Ca2+ dependence in rat trigeminal ganglion cells. Journal of Neurophysiology, 75(4), 1503-1514.

Liu, M. L., Huang, Z. Y., Zhong, X. C., Liu, S. H., Xu, G., Jiang, T. Y., . . . Yan, W. Q. (2009). Th1 polarization and low-T3 syndrome are correlated with hyperleptinemia in hemodialysis patients. Journal of Nephrology, 22(4), 515-522.

Liu, X. R., Zheng, X. F., Ji, S. Z., Lv, Y. H., Zheng, D. Y., Xia, Z. F., & Zhang, W. D. (2010). Metabolomic analysis of thermally injured and/or septic rats. Burns, 36(7), 992-998. doi:10.1016/j.burns.2010.03.015

Liu, X. S., Luo, Z. H., Yang, Z. C., Huang, W. H., & Li, A. (1994). The significance of changes in serum tumour necrosis factor (TNF) activity in severely burned patients. Burns, 20(1), 40-44. doi:http://dx.doi.org/10.1016/0305-4179(94)90104-X

Liu, Y., Casey, L., & Pike, L. J. (1998). Compartmentalization of phosphatidylinositol 4,5-bisphosphate in low-density membrane domains in the absence of caveolin. Biochem Biophys Res Commun, 245(3), 684-690. doi:10.1006/bbrc.1998.8329

Locksley, R. M., Killeen, N., & Lenardo, M. J. (2001). The TNF and TNF receptor superfamilies: integrating mammalian biology. Cell, 104(4), 487-501.

Loffreda, S., Yang, S. Q., Lin, H. Z., Karp, C. L., Brengman, M. L., Wang, D. J., . . . Diehl, A. M. (1998). Leptin regulates proinflammatory immune responses. Faseb Journal, 12(1), 57-65.

Long, T. D., Cathers, T. A., Twillman, R., O'Donnell, T., Garrigues, N., & Jones, T. (2001). Morphine-Infused silver sulfadiazine (MISS) cream for burn analgesia: a pilot study. J Burn Care Rehabil, 22(2), 118-123.

Lonnroth, P., Jansson, P. A., & Smith, U. (1987). A microdialysis method allowing characterization of intercellular water space in humans. Am J Physiol, 253(2 Pt 1), E228-231.

Loose, L. D., Megirian, R., & Turinsky, J. (1984). Biochemical and functional alterations in macrophages after thermal injury. Infect Immun, 44(3), 554-558.

Lord, G. M., Matarese, G., Howard, J. K., Baker, R. J., Bloom, S. R., & Lechler, R. I. (1998). Leptin modulates the T-cell immune response and reverses starvation-induced immunosuppression. Nature, 394(6696), 897-901. doi:10.1038/29795

Loyd, D. R., Weiss, G., Henry, M. A., & Hargreaves, K. M. (2011). Serotonin increases the functional activity of capsaicin-sensitive rat trigeminal nociceptors via peripheral serotonin receptors. Pain, 152(10), 2267-2276. doi:10.1016/j.pain.2011.06.002

Lu, W., Bennett, B. D., Rabinowitz, J. D. (2008). Analytical strategies for LC-MS-based targeted metabolomics. J Chromatogr B Analyt Technol Biomed Life Sci 871(2): 236-242.

Lucas, A. D., Bursill, C., Guzik, T. J., Sadowski, J., Channon, K. M., & Greaves, D. R. (2003). Smooth muscle cells in human atherosclerotic plaques express the fractalkine receptor CX(3)CR1 and undergo chemotaxis to the CX3C chemokine fractalkine (CX3CL1). Circulation, 108(20), 2498-2504. doi:10.1161/01.Cir.0000097119.57756.Ef

Ludwig, A., Dietel, M., Schafer, G., Muller, K., & Hilz, H. (1990). Nicotinamide and nicotinamide analogues as antitumor promoters in mouse skin. Cancer Research, 50(8), 2470-2475.

Lumpkin, E. A., & Caterina, M. J. (2007). Mechanisms of sensory transduction in the skin. Nature, 445(7130), 858-865.

Lund, T., Onarheim, H., & Reed, R. K. (1992). Pathogenesis of edema formation in burn injuries. World J Surg, 16(1), 2-9.

Lundbaek, J. A., & Andersen, O. S. (1994). Lysophospholipids modulate channel function by altering the mechanical properties of lipid bilayers. J Gen Physiol, 104(4), 645-673. doi:10.1085/jgp.104.4.645

Lundbaek, J. A., Birn, P., Tape, S. E., Toombes, G. E., Sogaard, R., Koeppe, R. E., 2nd, . . . Andersen, O. S. (2005). Capsaicin regulates voltage-dependent sodium channels by altering lipid bilayer elasticity. Mol Pharmacol, 68(3), 680-689. doi:10.1124/mol.105.013573

Ma, W. (2010). Chronic prostaglandin E2 treatment induces the synthesis of the pain-related peptide substance P and calcitonin gene-related peptide in cultured sensory ganglion explants. Journal of Neurochemistry, 115(2), 363-372. doi:10.1111/j.1471-4159.2010.06927.x

Maass, D. L., White, J., & Horton, J. W. (2002). IL-1beta and IL-6 act synergistically with TNF-alpha to alter cardiac contractile function after burn trauma. Shock, 18(4), 360-366.

Machens, H. G., Pabst, A., Dreyer, M., Gliemroth, J., Gorg, S., Bahlmann, L., . . . Mailander, P. (2006). C3a levels and occurrence of subdermal vascular thrombosis are age-related in deep second-degree burn wounds. Surgery, 139(4), 550-555. doi:10.1016/j.surg.2005.09.001

MacMicking, J., Xie, Q. W., & Nathan, C. (1997). Nitric oxide and macrophage function. Annu Rev Immunol, 15, 323-350. doi:10.1146/annurev.immunol.15.1.323

Madianos, M. G., Papaghelis, M., Ioannovich, J., & Dafni, R. (2001). Psychiatric disorders in burn patients: a follow-up study. Psychother Psychosom, 70(1), 30-37. doi:56222

Maeda, T., Kiguchi, N., Kobayashi, Y., Ikuta, T., Ozaki, M., & Kishioka, S. (2009). Leptin derived from adipocytes in injured peripheral nerves facilitates development of neuropathic pain via macrophage stimulation. Proc Natl Acad Sci U S A, 106(31), 13076-13081. doi:10.1073/pnas.0903524106

Magalhaes, K., Almeida, P. E., Atella, G., Maya-Monteiro, C. M., Castro-Faria-Neto, H., Pelajo-Machado, M., . . . Bozza, P. T. (2010). Schistosomal-derived lysophosphatidylcholine are involved in eosinophil activation and recruitment through Toll-like receptor-2-dependent mechanisms. J Infect Dis, 202(9), 1369-1379. doi:10.1086/656477

Maggi, C. A., & Meli, A. (1986a). Suitability of urethane anesthesia for physiopharmacological investigations in various systems. Part 2: Cardiovascular system. Experientia, 42(3), 292-297.

Maggi, C. A., & Meli, A. (1986b). Suitability of urethane anesthesia for physiopharmacological investigations. Part 3: Other systems and conclusions. Experientia, 42(5), 531-537.

Mahajan, A. L., Tenorio, X., Pepper, M. S., Baetens, D., Montandon, D., Schlaudraff, K. U., & Pittet, B. (2006). Progressive tissue injury in burns is reduced by rNAPc2. Burns, 32(8), 957-963. doi:10.1016/j.burns.2006.02.010

Maier, T., Güell, M., Serrano, L. (2009). Correlation of mRNA and protein in complex biological samples. FEBS Lett 583(24): 3966-3973.

Maingret, F., Lauritzen, I., Patel, A. J., Heurteaux, C., Reyes, R., Lesage, F., . . . Honore, E. (2000). TREK-1 is a heat-activated background K(+) channel. EMBO J, 19(11), 2483-2491. doi:10.1093/emboj/19.11.2483

Maingret, F., Patel, A. J., Lesage, F., Lazdunski, M., & Honoré, E. (2000). Lysophospholipids Open the Two-pore Domain Mechano-gated K+ Channels TREK-1 and TRAAK. Journal of Biological Chemistry, 275(14), 10128-10133.

Maingrette, F., & Renier, G. (2003). Leptin increases lipoprotein lipase secretion by macrophages: involvement of oxidative stress and protein kinase C. Diabetes, 52(8), 2121-2128.

Malan, T. P., Mata, H. P., & Porreca, F. (2002). Spinal GABA(A) and GABA(B) receptor pharmacology in a rat model of neuropathic pain. Anesthesiology, 96(5), 1161-1167.

Malek, N., Pajak, A., Kolosowska, N., Kucharczyk, M., & Starowicz, K. (2015). The importance of TRPV1-sensitisation factors for the development of neuropathic pain. Mol Cell Neurosci, 65, 1-10. doi:10.1016/j.mcn.2015.02.001

Malenfant, A., Forget, R., Amsel, R., Papillon, J., Frigon, J. Y., & Choiniere, M. (1998). Tactile, thermal and pain sensibility in burned patients with and without chronic pain and paresthesia problems. Pain, 77(3), 241-251.

Malenfant, A., Forget, R., Papillon, J., Amsel, R., Frigon, J. Y., & Choiniere, M. (1996). Prevalence and characteristics of chronic sensory problems in burn patients. Pain, 67(2-3), 493-500.

Malin, S. A., Davis, B. M., & Molliver, D. C. (2007). Production of dissociated sensory neuron cultures and considerations for their use in studying neuronal function and plasticity. Nat Protoc, 2(1), 152-160. doi:10.1038/nprot.2006.461

Malorni, W., Paradisi, S., Iosi, F., & Santini, M. T. (1993). Two different pathways for necrotic cell death induced by free radicals. Cell Biol Toxicol, 9(2), 119-130.

Mamet, J., Lazdunski, M., & Voilley, N. (2003). How nerve growth factor drives physiological and inflammatory expressions of acid-sensing ion channel 3 in sensory neurons. Journal of Biological Chemistry, 278(49), 48907-48913. doi:10.1074/jbc.M309468200

Mandadi, S., Numazaki, M., Tominaga, M., Bhat, M. B., Armati, P. J., & Roufogalis, B. D. (2004). Activation of protein kinase C reverses capsaicin-induced calcium-dependent desensitization of TRPV1 ion channels. Cell Calcium, 35(5), 471-478. doi:10.1016/j.ceca.2003.11.003

Mandadi, S., & Roufogalis, B. D. (2008). ThermoTRP channels in nociceptors: taking a lead from capsaicin receptor TRPV1. Curr Neuropharmacol, 6(1), 21-38. doi:10.2174/157015908783769680

Mannaioni, P. F., Di Bello, M. G., & Masini, E. (1997). Platelets and inflammation: role of platelet-derived growth factor, adhesion molecules and histamine. Inflamm Res, 46(1), 4-18. doi:10.1007/pl00000158

Marano, M. A., Moldawer, L. L., Fong, Y., Wei, H., Minei, J., Yurt, R., . . . Lowry, S. F. (1988). Cachectin/TNF production in experimental burns and Pseudomonas infection. Arch Surg, 123(11), 1383-1388.

Marceau, F., Hess, J. F., & Bachvarov, D. R. (1998). The B1 receptors for kinins. Pharmacol Rev, 50(3), 357-386.

March, R. E. (1997). An Introduction to Quadrupole Ion Trap Mass Spectrometry. Journal of Mass Spectrometry 32(4): 351-369.

Mark, A. L., Shaffer, R. A., Correia, M. L. G., Morgan, D. A., Sigmund, C. D., & Haynes, W. G. (1999). Contrasting blood pressure effects of obesity in leptin-deficient ob/ob mice and agouti yellow obese mice. Journal of Hypertension, 17(12), 1949-1953. doi:Doi 10.1097/00004872-199917121-00026

Marshall, A. G., Hendrickson, C. L., Jackson, G. S. (1998). Fourier transform ion cyclotron resonance mass spectrometry: a primer. Mass Spectrom Rev 17(1): 1-35.

Marshall, W. G., & Dimick, A. R. (1983). The Natural-History of Major Burns with Multiple Subsystem Failure. Journal of Trauma-Injury Infection and Critical Care, 23(2), 102-105. doi:Doi 10.1097/00005373-198302000-00005

Marshall, W. G., Jr., & Dimick, A. R. (1983). The natural history of major burns with multiple subsystem failure. J Trauma, 23(2), 102-105.

Martin-Romero, C., & Sanchez-Margalet, V. (2001). Human leptin activates PI3K and MAPK pathways in human peripheral blood mononuclear cells: Possible role of Sam68. Cellular Immunology, 212(2), 83-91. doi:10.1006/cimm.2001.1851

Martin-Romero, C., Santos-Alvarez, J., Goberna, R., & Sanchez-Margalet, V. (2000). Human leptin enhances activation and proliferation of human circulating T lymphocytes. Cellular Immunology, 199(1), 15-24. doi:DOI 10.1006/cimm.1999.1594

Martinac, B., Adler, J., & Kung, C. (1990). Mechanosensitive ion channels of E. coli activated by amphipaths. Nature, 348(6298), 261-263. doi:10.1038/348261a0

Martini, W. Z., Irtun, O., Chinkes, D. L., Rasmussen, B., Traber, D. L., Wolfe, R. R. (2001). Alteration of hepatic fatty acid metabolism after burn injury in pigs. JPEN J Parenter Enteral Nutr 25(6): 310-316.

Martinon, F. (2010). Mechanisms of uric acid crystal-mediated autoinflammation. Immunol Rev, 233(1), 218-232. doi:10.1111/j.0105-2896.2009.00860.x

Masamune, A., Sakai, Y., Satoh, A., Fujita, M., Yoshida, M., & Shimosegawa, T. (2001). Lysophosphatidylcholine induces apoptosis in AR42J cells. Pancreas, 22(1), 75-83.

Matarese, G., De Rosa, V., & La Cava, A. (2008). Regulatory CD4 T cells: sensing the environment. Trends in Immunology, 29(1), 12-17. doi:10.1016/j.it.2007.10.006

Matarese, G., Moschos, S., & Mantzoros, C. S. (2005). Leptin in immunology. J Immunol, 174(6), 3137-3142.

Matsumoto, T., Kobayashi, T., & Kamata, K. (2007). Role of lysophosphatidylcholine (LPC) in atherosclerosis. Curr Med Chem, 14(30), 3209-3220.

Matthys, E., Patel, Y., Kreisberg, J., Stewart, J. H., & Venkatachalam, M. (1984). Lipid alterations induced by renal ischemia: pathogenic factor in membrane damage. Kidney Int, 26(2), 153-161.
Mattioli, B., Straface, E., Quaranta, M. G., Giordani, L., & Viora, M. (2005). Leptin promotes differentiation and survival of human dendritic cells and licenses them for Th1 priming. J Immunol, 174(11), 6820-6828.
Mauel, J., Ransijn, A., Corradin, S. B., & Buchmuller-Rouiller, Y. (1995). Effect of PGE2 and of agents that raise cAMP levels on macrophage activation induced by IFN-gamma and TNF-alpha. J Leukoc Biol, 58(2), 217-224.
McHowat, J., & Corr, P. B. (1993). Thrombin-induced release of lysophosphatidylcholine from endothelial cells. Journal of Biological Chemistry, 268(21), 15605-15610.
McKemy, D. (2007). TRPM8: The Cold and Menthol Receptor. In: Liedtke WB, Heller S, editors. TRP Ion Channel Function in Sensory Transduction and Cellular Signaling Cascades: CRC Press/Taylor & Francis.
McKenney, J. (2003). Niacin for dyslipidemia: considerations in product selection. Am J Health Syst Pharm, 60(10), 995-1005.
McLure, H. A., & Rubin, A. P. (2005). Review of local anaesthetic agents. Minerva Anestesiol, 71(3), 59-74.
McMahon, H. T., & Gallop, J. L. (2005). Membrane curvature and mechanisms of dynamic cell membrane remodelling. Nature, 438(7068), 590-596. doi:10.1038/nature04396
McMahon, S. B., Armanini, M. P., Ling, L. H., & Phillips, H. S. (1994). Expression and coexpression of Trk receptors in subpopulations of adult primary sensory neurons projecting to identified peripheral targets. Neuron, 12(5), 1161-1171.
McMahon, S. B., & Bevan, S. (2005). Inflammatory mediators and modulators of pain Wall and Melzack's Textbook of Pain E-dition (pp. 49-72): Churchill Livingstone (Elsevier Health Sciences).
McMillen, M. A., Huribal, M., Cunningham, M. E., Bala, R. J., Pleban, W. E., & D'Aiuto, M. L. (1996). Endothelin-1, Interleukin-6, and Interleukin-8 Levels Increase in Patients With Burns. Journal of Burn Care & Research, 17(5), 384-389.
McNamara, A. R., Zamba, K. D., Sokolich, J. C., Jaskille, A. D., Light, T. D., Griffin, M. A., & Meyerholz, D. K. (2010). Apoptosis is differentially regulated by burn severity and dermal location. J Surg Res, 162(2), 258-263. doi:10.1016/j.jss.2009.01.038
Medina-Torres, C. E., van Eps, A. W., Nielsen, L. K., & Hodson, M. P. (2015). A liquid chromatography-tandem mass spectrometry-based investigation of the lamellar interstitial metabolome in healthy horses and during experimental laminitis induction. Vet J, 206(2), 161-169. doi:10.1016/j.tvjl.2015.07.031
Mehta, D., Gupta, S., Gaur, S. N., Gangal, S. V., & Agrawal, K. P. (1990). Increased leukocyte phospholipase A2 activity and plasma lysophosphatidylcholine levels in asthma and rhinitis and their relationship to airway sensitivity to histamine. Am Rev Respir Dis, 142(1), 157-161. doi:10.1164/ajrccm/142.1.157
Meier, C. A., Chicheportiche, R., Dreyer, M., & Dayer, J.-M. (2003). IP-10, but not RANTES, is upregulated by leptin in monocytic cells. Cytokine, 21(1), 43-47. doi:http://dx.doi.org/10.1016/S1043-4666(02)00491-X
Melgaard, L., Hersini, K. J., Gazerani, P., & Petersen, L. J. (2013). Retrodialysis: a review of experimental and clinical applications of reverse microdialysis in the skin. Skin Pharmacol Physiol, 26(3), 160-174. doi:10.1159/000351341
Menten, P., Wuyts, A., & Van Damme, J. (2002). Macrophage inflammatory protein-1. Cytokine Growth Factor Rev, 13(6), 455-481.
Mery, L., Girot, R., & Aractingi, S. (2004). Topical effectiveness of molgramostim (GM-CSF) in sickle cell leg ulcers. Dermatology, 208(2), 135-137. doi:10.1159/000076487
Metz, T. O., Zhang, Q., Page, J. S., Shen, Y., Callister, S. J., Jacobs, J. M., & Smith, R. D. (2007). The future of liquid chromatography-mass spectrometry (LC-MS) in metabolic profiling and metabolomic studies for biomarker discovery. Biomark Med, 1(1), 159-185. doi:10.2217/17520363.1.1.159
Metzger, Z., Hoffeld, J. T., & Oppenheim, J. J. (1980). Macrophage-mediated suppression. I. Evidence for participation of both hdyrogen peroxide and prostaglandins in suppression of murine lymphocyte proliferation. J Immunol, 124(2), 983-988.
Meyer Iii, W. J., Wiechman, S., Woodson, L., Jaco, M., & Thomas, C. R. (2012). Chapter 64 - Management of pain and other discomforts in burned patients A2 - Herndon, David N Total Burn Care (Fourth Edition) (pp. 715-731.e716). London: W.B. Saunders.
Meyer, R. A., Davis, K. D., Cohen, R. H., Treede, R. D., & Campbell, J. N. (1991). Mechanically insensitive afferents (MIAs) in cutaneous nerves of monkey. Brain Res, 561(2), 252-261.
Milano, S., Arcoleo, F., Dieli, M., D'Agostino, R., D'Agostino, P., De Nucci, G., & Cillari, E. (1995). Prostaglandin E2 regulates inducible nitric oxide synthase in the murine macrophage cell line J774. Prostaglandins, 49(2), 105-115.

Milewski, L., Barcz, E., Dziunycz, P., Radomski, D., Kaminski, P., Roszkowski, P. I., . . . Malejczyk, J. (2008). Association of leptin with inflammatory cytokines and lymphocyte subpopulations in peritoneal fluid of patients with endometriosis. J Reprod Immunol, 79(1), 111-117. doi:10.1016/j.jri.2008.08.007

Miller, C. (2001) Ionic channels of excitable membranes. Second edition. Cell, 69(4), 579. doi:10.1016/0092-8674(92)90220-7

Miller, J. A. (1991). The need for epidemiological studies of the medical exposures of Japanese patients to the carcinogen ethyl carbamate (urethane) from 1950 to 1975. Jpn J Cancer Res 82(12): 1323-1324.

Miller, T., Bhattacharya, S., Zamula, W., Lezotte, D., Kowalske, K., Herndon, D., . . . Engrav, L. (2013). Quality-of-life loss of people admitted to burn centers, United States. Quality of Life Research, 22(9), 2293-2305. doi:10.1007/s11136-012-0321-5

Milligan, E. D., Zapata, V., Chacur, M., Schoeniger, D., Biedenkapp, J., O'Connor, K. A., . . . Watkins, L. R. (2004). Evidence that exogenous and endogenous fractalkine can induce spinal nociceptive facilitation in rats. European Journal of Neuroscience, 20(9), 2294-2302. doi:10.1111/j.1460-9568.2004.03709.x

Mills, C. D. (1991). Molecular basis of "suppressor" macrophages. Arginine metabolism via the nitric oxide synthetase pathway. J Immunol, 146(8), 2719-2723.

Mitra, B., Fitzgerald, M., Cameron, P., & Cleland, H. (2006). Fluid resuscitation in major burns. ANZ J Surg, 76(1-2), 35-38. doi:10.1111/j.1445-2197.2006.03641.x

Moatti, D., Faure, S., Fumeron, F., Amara Mel, W., Seknadji, P., McDermott, D. H., . . . Combadiere, C. (2001). Polymorphism in the fractalkine receptor CX3CR1 as a genetic risk factor for coronary artery disease. Blood, 97(7), 1925-1928.

Mock, T., & Man, R. Y. (1990). Mechanism of lysophosphatidylcholine accumulation in the ischemic canine heart. Lipids, 25(7), 357-362.

Moghaddam, B., & Bunney, B. S. (1989). Differential effect of cocaine on extracellular dopamine levels in rat medial prefrontal cortex and nucleus accumbens: comparison to amphetamine. Synapse, 4(2), 156-161. doi:10.1002/syn.890040209

Mohandas, N., Wyatt, J., Mel, S. F., Rossi, M. E., & Shohet, S. B. (1982). Lipid translocation across the human erythrocyte membrane. Regulatory factors. Journal of Biological Chemistry, 257(11), 6537-6543.

Mohapatra, D. P., & Nau, C. (2005). Regulation of Ca2+-dependent desensitization in the vanilloid receptor TRPV1 by calcineurin and cAMP-dependent protein kinase. Journal of Biological Chemistry, 280(14), 13424-13432. doi:10.1074/jbc.M410917200

Moiniche, S., Dahl, J. B., & Kehlet, H. (1993). Peripheral antinociceptive effects of morphine after burn injury. Acta Anaesthesiol Scand, 37(7), 710-712.

Moiniche, S., Pedersen, J. L., & Kehlet, H. (1994). Topical ketorolac has no antinociceptive or anti-inflammatory effect in thermal injury. Burns, 20(6), 483-486.

Monet, M., Gkika, D., Lehen'kyi, V., Pourtier, A., Vanden Abeele, F., Bidaux, G., . . . Prevarsakaya, N. (2009). Lysophospholipids stimulate prostate cancer cell migration via TRPV2 channel activation. Biochim Biophys Acta, 1793(3), 528-539. doi:10.1016/j.bbamcr.2009.01.003

Montana, G., Berk, M., & Ebbels, T. (2011). Modelling short time series in metabolomics: a functional data analysis approach. Adv Exp Med Biol, 696, 307-315. doi:10.1007/978-1-4419-7046-6_31

Montell, C., Birnbaumer, L., & Flockerzi, V. (2002). The TRP channels, a remarkably functional family. Cell, 108(5), 595-598.

Moran, K., & Munster, A. M. (1987). Alterations of the host defense mechanism in burned patients. Surg Clin North Am, 67(1), 47-56.

Moreau, M. E., Garbacki, N., Molinaro, G., Brown, N. J., Marceau, F., & Adam, A. (2005). The kallikrein-kinin system: current and future pharmacological targets. J Pharmacol Sci, 99(1), 6-38.

Morenilla-Palao, C., Planells-Cases, R., Garcia-Sanz, N., & Ferrer-Montiel, A. (2004). Regulated exocytosis contributes to protein kinase C potentiation of vanilloid receptor activity. Journal of Biological Chemistry, 279(24), 25665-25672. doi:10.1074/jbc.M311515200

Morita, M., Sekine, A., Urano, Y., Nishimura, T., Takabe, W., Arai, H., . . . Noguchi, N. (2015). Lysophosphatidylcholine promotes SREBP-2 activation via rapid cholesterol efflux and SREBP-2-independent cytokine release in human endothelial cells. J Biochem, 158(4), 331-338. doi:10.1093/jb/mvv044

Moriyama, T., Higashi, T., Togashi, K., Iida, T., Segi, E., Sugimoto, Y., . . . Tominaga, M. (2005). Sensitization of TRPV1 by EP1 and IP reveals peripheral nociceptive mechanism of prostaglandins. Mol Pain, 1, 3. doi:10.1186/1744-8069-1-3

Morris, C. E., & Juranka, P. F. (2007). Nav channel mechanosensitivity: activation and inactivation accelerate reversibly with stretch. Biophys J, 93(3), 822-833. doi:10.1529/biophysj.106.101246

Motter, A. L., & Ahern, G. P. (2012). TRPA1 is a polyunsaturated fatty acid sensor in mammals. PLoS One, 7(6), e38439. doi:10.1371/journal.pone.0038439

Mruwat, R., Cohen, Y., & Yedgar, S. (2013). Phospholipase A(2) inhibition as potential therapy for inflammatory skin diseases. Immunotherapy, 5(4), 315-317. doi:10.2217/imt.13.18

Muraki, K., Iwata, Y., Katanosaka, Y., Ito, T., Ohya, S., Shigekawa, M., & Imaizumi, Y. (2003). TRPV2 is a component of osmotically sensitive cation channels in murine aortic myocytes. Circ Res, 93(9), 829-838. doi:10.1161/01.res.0000097263.10220.0c

Murohara, T., Kugiyama, K., Ohgushi, M., Sugiyama, S., Ohta, Y., & Yasue, H. (1994). LPC in oxidized LDL elicits vasocontraction and inhibits endothelium- dependent relaxation. Am J Physiol, 267(6 Pt 2), H2441-2449.

Myers, M. G. (2004). Leptin receptor signaling and the regulation of mammalian physiology. Recent Progress in Hormone Research, Vol 59, 59, 287-304. doi:Doi 10.1210/Rp.59.1.287

Nagai, J., Uchida, H., Matsushita, Y., Yano, R., Ueda, M., Niwa, M., . . . Ueda, H. (2010). Autotaxin and lysophosphatidic acid1 receptor-mediated demyelination of dorsal root fibers by sciatic nerve injury and intrathecal lysophosphatidylcholine. Mol Pain, 6, 78. doi:10.1186/1744-8069-6-78

Nagy, I., Friston, D., Valente, J. S., Torres Perez, J. V., & Andreou, A. P. (2014). Pharmacology of the capsaicin receptor, transient receptor potential vanilloid type-1 ion channel. Prog Drug Res, 68, 39-76.

Nagy, I., & Rang, H. (1999a). Noxious heat activates all capsaicin-sensitive and also a sub-population of capsaicin-insensitive dorsal root ganglion neurons. Neuroscience, 88(4), 995-997.

Najib, S., & Sanchez-Margalet, V. (2002). Human leptin promotes survival of human circulating blood monocytes prone to apoptosis by activation of p42/44 MAPK pathway. Cellular Immunology, 220(2), 143-149.

Nakae, H., Endo, S., Inada, K., Yamashita, H., Yamada, Y., Takakuwa, T., . . . Uchida, K. (1995). Plasma concentrations of type II phospholipase A2, cytokines and eicosanoids in patients with burns. Burns, 21(6), 422-426.

Nakamura, Y., Yasukochi, M., Kobayashi, S., Uehara, K., Honda, A., Inoue, R., . . . Uehara, A. (2007). Cell membrane-derived lysophosphatidylcholine activates cardiac ryanodine receptor channels. Pflugers Arch, 453(4), 455-462. doi:10.1007/s00424-006-0141-y

Nanki, T., Imai, T., Nagasaka, K., Urasaki, Y., Nonomura, Y., Taniguchi, K., . . . Miyasaka, N. (2002). Migration of CX3CR1-positive T cells producing type 1 cytokines and cytotoxic molecules into the synovium of patients with rheumatoid arthritis. Arthritis and Rheumatism, 46(11), 2878-2883. doi:10.1002/art.10622

Napoleone, E., Di Santo, A., Amore, C., Baccante, G., Di Febbo, C., Porreca, E., . . . Lorenzet, R. (2007). Leptin induces tissue factor expression in human peripheral blood mononuclear cells: a possible link between obesity and cardiovascular risk? Journal of Thrombosis and Haemostasis, 5(7), 1462-1468. doi:DOI 10.1111/j.1538-7836.2007.02578.x

Nassar, M. A., Levato, A., Stirling, L. C., & Wood, J. N. (2005). Neuropathic pain develops normally in mice lacking both Na(v)1.7 and Na(v)1.8. Mol Pain, 1, 24. doi:10.1186/1744-8069-1-24

Natura, G., von Banchet, G. S., & Schaible, H. G. (2005). Calcitonin gene-related peptide enhances TTX-resistant sodium currents in cultured dorsal root ganglion neurons from adult rats. Pain, 116(3), 194-204. doi:10.1016/j.pain.2005.04.002

Nawroth, P. P., & Stern, D. M. (1986). Modulation of endothelial cell hemostatic properties by tumor necrosis factor. Journal of Experimental Medicine, 163(3), 740-745.

Nicholson, J. K., Lindon, J. C., & Holmes, E. (1999). 'Metabonomics': understanding the metabolic responses of living systems to pathophysiological stimuli via multivariate statistical analysis of biological NMR spectroscopic data. Xenobiotica, 29(11), 1181-1189. doi:10.1080/004982599238047

Nicol, G. D., Lopshire, J. C., & Pafford, C. M. (1997). Tumor necrosis factor enhances the capsaicin sensitivity of rat sensory neurons. J Neurosci, 17(3), 975-982.

Nicolson, T. A., Bevan, S., & Richards, C. D. (2002). Characterisation of the calcium responses to histamine in capsaicin-sensitive and capsaicin-insensitive sensory neurones. Neuroscience, 110(2), 329-338.

Nicolson, T. A., Foster, A. F., Bevan, S., & Richards, C. D. (2007). Prostaglandin E2 sensitizes primary sensory neurons to histamine. Neuroscience, 150(1), 22-30. doi:10.1016/j.neuroscience.2007.09.003

Niederbichler, A. D., Hoesel, L. M., Ipaktchi, K., Olivarez, L., Erdmann, M., Vogt, P. M., Su, G. L., Arbabi, S., Westfall, M. V., Wang, S. C., Hemmila, M. R. (2011). Burn-induced heart failure: lipopolysaccharide binding protein improves burn and endotoxin-induced cardiac contractility deficits. J Surg Res 165(1): 128-135.

Nielsen, N-P. V., Carstensen, J. M., Smedsgaard, J. (1998). Aligning of single and multiple wavelength chromatographic. Journal of Chromatography A, 805(1-2), 17-35.

Nieto-Posadas, A., Picazo-Juárez, G., Llorente, I., Jara-Oseguera, A., Morales-Lázaro, S., Escalante-Alcalde, D., . . . Rosenbaum, T. (2012). Lysophosphatidic acid directly activates TRPV1 through a C-terminal binding site. Nat Chem Biol, 8(1), 78-85. doi:http://www.nature.com/nchembio/journal/v8/n1/abs/nchembio.712.html#supplementary-information

NIH. (2013). Burns and Traumatic Injury. NIH Facts Sheet. Retrieved from https://report.nih.gov/nihfactsheets/ViewFactSheet.aspx?csid=33

Nilius, B., & Voets, T. (2005). TRP channels: a TR(I)P through a world of multifunctional cation channels. Pflugers Arch, 451(1), 1-10. doi:10.1007/s00424-005-1462-y

Nisanci, M., Eski, M., Sahin, I., Ilgan, S., & Isik, S. (2010). Saving the zone of stasis in burns with activated protein C: an experimental study in rats. Burns, 36(3), 397-402. doi:10.1016/j.burns.2009.06.208

Nishi, E., Kume, N., Ueno, Y., Ochi, H., Moriwaki, H., & Kita, T. (1998). Lysophosphatidylcholine enhances cytokine-induced interferon gamma expression in human T lymphocytes. Circ Res, 83(5), 508-515.

Nishimoto, S., Tanaka, H., Okamoto, M., Okada, K., Murase, T., & Yoshikawa, H. (2015). Methylcobalamin promotes the differentiation of Schwann cells and remyelination in lysophosphatidylcholine-induced demyelination of the rat sciatic nerve. Front Cell Neurosci, 9, 298. doi:10.3389/fncel.2015.00298

Noble, H. G., Robson, M. C., & Krizek, T. J. (1977). Dermal ischemia in the burn wound. J Surg Res, 23(2), 117-125.

Noel, J., Zimmermann, K., Busserolles, J., Deval, E., Alloui, A., Diochot, S., . . . Lazdunski, M. (2009). The mechano-activated K+ channels TRAAK and TREK-1 control both warm and cold perception. EMBO J, 28(9), 1308-1318. doi:10.1038/emboj.2009.57

Nordström, A., O'Maille, G., Qin, C., Siuzdak, G. (2006). Nonlinear data alignment for UPLC-MS and HPLC-MS based metabolomics: quantitative analysis of endogenous and exogenous metabolites in human serum. Anal Chem 78(10): 3289-3295.

Nørgaard, L., Bro, R., Westad, F., & Engelsen, S. B. (2006). A modification of canonical variates analysis to handle highly collinear multivariate data. Journal of Chemometrics, 20(8-10), 425-435. doi:10.1002/cem.1017

North, R. A. (2004). P2X3 receptors and peripheral pain mechanisms. J Physiol, 554(Pt 2), 301-308. doi:10.1113/jphysiol.2003.048587

Noto, C., Pappagallo, M., & Szallasi, A. (2009). NGX-4010, a high-concentration capsaicin dermal patch for lasting relief of peripheral neuropathic pain. Curr Opin Investig Drugs, 10(7), 702-710.

Numazaki, M., Tominaga, T., Takeuchi, K., Murayama, N., Toyooka, H., & Tominaga, M. (2003). Structural determinant of TRPV1 desensitization interacts with calmodulin. Proc Natl Acad Sci U S A, 100(13), 8002-8006. doi:10.1073/pnas.1337252100

Numazaki, M., Tominaga, T., Toyooka, H., & Tominaga, M. (2002). Direct phosphorylation of capsaicin receptor VR1 by protein kinase Cepsilon and identification of two target serine residues. Journal of Biological Chemistry, 277(16), 13375-13378. doi:10.1074/jbc.C200104200

Nuytinck, H. K., Offermans, X. J., Kubat, K., & Goris, J. A. (1988). Whole-body inflammation in trauma patients. An autopsy study. Arch Surg, 123(12), 1519-1524.

Nwariaku, F. E., Sikes, P. J., Lightfoot, E., Mileski, W. J., & Baxter, C. (1996). Effect of a bradykinin antagonist on the local inflammatory response following thermal injury. Burns, 22(4), 324-327.

Obata, K., Katsura, H., Mizushima, T., Yamanaka, H., Kobayashi, K., Dai, Y., . . . Noguchi, K. (2005). TRPA1 induced in sensory neurons contributes to cold hyperalgesia after inflammation and nerve injury. Journal of Clinical Investigation, 115(9), 2393-2401. doi:10.1172/jci25437

Obreja, O., Biasio, W., Andratsch, M., Lips, K. S., Rathee, P. K., Ludwig, A., . . . Kress, M. (2005). Fast modulation of heat-activated ionic current by proinflammatory interleukin 6 in rat sensory neurons. Brain, 128(Pt 7), 1634-1641. doi:10.1093/brain/awh490

Obreja, O., Schmelz, M., Poole, S., & Kress, M. (2002). Interleukin-6 in combination with its soluble IL-6 receptor sensitises rat skin nociceptors to heat, in vivo. Pain, 96(1-2), 57-62.

Oh, E. J., & Weinreich, D. (2004). Bradykinin decreases K(+) and increases Cl(-) conductances in vagal afferent neurones of the guinea pig. J Physiol, 558(Pt 2), 513-526. doi:10.1113/jphysiol.2004.066381

Okajima, F., Sato, K., Tomura, H., Kuwabara, A., Nochi, H., Tamoto, K., . . . Ui, M. (1998). Stimulatory and inhibitory actions of lysophosphatidylcholine, depending on its fatty acid residue, on the phospholipase C/Ca2+ system in HL-60 leukaemia cells. Biochemical Journal, 336 (Pt 2), 491-500.

Okita, M., Gaudette, D. C., Mills, G. B., & Holub, B. J. (1997). Elevated levels and altered fatty acid composition of plasma lysophosphatidylcholine(lysoPC) in ovarian cancer patients. Int J Cancer, 71(1), 31-34.

Oksuz, S., Ulkur, E., Oncul, O., Kose, G. T., Kucukodaci, Z., & Urhan, M. (2013). The Effect of Subcutaneous Mesenchymal Stem Cell Injection on Statis Zone and Apoptosis in an Experimental Burn Model. Plast Reconstr Surg, 131(3), 463-471. doi:Doi 10.1097/Prs.0b013e31827c6d6f

Okudaira, S., Yukiura, H., & Aoki, J. (2010). Biological roles of lysophosphatidic acid signaling through its production by autotaxin. Biochimie, 92(6), 698-706. doi:10.1016/j.biochi.2010.04.015

Oldham, K. T., Guice, K. S., Till, G. O., & Ward, P. A. (1988). Activation of complement by hydroxyl radical in thermal injury. Surgery, 104(2), 272-279.

Oliveira, M. C., Pelegrini-da-Silva, A., Parada, C. A., & Tambeli, C. H. (2007). 5-HT acts on nociceptive primary afferents through an indirect mechanism to induce hyperalgesia in the subcutaneous tissue. Neuroscience, 145(2), 708-714. doi:10.1016/j.neuroscience.2006.12.021

Oliveira, H. M., Sallam, H. S., Espana-Tenorio, J., Chinkes, D., Chung, D. H., Chen, J. D., Herndon, D. N. (2009). Gastric and small bowel ileus after severe burn in rats: the effect of cyclooxygenase-2 inhibitors. Burns 35(8): 1180-1184.

Olofsson, K. E., Andersson, L., Nilsson, J., & Bjorkbacka, H. (2008). Nanomolar concentrations of lysophosphatidylcholine recruit monocytes and induce pro-inflammatory cytokine production in macrophages. Biochem Biophys Res Commun, 370(2), 348-352. doi:10.1016/j.bbrc.2008.03.087

Ong, Y. S., Samuel, M., & Song, C. (2006). Meta-analysis of early excision of burns. Burns, 32(2), 145-150. doi:10.1016/j.burns.2005.09.005

Onjiko, R. M., Moody, S. A., & Nemes, P. (2015). Single-cell mass spectrometry reveals small molecules that affect cell fates in the 16-cell embryo. Proc Natl Acad Sci U S A, 112(21), 6545-6550. doi:10.1073/pnas.1423682112

Ono, I., Gunji, H., Zhang, J. Z., Maruyama, K., & Kaneko, F. (1995). A study of cytokines in burn blister fluid related to wound healing. Burns, 21(5), 352-355.

Onofrio, B. M., Yaksh, T. L., & Arnold, P. G. (1981). Continuous low-dose intrathecal morphine administration in the treatment of chronic pain of malignant origin. Mayo Clin Proc, 56(8), 516-520.

Onuoha, G. N., & Alpar, E. K. (2001). Levels of vasodilators (SP, CGRP) and vasoconstrictor (NPY) peptides in early human burns. European Journal of Clinical Investigation, 31(3), 253-257. doi:DOI 10.1046/j.1365-2362.2001.00787.x

Oremus, M., Hanson, M. D., Whitlock, R., Young, E., Archer, C., Dal Cin, A., . . . Raina, P. (2007). A systematic review of heparin to treat burn injury. J Burn Care Res, 28(6), 794-804. doi:10.1097/BCR.0b013e3181599b9b

Orman, M. A., Nguyen, T. T., Ierapetritou, M. G., Berthiaume, F., & Androulakis, I. P. (2011). Comparison of the cytokine and chemokine dynamics of the early inflammatory response in models of burn injury and infection. Cytokine, 55(3), 362-371. doi:DOI 10.1016/j.cyto.2011.05.010

Orrenius, S., Zhivotovsky, B., & Nicotera, P. (2003). Regulation of cell death: the calcium-apoptosis link. Nat Rev Mol Cell Biol, 4(7), 552-565. doi:10.1038/nrm1150

Osborne, P. G., O'Connor, W. T., Drew, K. L., & Ungerstedt, U. (1990). An in vivo microdialysis characterization of extracellular dopamine and GABA in dorsolateral striatum of awake freely moving and halothane anaesthetised rats. J Neurosci Methods, 34(1-3), 99-105.

Oster, C., Willebrand, M., & Ekselius, L. (2011). Health-Related Quality of Life 2 Years to 7 Years After Burn Injury. Journal of Trauma-Injury Infection and Critical Care, 71(5), 1435-1441. doi:Doi 10.1097/Ta.0b013e318208fc74

Ottonello, L., Gnerre, P., Bertolotto, M., Mancini, M., Dapino, P., Russo, R., . . . Dallegri, F. (2004). Leptin as a uremic toxin interferes with neutrophil chemotaxis. Journal of the American Society of Nephrology, 15(9), 2366-2372. doi:10.1097/01.Asn.0000139321.98028.40

Otuki, M. F., Schwob, O., Silveira Prudente, A., Zaltsman, I., Meretski, S., Segal, J., . . . Rosenblat, G. (2011). Attenuation of experimental TPA-induced dermatitis by acetylenic acetogenins is associated with inhibition of PLA(2) activity. European Journal of Pharmacology, 672(1-3), 175-179. doi:10.1016/j.ejphar.2011.09.184

Ousman, S. S., & David, S. (2000). Lysophosphatidylcholine induces rapid recruitment and activation of macrophages in the adult mouse spinal cord. Glia, 30(1), 92-104.

Ouyang, W., Rutz, S., Crellin, N. K., Valdez, P. A., & Hymowitz, S. G. (2011). Regulation and functions of the IL-10 family of cytokines in inflammation and disease. Annu Rev Immunol, 29, 71-109. doi:10.1146/annurev-immunol-031210-101312

Oz-Arslan, D., Ruscher, W., Myrtek, D., Ziemer, M., Jin, Y., Damaj, B. B., . . . Maghazachi, A. A. (2006). IL-6 and IL-8 release is mediated via multiple signaling pathways after stimulating dendritic cells with lysophospholipids. J Leukoc Biol, 80(2), 287-297. doi:10.1189/jlb.1205751

Palmieri, T. L., Przkora, R., Meyer, W. J., 3rd, & Carrougher, G. J. (2014). Measuring burn injury outcomes. Surg Clin North Am, 94(4), 909-916. doi:10.1016/j.suc.2014.05.010

Pan, H. L., Zhang, Y. Q., & Zhao, Z. Q. (2010). Involvement of lysophosphatidic acid in bone cancer pain by potentiation of TRPV1 via PKCepsilon pathway in dorsal root ganglion neurons. Mol Pain, 6, 85. doi:10.1186/1744-8069-6-85

Papazian, D. M., Timpe, L. C., Jan, Y. N., & Jan, L. Y. (1991). Alteration of voltage-dependence of Shaker potassium channel by mutations in the S4 sequence. Nature, 349(6307), 305-310. doi:10.1038/349305a0

Papp, A., Harma, M., Harvima, R., Lahtinen, T., Uusaro, A., & Alhava, E. (2005). Microdialysis for detection of dynamic changes in tissue histamine levels in experimental thermal injury. Burns, 31(4), 476-481. doi:10.1016/j.burns.2004.12.004

Papp, A., Uusaro, A., Parviainen, I., Hartikainen, J., & Ruokonen, E. (2003). Myocardial function and haemodynamics in extensive burn trauma: evaluation by clinical signs, invasive monitoring, echocardiography and cytokine concentrations. A prospective clinical study. Acta Anaesthesiol Scand, 47(10), 1257-1263.

Parihar, A., Parihar, M. S., Milner, S., & Bhat, S. (2008). Oxidative stress and anti-oxidative mobilization in burn injury. Burns, 34(1), 6-17. doi:10.1016/j.burns.2007.04.009

Patapoutian, A., Peier, A. M., Story, G. M., & Viswanath, V. (2003). ThermoTRP channels and beyond: mechanisms of temperature sensation. Nat Rev Neurosci, 4(7), 529-539. doi:10.1038/nrn1141

Patel, A. J., Lazdunski, M., & Honoré, E. (2001). Lipid and mechano-gated 2P domain K+ channels. Curr Opin Cell Biol, 13(4), 422-428. doi:http://dx.doi.org/10.1016/S0955-0674(00)00231-3

Patti, G. J. (2011). Separation strategies for untargeted metabolomics. J Sep Sci 34(24): 3460-3469.

Patwardhan, A. M., Akopian, A. N., Ruparel, N. B., Diogenes, A., Weintraub, S. T., Uhlson, C., . . . Hargreaves, K. M. (2010). Heat generates oxidized linoleic acid metabolites that activate TRPV1 and produce pain in rodents. Journal of Clinical Investigation, 120(5), 1617-1626. doi:10.1172/jci41678

Pavoni, V., Gianesello, L., Paparella, L., Buoninsegni, L. T., & Barboni, E. (2010). Outcome predictors and quality of life of severe burn patients admitted to intensive care unit. Scand J Trauma Resusc Emerg Med, 18, 24. doi:10.1186/1757-7241-18-24

Payne, W. G., Wachtel, T. L., Smith, C. A., Uberti, M. G., Ko, F., & Robson, M. C. (2010). Effect of amnion-derived cellular cytokine solution on healing of experimental partial-thickness burns. World J Surg, 34(7), 1663-1668. doi:10.1007/s00268-010-0420-9

Peck, M., & Pressman, M. A. (2013). The correlation between burn mortality rates from fire and flame and economic status of countries. Burns, 39(6), 1054-1059. doi:DOI 10.1016/j.burns.2013.04.010

Pedersen, J. L., Galle, T. S., & Kehlet, H. (1998). Peripheral analgesic effects of ketamine in acute inflammatory pain. Anesthesiology, 89(1), 58-66.

Peier, A. M., Moqrich, A., Hergarden, A. C., Reeve, A. J., Andersson, D. A., Story, G. M., . . . Patapoutian, A. (2002). A TRP channel that senses cold stimuli and menthol. Cell, 108(5), 705-715.

Pereira, C., Murphy, K., & Herndon, D. (2004). Outcome measures in burn care - Is mortality dead? Burns, 30(8), 761-771. doi:DOI 10.1016/j.burns.2004.05.012

Perozo, E., Kloda, A., Cortes, D. M., & Martinac, B. (2002). Physical principles underlying the transduction of bilayer deformation forces during mechanosensitive channel gating. Nat Struct Biol, 9(9), 696-703. doi:10.1038/nsb827

Perry, S., Difede, J., Musngi, G., Frances, A. J., & Jacobsberg, L. (1992). Predictors of posttraumatic stress disorder after burn injury. Am J Psychiatry, 149(7), 931-935.

Perry, S., Heidrich, G., & Ramos, E. (1981). Assessment of Pain by Burn Patients. Journal of Burn Care & Research, 2(6), 322-326.

Perry, S. W. (1984). Undermedication for pain on a burn unit. Gen Hosp Psychiatry, 6(4), 308-316.

Petersen, L. J., Pedersen, J. L., Skov, P. S., Nielsen, H. J., & Kehlet, H. (2009). Histamine is not released in acute thermal injury in human skin in vivo: a microdialysis study. Inflamm Res, 58(7), 395-399. doi:10.1007/s00011-009-0004-z

Petersen, L. J., Poulsen, L. K., Sondergaard, J., & Skov, P. S. (1994). The use of cutaneous microdialysis to measure substance P-induced histamine release in intact human skin in vivo. J Allergy Clin Immunol, 94(4), 773-783.

Petersen, L. J., Skov, P. S., Bindslev-Jensen, C., & Sondergaard, J. (1992). Histamine release in immediate-type hypersensitivity reactions in intact human skin measured by microdialysis. A preliminary study. Allergy, 47(6), 635-637.

Peterson, S. L., Mani, M. M., Crawford, C. M., Neff, J. R., & Hiebert, J. M. (1989). Postburn heterotopic ossification: insights for management decision making. J Trauma, 29(3), 365-369.

Phillips, R., Ursell, T., Wiggins, P., & Sens, P. (2009). Emerging roles for lipids in shaping membrane-protein function. Nature, 459(7245), 379-385. doi:10.1038/nature08147

Picazo-Juarez, G., Romero-Suarez, S., Nieto-Posadas, A., Llorente, I., Jara-Oseguera, A., Briggs, M., . . . Rosenbaum, T. (2011). Identification of a binding motif in the S5 helix that confers cholesterol sensitivity to the TRPV1 ion channel. Journal of Biological Chemistry, 286(28), 24966-24976. doi:10.1074/jbc.M111.237537

Piguet, P. F., Grau, G. E., & Vassalli, P. (1991). Tumor necrosis factor and immunopathology. Immunol Res, 10(2), 122-140.

Pileri, D., Accardo Palombo, A., D'Amelio, L., D'Arpa, N., Amato, G., Masellis, A., . . . Conte, C. (2008). Concentrations of cytokines IL-6 and IL-10 in plasma of burn patients: their relationship to sepsis and outcome. Ann Burns Fire Disasters, 21(4), 182-185.

Piper, A. S., Yeats, J. C., Bevan, S., & Docherty, R. J. (1999). A study of the voltage dependence of capsaicin-activated membrane currents in rat sensory neurones before and after acute desensitization. J Physiol, 518 (Pt 3), 721-733.

Planas, M., Wachtel, T., Frank, H., & Henderson, L. W. (1982). Characterization of acute renal failure in the burned patient. Arch Intern Med, 142(12), 2087-2091.

Planells-Cases, R., Garcia-Sanz, N., Morenilla-Palao, C., & Ferrer-Montiel, A. (2005). Functional aspects and mechanisms of TRPV1 involvement in neurogenic inflammation that leads to thermal hyperalgesia. Pflugers Arch, 451(1), 151-159. doi:10.1007/s00424-005-1423-5

Plumb, R., Castro-Perez, J., Granger, J., Beattie, I., Joncour, K., Wright, A. (2004). Ultra-performance liquid chromatography coupled to quadrupole-orthogonal time-of-flight mass spectrometry. Rapid Commun Mass Spectrom 18(19): 2331-2337.

Plumb, R. S., Stumpf, C.L., Gorenstein, M. V., Castro-Perez, J. M., Dear, G. J., Anthony, M., Sweatman, B. C., Connor, S. C., Haselden, J. N. (2002). Metabonomics: the use of electrospray mass spectrometry coupled to reversed-phase liquid chromatography shows potential for the screening of rat urine in drug development. Rapid Commun Mass Spectrom 16(20): 1991-1996.

Pluskal, T., Castillo, S., Villar-Briones, A., & Oresic, M. (2010). MZmine 2: modular framework for processing, visualizing, and analyzing mass spectrometry-based molecular profile data. Bmc Bioinformatics, 11, 395. doi:10.1186/1471-2105-11-395

Pollins, A. C., Friedman, D. B., & Nanney, L. B. (2007). Proteomic investigation of human burn wounds by 2D-difference gel electrophoresis and mass spectrometry. J Surg Res, 142(1), 143-152. doi:10.1016/j.jss.2007.01.001

Portenoy, R. K., & Hagen, N. A. (1990). Breakthrough pain: definition, prevalence and characteristics. Pain, 41(3), 273-281.

Povlsen, J. A., Lofgren, B., Dalgas, C., Birkler, R. I., Johannsen, M., Stottrup, N. B., & Botker, H. E. (2013). Protection against myocardial ischemia-reperfusion injury at onset of type 2 diabetes in Zucker diabetic fatty rats is associated with altered glucose oxidation. PLoS One, 8(5), e64093. doi:10.1371/journal.pone.0064093

Pratt, V. C., Tredget, E. E., Clandinin, M. T., & Field, C. J. (2001). Fatty acid content of plasma lipids and erythrocyte phospholipids are altered following burn injury. Lipids, 36(7), 675-682.

Premkumar, L. S., & Ahern, G. P. (2000). Induction of vanilloid receptor channel activity by protein kinase C. Nature, 408(6815), 985-990. doi:10.1038/35050121

Prescott, E. D., & Julius, D. (2003). A modular PIP2 binding site as a determinant of capsaicin receptor sensitivity. Science, 300(5623), 1284-1288. doi:10.1126/science.1083646

Price, D. D., & Dubner, R. (1977). Mechanisms of first and second pain in the peripheral and central nervous systems. Journal of Investigative Dermatology, 69(1), 167-171.

Price, M. P., Lewin, G. R., McIlwrath, S. L., Cheng, C., Xie, J., Heppenstall, P. A., . . . Welsh, M. J. (2000). The mammalian sodium channel BNC1 is required for normal touch sensation. Nature, 407(6807), 1007-1011. doi:10.1038/35039512

Price, M. P., McIlwrath, S. L., Xie, J., Cheng, C., Qiao, J., Tarr, D. E., . . . Welsh, M. J. (2001). The DRASIC Cation Channel Contributes to the Detection of Cutaneous Touch and Acid Stimuli in Mice. Neuron, 35(2), 407. doi:10.1016/S0896-6273(02)00772-9

Prommer, E. E. (2010). Tapentadol: an initial analysis. J Opioid Manag, 6(3), 223-226.
Prout, J. (2014). Advanced training in anaesthesia (T. J. Jeremy Prout, Daniel Martin Ed.). Oxford: Oxford University Press, USA.
Qian, W. J., Petritis, B. O., Kaushal, A., Finnerty, C. C., Jeschke, M. G., Monroe, M. E., . . . Smith, R. D. (2010). Plasma proteome response to severe burn injury revealed by 18O-labeled "universal" reference-based quantitative proteomics. J Proteome Res, 9(9), 4779-4789. doi:10.1021/pr1005026
Qiao, J., Huang, F., Naikawadi, R. P., Kim, K. S., Said, T., & Lum, H. (2006). Lysophosphatidylcholine impairs endothelial barrier function through the G protein-coupled receptor GPR4. Am J Physiol Lung Cell Mol Physiol, 291(1), L91-101. doi:10.1152/ajplung.00508.2005
Qin, F. (2007). Regulation of TRP ion channels by phosphatidylinositol-4,5-bisphosphate. Handb Exp Pharmacol(179), 509-525. doi:10.1007/978-3-540-34891-7_30
Qin, Z. X., Zhu, H. Y., & Hu, Y. H. (2009). Effects of lysophosphatidylcholine on beta-amyloid-induced neuronal apoptosis. Acta Pharmacol Sin, 30(4), 388-395. doi:10.1038/aps.2009.25
Qiu, F., Qiu, C. Y., Liu, Y. Q., Wu, D., Li, J. D., & Hu, W. P. (2012). Potentiation of acid-sensing ion channel activity by the activation of 5-HT(2) receptors in rat dorsal root ganglion neurons. Neuropharmacology, 63(3), 494-500. doi:10.1016/j.neuropharm.2012.04.034
Quinn, M. T., Parthasarathy, S., & Steinberg, D. (1988). Lysophosphatidylcholine: a chemotactic factor for human monocytes and its potential role in atherogenesis. Proc Natl Acad Sci U S A, 85(8), 2805-2809.
Rabinowitz, J. D. and E. Kimball (2007). Acidic acetonitrile for cellular metabolome extraction from Escherichia coli. Anal Chem 79(16): 6167-6173.
Rackow, E. C., Astiz, M. E., & Weil, M. H. (1987). Increases in oxygen extraction during rapidly fatal septic shock in rats. J Lab Clin Med, 109(6), 660-664.
Radu, C. G., Yang, L. V., Riedinger, M., Au, M., & Witte, O. N. (2004). T cell chemotaxis to lysophosphatidylcholine through the G2A receptor. Proc Natl Acad Sci U S A, 101(1), 245-250. doi:10.1073/pnas.2536801100
Ramanathan, A., Nelson, A. R., Sagare, A. P., Zlokovic, B. V. (2015). Impaired vascular-mediated clearance of brain amyloid beta in Alzheimer's disease: the role, regulation and restoration of LRP1. Front Aging Neurosci. (7), 136.
Ramautar, R., Somsen, G. W., de Jong, G. J. (2009). CE-MS in metabolomics. Electrophoresis 30(1): 276-291.
Ramer, M. S., Bradbury, E. J., & McMahon, S. B. (2001). Nerve growth factor induces P2X(3) expression in sensory neurons. Journal of Neurochemistry, 77(3), 864-875.
Rand, J. H., Wu, X. X., Quinn, A. S., Chen, P. P., McCrae, K. R., Bovill, E. G., & Taatjes, D. J. (2003). Human Monoclonal Antiphospholipid Antibodies Disrupt the Annexin A5 Anticoagulant Crystal Shield on Phospholipid Bilayers: Evidence from Atomic Force Microscopy and Functional Assay. Am J Pathol, 163(3), 1193-1200.
Rao, P., & Knaus, E. E. (2008). Evolution of nonsteroidal anti-inflammatory drugs (NSAIDs): cyclooxygenase (COX) inhibition and beyond. J Pharm Pharm Sci, 11(2), 81s-110s.
Rashid, A., Khanna, A., Gowar, J. P., & Bull, J. P. (2001). Revised estimates of mortality from burns in the last 20 years at the Birmingham Burns Centre. Burns, 27(7), 723-730.
Rathee, P. K., Distler, C., Obreja, O., Neuhuber, W., Wang, G. K., Wang, S. Y., . . . Kress, M. (2002). PKA/AKAP/VR-1 module: A common link of Gs-mediated signaling to thermal hyperalgesia. J Neurosci, 22(11), 4740-4745. doi:20026461
Rau, K. K., Jiang, N., Johnson, R. D., & Cooper, B. Y. (2007). Heat sensitization in skin and muscle nociceptors expressing distinct combinations of TRPV1 and TRPV2 protein. Journal of Neurophysiology, 97(4), 2651-2662. doi:10.1152/jn.00840.2006
Ravage, Z. B., Gomez, H. F., Czermak, B. J., Watkins, S. A., & Till, G. O. (1998). Mediators of microvascular injury in dermal burn wounds. Inflammation, 22(6), 619-629.
Ravichandran, K. S. (2010). Find-me and eat-me signals in apoptotic cell clearance: progress and conundrums. Journal of Experimental Medicine, 207(9), 1807-1817. doi:10.1084/jem.20101157
Rawlingson, A. (2003). Nitric oxide, inflammation and acute burn injury. Burns, 29(7), 631-640.
Rehberg, S., Enkhbaatar, P., Cox, R. A., & Traber, D. L. (2012). Coagulopathy after burn and smoke inhalation injury: the evidence is there, let's take advantage of it! J Trauma Acute Care Surg, 72(4), 1121-1122; author reply 1122-1123. doi:10.1097/TA.0b013e318246dc21
Reichard, P., & Ehrenberg, A. (1983). Ribonucleotide reductase--a radical enzyme. Science, 221(4610), 514-519.
Reif, S., Lang, A., Lindquist, J. N., Yata, Y., Gabele, E., Scanga, A., Brenner, D. A., Rippe, R. A. (2003). The role of focal adhesion kinase-phosphatidylinositol 3-kinase-akt signaling in hepatic stellate cell proliferation and type I collagen expression. J Biol Chem 278(10): 8083-8090.

Ren, H., Zhou, X., Dai, D., Liu, X., Wang, L., Zhou, Y., . . . Cai, Q. (2015). Assessment of urinary kidney injury molecule-1 and interleukin-18 in the early post-burn period to predict acute kidney injury for various degrees of burn injury. BMC Nephrol, 16, 142. doi:10.1186/s12882-015-0140-3

Renz, H., Gong, J. H., Schmidt, A., Nain, M., & Gemsa, D. (1988). Release of tumor necrosis factor-alpha from macrophages. Enhancement and suppression are dose-dependently regulated by prostaglandin E2 and cyclic nucleotides. J Immunol, 141(7), 2388-2393.

Rhodes, L. E., Hashim, I.A., McLaughlin, P. J., Friedmann, P. S. (1999). Blister fluid cytokines in cutaneous inflammatory bullous disorders. Acta Derm Venereol., 79(4), 288-90.

Ricciotti, E., & FitzGerald, G. A. (2011). Prostaglandins and Inflammation. Arterioscler Thromb Vasc Biol, 31(5), 986-1000. doi:10.1161/atvbaha.110.207449

Richardson, J. D., & Vasko, M. R. (2002). Cellular Mechanisms of Neurogenic Inflammation. Journal of Pharmacology and Experimental Therapeutics, 302(3), 839-845. doi:10.1124/jpet.102.032797

Riley, J. F., & West, G. B. (1953). The presence of histamine in tissue mast cells. J Physiol, 120(4), 528-537.

Ring, B. D., Scully, S., Davis, C. R., Baker, M. B., Cullen, M. J., Pelleymounter, M. A., & Danilenko, D. M. (2000). Systemically and topically administered leptin both accelerate wound healing in diabetic ob/ob mice. Endocrinology, 141(1), 446-449. doi:10.1210/endo.141.1.7373

Ritchie, M. E., Phipson, B., Wu, D., Hu, Y., Law, C. W., Shi, W., & Smyth, G. K. (2015). limma powers differential expression analyses for RNA-sequencing and microarray studies. Nucleic Acids Res, 43(7), e47. doi:10.1093/nar/gkv007

Robertson, D. G. (2005). Metabonomics in toxicology: a review. Toxicol Sci 85(2): 809-822.

Rockwell, W. B., & Ehrlich, H. P. (1990). Fibrinolysis inhibition in human burn blister fluid. J Burn Care Rehabil, 11(1), 1-6.

Rodeberg, D. A., Meyer, J. G., & Babcock, G. F. (1999). Heat shock response: presence and effects in burn patient neutrophils. J Leukoc Biol, 66(5), 773-780.

Rodriguez, J. L., Miller, C. G., Garner, W. L., Till, G. O., Guerrero, P., Moore, N. P., . . . Remick, D. G. (1993). Correlation of the local and systemic cytokine response with clinical outcome following thermal injury. J Trauma, 34(5), 684-694; discussion 694-685.

Rodt, S. A., Reed, R. K., Ljungstrom, M., Gustafsson, T. O., & Rubin, K. (1994). The anti-inflammatory agent alpha-trinositol exerts its edema-preventing effects through modulation of beta 1 integrin function. Circ Res, 75(5), 942-948.

Roessner, U., & Bowne, J. (2009). What is metabolomics all about? Biotechniques, 46(5), 363-365. doi:10.2144/000113133

Rohacs, T., Lopes, C. M. B., Michailidis, I., & Logothetis, D. E. (2005). PI(4,5)P2 regulates the activation and desensitization of TRPM8 channels through the TRP domain. Nature Neuroscience, 8(5), 626-634. doi:http://www.nature.com/neuro/journal/v8/n5/suppinfo/nn1451_S1.html

Rolin, J., Al-Jaderi, Z., & Maghazachi, A. A. (2013). Oxidized lipids and lysophosphatidylcholine induce the chemotaxis and intracellular calcium influx in natural killer cells. Immunobiology, 218(6), 875-883. doi:10.1016/j.imbio.2012.10.009

Rosen, G. M., Pou, S., Ramos, C. L., Cohen, M. S., & Britigan, B. E. (1995). Free radicals and phagocytic cells. Faseb Journal, 9(2), 200-209.

Rosenbaum, T., Gordon-Shaag, A., Munari, M., & Gordon, S. E. (2004). Ca2+/calmodulin modulates TRPV1 activation by capsaicin. J Gen Physiol, 123(1), 53-62. doi:10.1085/jgp.200308906

Ross, R. A. (2003). Anandamide and vanilloid TRPV1 receptors. Br J Pharmacol, 140(5), 790-801. doi:10.1038/sj.bjp.0705467

Roth, G. B. (1935). Barbiturates on the mammalian heart. Arch. Intern. Pharmacodyn. 51, 179-184.

Rowan, M. P., Cancio, L. C., Elster, E. A., Burmeister, D. M., Rose, L. F., Natesan, S., . . . Chung, K. K. (2015). Burn wound healing and treatment: review and advancements. Crit Care, 19(1), 243. doi:10.1186/s13054-015-0961-2

Roza, C., Puel, J. L., Kress, M., Baron, A., Diochot, S., Lazdunski, M., & Waldmann, R. (2004). Knockout of the ASIC2 channel in mice does not impair cutaneous mechanosensation, visceral mechanonociception and hearing. J Physiol, 558(Pt 2), 659-669. doi:10.1113/jphysiol.2004.066001

Runnels, L. W., Yue, L., & Clapham, D. E. (2002). The TRPM7 channel is inactivated by PIP(2) hydrolysis. Nat Cell Biol, 4(5), 329-336. doi:10.1038/ncb781

Russell, F. A., Veldhoen, V. E., Tchitchkan, D., & McDougall, J. J. (2010). Proteinase-Activated Receptor-4 (PAR(4)) Activation Leads to Sensitization of Rat Joint Primary Afferents Via a Bradykinin B-2 Receptor-Dependent Mechanism. Journal of Neurophysiology, 103(1), 155-163. doi:DOI 10.1152/jn.00486.2009

Ruth, J. H., Volin, M. V., Haines, G. K., Woodruff, D. C., Katschke, K. J., Woods, J. M., . . . Koch, A. E. (2001). Fractalkine, a novel chemokine in rheumatoid arthritis and in rat adjuvant-induced arthritis. Arthritis and Rheumatism, 44(7), 1568-1581. doi:Doi 10.1002/1529-0131(200107)44:7<1568::Aid-Art280>3.0.Co;2-1

Rutter, A. R., Ma, Q. P., Leveridge, M., & Bonnert, T. P. (2005). Heteromerization and colocalization of TrpV1 and TrpV2 in mammalian cell lines and rat dorsal root ganglia. Neuroreport, 16(16), 1735-1739.

Ryborg, A. K., Deleuran, B., Sogaard, H., & Kragballe, K. (2000). Intracutaneous injection of lysophosphatidylcholine induces skin inflammation and accumulation of leukocytes. Acta Derm Venereol, 80(4), 242-246.

Ryborg, A. K., Gron, B., & Kragballe, K. (1995). Increased lysophosphatidylcholine content in lesional psoriatic skin. Br J Dermatol, 133(3), 398-402.

Ryu, S., Liu, B., Yao, J., Fu, Q., & Qin, F. (2007). Uncoupling proton activation of vanilloid receptor TRPV1. J Neurosci, 27(47), 12797-12807. doi:10.1523/jneurosci.2324-07.2007

Sachs, D., Cunha, F. Q., Poole, S., & Ferreira, S. H. (2002). Tumour necrosis factor-alpha, interleukin-1beta and interleukin-8 induce persistent mechanical nociceptor hypersensitivity. Pain, 96(1-2), 89-97.

Safieh-Garabedian, B., Poole, S., Allchorne, A., Winter, J., & Woolf, C. J. (1995). Contribution of interleukin-1 beta to the inflammation-induced increase in nerve growth factor levels and inflammatory hyperalgesia. Br J Pharmacol, 115(7), 1265-1275.

Sakai, M., Miyazaki, A., Hakamata, H., Sato, Y., Matsumura, T., Kobori, S., . . . Horiuchi, S. (1996). Lysophosphatidylcholine potentiates the mitogenic activity of modified LDL for human monocyte-derived macrophages. Arterioscler Thromb Vasc Biol, 16(4), 600-605.

Salazar, H., Jara-Oseguera, A., Hernandez-Garcia, E., Llorente, I., Arias, O., II, Soriano-Garcia, M., . . . Rosenbaum, T. (2009). Structural determinants of gating in the TRPV1 channel. Nat Struct Mol Biol, 16(7), 704-710. doi:10.1038/nsmb.1633

Salcedo, R., Young, H. A., Ponce, M. L., Ward, J. M., Kleinman, H. K., Murphy, W. J., & Oppenheim, J. J. (2001). Eotaxin (CCL11) induces in vivo angiogenic responses by human CCR3+ endothelial cells. J Immunol, 166(12), 7571-7578.

Salvemini, D., Seibert, K., Masferrer, J. L., Settle, S. L., Misko, T. P., Currie, M. G., & Needleman, P. (1995). Nitric oxide and the cyclooxygenase pathway. Adv Prostaglandin Thromboxane Leukot Res, 23, 491-493.

Samuelsson, A., Abdiu, A., Wackenfors, A., & Sjoberg, F. (2008). Serotonin kinetics in patients with burn injuries: a comparison between the local and systemic responses measured by microdialysis-a pilot study. Burns, 34(5), 617-622. doi:10.1016/j.burns.2007.08.003

Samuelsson, A., Steinvall, I., & Sjoberg, F. (2006). Microdialysis shows metabolic effects in skin during fluid resuscitation in burn-injured patients. Crit Care, 10(6), R172. doi:10.1186/cc5124

Sanchez-Lozada, L. G., Tapia, E., Santamaria, J., Avila-Casado, C., Soto, V., Nepomuceno, T., . . . Herrera-Acosta, J. (2005). Mild hyperuricemia induces vasoconstriction and maintains glomerular hypertension in normal and remnant kidney rats. Kidney Int, 67(1), 237-247. doi:10.1111/j.1523-1755.2005.00074.x

Sanchez-Margalet, V., & Martin-Romero, C. (2001). Human leptin signaling in human peripheral blood mononuclear cells: Activation of the JAK-STAT pathway. Cellular Immunology, 211(1), 30-36. doi:10.1006/cimm.2001.1815

Sanchez-Margalet, V., Martin-Romero, C., Gonzalez-Yanes, C., Goberna, R., Rodriguez-Bano, J., & Muniain, M. A. (2002). Leptin receptor (Ob-R) expression is induced in peripheral blood mononuclear cells by in vitro activation and in vivo in HIV-infected patients. Clin Exp Immunol, 129(1), 119-124. doi:DOI 10.1046/j.1365-2249.2002.01900.x

Sanchez-Pozo, C., Rodriguez-Bano, J., Dominguez-Castellano, A., Muniain, M. A., Goberna, R., & Sanchez-Margalet, V. (2003). Leptin stimulates the oxidative burst in control monocytes but attenuates the oxidative burst in monocytes from HIV-infected patients. Clin Exp Immunol, 134(3), 464-469.

Sano, S., Itami, S., Takeda, K., Tarutani, M., Yamaguchi, Y., Miura, H., . . . Takeda, J. (1999). Keratinocyte-specific ablation of Stat3 exhibits impaired skin remodeling, but does not affect skin morphogenesis. Embo Journal, 18(17), 4657-4668. doi:DOI 10.1093/emboj/18.17.4657

Santos-Alvarez, J., Goberna, R., & Sanchez-Margalet, V. (1999). Human leptin stimulates proliferation and activation of human circulating monocytes. Cellular Immunology, 194(1), 6-11. doi:DOI 10.1006/cimm.1999.1490

Santos Heredero, F. X., Hamann, C., Obispo Martin, J. M., Rodriguez Arias, C., Coca Menchero, S. (1996). Experimental burn models. Annals of Burns and Fire Disasters, 9(2), 96-100.

Sanz-Salvador, L., Andres-Borderia, A., Ferrer-Montiel, A., & Planells-Cases, R. (2012). Agonist- and Ca2+-dependent desensitization of TRPV1 channel targets the receptor to lysosomes for degradation. Journal of Biological Chemistry, 287(23), 19462-19471. doi:10.1074/jbc.M111.289751

Saraf, M. K., Herndon, D. N., Porter, C., Toliver-Kinsky, T., Radhakrishnan, R., Chao, T., . . . Sidossis, L. S. (2016). Morphological Changes in Subcutaneous White Adipose Tissue After Severe Burn Injury. J Burn Care Res, 37(2), e96-103. doi:10.1097/bcr.0000000000000292

Sarraf, P., Frederich, R. C., Turner, E. M., Ma, G., Jaskowiak, N. T., Rivet, D. J., . . . Alexander, H. R. (1997). Multiple cytokines and acute inflammation raise mouse leptin levels: Potential role in inflammatory anorexia. Journal of Experimental Medicine, 185(1), 171-175. doi:DOI 10.1084/jem.185.1.171

Sasagawa, T., Okita, M., Murakami, J., Kato, T., & Watanabe, A. (1999). Abnormal serum lysophospholipids in multiple myeloma patients. Lipids, 34(1), 17-21.

Saunders, L. (1966). [Phospholipid micelles]. Ann Pharm Fr, 24(2), 89-92.

Saxe, G., Stoddard, F., Courtney, D., Cunningham, K., Chawla, N., Sheridan, R., . . . King, L. (2001). Relationship between acute morphine and the course of PTSD in children with burns. J Am Acad Child Adolesc Psychiatry, 40(8), 915-921. doi:10.1097/00004583-200108000-00013

Sayeed, M. M. (2005). Inflammatory/cardiovascular-metabolic responses in a rat model of burn injury with superimposed infection. Shock, 24, 40-44. doi:DOI 10.1097/01.shk.0000191412.56343.1e

Scheller, J., Chalaris, A., Schmidt-Arras, D., & Rose-John, S. (2011). The pro- and anti-inflammatory properties of the cytokine interleukin-6. Biochim Biophys Acta, 1813(5), 878-888. doi:10.1016/j.bbamcr.2011.01.034

Schiavon, M., Di Landro, D., Baldo, M., De Silvestro, G., & Chiarelli, A. (1988). A study of renal damage in seriously burned patients. Burns Incl Therm Inj, 14(2), 107-112.

Schiller, W. R., & Bay, R. C. (1996). Hemodynamic and oxygen transport monitoring in management of burns. New Horiz, 4(4), 475-482.

Schilling, T., & Eder, C. (2009a). Lysophosphatidylcholine- and MCP-1-induced chemotaxis of monocytes requires potassium channel activity. Pflugers Arch, 459(1), 71-77. doi:10.1007/s00424-009-0710-y

Schilling, T., & Eder, C. (2009b). Non-selective cation channel activity is required for lysophosphatidylcholine-induced monocyte migration. J Cell Physiol, 221(2), 325-334. doi:10.1002/jcp.21857

Schilling, T., & Eder, C. (2010). Stimulus-dependent requirement of ion channels for microglial NADPH oxidase-mediated production of reactive oxygen species. J Neuroimmunol, 225(1-2), 190-194. doi:10.1016/j.jneuroim.2010.05.024

Schmelz, M., & Petersen, L. J. (2001). Neurogenic inflammation in human and rodent skin. News Physiol Sci, 16, 33-37.

Schmidt, D., & MacKinnon, R. (2008). Voltage-dependent K+ channel gating and voltage sensor toxin sensitivity depend on the mechanical state of the lipid membrane. Proc Natl Acad Sci U S A, 105(49), 19276-19281. doi:10.1073/pnas.0810187105

Schmidt, R., Schmelz, M., Forster, C., Ringkamp, M., Torebjork, E., & Handwerker, H. (1995). Novel classes of responsive and unresponsive C nociceptors in human skin. J Neurosci, 15(1 Pt 1), 333-341.

Schneider, J. C., Holavanahalli, R., Helm, P., Goldstein, R., & Kowalske, K. (2006). Contractures in burn injury: defining the problem. J Burn Care Res, 27(4), 508-514. doi:10.1097/01.BCR.0000225994.75744.9D

Scholzen, T., Armstrong, C. A., Bunnett, N. W., Luger, T. A., Olerud, J. E., & Ansel, J. C. (1998). Neuropeptides in the skin: interactions between the neuroendocrine and the skin immune systems. Experimental Dermatology, 7(2-3), 81-96.

Schroder, K., Hertzog, P. J., Ravasi, T., & Hume, D. A. (2004). Interferon-gamma: an overview of signals, mechanisms and functions. J Leukoc Biol, 75(2), 163-189. doi:10.1189/jlb.0603252

Schulte, W., Bernhagen, J., & Bucala, R. (2013). Cytokines in sepsis: potent immunoregulators and potential therapeutic targets--an updated view. Mediators Inflamm, 2013, 165974. doi:10.1155/2013/165974

Schultz, A. M., Werba, A., & Wolrab, C. (1997). Early cardiorespiratory patterns in severely burned patients with concomitant inhalation injury. Burns, 23(5), 421-425.

Schulz, D. J., Temporal, S., Barry, D. M., & Garcia, M. L. (2008). Mechanisms of voltage-gated ion channel regulation: from gene expression to localization. Cell Mol Life Sci, 65(14), 2215-2231. doi:10.1007/s00018-008-8060-z

Schwacha, M. G. (2003). Macrophages and post-burn immune dysfunction. Burns, 29(1), 1-14.

Sedlis, S. P., Hom, M., Sequeira, J. M., & Esposito, R. (1993). Lysophosphatidylcholine accumulation in ischemic human myocardium. J Lab Clin Med, 121(1), 111-117.

Sedlis, S. P., Hom, M., Sequeira, J. M., Tritel, M., Gindea, A., Ladenson, J. H., . . . Esposito, R. (1997). Time course of lysophosphatidylcholine release from ischemic human myocardium parallels the time course of early ischemic ventricular arrhythmia. Coron Artery Dis, 8(1), 19-27.

Segond von Banchet, G., Pastor, A., Biskup, C., Schlegel, C., Benndorf, K., & Schaible, H. G. (2002). Localization of functional calcitonin gene-related peptide binding sites in a subpopulation of cultured dorsal root ganglion neurons. Neuroscience, 110(1), 131-145.

Segond von Banchet, G., Scholze, A., & Schaible, H. G. (2003). Prostaglandin E2 increases the expression of the neurokinin1 receptor in adult sensory neurones in culture: a novel role of prostaglandins. Br J Pharmacol, 139(3), 672-680. doi:10.1038/sj.bjp.0705278

Sekine, K., Fujishima, S., Sasaki, J., Ishizaka, A., Aiso, S., & Aikawa, N. (2009). In vivo IL-18 supplementation ameliorates lethal acute lung injury in burn-primed endotoxemic mice: a novel anti-inflammatory role of IL-18. Shock, 32(5), 554-562. doi:10.1097/SHK.0b013e31819e2db6

Senatore, A., Boone, A. N., & Spafford, J. D. (2011). Optimized transfection strategy for expression and electrophysiological recording of recombinant voltage-gated ion channels in HEK-293T cells. J Vis Exp(47). doi:10.3791/2314

Sener, G., Sehirli, A. O., Satiroglu, H., Keyer-Uysal, M., & Yegen, B. C. (2002). Melatonin improves oxidative organ damage in a rat model of thermal injury. Burns, 28(5), 419-425.

Shackleton C. H. L., Marcos P. G. M. (2006). Steroid profiling: diagnosis of disorders affecting steroid synthesis and metabolism. In: Gross, M., Caprioli, R. (Eds.), The Encyclopedia of Mass Spectrometry (pp. 789-813). Amsterdam: Elsevier.

Shalaby, M. R., Waage, A., Aarden, L., & Espevik, T. (1989). Endotoxin, tumor necrosis factor-alpha and interleukin 1 induce interleukin 6 production in vivo. Clin Immunol Immunopathol, 53(3), 488-498.

Shalita, A. R., Smith, J. G., Parish, L. C., Sofman, M. S., & Chalker, D. K. (1995). Topical nicotinamide compared with clindamycin gel in the treatment of inflammatory acne vulgaris. Int J Dermatol, 34(6), 434-437.

Shallo, H., Plackett, T. P., Heinrich, S. A., & Kovacs, E. J. (2003). Monocyte chemoattractant protein-1 (MCP-1) and macrophage infiltration into the skin after burn injury in aged mice. Burns, 29(7), 641-647.

Shehab El-Din, A., Salama, Shouman. (1996). Serum cytokines following thermal injury. Ann Burns Fire Disasters, 9, 18-23.

Shelhamer, M. C., Rowan, M. P., Cancio, L. C., Aden, J. K., Rhie, R. Y., Merrill, G. A., . . . Chung, K. K. (2015). Elevations in inflammatory cytokines are associated with poor outcomes in mechanically ventilated burn patients. J Trauma Acute Care Surg, 79(3), 431-436. doi:10.1097/TA.0000000000000786

Shen, H., de Almeida, P. E., Kang, K. H., Yao, P., & Chan, C. W. (2012). Burn injury triggered dysfunction in dendritic cell response to TLR9 activation and resulted in skewed T cell functions. PLoS One, 7(11), e50238. doi:10.1371/journal.pone.0050238

Shih, B., Garside, E., McGrouther, D. A., & Bayat, A. (2010). Molecular dissection of abnormal wound healing processes resulting in keloid disease. Wound Repair Regen, 18(2), 139-153. doi:10.1111/j.1524-475X.2009.00553.x

Shimizu, H., Oh, I. S., Okada, S., & Mori, M. (2005). Inhibition of appetite by nasal leptin administration in rats. Int J Obes (Lond), 29(7), 858-863. doi:10.1038/sj.ijo.0802951

Shin, J., Cho, H., Hwang, S. W., Jung, J., Shin, C. Y., Lee, S. Y., . . . Oh, U. (2002). Bradykinin-12-lipoxygenase-VR1 signaling pathway for inflammatory hyperalgesia. Proc Natl Acad Sci U S A, 99(15), 10150-10155. doi:10.1073/pnas.152002699

Shoup, M., He, L. K., Liu, H., Shankar, R., & Gamelli, R. (1998). Cyclooxygenase-2 inhibitor NS-398 improves survival and restores leukocyte counts in burn infection. J Trauma, 45(2), 215-220; discussion 220-211.

Shults, J. A., Curtis, B. J., Chen, M. M., O'Halloran, E. B., Ramirez, L., & Kovacs, E. J. (2015). Impaired respiratory function and heightened pulmonary inflammation in episodic binge ethanol intoxication and burn injury. Alcohol, 49(7), 713-720. doi:10.1016/j.alcohol.2015.06.006

Shupp, J. W., Nasabzadeh, T. J., Rosenthal, D. S., Jordan, M. H., Fidler, P., & Jeng, J. C. (2010). A review of the local pathophysiologic bases of burn wound progression. J Burn Care Res, 31(6), 849-873.

Sierra-Honigmann, M. R., Nath, A. K., Murakami, C., Garcia-Cardena, G., Papapetropoulos, A., Sessa, W. C., . . . Flores-Riveros, J. R. (1998). Biological action of leptin as an angiogenic factor. Science, 281(5383), 1683-1686.

Silliman, C. C., Elzi, D. J., Ambruso, D. R., Musters, R. J., Hamiel, C., Harbeck, R. J., . . . Bannerjee, A. (2003). Lysophosphatidylcholines prime the NADPH oxidase and stimulate multiple neutrophil functions through changes in cytosolic calcium. J Leukoc Biol, 73(4), 511-524.

Singaravelu, K., Lohr, C., & Deitmer, J. W. (2006). Regulation of store-operated calcium entry by calcium-independent phospholipase A2 in rat cerebellar astrocytes. J Neurosci, 26(37), 9579-9592. doi:10.1523/jneurosci.2604-06.2006

Singer, A. J., & Clark, R. A. (1999). Cutaneous wound healing. N Engl J Med, 341(10), 738-746. doi:10.1056/nejm199909023411006

Singer, A. J., McClain, S. A., Taira, B. R., Guerriero, J. L., & Zong, W. (2008). Apoptosis and necrosis in the ischemic zone adjacent to third degree burns. Acad Emerg Med, 15(6), 549-554. doi:10.1111/j.1553-2712.2008.00115.x

Singh, V., Devgan, L., Bhat, S., & Milner, S. M. (2007). The pathogenesis of burn wound conversion. Ann Plast Surg, 59(1), 109-115. doi:10.1097/01.sap.0000252065.90759.e6

Sivilotti, L., & Woolf, C. J. (1994). The contribution of GABAA and glycine receptors to central sensitization: disinhibition and touch-evoked allodynia in the spinal cord. Journal of Neurophysiology, 72(1), 169-179.

Sluka, K. A., Price, M. P., Breese, N. M., Stucky, C. L., Wemmie, J. A., & Welsh, M. J. (2003). Chronic hyperalgesia induced by repeated acid injections in muscle is abolished by the loss of ASIC3, but not ASIC1. Pain, 106(3), 229-239.

Smith, C. A., O'Maille, G., Want, E. J., Qin, C., Trauger, S. A., Brandon, T. R., . . . Siuzdak, G. (2005). METLIN: a metabolite mass spectral database. Ther Drug Monit, 27(6), 747-751.

Smith, C. A., Want, E. J., O'Maille, G., Abagyan, R., & Siuzdak, G. (2006). XCMS: processing mass spectrometry data for metabolite profiling using nonlinear peak alignment, matching, and identification. Analytical Chemistry, 78(3), 779-787. doi:10.1021/ac051437y

Smith, E. S., & Lewin, G. R. (2009). Nociceptors: a phylogenetic view. J Comp Physiol A Neuroethol Sens Neural Behav Physiol, 195(12), 1089-1106. doi:10.1007/s00359-009-0482-z

Smith, G. D., Gunthorpe, M. J., Kelsell, R. E., Hayes, P. D., Reilly, P., Facer, P., . . . Davis, J. B. (2002). TRPV3 is a temperature-sensitive vanilloid receptor-like protein. Nature, 418(6894), 186-190. doi:10.1038/nature00894

Smith, K. J., Hall, S. M., & Schauf, C. L. (1985). Vesicular demyelination induced by raised intracellular calcium. J Neurol Sci, 71(1), 19-37.

Smith, Y. R., Klitzman, B., Ellis, M. N., & Kull, F. C., Jr. (1989). The effect of nicotinamide on microvascular density and thermal injury in rats. J Surg Res, 47(5), 465-469.

Sneve, H. (1905). The treatment of burns and skin grafting. JAMA Neurol, 45, 1.

Snider, W. D., & McMahon, S. B. (1998). Tackling pain at the source: new ideas about nociceptors. Neuron, 20(4), 629-632.

So, I., Chae, M. R., Kim, S. J., & Lee, S. W. (2005). Lysophosphatidylcholine, a component of atherogenic lipoproteins, induces the change of calcium mobilization via TRPC ion channels in cultured human corporal smooth muscle cells. Int J Impot Res, 17(6), 475-483. doi:10.1038/sj.ijir.3901356

Song, J., Liu, K., Yi, J., Zhu, D., Liu, G., & Liu, B. (2010). Luteolin inhibits lysophosphatidylcholine-induced apoptosis in endothelial cells by a calcium/mitocondrion/caspases-dependent pathway. Planta Med, 76(5), 433-438. doi:10.1055/s-0029-1186197

Souslova, V., Cesare, P., Ding, Y., Akopian, A. N., Stanfa, L., Suzuki, R., . . . Wood, J. N. (2000). Warm-coding deficits and aberrant inflammatory pain in mice lacking P2X3 receptors. Nature, 407(6807), 1015-1017. doi:10.1038/35039526

Spagou, K., Tsoukali, H., Raikos, N., Gika, H., Wilson, I. D., Theodoridis, G. (2010). Hydrophilic interaction chromatography coupled to MS for metabonomic/metabolomic studies. J Sep Sci 33(6-7): 716-727.

St-Jacques, B., & Ma, W. (2011). Role of prostaglandin E2 in the synthesis of the pro-inflammatory cytokine interleukin-6 in primary sensory neurons: an in vivo and in vitro study. Journal of Neurochemistry, 118(5), 841-854. doi:10.1111/j.1471-4159.2011.07230.x

St Pierre, M., Reeh, P. W., & Zimmermann, K. (2009). Differential effects of TRPV channel block on polymodal activation of rat cutaneous nociceptors in vitro. Exp Brain Res, 196(1), 31-44. doi:10.1007/s00221-009-1808-3

Stahlman, M., Fagerberg, B., Adiels, M., Ekroos, K., Chapman, J. M., Kontush, A., & Boren, J. (2013). Dyslipidemia, but not hyperglycemia and insulin resistance, is associated with marked alterations in the HDL lipidome in type 2 diabetic subjects in the DIWA cohort: impact on small HDL particles. Biochim Biophys Acta, 1831(11), 1609-1617. doi:10.1016/j.bbalip.2013.07.009

Steen, K. H., Reeh, P. W., Anton, F., & Handwerker, H. O. (1992). Protons selectively induce lasting excitation and sensitization to mechanical stimulation of nociceptors in rat skin, in vitro. J Neurosci, 12(1), 86-95.

Steffey, E. P. and D. Howland, Jr. (1980). Comparison of circulatory and respiratory effects of isoflurane and halothane anesthesia in horses. Am J Vet Res 41(5): 821-825.
Stein, A. T., Ufret-Vincenty, C. A., Hua, L., Santana, L. F., & Gordon, S. E. (2006). Phosphoinositide 3-kinase binds to TRPV1 and mediates NGF-stimulated TRPV1 trafficking to the plasma membrane. J Gen Physiol, 128(5), 509-522. doi:10.1085/jgp.200609576
Stenken, J. A., Church, M. K., Gill, C. A., & Clough, G. F. (2010). How minimally invasive is microdialysis sampling? A cautionary note for cytokine collection in human skin and other clinical studies. Aaps j, 12(1), 73-78. doi:10.1208/s12248-009-9163-7
Stenson, W. F., & Parker, C. W. (1980). Monohydroxyeicosatetraenoic acids (HETEs) induce degranulation of human neutrophils. J Immunol, 124(5), 2100-2104.
Stoddard, F. J., Jr., Ryan, C. M., & Schneider, J. C. (2014). Physical and psychiatric recovery from burns. Surg Clin North Am, 94(4), 863-878. doi:10.1016/j.suc.2014.05.007
Stokes, E. L., Flecknell, P. A., Richardson, C. A. (2009). Reported analgesic and anaesthetic administration to rodents undergoing experimental surgical procedures. Lab Anim 43(2): 149-154.
Story, G. M., Peier, A. M., Reeve, A. J., Eid, S. R., Mosbacher, J., Hricik, T. R., . . . Patapoutian, A. (2003). ANKTM1, a TRP-like channel expressed in nociceptive neurons, is activated by cold temperatures. Cell, 112(6), 819-829.
Strong, V. E., Mackrell, P. J., Concannon, E. M., Naama, H. A., Schaefer, P. A., Shaftan, G. W., . . . Daly, J. M. (2000). Blocking prostaglandin E2 after trauma attenuates pro-inflammatory cytokines and improves survival. Shock, 14(3), 374-379.
Struzyna, J., Pojda, Z., Braun, B., Chomicka, M., Sobiczewska, E., & Wrembel, J. (1995). Serum cytokine levels (IL-4, IL-6, IL-8, G-CSF, GM-CSF) in burned patients. Burns, 21(6), 437-440.
Stubbe, J. (1990). Ribonucleotide reductases: amazing and confusing. Journal of Biological Chemistry, 265(10), 5329-5332.
Stuhmer, W., Conti, F., Suzuki, H., Wang, X. D., Noda, M., Yahagi, N., . . . Numa, S. (1989). Structural parts involved in activation and inactivation of the sodium channel. Nature, 339(6226), 597-603. doi:10.1038/339597a0
Subbaiah, P. V., & Liu, M. (1996). Comparative studies on the substrate specificity of lecithin:cholesterol acyltransferase towards the molecular species of phosphatidylcholine in the plasma of 14 vertebrates. J Lipid Res, 37(1), 113-122.
Sugiura, T., Tominaga, M., Katsuya, H., & Mizumura, K. (2002). Bradykinin lowers the threshold temperature for heat activation of vanilloid receptor 1. Journal of Neurophysiology, 88(1), 544-548.
Sukharev, S. I., Blount, P., Martinac, B., Blattner, F. R., & Kung, C. (1994). A large-conductance mechanosensitive channel in E. coli encoded by mscL alone. Nature, 368(6468), 265-268. doi:10.1038/368265a0
Sukharev, S. I., Martinac, B., Arshavsky, V. Y., & Kung, C. (1993). Two types of mechanosensitive channels in the Escherichia coli cell envelope: solubilization and functional reconstitution. Biophys J, 65(1), 177-183. doi:10.1016/s0006-3495(93)81044-0
Summer, G. J., Puntillo, K. A., Miaskowski, C., Green, P. G., & Levine, J. D. (2007). Burn injury pain: the continuing challenge. J Pain, 8(7), 533-548. doi:10.1016/j.jpain.2007.02.426
Summer, G. J., Romero-Sandoval, E. A., Bogen, O., Dina, O. A., Khasar, S. G., & Levine, J. D. (2008). Proinflammatory cytokines mediating burn-injury pain. Pain, 135(1-2), 98-107. doi:10.1016/j.pain.2007.05.012
Sundaram, J. R., Chan, E. S., Poore, C. P., Pareek, T. K., Cheong, W. F., Shui, G., . . . Kesavapany, S. (2012). Cdk5/p25-induced cytosolic PLA2-mediated lysophosphatidylcholine production regulates neuroinflammation and triggers neurodegeneration. J Neurosci, 32(3), 1020-1034. doi:10.1523/jneurosci.5177-11.2012
Suzuki, M., Mizuno, A., Kodaira, K., & Imai, M. (2003). Impaired pressure sensation in mice lacking TRPV4. Journal of Biological Chemistry, 278(25), 22664-22668. doi:10.1074/jbc.M302561200
Swartz, M. E. (2005). UPLC™: An Introduction and Review. Journal of Liquid Chromatography & Related Technologies 28(7-8): 1253-1263.
Sysi-Aho, M., Katajamaa, M., Yetukuri, L., Oresic, M. (2007). Normalization method for metabolomics data using optimal selection of multiple internal standards. BMC Bioinformatics 8: 93.
Szucs, P., Polgar, E., Spigelman, I., Porszasz, R., & Nagy, I. (1999). Neurokinin-1 receptor expression in dorsal root ganglion neurons of young rats. J Peripher Nerv Syst, 4(3-4), 270-278.
Tabas, I., & Glass, C. K. (2013). Anti-inflammatory therapy in chronic disease: challenges and opportunities. Science, 339(6116), 166-172. doi:10.1126/science.1230720

Taheri, P. A., Lippton, H. L., Force, S. D., Franklin, E. W., Hyman, A. L., Flint, L. M., & Ferrara, J. J. (1994). Analysis of regional hemodynamic regulation in response to scald injury. Journal of Clinical Investigation, 93(1), 147-154. doi:10.1172/jci116938

Takabe, W., Kanai, Y., Chairoungdua, A., Shibata, N., Toi, S., Kobayashi, M., . . . Noguchi, N. (2004). Lysophosphatidylcholine enhances cytokine production of endothelial cells via induction of L-type amino acid transporter 1 and cell surface antigen 4F2. Arterioscler Thromb Vasc Biol, 24(9), 1640-1645. doi:10.1161/01.atv.0000134377.17680.26

Takahara, N., Kashiwagi, A., Maegawa, H., & Shigeta, Y. (1996). Lysophosphatidylcholine stimulates the expression and production of MCP-1 by human vascular endothelial cells. Metabolism, 45(5), 559-564.

Takahashi, M., Okazaki, H., Ogata, Y., Takeuchi, K., Ikeda, U., & Shimada, K. (2002). Lysophosphatidylcholine induces apoptosis in human endothelial cells through a p38-mitogen-activated protein kinase-dependent mechanism. Atherosclerosis, 161(2), 387-394.

Takeda, M., Kitagawa, J., Takahashi, M., & Matsumoto, S. (2008). Activation of interleukin-1beta receptor suppresses the voltage-gated potassium currents in the small-diameter trigeminal ganglion neurons following peripheral inflammation. Pain, 139(3), 594-602. doi:10.1016/j.pain.2008.06.015

Takeshita, S., Inoue, N., Gao, D., Rikitake, Y., Kawashima, S., Tawa, R., . . . Yokoyama, M. (2000). Lysophosphatidylcholine enhances superoxide anions production via endothelial NADH/NADPH oxidase. Journal of Atherosclerosis and Thrombosis, 7(4), 238-246.

Talavera, K., Yasumatsu, K., Voets, T., Droogmans, G., Shigemura, N., Ninomiya, Y., . . . Nilius, B. (2005). Heat activation of TRPM5 underlies thermal sensitivity of sweet taste. Nature, 438(7070), 1022-1025. doi:10.1038/nature04248

Tamam, Y., Tamam, C., Tamam, B., Ustundag, M., Orak, M., & Tasdemir, N. (2013). Peripheral neuropathy after burn injury. Eur Rev Med Pharmacol Sci, 17 Suppl 1, 107-111.

Tambeli, C. H., Oliveira, M. C., Clemente, J. T., Pelegrini-da-Silva, A., & Parada, C. A. (2006). A novel mechanism involved in 5-hydroxytryptamine-induced nociception: the indirect activation of primary afferents. Neuroscience, 141(3), 1517-1524. doi:10.1016/j.neuroscience.2006.04.030

Tan, J., He, W., Luo, G., & Wu, J. (2015). iTRAQ-based proteomic profiling reveals different protein expression between normal skin and hypertrophic scar tissue. Burns Trauma, 3, 13. doi:10.1186/s41038-015-0016-6

Tan, M., Hao, F., Xu, X., Chisolm, G. M., & Cui, M. Z. (2009). Lysophosphatidylcholine activates a novel PKD2-mediated signaling pathway that controls monocyte migration. Arterioscler Thromb Vasc Biol, 29(9), 1376-1382. doi:10.1161/atvbaha.109.191585

Tan, Q., Lin, Z., Ma, W., Chen, H., Wang, L., Ning, G., & Zhou, X. (2002). Failure of Ibuprofen to prevent progressive dermal ischemia after burning in guinea pigs. Burns, 28(5), 443-448.

Tanaka, T., Ikeda, K., Yamamoto, Y., Iida, H., Kikuchi, H., Morita, T., . . . Nakajima, T. (2011). Effects of serum amyloid a and lysophosphatidylcholine on intracellular calcium concentration in human coronary artery smooth muscle cells. Int Heart J, 52(3), 185-193.

Tannenbaum, A. and H. Silverstone (1958). Urethan (ethyl carbamate) as a multipotential carcinogen. Cancer Res 18(10): 1225-1231.

Tautenhahn, R., Böttcher, C., Neumann, S. (2008). Highly sensitive feature detection for high resolution LC/MS. BMC Bioinformatics, 1(9), 504-519.

Thombs, B. D., Haines, J. M., Bresnick, M. G., Magyar-Russell, G., Fauerbach, J. A., & Spence, R. J. (2007). Depression in burn reconstruction patients: symptom prevalence and association with body image dissatisfaction and physical function. Gen Hosp Psychiatry, 29(1), 14-20. doi:10.1016/j.genhosppsych.2006.09.002

Thompson, S. W., Dray, A., McCarson, K. E., Krause, J. E., & Urban, L. (1995). Nerve growth factor induces mechanical allodynia associated with novel A fibre-evoked spinal reflex activity and enhanced neurokinin-1 receptor activation in the rat. Pain, 62(2), 219-231.

Tian, Y. H., Wang, S. X., Ma, Y. X., Lim, G., Kim, H., & Mao, J. R. (2011). Leptin enhances NMDA-induced spinal excitation in rats: A functional link between adipocytokine and neuropathic pain. Pain, 152(6), 1263-1271. doi:10.1016/j.pain.2011.01.054

Tigyi, G. (2011). Lipids: LPA activates TRPV1--and it hurts. Nat Chem Biol, 8(1), 22-23. doi:10.1038/nchembio.738

Tilg, H., Dinarello, C. A., & Mier, J. W. (1997). IL-6 and APPs: anti-inflammatory and immunosuppressive mediators. Immunol Today, 18(9), 428-432.

Till, G. O., Beauchamp, C., Menapace, D., Tourtellotte, W., Jr., Kunkel, R., Johnson, K. J., & Ward, P. A. (1983). Oxygen radical dependent lung damage following thermal injury of rat skin. J Trauma, 23(4), 269-277.

Ting, E., Roveroni, R. C., Ferrari, L. F., Lotufo, C. M., Veiga, M. C., Parada, C. A., & Tambeli, C. H. (2007). Indirect mechanism of histamine-induced nociception in temporomandibular joint of rats. Life Sci, 81(9), 765-771. doi:10.1016/j.lfs.2007.07.012

Tirumala N, Kumar S. V., Sathyadev M., Ande J. D., Guguloth K., Kiran C. R., & N., C. (2013). Assessment of quality of life in Thermal (flame) burn patients: An observational study at Tertiary Care Teaching Hospital in Warangal, A.P., India International Journal of Pharmacy and Life Sciences, 4(12), 3151-3158.

Todaka, H., Taniguchi, J., Satoh, J., Mizuno, A., & Suzuki, M. (2004). Warm temperature-sensitive transient receptor potential vanilloid 4 (TRPV4) plays an essential role in thermal hyperalgesia. Journal of Biological Chemistry, 279(34), 35133-35138. doi:10.1074/jbc.M406260200

Toliver-Kinsky, T. E., Varma, T. K., Lin, C. Y., Herndon, D. N., & Sherwood, E. R. (2002). Interferon-gamma production is suppressed in thermally injured mice: decreased production of regulatory cytokines and corresponding receptors. Shock, 18(4), 322-330.

Tolstikov, V. V. and O. Fiehn (2002). Analysis of highly polar compounds of plant origin: combination of hydrophilic interaction chromatography and electrospray ion trap mass spectrometry. Anal Biochem 301(2): 298-307.

Tomera, J. F., Martyn, J., & Hoaglin, D. C. (1988). Neuromuscular dysfunction in burns and its relationship to burn size, hypermetabolism, and immunosuppression. J Trauma, 28(10), 1499-1504.

Tong, N., Perry, S. W., Zhang, Q., James, H. J., Guo, H., Brooks, A., . . . Gelbard, H. A. (2000). Neuronal fractalkine expression in HIV-1 encephalitis: Roles for macrophage recruitment and neuroprotection in the central nervous system. J Immunol, 164(3), 1333-1339.

Török, Z., Crul, T., Maresca, B., Schütz, G. J., Viana, F., Dindia, L., . . . Vigh, L. (2014). Plasma membranes as heat stress sensors: From lipid-controlled molecular switches to therapeutic applications. Biochimica et Biophysica Acta (BBA) - Biomembranes, 1838(6), 1594-1618. doi:http://dx.doi.org/10.1016/j.bbamem.2013.12.015

Torok, Z., Crul, T., Maresca, B., Schutz, G. J., Viana, F., Dindia, L., . . . Vigh, L. (2014). Plasma membranes as heat stress sensors: from lipid-controlled molecular switches to therapeutic applications. Biochim Biophys Acta, 1838(6), 1594-1618. doi:10.1016/j.bbamem.2013.12.015

Torpy, D. J., Bornstein, S. R., & Chrousos, G. P. (1998). Leptin and interleukin-6 in sepsis. Hormone and Metabolic Research, 30(12), 726-729. doi:DOI 10.1055/s-2007-978967

Torsney, C., & MacDermott, A. B. (2006). Disinhibition opens the gate to pathological pain signaling in superficial neurokinin 1 receptor-expressing neurons in rat spinal cord. J Neurosci, 26(6), 1833-1843. doi:10.1523/jneurosci.4584-05.2006

Toyomoto, M., Ohta, M., Okumura, K., Yano, H., Matsumoto, K., Inoue, S., . . . Ikeda, K. (2004). Prostaglandins are powerful inducers of NGF and BDNF production in mouse astrocyte cultures. FEBS Lett, 562(1-3), 211-215. doi:10.1016/s0014-5793(04)00246-7

Tranbaugh, R. F., Lewis, F. R., Christensen, J. M., & Elings, V. B. (1980). Lung water changes after thermal injury. The effects of crystalloid resuscitation and sepsis. Ann Surg, 192(4), 479-490.

Tredget, E. E., & Yu, Y. M. (1992). The metabolic effects of thermal injury. World J Surg, 16(1), 68-79.

Trevisani, M., Smart, D., Gunthorpe, M. J., Tognetto, M., Barbieri, M., Campi, B., . . . Geppetti, P. (2002). Ethanol elicits and potentiates nociceptor responses via the vanilloid receptor-1. Nature Neuroscience, 5(6), 546-551. doi:10.1038/nn852

Tsuboi, R., Shi, C. M., Rifkin, D. B., & Ogawa, H. (1992). A wound healing model using healing-impaired diabetic mice. J Dermatol, 19(11), 673-675.

Tsuchiya, T., Shimizu, H., Horie, T., & Mori, M. (1999). Expression of leptin receptor in lung: leptin as a growth factor. European Journal of Pharmacology, 365(2-3), 273-279.

Tsuda, M., Shigemoto-Mogami, Y., Koizumi, S., Mizokoshi, A., Kohsaka, S., Salter, M. W., & Inoue, K. (2003). P2X4 receptors induced in spinal microglia gate tactile allodynia after nerve injury. Nature, 424(6950), 778-783. doi:10.1038/nature01786

Tsuji, F., & Aono, H. (2012). Role of transient receptor potential vanilloid 1 in inflammation and autoimmune diseases. Pharmaceuticals (Basel), 5(8), 837-852. doi:10.3390/ph5080837

Tsujimoto, Y. (1997). Apoptosis and necrosis: intracellular ATP level as a determinant for cell death modes. Cell Death Differ, 4(6), 429-434. doi:10.1038/sj.cdd.4400262

Turinsky, J., & Chaudry, I. H. (1985). Phospholipid and adenine nucleotide metabolism in muscle after burn injury. Am J Physiol, 249(5 Pt 2), R603-610.

Turnage, R. H., Nwariaku, F., Murphy, J., Schulman, C., Wright, K., & Yin, H. (2002). Mechanisms of pulmonary microvascular dysfunction during severe burn injury. World J Surg, 26(7), 848-853. doi:10.1007/s00268-002-4063-3

Turner, H., Fleig, A., Stokes, A., Kinet, J. P., & Penner, R. (2003). Discrimination of intracellular calcium store subcompartments using TRPV1 (transient receptor potential channel, vanilloid subfamily member 1) release channel activity. Biochemical Journal, 371(Pt 2), 341-350. doi:10.1042/bj20021381

Twine, N. A., Janitz, K., Wilkins, M. R., & Janitz, M. (2011). Whole Transcriptome Sequencing Reveals Gene Expression and Splicing Differences in Brain Regions Affected by Alzheimer's Disease. PLoS One, 6(1), e16266. doi:10.1371/journal.pone.0016266

Uhlen, M., Fagerberg, L., Hallström, B. M., Lindskog, C., Oksvold, P., Mardinoglu, A., Sivertsson, Å., Kampf, C., Sjöstedt, E., Asplund, A., Olsson, I., Edlund, K., Lundberg, E., Navani, S., Szigyarto, C. A., Odeberg, J., Djureinovic, D., Takanen, J. O., Hober, S., Alm, T., Edqvist, P. H., Berling, H., Tegel, H., Mulder, J., Rockberg, J., Nilsson, P., Schwenk, J. M., Hamsten, M., von Feilitzen, K., Forsberg, M., Persson, L., Johansson, F., Zwahlen, M., von Heijne, G., Nielsen, J., Pontén, F. (2015). Proteomics. Tissue-based map of the human proteome. Science 347(6220): 1260419.

Umehara, H., Bloom, E. T., Okazaki, T., Nagano, Y., Yoshie, O., & Imai, T. (2004). Fractalkine in vascular biology - From basic research to clinical disease. Arteriosclerosis Thrombosis and Vascular Biology, 24(1), 34-40. doi:10.1161/01.Atv.0000095360.62479.1f

Ungerstedt, U. (1991). Microdialysis--principles and applications for studies in animals and man. J Intern Med, 230(4), 365-373.

Ungerstedt, U., & Pycock, C. (1974). Functional correlates of dopamine neurotransmission. Bull Schweiz Akad Med Wiss, 30(1-3), 44-55.

Uygur, F., Evinc, R., Urhan, M., Celikoz, B., & Haholu, A. (2009). Salvaging the zone of stasis by simvastatin: an experimental study in rats. J Burn Care Res, 30(5), 872-879. doi:10.1097/BCR.0b013e3181b47eb8

Vaisse, C., Halaas, J. L., Horvath, C. M., Darnell, J. E., Stoffel, M., & Friedman, J. M. (1996). Leptin activation of Stat3 in the hypothalamus of wildtype and ob/ob mice but not db/db mice. Nature Genetics, 14(1), 95-97. doi:Doi 10.1038/Ng0996-95

Valente, P., Garcia-Sanz, N., Gomis, A., Fernandez-Carvajal, A., Fernandez-Ballester, G., Viana, F., . . . Ferrer-Montiel, A. (2008). Identification of molecular determinants of channel gating in the transient receptor potential box of vanilloid receptor I. Faseb Journal, 22(9), 3298-3309. doi:10.1096/fj.08-107425

van de Goot, F., Krijnen, P. A., Begieneman, M. P., Ulrich, M. M., Middelkoop, E., & Niessen, H. W. (2009). Acute inflammation is persistent locally in burn wounds: a pivotal role for complement and C-reactive protein. J Burn Care Res, 30(2), 274-280. doi:10.1097/BCR.0b013e318198a252

van den Berg, R. A., Hoefsloot, H. C. J., Westerhuis, J. A., Smilde, A. K., & van der Werf Më, J. (2006). Centering, scaling, and transformations: improving the biological information content of metabolomics data. BMC Genomics, 7, 142. doi:10.1186/1471-2164-7-142

van den Brink-van der Laan, E., Killian, J. A., & de Kruijff, B. (2004). Nonbilayer lipids affect peripheral and integral membrane proteins via changes in the lateral pressure profile. Biochim Biophys Acta, 1666(1-2), 275-288. doi:10.1016/j.bbamem.2004.06.010

Vanden Abeele, F., Kondratskyi, A., Dubois, C., Shapovalov, G., Gkika, D., Busserolles, J., . . . Prevarskaya, N. (2013). Complex modulation of the cold receptor TRPM8 by volatile anaesthetics and its role in complications of general anaesthesia. Journal of Cell Science, 126(19), 4479-4489. doi:10.1242/jcs.131631

Veenstra, T. D. (2012). Metabolomics: the final frontier? Genome Med, 4(4), 40. doi:10.1186/gm339

Veldhuis, N. A., Lew, M. J., Abogadie, F. C., Poole, D. P., Jennings, E. A., Ivanusic, J. J., . . . McIntyre, P. (2012). N-glycosylation determines ionic permeability and desensitization of the TRPV1 capsaicin receptor. Journal of Biological Chemistry, 287(26), 21765-21772. doi:10.1074/jbc.M112.342022

Vellani, V., Kinsey, A. M., Prandini, M., Hechtfischer, S. C., Reeh, P., Magherini, P. C., . . . McNaughton, P. A. (2010). Protease activated receptors 1 and 4 sensitize TRPV1 in nociceptive neurones. Mol Pain, 6, 61. doi:10.1186/1744-8069-6-61

Vellani, V., Mapplebeck, S., Moriondo, A., Davis, J. B., & McNaughton, P. A. (2001). Protein kinase C activation potentiates gating of the vanilloid receptor VR1 by capsaicin, protons, heat and anandamide. J Physiol, 534(Pt 3), 813-825.

Venkatachalam, K., & Montell, C. (2007). TRP channels. Annu Rev Biochem, 76, 387-417. doi:10.1146/annurev.biochem.75.103004.142819

Vennekens, R., Voets, T., Bindels, R. J., Droogmans, G., & Nilius, B. (2002). Current understanding of mammalian TRP homologues. Cell Calcium, 31(6), 253-264.

Vereyken, E. J., Fluitsma, D. M., Bolijn, M. J., Dijkstra, C. D., & Teunissen, C. E. (2009). An in vitro model for de- and remyelination using lysophosphatidyl choline in rodent whole brain spheroid cultures. Glia, 57(12), 1326-1340. doi:10.1002/glia.20852

Veselkov, K. A., Vingara, L. K., Masson, P., Robinette, S. L., Want, E., Li, J. V., . . . Nicholson, J. K. (2011). Optimized preprocessing of ultra-performance liquid chromatography/mass spectrometry urinary metabolic profiles for improved information recovery. Analytical Chemistry, 83(15), 5864-5872. doi:10.1021/ac201065j

Villas-Boas, S. G., Roessner, U., Hansen, M. A. E., Smedsgaard, J., and Nielsen, J. (2007). Metabolome Analysis: An Introduction. New York: John Wiley and Sons Inc.

Vindenes, H., Ulvestad, E., & Bjerknes, R. (1995). Increased levels of circulating interleukin-8 in patients with large burns: relation to burn size and sepsis. J Trauma, 39(4), 635-640.

Vlachova, V., Teisinger, J., Susankova, K., Lyfenko, A., Ettrich, R., & Vyklicky, L. (2003). Functional role of C-terminal cytoplasmic tail of rat vanilloid receptor 1. J Neurosci, 23(4), 1340-1350.

Volin, M. V., Woods, J. M., Amin, M. A., Connors, M. A., Harlow, L. A., & Koch, A. E. (2001). Fractalkine: A novel angiogenic chemokine in rheumatoid arthritis. American Journal of Pathology, 159(4), 1521-1530. doi:Doi 10.1016/S0002-9440(10)62537-0

von Banchet, G. S., Fischer, N., Uhlig, B., Hensellek, S., Eitner, A., & Schaible, H. G. (2011). Molecular effects of interleukin-1beta on dorsal root ganglion neurons: prevention of ligand-induced internalization of the bradykinin 2 receptor and downregulation of G protein-coupled receptor kinase 2. Mol Cell Neurosci, 46(1), 262-271. doi:10.1016/j.mcn.2010.09.009

Von Hoegen, I., Falk, W., Kojouharoff, G., & Krammer, P. H. (1989). Internalization of interleukin 1 (IL 1) correlates with IL 1-induced IL 2 receptor expression and IL 2 secretion of EL4 thymoma cells. Eur J Immunol, 19(2), 329-334. doi:10.1002/eji.1830190217

Vuong, T. D., de Kimpe, S., de Roos, R., Rabelink, T. J., Koomans, H. A., & Joles, J. A. (2001). Albumin restores lysophosphatidylcholine-induced inhibition of vasodilation in rat aorta. Kidney Int, 60(3), 1088-1096. doi:10.1046/j.1523-1755.2001.0600031088.x

Wade, C. E., Baer, L. A., Wu, X., Silliman, D. T., Walters, T. J., & Wolf, S. E. (2013). Severe burn and disuse in the rat independently adversely impact body composition and adipokines. Crit Care, 17(5), R225. doi:10.1186/cc13048

Wall, P. D. (1992). Sensory Mechanisms of the Spinal Cord: J Anat. 1992 Apr;180(Pt 2):352.

Wallace, A. M., Sattar, N., & McMillan, D. C. (2000). The co-ordinated cytokine/hormone response to acute injury incorporates leptin. Cytokine, 12(7), 1042-1045. doi:DOI 10.1006/cyto.2000.0674

Wallace, M. S., Quessy, S., & Schulteis, G. (2004). Lack of effect of two oral sodium channel antagonists, lamotrigine and 4030W92, on intradermal capsaicin-induced hyperalgesia model. Pharmacol Biochem Behav, 78(2), 349-355. doi:10.1016/j.pbb.2004.04.007

Wallace, V. C., Cottrell, D. F., Brophy, P. J., & Fleetwood-Walker, S. M. (2003). Focal lysolecithin-induced demyelination of peripheral afferents results in neuropathic pain behavior that is attenuated by cannabinoids. J Neurosci, 23(8), 3221-3233.

Wan, Y., & Evans, R. M. (2010). Rosiglitazone activation of PPARgamma suppresses fractalkine signaling. J Mol Endocrinol, 44(2), 135-142. doi:10.1677/JME-09-0090

Wang, H., Li, R., Zhou, X., Xue, L., Xu, X., & Liu, B. (2016). Genome-Wide Analysis and Functional Characterization of the Polyadenylation Site in Pigs Using RNAseq Data. Sci Rep, 6, 36388. doi:10.1038/srep36388

Wang, H. Y., Tsai, Y. J., Chen, S. H., Lin, C. T., & Lue, J. H. (2013). Lysophosphatidylcholine causes neuropathic pain via the increase of neuronal nitric oxide synthase in the dorsal root ganglion and cuneate nucleus. Pharmacol Biochem Behav, 106, 47-56. doi:10.1016/j.pbb.2013.03.002

Wang, P., Wang, Q., Yang, L., Qin, Q. L., & Wu, Y. J. (2015). Characterization of lysophosphatidylcholine-induced changes of intracellular calcium in Drosophila S2 cells. Life Sci, 131, 57-62. doi:10.1016/j.lfs.2015.02.014

Wang, W., Zhou, H., Lin, H., Roy, S., Shaler, T. A., Hill, L. R., Norton, S., Kumar, P., Anderle, M., Becker, C. H. (2003). Quantification of proteins and metabolites by mass spectrometry without isotopic labeling or spiked standards. Anal Chem 75(18): 4818-4826.

Wang, Y., Wang, Y., & Li, G. R. (2016). TRPC1/TRPC3 channels mediate lysophosphatidylcholine-induced apoptosis in cultured human coronary artery smooth muscles cells. Oncotarget. doi:10.18632/oncotarget.10853

Wang, Z., Gerstein, M., & Snyder, M. (2009). RNA-Seq: a revolutionary tool for transcriptomics. Nat Rev Genet, 10(1), 57-63. doi:10.1038/nrg2484
Want, E., & Masson, P. (2011). Processing and analysis of GC/LC-MS-based metabolomics data. Methods Mol Biol, 708, 277-298. doi:10.1007/978-1-61737-985-7_17
Want, E. J., Wilson, I. D., Gika, H., Theodoridis, G., Plumb, R. S., Shockcor, J., . . . Nicholson, J. K. (2010a). Global metabolic profiling procedures for urine using UPLC-MS. Nat Protoc, 5(6), 1005-1018. doi:10.1038/nprot.2010.50
Want, E. M., Metz, T. O. (2010b). MS Based Metabonomics. In: Encyclopedia of Spectroscopy and Spectrometry.
Warrack, B. M., Hnatyshyn, S., Ott, K. H., Reily, M. D., Sanders, M., Zhang, H., Drexler, D. M. (2009). Normalization strategies for metabonomic analysis of urine samples. J Chromatogr B Analyt Technol Biomed Life Sci 877(5-6): 547-552.
Wasiak, J., Paul, E., Lee, S. J., Mahar, P., Pfitzer, B., Spinks, A., . . . Gabbe, B. (2014). Patterns of recovery over 12 months following a burn injury in Australia. Injury-International Journal of the Care of the Injured, 45(9), 1459-1464. doi:DOI 10.1016/j.injury.2014.02.018
Watanabe, M., & Okada, T. (2003). Lysophosphatidylcholine-induced myocardial damage is inhibited by pretreatment with poloxamer 188 in isolated rat heart. Mol Cell Biochem, 248(1-2), 209-215.
Watson, J. J., Allen, S. J., & Dawbarn, D. (2008). Targeting nerve growth factor in pain: what is the therapeutic potential? BioDrugs, 22(6), 349-359. doi:10.2165/0063030-200822060-00002
Wearn, C. H. P. H., J; Bamford, A; Lord, J; Young, S; Moiemen, N. (2015). Metabolomic profiling to predict clinical outcomes following severe burn injury. Ann Burns Fire Disasters, 28.
Weinberg, G. L., Hertz, P. H., & Newman, J. (2004). Local anesthetic cardiac toxicity can present as late-onset hypotension, bradycardia, and asystole. Anesthesiology, 101(2), 553.
Weiss, S. J. (1986). Oxygen, ischemia and inflammation. Acta Physiol Scand Suppl, 548, 9-37.
Wells, I. C., Peitzmeier, G., & Vincent, J. K. (1986). Lecithin: cholesterol acyltransferase and lysolecithin in coronary atherosclerosis. Exp Mol Pathol, 45(3), 303-310.
Weltzien, H. U. (1979). Cytolytic and membrane-perturbing properties of lysophosphatidylcholine. Biochim Biophys Acta, 559(2-3), 259-287.
Westerink, B. H., & De Vries, J. B. (1988). Characterization of in vivo dopamine release as determined by brain microdialysis after acute and subchronic implantations: methodological aspects. Journal of Neurochemistry, 51(3), 683-687.
Westerink, B. H., Hofsteede, H. M., Damsma, G., & de Vries, J. B. (1988). The significance of extracellular calcium for the release of dopamine, acetylcholine and amino acids in conscious rats, evaluated by brain microdialysis. Naunyn Schmiedebergs Arch Pharmacol, 337(4), 373-378.
Wetzel, C., Hu, J., Riethmacher, D., Benckendorff, A., Harder, L., Eilers, A., . . . Lewin, G. R. (2007). A stomatin-domain protein essential for touch sensation in the mouse. Nature, 445(7124), 206-209. doi:10.1038/nature05394
White, J. P., Ko, C. W., Fidalgo, A. R., Cibelli, M., Paule, C. C., Anderson, P. J., Nagy, I. (2011). Severe burn injury induces a characteristic activation of extracellular signal-regulated kinase 1/2 in spinal dorsal horn neurons. European Journal of Pain, 15(7), 683-690. doi:10.1016/j.ejpain.2010.12.006
White, J. P. M., Cibelli, M., Fidalgo, A. R., Paule, C. C., Noormohamed, F., Urban, L., Nagy, I. (2010). Role of Transient Receptor Potential and Acid-sensing Ion Channels in Peripheral Inflammatory Pain. Anesthesiology, 112(3), 729-741. doi:Doi 10.1097/Aln.0b013e3181ca3179
Whitfield, P. D., German, A. J., & Noble, P. J. (2004). Metabolomics: an emerging post-genomic tool for nutrition. Br J Nutr, 92(4), 549-555.
WHO. (2008). The Global Burden of Disease - 2004 Update. Retrieved from http://www.who.int/healthinfo/global_burden_disease/GBD_report_2004update_full.pdf
WHO. (2014, 04/2014). Fact sheet N°365. Retrieved from http://www.who.int/mediacentre/factsheets/fs365/en/
Wibom, C., Surowiec, I., Moren, L., Bergstrom, P., Johansson, M., Antti, H., & Bergenheim, A. T. (2010). Metabolomic patterns in glioblastoma and changes during radiotherapy: a clinical microdialysis study. J Proteome Res, 9(6), 2909-2919. doi:10.1021/pr901088r
Wicks, I. P., & Roberts, A. W. (2016). Targeting GM-CSF in inflammatory diseases. Nat Rev Rheumatol, 12(1), 37-48. doi:10.1038/nrrheum.2015.161
Wiechman, S. A., & Patterson, D. R. (2004). Psychosocial aspects of burn injuries. BMJ, 329(7462), 391-393.
Williams, E. E., & Griffiths, T. A. (1991). Psychological consequences of burn injury. Burns, 17(6), 478-480.

Williams, F. N., Herndon, D. N., Hawkins, H. K., Lee, J. O., Cox, R. A., Kulp, G. A., M. G. (2009). The leading causes of death after burn injury in a single pediatric burn center. Crit Care, 13(6), R183. doi:10.1186/cc8170

Williams, F. N., Herndon, D. N., & Jeschke, M. G. (2009). The Hypermetabolic Response to Burn Injury and Interventions to Modify this Response. Clin Plast Surg, 36(4), 583-+. doi:DOI 10.1016/j.cps.2009.05.001

Williams, K. N., Szilagyi, A., He, L. K., Conrad, P., Halerz, M., Gamelli, R. L., Muthumalaiappan, K. (2012). Dendritic cell depletion in burn patients is regulated by MafB expression. J Burn Care Res, 33(6), 747-758. doi:10.1097/BCR.0b013e318250457f

Williams, P. I., Sarginson, R. E., & Ratcliffe, J. M. (1998). Use of methadone in the morphine-tolerant burned paediatric patient. Br J Anaesth, 80(1), 92-95.

Willis, M. S., Carlson, D. L., Dimaio, J. M., White, M. D., White, D. J., Adams, G. A. t., Giroir, B. P. (2005). Macrophage migration inhibitory factor mediates late cardiac dysfunction after burn injury. Am J Physiol Heart Circ Physiol, 288(2), H795-804. doi:10.1152/ajpheart.00189.2004

Williams, R. E., Major, H., Lock, E. A., Lenz, E. M., Wilson, I. D. (2005). D-Serine-induced nephrotoxicity: a HPLC-TOF/MS-based metabonomics approach. Toxicology 207(2): 179-190.

Wilson-Ashworth, H. A., Judd, A. M., Law, R. M., Freestone, B. D., Taylor, S., Mizukawa, M. K., Bell, J. D. (2004). Formation of transient non-protein calcium pores by lysophospholipids in S49 Lymphoma cells. J Membr Biol, 200(1), 25-33. doi:10.1007/s00232-004-0691-x

Wilson, I. D., Nicholson, J. K., Castro-Perez, J., Granger, J. H., Johnson, K. A., Smith, B. W., & Plumb, R. S. (2005). High resolution "ultra performance" liquid chromatography coupled to oa-TOF mass spectrometry as a tool for differential metabolic pathway profiling in functional genomic studies. J Proteome Res, 4(2), 591-598. doi:10.1021/pr049769r

Wilson, I. D., Plumb, R., Granger, J., Major, H., Williams, R., Lenz, E. M. (2005). HPLC-MS-based methods for the study of metabonomics. J Chromatogr B Analyt Technol Biomed Life Sci 817(1): 67-76.

Winslow, G. A., Shelby, J., Nelson, E. W., & Saffle, J. R. (1996). Influence of allogeneic blood transfusion on natural killer cell activity in burn-injured mice. J Burn Care Rehabil, 17(2), 117-123.

Wishart, D. S., Jewison, T., Guo, A. C., Wilson, M., Knox, C., Liu, Y., Scalbert, A. (2013). HMDB 3.0--The Human Metabolome Database in 2013. Nucleic Acids Res, 41(Database issue), D801-807. doi:10.1093/nar/gks1065

Wishart, D. S., Knox, C., Guo, A. C., Eisner, R., Young, N., Gautam, B., Forsythe, I. (2009). HMDB: a knowledgebase for the human metabolome. Nucleic Acids Res, 37(Database issue), D603-610. doi:10.1093/nar/gkn810

Wisnoskey, B. J., Sinkins, W. G., & Schilling, W. P. (2003). Activation of vanilloid receptor type I in the endoplasmic reticulum fails to activate store-operated Ca2+ entry. Biochemical Journal, 372(Pt 2), 517-528. doi:10.1042/bj20021574

Wohlrab, J., & Kreft, D. (2014). Niacinamide - mechanisms of action and its topical use in dermatology. Skin Pharmacol Physiol, 27(6), 311-315. doi:10.1159/000359974

Wolf, J., Curtis, N., Worth, L. J., & Flynn, P. M. (2013). Central line-associated bloodstream infection in children: an update on treatment. Pediatr Infect Dis J, 32(8), 905-910. doi:10.1097/INF.0b013e3182996b6e

Wong, C. K., Cheung, P. F., & Lam, C. W. (2007). Leptin-mediated cytokine release and migration of eosinophils: implications for immunopathophysiology of allergic inflammation. Eur J Immunol, 37(8), 2337-2348. doi:10.1002/eji.200636866

Woo, D. H., Jung, S. J., Zhu, M. H., Park, C. K., Kim, Y. H., Oh, S. B., & Lee, C. J. (2008). Direct activation of transient receptor potential vanilloid 1(TRPV1) by diacylglycerol (DAG). Mol Pain, 4, 42. doi:10.1186/1744-8069-4-42

Woolf, C. J., Allchorne, A., Safieh-Garabedian, B., & Poole, S. (1997). Cytokines, nerve growth factor and inflammatory hyperalgesia: the contribution of tumour necrosis factor alpha. Br J Pharmacol, 121(3), 417-424. doi:10.1038/sj.bjp.0701148

Woolf, C. J., & Ma, Q. (2007). Nociceptors--noxious stimulus detectors. Neuron, 55(3), 353-364. doi:10.1016/j.neuron.2007.07.016

Woolf, C. J., & Mannion, R. J. (1999). Neuropathic pain: aetiology, symptoms, mechanisms, and management. Lancet, 353(9168), 1959-1964. doi:10.1016/s0140-6736(99)01307-0

Worley, B., & Powers, R. (2013). Multivariate Analysis in Metabolomics. Curr Metabolomics, 1(1), 92-107. doi:10.2174/2213235x11301010092

Wozniak, M. A., Modzelewska, K., Kwong, L., Keely, P. J. (2004). Focal adhesion regulation of cell behavior. Biochim Biophys Acta 1692(2-3): 103-119.

Wray, C. J., Mammen, J. M., & Hasselgren, P. O. (2002). Catabolic response to stress and potential benefits of nutrition support. Nutrition, 18(11-12), 971-977.
Wu, J. C., Rose, L. F., Christy, R. J., Leung, K. P., & Chan, R. K. (2015). Full-Thickness Thermal Injury Delays Wound Closure in a Murine Model. Adv Wound Care (New Rochelle), 4(2), 83-91. doi:10.1089/wound.2014.0570
Wu, X., Baer, L. A., Wolf, S. E., Wade, C. E., Walters, T. J. (2010a). The impact of muscle disuse on muscle atrophy in severely burned rats. J Surg Res 164(2): e243-251.
Wu, X., Wolf, S. E., Walters, T.J. (2010b). Muscle contractile properties in severely burned rats. Burns 36(6): 905-911.
Wu, X., Walters, T. J., Rathbone, C. R. (2013). Skeletal muscle satellite cell activation following cutaneous burn in rats. Burns 39(4): 736-744.
Wuhanqimuge, Itakura, A., Matsuki, Y., Tanaka, M., & Arioka, M. (2013). Lysophosphatidylcholine enhances NGF-induced MAPK and Akt signals through the extracellular domain of TrkA in PC12 cells. FEBS Open Bio, 3, 243-251. doi:10.1016/j.fob.2013.05.003
Xia, P., Gamble, J. R., Rye, K. A., Wang, L., Hii, C. S., Cockerill, P., Vadas, M. A. (1998). Tumor necrosis factor-alpha induces adhesion molecule expression through the sphingosine kinase pathway. Proc Natl Acad Sci U S A, 95(24), 14196-14201.
Xiao, M., Li, L., Hu, Q., Ma, L., Liu, L., Chu, W., & Zhang, H. (2013). Rapamycin reduces burn wound progression by enhancing autophagy in deep second-degree burn in rats. Wound Repair Regen, 21(6), 852-859. doi:10.1111/wrr.12090
Xiao, W., Mindrinos, M. N., Seok, J., Cuschieri, J., Cuenca, A. G., Gao, H., Tompkins, R. G. (2011). A genomic storm in critically injured humans. Journal of Experimental Medicine, 208(13), 2581-2590. doi:10.1084/jem.20111354
Xie, B., Xiao, S. C., Zhu, S. H., & Xia, Z. F. (2012). Evaluation of long term health-related quality of life in extensive burns: a 12-year experience in a burn center. Burns, 38(3), 348-355. doi:10.1016/j.burns.2011.09.003
Xie, H., & He, S. H. (2005). Roles of histamine and its receptors in allergic and inflammatory bowel diseases. World J Gastroenterol, 11(19), 2851-2857. doi:10.3748/wjg.v11.i19.2851
Xu, C., Li, G., Gao, Y., Liu, S., Lin, J., Zhang, J., Liang, S. (2009). Effect of puerarin on P2X3 receptor involved in hyperalgesia after burn injury in the rat. Brain Res Bull, 80(6), 341-346. doi:10.1016/j.brainresbull.2009.08.027
Xue, Q., Jong, B., Chen, T., & Schumacher, M. A. (2007). Transcription of rat TRPV1 utilizes a dual promoter system that is positively regulated by nerve growth factor. Journal of Neurochemistry, 101(1), 212-222. doi:10.1111/j.1471-4159.2006.04363.x
Yaksh, T. L. (1989). Behavioral and autonomic correlates of the tactile evoked allodynia produced by spinal glycine inhibition: effects of modulatory receptor systems and excitatory amino acid antagonists. Pain, 37(1), 111-123. doi:http://dx.doi.org/10.1016/0304-3959(89)90160-7
Yaksh, T. L., & Rudy, T. A. (1976). Analgesia mediated by a direct spinal action of narcotics. Science, 192(4246), 1357-1358.
Yamada, K., Lim, J., Dale, J. M., Chen, H., Shinn, P., Palm, C. J., Ecker, J. R. (2003). Empirical analysis of transcriptional activity in the Arabidopsis genome. Science, 302(5646), 842-846. doi:10.1126/science.1088305
Yamada, Y., Endo, S., Kamei, Y., Minato, T., Yokoyama, M., Taniguchi, S., Ogawa, M. (1998). Plasma levels of type II phospholipase A2 and nitrite/nitrate in patients with burns. Burns, 24(6), 513-517.
Yamamoto, N., Ngwenya, B. Z., Sery, T. W., & Pieringer, R. A. (1987). Activation of macrophages by ether analogues of lysophospholipids. Cancer Immunol Immunother, 25(3), 185-192.
Yamashita, M., & Fenn, J. B. (1984). Electrospray ion source. Another variation on the free-jet theme. The Journal of Physical Chemistry, 88(20), 4451-4459. doi:10.1021/j150664a002
Yan, S., Tsurumi, A., Que, Y. A., Ryan, C. M., Bandyopadhaya, A., Morgan, A. A., Rahme, L. G. (2015). Prediction of multiple infections after severe burn trauma: a prospective cohort study. Ann Surg, 261(4), 781-792. doi:10.1097/sla.0000000000000759
Yang, Q., Orman, M. A., Berthiaume, F., Ierapetritou, M. G., Androulakis, I. P. (2012). Dynamics of short-term gene expression profiling in liver following thermal injury. J Surg Res 176(2): 549-558.
Yarla, N. (2015). Phospholipase A2: A Potential Therapeutic Target in Inflammation and Cancer (In silico, In vitro, In vivo and Clinical Approach). J Cancer Sci Ther, 7, 249-252.

Yasuhara, S., Kaneki, M., Sugita, H., Sugita, M., Asai, A., Sahani, N., Martyn, J. A. (2006). Adipocyte apoptosis after burn injury is associated with altered fat metabolism. J Burn Care Res, 27(3), 367-376. doi:10.1097/01.bcr.0000216777.94365.47

Yasuhara, S., Perez, M. E., Kanakubo, E., Yasuhara, Y., Shin, Y. S., Kaneki, M., Martyn, J. A. (2000). Skeletal muscle apoptosis after burns is associated with activation of proapoptotic signals. Am J Physiol Endocrinol Metab, 279(5), E1114-1121.

Yeh, F. L., Lin, W. L., Shen, H. D., & Fang, R. H. (1997a). Changes in levels of serum IL-8 in burned patients. Burns, 23(7-8), 555-559.

Yeh, F. L., Lin, W. L., Shen, H. D., & Fang, R. H. (1997b). Changes in serum tumour necrosis factor-alpha in burned patients. Burns, 23(1), 6-10.

Yeh, F. L., Lin, W. L., Shen, H. D., & Fang, R. H. (1999). Changes in circulating levels of interleukin 6 in burned patients. Burns, 25(2), 131-136.

Yin, J., & Kuebler, W. M. (2010). Mechanotransduction by TRP channels: general concepts and specific role in the vasculature. Cell Biochem Biophys, 56(1), 1-18. doi:10.1007/s12013-009-9067-2

Yoder, M., Zhuge, Y., Yuan, Y., Holian, O., Kuo, S., van Breemen, R., Lum, H. (2014). Bioactive lysophosphatidylcholine 16:0 and 18:0 are elevated in lungs of asthmatic subjects. Allergy Asthma Immunol Res, 6(1), 61-65. doi:10.4168/aair.2014.6.1.61

Yoneda, O., Imai, T., Goda, S., Inoue, H., Yamauchi, A., Okazaki, T., Umehara, H. (2000). Fractalkine-mediated endothelial cell injury by NK cells. J Immunol, 164(8), 4055-4062.

Yowler, C. J., & Fratianne, R. B. (2000). Current status of burn resuscitation. Clin Plast Surg, 27(1), 1-10.

Yu, B. H., & Dimsdale, J. E. (1999). Posttraumatic stress disorder in patients with burn injuries. J Burn Care Rehabil, 20(5), 426-433; discussion 422-425.

Yu, L., Netticadan, T., Xu, Y. J., Panagia, V., & Dhalla, N. S. (1998). Mechanisms of lysophosphatidylcholine-induced increase in intracellular calcium in rat cardiomyocytes. J Pharmacol Exp Ther, 286(1), 1-8.

Zalewski, A., & Macphee, C. (2005). Role of lipoprotein-associated phospholipase A2 in atherosclerosis: biology, epidemiology, and possible therapeutic target. Arterioscler Thromb Vasc Biol, 25(5), 923-931. doi:10.1161/01.ATV.0000160551.21962.a7

Zapata, A., Chefer, V. I., & Shippenberg, T. S. (2009). Microdialysis in rodents. Curr Protoc Neurosci, Chapter 7, Unit7.2. doi:10.1002/0471142301.ns0702s47

Zarkesh-Esfahani, H., Pockley, A. G., Wu, Z., Hellewell, P. G., Weetman, A. P., & Ross, R. J. (2004). Leptin indirectly activates human neutrophils via induction of TNF-alpha. J Immunol, 172(3), 1809-1814.

Zelt, R. G., Daniel, R. K., Ballard, P. A., Brissette, Y., Heroux, P. (1988). High-voltage electrical injury: chronic wound evolution. Plast Reconstr Surg 82(6): 1027-1041.

Zemtsov, A., & Neldner, K. H. (1993). Successful treatment of dermatitis herpetiformis with tetracycline and nicotinamide in a patient unable to tolerate dapsone. J Am Acad Dermatol, 28(3), 505-506.

Zeng, F., Xu, S. Z., Jackson, P. K., McHugh, D., Kumar, B., Fountain, S. J., & Beech, D. J. (2004). Human TRPC5 channel activated by a multiplicity of signals in a single cell. J Physiol, 559(Pt 3), 739-750. doi:10.1113/jphysiol.2004.065391

Zhang, H. H., Halbleib, M., Ahmad, F., Manganiello, V. C., & Greenberg, A. S. (2002). Tumor necrosis factor-alpha stimulates lipolysis in differentiated human adipocytes through activation of extracellular signal-related kinase and elevation of intracellular cAMP. Diabetes, 51(10), 2929-2935.

Zhang, J. P., Liang, W. Y., Luo, Z. H., Yang, Z. C., Chan, H. C., & Huang, Y. S. (2007). Involvement of p38 MAP kinase in burn-induced degradation of membrane phospholipids and upregulation of cPLA2 in cardiac myocytes. Shock, 28(1), 86-93. doi:10.1097/SHK.0b013e31802f9d9a

Zhang, X., Huang, J., & McNaughton, P. A. (2005). NGF rapidly increases membrane expression of TRPV1 heat-gated ion channels. EMBO J, 24(24), 4211-4223. doi:10.1038/sj.emboj.7600893

Zhang, Y., Cai, B., Jiang, H., Yan, H., Yang, H., Peng, J., Peng, X. (2014). Use of 1H-nuclear magnetic resonance to screen a set of biomarkers for monitoring metabolic disturbances in severe burn patients. Crit Care, 18(4), R159. doi:10.1186/cc13999

Zhang, Y., Wang, T., He, J., & Dong, J. (2016). Growth factor therapy in patients with partial-thickness burns: a systematic review and meta-analysis. International Wound Journal, 13(3), 354-366. doi:10.1111/iwj.12313

Zhao, J., Chen, L., Shu, B., Tang, J., Zhang, L., Xie, J., Qi, S. (2015). Granulocyte/macrophage colony-stimulating factor attenuates endothelial hyperpermeability after thermal injury. Am J Transl Res, 7(3), 474-488.

Zhao, J., Chen, L., Shu, B., Tang, J., Zhang, L., Xie, J., Xu, Y. (2014). Granulocyte/macrophage colony-stimulating factor influences angiogenesis by regulating the coordinated expression of VEGF and the Ang/Tie system. PLoS One, 9(3), e92691. doi:10.1371/journal.pone.0092691

Zhao, Q., Wu, K., Geng, J., Chi, S., Wang, Y., Zhi, P., Xiao, B. (2016). Ion Permeation and Mechanotransduction Mechanisms of Mechanosensitive Piezo Channels. Neuron, 89(6), 1248-1263. doi:10.1016/j.neuron.2016.01.046

Zhao, W., He, X., Hoadley, K. A., Parker, J. S., Hayes, D. N., & Perou, C. M. (2014). Comparison of RNA-Seq by poly (A) capture, ribosomal RNA depletion, and DNA microarray for expression profiling. BMC Genomics, 15, 419. doi:10.1186/1471-2164-15-419

Zhi, L., Hu, X., & Han, C. (2014). Biphasic changes (overreduction and overoxidation) of plasma redox status and clinical implications in early stage of severe burns. J Crit Care, 29(6), 1063-1068. doi:10.1016/j.jcrc.2014.06.013

Zhou, L., Shi, M., Guo, Z., Brisbon, W., Hoover, R., & Yang, H. (2006). Different cytotoxic injuries induced by lysophosphatidylcholine and 7-ketocholesterol in mouse endothelial cells. Endothelium, 13(3), 213-226. doi:10.1080/10623320600780926

Zhu, W., & Oxford, G. S. (2007). Phosphoinositide-3-kinase and mitogen activated protein kinase signaling pathways mediate acute NGF sensitization of TRPV1. Mol Cell Neurosci, 34(4), 689-700. doi:10.1016/j.mcn.2007.01.005

Zhuang, Z. Y., Xu, H., Clapham, D. E., & Ji, R. R. (2004). Phosphatidylinositol 3-kinase activates ERK in primary sensory neurons and mediates inflammatory heat hyperalgesia through TRPV1 sensitization. J Neurosci, 24(38), 8300-8309. doi:10.1523/jneurosci.2893-04.2004

Zimmermann, K., Leffler, A., Babes, A., Cendan, C. M., Carr, R. W., Kobayashi, J., Reeh, P. W. (2007). Sensory neuron sodium channel Nav1.8 is essential for pain at low temperatures. Nature, 447(7146), 855-858. doi:10.1038/nature05880

Zimmermann, K., Leffler, A., Fischer, M. M., Messlinger, K., Nau, C., & Reeh, P. W. (2005). The TRPV1/2/3 activator 2-aminoethoxydiphenyl borate sensitizes native nociceptive neurons to heat in wildtype but not TRPV1 deficient mice. Neuroscience, 135(4), 1277-1284. doi:10.1016/j.neuroscience.2005.07.018

Zou, Y., Kim, C. H., Chung, J. H., Kim, J. Y., Chung, S. W., Kim, M. K., Chung, H. Y. (2007). Upregulation of endothelial adhesion molecules by lysophosphatidylcholine. Involvement of G protein-coupled receptor GPR4. Febs Journal, 274(10), 2573-2584. doi:10.1111/j.1742-4658.2007.05792.x

Zylka, M. J., Rice, F. L., & Anderson, D. J. (2005). Topographically distinct epidermal nociceptive circuits revealed by axonal tracers targeted to Mrgprd. Neuron, 45(1), 17-25. doi:10.1016/j.neuron.2004.12.015

10 Appendix

Supplementary Table 1. All genes differentially expressed between burn and control microdialysate site skin, presented with the Fold Change (FC) in signal (Burn vs. Control) and false discovery rate-adjusted p-value.

Ensembl ID	FC	FDR	Gene symbol
ENSRNOG00000029042	8.296579744	2.42E-05	Mt-nd6
ENSRNOG0000000143	5.199951882	2.42E-05	Rasa4
ENSRNOG0000000016	82.68824155	3.41E-05	Alas2
ENSRNOG0000002988	76.1048102	3.41E-05	Hba1
ENSRNOG0000002124	4.059481101	3.41E-05	RGD1311739
ENSRNOG0000001974	3.962003942	3.64E-05	Isyna1
ENSRNOG0000004942	102.0500321	3.73E-05	Hbb
ENSRNOG0000003288	69.4376832	3.73E-05	AY172581.19
ENSRNOG0000003168	12.74930475	3.73E-05	AY172581.12
ENSRNOG0000000723	6.976766405	3.73E-05	Kank3
ENSRNOG0000003726	4.784792815	3.73E-05	Scarf1
ENSRNOG0000000456	4.731833945	3.73E-05	Arhgef15
ENSRNOG0000001564	4.613617036	3.73E-05	Exoc3l1
ENSRNOG0000000283	4.49701336	3.73E-05	Luc7l3
ENSRNOG0000002463	-	3.73E-05	Atf6
ENSRNOG0000002946	7.550977822	3.98E-05	Slc26a10
ENSRNOG0000004942	7.486637995	4.05E-05	Fam167b
ENSRNOG0000001576	4.221222437	4.58E-05	Abtb1
ENSRNOG0000002124	3.502536529	4.58E-05	Hspa12b
ENSRNOG0000000406	2.696628774	4.58E-05	Pnn
ENSRNOG0000001938	6.430444386	5.46E-05	Egfl7
ENSRNOG0000003123	60.42586919	5.58E-05	LOC100134871
ENSRNOG0000004732	51.45159815	5.58E-05	Hba2
ENSRNOG0000002348	6.246693819	5.58E-05	Ushbp1
ENSRNOG0000000132	5.169978805	5.58E-05	Il3ra
ENSRNOG0000004973	4.254541777	5.58E-05	AABR06030183.1
ENSRNOG0000000919	7.594278221	6.38E-05	RGD1305202
ENSRNOG0000001964	-	6.80E-05	Col6a3
ENSRNOG0000002040	5.554793128	7.45E-05	Adcy4
ENSRNOG0000000158	-3.80357376	7.45E-05	Nrip1
ENSRNOG0000000796	-	7.45E-05	B4galt1
ENSRNOG0000001543	-	7.45E-05	Man2a1
ENSRNOG0000004600	2.507388778	8.00E-05	Clasrp
ENSRNOG0000000077	3.108659648	8.05E-05	Gabbr1
ENSRNOG0000001164	33.24229025	8.76E-05	Epb42
ENSRNOG0000002207	11.02222937	8.76E-05	Itga2b
ENSRNOG0000001418	6.549589286	8.76E-05	AABR06058720.1
ENSRNOG0000004632	-	8.76E-05	Rbpj
ENSRNOG0000000504	2.146017273	8.76E-05	Crip2
ENSRNOG0000001866	4.177134852	9.02E-05	Jak3
ENSRNOG0000003854	48.10377469	9.51E-05	LOC100911551
ENSRNOG0000003896	4.292884873	9.51E-05	AABR06063297.1
ENSRNOG0000001911	4.212142381	9.51E-05	Chp2
ENSRNOG0000001844	2.278182184	9.51E-05	Arfip2
ENSRNOG0000000938	-	9.67E-05	Mapk6
ENSRNOG0000000922	8.590629297	0.00010550	Aplnr
ENSRNOG0000003999	2.323870375	0.00010550	Upf3b
ENSRNOG0000001918	78.72116862	0.00010937	Alox15
ENSRNOG0000000043	5.095765087	0.00011286	Egfl8
ENSRNOG0000004010	42.48612609	0.00011347	Treml1
ENSRNOG0000002702	5.382048297	0.00011347	Arap3
ENSRNOG0000004758	3.874354362	0.00011347	AABR06049893.1
ENSRNOG0000000112	-	0.00011347	Med13l
ENSRNOG0000003293	2.514059601	0.00011347	Shank3
ENSRNOG0000001796	2.803893238	0.00011627	Deaf1
ENSRNOG0000001013	8.245765437	0.00011892	Bpgm
ENSRNOG0000000564	-	0.00012002	Frs2
ENSRNOG0000001841	-	0.0001511	Csf1r
ENSRNOG0000001557	-	0.0001511	Rab11fip5
ENSRNOG0000000254	-	0.0001511	Pds5a
ENSRNOG0000002589	2.474527697	0.00015682	Pkn3
ENSRNOG0000000715	-	0.00016064	Bhlhe40
ENSRNOG0000000587	4.289173879	0.00016397	Tle2
ENSRNOG0000000642	17.318746	0.00016574	Rbm38
ENSRNOG0000000654	-	0.00016858	Mrc2
ENSRNOG0000003014	228.9517303	0.00017313	LOC685793
ENSRNOG0000004958	-	0.00017340	Tnc
ENSRNOG0000000055	-	0.00017839	Eif4ebp2
ENSRNOG0000000667	2.929955772	0.00017839	Fam101b
ENSRNOG0000000030	-	0.00017839	Cd164
ENSRNOG0000002100	4.129586859	0.00018345	Rasip1
ENSRNOG0000002060	2.838864636	0.00018345	Hmg20b
ENSRNOG0000000299	3.000767655	0.00018357	Slc9a3r2
ENSRNOG0000002961	-	0.00018717	Robo1
ENSRNOG0000001130	-	0.00018717	AABR06093716.1
ENSRNOG0000004262	-	0.00019164	Marveld1
ENSRNOG0000001559	4.414236235	0.00019167	Sigirr
ENSRNOG0000003072	-	0.00020531	C4b
ENSRNOG0000004867	12.98416844	0.00020784	Slfn3
ENSRNOG0000004222	9.415996604	0.00020784	Gimap1
ENSRNOG0000005038	2.30006256	0.00020784	Dus3l
ENSRNOG0000000928	3.92959022	0.00020822	Mkrn1
ENSRNOG0000003166	36.43990751	0.00023224	AY172581.11
ENSRNOG0000000056	-	0.00024144	Sgpl1
ENSRNOG0000001517	11.354147	0.00024913	Dhh
ENSRNOG0000000867	-	0.00024913	Antxr1
ENSRNOG0000001878	2.374819469	0.00024913	Bcas2
ENSRNOG0000002925	27.88605199	0.00025090	LOC690435
ENSRNOG0000000182	-	0.00025090	Adipoq
ENSRNOG0000000753	52.6760121	0.00025535	Rsad2
ENSRNOG0000001805	4.353139175	0.00025955	Fech
ENSRNOG0000004881	3.986927022	0.00025955	AABR06059226.1
ENSRNOG0000000674	2.966624004	0.00026484	Gatsl3
ENSRNOG0000003889	9.712349196	0.00027251	Upk3bl
ENSRNOG0000000953	8.108072818	0.00027251	Col9a3
ENSRNOG0000000734	4.890691239	0.00027251	Grasp
ENSRNOG0000001924	3.235202015	0.00027251	Plekhj1
ENSRNOG0000000037	2.812684786	0.00027251	Ctnna3
ENSRNOG0000003895	2.445885137	0.00027251	Cox17
ENSRNOG0000001384	-2.19058863	0.00027251	Arcn1
ENSRNOG0000000387	-	0.00028297	Cpd
ENSRNOG0000000649	-	0.00028297	Neo1
ENSRNOG0000003337	2.069954853	0.00028297	Rnf123
ENSRNOG0000002124	7.009124195	0.00028366	Cdc25b
ENSRNOG0000000463	-	0.00028366	Traf6
ENSRNOG0000001581	3.047306907	0.00028366	Tm4sf1
ENSRNOG0000001861	-	0.00028366	Nfatc3
ENSRNOG0000002101	3.730354423	0.00028758	Car11
ENSRNOG0000000703	-2.34092572	0.00030181	Tgfbr1
ENSRNOG0000003680	-	0.00030181	Psme3
ENSRNOG0000001373	-2.54664678	0.00030260	Bcar3
ENSRNOG0000001798	2.178854576	0.00032898	Ubac1
ENSRNOG0000001825	-	0.00032931	Mrc1
ENSRNOG0000004757	3.762087648	0.00033577	Ccdc28b
ENSRNOG0000000524	-	0.00035317	Slc1a4
ENSRNOG0000002002	2.325437663	0.00035317	Arhgef2
ENSRNOG0000001280	-	0.00036627	C1qa
ENSRNOG0000003356	-	0.00036627	Cfd
ENSRNOG0000002953	2.881997606	0.00036627	Nrbp2
ENSRNOG0000001715	-	0.00036861	Dsc3
ENSRNOG0000000994	-	0.00036906	Ldlr
ENSRNOG0000002832	3.201604226	0.00036906	Dhrsx
ENSRNOG0000000624	-	0.00036906	39142
ENSRNOG0000002099	3.131299009	0.00037115	Slc25a39
ENSRNOG0000001828	-	0.00037115	Ncoa6
ENSRNOG0000000962	22.96807689	0.00037353	Car2
ENSRNOG0000000101	-19.1618682	0.00037353	Clec4m
ENSRNOG0000001113	-	0.00037353	Lama2
ENSRNOG0000000874	-	0.00037353	Col5a1
ENSRNOG0000002339	4.740637624	0.00037353	LOC100911104
ENSRNOG0000000987	4.57555408	0.00037353	Tmem88
ENSRNOG0000002076	3.525238213	0.00037353	Snrnp70
ENSRNOG0000004966	3.103009089	0.00037353	AABR06007110.1
ENSRNOG0000004827	3.003651005	0.00037353	Srrt
ENSRNOG0000004338	2.981189536	0.00037353	Irf3
ENSRNOG0000000048	2.79044628	0.00037353	Phf1
ENSRNOG0000003249	-	0.00037353	Usp22
ENSRNOG0000002414	2.473010089	0.00037353	Arglu1
ENSRNOG0000000287	2.467763084	0.00037353	Rbm25l1
ENSRNOG0000002822	-	0.00037353	Pbrm1
ENSRNOG0000001408	-	0.00037353	Sp1
ENSRNOG0000000540	-	0.00037353	Clint1
ENSRNOG0000000158	3.221189605	0.00037543	Hoxd9
ENSRNOG0000000189	3.638945392	0.00038076	Tbx1
ENSRNOG0000001274	-	0.00038581	C1qb
ENSRNOG0000001068	11.37503569	0.00038581	Nrgn
ENSRNOG0000002512	4.601271059	0.00038581	Gli1
ENSRNOG0000000682	3.607883704	0.00038581	Tmem198b
ENSRNOG0000000905	2.1239558	0.00038581	Sec62
ENSRNOG0000001101	-	0.00038790	Hivep2
ENSRNOG0000002938	24.71189497	0.00038871	AY172581.5
ENSRNOG0000001439	-	0.00039567	Gli3
ENSRNOG0000001730	3.402471629	0.00040021	Rsrp1
ENSRNOG0000001912	-	0.00040021	Fcgbp
ENSRNOG0000002606	-	0.00040807	RGD1566226
ENSRNOG0000001883	-	0.00040807	Ntrk2
ENSRNOG0000002051	-	0.00040881	Sox6
ENSRNOG0000004579	-	0.00040954	Lep
ENSRNOG0000002893	-6.08144412	0.00040954	Dab2
ENSRNOG0000001276	4.08450801	0.00040954	Cwf19l1
ENSRNOG0000002835	-	0.00040954	Exoc6b
ENSRNOG0000001389	2.378051443	0.00040954	Npdc1
ENSRNOG0000001580	-	0.00040954	Prkrir
ENSRNOG0000001130	-	0.00041003	Slmap
ENSRNOG0000001380	-	0.00042966	Exoc5
ENSRNOG0000001629	-	0.00043048	Cd4
ENSRNOG0000003087	4.226247723	0.00043414	LOC102550396
ENSRNOG0000003033	2.206071728	0.00044135	Adck5
ENSRNOG0000002489	-	0.00044719	Cxcl13
ENSRNOG0000004709	45.64899616	0.00044719	Hbb-b1
ENSRNOG0000003401	-	0.00046800	Acaca
ENSRNOG0000001989	-	0.00047374	Folr2
ENSRNOG0000002467	-	0.00047374	Dmxl1
ENSRNOG0000002057	3.519080197	0.00047776	Catsperg1
ENSRNOG0000002045	2.425843283	0.00047776	Slc26a6
ENSRNOG0000002120	-	0.00048865	Atl3
ENSRNOG0000002641	-5.90328166	0.00050961	Col14a1
ENSRNOG0000002505	-	0.00050961	Lrp1
ENSRNOG0000002021	2.478613894	0.00050961	RGD1305592
ENSRNOG0000002821	2.140789268	0.00050961	Akap17a
ENSRNOG0000000441	3.187128025	0.00051023	Fam117a
ENSRNOG0000001875	11.13763407	0.00051029	Insl3
ENSRNOG0000004793	2.695457447	0.00051084	Tmsb4x
ENSRNOG0000000884	76.97794838	0.00052984	Cyp4a8
ENSRNOG0000001969	2.385571253	0.00053217	Ssbp4
ENSRNOG0000000047	2.359887315	0.00053747	Rgl2

ENSRNOG0000000630	-	0.00053747	Slc38a2
ENSRNOG0000000483	-	0.00053747	Arid2
ENSRNOG0000001577	-	0.00053747	Mex3c
ENSRNOG0000001773	2.049578172	0.00053835	Dgkz
ENSRNOG0000000696	-	0.00054001	Aff4
ENSRNOG0000003729	3.802291865	0.00054999	Smpd5
ENSRNOG0000004306	2.826982284	0.00055596	Prpf40b
ENSRNOG0000001280	-	0.000575	C1qc
ENSRNOG0000000433	-	0.00058459	Egfr
ENSRNOG0000001025	-	0.00059032	Cd163
ENSRNOG0000002995	51.76911657	0.00059730	AY172581.7
ENSRNOG0000001137	2.225142824	0.00060070	Ccndbp1
ENSRNOG0000002087	2.52496977	0.00060227	Bax
ENSRNOG0000005072	-	0.00060511	AABR06061565.1
ENSRNOG0000001836	6.144579684	0.00060511	Prx
ENSRNOG0000001582	-	0.00060511	Klf13
ENSRNOG0000001346	-	0.00060511	Txndc5
ENSRNOG0000000915	2.299518417	0.00060511	Tra2a
ENSRNOG0000002093	19.01212083	0.00060554	AABR06009772.1
ENSRNOG0000000044	-	0.00061177	C4a
ENSRNOG0000001654	-	0.00061177	Enc1
ENSRNOG0000003299	25.77729917	0.00061618	AY172581.20
ENSRNOG0000001633	-	0.00062596	Ptbp3
ENSRNOG0000000004	2.090343373	0.00062596	Idua
ENSRNOG0000003354	40.38098787	0.00063121	AY172581.21
ENSRNOG0000004965	-	0.00064568	Errfi1
ENSRNOG0000000326	-	0.00064568	Maml1
ENSRNOG0000004951	2.012612332	0.00064568	Safb2
ENSRNOG0000001135	-	0.00065532	Hipk3
ENSRNOG0000003191	2.547677099	0.00065532	Hdac10
ENSRNOG0000001454	-2.09229244	0.00065532	Tbc1d2b
ENSRNOG0000000529	-	0.00066483	Trip11
ENSRNOG0000001741	5.564937178	0.00067131	Irf7
ENSRNOG0000000406	-	0.00067131	Sh3pxd2b
ENSRNOG0000004348	3.950841657	0.00067131	Tnfrsf26
ENSRNOG0000004577	-	0.00067131	Chl1
ENSRNOG0000000801	2.297107925	0.00067131	Cdk5
ENSRNOG0000000325	-	0.00067131	Ccng1
ENSRNOG0000000796	30.79341686	0.00067493	Klre1
ENSRNOG0000001871	-	0.00068295	Arl5b
ENSRNOG0000000303	2.317920232	0.00068330	Plcd3
ENSRNOG0000004825	-	0.00068886	Fam160a1
ENSRNOG0000000994	-	0.00068886	Kremen1
ENSRNOG0000000044	4.845260071	0.00069465	Notch4
ENSRNOG0000002167	-	0.00069465	Frem2
ENSRNOG0000001004	-	0.00069719	Clec4a
ENSRNOG0000003687	16.70572785	0.00069891	Bpifa2f
ENSRNOG0000002125	3.912209915	0.00069975	Smox
ENSRNOG0000001334	-	0.00069975	LOC100910454
ENSRNOG0000002136	3.282047508	0.00069975	Ybey
ENSRNOG0000001080	3.671825147	0.00070472	Fabp4
ENSRNOG0000002454	2.319757541	0.00070477	Mum1
ENSRNOG0000002643	110.603835	0.00070652	Trim58
ENSRNOG0000000881	-	0.00070652	Gpnmb
ENSRNOG0000001532	-	0.00070652	Moxd1
ENSRNOG0000002269	2.220305254	0.00070935	Plekhg5
ENSRNOG0000001486	-	0.0007212	Synpo2
ENSRNOG0000002223	-	0.0007212	Tusc5
ENSRNOG0000000343	3.575861194	0.0007212	Il15
ENSRNOG0000000803	-	0.0007212	Dennd4c
ENSRNOG0000004818	5.496621828	0.00073224	LOC100911042
ENSRNOG0000004947	-	0.00073247	Steap3
ENSRNOG0000000502	-	0.00073247	Rab5al1
ENSRNOG0000000557	4.554079146	0.00073825	Abi3
ENSRNOG0000002028	4.504572134	0.00074299	Syt15
ENSRNOG0000000707	-	0.00074299	Met
ENSRNOG0000001446	-	0.00074454	Hivep1
ENSRNOG0000000110	-	0.00075290	Sdk1
ENSRNOG0000000414	-	0.00076706	Vasn
ENSRNOG0000000732	-	0.00076878	Frmd6
ENSRNOG0000004277	3.584424015	0.00076991	Apol3
ENSRNOG0000000439	5.963450472	0.00077314	Aatk
ENSRNOG0000000003	34.5412739	0.00077426	Tmcc2
ENSRNOG0000001338	2.64259124	0.00077501	Tpcn2
ENSRNOG0000000372	-	0.00078519	Prrx1
ENSRNOG0000000632	-	0.00078519	Ptges
ENSRNOG0000001869	2.683112224	0.00079222	Ccnl2
ENSRNOG0000003305	-	0.00080419	Galnt6
ENSRNOG0000001407	-	0.00080419	Mbnl1
ENSRNOG0000001668	-	0.00080942	Nsd1
ENSRNOG0000000737	-4.76978759	0.00081114	Slit3
ENSRNOG0000003283	-	0.00083123	Mmp10
ENSRNOG0000000593	-	0.00083123	Yap1
ENSRNOG0000002801	3.142924207	0.00083833	Pf4
ENSRNOG0000000561	3.648347596	0.00084063	Fmc1
ENSRNOG0000001667	-	0.00084063	Angptl2
ENSRNOG0000002486	2.539126171	0.00084063	Eme2
ENSRNOG0000000460	-2.35887591	0.00084063	Slc38a10
ENSRNOG0000001726	-	0.00084063	Tmem131
ENSRNOG0000000054	-	0.00084522	Frk
ENSRNOG0000001712	-	0.00084522	Abhd2
ENSRNOG0000001750	3.126380698	0.00084522	Suv420h2
ENSRNOG0000001669	-	0.00085095	Mmp2
ENSRNOG0000000601	4.419960649	0.00085095	G0s2
ENSRNOG0000004691	-	0.00086165	Nr1d2
ENSRNOG0000003311	-	0.00086188	Svep1
ENSRNOG0000001358	-2.65833802	0.00086347	Extl3
ENSRNOG0000001205	26.81668393	0.000866	Olig3
ENSRNOG0000002776	17.85755004	0.000866	Slc38a5
ENSRNOG0000000934	6.018222468	0.000866	Nos3
ENSRNOG0000002244	2.290833428	0.000866	Htra2
ENSRNOG0000002310	-	0.00087028	Icoslg
ENSRNOG0000001722	2.832019142	0.00087743	Tcirg1
ENSRNOG0000004212	23.46735511	0.00088091	RGD1564129
ENSRNOG0000000497	4.291775005	0.00090117	Upp1
ENSRNOG0000001785	4.17925601	0.00090117	Ucp2
ENSRNOG0000002086	-	0.00090643	Ano1
ENSRNOG0000001936	2.091700375	0.00090643	Slx1b
ENSRNOG0000003859	-	0.00090643	Dlg1
ENSRNOG0000003546	12.25343565	0.00092715	Mirlet7c-2
ENSRNOG0000003980	3.164697274	0.00092715	Fam193b
ENSRNOG0000004565	2.364537457	0.00092715	LOC100909983
ENSRNOG0000002007	-	0.00092869	Pcdhb8
ENSRNOG0000004775	-	0.00092869	Mef2a
ENSRNOG0000004309	-	0.00092869	Ddx21
ENSRNOG0000000730	-	0.00093141	Fbn1
ENSRNOG0000004592	5.189266288	0.00093611	RT1-T24-3
ENSRNOG0000002345	-	0.00093676	Lrba
ENSRNOG0000001311	2.322724505	0.00094084	Mettl3
ENSRNOG0000001192	-	0.00094495	Fam83b
ENSRNOG0000004231	-	0.00094900	Cd209f
ENSRNOG0000000531	3.311363663	0.00095026	Ahsa2
ENSRNOG0000002016	4.708802409	0.00095189	Gimap8
ENSRNOG0000001624	-	0.00095627	Tshz1
ENSRNOG0000000459	21.09443962	0.00095981	Sec14l3
ENSRNOG0000000241	-	0.00096071	Tfcp2l1
ENSRNOG0000001107	-	0.00096071	Nt5e
ENSRNOG0000002110	2.857311251	0.00096195	Gramd1a
ENSRNOG0000000273	-	0.00097033	Rgs5
ENSRNOG0000001616	-	0.00097033	Slc1a3
ENSRNOG0000002068	4.091251506	0.00097033	Dpf1
ENSRNOG0000003123	3.242436245	0.00097033	Mapk12
ENSRNOG0000000647	3.216470642	0.00097033	Hspa2
ENSRNOG0000002085	2.83951568	0.00097033	APLP1
ENSRNOG0000000708	-	0.00097033	Xpot
ENSRNOG0000000561	-	0.00097033	Ncoa3
ENSRNOG0000001021	-	0.00097913	Prrc2b
ENSRNOG0000004015	-	0.00098114	Sdr16c6
ENSRNOG0000003351	15.54711028	0.00098623	LOC100361767
ENSRNOG0000000056	10.23300197	0.00098623	Prf1
ENSRNOG0000000958	-	0.00098777	Tcf20
ENSRNOG0000000456	-	0.00099113	Sec24a
ENSRNOG0000002034	-	0.00099113	Nup98
ENSRNOG0000002028	-	0.00099523	Prkar2a
ENSRNOG0000001455	-	0.00099946	Aox4
ENSRNOG0000001822	-	0.00099946	Zcchc14
ENSRNOG0000001957	3.555397354	0.00100828	Lcat
ENSRNOG0000004872	-	0.00100828	Pros1
ENSRNOG0000003800	-	0.00100873	RGD1311318
ENSRNOG0000000897	-	0.00102731	Cdh4
ENSRNOG0000000224	-	0.00102731	Pdgfra
ENSRNOG0000003930	-	0.00102731	Ahcyl2
ENSRNOG0000001952	-	0.00103065	Hspa9
ENSRNOG0000001459	-	0.00103068	Abhd13
ENSRNOG0000004625	2.08318727	0.00103647	AABR06041318.1
ENSRNOG0000001767	2.953938059	0.00103938	Plvap
ENSRNOG0000004713	-	0.00104101	Erbb2ip
ENSRNOG0000000130	-	0.00104101	Bcr
ENSRNOG0000001200	-	0.00104101	Iqgap1
ENSRNOG0000004259	18.67050294	0.00104131	AABR06084916.1
ENSRNOG0000000818	-	0.00104131	Htra3
ENSRNOG0000003429	5.528617964	0.00104131	Sptbn5
ENSRNOG0000000932	3.704207413	0.00104131	Wdr54
ENSRNOG0000000223	-	0.00104131	Aff1
ENSRNOG0000004569	-	0.00104131	Lin7c
ENSRNOG0000000449	-	0.00104264	Scin
ENSRNOG0000001999	-2.07093971	0.00104361	Slc16a1
ENSRNOG0000001205	-	0.00105307	Zmpste24
ENSRNOG0000001649	-	0.00106025	Ctsc
ENSRNOG0000002991	-	0.00106025	Cilp
ENSRNOG0000001776	-	0.00106025	Mrvi1
ENSRNOG0000000900	-	0.00106025	Mtss1
ENSRNOG0000001081	-	0.00106205	Bmpr1a
ENSRNOG0000004762	2.574072578	0.00106252	Atg4d
ENSRNOG0000000173	-	0.00106252	Acap2
ENSRNOG0000000077	2.172941998	0.00107165	Znrd1
ENSRNOG0000002008	4.091368735	0.00108646	Klhl26
ENSRNOG0000000761	4.039290445	0.00108646	Hoxb7
ENSRNOG0000003724	2.0218689	0.00108646	Gdi1
ENSRNOG0000003974	4.05784413	0.00110227	RT1-CE4
ENSRNOG0000003874	7.072213746	0.00111241	Gimap7
ENSRNOG0000001860	5.171819956	0.00111241	Carns1
ENSRNOG0000000441	2.789801358	0.00111416	Tspan8
ENSRNOG0000001187	-	0.00112015	Itga2
ENSRNOG0000001894	-	0.00112015	Trim33
ENSRNOG0000000635	2.468259074	0.00112015	Akap8l
ENSRNOG0000003726	-	0.00112015	Hcfc1
ENSRNOG0000002095	82.84151925	0.00113208	Slc4a1
ENSRNOG0000003259	-	0.00113208	Ttc28
ENSRNOG0000000291	2.06889962	0.00113208	Trmt1
ENSRNOG0000004679	-	0.00114667	Sh3rf3
ENSRNOG0000004706	13.55225488	0.00114667	AABR06099364.2
ENSRNOG0000001816	2.269727284	0.00114667	Klc4
ENSRNOG0000004960	8.728117494	0.00115184	AABR06088414.1
ENSRNOG0000005030	51.80795665	0.00116110	LOC100911854
ENSRNOG0000000495	-	0.00116563	Kif16b
ENSRNOG0000000664	-	0.00116643	Thrb
ENSRNOG0000002842	-	0.00116909	Rmnd5a
ENSRNOG0000002003	-	0.00118829	Chpf
ENSRNOG0000001561	4.442819908	0.00119354	Rgs14
ENSRNOG0000003355	-	0.00119976	Spen
ENSRNOG0000002403	3.393067632	0.00120281	Fam98c
ENSRNOG0000004797	3.283149824	0.00120420	LOC100910163
ENSRNOG0000000719	23.70567108	0.00120491	Nr1h4
ENSRNOG0000004731	17.0190707	0.00120491	AABR06032074.1
ENSRNOG0000002153	-	0.00120491	Rai1
ENSRNOG0000001115	-	0.00121422	Tenm4
ENSRNOG0000001499	-	0.00121422	Tnpo1
ENSRNOG0000001721	-2.65919757	0.00121671	LOC100909715
ENSRNOG0000001447	-	0.00121716	Slc31a1
ENSRNOG0000000131	2.281775038	0.00121720	Pdgfa
ENSRNOG0000000569	2.553221263	0.00122155	Lmcd1
ENSRNOG0000001442	-	0.00122412	Lox
ENSRNOG0000004852	15.90531969	0.00122514	AABR06027158.1
ENSRNOG0000002095	-	0.00123241	Ms4a7
ENSRNOG0000001653	-	0.00123498	Itga8
ENSRNOG0000002735	-	0.00123498	Tns4
ENSRNOG0000003262	-	0.00123613	Mmp3
ENSRNOG0000004605	3.255272125	0.00123834	AABR06086725.1
ENSRNOG0000001099	-	0.00123834	Mob1b
ENSRNOG0000001210	2.677284657	0.00123834	Thsd1
ENSRNOG0000000503	-	0.00123834	Ppp1r12b
ENSRNOG0000001380	2.580111148	0.00123834	Tnip2
ENSRNOG0000000668	-	0.00123834	Nedd4
ENSRNOG0000000862	-	0.00125136	Smad3
ENSRNOG0000000683	-	0.00125379	Arl5a
ENSRNOG0000001828	-	0.00125864	Gda
ENSRNOG0000002789	3.93515933	0.00126262	Dhrs11
ENSRNOG0000003559	17.17835335	0.00126357	Mir27a
ENSRNOG0000001585	-	0.00126357	Arhgap35
ENSRNOG0000000443	-	0.00127814	Cntn1
ENSRNOG0000000386	-	0.00129522	Sod3
ENSRNOG0000000232	2.583354803	0.00130126	RGD1310587
ENSRNOG0000003430	-	0.00131497	Spon1
ENSRNOG0000000039	2.286074151	0.00131497	Zufsp
ENSRNOG0000000794	-	0.00131937	Edem1
ENSRNOG0000000416	2.008088374	0.00132474	Mtif2
ENSRNOG0000004882	35.82009343	0.00134483	AABR06084922.1
ENSRNOG0000000976	20.42949654	0.00134483	Npy
ENSRNOG0000002880	-	0.00134483	Cd209e
ENSRNOG0000001423	-	0.00134483	P2ry1
ENSRNOG0000003133	73.43956359	0.00135132	AY172581.10
ENSRNOG0000000369	-	0.00135132	Prkx
ENSRNOG0000001648	-5.73377545	0.00135204	Pltp
ENSRNOG0000002834	-	0.00135204	Alkbh5
ENSRNOG0000001768	-	0.00135669	Pi15

ENSRNOG0000000801	8.552901396	0.00135669	Hoxb5
ENSRNOG0000000369	-	0.00135745	Tmed7
ENSRNOG0000000658	-	0.00138004	Hpgds
ENSRNOG0000002736	2.164009486	0.00138004	Srsf7
ENSRNOG0000000719	5.019389158	0.00138781	Rapgef3
ENSRNOG0000000864	37.94790575	0.00138822	Nkx2-1
ENSRNOG0000003076	-	0.00138898	Dpp4
ENSRNOG0000000516	-3.53124083	0.00139784	Smcr8
ENSRNOG0000001447	2.530813218	0.00139784	Evl
ENSRNOG0000000383	-	0.00139784	Map2k4
ENSRNOG0000000529	2.330991707	0.00139784	Zfp513
ENSRNOG0000003683	60.84218781	0.00140570	Nfe2
ENSRNOG0000001784	3.36406364	0.00140570	Apbb3
ENSRNOG0000001918	-	0.00140570	Acsl4
ENSRNOG0000001890	-	0.00141599	Pik3r1
ENSRNOG0000001074	-	0.00141847	Nrp1
ENSRNOG0000001272	-	0.00142034	Ednra
ENSRNOG0000001743	-	0.00142270	Gfra1
ENSRNOG0000001597	-	0.00142661	Zfp609
ENSRNOG0000001188	-	0.00143493	RGD1307929
ENSRNOG0000000790	12.60079914	0.00145311	Tspan33
ENSRNOG0000001926	-	0.00145311	Sp3
ENSRNOG0000001649	5.26554608	0.00145888	Fam110d
ENSRNOG0000004219	2.967383768	0.00146053	Pabpn1
ENSRNOG0000000287	23.74745945	0.00147190	Afm
ENSRNOG0000001940	2.545598381	0.00147190	Afap1l1
ENSRNOG0000000182	-	0.00147386	Masp1
ENSRNOG0000002350	-	0.00147386	Irs2
ENSRNOG0000001090	15.88416742	0.00147863	Ccl5
ENSRNOG0000001339	-	0.00148109	Foxo1
ENSRNOG0000002456	4.020330204	0.00148463	Gimap9
ENSRNOG0000005026	4.681370272	0.00149054	AABR06107429.1
ENSRNOG0000000029	-	0.00149054	Foxo3
ENSRNOG0000001185	-	0.00149665	Mtpn
ENSRNOG0000001565	-	0.00149984	Ptgfrn
ENSRNOG0000000674	-	0.00150657	Tmtc3
ENSRNOG0000000911	2.962291171	0.00151587	Marcksl1
ENSRNOG0000001316	-	0.00151814	Sash1
ENSRNOG0000000973	-	0.00152028	Cyp7b1
ENSRNOG0000000245	-	0.00152455	Rnf2
ENSRNOG0000004612	22.74019813	0.00152577	AABR06016101.1
ENSRNOG0000001013	-	0.00153706	Rin2
ENSRNOG0000001756	2.039128012	0.00154162	Mib2
ENSRNOG0000001307	2.181512356	0.00154505	Zcchc7
ENSRNOG0000004785	16.23873756	0.00156158	AABR06065479.1
ENSRNOG0000004251	-	0.00156158	Peak1
ENSRNOG0000000548	2.330385532	0.00156158	Ybx3
ENSRNOG0000000250	-	0.00156931	Gnl3l
ENSRNOG0000000041	-4.45125498	0.00157008	C2
ENSRNOG0000000495	-	0.00157820	Actr2
ENSRNOG0000001151	-	0.00157823	Tnfrsf21
ENSRNOG0000000836	6.355487248	0.00159192	Gimap4
ENSRNOG0000003033	35.95007945	0.00159819	AY172581.8
ENSRNOG0000001052	-	0.00162383	Thbs2
ENSRNOG0000000137	4.313047105	0.00162558	Rasal1
ENSRNOG0000002945	24.80689063	0.00162645	AABR06010514.1
ENSRNOG0000003273	2.712274143	0.00162645	Srek1
ENSRNOG0000001526	-	0.00163206	Atf7
ENSRNOG0000000116	2.343318375	0.00163206	Srsf9
ENSRNOG0000002017	2.277212124	0.00163206	Tie1
ENSRNOG0000004754	-	0.00164067	Adra2a
ENSRNOG0000002401	-	0.00164067	Ccdc6
ENSRNOG0000003660	20.75287846	0.00164212	Ifit1lb
ENSRNOG0000004879	-	0.00164740	Top2b
ENSRNOG0000001624	2.611861908	0.00165036	Fhod1
ENSRNOG0000001330	2.621989342	0.00165345	Atpif1
ENSRNOG0000001140	2.121597717	0.00165345	Chkb
ENSRNOG0000004182	-	0.00166183	AABR06025204.1
ENSRNOG0000005052	31.14612856	0.00166651	Tspo2
ENSRNOG0000002611	8.252202155	0.00166651	Scml4
ENSRNOG0000002408	-	0.00166651	Fndc3b
ENSRNOG0000002798	-	0.00166651	Zhx3
ENSRNOG0000001059	2.841414597	0.00166651	Ctnnal1
ENSRNOG0000001376	2.70672271	0.00166651	Ccdc61
ENSRNOG0000002054	2.695793216	0.00166651	Nosip
ENSRNOG0000001133	-	0.00166651	Slk
ENSRNOG0000005025	2.125812696	0.00166651	MGC105649
ENSRNOG0000001487	-	0.00168003	Sec24d
ENSRNOG0000003239	-	0.00168392	Esyt2
ENSRNOG0000001883	-	0.00169295	Notch2
ENSRNOG0000003049	-	0.00170464	AABR06019264.1
ENSRNOG0000002919	5.108013713	0.00170464	Uba7
ENSRNOG0000001034	28.78849278	0.00171522	Ssmem1
ENSRNOG0000004961	5.804440223	0.00171522	AABR06062470.1
ENSRNOG0000001047	-	0.00171522	Copg1
ENSRNOG0000001809	-	0.00174043	Itch
ENSRNOG0000001100	3.315439561	0.00174843	Ube2o
ENSRNOG0000004832	-	0.00175172	Lrba
ENSRNOG0000001887	-	0.00175941	Fam168a
ENSRNOG0000001700	-	0.00176051	Plxna1
ENSRNOG0000000317	61.09624496	0.0017631	LOC100912275
ENSRNOG0000000806	2.898320306	0.00178892	Dqx1
ENSRNOG0000001339	-15.0849903	0.00178983	LOC501033
ENSRNOG0000003036	38.13228205	0.00179578	Psma8
ENSRNOG0000000017	-	0.00179578	Slc30a4
ENSRNOG0000004683	27.26563927	0.00180104	AABR06033357.1
ENSRNOG0000000358	-	0.00180104	Figf
ENSRNOG0000003278	2.422560738	0.00180104	Dysf
ENSRNOG0000001045	-	0.00181270	Elovl7
ENSRNOG0000000811	-2.49501551	0.00181385	RGD1561149
ENSRNOG0000002042	19.1131606	0.00181878	Pklr
ENSRNOG0000002511	-	0.00181878	Exph5
ENSRNOG0000001949	2.523774179	0.00181878	Psmb10
ENSRNOG0000000516	3.525526865	0.00182357	Surf2
ENSRNOG0000000092	-	0.00182847	Slc7a1
ENSRNOG0000003107	-	0.00184051	Calcoco2
ENSRNOG0000001570	-	0.00186257	Rreb1
ENSRNOG0000004970	20.14896798	0.00186570	AABR06079877.1
ENSRNOG0000001478	9.924505379	0.00187477	Ddn
ENSRNOG0000001491	-	0.00187477	Lats1
ENSRNOG0000001376	-	0.00187477	Erlin2
ENSRNOG0000001610	2.183491807	0.00187477	Nkd2
ENSRNOG0000004287	-	0.00187957	Seh1l
ENSRNOG0000002570	-	0.00188149	Yod1
ENSRNOG0000001239	-	0.00188734	Bcl2l13
ENSRNOG0000004355	19.70435683	0.00189604	AABR06042281.1
ENSRNOG0000001239	2.472483401	0.00189604	S100a13
ENSRNOG0000002338	21.78447901	0.00190334	Ephx4
ENSRNOG0000002504	-16.6087801	0.00190334	Pde3a
ENSRNOG0000002633	4.33262448	0.00190334	Tmem255b
ENSRNOG0000003195	4.126639453	0.00190334	Izumo4
ENSRNOG0000001435	3.226239559	0.00190334	Cep95
ENSRNOG0000005021	2.922277778	0.00190334	Amt
ENSRNOG0000000690	2.817234121	0.00190334	Cd320
ENSRNOG0000000446	-	0.00190334	Sel1l
ENSRNOG0000005073	2.182100456	0.00191054	Cd99
ENSRNOG0000001179	-	0.00191783	C1r
ENSRNOG0000001590	43.83397946	0.00191807	Add2
ENSRNOG0000001740	-	0.00191807	Atrnl1
ENSRNOG0000000810	2.125933873	0.00192524	RGD1304868
ENSRNOG0000000440	-	0.00192720	Lpgat1
ENSRNOG0000000318	2.156176803	0.00192898	Anks3
ENSRNOG0000001251	-	0.00193858	C7
ENSRNOG0000002128	-	0.00195362	Celsr1
ENSRNOG0000000192	-	0.00196762	Leprel1
ENSRNOG0000000847	-	0.00196931	Slc8a1
ENSRNOG0000001035	-	0.00196931	Sh3rf1
ENSRNOG0000002976	7.53997466	0.00198321	Acr
ENSRNOG0000000977	-	0.00198321	Elovl4
ENSRNOG0000002071	-	0.00198321	Axl
ENSRNOG0000001866	-	0.00198321	Glg1
ENSRNOG0000001361	18.55070843	0.00199198	Chrna5
ENSRNOG0000001871	-	0.00202750	Clec10a
ENSRNOG0000005098	4.416069962	0.00203277	AABR06009228.1
ENSRNOG0000002485	-	0.00204809	Tmx4
ENSRNOG0000002023	2.343891484	0.00204809	Pias4
ENSRNOG0000001121	2.068817337	0.00204809	Polr2f
ENSRNOG0000000188	2.050745854	0.00204837	Trmt2a
ENSRNOG0000005024	-	0.00205503	AABR06016922.1
ENSRNOG0000000125	-	0.00205503	Mlxip
ENSRNOG0000002521	-	0.00205681	RGD1559622
ENSRNOG0000000274	-	0.00205681	Fstl1
ENSRNOG0000000057	-	0.00205681	Spock2
ENSRNOG0000000497	-3.76410462	0.00205681	Prkacb
ENSRNOG0000000458	-	0.00206634	Galnt16
ENSRNOG0000001065	47.64348328	0.00206906	LOC100363289
ENSRNOG0000000399	-	0.00207954	Adcy3
ENSRNOG0000001168	3.268333977	0.00208110	Fes
ENSRNOG0000001343	2.074681157	0.00208110	Exosc8
ENSRNOG0000001094	-	0.00209009	Mmp14
ENSRNOG0000004607	13.29149466	0.00209439	AABR06014073.1
ENSRNOG0000000819	4.701537749	0.00209439	Hoxb4
ENSRNOG0000000064	-	0.00209439	Reep3
ENSRNOG0000001663	2.234082088	0.00209439	Lpin3
ENSRNOG0000000428	-	0.00209439	Kdm6a
ENSRNOG0000000980	-	0.00209439	Wasf2
ENSRNOG0000001956	-	0.00209496	Tbx15
ENSRNOG0000001051	-	0.00209496	Col12a1
ENSRNOG0000002499	-	0.00209923	Trps1
ENSRNOG0000000733	-	0.00209923	Fbln2
ENSRNOG0000004991	4.107632369	0.00210354	Lrg1
ENSRNOG0000000217	-	0.00212066	LOC100911602
ENSRNOG0000001891	-	0.00212634	Pfkfb3
ENSRNOG0000000620	-	0.00213111	St18
ENSRNOG0000001444	-	0.00213111	Pde5a
ENSRNOG0000000093	6.037670076	0.00213187	Piwil1
ENSRNOG0000003058	3.919739888	0.00213187	LOC317588
ENSRNOG0000001073	-	0.00213187	Mbnl2
ENSRNOG0000000747	-	0.00213187	ST7
ENSRNOG0000000922	2.047546153	0.00213187	E4f1
ENSRNOG0000000528	-	0.00214240	Coch
ENSRNOG0000003166	-	0.00214668	Lpp
ENSRNOG0000001788	2.998289054	0.00216286	Mutyh
ENSRNOG0000002835	-	0.00218051	Edem3
ENSRNOG0000004664	-	0.00218051	Impad1
ENSRNOG0000003018	-	0.00218621	Cyp2d1
ENSRNOG0000003891	21.85125401	0.00218621	AABR06032064.2
ENSRNOG0000003152	-	0.00218621	LOC689840
ENSRNOG0000004847	-	0.00218621	Kcne4
ENSRNOG0000000470	-	0.00218621	Foxn3
ENSRNOG0000001713	59.57757354	0.00218698	Rhd
ENSRNOG0000000553	8.159788035	0.00219013	Rps6kl1
ENSRNOG0000001494	-	0.00219013	Kpna3
ENSRNOG0000002722	2.152792011	0.00219013	Slc35d2
ENSRNOG0000001154	-	0.00219072	Cygb
ENSRNOG0000002684	2.80339208	0.00219461	Thap3
ENSRNOG0000004847	9.888281323	0.00222910	AABR06062861.1
ENSRNOG0000000619	-2.21694251	0.00222910	Calu
ENSRNOG0000003071	-	0.00223576	Cfh
ENSRNOG0000000078	2.321128919	0.00225650	Trim39
ENSRNOG0000005026	4.040596991	0.00225998	AABR06028510.1
ENSRNOG0000001262	2.435576083	0.00226528	Mmp15
ENSRNOG0000001895	-	0.00227078	Col4a5
ENSRNOG0000001706	-	0.00227839	Fcna
ENSRNOG0000000379	-	0.00228002	Med14
ENSRNOG0000001391	-	0.00228002	Slc30a7
ENSRNOG0000000367	-2.49786862	0.00229027	Med13
ENSRNOG0000000229	-	0.00229027	Snx29
ENSRNOG0000002283	10.97429402	0.00229417	Ifit3
ENSRNOG0000003729	6.531763683	0.00233493	Plxnb3
ENSRNOG0000000335	2.18609929	0.00233493	Ogt
ENSRNOG0000002870	-	0.00235397	Ntsr1
ENSRNOG0000000015	-	0.00235397	Cdo1
ENSRNOG0000001560	-	0.00236696	PTPRK
ENSRNOG0000000465	2.995802237	0.00238351	Begain
ENSRNOG0000002940	13.10448606	0.00238585	LOC499407
ENSRNOG0000001211	-	0.00238585	Col17a1
ENSRNOG0000002291	2.977222846	0.00239293	Emcn
ENSRNOG0000002102	7.327550264	0.00239683	Mag
ENSRNOG0000000420	2.517865097	0.00239683	Glrx5
ENSRNOG0000004031	25.82555874	0.00240206	AABR06062637.1
ENSRNOG0000003091	7.932446436	0.00240206	Grik4
ENSRNOG0000001485	-	0.00241453	Fbxo30
ENSRNOG0000001658	8.546043161	0.00244494	Mamdc4
ENSRNOG0000000609	-	0.00245260	Cd44
ENSRNOG0000002853	-	0.00245828	AABR06099253.1
ENSRNOG0000001926	11.96385755	0.00247881	Dkk4
ENSRNOG0000000946	-6.61746001	0.00248111	Sfrp2
ENSRNOG0000002088	2.313780208	0.00248415	Tmem101
ENSRNOG0000000444	-	0.00252896	Faim3
ENSRNOG0000000560	-	0.00253829	Med1
ENSRNOG0000002503	16.8718064	0.00254293	RGD1561635
ENSRNOG0000001252	2.471814888	0.00254293	Zfyve19
ENSRNOG0000003260	42.71773151	0.00254469	AY172581.18
ENSRNOG0000002775	-	0.00254469	RGD1560175
ENSRNOG0000001418	-	0.00254469	Tns1
ENSRNOG0000000142	2.122157821	0.00254469	Lrwd1
ENSRNOG0000000083	7.13463628	0.00254583	Ltb
ENSRNOG0000002030	19.01579384	0.00254763	RGD1309139
ENSRNOG0000000241	-	0.00256594	Tgfb2
ENSRNOG0000001430	-	0.00257293	Fbxo42
ENSRNOG0000002998	-	0.00260652	Insr
ENSRNOG0000003876	-	0.00261794	Atxn1l
ENSRNOG0000000865	-	0.00261794	Arhgap21
ENSRNOG0000001522	-	0.00261794	Man1a2
ENSRNOG0000002041	2.903173525	0.00262993	Ramp2

ENSRNOG0000000891	-	0.00262993	Aqr
ENSRNOG0000000652	-	0.00263196	Sema3c
ENSRNOG0000000606	-	0.00263823	Tfec
ENSRNOG0000001053	-	0.00263823	Ankrd50
ENSRNOG0000000976	-	0.00263893	Lamc3
ENSRNOG0000000233	-2.1277945	0.00263893	Aldh3a1
ENSRNOG0000001582	3.384036195	0.00264017	Aurkc
ENSRNOG0000001439	-	0.00265425	Scara5
ENSRNOG0000002155	4.313217969	0.00265425	Mis18a
ENSRNOG0000001675	6.577964783	0.00266159	Slc14a1
ENSRNOG0000000933	18.55682972	0.00266790	Rec114
ENSRNOG0000001123	-	0.00268304	Tiparp
ENSRNOG0000004774	4.641846184	0.00270772	AABR06104557.1
ENSRNOG0000000038	3.437084	0.00272429	Pbld1
ENSRNOG0000001919	-	0.00273013	Arhgef17
ENSRNOG0000000597	-	0.00273819	Gpr176
ENSRNOG0000003674	-	0.00273819	Gna13
ENSRNOG0000001868	-	0.00273819	RGD1305464
ENSRNOG0000000539	-	0.00274398	Sertad2
ENSRNOG0000003095	-	0.00275542	Fat1
ENSRNOG0000002779	5.75731958	0.00275775	Tmie
ENSRNOG0000003898	18.25011977	0.00276644	AABR06029798.2
ENSRNOG0000002755	3.989948771	0.00279924	Mzf1
ENSRNOG0000001846	-	0.00280026	Pdgfrb
ENSRNOG0000001213	2.631085541	0.00280812	Ccdc84
ENSRNOG0000000061	-4.67768793	0.00282970	Bicc1
ENSRNOG0000000812	-	0.00283556	Pla2r1
ENSRNOG0000002385	-	0.00283556	Igsf3
ENSRNOG0000000999	-	0.00284495	Rapgef6
ENSRNOG0000004743	-	0.00284934	AABR06041411.1
ENSRNOG0000001723	-	0.00284934	Adam9
ENSRNOG0000000045	-	0.00285974	RT1-Ba
ENSRNOG0000001414	-	0.00286042	Npy1r
ENSRNOG0000000146	-	0.00286253	Ids
ENSRNOG0000000861	-	0.00286439	Ubr3
ENSRNOG0000001913	-	0.00286684	Clec11a
ENSRNOG0000001508	-	0.00290337	Plin1
ENSRNOG0000004753	3.683263227	0.00290337	AABR06067563.1
ENSRNOG0000002144	4.405491388	0.00295692	Prr7
ENSRNOG0000000411	-	0.00297439	Soat1
ENSRNOG0000001675	-	0.00299703	Crispld2
ENSRNOG0000000469	-	0.00300086	Arhgap5
ENSRNOG0000004305	2.743624189	0.00301404	Aplf
ENSRNOG0000001197	-	0.00304216	C1s
ENSRNOG0000000158	-	0.00306457	Hoxd13
ENSRNOG0000002115	-	0.00307127	Ctss
ENSRNOG0000002072	-	0.00307449	Pten
ENSRNOG0000003743	-	0.00308204	Golga3
ENSRNOG0000002426	2.083610004	0.00308204	Haus5
ENSRNOG0000001382	2.683148671	0.00309164	Rap1gap
ENSRNOG0000001060	2.280553658	0.00309357	Taf15
ENSRNOG0000001299	-	0.00309840	Gpr165
ENSRNOG0000001326	-	0.00310486	Tgfbr2
ENSRNOG0000001617	-2.21456127	0.00311037	RGD1310016
ENSRNOG0000004240	2.894699494	0.00313764	Obp2a
ENSRNOG0000004958	8.930790496	0.00316051	AABR06096154.1
ENSRNOG0000004695	4.286844023	0.00316051	AABR06043416.1
ENSRNOG0000001361	5.59888709	0.00316274	Krt32
ENSRNOG0000003791	11.69931598	0.00316800	LOC680227
ENSRNOG0000001572	-	0.00319077	Loxl4
ENSRNOG0000001089	36.48316501	0.00320198	Prok2
ENSRNOG0000002816	2.021357166	0.00320470	Asmtl
ENSRNOG0000003184	23.04813545	0.00322996	LOC100362172
ENSRNOG0000000765	2.850581958	0.00323074	Col27a1
ENSRNOG0000000080	-4.31774617	0.00323258	Man1a1
ENSRNOG0000000701	-	0.00323258	Mapkbp1
ENSRNOG0000002552	-	0.00323258	Efr3a
ENSRNOG0000001984	2.132827946	0.00323684	Mdp1
ENSRNOG0000000952	-	0.00327001	Adra1a
ENSRNOG0000002815	-	0.00329952	Pld1
ENSRNOG0000004890	7.674468648	0.00331473	AABR06003226.1
ENSRNOG0000004797	5.645964164	0.00332454	AABR06008887.2
ENSRNOG0000004796	-	0.00332454	AABR06056275.2
ENSRNOG0000002160	3.812060759	0.00332454	Zmynd10
ENSRNOG0000001265	3.80099965	0.00332454	Vamp5
ENSRNOG0000002943	3.769341019	0.00332454	AABR06020182.1
ENSRNOG0000002701	-	0.00332454	Cobll1
ENSRNOG0000000076	5.935804489	0.00333486	Ubd
ENSRNOG0000001987	2.329874325	0.00335378	Eml3
ENSRNOG0000001080	2.162568221	0.00335378	Cox6c
ENSRNOG0000001979	-	0.00335499	Pcdhga12
ENSRNOG0000000168	-	0.00336136	Hlcs
ENSRNOG0000003260	3.295672572	0.00338138	Bcdin3d
ENSRNOG0000000724	-	0.00338138	Atxn7
ENSRNOG0000004721	-	0.00338138	Gnpda1
ENSRNOG0000000060	-	0.00338444	Ipmk
ENSRNOG0000000039	-	0.00338444	Kpna1
ENSRNOG0000001051	-	0.00338444	Cachd1
ENSRNOG0000001906	2.036872146	0.00338444	Pura
ENSRNOG0000001186	2.024525452	0.00338444	Fam96b
ENSRNOG0000004875	16.73295418	0.00338547	AABR06044840.1
ENSRNOG0000002735	3.379121413	0.00338547	Sox17
ENSRNOG0000000465	-	0.00338547	Sec23a
ENSRNOG0000002370	2.39948859	0.00338547	Tmem176a
ENSRNOG0000000083	2.033076643	0.00339179	Vars2
ENSRNOG0000004591	-	0.00339785	Jarid2
ENSRNOG0000002106	6.266275788	0.00340284	Fxyd7
ENSRNOG0000000901	-2.33526143	0.00341660	Slc6a6
ENSRNOG0000004238	82.16482747	0.00342985	LOC690386
ENSRNOG0000000633	-	0.00342985	Elovl5
ENSRNOG0000001253	-	0.00342985	Ephb2
ENSRNOG0000004734	3.607968411	0.00344244	AABR06065179.1
ENSRNOG0000001924	-	0.00344403	Glb1l
ENSRNOG0000001021	-	0.00346700	Vwa8
ENSRNOG0000001935	-	0.00347625	Esr1
ENSRNOG0000001929	-	0.00347625	Dctn4
ENSRNOG0000003563	20.0802946	0.00348164	Mir142
ENSRNOG0000001622	-	0.00348949	Gltscr1l
ENSRNOG0000001515	-	0.00350949	Pikfyve
ENSRNOG0000001066	19.03074006	0.00351766	Gzmk
ENSRNOG0000001833	3.492311145	0.00351766	Vwa1
ENSRNOG0000000937	2.519993679	0.00351864	Tbkbp1
ENSRNOG0000000173	-	0.00351864	Eif4g1
ENSRNOG0000001374	2.208812865	0.00352842	Akip1
ENSRNOG0000000932	-	0.00353677	Nr1d1
ENSRNOG0000000288	-	0.00354140	Ddr2
ENSRNOG0000004615	58.30943872	0.00355373	Tubb1
ENSRNOG0000000078	28.17129397	0.00355373	Trim10
ENSRNOG0000001210	-	0.00357476	Tbc1d8b
ENSRNOG0000005074	-	0.00357476	Dnmbp
ENSRNOG0000002259	-	0.00357476	Trerf1
ENSRNOG0000001653	2.470017812	0.00359691	Rab24
ENSRNOG0000003756	-	0.00361616	Cd68
ENSRNOG0000000981	17.99898764	0.00362222	Pnma2
ENSRNOG0000001847	4.0461974	0.00362222	Fuom
ENSRNOG0000005008	-	0.00363602	RGD1563334
ENSRNOG0000000362	-	0.00363602	Cybb
ENSRNOG0000001420	2.865168487	0.00363602	Klf2
ENSRNOG0000004919	9.746701565	0.00364319	AABR06099361.1
ENSRNOG0000004738	-	0.00364319	Smg1
ENSRNOG0000000063	-	0.00365276	Arid5b
ENSRNOG0000000154	-	0.00365582	Gabpa
ENSRNOG0000004572	-	0.00365935	LOC100360726
ENSRNOG0000000219	-2.29589963	0.00367655	Rell1
ENSRNOG0000000836	2.091331435	0.00367655	Pcgf1
ENSRNOG0000000282	13.57921618	0.00369841	Ppbp
ENSRNOG0000000259	3.721041049	0.00370223	Grap
ENSRNOG0000000355	2.654446683	0.00370223	B4galt3
ENSRNOG0000003563	15.90707372	0.00371421	Mirlet7b
ENSRNOG0000002020	3.394298945	0.00371421	Asrgl1
ENSRNOG0000002811	54.40045306	0.00375279	Hbq1
ENSRNOG0000002346	2.875414287	0.00375279	LOC500300
ENSRNOG0000005074	2.787409009	0.00375279	Rn50_16_0006.1
ENSRNOG0000002075	2.537134786	0.00375279	Rdm1
ENSRNOG0000000858	2.124628107	0.00375279	Rnaseh1
ENSRNOG0000000492	-	0.00375279	Map4k5
ENSRNOG0000000995	-	0.00375568	Cacul1
ENSRNOG0000001628	2.492578614	0.00375577	Tcea2
ENSRNOG0000003874	2.162794011	0.00375779	Atp5hl1
ENSRNOG0000001699	7.301640371	0.00376749	LOC687441
ENSRNOG0000000862	-3.2912312	0.00377167	Manea
ENSRNOG0000000899	-	0.00378453	Amotl1
ENSRNOG0000004592	-	0.00379117	Mcu
ENSRNOG0000002338	2.392186221	0.00380036	Rpl37a
ENSRNOG0000000059	5.585108031	0.00381350	Naglt1
ENSRNOG0000002588	-	0.00384034	Nipal1
ENSRNOG0000001068	6.851501794	0.00384207	Med12l
ENSRNOG0000002785	35.95295135	0.00386704	Fcar
ENSRNOG0000000801	3.350339057	0.00387940	Fos
ENSRNOG0000001238	-	0.00390245	Zbtb38
ENSRNOG0000000082	-	0.00392144	Dse
ENSRNOG0000001490	-2.33761385	0.00392164	Uggt1
ENSRNOG0000001862	5.015292964	0.00393215	Plekhb1
ENSRNOG0000003357	-	0.00393215	Glt8d2
ENSRNOG0000001899	3.272848907	0.00393215	Cdc14b
ENSRNOG0000000910	-	0.00393215	Fnip1
ENSRNOG0000001513	2.648389962	0.00393215	Map3k12
ENSRNOG0000002484	-	0.00393345	Tor1aip2
ENSRNOG0000001712	4.790115202	0.00393373	LOC100912128
ENSRNOG0000000811	-	0.00393373	Ppap2b
ENSRNOG0000000325	-	0.00393373	C1qtnf1
ENSRNOG0000004625	-	0.00394512	Emr1
ENSRNOG0000001562	-	0.00397385	Slc35a3
ENSRNOG0000000433	-	0.00400699	Chrdl1
ENSRNOG0000000482	-	0.00400699	Acvr1c
ENSRNOG0000003021	-	0.00400699	Fndc1
ENSRNOG0000002048	2.044126185	0.00401583	Luc7l
ENSRNOG0000000778	21.31396689	0.00401946	Ghrh
ENSRNOG0000001461	-	0.00401946	Tgoln2
ENSRNOG0000000262	-	0.00404023	Ptpn4
ENSRNOG0000000474	-	0.00404957	Cdcp1
ENSRNOG0000001293	2.614380491	0.00405837	Abca7
ENSRNOG0000002046	-	0.00406272	Nrep
ENSRNOG0000003907	3.806956168	0.00406475	LOC688452
ENSRNOG0000000547	-	0.00407329	Fkbp9
ENSRNOG0000000962	-	0.00410336	Cybrd1
ENSRNOG0000003333	2.611867195	0.00413547	Gimap6
ENSRNOG0000000541	-4.28840127	0.00413721	Creb3l1
ENSRNOG0000003270	-	0.00413728	LOC688090
ENSRNOG0000001299	-	0.00413922	Gpr124
ENSRNOG0000002650	6.375703201	0.00414051	Vmo1
ENSRNOG0000000298	-	0.00414051	Nfix
ENSRNOG0000001471	-	0.00416124	Csgalnact2
ENSRNOG0000001722	-	0.00418939	Fam160b1
ENSRNOG0000001522	4.64014981	0.00420201	Fam46c
ENSRNOG0000002874	14.45317945	0.00420206	Gal3st3
ENSRNOG0000000841	4.344397425	0.00421184	Gimap5
ENSRNOG0000001096	-	0.00421184	Itgb1
ENSRNOG0000001676	2.188330439	0.00421689	Ggps1
ENSRNOG0000004712	4.945202292	0.00423310	Tstd1
ENSRNOG0000004587	8.188768255	0.00423972	AABR06100660.1
ENSRNOG0000000130	-	0.00423972	Specc1l
ENSRNOG0000000859	-	0.00424821	Btbd7
ENSRNOG0000002862	-	0.00427043	Hmcn1
ENSRNOG0000002794	10.51565478	0.00427395	Lppr3
ENSRNOG0000003319	-	0.00428151	Osmr
ENSRNOG0000001981	-	0.00430416	Des
ENSRNOG0000000782	2.020506937	0.00431277	Vgll4
ENSRNOG0000000148	2.865807722	0.00432853	Gtf2ird2
ENSRNOG0000003232	2.96371404	0.00433105	Pdia5
ENSRNOG0000001388	-	0.00433156	Adra2b
ENSRNOG0000001751	2.897668398	0.00433517	Aldh3b1
ENSRNOG0000000946	-	0.00433517	Pdzd8
ENSRNOG0000001184	17.93402224	0.00433721	Krt28
ENSRNOG0000003564	8.252836288	0.00433721	Mirlet7i
ENSRNOG0000000294	2.564126554	0.00433721	RGD1304587
ENSRNOG0000001767	-	0.00433721	Pard6g
ENSRNOG0000003200	-	0.00435599	Cyp2b21
ENSRNOG0000001638	2.41371977	0.00435599	Ptms
ENSRNOG0000001294	4.878737551	0.00437807	Mov10
ENSRNOG0000002225	-	0.00437807	Tmprss11e
ENSRNOG0000004968	4.306670172	0.00440457	AABR06082052.1
ENSRNOG0000004204	10.44887191	0.00441367	Gal3st1
ENSRNOG0000000573	-	0.00444263	Pcmtd1
ENSRNOG0000001371	7.064260531	0.00445670	LOC499240
ENSRNOG0000001026	-	0.00445670	Klhdc10
ENSRNOG0000000317	5.145712286	0.00445836	Mpz
ENSRNOG0000001209	-	0.00447974	Adcyap1r1
ENSRNOG0000003890	9.810007197	0.00448279	AABR06088060.1
ENSRNOG0000001720	-	0.00451023	Igfbp5
ENSRNOG0000001218	-	0.00451054	Lpl
ENSRNOG0000000865	8.26700717	0.00451309	Snca
ENSRNOG0000000552	-	0.00451679	Man2b2
ENSRNOG0000001580	2.586925108	0.00453781	Pyroxd2
ENSRNOG0000000750	9.82815146	0.00456599	Lrtm2
ENSRNOG0000001051	-	0.00457730	Fam126a
ENSRNOG0000003071	2.337448236	0.00457730	RT1-A2
ENSRNOG0000000600	-	0.00459243	Cdk12
ENSRNOG0000001957	4.194799954	0.00460394	Adamts19
ENSRNOG0000002179	3.402276754	0.00464274	Fam227a
ENSRNOG0000002424	6.223389943	0.00464615	Cadm4
ENSRNOG0000002533	-	0.00464615	Cd109
ENSRNOG0000000768	-	0.00464715	Fhl5
ENSRNOG0000001569	-	0.00464715	Taok1
ENSRNOG0000000312	-	0.00466526	Prelp
ENSRNOG0000004729	5.230219127	0.00469270	AABR06097607.1

ENSRNOG0000001203	-4.99009503	0.00469270	Pcsk5
ENSRNOG0000001083	-	0.00469930	Pdgfrl
ENSRNOG0000002852	-	0.00472963	Mansc1
ENSRNOG0000002488	-	0.00473198	Ext1
ENSRNOG0000001468	2.362121891	0.00476175	Npr1
ENSRNOG0000004553	3.894634974	0.00477253	AABR06049731.1
ENSRNOG0000003368	-	0.00479992	Cep170b
ENSRNOG0000000915	-	0.00481736	Cidec
ENSRNOG0000000117	2.182713866	0.00481736	Rnf10
ENSRNOG0000004599	3.322724688	0.00484434	Sema6b
ENSRNOG0000002411	-	0.00486875	C6
ENSRNOG0000002242	-	0.00486875	Flrt1
ENSRNOG0000004584	-	0.00486875	Rfx2
ENSRNOG0000003745	3.710136709	0.00487218	LOC100364989
ENSRNOG0000001129	-	0.00488791	Col1a2
ENSRNOG0000001327	-	0.00488791	Ireb2
ENSRNOG0000001663	-2.658077	0.00491960	Dsg3
ENSRNOG0000004556	6.574082535	0.00492460	AABR06007423.1
ENSRNOG0000004935	-	0.00492460	Nat8l
ENSRNOG0000001277	-	0.00492586	Msr1
ENSRNOG0000003284	-	0.00494771	RT1-Da
ENSRNOG0000001077	-	0.00494902	Arrdc4
ENSRNOG0000001357	6.704912555	0.00495352	Atp6v1b1
ENSRNOG0000000266	-	0.00495831	Lamc2
ENSRNOG0000002368	-	0.00496176	Upk3b
ENSRNOG0000001208	-	0.00496176	Itga1
ENSRNOG0000001289	-	0.00497983	Cyp2c11
ENSRNOG0000000846	2.087653559	0.00499106	Tmem176b
ENSRNOG0000002602	-3.39911005	0.00499151	Taf4b
ENSRNOG0000001001	-	0.00499325	Clec4a3
ENSRNOG0000000115	3.197770102	0.00499858	Sirt4
ENSRNOG0000002450	2.188367812	0.00502847	Rgs3
ENSRNOG0000003546	19.82616233	0.00503024	Mir23b
ENSRNOG0000004208	3.505856725	0.00505874	Rab26
ENSRNOG0000001873	-	0.00506291	Cd74
ENSRNOG0000002866	-	0.00508973	Arhgap35
ENSRNOG0000001869	-	0.00511242	Lipg
ENSRNOG0000001327	-	0.00511699	LOC681458
ENSRNOG0000000817	-	0.00511860	Jph2
ENSRNOG0000000505	-	0.00513136	Slc39a9
ENSRNOG0000000894	-	0.00513207	Cpz
ENSRNOG0000002998	-	0.00513207	Zbtb16
ENSRNOG0000000222	-	0.00513207	Adcy5
ENSRNOG0000000107	2.493029572	0.00513207	LOC100910427
ENSRNOG0000000012	-	0.00513207	Kpna6
ENSRNOG0000003975	-	0.00514959	Gpr34
ENSRNOG0000000464	-	0.00515146	Il10
ENSRNOG0000003326	12.20695653	0.00515146	AABR06002048.1
ENSRNOG0000000030	2.110589261	0.00515729	Smpd2
ENSRNOG0000002524	-	0.00517035	RGD1311946
ENSRNOG0000004324	2.581788803	0.00517741	AABR06002662.1
ENSRNOG0000005040	8.05089188	0.00518677	AABR06043689.1
ENSRNOG0000002675	-2.88217808	0.00524538	Mpzl3
ENSRNOG0000002749	-	0.00525190	Vldlr
ENSRNOG0000001841	2.320923798	0.00525190	Sfi1
ENSRNOG0000002797	-	0.00526742	Il22ra1
ENSRNOG0000001900	2.245380063	0.00526742	Arrdc2
ENSRNOG0000003666	2.017477881	0.00527327	Hexdc
ENSRNOG0000003890	4.590437196	0.00527386	Phf11b
ENSRNOG0000000246	-	0.00528446	Nid1
ENSRNOG0000002346	-2.98507969	0.00528937	Fam168b
ENSRNOG0000001135	29.71774112	0.00529317	Gfi1b
ENSRNOG0000003322	19.82208665	0.00530054	Oas1k
ENSRNOG0000001699	10.98878007	0.00530054	Grp
ENSRNOG0000001827	-	0.00530373	Sfxn1
ENSRNOG0000001755	-	0.00530636	Fbln7
ENSRNOG0000003224	-	0.00532068	Acsm3
ENSRNOG0000001899	-2.5257932	0.00532068	Gsn
ENSRNOG0000000860	-	0.00534796	Steap4
ENSRNOG0000001106	-	0.00534796	Dennd1b
ENSRNOG0000000612	8.865894278	0.00534977	Shh
ENSRNOG0000000222	-	0.00534977	Kit
ENSRNOG0000000016	-	0.00534977	Chm
ENSRNOG0000000470	-	0.00534977	Muc15
ENSRNOG0000002930	3.043394069	0.00535238	Lrmp
ENSRNOG0000001617	-	0.00536286	Scara3
ENSRNOG0000003740	2.194963114	0.00536675	Myeov2
ENSRNOG0000000494	-	0.00541026	LOC100364912
ENSRNOG0000001636	-9.45247814	0.00541814	Colec12
ENSRNOG0000000851	-	0.00541962	RGD1309079
ENSRNOG0000004616	4.248401085	0.00542008	AABR06009617.1
ENSRNOG0000002722	24.07133084	0.00542502	Ly6g6f
ENSRNOG0000004941	-	0.00542502	Mia3
ENSRNOG0000002827	2.040080672	0.00543958	Ctu2
ENSRNOG0000000821	2.069823115	0.00544108	Trim47
ENSRNOG0000001467	-	0.00549843	Pi4k2a
ENSRNOG0000000671	-	0.00549987	Rbm33
ENSRNOG0000001903	12.78909115	0.00550309	Neu4
ENSRNOG0000004617	3.541810876	0.00552289	AABR06028471.1
ENSRNOG0000000428	2.127136831	0.00552289	Camta2
ENSRNOG0000001502	-	0.00552289	Arhgef11
ENSRNOG0000000444	-	0.00552699	Sptlc3
ENSRNOG0000001130	7.367908839	0.00554685	Sox10
ENSRNOG0000001106	-	0.00554685	Mar-06
ENSRNOG0000001675	-	0.00554798	Loxl2
ENSRNOG0000004256	-	0.00554798	Bag4
ENSRNOG0000001801	-	0.00555095	Fam208b
ENSRNOG0000002289	3.731338597	0.00557039	Rimbp2
ENSRNOG0000002719	-	0.00559672	Birc6
ENSRNOG0000000666	-	0.00559672	Usp2
ENSRNOG0000002783	-	0.00559958	Fnip2
ENSRNOG0000004844	-	0.00562497	RGD1561998
ENSRNOG0000004630	14.50714619	0.00565070	AABR06025556.1
ENSRNOG0000000427	-	0.00565070	Itga3
ENSRNOG0000000429	-	0.00566431	Abca9
ENSRNOG0000002562	-	0.00566431	Rnase4
ENSRNOG0000001154	2.072513065	0.00566431	Zfp219
ENSRNOG0000002918	-	0.00566812	Rasa1
ENSRNOG0000002746	9.971941681	0.00568363	Cd27
ENSRNOG0000000855	-	0.00568363	Slc9a9
ENSRNOG0000001001	10.47864899	0.00568852	Gp9
ENSRNOG0000000346	5.532618715	0.00568852	Capn8
ENSRNOG0000003316	-	0.00568904	Cpeb4
ENSRNOG0000001425	-	0.00569664	Ces4a
ENSRNOG0000003877	42.98907444	0.00570260	Oscar
ENSRNOG0000004696	4.051891506	0.00570260	Ubxn7
ENSRNOG0000001921	-	0.00570343	Olfml3
ENSRNOG0000000471	-	0.00570807	Angptl1
ENSRNOG0000000678	2.199156431	0.00570807	Ddit3
ENSRNOG0000000194	34.37312634	0.00572144	Retnlg
ENSRNOG0000002219	-	0.00572147	Bmpr2
ENSRNOG0000002292	-	0.00574228	Slc25a12
ENSRNOG0000002733	3.583158774	0.00574321	Gemin6
ENSRNOG0000002640	-	0.00574321	LOC683565
ENSRNOG0000001124	2.584190741	0.00574321	Tfdp2
ENSRNOG0000000350	-	0.00574321	Ergic1
ENSRNOG0000001834	-	0.00576714	Agtr1a
ENSRNOG0000001159	4.153526433	0.00580110	Senp8
ENSRNOG0000001886	-	0.00581261	Adamts12
ENSRNOG0000001594	-	0.00581647	Fkbp10
ENSRNOG0000003756	5.228140542	0.00583824	RGD1560398
ENSRNOG0000001085	-	0.00585322	Zyg11b
ENSRNOG0000000469	-	0.00585322	Pbx1
ENSRNOG0000001065	-	0.00587897	Elmsan1
ENSRNOG0000000100	-	0.00588059	Retn
ENSRNOG0000000388	-	0.00589612	Cep350
ENSRNOG0000001397	-	0.00590018	Psat1
ENSRNOG0000001502	-	0.00590697	Dbt
ENSRNOG0000004631	3.119397299	0.00590697	Tomm6
ENSRNOG0000002456	2.246885156	0.00590697	Ndufs7
ENSRNOG0000002565	-	0.00591344	Ikzf5
ENSRNOG0000001450	-	0.00591344	Il1r1
ENSRNOG0000001007	-	0.00591865	Car3
ENSRNOG0000001931	10.07324622	0.00591865	Cplx3
ENSRNOG0000002378	-	0.00591865	LOC100909434
ENSRNOG0000003751	-	0.00591865	Qser1
ENSRNOG0000000314	-	0.00591865	Timp2
ENSRNOG0000004595	2.026540322	0.00593397	Tmc6
ENSRNOG0000002445	3.466494592	0.00594405	Rltpr
ENSRNOG0000001937	2.269149162	0.00594405	Zfp329
ENSRNOG0000003241	-2.09460839	0.00594405	Tmem161b
ENSRNOG0000004927	2.062925248	0.00594846	Ppp2r3b
ENSRNOG0000001857	2.069441348	0.00597463	Neil1
ENSRNOG0000002537	-	0.00597696	Glce
ENSRNOG0000000209	-	0.00597886	Tgfbr3
ENSRNOG0000001188	-2.59477964	0.00597886	Slc25a15
ENSRNOG0000003116	-	0.00598261	Ccl24
ENSRNOG0000000137	3.51722661	0.00598494	Oas1b
ENSRNOG0000003320	-	0.00599176	Entpd5
ENSRNOG0000000045	2.435970268	0.00599368	Psmb9
ENSRNOG0000002087	3.27147974	0.00600134	Nphs1
ENSRNOG0000003996	-	0.00600959	Dsc2
ENSRNOG0000000437	-	0.00601147	Lpin1
ENSRNOG0000001714	-	0.00603807	Zfp185
ENSRNOG0000001700	-	0.00604299	Zfp652
ENSRNOG0000003733	-	0.00604451	Siglec10
ENSRNOG0000001635	-	0.00604451	Cbfa2t2
ENSRNOG0000000907	-	0.00605908	Prkar2b
ENSRNOG0000000332	-	0.00605908	LOC100910121
ENSRNOG0000001445	5.78400672	0.00607795	LOC499136
ENSRNOG0000004805	-	0.00609604	Zfp106
ENSRNOG0000000941	-	0.00611443	Ptprg
ENSRNOG0000000691	15.67459291	0.00612588	Sptb
ENSRNOG0000000974	3.546749784	0.00612588	Cyp4b1
ENSRNOG0000003696	-	0.00613996	Abcc9
ENSRNOG0000001486	-3.58479746	0.00613996	Reck
ENSRNOG0000001942	-	0.00613996	Dip2b
ENSRNOG0000001733	2.047786597	0.00614063	Dapk2
ENSRNOG0000002072	-	0.00615526	Stc2
ENSRNOG0000002778	3.289701157	0.00615526	Cdc6
ENSRNOG0000001609	-	0.00615526	Mtmr10
ENSRNOG0000002959	2.157913818	0.00616290	Srsf11
ENSRNOG0000000098	2.475724736	0.00616650	Scarb1
ENSRNOG0000000768	2.849965211	0.00621770	Sema7a
ENSRNOG0000003046	2.375174617	0.00621770	Ube2l6
ENSRNOG0000001844	-	0.00621995	Agt
ENSRNOG0000000846	2.098923808	0.00622779	Smdt1
ENSRNOG0000000227	-	0.00622779	Naaa
ENSRNOG0000001809	-	0.00625722	Cd83
ENSRNOG0000000545	5.452180545	0.00627433	Ppp2r2c
ENSRNOG0000003321	-	0.00629601	RT1-Db1
ENSRNOG0000000184	-	0.00635757	Klhl42
ENSRNOG0000002000	-2.37278346	0.00635757	Epb41l1
ENSRNOG0000003795	3.601088985	0.00636113	Aifm3
ENSRNOG0000001317	19.00657001	0.00637081	Grm2
ENSRNOG0000000563	-	0.00637747	Ar
ENSRNOG0000000002	-	0.00637747	Myh11
ENSRNOG0000001585	-	0.00641171	Chdh
ENSRNOG0000000429	-	0.00642427	Cltc
ENSRNOG0000000357	-	0.0064313	Adamts2
ENSRNOG0000000088	-	0.00643308	Auts2
ENSRNOG0000003349	-	0.00645491	Igdcc4
ENSRNOG0000001797	7.888441075	0.00645557	Dnajb13
ENSRNOG0000000335	-	0.00645557	Col3a1
ENSRNOG0000004661	8.896988396	0.00647486	Dzip1-ps1
ENSRNOG0000001055	4.491536647	0.00647486	Lhx2
ENSRNOG0000002029	2.141771212	0.00647486	Usmg5
ENSRNOG0000002660	4.025354123	0.00649135	Ifi27l2b
ENSRNOG0000001571	-	0.00649135	Parva
ENSRNOG0000002973	-	0.00655619	Pid1
ENSRNOG0000004628	10.78549844	0.00657910	Mir6326
ENSRNOG0000004887	19.91819297	0.00659635	Gm20721
ENSRNOG0000001389	43.9032433	0.00660275	Krt40
ENSRNOG0000000727	11.12766114	0.00661541	Il12rb2
ENSRNOG0000001475	-	0.00661655	Fam208a
ENSRNOG0000000994	-	0.00661690	Pcdh18
ENSRNOG0000000394	-	0.00662089	Ntn1
ENSRNOG0000004286	-	0.00662394	Pappa2
ENSRNOG0000003043	-	0.00662394	RT1-Db2
ENSRNOG0000003679	-10.9746351	0.00665212	Olfml1
ENSRNOG0000002184	-5.37497115	0.00665576	Cped1
ENSRNOG0000000500	-	0.00665576	Angpt4
ENSRNOG0000000166	-	0.00666908	Dyrk1a
ENSRNOG0000004890	-	0.00669489	AABR06016611.1
ENSRNOG0000001471	3.217625828	0.00671549	Zfp39
ENSRNOG0000001793	-	0.00672379	Ccdc3
ENSRNOG0000001867	-	0.00675001	Rptn
ENSRNOG0000000760	14.92813932	0.00675058	Inhbe
ENSRNOG0000001475	-	0.00676386	Ret
ENSRNOG0000000871	-	0.00677051	Slc41a2
ENSRNOG0000004920	2.323369143	0.00680338	AABR06045579.1
ENSRNOG0000001876	-	0.00681140	Mpp7
ENSRNOG0000001372	-	0.00681283	Aebp1
ENSRNOG0000000268	-	0.00683630	Lamc1
ENSRNOG0000002132	-	0.00683630	Car13
ENSRNOG0000001060	10.48108118	0.00685224	Gzma
ENSRNOG0000001483	-	0.00685447	Ralgapb
ENSRNOG0000001750	2.366968065	0.00685975	Npepo
ENSRNOG0000000389	-	0.00688405	Krt14
ENSRNOG0000000943	55.36696349	0.00688809	Hemgn
ENSRNOG0000002180	10.65525535	0.00689293	Isg15
ENSRNOG0000002856	-	0.00689293	Pld4
ENSRNOG0000001536	5.871587234	0.00689293	9330171B17Rik
ENSRNOG0000000745	-5.3205975	0.00689293	Serping1
ENSRNOG0000000295	5.261338651	0.00689293	Lyl1
ENSRNOG0000004794	3.394062022	0.00689293	AABR06029450.1

ENSRNOG0000001869	-	0.00689293	Wac
ENSRNOG0000001008	-	0.00689293	Ythdf3
ENSRNOG0000000419	2.109133549	0.00690507	Rps29
ENSRNOG0000001424	2.006354085	0.00691056	Pear1
ENSRNOG0000003077	-	0.00694197	Dgkb
ENSRNOG0000004750	-11.3643759	0.00694893	NA
ENSRNOG0000001968	2.272001855	0.00694893	Timm13
ENSRNOG0000000175	2.216936144	0.00694893	Tctex1d2
ENSRNOG0000001918	2.201151329	0.00697236	Tmem53
ENSRNOG0000000317	-	0.0069846	Tapt1
ENSRNOG0000005027	5.074489471	0.00699366	AABR06006741.1
ENSRNOG0000001457	5.271257997	0.0070436	Fxyd4
ENSRNOG0000004843	3.480844487	0.0070436	AABR06098023.1
ENSRNOG0000002437	2.069785448	0.0070436	Cwf19l2
ENSRNOG0000001500	8.65075348	0.00704505	Gcm2
ENSRNOG0000002754	-	0.00707120	Fam102b
ENSRNOG0000001195	2.261659666	0.00711092	Plk2
ENSRNOG0000000268	2.64923448	0.00711391	Zfp692
ENSRNOG0000000027	2.309513185	0.00718001	Fam13c
ENSRNOG0000001824	14.55525167	0.00725936	Ank1
ENSRNOG0000004646	2.44197104	0.00730395	Tatdn3
ENSRNOG0000001474	2.102477073	0.00731878	Hagh
ENSRNOG0000000766	-	0.00733884	Zfp800
ENSRNOG0000000517	-	0.00733884	Sgpp1
ENSRNOG0000000633	-	0.00733884	Lrp6
ENSRNOG0000000707	-	0.00734613	Fem1b
ENSRNOG0000002094	2.017430046	0.00734613	Ccdc12
ENSRNOG0000000540	-	0.00735050	Rasgrp1
ENSRNOG0000001786	-	0.00736596	Bdp1
ENSRNOG0000001941	2.378825404	0.00736596	Atg16l2
ENSRNOG0000004226	-	0.00738824	Sprr4
ENSRNOG0000000715	-	0.00740502	Cdk14
ENSRNOG0000002553	26.93482266	0.00741067	LOC100911167
ENSRNOG0000004982	2.198563565	0.00741067	Crlf2
ENSRNOG0000000124	-	0.00741067	Clip1
ENSRNOG0000001221	-	0.00741321	Tgfbi
ENSRNOG0000000125	-	0.00741449	Col6a2
ENSRNOG0000000397	-	0.00746507	Tshr
ENSRNOG0000003219	-	0.00748487	RGD1307325
ENSRNOG0000001651	4.745829647	0.00748565	Mbp
ENSRNOG0000000430	-	0.00748565	Abl2
ENSRNOG0000002353	-	0.00748565	Fam69a
ENSRNOG0000001459	-	0.00753986	Irs1
ENSRNOG0000001078	-	0.00754930	Dlc1
ENSRNOG0000002894	-	0.00755268	Tmem182
ENSRNOG0000000019	-	0.00755268	Ep300
ENSRNOG0000000356	2.069140245	0.00755268	Ppox
ENSRNOG0000001541	-	0.00755693	Rhoq
ENSRNOG0000000623	6.344997342	0.00756052	Gpr37l1
ENSRNOG0000001474	-	0.00756584	Nbea
ENSRNOG0000000230	2.307578206	0.00757140	Hlx
ENSRNOG0000001001	-	0.00758262	Wee1
ENSRNOG0000000631	2.125837638	0.00758262	Zfp202
ENSRNOG0000005004	7.927455345	0.00762315	AABR06015425.1
ENSRNOG0000000136	4.817410843	0.00762315	Gpc2
ENSRNOG0000001547	2.317178564	0.00768301	Ubxn11
ENSRNOG0000001662	-	0.00769667	Tmeff2
ENSRNOG0000000958	-	0.00770346	Angptl7
ENSRNOG0000000646	4.71403276	0.00771374	Hoxa5
ENSRNOG0000000610	2.921999523	0.00771374	Gngt2
ENSRNOG0000001221	2.513290944	0.00771374	Nthl1
ENSRNOG0000003087	36.49754906	0.00776523	Krt72
ENSRNOG0000003668	-	0.00782235	Pycr1
ENSRNOG0000001563	2.086880803	0.00782861	Taf1c
ENSRNOG0000000538	-	0.00785488	Kitlg
ENSRNOG0000001533	-	0.00785488	Fcho2
ENSRNOG0000002115	2.420272295	0.00786702	Vegfb
ENSRNOG0000003054	-	0.00787429	Dpp6
ENSRNOG0000001570	4.640317858	0.00789211	AABR06003301.1
ENSRNOG0000000344	13.92770732	0.00794794	Klf1
ENSRNOG0000002914	9.881699933	0.00794794	AY172581.2
ENSRNOG0000000303	-	0.00794794	Atp2b4
ENSRNOG0000002986	2.882507641	0.00796217	Dennd6b
ENSRNOG0000003985	6.052295754	0.00798496	AABR06053663.2
ENSRNOG0000001204	-	0.00799339	Slc25a48
ENSRNOG0000000453	2.413276326	0.00799769	Fam69b
ENSRNOG0000003142	10.77524018	0.00803217	LOC500846
ENSRNOG0000002930	15.09534217	0.00805976	AY172581.4
ENSRNOG0000001840	-	0.00805976	Apoc4
ENSRNOG0000002695	-	0.00805976	Gpr88
ENSRNOG0000000317	-	0.00805976	Serpinf1
ENSRNOG0000001402	-	0.00805976	Klhl13
ENSRNOG0000001640	-	0.00805976	Kirrel
ENSRNOG0000000233	-	0.00805976	Mospd1
ENSRNOG0000000362	-5.19147355	0.00806220	Fmo3
ENSRNOG0000004330	30.78405633	0.00808825	LOC690478
ENSRNOG0000001981	2.784486181	0.00809297	Dus2
ENSRNOG0000004297	-	0.00811018	Tmem45al
ENSRNOG0000001687	2.298324398	0.00811018	Cbx7
ENSRNOG0000002256	8.221058896	0.00811237	AABR06058786.1
ENSRNOG0000001341	4.170037649	0.00811766	Ptpn18
ENSRNOG0000000343	-	0.00811766	Trove2
ENSRNOG0000000702	-	0.00811908	Hgf
ENSRNOG0000000322	-	0.00811908	Myoc
ENSRNOG0000004851	-	0.00811908	Garem
ENSRNOG0000000165	-	0.00814158	Kcnj15
ENSRNOG0000001138	-	0.00814158	Tet3
ENSRNOG0000004819	-	0.00814158	Rgmb
ENSRNOG0000000389	-	0.00814193	Col1a1
ENSRNOG0000004767	9.93956526	0.00814265	AABR06033358.1
ENSRNOG0000004962	6.651626168	0.00819360	AABR06057042.1
ENSRNOG0000003068	6.799689098	0.00823081	Lrrc2
ENSRNOG0000001885	-	0.00823081	Col4a6
ENSRNOG0000001781	-	0.00823081	Cd14
ENSRNOG0000002836	10.89171335	0.00823278	Etnk2
ENSRNOG0000003342	10.65043565	0.00823736	LOC100363112
ENSRNOG0000000141	-	0.00823736	Serpine1
ENSRNOG0000002833	-	0.00823736	Fat4
ENSRNOG0000001286	-	0.00824545	Ern1
ENSRNOG0000000373	-	0.00826720	Col5a2
ENSRNOG0000000158	3.787575606	0.00827537	Hoxd10
ENSRNOG0000001606	2.136202165	0.00827537	Bambi
ENSRNOG0000000384	-	0.00827719	Kcnh1
ENSRNOG0000003028	-13.7815237	0.00830115	Epha3
ENSRNOG0000000759	-	0.00830115	Afap1
ENSRNOG0000001188	2.623676397	0.00831482	Rhpn2
ENSRNOG0000002447	-	0.00833275	Lman1
ENSRNOG0000001369	-	0.00835844	Ntng2
ENSRNOG0000001084	-	0.00836545	Nhlrc3
ENSRNOG0000000064	2.13241608	0.00836591	Egr2
ENSRNOG0000001620	-	0.00837306	Setbp1
ENSRNOG0000002109	2.669235493	0.00837306	Rasgrp2
ENSRNOG0000003983	-	0.00837369	Jade3
ENSRNOG0000000090	-	0.00837589	Medag
ENSRNOG0000001586	2.055937312	0.00843960	Hint2
ENSRNOG0000001692	-	0.00844286	Klhl11
ENSRNOG0000001391	-	0.00844757	Igsf10
ENSRNOG0000002837	17.78214421	0.00849806	Mpl
ENSRNOG0000001278	-	0.00849806	Gtf3c4
ENSRNOG0000004574	-	0.00850908	Tmx3
ENSRNOG0000000180	-	0.00851788	Fetub
ENSRNOG0000002936	3.437508405	0.00851788	Prrt2
ENSRNOG0000005065	-	0.00851788	P4ha1
ENSRNOG0000002157	-	0.00854585	Dpy19l3
ENSRNOG0000004216	2.183799253	0.00858834	Btbd19
ENSRNOG0000000277	-	0.00862593	Rgs4
ENSRNOG0000000461	-	0.00864342	Lum
ENSRNOG0000001535	3.251383347	0.00866873	Prss12
ENSRNOG0000002809	-	0.00869074	Marveld1
ENSRNOG0000001747	-	0.00869605	Tcf12
ENSRNOG0000000652	8.926771737	0.00871415	Slc6a1
ENSRNOG0000001018	-7.80057714	0.00871799	Satb2
ENSRNOG0000002997	3.179024017	0.00871799	Mt-nd5
ENSRNOG0000003295	-	0.00871799	Adh7
ENSRNOG0000004385	10.22312557	0.00872609	AABR06062867.1
ENSRNOG0000002517	-	0.00873751	Kat6a
ENSRNOG0000000151	-	0.00874342	Itga6
ENSRNOG0000000254	-	0.00874504	Tnn
ENSRNOG0000000593	-	0.00874578	Cpq
ENSRNOG0000002658	-	0.00874578	Dpy19l1
ENSRNOG0000000966	2.002088214	0.00874578	Tgds
ENSRNOG0000002514	-	0.00877177	Zfat
ENSRNOG0000004821	3.169278829	0.00881206	Bbc3
ENSRNOG0000000927	-	0.00882279	Obp3
ENSRNOG0000001791	2.051633595	0.00882279	Prkcdbp
ENSRNOG0000000542	-	0.00884257	Foxp2
ENSRNOG0000004198	12.70392357	0.00884571	AABR06015851.1
ENSRNOG0000000806	-	0.00891846	LOC102554884
ENSRNOG0000001774	15.09477476	0.00896864	Nkg7
ENSRNOG0000001375	30.37997973	0.00897630	Krt35
ENSRNOG0000000436	2.231518031	0.00897737	Gemin2
ENSRNOG0000002015	2.025594193	0.00899963	Dalrd3
ENSRNOG0000005015	-13.5908668	0.00900372	Chsy3
ENSRNOG0000002579	-	0.00901521	Usp31
ENSRNOG0000005039	8.60211188	0.00902398	AABR06005880.1
ENSRNOG0000000221	-2.94593224	0.00903836	Mylk
ENSRNOG0000000590	2.578506937	0.00908640	Ccdc34
ENSRNOG0000003898	19.72174791	0.00912710	LOC498084
ENSRNOG0000001968	2.531668644	0.00915360	Fam173a
ENSRNOG0000000121	7.565643851	0.00916791	Trpm2
ENSRNOG0000003287	7.547533406	0.00916791	AABR06016949.1
ENSRNOG0000001585	3.497670674	0.00916791	Nat8b
ENSRNOG0000001481	17.66704048	0.00918726	Nlrp12
ENSRNOG0000000771	-	0.00919776	Tmcc3
ENSRNOG0000001430	8.261342426	0.00920303	Dlgap3
ENSRNOG0000001461	-	0.00920303	Anpep
ENSRNOG0000002792	-	0.00927417	Rlf
ENSRNOG0000003251	-11.8577136	0.00928509	AABR06095360.1
ENSRNOG0000002168	2.164924168	0.00930074	Rps6kb2
ENSRNOG0000000664	-	0.00930427	Yipf6
ENSRNOG0000000121	7.844358726	0.00933752	Dnmt3l
ENSRNOG0000000478	-	0.00933881	Fam171b
ENSRNOG0000002853	-	0.00933881	Zfp518b
ENSRNOG0000001808	-	0.00936414	Slc26a2
ENSRNOG0000002373	7.712530445	0.00936930	RGD1560821
ENSRNOG0000000056	-	0.00937919	Unc5b
ENSRNOG0000000824	-	0.00938806	Ikbip
ENSRNOG0000001771	-	0.00938806	AABR06055554.1
ENSRNOG0000004337	2.005537038	0.00938806	RGD1566099
ENSRNOG0000001151	-2.75645495	0.00941021	Ccnt1
ENSRNOG0000000284	-	0.00943242	Cdc42bpa
ENSRNOG0000001845	-	0.00943863	Xylt1
ENSRNOG0000000124	-	0.00943863	Col6a1
ENSRNOG0000001565	-	0.00943863	Ghr
ENSRNOG0000000600	-	0.00943863	Stk35
ENSRNOG0000004234	9.314925535	0.00946391	Smim22
ENSRNOG0000002803	15.03557598	0.00946659	RT1-M1-5
ENSRNOG0000001688	-	0.00946659	Hrh4
ENSRNOG0000001567	2.480599545	0.00946796	Acap1
ENSRNOG0000001999	2.339463565	0.00950079	Cnbd2
ENSRNOG0000003265	-	0.00952757	Plcl1
ENSRNOG0000001428	-	0.00953115	Fn1
ENSRNOG0000000527	-	0.00953115	Shmt1
ENSRNOG0000004840	14.79982641	0.00956133	IGH-1A
ENSRNOG0000001468	-	0.00960241	Il1rl2
ENSRNOG0000003682	-	0.00960980	Pde1b
ENSRNOG0000000573	-	0.00960980	Asap1
ENSRNOG0000001895	3.480804484	0.00961140	Mt3
ENSRNOG0000004890	7.998351529	0.00962251	AABR06012582.1
ENSRNOG0000000780	-	0.00963601	C1galt1
ENSRNOG0000000988	-	0.00963601	Fkbp14
ENSRNOG0000003047	5.792356442	0.00963620	AY172581.9
ENSRNOG0000001776	-	0.00965124	Car12
ENSRNOG0000003230	-12.027472	0.00965406	Dsel
ENSRNOG0000001339	7.308070693	0.00969356	Pglyrp1
ENSRNOG0000001944	5.382348155	0.00969356	Ecel1
ENSRNOG0000002479	-	0.00970550	Zfp862
ENSRNOG0000002508	13.68622461	0.00970927	Krt73
ENSRNOG0000000747	3.858318407	0.00972479	Gpihbp1
ENSRNOG0000000042	2.320742909	0.00974374	LOC100360835
ENSRNOG0000002889	2.508138613	0.00978892	Rtp4
ENSRNOG0000004308	-	0.00979752	Clstn2
ENSRNOG0000003136	-	0.00980096	LOC499235
ENSRNOG0000002293	-	0.00986031	Ap4e1
ENSRNOG0000002514	2.840820358	0.00987383	Icam2
ENSRNOG0000001022	-	0.00987403	Rab30
ENSRNOG0000005072	4.275963708	0.00987756	AABR06053494.1
ENSRNOG0000003144	-	0.00992294	Havcr2
ENSRNOG0000004883	-	0.00992756	Sowahc
ENSRNOG0000000283	-	0.00995210	Gsk3b
ENSRNOG0000000926	2.006270913	0.00995210	Ifi27
ENSRNOG0000000782	4.567784753	0.00995854	Hoxb6
ENSRNOG0000000413	-	0.00995974	Ubtd2
ENSRNOG0000001708	-2.19370817	0.00997219	Man1c1
ENSRNOG0000002462	-	0.01003997	MAMDC2
ENSRNOG0000001544	3.652389005	0.01011787	Mal
ENSRNOG0000001035	-	0.01018111	Rcan2
ENSRNOG0000001413	-	0.01018379	Fbln1
ENSRNOG0000001919	3.043194955	0.01018384	Cracr2b
ENSRNOG0000001788	-	0.01022538	Camk1d
ENSRNOG0000002695	-	0.01026586	Susd5
ENSRNOG0000002617	17.74528798	0.01027228	Mgam
ENSRNOG0000000580	-	0.01034652	Oxtr
ENSRNOG0000001619	3.653909254	0.01036101	Hoxc9
ENSRNOG0000002472	10.53177318	0.01036240	LOC100909834
ENSRNOG0000000221	4.084819325	0.01042320	Plac8

ENSRNOG0000000240	-	0.01042671	Fam129a
ENSRNOG0000003134	3.596523051	0.01043228	Nxpe4
ENSRNOG0000000176	-	0.01043228	RGD1562339
ENSRNOG0000000197	-	0.01043228	LOC100911172
ENSRNOG0000004213	2.052417067	0.01043228	Tmem173
ENSRNOG0000000205	2.017069673	0.01043228	Igfbp7
ENSRNOG0000000640	-	0.01045290	Pvrl1
ENSRNOG0000002030	3.026816534	0.01054430	Klhl17
ENSRNOG0000000835	28.22445949	0.01057114	Myo5c
ENSRNOG0000001158	4.212731592	0.01058649	Phf11
ENSRNOG0000001197	-2.61617047	0.01059178	Crtc3
ENSRNOG0000000613	-	0.01059178	Pdpk1
ENSRNOG0000005023	2.106123262	0.01061435	Cchcr1
ENSRNOG0000000391	-	0.01064091	Uck2
ENSRNOG0000000792	-	0.01070360	Mettl7b
ENSRNOG0000000283	-	0.01075480	Slc16a2
ENSRNOG0000000720	-	0.01075600	Sema3d
ENSRNOG0000000737	-	0.01076184	Rnf144a
ENSRNOG0000001492	-5.10576863	0.01077468	Apba1
ENSRNOG0000001796	-2.05660204	0.01077468	Asb13
ENSRNOG0000002917	7.883305197	0.01080487	AY172581.3
ENSRNOG0000003272	-	0.01080721	LOC684499
ENSRNOG0000002497	-	0.01088985	LOC687381
ENSRNOG0000001621	-	0.01100419	Ankfy1
ENSRNOG0000001741	-2.57410402	0.01102836	Ppic
ENSRNOG0000002045	4.401100552	0.01106018	Rgs11
ENSRNOG0000002682	-	0.01110015	Arhgap42
ENSRNOG0000000491	-	0.01112926	Itgav
ENSRNOG0000001013	2.472417535	0.01114376	Acot2
ENSRNOG0000001719	2.793868766	0.01115493	Pdgfb
ENSRNOG0000000424	-	0.01116549	Tlr7
ENSRNOG0000000276	-	0.01116549	Ulk2
ENSRNOG0000001458	-	0.01120335	Mid2
ENSRNOG0000002402	2.110234441	0.01123352	Edc4
ENSRNOG0000002117	2.540077066	0.01123529	Plekho1
ENSRNOG0000001760	-	0.0112507	Cnga4
ENSRNOG0000000294	-	0.0112507	RGD1561897
ENSRNOG0000004253	-	0.01129422	Pde4d
ENSRNOG0000005075	8.24535031	0.01130974	AABR06009537.6
ENSRNOG0000000001	-	0.01132615	Cbln1
ENSRNOG0000000903	-8.74312352	0.01136609	Sulf1
ENSRNOG0000000890	-	0.01136609	Coro2a
ENSRNOG0000001230	-	0.01136609	Gucy1a3
ENSRNOG0000000949	-	0.01136609	Phc3
ENSRNOG0000001503	-	0.01136609	Ctgf
ENSRNOG0000004386	3.758738053	0.01142827	AY172581.24
ENSRNOG0000002015	-	0.01142827	Mapk8
ENSRNOG0000003966	-	0.01144000	Srpx
ENSRNOG0000000361	-	0.01145087	Grem2
ENSRNOG0000000786	-	0.01145087	Clec2dl1
ENSRNOG0000002312	4.714551614	0.01145087	Apol11a
ENSRNOG0000001184	-	0.01145087	Map2
ENSRNOG0000000175	-	0.01146173	Fbxo45
ENSRNOG0000004980	-	0.01152861	LOC100363436
ENSRNOG0000002907	11.18552632	0.01155421	AY172581.1
ENSRNOG0000002349	4.85164272	0.01157236	Foxe1
ENSRNOG0000004704	-	0.01157847	Plin4
ENSRNOG0000002660	-	0.01165541	Cercam
ENSRNOG0000003564	7.435615319	0.01167811	Mir23a
ENSRNOG0000001358	-	0.01167811	Cxcl12
ENSRNOG0000002500	-	0.01167958	Pcolce
ENSRNOG0000001568	55.75457279	0.01173298	Kel
ENSRNOG0000004677	-	0.01173298	Fam83c
ENSRNOG0000001485	-	0.01174288	Col4a4
ENSRNOG0000001630	-	0.01174288	Cnnm1
ENSRNOG0000003422	-	0.01174288	Pik3c2g
ENSRNOG0000002891	12.05508408	0.01175139	LOC688970
ENSRNOG0000001190	-2.15100159	0.01177109	Asxl2
ENSRNOG0000004666	17.4723666	0.01179263	AABR06052098.1
ENSRNOG0000004637	4.467712709	0.01179263	LOC684480
ENSRNOG0000001635	-	0.01179263	Frrs1
ENSRNOG0000002399	2.636754095	0.01179263	Ankrd39
ENSRNOG0000001266	-	0.01179263	Postn
ENSRNOG0000004650	-2.46327878	0.01179263	Rprd2
ENSRNOG0000004292	-	0.01184554	Tas1r2
ENSRNOG0000000132	8.554197606	0.01188871	Gjc3
ENSRNOG0000000995	2.185506733	0.01193392	MSANTD2
ENSRNOG0000001010	-	0.01193855	Pofut1
ENSRNOG0000001999	2.144823705	0.01194918	RGD1566239
ENSRNOG0000001983	2.218358812	0.01196651	Gmfg
ENSRNOG0000001091	-	0.01199633	Tmem108
ENSRNOG0000002987	-	0.01201176	Slc8a3
ENSRNOG0000002696	-	0.01201838	Osbpl8
ENSRNOG0000001655	5.510059456	0.01211693	Pllp
ENSRNOG0000002881	4.864738705	0.01211693	Oasl2
ENSRNOG0000003893	-	0.01213308	Spcs3
ENSRNOG0000001573	-	0.01214509	Zswim1
ENSRNOG0000000673	-	0.01214509	Fbxo32
ENSRNOG0000001744	-	0.01216818	Bgn
ENSRNOG0000000395	2.309086262	0.01217087	Il2rg
ENSRNOG0000003366	2.169624582	0.01217087	Lmbr1l
ENSRNOG0000002821	-	0.01218522	Nup160
ENSRNOG0000001889	-	0.01219034	Sfrp4
ENSRNOG0000002580	-	0.01220796	AABR06026181.1
ENSRNOG0000001683	19.61727453	0.01221032	Sycp1
ENSRNOG0000002024	17.69253418	0.01221122	Ina
ENSRNOG0000003550	16.58842534	0.01221122	Mir24-2
ENSRNOG0000004561	-	0.01221122	LOC100911403
ENSRNOG0000003227	13.08773403	0.01221122	AY172581.15
ENSRNOG0000004020	-	0.01221122	Mmp27
ENSRNOG0000002467	2.564756215	0.01221122	Arhgap33
ENSRNOG0000001401	2.443939718	0.01221122	Dll4
ENSRNOG0000000593	-	0.01221122	Megf9
ENSRNOG0000000679	-	0.01221122	Zfp146
ENSRNOG0000000728	-	0.01225106	Flnc
ENSRNOG0000000110	-	0.01225106	Foxk1
ENSRNOG0000000011	2.522125991	0.01229616	Coprs
ENSRNOG0000004288	2.186049897	0.01229616	Rps28
ENSRNOG0000001022	2.036202298	0.01229616	Gpatch2l
ENSRNOG0000002629	2.57225559	0.01230189	Rbpjl
ENSRNOG0000004982	16.7865128	0.01232037	Igkc
ENSRNOG0000002703	-	0.01232037	Adm
ENSRNOG0000002825	21.30357325	0.01238524	Mcemp1
ENSRNOG0000003023	-	0.01243123	Fndc5
ENSRNOG0000001838	-	0.01243310	Inpp4b
ENSRNOG0000000205	-	0.01243310	Ccdc80
ENSRNOG0000000885	-2.21185165	0.01243310	Tank
ENSRNOG0000002684	-	0.01244763	Nnt
ENSRNOG0000000773	-	0.01245296	Pigm
ENSRNOG0000004216	3.807023535	0.01245825	Wfdc3
ENSRNOG0000002516	-	0.01250197	Sema4b
ENSRNOG0000004648	-	0.01250441	Znf750
ENSRNOG0000002585	5.350348555	0.01253563	LOC500712
ENSRNOG0000000117	3.424766423	0.01253563	Pde9a
ENSRNOG0000001282	4.963936369	0.01256406	Lect1
ENSRNOG0000004820	3.94422312	0.01258054	AABR06088247.1
ENSRNOG0000001141	-	0.01258093	Pde3b
ENSRNOG0000001801	-	0.01262313	Tulp4
ENSRNOG0000004247	78.76615767	0.01263547	Krtap17-1
ENSRNOG0000002058	2.665900586	0.01264435	LOC500956
ENSRNOG0000001561	-	0.01264932	Wnt5a
ENSRNOG0000004339	2.391896557	0.01264932	Pecam1
ENSRNOG0000001239	4.83216843	0.01265261	Npw
ENSRNOG0000001627	3.457801147	0.01268751	Zfp865
ENSRNOG0000001062	-	0.01274114	Ndc1
ENSRNOG0000000160	-	0.01276598	Adamts5
ENSRNOG0000000224	2.280273969	0.01279410	Hspbap1
ENSRNOG0000004672	17.6350913	0.01285653	Abcc2
ENSRNOG0000002235	-	0.01289411	AABR06088579.1
ENSRNOG0000004760	9.961078544	0.01289411	AABR06075699.1
ENSRNOG0000004875	8.924909513	0.01289411	AABR06075522.1
ENSRNOG0000000623	-	0.01289411	Nell2
ENSRNOG0000002229	3.178109066	0.01289411	Kcnmb4
ENSRNOG0000002553	-2.56899281	0.01289411	Vps13a
ENSRNOG0000001707	-	0.01289411	Slc16a14
ENSRNOG0000000759	5.108316226	0.01290582	Rhpn1
ENSRNOG0000002470	-	0.01290663	Dock5
ENSRNOG0000001595	-3.69726201	0.01292218	F13a1
ENSRNOG0000001491	15.25215567	0.01294661	Klrg1
ENSRNOG0000003239	-3.82751706	0.01294661	RGD1559575
ENSRNOG0000000198	-	0.01294661	Cblb
ENSRNOG0000001998	2.081725988	0.01294661	Scand1
ENSRNOG0000001757	3.878308406	0.01295010	Gins2
ENSRNOG0000002499	38.56518586	0.01298323	Krtap5-1
ENSRNOG0000003847	2.635717253	0.01299604	RGD1563668
ENSRNOG0000002097	4.20650294	0.01300593	Rundc3a
ENSRNOG0000004684	-	0.01306003	PCOLCE2
ENSRNOG0000003774	-	0.01307283	LOC299277
ENSRNOG0000000845	2.218577338	0.01311948	Anapc13
ENSRNOG0000001980	3.371765198	0.01313704	Zfp428
ENSRNOG0000000473	-	0.01317342	Ralgps2
ENSRNOG0000002115	-	0.01318575	Ctsk
ENSRNOG0000002563	-	0.01318575	RGD1563300
ENSRNOG0000000464	5.575058251	0.01319049	Il1b
ENSRNOG0000001588	-3.40335995	0.01319049	Dpep1
ENSRNOG0000001071	-	0.01319049	Gpr153
ENSRNOG0000003843	-	0.01319049	RGD1307100
ENSRNOG0000002000	2.342978976	0.01320644	Wdr90
ENSRNOG0000002131	-	0.01322666	Epas1
ENSRNOG0000001458	2.13100844	0.01323271	Trappc2l
ENSRNOG0000001446	-	0.01323395	Galns
ENSRNOG0000000836	17.40130131	0.01327562	Nanog
ENSRNOG0000001784	2.745797285	0.01328161	Rps19bp1
ENSRNOG0000004823	3.546664841	0.01333072	AABR06106055.2
ENSRNOG0000002060	2.658923955	0.01333452	B3gnt8
ENSRNOG0000002555	-	0.01339820	Palm2
ENSRNOG0000004561	5.303860295	0.01339820	LOC688286
ENSRNOG0000000149	9.259854359	0.01340106	Mia
ENSRNOG0000000730	-	0.01340106	C1qtnf6
ENSRNOG0000004889	-	0.01340106	Prr14l
ENSRNOG0000000281	-	0.01349362	F5
ENSRNOG0000000792	-	0.01352758	Pak6
ENSRNOG0000001101	-	0.01353089	Slc7a2
ENSRNOG0000001118	-	0.01353089	Cpa3
ENSRNOG0000004773	3.955226037	0.01353157	Npff
ENSRNOG0000000792	-	0.01353157	Cgref1
ENSRNOG0000004962	3.438334895	0.01355866	Reep2
ENSRNOG0000001512	-	0.01361845	Gpam
ENSRNOG0000002353	-	0.01364823	Gpr133
ENSRNOG0000000733	5.558168923	0.01364823	Sstr3
ENSRNOG0000000189	2.236133132	0.01364823	Gnb1l
ENSRNOG0000000926	3.126175184	0.01369827	Cnr2
ENSRNOG0000001819	-	0.01369827	Dapk1
ENSRNOG0000004680	4.985034652	0.01374704	AABR06042817.2
ENSRNOG0000002215	-	0.01377168	Serpinb6e
ENSRNOG0000000045	2.000273005	0.01377168	Psmb8
ENSRNOG0000001838	-	0.01377311	Adam12
ENSRNOG0000003771	17.44504299	0.01379481	Mfsd6l
ENSRNOG0000000470	-	0.01384468	Vit
ENSRNOG0000004599	-	0.01384468	Tlr8
ENSRNOG0000002206	-	0.01384468	Fam117b
ENSRNOG0000000238	-	0.01386903	Bmp3
ENSRNOG0000002436	2.503980132	0.01388144	Enkd1
ENSRNOG0000002700	-	0.01388308	Mast4
ENSRNOG0000004564	-	0.01389872	Arrdc3
ENSRNOG0000000705	-	0.01390523	Dhx33
ENSRNOG0000002376	-3.88717068	0.01392886	Plekhm3
ENSRNOG0000002353	2.374242546	0.01392886	Haus8
ENSRNOG0000000820	-	0.01394904	St3gal1
ENSRNOG0000004137	5.143997611	0.01395261	AABR06066677.1
ENSRNOG0000004704	4.890988139	0.01395261	AABR06094734.1
ENSRNOG0000000798	-	0.01395261	Amer1
ENSRNOG0000000192	-	0.01395261	Tp63
ENSRNOG0000000349	-	0.01401646	Prp2l1
ENSRNOG0000000090	-	0.01403311	Tpst1
ENSRNOG0000001178	-	0.01405735	Cdon
ENSRNOG0000004808	4.754684292	0.01412677	AABR06011601.1
ENSRNOG0000001868	3.673747268	0.01414074	Nes
ENSRNOG0000000583	-	0.01417619	Fam49a
ENSRNOG0000001064	-	0.01417619	Kank2
ENSRNOG0000000279	-2.13298029	0.01420827	Abcb7
ENSRNOG0000001247	-	0.01424686	Thbs4
ENSRNOG0000004731	-	0.01424938	AABR06071064.1
ENSRNOG0000003116	-	0.01426803	Srxn1
ENSRNOG0000004656	-	0.01426803	LOC102552895
ENSRNOG0000001428	-	0.01428511	Ssh2
ENSRNOG0000004745	-	0.01433798	Vipr1
ENSRNOG0000001618	-	0.01433798	Zfp709
ENSRNOG0000004996	4.844734796	0.014345	AABR06103741.2
ENSRNOG0000000670	-	0.014345	Zfp398
ENSRNOG0000001104	-	0.014345	Tmem185a
ENSRNOG0000001882	-	0.01435577	Htr7
ENSRNOG0000004816	-	0.01436886	Tlr9
ENSRNOG0000002400	8.050599491	0.01442804	AABR06107055.2
ENSRNOG0000002032	3.954586574	0.01442804	Asb1
ENSRNOG0000005076	-	0.01445585	Tgfbr1
ENSRNOG0000004979	-	0.01455953	AABR06033538.1
ENSRNOG0000001636	2.058997145	0.01455953	Gba2
ENSRNOG0000000497	2.119802319	0.01462061	Txlng
ENSRNOG0000001052	-	0.01462469	Tlr4
ENSRNOG0000002042	4.386279222	0.01462553	Fndc7
ENSRNOG0000003361	25.08830639	0.01462723	Krt26
ENSRNOG0000002811	9.86488331	0.01463521	LOC499796
ENSRNOG0000001668	-	0.01465437	Ssc5d
ENSRNOG0000002516	-	0.01468635	Tmem56
ENSRNOG0000000869	-	0.01469235	Nov

ENSRNOG0000000277	-	0.01473425	Ereg
ENSRNOG0000000432	5.927875809	0.01477920	Tgm4
ENSRNOG0000001112	-5.55425004	0.01483078	LOC501116
ENSRNOG0000003948	-	0.01486674	AABR06070618.1
ENSRNOG0000000741	-	0.01489276	LOC100362038
ENSRNOG0000004909	-	0.01489522	Larp4
ENSRNOG0000001235	-	0.01489522	Slc36a1
ENSRNOG0000000045	2.389616693	0.01490526	Tap2
ENSRNOG0000004911	-	0.01491944	Dchs2
ENSRNOG0000000935	5.335134519	0.01492408	Sez6
ENSRNOG0000000241	3.44531399	0.01492630	Plp1
ENSRNOG0000000650	-	0.01501676	Srgap3
ENSRNOG0000000400	-	0.01504666	Xpnpep2
ENSRNOG0000004793	-	0.01505485	Chsy3
ENSRNOG0000001536	2.102453056	0.01505647	Neurl3
ENSRNOG0000001824	2.42383654	0.01508125	Dhx58
ENSRNOG0000004220	2.653698794	0.01509804	Efcab2
ENSRNOG0000001392	-2.73821428	0.01511231	Dsp
ENSRNOG0000001380	-	0.01516115	Slc25a36l1
ENSRNOG0000002262	2.701801051	0.01519538	Mroh7
ENSRNOG0000002714	-	0.01519538	Rora
ENSRNOG0000002979	-	0.01521505	Ogn
ENSRNOG0000005059	-	0.01521505	LOC100912565
ENSRNOG0000004594	2.355087951	0.01530964	Arl10
ENSRNOG0000000535	-	0.01533476	Elf4
ENSRNOG0000001924	-	0.01534269	Mxra8
ENSRNOG0000002895	41.58456554	0.01534559	AABR06009373.1
ENSRNOG0000000660	-	0.01534559	Thy1
ENSRNOG0000001551	-	0.01535861	Rbp4
ENSRNOG0000001462	-	0.01535861	Rhbdd1
ENSRNOG0000001150	7.316252385	0.01537340	Col9a2
ENSRNOG0000000725	2.927218117	0.01537340	Zpbp2
ENSRNOG0000004254	-	0.01541341	Ism1
ENSRNOG0000003364	-	0.01547684	Prkg1
ENSRNOG0000000844	2.166088934	0.01548169	Cttnbp2
ENSRNOG0000002940	-	0.01551470	Actg2
ENSRNOG0000002660	-	0.01552428	Tnfsf18
ENSRNOG0000004280	-	0.01555973	RGD1559644
ENSRNOG0000001322	-	0.01555973	Cd207
ENSRNOG0000004966	4.045182775	0.01555973	Prr24
ENSRNOG0000002854	5.089109685	0.01556401	Ccl9
ENSRNOG0000000031	-	0.01557847	Sobp
ENSRNOG0000003247	-	0.01557988	Gpr64
ENSRNOG0000003358	-2.0753424	0.01561423	Tnxb
ENSRNOG0000001169	-	0.01567227	Lifr
ENSRNOG0000000485	18.49619157	0.01570076	LOC257643
ENSRNOG0000004221	3.713095356	0.0157214	Tmem240
ENSRNOG0000000044	2.269630556	0.01573413	Gpsm3
ENSRNOG0000002567	-	0.01574682	Fam198a
ENSRNOG0000004662	-	0.01576593	Zfp37
ENSRNOG0000001745	4.602714938	0.01578020	C1ql3
ENSRNOG0000004899	-	0.01579593	AABR06103058.1
ENSRNOG0000000488	-	0.01582134	Capn6
ENSRNOG0000004314	2.193492422	0.01591944	LOC100360056
ENSRNOG0000004769	6.544384952	0.01593746	Ggt1
ENSRNOG0000001961	3.565182099	0.01593746	Haghl
ENSRNOG0000001973	-3.27064409	0.01594021	LOC100910486
ENSRNOG0000000615	-	0.01597262	Pde1a
ENSRNOG0000003331	2.160992266	0.01604847	Rfxank
ENSRNOG0000002221	2.584037534	0.01606026	Ifi44
ENSRNOG0000001461	2.066478349	0.01613953	Med31
ENSRNOG0000003026	19.99460591	0.01617881	Atp2b2
ENSRNOG0000004724	-	0.01617881	AABR06034751.1
ENSRNOG0000000174	3.590134786	0.01617881	Clcn2
ENSRNOG0000001641	2.893784017	0.01619875	Fxyd6
ENSRNOG0000002002	2.179603303	0.01621812	Psmc3ip
ENSRNOG0000004349	-	0.01621812	Sik2
ENSRNOG0000000306	-	0.01625751	Phka1
ENSRNOG0000002090	6.945103163	0.01627107	Prodh2
ENSRNOG0000000117	5.601231686	0.01627107	Cabp1
ENSRNOG0000000636	4.241423502	0.01629859	Lrrn3
ENSRNOG0000000087	-	0.01648533	Slc9a6
ENSRNOG0000001899	-	0.01648550	Dpysl3
ENSRNOG0000000578	13.2677259	0.01653903	Erp27
ENSRNOG0000002206	-	0.01658921	Tlr5
ENSRNOG0000001975	7.187818042	0.01662104	Dpep3
ENSRNOG0000001393	-	0.01662104	Tshz3
ENSRNOG0000004943	5.224072717	0.01666078	AABR06105117.1
ENSRNOG0000002269	11.65742379	0.01668766	Rn50_10_0644.1
ENSRNOG0000001901	-2.42389638	0.01669879	Ndst1
ENSRNOG0000002155	-	0.01673321	Uprt
ENSRNOG0000000052	-3.61756327	0.01675608	Pi16
ENSRNOG0000001206	-	0.01676683	Gucy1b3
ENSRNOG0000002063	-	0.01677186	Il9r
ENSRNOG0000001119	16.44051568	0.01677765	Krt25
ENSRNOG0000003242	3.067343568	0.01677765	Hmgb1-ps3
ENSRNOG0000001182	-	0.01677765	Acpp
ENSRNOG0000002463	-	0.01677765	Cramp1l
ENSRNOG0000003062	49.20149293	0.01679964	LOC102557415
ENSRNOG0000000277	29.67717069	0.01679964	Sell
ENSRNOG0000000421	-	0.01681843	Osr1
ENSRNOG0000001850	-2.74801155	0.01686545	Gfpt1
ENSRNOG0000001918	-	0.01688133	Synpo
ENSRNOG0000003229	-	0.01688133	Msmo1
ENSRNOG0000001837	-2.15382815	0.0169303	Tln2
ENSRNOG0000003950	8.984659583	0.01694311	LOC360919
ENSRNOG0000002414	5.253270532	0.01694558	Prr18
ENSRNOG0000001023	-	0.01696672	Cald1
ENSRNOG0000000464	-	0.01699896	Galnt5
ENSRNOG0000003053	11.50500375	0.01699948	Slco1b2
ENSRNOG0000004897	-	0.01699948	Nphp3
ENSRNOG0000001496	-	0.01703140	Pdpn
ENSRNOG0000000779	8.25812933	0.01705884	Fam151a
ENSRNOG0000000698	-	0.01706414	Vcpip1
ENSRNOG0000002928	11.18400345	0.01715000	Hbe1
ENSRNOG0000001031	-	0.01715000	Astn2
ENSRNOG0000000858	-	0.01715000	Aldh1l2
ENSRNOG0000001784	2.180968684	0.01716652	Polr3k
ENSRNOG0000002878	5.170103035	0.01717763	Abcc6
ENSRNOG0000000698	-	0.01717763	Tmem263
ENSRNOG0000001342	-	0.01717763	Mrgprf
ENSRNOG0000000797	-	0.01722788	Ncoa2
ENSRNOG0000004810	4.607051643	0.01726760	AABR06028897.1
ENSRNOG0000001106	-	0.01727597	Papss2
ENSRNOG0000004599	5.82116603	0.01728605	Tnfaip8l1
ENSRNOG0000000630	-	0.01728605	Soga1
ENSRNOG0000002337	2.244087531	0.01728605	Bst2
ENSRNOG0000002092	2.204966043	0.01728605	Lin37
ENSRNOG0000002143	-	0.01728605	Hspg2
ENSRNOG0000002812	13.0671536	0.01734705	Otop2
ENSRNOG0000002237	12.46244618	0.01740122	Sgcz
ENSRNOG0000001500	-	0.01740122	Abhd15
ENSRNOG0000000008	-	0.01741205	Antxr2
ENSRNOG0000000185	-	0.01741957	Tmtc1
ENSRNOG0000001581	2.115772632	0.01741957	Bbs7
ENSRNOG0000001206	-	0.01745701	Prkcb
ENSRNOG0000004260	-	0.01751688	Ttc39b
ENSRNOG0000005053	-	0.01757644	Fbln5
ENSRNOG0000001161	-	0.01759633	Tmcc1
ENSRNOG0000004895	6.161070534	0.01770944	LOC689064
ENSRNOG0000001690	2.249797455	0.01777092	Lipt2
ENSRNOG0000002417	8.60738448	0.01783334	T2
ENSRNOG0000001346	-4.3323834	0.01789959	Kcnj8
ENSRNOG0000000672	-	0.01790430	Itga11
ENSRNOG0000000528	-2.39125434	0.01790434	Prkd3
ENSRNOG0000001616	-	0.01791833	Fcrl2
ENSRNOG0000000695	-	0.01791833	Adamtsl1
ENSRNOG0000000364	-	0.01792182	Tab3
ENSRNOG0000001465	2.580784778	0.01792182	Sema4g
ENSRNOG0000002035	-	0.01792182	Sh3pxd2a
ENSRNOG0000000455	-	0.01798877	Dcn
ENSRNOG0000004914	15.30791677	0.01799412	5S_rRNA
ENSRNOG0000000353	21.54519742	0.01801373	Spta1
ENSRNOG0000002295	2.238645102	0.01801373	Ccdc163
ENSRNOG0000002026	-	0.01803254	Fam53c
ENSRNOG0000001476	-	0.01805788	Glis3
ENSRNOG0000002923	-	0.01809615	Sfmbt2
ENSRNOG0000003280	-	0.01811494	Cyp2f4
ENSRNOG0000004222	9.906889636	0.01815018	Vsx1
ENSRNOG0000002037	6.559523155	0.01823608	Cideb
ENSRNOG0000000630	7.789964233	0.01833492	Mycn
ENSRNOG0000002907	-	0.01833576	Hspb7
ENSRNOG0000002302	2.066257228	0.01837024	Trpt1
ENSRNOG0000003816	-	0.01837882	Spin4
ENSRNOG0000001020	21.87787253	0.01842876	Clec4e
ENSRNOG0000002709	7.93847889	0.01849757	Fbxl2
ENSRNOG0000001500	-	0.01850705	Ski
ENSRNOG0000001707	-	0.01857451	Sepn1
ENSRNOG0000000313	5.849181341	0.01859101	Fcrla
ENSRNOG0000004784	5.501511092	0.01859101	Cbr1
ENSRNOG0000003321	2.402202179	0.01859101	Esam
ENSRNOG0000004588	2.313265537	0.01864449	AABR06065806.1
ENSRNOG0000004011	-	0.01865782	Foxn2
ENSRNOG0000001445	5.176700439	0.01872608	AABR06019754.1
ENSRNOG0000001372	-	0.01872608	RGD1306271
ENSRNOG0000000159	-	0.01872608	Lnp
ENSRNOG0000000784	-	0.01880151	Wnt2
ENSRNOG0000005083	-	0.01884418	Fam102a
ENSRNOG0000002021	2.19379908	0.01885224	Gmpr2
ENSRNOG0000002559	-	0.01888066	Ago4
ENSRNOG0000001018	12.73648061	0.01890550	Clec4d
ENSRNOG0000001467	-	0.01903513	AABR06060748.1
ENSRNOG0000001683	-	0.01907974	Ide
ENSRNOG0000003360	-2.80831634	0.01909061	Cd276
ENSRNOG0000005061	2.266864539	0.01915962	AABR06041255.1
ENSRNOG0000004556	2.04874392	0.01925090	LOC690344
ENSRNOG0000000843	-	0.01928311	Ss18l1
ENSRNOG0000001219	-	0.01931973	NA
ENSRNOG0000000609	5.446957214	0.01932762	LRRTM1
ENSRNOG0000004558	7.812189459	0.01939819	Erv3
ENSRNOG0000000057	-	0.01944649	Chst3
ENSRNOG0000000796	-	0.01945815	Tp53inp1
ENSRNOG0000002210	-	0.01951760	RT1-M4
ENSRNOG0000000530	-	0.01959296	Slc2a9
ENSRNOG0000000951	-	0.01971002	Mme
ENSRNOG0000003392	37.42801809	0.01972574	Gm10100
ENSRNOG0000001652	-	0.01972574	Dsg2
ENSRNOG0000001681	2.400786631	0.01972574	Stmn1
ENSRNOG0000002890	2.052027222	0.01972574	Vps9d1
ENSRNOG0000001618	-	0.01972574	Pdp1
ENSRNOG0000004030	2.015064221	0.01972574	Cebpzos
ENSRNOG0000000545	-	0.01972574	Lsm11
ENSRNOG0000000318	-11.4193717	0.01975401	Fmod
ENSRNOG0000000259	-	0.01975401	Esrrg
ENSRNOG0000004949	9.643714708	0.01978571	Krt71
ENSRNOG0000002069	3.33565536	0.01985065	Tead2
ENSRNOG0000000595	-	0.01985623	Slc4a7
ENSRNOG0000001243	-	0.01986875	Larp6
ENSRNOG0000000079	2.145031572	0.01986875	RT1-N3
ENSRNOG0000000065	-	0.01990168	Acacb
ENSRNOG0000002198	10.88465505	0.01997114	Olfr225
ENSRNOG0000002128	2.592350843	0.01998625	Hexim2
ENSRNOG0000000185	-	0.02000318	Far2
ENSRNOG0000000911	-	0.02002300	Sprr2g
ENSRNOG0000003329	4.244247053	0.02003882	Mt-atp8
ENSRNOG0000001103	-	0.02003882	Lhfpl2
ENSRNOG0000004271	-2.44277243	0.02003882	Ciart
ENSRNOG0000001836	-	0.02010751	RGD1310819
ENSRNOG0000000283	-	0.02018076	Klb
ENSRNOG0000002944	-	0.02018076	Ror1
ENSRNOG0000001895	8.824628121	0.02021037	Tsnaxip1
ENSRNOG0000004006	38.78139048	0.02022456	LOC684744
ENSRNOG0000000290	2.688402111	0.02022456	Specc1
ENSRNOG0000004303	-	0.02030491	Zfp770
ENSRNOG0000000729	-	0.02033720	Atp1a2
ENSRNOG0000001164	2.193574412	0.02042227	S100a6
ENSRNOG0000000159	-	0.02046696	Atf2
ENSRNOG0000000081	-	0.02046696	Pkib
ENSRNOG0000004792	2.274359918	0.02046696	LOC102557117
ENSRNOG0000001668	-	0.02050553	Wnk2
ENSRNOG0000005071	-	0.02050846	LOC100910729
ENSRNOG0000005072	-	0.02052259	AABR06039771.1
ENSRNOG0000001682	-	0.02058074	Pla2g2d
ENSRNOG0000003641	13.66499437	0.02066209	AABR06097721.2
ENSRNOG0000004021	2.193045521	0.02067578	RGD1564792
ENSRNOG0000001995	11.27021017	0.02073388	Kcnc3
ENSRNOG0000004930	11.17561825	0.02073388	Marco
ENSRNOG0000002538	-4.58695653	0.02073388	Slc2a10
ENSRNOG0000000607	-	0.02073388	Steap2
ENSRNOG0000000301	-	0.02074745	Olfml2b
ENSRNOG0000002099	-	0.02074745	Ms4a2
ENSRNOG0000002016	47.31101152	0.02076152	Ahsp
ENSRNOG0000000444	-	0.02076152	Acss3
ENSRNOG0000004632	45.75905787	0.02077012	AABR06100209.1
ENSRNOG0000002108	-	0.02082645	Dtx4
ENSRNOG0000001746	3.105796605	0.02082645	Bloc1s3
ENSRNOG0000000761	-	0.02084684	C1qtnf5
ENSRNOG0000004005	23.42548799	0.02084723	LOC102551168
ENSRNOG0000004282	-	0.02084723	Cd300le
ENSRNOG0000000534	-	0.02086573	Pamr1
ENSRNOG0000004683	2.848867198	0.02086991	AABR06068952.1
ENSRNOG0000001742	2.380134156	0.02096251	Lat
ENSRNOG0000000747	-	0.02097744	Clmp
ENSRNOG0000000406	-	0.02102402	C4bpa
ENSRNOG0000001154	-	0.02102402	Ebf2
ENSRNOG0000004895	4.367337159	0.02102402	AABR06062061.1

ENSRNOG0000000162	-	0.02102402	Abi3bp
ENSRNOG0000001941	2.833348087	0.02102402	Zfp94
ENSRNOG0000000189	2.03695085	0.02102402	Txnrd2
ENSRNOG0000002437	2.387278302	0.02103457	Sorl1
ENSRNOG0000000463	-16.5679484	0.02104480	Kera
ENSRNOG0000004765	-	0.02111255	Gaa
ENSRNOG0000001026	2.100741605	0.02111255	Ada
ENSRNOG0000002094	3.051805207	0.02112365	Plekha4
ENSRNOG0000001659	2.343375992	0.02112852	Hhex
ENSRNOG0000001685	-	0.02118968	Dsg1
ENSRNOG0000000219	-	0.02121155	AABR06078960.1
ENSRNOG0000001122	-	0.02124944	Atp1b2
ENSRNOG0000000587	-	0.02126362	Maml2
ENSRNOG0000000204	2.684503818	0.02129132	Anxa3
ENSRNOG0000000792	5.480585051	0.02131411	Cldn19
ENSRNOG0000004330	-	0.02131411	Apcdd1
ENSRNOG0000003392	-	0.02132068	Stfa2l1
ENSRNOG0000000248	-	0.02136577	Mbnl3
ENSRNOG0000003105	3.243886554	0.02138148	Mt-nd4l
ENSRNOG0000001053	-	0.02142127	Nr2c2
ENSRNOG0000000748	-	0.02142723	Ehf
ENSRNOG0000000225	2.220618656	0.02153933	Tmem150c
ENSRNOG0000004993	-	0.02153979	Pdxk
ENSRNOG0000000227	-	0.02156353	Lnx1
ENSRNOG0000001365	6.521471898	0.02158472	AABR06011532.1
ENSRNOG0000000219	-	0.02159904	Ociad2
ENSRNOG0000001683	-	0.02159904	Serpinh1
ENSRNOG0000001200	11.65864903	0.02171991	S100a3
ENSRNOG0000004218	-2.79406387	0.02175082	Rab31
ENSRNOG0000005040	2.203630825	0.02175621	Vbp1
ENSRNOG0000001595	-	0.02177556	Slc19a3
ENSRNOG0000001416	-	0.02178529	Smoc2
ENSRNOG0000002715	-	0.02178716	N4bp2
ENSRNOG0000003662	-	0.02182790	LOC100911469
ENSRNOG0000000294	-	0.02184309	Dpt
ENSRNOG0000003201	-	0.02186725	Tmem200b
ENSRNOG0000004205	3.527266161	0.02196364	Rccd1
ENSRNOG0000000649	6.730058031	0.02197127	Foxi3
ENSRNOG0000002760	-	0.02197127	Lhfpl1
ENSRNOG0000001549	2.655472006	0.02203010	Slc25a37
ENSRNOG0000004813	-	0.02203010	Senp5
ENSRNOG0000004892	-	0.02213107	CEP170
ENSRNOG0000003420	-	0.02220496	Atp8a1
ENSRNOG0000000468	-	0.02224189	Rbfox2
ENSRNOG0000001380	-	0.02226872	Ces2g
ENSRNOG0000000803	6.576842326	0.02241866	Wbp2nl
ENSRNOG0000001423	-	0.02242589	Hif1an
ENSRNOG0000001042	9.885973686	0.02246824	Misp
ENSRNOG0000004646	-	0.02246824	Ptgfr
ENSRNOG0000001684	-	0.02246824	Bace1
ENSRNOG0000001175	-	0.02247637	Fam180a
ENSRNOG0000002419	-	0.02247823	LOC683719
ENSRNOG0000002921	-	0.02250864	Vcan
ENSRNOG0000000876	-	0.02253286	Zfhx4
ENSRNOG0000000227	-	0.02254840	Phf6
ENSRNOG0000000875	-	0.02254840	Tspan18
ENSRNOG0000000240	-	0.02254840	Rbm47
ENSRNOG0000000056	-	0.02254840	Lrrc20
ENSRNOG0000004726	-	0.02254840	LOC100911918
ENSRNOG0000000989	-	0.02254840	Skil
ENSRNOG0000000395	-	0.02261843	Lvrn
ENSRNOG0000004320	3.051588045	0.02261843	Krt75
ENSRNOG0000003841	7.910691366	0.02262799	AABR06099221.1
ENSRNOG0000004614	4.526108642	0.02262853	AABR06044270.1
ENSRNOG0000004213	-	0.02263989	Clec4a1
ENSRNOG0000003966	-	0.02263989	Col8a1
ENSRNOG0000003340	19.42418298	0.02266755	Krt82
ENSRNOG0000004773	11.88295573	0.02267817	Tnfsf14
ENSRNOG0000001944	3.135495767	0.02267817	Kcnn4
ENSRNOG0000004620	3.032212464	0.02271140	Tspan15
ENSRNOG0000001323	2.136609469	0.02271140	Tmem14a
ENSRNOG0000001834	-	0.02272909	Ctif
ENSRNOG0000001681	-	0.02273379	Tmem135
ENSRNOG0000000403	8.140503901	0.02275465	Nphs2
ENSRNOG0000001286	2.094715757	0.02294759	Nek8
ENSRNOG0000000352	-	0.02298860	Lrrc59
ENSRNOG0000002889	-	0.02299815	Zbtb33
ENSRNOG0000003723	-	0.02313772	Pla2g4d
ENSRNOG0000000934	-	0.02322013	Zbtb6
ENSRNOG0000001625	2.122261217	0.02325766	Sema4c
ENSRNOG0000001039	2.411436196	0.02325911	Agbl3
ENSRNOG0000003960	13.54454781	0.02331011	LOC100360411
ENSRNOG0000000715	2.150162599	0.02331011	Qtrt1
ENSRNOG0000002695	2.22084942	0.02336296	LOC500077
ENSRNOG0000000685	3.12410319	0.02339606	Padi4
ENSRNOG0000001487	3.69855431	0.02347905	Zfyve28
ENSRNOG0000000245	-	0.02350702	Hlf
ENSRNOG0000000333	2.743246137	0.02353001	Pmp22
ENSRNOG0000002917	-	0.02353674	AABR06019066.1
ENSRNOG0000004654	2.876724096	0.02362022	AABR06023331.2
ENSRNOG0000001928	-	0.02366198	Ogfod1
ENSRNOG0000000979	-	0.02367859	Kcnk3
ENSRNOG0000001472	-	0.02367859	Raph1
ENSRNOG0000000698	3.600368318	0.02382039	Mapk11
ENSRNOG0000002871	2.194435023	0.02382039	Ndufb7
ENSRNOG0000005038	13.08133158	0.02385154	Pfn4
ENSRNOG0000001138	-	0.02391069	Nhsl1
ENSRNOG0000001795	4.786101379	0.02392629	Ccdc37
ENSRNOG0000002696	2.127306844	0.02394572	Tmem140
ENSRNOG0000000868	-	0.02398251	Loxl1
ENSRNOG0000003743	3.285142305	0.02399971	Exo5
ENSRNOG0000000286	-	0.02402957	Clcn5
ENSRNOG0000000451	-	0.02405931	Itgbl1
ENSRNOG0000000565	-	0.02412615	Pgf
ENSRNOG0000004917	-	0.02412944	AABR06087018.1
ENSRNOG0000003211	8.251359627	0.02412944	AY172581.14
ENSRNOG0000005068	-	0.02413142	Rn50_5_0815.3
ENSRNOG0000000257	-	0.02413142	Parm1
ENSRNOG0000001483	-	0.02413426	Il1rl1
ENSRNOG0000003297	-	0.02417481	Il13ra2
ENSRNOG0000001777	-	0.02421753	Slc5a1
ENSRNOG0000000586	-	0.02434972	AABR06082101.1
ENSRNOG0000003199	-3.55474621	0.02443614	Ttll7
ENSRNOG0000001357	-	0.02444005	Trem2
ENSRNOG0000000688	-	0.02444005	Dbx2
ENSRNOG0000001752	-	0.02444005	H6pd
ENSRNOG0000000535	-	0.02445999	Rybp
ENSRNOG0000001092	2.106268545	0.02446413	Taf1d
ENSRNOG0000000757	-	0.02448457	Zfp597
ENSRNOG0000002546	-	0.02449576	LOC100125362
ENSRNOG0000000205	-	0.02450272	Fras1
ENSRNOG0000002731	6.821706482	0.02452552	4930562C15Rik
ENSRNOG0000000786	2.058193494	0.02452552	Ephb1
ENSRNOG0000003402	-	0.02455150	Lclat1
ENSRNOG0000001927	-	0.02457508	P2ry6
ENSRNOG0000003800	2.29927643	0.02457508	Ccdc62
ENSRNOG0000002078	2.526306905	0.02458229	LOC100911774
ENSRNOG0000000702	9.787944933	0.02464215	Gm5218
ENSRNOG0000000825	-	0.02466105	Mfap2
ENSRNOG0000000798	2.559015866	0.02468484	Klhl23
ENSRNOG0000001750	-	0.02468484	Ppargc1b
ENSRNOG0000003955	2.22682151	0.02474514	Rpp25l
ENSRNOG0000004876	6.164989086	0.02474878	Nek5
ENSRNOG0000001046	-	0.02476585	Cpa4
ENSRNOG0000005084	4.717959798	0.02477300	AABR06091708.2
ENSRNOG0000001574	-	0.02477321	Slc2a13
ENSRNOG0000001937	-	0.02477524	Pc
ENSRNOG0000002715	2.198148735	0.02477524	Morn4
ENSRNOG0000001805	4.958204441	0.02477666	F2rl2
ENSRNOG0000000520	-	0.02477666	Spred1
ENSRNOG0000000830	-	0.02477666	Nanp
ENSRNOG0000002615	2.047665322	0.02477666	RGD1562200
ENSRNOG0000003898	-	0.0249078	Lypd6
ENSRNOG0000000228	4.742279823	0.02494599	Ppef2
ENSRNOG0000000620	-	0.02496253	Rel
ENSRNOG0000000934	2.717146488	0.02509038	Arhgap25
ENSRNOG0000002315	-	0.02510174	Tmem201
ENSRNOG0000001887	3.631971063	0.02512720	Hapln2
ENSRNOG0000000743	2.867750658	0.02515236	LOC100158225
ENSRNOG0000000850	3.087553235	0.02516882	Cradd
ENSRNOG0000001333	-	0.02521251	Clca5
ENSRNOG0000000033	25.08592462	0.02522219	Ermap
ENSRNOG0000001476	2.256911177	0.02528422	Galt
ENSRNOG0000002122	-	0.02530209	Cpxm1
ENSRNOG0000003687	2.444990005	0.02530693	RGD1308923
ENSRNOG0000003341	2.663319647	0.02540249	Plscr2
ENSRNOG0000002099	9.807709243	0.02540383	Ms4a4c
ENSRNOG0000000212	-	0.02540383	Lrrc8b
ENSRNOG0000001483	-	0.02552718	Emilin2
ENSRNOG0000001247	-	0.02562684	Zc3h12c
ENSRNOG0000001496	-13.6578849	0.02564495	Mrgprh
ENSRNOG0000001956	2.328117797	0.02565557	Pde2a
ENSRNOG0000002452	3.407157615	0.02567062	Dnai2
ENSRNOG0000000665	5.677582129	0.02570567	RGD1563015
ENSRNOG0000003681	10.11941302	0.02575620	Hspb9
ENSRNOG0000001855	-	0.02578057	Olr63
ENSRNOG0000002366	-	0.02581811	Celf2
ENSRNOG0000001113	-	0.02583062	Zbtb41
ENSRNOG0000004709	5.639912175	0.02584326	Psmb11
ENSRNOG0000003402	-	0.02584326	Ptprj
ENSRNOG0000001940	-	0.02589060	Dag1
ENSRNOG0000002125	-4.25744326	0.02591784	Rnf24
ENSRNOG0000004682	2.040860576	0.02592862	Kdr
ENSRNOG0000004791	3.392392884	0.02595393	AABR06069908.1
ENSRNOG0000001625	-	0.02597185	Zfp516
ENSRNOG0000001415	-	0.02600619	Lhfp
ENSRNOG0000003703	-	0.02602213	Aadacl4
ENSRNOG0000001661	2.345323714	0.02602213	Hoxc4
ENSRNOG0000001284	-	0.02603467	Sparc
ENSRNOG0000001326	2.403478649	0.02610601	Helz2
ENSRNOG0000002134	3.496669793	0.02612968	Timd2
ENSRNOG0000004904	4.600634688	0.02620190	AABR06042928.1
ENSRNOG0000002932	-	0.02625684	Ccser1
ENSRNOG0000003707	10.76500748	0.02639246	Clec12b
ENSRNOG0000003670	2.881127232	0.02641173	Itgax
ENSRNOG0000001240	2.194291618	0.02641324	Exosc3
ENSRNOG0000000445	-	0.02643594	Ston2
ENSRNOG0000004567	4.160785853	0.02650017	Apoa1
ENSRNOG0000001518	2.095399725	0.02652079	Acot8
ENSRNOG0000000451	-	0.02656945	Igf1
ENSRNOG0000002161	-	0.02659480	Cela3b
ENSRNOG0000001304	-	0.02665913	Htr1b
ENSRNOG0000001451	-	0.02665913	Alg10
ENSRNOG0000001503	-	0.02670933	Myo7b
ENSRNOG0000002053	10.97128693	0.02674065	4732471J01Rik
ENSRNOG0000001664	-	0.02674065	Dner
ENSRNOG0000000634	2.577313073	0.02681971	Saysd1
ENSRNOG0000000312	-	0.02691697	Zfp496
ENSRNOG0000000377	2.124247499	0.02692256	Csrp2
ENSRNOG0000004771	30.31391853	0.02694473	LOC102557415
ENSRNOG0000001143	-	0.02694515	Mfhas1
ENSRNOG0000004353	10.6377296	0.02701175	AABR06026104.1
ENSRNOG0000003021	-2.01520639	0.02702282	Vps13c
ENSRNOG0000000272	3.093338544	0.02704332	Sele
ENSRNOG0000000434	-	0.02704419	Notch3
ENSRNOG0000000562	-	0.02716526	Gxylt2
ENSRNOG0000003408	-	0.02718938	Krt42
ENSRNOG0000003281	-	0.02723614	Mdc1
ENSRNOG0000001673	9.051219255	0.02730429	Tcerg1l
ENSRNOG0000001477	-	0.02732255	Adcy7
ENSRNOG0000001846	6.324985068	0.02738958	Lipt1
ENSRNOG0000001869	-	0.02741557	Rgs17
ENSRNOG0000000174	-	0.02742487	Pak2
ENSRNOG0000001134	-	0.02743038	Rictor
ENSRNOG0000001406	-	0.02743038	Ctsh
ENSRNOG0000000704	-	0.02743038	Eps8
ENSRNOG0000004638	2.105525164	0.02743038	AABR06064957.2
ENSRNOG0000001434	-	0.02743665	Anln
ENSRNOG0000001236	-	0.02743939	Pcdh7
ENSRNOG0000002678	-	0.02755188	RGD1308878
ENSRNOG0000002427	-2.31051252	0.02756086	Ino80d
ENSRNOG0000001794	5.643450409	0.02770206	Tbx10
ENSRNOG0000000533	5.344237077	0.02770206	Csdc2
ENSRNOG0000000636	-2.6416271	0.02770206	Slc5a8
ENSRNOG0000000658	2.179837268	0.02771997	Meox2
ENSRNOG0000000571	-8.13004732	0.02772940	Ptprd
ENSRNOG0000000312	-	0.02773409	Rtn4rl1
ENSRNOG0000004296	2.034389387	0.02777716	Rgcc
ENSRNOG0000001558	-	0.02778213	Suv39h2
ENSRNOG0000002773	-	0.02779409	Cnn1
ENSRNOG0000005010	-	0.02779409	LOC100911319
ENSRNOG0000003002	3.282068847	0.02785311	Ccl6
ENSRNOG0000001465	-	0.02785311	Arl11
ENSRNOG0000000235	-	0.02787542	Slc47a1
ENSRNOG0000003945	-	0.02788203	Pcdhgb5
ENSRNOG0000003185	-	0.02788203	Ndufa4l2
ENSRNOG0000001388	-	0.02791801	Psd3
ENSRNOG0000002333	-	0.02800367	Aff2
ENSRNOG0000000981	-	0.02800709	Vezf1
ENSRNOG0000001575	-	0.02805050	Wnt7b
ENSRNOG0000001863	-	0.02806261	Srcap
ENSRNOG0000001598	-	0.02808736	Rassf8
ENSRNOG0000000175	2.458242583	0.02808736	Nrros
ENSRNOG0000004573	7.273370697	0.02814494	AABR06053391.1
ENSRNOG0000001826	2.534960549	0.02822376	Slc23a3
ENSRNOG0000004568	-	0.02825618	AABR06090530.1

ENSRNOG0000001395	-	0.02838097	Aadac
ENSRNOG0000004563	-2.46396326	0.02846488	Fasn
ENSRNOG0000002153	-	0.02850499	Plxdc1
ENSRNOG0000001137	-	0.02852143	Socs4
ENSRNOG0000000974	2.988767319	0.02853608	Akap17b
ENSRNOG0000005086	6.843188062	0.02856228	AABR06107000.1
ENSRNOG0000000852	2.734099978	0.02870227	Pdzd3
ENSRNOG0000004708	2.349718277	0.02870227	Alkbh7
ENSRNOG0000000707	2.210777138	0.02870227	LOC691422
ENSRNOG0000004798	2.739984594	0.02870439	LOC100363408
ENSRNOG0000000169	11.16477668	0.02870971	Cldn14
ENSRNOG0000001180	5.449096619	0.02882147	Ghrhr
ENSRNOG0000000001	-	0.02882147	AABR06027248.1
ENSRNOG0000000111	-	0.02884302	Fbxl18
ENSRNOG0000002773	-	0.02885529	Cndp1
ENSRNOG0000001205	-	0.02885529	Egflam
ENSRNOG0000000903	-	0.02892346	Cntn2
ENSRNOG0000000455	2.030735899	0.02892583	Cox20
ENSRNOG0000004998	4.326515389	0.02894764	AABR06025244.2
ENSRNOG0000004998	7.823121209	0.02894871	AABR06077911.1
ENSRNOG0000001066	-	0.02896413	Wisp2
ENSRNOG0000002475	-	0.02896985	RGD1562107
ENSRNOG0000004846	4.956596435	0.02898467	AABR06062965.1
ENSRNOG0000001892	-	0.02909928	Sprn
ENSRNOG0000001749	2.613909531	0.02913085	Cnp
ENSRNOG0000001131	-	0.02925973	Zbtb10
ENSRNOG0000001964	2.14765942	0.02933622	Pcyox1l
ENSRNOG0000001001	-	0.02938052	Osbpl3
ENSRNOG0000001884	3.806746264	0.02938247	Sox8
ENSRNOG0000003585	14.24930355	0.02952793	5S_rRNA
ENSRNOG0000003423	3.325755504	0.02957472	Mt-co1
ENSRNOG0000003557	12.11934166	0.02966711	Mir27b
ENSRNOG0000001087	2.168378281	0.02966711	LOC691931
ENSRNOG0000000603	-	0.02974038	Ptprz1
ENSRNOG0000001139	2.042741264	0.02978947	Kif3c
ENSRNOG0000000133	-	0.02979759	Zkscan1
ENSRNOG0000002383	11.59311884	0.02981947	Sycp2l
ENSRNOG0000001331	-	0.02981947	Kcnt2
ENSRNOG0000002074	4.325654847	0.02981947	Lin7b
ENSRNOG0000001865	-	0.02981947	Csf1
ENSRNOG0000001191	-	0.02984894	Cp
ENSRNOG0000003920	6.265413955	0.02988058	Pram1
ENSRNOG0000003336	4.706109288	0.02997011	Slc39a5
ENSRNOG0000001001	5.664800416	0.02998617	Fam166a
ENSRNOG0000004833	6.014289155	0.03010377	AABR06013100.1
ENSRNOG0000001642	5.388145947	0.03012718	Tyr
ENSRNOG0000002011	-	0.03020133	Pcdhac1
ENSRNOG0000004674	-	0.03022654	Ankrd29
ENSRNOG0000001638	-	0.03023979	Ust
ENSRNOG0000001012	5.411077119	0.03028796	Lef1
ENSRNOG0000001451	-	0.03028796	Cdc14a
ENSRNOG0000004833	4.182056932	0.03036898	AABR06033087.1
ENSRNOG0000000527	2.669517784	0.03036898	Ptprv
ENSRNOG0000004896	5.956859981	0.03037386	AABR06064747.2
ENSRNOG0000000718	-	0.03037556	Lmod1
ENSRNOG0000004646	-	0.03039222	En1
ENSRNOG0000000948	-	0.03039222	Slc24a3
ENSRNOG0000004761	5.017369369	0.03041364	AABR06103642.3
ENSRNOG0000001857	-	0.03042598	C1qtnf3
ENSRNOG0000001432	-	0.03049198	Extl2
ENSRNOG0000002271	-	0.03049411	Abcb1b
ENSRNOG0000004613	7.358685577	0.03056602	LOC316935
ENSRNOG0000001969	-	0.03059310	Ankrd28
ENSRNOG0000000461	-	0.03059310	Fmnl2
ENSRNOG0000002125	-	0.03069156	Adra1d
ENSRNOG0000001061	7.236805433	0.03075199	AABR06012068.1
ENSRNOG0000002418	-	0.03084675	Tpsab1
ENSRNOG0000001670	3.689569527	0.03088462	Gng8
ENSRNOG0000000282	-	0.03088462	Hsd17b7
ENSRNOG0000000996	2.210285265	0.03115861	Pih1d2
ENSRNOG0000000697	-	0.03124481	Zfp189
ENSRNOG0000002453	-	0.03129756	Ccbe1
ENSRNOG0000000251	-	0.03135079	Atp7a
ENSRNOG0000004632	-	0.03157165	LOC683404
ENSRNOG0000001091	-	0.03166487	Bmp5
ENSRNOG0000002147	4.783030633	0.03167377	Ermn
ENSRNOG0000004915	2.326616199	0.03172983	Nme4
ENSRNOG0000003195	3.007918713	0.03189983	LOC100361645
ENSRNOG0000001822	-	0.03206506	Tp53inp2
ENSRNOG0000000364	4.177920795	0.03207224	Cldn6
ENSRNOG0000003185	-2.53592345	0.03207955	Lsamp
ENSRNOG0000000691	2.055563277	0.03207955	Rpain
ENSRNOG0000000275	-	0.03209531	Rc3h1
ENSRNOG0000001264	-	0.03209531	Dpp7
ENSRNOG0000004592	2.981536639	0.03212330	LOC100910474
ENSRNOG0000004638	5.217197469	0.03217425	AABR06081235.1
ENSRNOG0000003300	9.48807992	0.03221839	AABR06026204.1
ENSRNOG0000001386	2.677574797	0.03221929	Dusp2
ENSRNOG0000002151	-	0.03224524	Tmem231
ENSRNOG0000001759	5.124393284	0.03239299	Fbp1
ENSRNOG0000000775	-	0.03240884	Pm20d2
ENSRNOG0000000086	-	0.03251922	Arhgef6
ENSRNOG0000005063	-4.20211956	0.03257266	AABR06044678.1
ENSRNOG0000000948	-	0.03257266	Emx2
ENSRNOG0000004625	-3.31999216	0.03262739	Tbl2
ENSRNOG0000002976	-	0.03262911	AABR06019060.1
ENSRNOG0000005086	3.436676388	0.03269393	AABR06023614.1
ENSRNOG0000001921	3.695646792	0.03278614	Il12rb1
ENSRNOG0000004012	-	0.03280364	Cd209a
ENSRNOG0000004568	2.714167672	0.03287048	AABR06103586.1
ENSRNOG0000001556	-	0.03288312	RGD1310712
ENSRNOG0000001481	-	0.03288312	Slc1a1
ENSRNOG0000001612	-	0.03295086	Hmgcr
ENSRNOG0000004251	-	0.03297389	LOC102550512
ENSRNOG0000001887	2.469530955	0.03297468	Phf19
ENSRNOG0000003945	-2.93294661	0.03298335	LOC102552705
ENSRNOG0000004825	-	0.03298335	NA
ENSRNOG0000000606	-2.04421418	0.03313771	Tmem117
ENSRNOG0000000596	-	0.03317188	Nr4a3
ENSRNOG0000004892	-	0.03317434	Islr
ENSRNOG0000000853	4.002973047	0.03321655	Dusp15
ENSRNOG0000001660	2.138957827	0.03328091	Zfp579
ENSRNOG0000002357	-	0.03332747	Tet2
ENSRNOG0000000707	-	0.03333598	Wisp1
ENSRNOG0000004775	2.554673306	0.03339796	Epc1
ENSRNOG0000001505	-2.34946436	0.03340074	Mcfd2
ENSRNOG0000003561	4.109122836	0.03343988	Mir7a-1
ENSRNOG0000000533	13.17215638	0.03358853	Galnt13
ENSRNOG0000001180	8.744159253	0.03358853	Rpgrip1
ENSRNOG0000000675	-	0.03363221	Tgm3
ENSRNOG0000001894	-	0.03364658	Pank1
ENSRNOG0000000764	6.030169853	0.03369448	Oprk1
ENSRNOG0000004335	-	0.03369613	Cap2
ENSRNOG0000000872	8.744319804	0.03380911	Crnn
ENSRNOG0000003365	2.946666147	0.03380911	Mpp3
ENSRNOG0000001229	2.325714553	0.03381646	Gchfr
ENSRNOG0000000207	-	0.03388149	Rest
ENSRNOG0000003419	-	0.03395702	Fmo1
ENSRNOG0000001400	-	0.03396754	Gfod1
ENSRNOG0000000150	2.169589362	0.03397845	Tmem35
ENSRNOG0000000829	-	0.03410080	Dock7
ENSRNOG0000003140	-	0.03410080	Hps3
ENSRNOG0000002191	-	0.03416432	Slc16a12
ENSRNOG0000000303	-3.49325955	0.03426485	Awat2
ENSRNOG0000001540	12.15421666	0.03428596	Cd52
ENSRNOG0000003018	-	0.03430320	Mmp12
ENSRNOG0000003037	3.911937468	0.03430320	Mt-co2
ENSRNOG0000003664	5.113987634	0.03435016	LOC689065
ENSRNOG0000000518	-	0.03435016	Tspan11
ENSRNOG0000000401	2.033896711	0.03435016	Phlda1
ENSRNOG0000004835	-	0.03443754	AABR06016929.1
ENSRNOG0000004939	116.5385161	0.03449355	Krtap13
ENSRNOG0000002057	2.885360823	0.03449355	Spred3
ENSRNOG0000002636	-	0.03451473	Tanc2
ENSRNOG0000004015	4.881854263	0.03451550	Rdh5
ENSRNOG0000001333	-	0.03451550	Maml3
ENSRNOG0000004838	2.421698772	0.03451550	Fgf18
ENSRNOG0000003668	5.452530166	0.03458156	Npb
ENSRNOG0000004745	4.684446396	0.03458156	AABR06090814.1
ENSRNOG0000005021	3.293376796	0.03470539	RT1-CE10
ENSRNOG0000000695	22.67881952	0.03470748	Padi3
ENSRNOG0000003031	-	0.03473142	Bend6
ENSRNOG0000000770	2.089565844	0.03473404	Zfp467
ENSRNOG0000002478	2.199422146	0.03481522	MGC95210
ENSRNOG0000004880	-	0.03481522	Nr3c1
ENSRNOG0000004751	3.018804992	0.03482662	Oxld1
ENSRNOG0000002124	2.127475302	0.03488782	Spef1
ENSRNOG0000000909	-	0.03490715	Pon3
ENSRNOG0000001891	-	0.03497630	Tagap
ENSRNOG0000001282	-	0.03497630	Creb3l2
ENSRNOG0000000344	7.009965766	0.03499473	Asb9
ENSRNOG0000003361	3.385586556	0.03499473	ND3
ENSRNOG0000004863	3.368233371	0.03507037	AABR06011509.1
ENSRNOG0000003686	4.420745271	0.03525645	Tmem88b
ENSRNOG0000003708	-	0.03526957	LOC100910104
ENSRNOG0000002825	11.82258856	0.03534984	Lax1
ENSRNOG0000001554	-	0.03536441	RGD1305938
ENSRNOG0000002011	-	0.03538714	Cnnm2
ENSRNOG0000002763	2.175121961	0.03545010	Casc1
ENSRNOG0000000590	-	0.03547153	Pde4b
ENSRNOG0000000053	2.47591571	0.03574591	Ccdc167
ENSRNOG0000002083	2.299107363	0.03574591	Cspg5
ENSRNOG0000001687	-	0.03584341	Lppr5
ENSRNOG0000001332	-	0.03590062	Hmbox1
ENSRNOG0000004316	-2.23565982	0.03590062	Itga9
ENSRNOG0000002431	2.291368449	0.03590504	Xkr8
ENSRNOG0000004821	43.83255479	0.03591882	Krtap26-1
ENSRNOG0000001480	2.22914788	0.03591882	Exog
ENSRNOG0000000389	-	0.03603221	Tnmd
ENSRNOG0000000273	-2.73212671	0.03612447	Rabgap1l
ENSRNOG0000003779	2.784556695	0.03625862	Ldlrad1
ENSRNOG0000002479	2.001971493	0.03629230	Bora
ENSRNOG0000004682	6.221706737	0.03634805	AABR06089746.1
ENSRNOG0000000890	2.147149321	0.03639490	Fli1
ENSRNOG0000001642	-	0.03646379	Tacc1
ENSRNOG0000002905	-	0.03665725	AABR06101755.1
ENSRNOG0000004553	-	0.03676639	Gpr1
ENSRNOG0000000085	4.207258641	0.03678644	Lst1
ENSRNOG0000002389	2.464934204	0.03683980	Ube2u
ENSRNOG0000001317	-3.35457245	0.03689423	Far1
ENSRNOG0000004589	-	0.03690979	NA
ENSRNOG0000000440	-8.66262224	0.03691611	Avpr1a
ENSRNOG0000001219	5.746272589	0.03691611	Sox2
ENSRNOG0000000082	2.065519695	0.03691611	Ier3
ENSRNOG0000001785	8.564803857	0.03698080	Fev
ENSRNOG0000001120	-	0.03698080	Socs7
ENSRNOG0000003872	2.137532125	0.03698080	Cdkl1
ENSRNOG0000004647	5.234570078	0.03700812	Fmn2
ENSRNOG0000002019	2.805912329	0.03700812	Scgb1a1
ENSRNOG0000002558	-	0.03700812	Plagl1
ENSRNOG0000000583	-	0.03706497	AABR06031707.1
ENSRNOG0000002006	-	0.03709969	Pcdhb13
ENSRNOG0000002776	-	0.03712571	LOC100365826
ENSRNOG0000002796	-	0.03712571	Rn50_6_1181.1
ENSRNOG0000000121	33.20598949	0.03720886	LOC100365646
ENSRNOG0000001116	-2.63746537	0.03720886	Slc2a12
ENSRNOG0000002167	6.624155209	0.03741101	Ifitm7
ENSRNOG0000004294	2.005596539	0.03743467	Cenpw
ENSRNOG0000002300	-	0.03743858	Col6a6
ENSRNOG0000000282	-	0.03747394	Rlim
ENSRNOG0000002357	-	0.03749653	RGD1305645
ENSRNOG0000004265	2.188788556	0.03750173	LOC690871
ENSRNOG0000000175	-	0.03754678	LOC100911374
ENSRNOG0000004608	5.317909515	0.03756212	Tmc8
ENSRNOG0000004241	2.768133556	0.03756241	Nat14
ENSRNOG0000001411	-	0.03761686	Hmox1
ENSRNOG0000003883	-	0.03763003	Cd86
ENSRNOG0000001575	3.8326429	0.03763003	Cyp4f18
ENSRNOG0000001551	-	0.03763003	Bcat1
ENSRNOG0000000921	-	0.03771525	C3ar1
ENSRNOG0000000213	2.14466996	0.03802804	Aasdh
ENSRNOG0000003047	72.48788745	0.03803484	LOC100910814
ENSRNOG0000001115	-	0.03805300	Arsb
ENSRNOG0000000768	3.729269666	0.03817713	Sep-03
ENSRNOG0000000128	-	0.03823758	Gper1
ENSRNOG0000002992	-2.20382188	0.03836399	Tpk1
ENSRNOG0000002670	4.383191738	0.03838546	Drp2
ENSRNOG0000001597	-	0.03847140	Ano5
ENSRNOG0000004203	5.272022881	0.03847140	AABR06092315.1
ENSRNOG0000002013	30.92580625	0.03850146	LOC685544
ENSRNOG0000000003	3.516183866	0.0385156	Klhdc8a
ENSRNOG0000004247	-	0.03880216	RGD1560324
ENSRNOG0000003946	-5.64259188	0.03887990	Pcdhga3
ENSRNOG0000004846	4.226855525	0.03892525	AABR06010073.2
ENSRNOG0000002098	-9.31853625	0.03895444	AABR06009795.1
ENSRNOG0000002399	2.772894145	0.03897256	Kif1a
ENSRNOG0000000886	-	0.03897747	Stac
ENSRNOG0000004813	6.259141798	0.03897747	Ncmap
ENSRNOG0000000500	-	0.03911050	Scn3a
ENSRNOG0000000469	-	0.03912156	Fibin
ENSRNOG0000004028	-	0.03912733	Cyp1b1
ENSRNOG0000002862	-	0.03912733	Pnpla1
ENSRNOG0000001930	2.767369691	0.03912733	Sh3tc2
ENSRNOG0000000361	-	0.03912733	Mid1
ENSRNOG0000003061	4.979740158	0.03923279	LOC689899
ENSRNOG0000000384	-	0.03926003	Slit2

ENSRNOG0000000982	-	0.03927711	Bche
ENSRNOG0000000238	-	0.03964102	LOC100911714
ENSRNOG0000003986	4.568304743	0.03967827	LOC690617
ENSRNOG0000003122	3.392548294	0.03969291	LOC100910651
ENSRNOG0000004816	2.767828729	0.03969291	Arhgap19
ENSRNOG0000001197	-	0.03969291	Sema5a
ENSRNOG0000001421	-	0.03977897	Klf9
ENSRNOG0000005039	-	0.03980800	AABR06051781.1
ENSRNOG0000004223	2.102941776	0.03986452	Rpl41
ENSRNOG0000001971	6.027082641	0.03987803	Kcna5
ENSRNOG0000003113	-	0.03994155	Serpinb3
ENSRNOG0000001494	3.539307421	0.03997196	Sfrp5
ENSRNOG0000000902	4.802037015	0.0399915	Foxd3
ENSRNOG0000001528	-	0.04006729	Nt5c1a
ENSRNOG0000003309	4.839086942	0.04009479	Agbl4
ENSRNOG0000000084	20.58646597	0.04011011	Ly6g6d
ENSRNOG0000002729	-	0.04011011	Pcdhga7
ENSRNOG0000000196	2.241995455	0.04011011	Mx2
ENSRNOG0000004660	4.244500937	0.04012372	Muc2
ENSRNOG0000001677	-	0.04014601	Sap130
ENSRNOG0000002421	2.973400624	0.04018346	LOC679924
ENSRNOG0000001689	8.11651544	0.04024942	Rlbp1
ENSRNOG0000000541	-	0.04027738	Zhx2
ENSRNOG0000003731	7.713681234	0.04034799	Riiad1
ENSRNOG0000000408	-2.42667989	0.04043025	Enpp2
ENSRNOG0000004656	39.72237733	0.04044117	RGD1561684
ENSRNOG0000000836	2.234607009	0.04050561	Zfp775
ENSRNOG0000004345	3.087545887	0.04060036	Spp1
ENSRNOG0000002422	-	0.04070683	Mettl24
ENSRNOG0000001436	-	0.04076447	Shc3
ENSRNOG0000002691	2.334754787	0.04076447	Bbs10
ENSRNOG0000003120	5.282544697	0.04078544	LOC500035
ENSRNOG0000002077	2.413475623	0.04090166	Zfp382
ENSRNOG0000002861	-	0.04094801	Pck1
ENSRNOG0000003105	3.553974076	0.04094801	LOC100362751
ENSRNOG0000000314	-	0.04094801	Gprc5c
ENSRNOG0000003368	15.72226476	0.04103711	Elane
ENSRNOG0000001792	-	0.04108885	Tpbgl
ENSRNOG0000001524	-	0.04108885	Abca12
ENSRNOG0000003681	-	0.04108885	Ndrg3
ENSRNOG0000001107	-	0.04115956	Ank2
ENSRNOG0000004775	-	0.04119792	AABR06044018.1
ENSRNOG0000000155	-	0.04122295	Cxadr
ENSRNOG0000004963	7.378375421	0.04127681	AABR06075883.1
ENSRNOG0000004631	2.426133488	0.04127681	AABR06014093.1
ENSRNOG0000000875	12.91611754	0.04134088	Csf3r
ENSRNOG0000004334	-	0.04134088	LOC290595
ENSRNOG0000002917	11.22717443	0.04136560	LOC100361944
ENSRNOG0000004791	2.467944183	0.04136564	LOC100911456
ENSRNOG0000002580	-	0.04140300	Ms4a14
ENSRNOG0000000455	-	0.04141966	Sec14l4
ENSRNOG0000001743	-	0.04141966	Cgnl1
ENSRNOG0000004882	3.290055112	0.04142438	Rnf165
ENSRNOG0000004764	7.626377817	0.04143800	AABR06013759.1
ENSRNOG0000004896	-2.57897925	0.04150226	Bhlhe41
ENSRNOG0000001167	-	0.04158109	Tph1
ENSRNOG0000002126	-	0.04162013	Rassf2
ENSRNOG0000005063	-	0.04177025	AABR06045205.1
ENSRNOG0000002108	-	0.04178112	Mpeg1
ENSRNOG0000001848	2.043445786	0.04189632	Cd40
ENSRNOG0000004753	16.22736624	0.04191361	AABR06100208.3
ENSRNOG0000001972	-	0.04191361	Itgam
ENSRNOG0000002019	-	0.04191361	Cd248
ENSRNOG0000000835	2.017196091	0.04198439	RGD1308117
ENSRNOG0000000938	-	0.04203709	Pik3cg
ENSRNOG0000000810	40.63438758	0.04210210	Clec1b
ENSRNOG0000001175	-	0.04218698	Fkbp7
ENSRNOG0000001521	-	0.04222916	Sass6
ENSRNOG0000004229	8.282534052	0.04228128	Kpna7
ENSRNOG0000001263	-	0.04228988	Fbxo10
ENSRNOG0000001702	5.53805241	0.04231651	Pla2g2e
ENSRNOG0000004633	6.499298981	0.04244757	AABR06007382.1
ENSRNOG0000004789	3.671167507	0.04244757	AABR06051863.1
ENSRNOG0000000078	2.770288136	0.04244757	AABR06099817.1
ENSRNOG0000003958	-	0.04249104	RGD1561161
ENSRNOG0000000499	4.327572278	0.04250500	Jakmip1
ENSRNOG0000001624	3.898559332	0.04253023	Sox18
ENSRNOG0000003915	5.256160616	0.04253678	Acnat2
ENSRNOG0000002258	-	0.04253678	Atp10a
ENSRNOG0000002276	2.958197899	0.04256086	Evi2a
ENSRNOG0000000570	-	0.04263086	Mmp16
ENSRNOG0000001805	-	0.0426667	Runx3
ENSRNOG0000000843	29.74145216	0.04269830	Krt85
ENSRNOG0000001068	-	0.04269830	Pitx2
ENSRNOG0000000391	3.497279404	0.04278343	Fam78b
ENSRNOG0000000567	-	0.04278343	Fap
ENSRNOG0000001217	-	0.04285516	Rab27b
ENSRNOG0000001655	2.659196547	0.04289969	Dclk2
ENSRNOG0000002135	3.433129195	0.04294341	Dnah2
ENSRNOG0000003808	5.490033951	0.04297884	Nanos2
ENSRNOG0000001246	2.656533956	0.04300548	Cntf
ENSRNOG0000003668	5.555797842	0.04313568	Notum
ENSRNOG0000001174	2.007381712	0.04320702	Tmem205
ENSRNOG0000000395	-	0.04325280	Arhgap6
ENSRNOG0000004701	-	0.04325284	Homer1
ENSRNOG0000001012	-	0.04332694	Trim2
ENSRNOG0000004295	25.88421871	0.04335507	Krtap12-2
ENSRNOG0000000700	-	0.04345556	Lif
ENSRNOG0000004326	2.172372069	0.04355626	Ftsj2
ENSRNOG0000001051	-	0.04355626	Plau
ENSRNOG0000004207	-	0.04360807	Ticam2
ENSRNOG0000000402	4.179706806	0.04364509	Klhdc9
ENSRNOG0000000379	2.101731762	0.04366356	Nmral1
ENSRNOG0000005046	7.948914701	0.04371100	AABR06007815.1
ENSRNOG0000000020	6.238117672	0.04374369	Gsta5
ENSRNOG0000000934	5.079335699	0.04374369	Fcnb
ENSRNOG0000001088	-	0.04374728	Ankrd33b
ENSRNOG0000002726	-	0.04381094	AABR06009501.1
ENSRNOG0000002386	-	0.04381094	Snap91
ENSRNOG0000003051	2.732013708	0.04381094	Nfasc
ENSRNOG0000000546	-	0.04384381	Kcnmb1
ENSRNOG0000004744	2.405863032	0.04387536	Foxc2
ENSRNOG0000000698	2.10168711	0.04387536	RGD1304624
ENSRNOG0000003410	3.807737582	0.04402919	Plk5
ENSRNOG0000002069	5.200893188	0.04403556	Icam5
ENSRNOG0000002040	8.573991021	0.04407964	Atcay
ENSRNOG0000000799	2.013993892	0.04408798	Sh3tc1
ENSRNOG0000000344	-	0.04420892	Adora1
ENSRNOG0000004288	3.548587071	0.04421831	Alppl2
ENSRNOG0000004270	-2.75186135	0.04430318	Nipa1
ENSRNOG0000000934	4.827554962	0.04432409	Ugt8
ENSRNOG0000000378	2.658620825	0.04432409	Rilp
ENSRNOG0000004206	3.908222664	0.04442889	LOC680656
ENSRNOG0000004616	-	0.04443413	Ppm1l
ENSRNOG0000005056	-	0.04446638	Zfp449
ENSRNOG0000001275	2.643204111	0.04458134	Cklf
ENSRNOG0000001486	-	0.04462746	Pign
ENSRNOG0000003393	13.3478102	0.04478953	AY172581.22
ENSRNOG0000003736	-	0.04482435	Zfp939
ENSRNOG0000003933	3.251473325	0.04484141	Mslnl
ENSRNOG0000002113	2.067903317	0.0449438	Trmt112
ENSRNOG0000001548	-	0.04499237	Tead1
ENSRNOG0000001357	-	0.04499704	Kdelr3
ENSRNOG0000001324	-	0.04505487	Ptger4
ENSRNOG0000003933	2.582968523	0.04514683	Hrct1
ENSRNOG0000001396	3.107168374	0.04515334	Magi2
ENSRNOG0000000236	-2.83564436	0.04515334	Itm2a
ENSRNOG0000000844	-	0.04517368	Cbl
ENSRNOG0000002109	2.471113981	0.04533323	Scnm1
ENSRNOG0000000831	3.395904925	0.04536550	Hoxb3
ENSRNOG0000002007	-	0.04550295	Pcdhb9
ENSRNOG0000004558	3.942282921	0.04565604	AABR06008620.1
ENSRNOG0000001394	-7.82753682	0.04573681	RGD1565989
ENSRNOG0000001897	2.460526629	0.04605349	Cd163l1
ENSRNOG0000002230	-	0.04606088	Frem1
ENSRNOG0000003794	2.484681112	0.04611539	LOC100909581
ENSRNOG0000003244	-	0.04613769	Zfp641
ENSRNOG0000001722	-	0.04613769	Slc2a4
ENSRNOG0000004698	2.678972415	0.04614215	Gp1bb
ENSRNOG0000002679	-	0.04620184	Nt5dc3
ENSRNOG0000001188	-	0.04622375	Gab2
ENSRNOG0000001882	-	0.04622375	Slc5a5
ENSRNOG0000000756	-	0.04622375	Rem1
ENSRNOG0000004717	-	0.04632496	AABR06038420.1
ENSRNOG0000000910	-	0.04648327	Kb15
ENSRNOG0000000766	5.438326263	0.04650530	LOC100911372
ENSRNOG0000001944	2.052985183	0.04651252	Josd2
ENSRNOG0000000861	-	0.04657032	Mal2
ENSRNOG0000002464	2.177823295	0.04657032	LOC100910838
ENSRNOG0000001152	6.059142091	0.04657887	Hcn1
ENSRNOG0000004761	-	0.04663075	Mup5
ENSRNOG0000000732	-	0.04688714	Pars2
ENSRNOG0000002684	2.205053979	0.04698160	Hnrnph3
ENSRNOG0000004325	13.33851731	0.04704138	Bpifa6
ENSRNOG0000004666	2.556580771	0.04704138	Fosb
ENSRNOG0000000961	3.830376839	0.04711929	Bricd5
ENSRNOG0000000230	-	0.04713590	Slc15a2
ENSRNOG0000004038	7.513172488	0.04719063	rno-mir-762
ENSRNOG0000000039	2.754139631	0.04733087	Srgn
ENSRNOG0000000373	-	0.04733087	Flrt2
ENSRNOG0000004333	6.439916315	0.04736422	AABR06053812.2
ENSRNOG0000000157	8.132652472	0.04742282	Hoxd4
ENSRNOG0000002124	-	0.04744043	Siglec1
ENSRNOG0000004006	121.0940222	0.04768684	Krtap16-5
ENSRNOG0000001974	-	0.04768684	Prr16
ENSRNOG0000001816	-	0.04768684	Prkab2
ENSRNOG0000004671	3.547005268	0.04780674	AABR06074252.1
ENSRNOG0000000001	5.723936221	0.04800833	Tcf15
ENSRNOG0000001053	5.739593581	0.04815090	Oprd1
ENSRNOG0000004691	3.061000662	0.04828013	Ceacam9
ENSRNOG0000000261	3.529469583	0.04828365	Slc5a10
ENSRNOG0000002650	-	0.04831726	Fam114a1
ENSRNOG0000001590	-2.50953537	0.04834459	Cpxm2
ENSRNOG0000001835	2.237828541	0.04838285	Msx2
ENSRNOG0000003349	4.818693173	0.04838518	Vom2r52
ENSRNOG0000001374	9.568831766	0.04839129	Trem3
ENSRNOG0000000869	-	0.04839129	RGD1563365
ENSRNOG0000002797	12.2118196	0.04856042	LOC500354
ENSRNOG0000001120	6.334235938	0.04856042	Ccl3
ENSRNOG0000004930	-	0.04858460	AABR06056850.1
ENSRNOG0000000509	-3.03869111	0.04858460	C1qtnf7
ENSRNOG0000002395	2.93314875	0.04858460	Tbc1d30
ENSRNOG0000001258	-	0.04866036	Ccdc141
ENSRNOG0000004661	9.224313075	0.04871600	AABR06107475.1
ENSRNOG0000000898	-	0.04872298	Diaph3
ENSRNOG0000001159	4.978940986	0.04888346	Gldc
ENSRNOG0000002532	-	0.04892046	Tert
ENSRNOG0000001522	-	0.04892046	Myo1b
ENSRNOG0000004669	-	0.04892046	Mkl2
ENSRNOG0000002108	2.12757378	0.04895493	Lgi4
ENSRNOG0000003014	-2.07827056	0.04909319	Lphn3
ENSRNOG0000002927	-	0.04920662	E2f3
ENSRNOG0000001707	-	0.04927738	Pgm2l1
ENSRNOG0000001618	3.710892814	0.04950877	Mxd3
ENSRNOG0000005029	6.425104047	0.04952906	AABR06038744.1
ENSRNOG0000002535	2.155072886	0.04964070	Rinl
ENSRNOG0000002677	3.052258092	0.0498699	Tspyl3
ENSRNOG0000001390	-6.27544296	0.04987476	Sall1
ENSRNOG0000002873	4.00218213	0.04987476	Lcn12
ENSRNOG0000001156	-	0.04989869	Mtmr9

Supplementary Table 2. GO terms with significantly different expression between burn and control data. GO terms organise genes by hierarchies based on their involvement in biological processes, molecular functions and cellular components; a significant result indicates that the respective genes were among those represented in the experimental effect.

GO ID	Term	Annotated	Significant	P-Value
GO:0005518	collagen binding	55	30	1.00E-11
GO:0005539	glycosaminoglycan binding	154	55	1.40E-10
GO:0005178	integrin binding	89	35	1.80E-08
GO:0019838	growth factor binding	124	43	3.80E-08
GO:0005102	receptor binding	1188	239	3.30E-07
GO:0008201	heparin binding	121	40	4.80E-07
GO:0048407	platelet-derived growth factor binding	11	9	1.60E-06
GO:0050840	extracellular matrix binding	48	21	1.70E-06
GO:0030551	cyclic nucleotide binding	32	16	3.40E-06
GO:0005509	calcium ion binding	546	121	3.40E-06
GO:0004872	receptor activity	861	175	7.70E-06
GO:0060089	molecular transducer activity	861	175	7.70E-06
GO:1901681	sulfur compound binding	200	53	1.50E-05
GO:0001071	nucleic acid binding transcription factor activity	769	157	1.80E-05
GO:0003700	transcription factor activity, sequence-specific DNA binding	769	157	1.80E-05
GO:0050839	cell adhesion molecule binding	167	46	1.90E-05
GO:0005344	oxygen transporter activity	11	8	2.70E-05
GO:0015924	mannosyl-oligosaccharide mannosidase activity	9	7	4.60E-05
GO:0000981	RNA polymerase II transcription factor activity, sequence-specific DNA binding	493	106	5.20E-05
GO:0033218	amide binding	261	63	6.00E-05

GO:0005161	platelet-derived growth factor receptor binding	12	8	7.10E-05
GO:0030246	carbohydrate binding	206	52	7.60E-05
GO:0042277	peptide binding	237	58	7.70E-05
GO:0038023	signaling receptor activity	697	141	7.70E-05
GO:0004559	alpha-mannosidase activity	15	9	8.00E-05
GO:0030552	cAMP binding	22	11	0.00012
GO:0005201	extracellular matrix structural constituent	33	14	0.00014
GO:0071813	lipoprotein particle binding	19	10	0.00014
GO:0071814	protein-lipid complex binding	19	10	0.00014
GO:0001968	fibronectin binding	26	12	0.00016
GO:0015923	mannosidase activity	16	9	0.00016
GO:0043565	sequence-specific DNA binding	764	150	2.00E-04
GO:0004871	signal transducer activity	913	175	0.00022
GO:0004571	mannosyl-oligosaccharide 1,2-alpha-mannosidase activity	8	6	0.00024
GO:0046872	metal ion binding	2895	494	0.00025
GO:0019199	transmembrane receptor protein kinase activity	69	22	0.00031
GO:0000982	transcription factor activity, RNA polymerase II core promoter proximal region sequence-specific binding	291	65	0.00049
GO:0009374	biotin binding	4	4	0.00051
GO:0042605	peptide antigen binding	29	12	0.00054
GO:0043169	cation binding	2967	501	6.00E-04
GO:0019825	oxygen binding	22	10	0.00064
GO:0004888	transmembrane signaling receptor activity	612	120	0.00092
GO:0044212	transcription regulatory region DNA binding	630	123	0.00094
GO:0001067	regulatory region nucleic acid binding	636	124	0.00095
GO:0000976	transcription regulatory region sequence-specific DNA binding	514	103	0.00098
GO:0004112	cyclic-nucleotide phosphodiesterase activity	23	10	0.00099
GO:0000975	regulatory region DNA binding	633	123	0.00113
GO:0030169	low-density lipoprotein particle binding	13	7	0.00126

GO:0043548	phosphatidylinositol 3-kinase binding	36	13	0.00146
GO:0000977	RNA polymerase II regulatory region sequence-specific DNA binding	453	91	0.00175
GO:0001012	RNA polymerase II regulatory region DNA binding	459	92	0.00178
GO:0005125	cytokine activity	122	31	0.00178
GO:0099600	transmembrane receptor activity	649	124	0.00205
GO:1990837	sequence-specific double-stranded DNA binding	537	105	0.00206
GO:0004936	alpha-adrenergic receptor activity	5	4	0.00222
GO:0019911	structural constituent of myelin sheath	5	4	0.00222
GO:0038085	vascular endothelial growth factor binding	5	4	0.00222
GO:0043237	laminin-1 binding	5	4	0.00222
GO:0098634	protein binding involved in cell-matrix adhesion	5	4	0.00222
GO:0098639	collagen binding involved in cell-matrix adhesion	5	4	0.00222
GO:0000987	core promoter proximal region sequence-specific DNA binding	287	61	0.00256
GO:0001159	core promoter proximal region DNA binding	287	61	0.00256
GO:0004016	adenylate cyclase activity	11	6	0.00265
GO:0005507	copper ion binding	47	15	0.0027
GO:0004114	3',5'-cyclic-nucleotide phosphodiesterase activity	22	9	0.00294
GO:0004720	protein-lysine 6-oxidase activity	3	3	0.00337
GO:0008823	cupric reductase activity	3	3	0.00337
GO:0031720	haptoglobin binding	3	3	0.00337
GO:0052851	ferric-chelate reductase (NADPH) activity	3	3	0.00337
GO:0070051	fibrinogen binding	3	3	0.00337
GO:0005355	glucose transmembrane transporter activity	15	7	0.00359
GO:0046332	SMAD binding	67	19	0.00361
GO:0000978	RNA polymerase II core promoter proximal region sequence-specific DNA binding	275	58	0.00383
GO:0008237	metallopeptidase activity	144	34	0.00405
GO:0043236	laminin binding	27	10	0.00412

GO:0045499	chemorepellent activity	27	10	0.00412
GO:0042056	chemoattractant activity	23	9	0.0042
GO:0005126	cytokine receptor binding	204	45	0.00431
GO:0004714	transmembrane receptor protein tyrosine kinase activity	54	16	0.00455
GO:0035497	cAMP response element binding	12	6	0.00463
GO:0001228	transcriptional activator activity, RNA polymerase II transcription regulatory region sequence-specific binding	273	57	0.00516
GO:0001077	transcriptional activator activity, RNA polymerase II core promoter proximal region sequence-specific binding	201	44	0.00547
GO:0038024	cargo receptor activity	55	16	0.00554
GO:0005537	mannose binding	16	7	0.00556
GO:0015149	hexose transmembrane transporter activity	16	7	0.00556
GO:0008239	dipeptidyl-peptidase activity	9	5	0.00562
GO:0005114	type II transforming growth factor beta receptor binding	6	4	0.00588
GO:0001664	G-protein coupled receptor binding	219	47	0.00619
GO:0008238	exopeptidase activity	81	21	0.00717
GO:0004115	3',5'-cyclic-AMP phosphodiesterase activity	13	6	0.00751
GO:0008235	metalloexopeptidase activity	38	12	0.00765
GO:0019955	cytokine binding	82	21	0.00831
GO:0030553	cGMP binding	10	5	0.00985
GO:0098631	protein binding involved in cell adhesion	10	5	0.00985
GO:0043394	proteoglycan binding	26	9	0.0105
GO:0008329	signaling pattern recognition receptor activity	14	6	0.0115
GO:0034185	apolipoprotein binding	14	6	0.0115
GO:0038187	pattern recognition receptor activity	14	6	0.0115
GO:0015145	monosaccharide transmembrane transporter activity	18	7	0.0118
GO:0043274	phospholipase binding	18	7	0.0118
GO:0030284	estrogen receptor activity	4	3	0.012
GO:0038064	collagen receptor activity	4	3	0.012

GO:0004935	adrenergic receptor activity	7	4	0.0121
GO:0016723	oxidoreductase activity, oxidizing metal ions, NAD or NADP as acceptor	7	4	0.0121
GO:0020037	heme binding	111	26	0.0122
GO:0001540	beta-amyloid binding	31	10	0.0123
GO:0001948	glycoprotein binding	106	25	0.0127
GO:0001076	transcription factor activity, RNA polymerase II transcription factor binding	117	27	0.0131
GO:0046906	tetrapyrrole binding	117	27	0.0131
GO:0030546	receptor activator activity	23	8	0.0151
GO:0008081	phosphoric diester hydrolase activity	71	18	0.0154
GO:0008009	chemokine activity	32	10	0.0155
GO:0004675	transmembrane receptor protein serine/threonine kinase activity	15	6	0.0168
GO:0017171	serine hydrolase activity	136	30	0.0174
GO:0003690	double-stranded DNA binding	608	110	0.0183
GO:0004177	aminopeptidase activity	33	10	0.0194
GO:0005520	insulin-like growth factor binding	24	8	0.0198
GO:0008083	growth factor activity	110	25	0.0199
GO:0044877	macromolecular complex binding	1366	231	0.0211
GO:0042379	chemokine receptor binding	43	12	0.0212
GO:0001223	transcription coactivator binding	8	4	0.0213
GO:0003810	protein-glutamine gamma-glutamyltransferase activity	8	4	0.0213
GO:0008046	axon guidance receptor activity	8	4	0.0213
GO:0043167	ion binding	4656	738	0.0214
GO:0009975	cyclase activity	20	7	0.0219
GO:0030215	semaphorin receptor binding	20	7	0.0219
GO:0001046	core promoter sequence-specific DNA binding	95	22	0.0227
GO:0016722	oxidoreductase activity, oxidizing metal ions	12	5	0.0239
GO:0036312	phosphatidylinositol 3-kinase regulatory subunit binding	12	5	0.0239

GO:0008236	serine-type peptidase activity	134	29	0.0244
GO:0004222	metalloendopeptidase activity	85	20	0.0246
GO:0008047	enzyme activator activity	313	60	0.0248
GO:0005044	scavenger receptor activity	39	11	0.0248
GO:0016504	peptidase activator activity	25	8	0.0254
GO:0004075	biotin carboxylase activity	5	3	0.0266
GO:0004887	thyroid hormone receptor activity	5	3	0.0266
GO:0004908	interleukin-1 receptor activity	5	3	0.0266
GO:0008035	high-density lipoprotein particle binding	5	3	0.0266
GO:0030492	hemoglobin binding	5	3	0.0266
GO:0048495	Roundabout binding	5	3	0.0266
GO:1990239	steroid hormone binding	5	3	0.0266
GO:0004553	hydrolase activity, hydrolyzing O-glycosyl compounds	70	17	0.0273
GO:0042562	hormone binding	70	17	0.0273
GO:0042169	SH2 domain binding	30	9	0.0276
GO:0016849	phosphorus-oxygen lyase activity	21	7	0.0287
GO:0017134	fibroblast growth factor binding	21	7	0.0287
GO:0004181	metallocarboxypeptidase activity	17	6	0.0318
GO:0031690	adrenergic receptor binding	17	6	0.0318
GO:0016857	racemase and epimerase activity, acting on carbohydrates and derivatives	9	4	0.0339
GO:0047555	3',5'-cyclic-GMP phosphodiesterase activity	9	4	0.0339
GO:0004180	carboxypeptidase activity	31	9	0.0339
GO:0045236	CXCR chemokine receptor binding	13	5	0.0341
GO:0030545	receptor regulator activity	36	10	0.035
GO:0070851	growth factor receptor binding	116	25	0.0364
GO:0046982	protein heterodimerization activity	435	79	0.0376
GO:0005179	hormone activity	62	15	0.0378
GO:0003705	transcription factor activity, RNA polymerase II distal enhancer	73	17	0.0397

	sequence-specific binding			
GO:0004896	cytokine receptor activity	73	17	0.0397
GO:0004713	protein tyrosine kinase activity	117	25	0.0399
GO:0004869	cysteine-type endopeptidase inhibitor activity	47	12	0.041
GO:0005112	Notch binding	18	6	0.0418
GO:0043395	heparan sulfate proteoglycan binding	18	6	0.0418
GO:0071837	HMG box domain binding	18	6	0.0418
GO:0005506	iron ion binding	158	32	0.0442
GO:0061134	peptidase regulator activity	158	32	0.0442
GO:0001227	transcriptional repressor activity, RNA polymerase II transcription regulatory region sequence-specific binding	141	29	0.0449
GO:0008252	nucleotidase activity	14	5	0.0467
GO:0010576	metalloenzyme regulator activity	14	5	0.0467
GO:0033612	receptor serine/threonine kinase binding	14	5	0.0467
GO:0050431	transforming growth factor beta binding	14	5	0.0467
GO:0070696	transmembrane receptor protein serine/threonine kinase binding	14	5	0.0467
GO:0004690	cyclic nucleotide-dependent protein kinase activity	6	3	0.0473
GO:0005021	vascular endothelial growth factor-activated receptor activity	6	3	0.0473
GO:0031726	CCR1 chemokine receptor binding	6	3	0.0473
GO:0033691	sialic acid binding	6	3	0.0473
GO:0030331	estrogen receptor binding	38	10	0.0492
GO:0016004	phospholipase activator activity	10	4	0.0499
GO:0070700	BMP receptor binding	10	4	0.0499

Supplementary Table 3. Significantly differentially expressed KEGG pathways, which associate genes by their shared pathways for biological interactions. A significant result indicates that the respective genes were among those represented in the experimental effect.

KEGG.ID	Term	Annotated	Significant	Expected	P.Value
4512	ECM-receptor interaction	65	30	10.27338744	6.23E-09
4974	Protein digestion and absorption	62	26	9.799231098	6.81E-07
4060	Cytokine-cytokine receptor interaction	156	48	24.65612986	1.45E-06
4510	Focal adhesion	174	51	27.50106792	3.38E-06
5150	Staphylococcus aureus infection	41	19	6.480136694	3.69E-06
4514	Cell adhesion molecules (CAMs)	124	39	19.5984622	7.98E-06
4640	Hematopoietic cell lineage	64	24	10.11533533	1.85E-05
5144	Malaria	45	18	7.112345152	7.69E-05
5320	Autoimmune thyroid disease	37	15	5.847928236	0.000255231
4610	Complement and coagulation cascades	54	19	8.534814182	0.000359087
4145	Phagosome	148	39	23.39171294	0.000571826
4270	Vascular smooth muscle contraction	101	29	15.96326356	0.000653453
4360	Axon guidance	117	32	18.49209739	0.000887947
5330	Allograft rejection	37	14	5.847928236	0.000932679
5310	Asthma	14	7	2.212729603	0.00296275
5323	Rheumatoid arthritis	68	20	10.74754378	0.003197688
5143	African trypanosomiasis	30	11	4.741563434	0.004335135
5332	Graft-versus-host disease	39	13	6.164032465	0.005149132
4672	Intestinal immune network for IgA production	27	10	4.267407091	0.005943466
4620	Toll-like receptor signaling pathway	81	22	12.80222127	0.005945663
5416	Viral myocarditis	69	19	10.9055959	0.008734295
4940	Type I diabetes mellitus	42	13	6.638188808	0.010258887
4630	Jak-STAT signaling pathway	110	27	17.38573259	0.01070756

4976	Bile secretion	61	17	9.641178983	0.011272773
5146	Amoebiasis	86	22	13.59248185	0.012455082
5140	Leishmaniasis	58	16	9.16702264	0.015165736
4910	Insulin signaling pathway	119	28	18.80820162	0.016778365
5020	Prion diseases	31	10	4.899615549	0.01724752
5414	Dilated cardiomyopathy	77	19	12.17001282	0.027900029
5142	Chagas disease (American trypanosomiasis)	89	21	14.06663819	0.034292071
4970	Salivary secretion	64	16	10.11533533	0.037132791
4960	Aldosterone-regulated sodium reabsorption	40	11	6.322084579	0.041283049
5200	Pathways in cancer	287	56	45.36095686	0.047888832
5322	Systemic lupus erythematosus	66	16	10.43143956	0.048017692

Supplementary Material 4. Demonstrating the use of identity matrices and Kronecker Tensor products in Matlab.

```
1. X  = kron(eye(2,2),eye(7,7));  % the effect of two sites measured seven times
2. X  = kron(ones(4,1),X);        % over four animals
3. X0  = kron(eye(8,8),ones(7,1)); % confounds are constants for each timeseries
```

Lines 2-4 serve to create the design matrix. In the Matlab environment, the term matrix refers to a type of array. An array is simply a grid of numbers. A 1x1 array is a scalar, an m x 1 array is a column vector, a 1 x n array is a row vector and a matrix is a two-dimensional grid such as:

```
7     2
5     4
7     2
```

A matrix is always rectangular, as the component vectors along one dimension are equal in length. In line 2, X is being defined as a type of matrix known as a Kronecker Tensor Product. This type of matrix, created with the syntax kron(X,Y), contains all possible products of the respective elements of two smaller arrays X and Y arranged as below:

```
[X(1,1)*Y  X(1,2)*Y  . . .  X(1,n)*Y
                . . .
X(m,1)*Y  X(m,2)*Y  . . .  X(m,n)*Y]
```

For example, the Kronecker product of the two matrices D and E are shown below.

```
  D =
1     2
2     2
  E =
1     3
3     3
```

```
kron(D,E)=

     1     3     2     6
     3     3     6     6
     2     6     2     6
     6     6     6     6

kron(E,D)=

     1     2     3     6
     2     2     6     6
     3     6     3     6
     6     6     6     6
```

Line 2 incorporates two identity matrices: eye(2,2) and eye(7,7). An identity matrix is a matrix with ones on the main diagonal and zeroes elsewhere. For example:

```
     1     0     0
     0     1     0
     0     0     1
```

An identity matrix with m rows and n columns is generated in Matlab via the syntax eye(m,n). Hence, the output of line 2 is the Kronecker product of two identity matrices. The first identity matrix is 2x2, representing the two sites, and the second is 7x7, representing the seven time points. The result is:

```
1  0  0  0  0  0  0  0  0  0  0  0  0  0
0  1  0  0  0  0  0  0  0  0  0  0  0  0
0  0  1  0  0  0  0  0  0  0  0  0  0  0
0  0  0  1  0  0  0  0  0  0  0  0  0  0
0  0  0  0  1  0  0  0  0  0  0  0  0  0
0  0  0  0  0  1  0  0  0  0  0  0  0  0
0  0  0  0  0  0  1  0  0  0  0  0  0  0
0  0  0  0  0  0  0  1  0  0  0  0  0  0
0  0  0  0  0  0  0  0  1  0  0  0  0  0
0  0  0  0  0  0  0  0  0  1  0  0  0  0
0  0  0  0  0  0  0  0  0  0  1  0  0  0
0  0  0  0  0  0  0  0  0  0  0  1  0  0
0  0  0  0  0  0  0  0  0  0  0  0  1  0
0  0  0  0  0  0  0  0  0  0  0  0  0  1
```

Line 3 generates another Kronecker Tensor product. Here, the ones function creates a 4 x 1 array of ones, such that the Kronecker product is the above matrix repeated four times (for four animals). The result is:

X=

1	0	0	0	0	0	0	0	0	0	0	0	0	0	0
0	1	0	0	0	0	0	0	0	0	0	0	0	0	0
0	0	1	0	0	0	0	0	0	0	0	0	0	0	0
0	0	0	1	0	0	0	0	0	0	0	0	0	0	0
0	0	0	0	1	0	0	0	0	0	0	0	0	0	0
0	0	0	0	0	1	0	0	0	0	0	0	0	0	0
0	0	0	0	0	0	1	0	0	0	0	0	0	0	0
0	0	0	0	0	0	0	1	0	0	0	0	0	0	0
0	0	0	0	0	0	0	0	1	0	0	0	0	0	0
0	0	0	0	0	0	0	0	0	1	0	0	0	0	0
0	0	0	0	0	0	0	0	0	0	1	0	0	0	0
0	0	0	0	0	0	0	0	0	0	0	1	0	0	0
0	0	0	0	0	0	0	0	0	0	0	0	1	0	0
0	0	0	0	0	0	0	0	0	0	0	0	0	1	0
0	0	0	0	0	0	0	0	0	0	0	0	0	0	1
1	0	0	0	0	0	0	0	0	0	0	0	0	0	0
0	1	0	0	0	0	0	0	0	0	0	0	0	0	0
0	0	1	0	0	0	0	0	0	0	0	0	0	0	0
0	0	0	1	0	0	0	0	0	0	0	0	0	0	0
0	0	0	0	1	0	0	0	0	0	0	0	0	0	0
0	0	0	0	0	1	0	0	0	0	0	0	0	0	0
0	0	0	0	0	0	1	0	0	0	0	0	0	0	0
0	0	0	0	0	0	0	1	0	0	0	0	0	0	0
0	0	0	0	0	0	0	0	1	0	0	0	0	0	0
0	0	0	0	0	0	0	0	0	1	0	0	0	0	0
0	0	0	0	0	0	0	0	0	0	1	0	0	0	0
0	0	0	0	0	0	0	0	0	0	0	1	0	0	0
0	0	0	0	0	0	0	0	0	0	0	0	1	0	0
0	0	0	0	0	0	0	0	0	0	0	0	0	1	0
0	0	0	0	0	0	0	0	0	0	0	0	0	0	1
1	0	0	0	0	0	0	0	0	0	0	0	0	0	0
0	1	0	0	0	0	0	0	0	0	0	0	0	0	0
0	0	1	0	0	0	0	0	0	0	0	0	0	0	0
0	0	0	1	0	0	0	0	0	0	0	0	0	0	0
0	0	0	0	1	0	0	0	0	0	0	0	0	0	0
0	0	0	0	0	1	0	0	0	0	0	0	0	0	0
0	0	0	0	0	0	1	0	0	0	0	0	0	0	0
0	0	0	0	0	0	0	1	0	0	0	0	0	0	0
0	0	0	0	0	0	0	0	1	0	0	0	0	0	0
0	0	0	0	0	0	0	0	0	1	0	0	0	0	0
0	0	0	0	0	0	0	0	0	0	1	0	0	0	0
0	0	0	0	0	0	0	0	0	0	0	1	0	0	0
0	0	0	0	0	0	0	0	0	0	0	0	1	0	0
0	0	0	0	0	0	0	0	0	0	0	0	0	1	0
0	0	0	0	0	0	0	0	0	0	0	0	0	0	1
1	0	0	0	0	0	0	0	0	0	0	0	0	0	0
0	1	0	0	0	0	0	0	0	0	0	0	0	0	0
0	0	1	0	0	0	0	0	0	0	0	0	0	0	0
0	0	0	1	0	0	0	0	0	0	0	0	0	0	0
0	0	0	0	1	0	0	0	0	0	0	0	0	0	0
0	0	0	0	0	1	0	0	0	0	0	0	0	0	0
0	0	0	0	0	0	1	0	0	0	0	0	0	0	0
0	0	0	0	0	0	0	1	0	0	0	0	0	0	0
0	0	0	0	0	0	0	0	1	0	0	0	0	0	0
0	0	0	0	0	0	0	0	0	1	0	0	0	0	0
0	0	0	0	0	0	0	0	0	0	1	0	0	0	0
0	0	0	0	0	0	0	0	0	0	0	1	0	0	0
0	0	0	0	0	0	0	0	0	0	0	0	1	0	0
0	0	0	0	0	0	0	0	0	0	0	0	0	1	0
0	0	0	0	0	0	0	0	0	0	0	0	0	0	1